# ASSESSMENT OF CLIMATE CHANGE IMPACT ON RUNOFF AND PEAK FLOW – A CASE STUDY ON KLANG WATERSHED IN WEST MALAYSIA

**Reza Kabiri**

**Thesis submitted to the University of Nottingham for the degree of Doctor of Philosophy**

**April 2014**

# ABSTRACT

Climate change is a consequence of changing in climate on environment over the worldwide. The increase in developmental activities and Greenhouse Gases ($GHG_S$) put a strain on environment, resulting in increased use of fuel resources. The consequence of such an emission to the atmosphere exacerbates climate pattern. There are numerous Climate Change Downscaling studies in coarse resolution, which have largely centred on employing the dynamic approaches, and in most of these investigations, the Regional Climate Model (RCM) has been reported to numerically predict the local climatic variables. The majority of previous investigations have failed to account for the spatial watershed scale, which could generate an average value of downscaled variables over the watershed scale.

To address shortcomings of previous investigations, the work undertaken in this project has two main objectives. The study first aims to implement a spatially distributed Statistical Downscaling Model (SDSM) to downscale the predictands, and second to evaluate the impact of climate changes on the future discharge and peak flow. It is conducted based on the IPCC Scenarios A2 (Medium–High Emission scenario) and B2 (Medium–Low Emission scenario). The main objectives of the study are as follows:

- To generate fine resolution climate change scenarios using Statistical Downscaling Model in the watershed scale,

- To project the variability in temperature, precipitation and evaporation for the three time slices, 2020s (2010 to 2039), 2050s (2040 to 2069) and 2080s (2070 to 2099), based on A2 and B2 scenarios,

- To calibrate and validate hydrological model using historical observed flow data to verify the performance of the hydrological model,

- To evaluate the impact of climate changes on the future discharge and future peak flow for three timeslices: 2020s (2010 to 2039), 2050s (2040 to 2069) and 2080s (2070 to 2099).

Thus, to meet the objectives of the study, projection of the future climate based on climate change scenarios from IPCC is carried out as the most important component in the research. The results of this research are presented as follows:

- The study indicates that there will be an increase of mean monthly precipitation but with an intensified decrease in the number of consecutive wet-days and can be concluded as a possibility of more precipitation amount in fewer days.

- The watershed is found to experience increased rainfall towards the end of the century. However, the analysis indicates that there will likely be a negative trend of mean precipitation in 2020s and with no difference in 2050s. The precipitation experiences a mean annual decrease by 7.9%, 0.6% in 2020s and 2050s and an increase by 12.4% in 2080s corresponding A2 scenario.

- The maximum and minimum temperatures are likely to be increased toward the end of the century by 2.7$^{o}$C and 0.8$^{o}$C respectively when compared to the current observed temperature (1975-2001) at the Subang temperature station.

- The average annual mean discharge is predicted to be decreasing by 9.4%, 4.9% and an increase of 3.4% for the A2 and a decrease of 17.3%, 13.6% and 5.1% for the B2 scenario, respectively in the 2020s, 2050s and 2080s.

- The average annual maximum discharge is projected to decrease by 7.7% in 2020s and an increase by 4.2% and 29% in A2 scenario for 2050s and 2080s, respectively. But there will most likely be a decrease in the maximum discharge for all the future under B2 scenario. It is projected a decrease of 32.3%, 19.5% and 2.3% for 2020s, 2050s and 2080s, respectively.

- The projected mean discharge indicates a decline in the months from January to April and also from July to August in all the three future periods for A2 and B2 scenarios. There is an increasing trend in the discharge of September and October in the 2020s according to the A2 and B2 scenarios.

- The highest increase in precipitation frequency occurs in 2080s under A2 scenario in which the increase in the magnitude of 100 Return Year is found to be 88% greater than the one of the maximum observed.

- The highest increase in flood frequency at Sulaiman streamflow station occurs in 2080s under A2 scenario. The increase in the magnitude of 100 Return Year is found to be 26.5% greater than the one of the maximum observed.

## PUBLICATIONS

### Journal

Kabiri, R., Ramani Bai V., and Chan, A. 2013. Comparison of SCS and Green-Ampt methods in surface runoff-Flooding simulation for Klang watershed in Malaysia. Open Journal of Modern Hydrology. 3 (3), PP. 102-114. doi: 10.4236/ojmh.2013.33014

Kabiri, R., Ramani Bai V., and Chan, A. 2013. Regional precipitation scenarios using a spatial statistical downscaling approach for Klang watershed in Malaysia, Journal of Environmental Research and Development. 8 (1), pp.126-134

Kabiri, R., Ramani Bai V., and Chan, A. 2013. Simulation of runoff using modified SCS-CN method using GIS system, case study: Klang watershed in Malaysia. Journal of Applied Sciences. (54651-RJES-AJ -In Press)

### Conference Proceeding

Kabiri, R., Ramani Bai V., and Chan, A. 2012. Estimation of Climate change impacts on frequency of precipitation extremes Case study: Klang watershed, Malaysia. International Conference on Environment, Chemistry and Biology-ICECB Hong Kong, 49, pp.144-149.

Kabiri, R., Ramani Bai V., and Chan, A. 2012.Using Green-Ampt loss method in surface runoff simulation, Case study: Klang watershed, Malaysia. 10th WSEAS International Conference on Environment, Ecosystems and Development (EED '12). Montreux, Switzerland, pp. 217-222.

Kabiri, R., Ramani Bai V., and Chan, A. 2012. Climate change impacts on river runoff in Klang watershed in Malaysia. 10th WSEAS International Conference on Environment, Ecosystems and Development (EED '12). Montreux, Switzerland, pp. 223-228.

**Book Chapter**

Ramani Bai V., S. Mohan and Kabiri, R. 2011. Towards a Database for an Information Management System on Climate Change: An Online Resource. Climate Change and the Sustainable Use of Water Resources, Climate Change Management, Springer, pp. 61-67. ISSN: 1610-2010, ISBN: 978-3-642-22265-8. www.springerlink.com/content/p38r44v1858t3538/

# ACKNOWLEDGEMENT

The author would like to take this opportunity to convey his deepest gratitude to the supervisor, Associate Professor Dr. Ramani Bai V., who has guided, encouraged and supported him throughout the completion of this research with her expertise in Water resources and Environmental Engineering. Moreover, the author would like to express his deepest gratitude to Professor Andrew Chan for his guidance and valuable advices.

The Author also takes this opportunity to express a deep sense of gratitude to Dr. Raju, National University of Singapore (NUS), for supporting the Climate Change Research and GIS system.

The author is obliged to the staff members of the government agencies, Engineers from the Hydrology Unit of the Department of Irrigation and Drainage (DID) Malaysia, as well as the Department of Survey and Mapping (JUPEM), Malaysia for the valuable information provided by them in their respective fields during the acquisition of data and supporting material for this research.

This thesis is done as a part of the big project which is currently conducting by the collaborator, Asia Pacific Network (APN), under a broad project title of "climate change and DIMS technology". It is appreciated to thank Science Fund, Ministry of Science, Technology and Innovation (MOSTI), Malaysia and APN, Japan for providing the research grant and their support in providing the required data for this research.

Lastly, the author would like to thank his family particularly his wife, Sara, for her constant encouragement to conduct his PhD at University of Nottingham.

# TABLE OF CONTENTS

# LIST of FIGURES

# LIST of TABLES

# 1- INTRODUCTION

Climate change can be defined as any changes in the mean or the variability of its properties throughout the long time. The Intergovernmental Panel on Climate Change, IPCC (2007) defines climate change as a significant change of climate which is attributed directly or indirectly to human activity that alters the composition of the global atmosphere and which is in addition to natural climate variability observed over comparable time periods. The climate system is connected with the water cycle. Hence any perturbation change in climate would result in the hydrological cycle. Climate is one of the most important components in the physical environment and can reflect the statistical characterisations of the average weather over a period of time (Arnell and Liu, 2001). Water resources studies assess streamflow responds in hydrological modelling to the climatic conditions and environmental changes (Compagnucci et al., 2007).

## 1-1- Problem Definition

Climate is a dynamic system in which changes are expected through the natural cycle. Some crucial natural causes that affect the climate are continental drift, volcanoes, earth's tilt and ocean currents. It has been confirmed through climate change researches as global warming is induced by anthropogenic forcing (IPCC, 2007). However, some believe the surface energy budget effects are the most important factor affecting the climate rather than carbon cycle effects (Pielke et al., 2002). Climate change is a consequence of changing in climate on environmental components on the earth. Obviously it is not homogeneous over the whole globe but depends on the geographical regions which face the impacts of climate changes.

IPCC responded the question on impacts of climate change on human activities and environment as follows: "Anthropogenic warming over the last three decades has likely had a discernible influence at the global and regional scales on observed changes in many physical and biological systems" (IPCC, 2007). Piechota et al., (2006) stated the activities which are capable to change climate are as follows: industrial activities, development of cities, dams and lakes, conversion of grassland

and forest to cropland activities, burning of fossil fuels and deforestation. The rise in greenhouse gas emissions for the late twentieth century is most likely attributed to anthropogenic causes (Hegerl et al., 2007). Since 1750, atmospheric concentrations of Green House Gases (GHGs) have been increased significantly (IPCC, 2007). Carbon dioxide has increased by 31 percent, methane by 151 percent and nitrous oxide by 17 percent (Prentice et al., 2001). The continuing of this greenhouse gas emissions phenomena at this rate, will lead to further warming and unexpected changes in the global climate system in the future (Solomon et al., 2007).

Obviously, climate change variables developed by IPCC are the most useful data to comprehend the climatic condition whether it is at global level or national level (Mearns et al., 2001). Projection of future climate trend will be highly essential for the environmental planning and management. Changes in climate conditions may promote the events of draught or flood extremes (IPCC, 2007). Therefore, the investigation on the climate change impacts on the present and future hydrological variability is highly demanded.

Hydrological variability is one of the most significant climate change impacts on watershed management (kabat et al., 2002). Therefore, it is essential to understand the hydrological processes existing within the watershed through hydrologic modelling which estimates surface runoff and its peak flow in the future, based on climate change scenarios at a watershed scale. Determination of the amount of flow through river would help the authorities and decision makers in planning the environmental hazardous and costs such as estimating the cost involved in flood protection (IPCC, 2007).

## 1-2- Literature Review

The issues related to the climate change and hydrology models have been studied through the literature review. The objectives of this study are identified and the significances of the research are outlined in the following sections.

### 1-2-1- Climate Change Model

The coupled Atmosphere-Ocean General Circulation Models (AOGCMs) which are continually evolving have been developed from the late 1990s. The models have been developed to include a holistic climate change effects such as solar activity fluctuations, volcanoes, shallow and deep ocean interactions, biosphere responses, airborne sulphates and parts of the atmospheric chemistry to project the future climate according to the different scenarios made by IPCC in 2001. GCMs are the most widely used models in climate change studies for evaluation, simulation and projection of the different climate change scenarios (IPCC, 2007).

GCMs reflect physical processes in the multi-sphere such as atmosphere, ocean, cryosphere and land surface. The atmospheric and oceanic models are the key components of GCMs (Guilyardi et al., 2004). GCMs illustrate the climate using a three dimensional grid over the globe of having horizontal resolution of 250 and 600 km, 10 to 20 vertical layers in the atmosphere and as many as 30 layers in the oceans (IPCC, 2009).

GCMs have been constructed based on the Navier–Stokes Equations which describes the motion of fluid .i.e.; the general circulation of the planetary atmosphere/ocean is modelled on a rotating sphere with thermodynamic terms for influxes of mass, energy and momentum from remote sources to the GCM model (Collins, 2007). The GCMs models pose few weaknesses and significant uncertainties in hydrology modelling to project the hydro-meteorological variables at watershed scale (Teng et al., 2012).

There are many studies describing the global climate change on environment (Parry et al., 2009). The impacts of climate change on global and regional scale are well documented (Solomon et al., 2007). Overall, all the GCMs reveal there will be a

warm rise, increasing hot days, sea level rise, changes in season patterns, occurrences in extreme rainfall and flooding, environmental damages and spreading of tropical diseases at the global scale in the century (IPCC, 2007).

On the other hand, GCMs are the currently most reliable tools to assess climate change at coarse scale but GCMs output do not meet the needed resolution to assess the climate change at regional or local scales which is required for hydrological modelling. The grid-boxes used by GCMs are too coarse especially for regions of complex topography, coastal or island locations, and in regions of highly heterogeneous land-cover (Wilby et al., 2004). Then, GCMs cannot present the local weather and micro-climate processes used in hydrology studies.

There are several GCMs with different resolutions such as HadCM3, CNCM3, MRCGCM, FGOALS, GFCM20, MIHR, MPEH5, NCPCM, CSMK3, CGMR, MIMR, GFDL-R30, CCSR/NIES, CGCM, CSIRO-MK2, ECHAM4, and NCAR-PCM with different grid resolution and process. The characterisation of the climate change models are listed in Appendix A. They are different based on the horizontal and vertical layers included in the models such as columns of momentum, heat and moisture in both atmosphere and oceanic parts.

Subsequent to these initial studies, the investigations were extended to a fairly coarse resolution, Regional Climate Model (RCM), to capture the variability of precipitation which is dependent on the physical nature of watershed. RCMs have been developed to assess the climate change impact in regional scale (IPCC, 2007). The use of RCMs for climate downscaling has been initiated by (Dickinson et al., 1989; Giorgi et al., 1990).

RCMs use the same parameters of GCMs in order to simulate the hydraulic processes. However, RCMs are highly dependent on the domain resolution and they are computationally more expensive. The advantage of RCMs to GCMs is to perform the regional redistribution of mass, energy and momentum in the fine domain which affects on quantitative relationships of the physical parameters through the land-atmosphere-ocean and convection-cloud-radiation interactions (e.g., Liang et al., 2004).

RCMs are able to produce downscaling results more accurately than GCMs due to the spatial resolution enhancement (Maurer and Hidalgo, 2008). Regional Climate Models project more accurately temperature data compared to GCMs, but reveal problems when downscaling maximum precipitation (Dankers et al., 2007).

### 1-2-2- Methods of Downscaling

It has been a crucial challenge to make a bridge for the gap between a coarse and a fine scale. Downscaling technique was emerged by a lot of efforts on the climate community to represent climate change at a regional and local scale. Downscaling is a technique of changing in climate data resolution from a coarse resolution into a fine resolution. It can be developed for an area and even a point. It is necessary to downscale the variables from large scale GCMs output into fine scale which are useful in hydrological modelling. Figure 1 illustrates various resolutions from coarse scale GCM to a watershed scale in climate change downscaling model.

There are several techniques available for downscaling coarse resolution GCM data to a fine resolution to use in hydrological studies. However, there is no specific approach to suggest for the most reliable method as different climate models give different results (Dibike and Coulibaly, 2005).

Downscaling techniques are generally categorised into two groups which are: dynamic downscaling and statistical downscaling (Fowler, 2007). Dynamic downscaling technique refers to the RCMs (Fowler et al., 2007). They were developed to overcome the very large resolution in GCMs (Gutmann et al., 2012). RCMs are a nested regional modelling technique that includes forcing of the large scale component of GCMs throughout the entire RCM domain (Diallo et al., 2012). Therefore, the resolution of RCMs is a sub-grid of GCM grid and is dependent on domain size which is usually of tens kilometres or less (IPCC, 2007). However, RCMs models are not able to predict the regular periodic monsoon currents and ocean-atmospheric oscillations (IPCC, 2007).

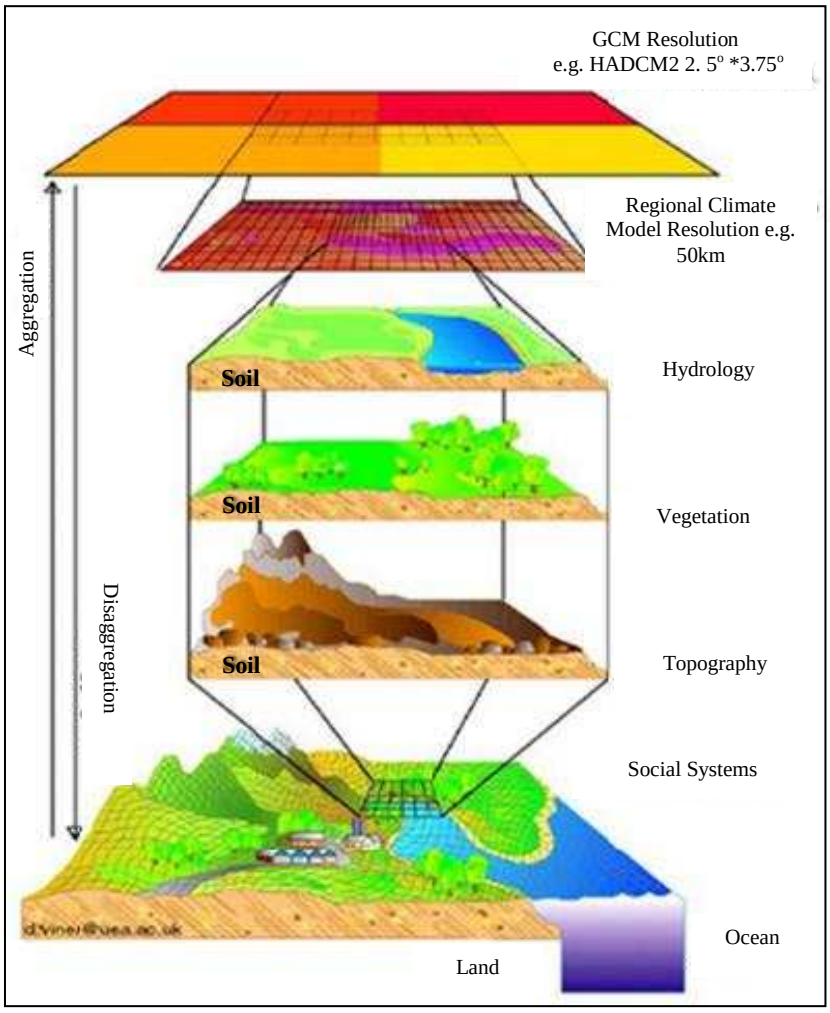


Figure 1 The schematic of downscaling spatial resolution (Source: http://www.cccsn.ec.gc.ca)

Although RCMs employ limited number of scenarios and also time periods, but it is highly dependent on the domain resolution and timely demanding in computational running. Due to inflexibility in nature, complicated design, sophisticated training for the modellers, difficulties in model calibration and validation, time consuming and cost needed for dynamic downscaling, RCM is not being highly used in climate change studies (Mearns, 2001; Wilby et al., 2009).

Owing to the difficulties and limitations in using RCM, statistical downscaling models have been emerged. They are based on the view that regional climate is mostly a result of the large scale climatic states and regional/local physiographic features, e.g. topography, land-sea distribution and landuse (Wilby, 2004). Statistical downscaling develops a statistical relationship between Predictors and Predictands variables. Recently, an interest has been increased in using statistical climate change downscaling to address the shortcomings of RCMs as it is not capable to project the

climate change scenarios at a local or point scale (Chen et al., 2012; Mearns et al., 2012; Meenu et al., 2012; Fiseha et al., 2012; Yang et al., 2012; Hassan and Haroun, 2012; Liu et al., 2011; Samadi et al., 2012).

There are many statistical downscaling methods in climate change studies. In Weather-Pattern Method, a link between observational point data and a weather classification schemes is developed (Yarnal et al., 2001; Anandhi et al., 2011). Weather-typing approaches categorise the various local predictand data to construct the Circulation Patterns (CPs) at the local scale. The weather state definition is archived directly by applying methods such as cluster analysis (PCA) to atmospheric fields (Huth, 2000).

The method developed by Bardossy et al. (2005) provides a basis daily classified circulation pattern for downscaling the most common climate data (temperature and precipitation). The presented classification is objective providing CPs that explain the dependency between the predictors and surface climate. Local climate change scenarios are then generated by resampling observed predictands from probability distributions conditioned on synthetic series of CPs. In spite of its applicability to a wide variety of atmosphere variables such as temperature and precipitation, have difficulty simulating extreme events, and must assume stationary circulation-to-surface climate conditioning (Wilby et al., 1999).

Stochastic Weather Generators (WG) as a statistical downscaling method has been used in water resource management (Wilks, 2012; Tan et al., 2008; Ivanov et al., 2007). The generators were developed by (Richardson, 1981; Richardson and Wright, 1984; Racsko et al., 1991 and Semenov et al., 1998). Daily precipitation occurrence is governed by a two-state (either precipitation occurs or it does not) and first-order Markov chain (the probability of precipitation depends only on whether or not precipitation occurred on the previous day). The key disadvantages of stochastic weather generators method in climate change downscaling relate to the underestimation of low frequency variance (Hansen and Mavromatis, 2001), the projection of unrealistic properties for extremes precipitation and limitation of the length of the synthetic climate data by length of the observed (Wilks and Wilby, 1999).

Regression Methods were developed by Wilby and Wigley (1997) which establishes a linear or non-linear regression between predictands and predictors. Therefore, this method is highly dependent on the empirical statistical relationships. The most famous statistical downscaling tools are LARS-WG and SDSM. LARS-WG is a sophisticated stochastic weather generator whereas SDSM is a hybrid between a stochastic weather generator and regression methods.

SDSM combined the regression models, weather typing schemes and weather generators (Vrac and Naveau, 2007). SDSM generates the unique meteorological characteristics at a single station scale which is a valuable ability in hydrology studies. SDSM downscaling method is recommended by Canadian Climate Impact Scenarios Project (CCIS) for climate change impact studies. It is one of the most efficient tools in downscaling of large scale daily GCMs climate variables into local scale, particularly in heterogeneous regions (Wilby, 2004).

The main advantage of Statistical Downscaling Model (SDSM) is simplicity, less computationally demanding and running the regression statistical method. However, it is limited to the locations where good regression results could be found. The major theoretical weakness of statistical downscaling is that their basic assumption is not verifiable, i.e., the statistical relationships developed for the present day climate will also hold for the different forcing conditions in the future climates (Fowler, 2007). The statistical downscaling technique is used in the present research and the details of this research are given in Chapter 2 (Section 2-2-4).

### 1-2-3- Hydrology Model

Hydrological models are generally categorised into deterministic and stochastic models (Beven, 2001). Deterministic models simulate runoff with a set of hydrological parameters require a large amount of data (Gosain et al., 2009), whereas stochastic models use mathematical techniques to link climate variables to runoff (Ahmad et al., 2001). Gosain et al. (2009) explained the development of various hydrological models. They simply defined hydrological models as a black-box or empirical model, statistically develops a relationship of input and output data (Nor et

al., 2007). Thus, Empirical models are invaluable in predicting streamflow in a watershed with no gauging data.

Cunderlik (2003) classified deterministic hydrologic models into three major categories: lumped model, semi-distributed model and distributed model. Lumped model is a simple approach to simulate runoff which is developed based on the water balance equation. It assumes the whole watershed system such as soli and landuse data as a single unit (Bormann et al., 2009). Thus, such this model does not provide the heterogeneity of physiographic properties in a large watershed. On the contrary, distributed hydrological models incorporate spatial variables of the hydrological parameters by dividing the watershed into the homogenous variables (Ghavidelfar et al., 2011).

Carpenter and Georgakakos (2006) have demonstrated the skill of distributed models compared to lumped models in simulation of runoff. As such, distributed models are able to provide a more representative description of watershed scale processes than lumped models (Collischonn et al., 2007). However, there are limitations related to resolution and nonlinearity of distributed models (Beven, 2001).

Conceptual models are divided into single event, for a short time period and continuous events, for long time series to simulate runoff (Salarpour, 2011). Conceptual models are highly dependent on spatial variability. Representative Element Area (REA), Hydrological Response Units (HRU) and Grouped Response Unit (GRU) are a few types of discretisation in the distributed conceptual model (Neitsch, 2005).

Semi distributed hydrological model have been developed to overcome the difficulties in using conceptual model (Beven, 2012). It performs less complex spatial resolution compared to fully distributed model by generating hydrological response units to simulate runoff in the watershed (Grayson and Blöschl, 2001).

There are literatures of hydrological models' application rang from small to large watershed scale (Singh and Frevert, 2002 a, b). Water resource management plans are generally performed at watershed scale. Then, a physically-based hydrologic model

can be employed to take into account the variety of climatic and physiographic parameters to simulate streamflow at the watershed scale (Praskievicz and Chang, 2009). For instance, the semi distributed DHSVM model is used for urbanised watersheds with representations of impervious surfaces and retention ponds in the model (Cuo et al., 2008) while rainfall-runoff HEC-HMS and SWAT models are usually used for regional watershed scale.

IHACRES (Jakeman et al. 1990; Jakeman and Hornberger, 1993), SRM (Rango, 1995), WATBAL (Knudsen et al., 1986) and Sacramento (Burnash, 1995) are the typical lumped models. Typical models of semi distributed physically based are HBV (Bergström, 1995), HEC-HMS (Ford et al., 2008), HSPF (Crawford and Linsley, 1966), SSARR (USGS-NPD, 1991), SWAT (Arnold et al., 1998; Arnold and Fohrer, 2005), SWMM (Huber and Dickinson, 1988), TOPMODEL (Beven and Kirkby, 1979), IHDM (Beven et al., 1987) and Thales (Grayson et al., 1992). The most famous distributed models are CASC2D (Ogden, 1998), CEQUEAU (Morin, 2002), GAWSER/GRIFFS (Schroeter et al., 1996), MIKE (DHI, 2000) and WATFLOOD (Kouwen, 2001).

The choice of a hydrological model is dependent on the many factors such as resolution, time series (daily or monthly) of climate variables to simulate the surface runoff (Xu and Singh, 1998). However, the physiographic features of watershed play a significant role in predicting the streamflow behaviour (Viessman and Lewis, 2003.).

Loss model is one of the most important components in hydrology models to estimate rainfall infiltrated by the ground. Green-Ampt (Mein and Larson 1973) and SCS Curve Number USDA-NRCS, 2000) are extensively used in hydrology modelling to calculate the rainfall loss rate (e.g., Kabiri et al., 2013; Petrosellia et al., 2013).

The SCS-CN method is the most popular methods for computing the volume of direct surface runoff for a given rainfall event (Mishra et al., 2006). Abood et al. (2012) have evaluated the performance of the two infiltration methods (SCS-CN and Green-Ampt) in rainfall-runoff simulation using HEC-HMS for the Kenyir and Berang watershed, Terengganu, in Malaysia which the storm events of September and

October through the year 1990 has been used for calibration simulation, whereas the storm events of November and December in the year 1990 data have been used for validation simulation. They found that the both loss methods have a good agreement with the observed data. However, the SCS-CN method was recommended for the watersheds due to its high accuracy in the modelling results.

Kabiri et al. (2013) have evaluated the performance of two loss models (Green-Ampt and SCS-CN) for some storm events in Klang watershed. They found out that there was no significant deference between two loss models in the rainfall-runoff model for Klang watershed. Many studies have conducted to improve the SCS-CN loss model and finding a better performance of rainfall loss estimation in runoff modelling (Huang et al., 2007; Sahu et al., 2010; Descheemaeker et al., 2008 and Shi et al., 2009). Fu et al. (2011) found out that the prediction accuracy for initial abstraction ratio equals to 0.05 was greater than the one for 0.2 to simulate surface runoff of 757 rainfall events in China.

Akbari et al. (2012) have investigated the assessment of the SCS-CN loss method on Klang watershed to evaluate the performance of SCS-CN loss method. They have concluded that the SCS-CN loss method can be used for Klang watershed due to its good agreement between observed and modelled in HEC-HMS. However, they have suggested a modified CN using initial abstraction ratio in value of 0.05 which gives a better fit than 0.2 (as default in HEC-HMS). It may produce the best performance of historical daily rainfall data compared to the other available loss models in HEC system.

### 1-2-4- Hydrology Modelling in Climate Change Study

Earlier studies on the projection of runoff corresponding to the climate change downscaling were conducted using a total coarse resolution GCM model. Only a handful of publications on assessing the climate change impacts on water resources by 2005 are available (Fowler et al., 2007). But lately, many studies have conducted statistical downscaling using GCMs models to estimate the hydrological behaviour based on climate change scenarios at a fine scale (e.g., Khazaei, et al., 2012; Randin et al., 2009; Day, 2013).

Numerous studies on climate change downscaling, ranging from small to large scale, have been conducted on the downscaling methods to make a link between GCMs output and hydrologic models at watershed scale (Fowler et al., 2007; Dibike and Coulibaly, 2007). A review on downscaling global climate models for hydrological analysis has been given by Prudhomme et al., (2002). All these studies deal with a coupled atmosphere-ocean general circulation model, since the resolution and certainties are considered to be most critical for climate change downscaling in the watershed scale.

A number of studies have been conducted for the runoff and flooding corresponding to the future climate for a region (e.g., Music and Caya, 2007; Bolle et al., 2008; Teng et al., 2012; Vaze and Teng, 2011; Zhang and Chiew, 2009) but the resolution remains the most widely examined configuration in climate change downscaling problems. For instance, rainfall-runoff modelling system has been used to simulate streamflow regime affected by climate change in many hydrologically heterogeneous regions (Qi et al., 2009).

The impact of climate variability on streamflow and peak flow is found in (e.g. .Chang et al., 2001; Rose and Peters, 2001; Brian et al., 2004; Brown et al., 2005; Qi et al., 2009; Miller and Russel, 2012; Petheram et al., 2012 ). The changes in climate potentially affect the regional hydrological processes and long-term water availability (Fu et al., 2007) changing in overall flow magnitude, variability and timing of the main flow event (Wurbs et al., 2005) and the occurrences of floods (Bronstert et al., 2007). Hydrological impacts on the intraannual variability over the annual cycle (Jasper et al., 2004; Graham et al., 2007; Bosshard et al., 2011; Teng et al., 2012) seasons (Tague et al., 2008; Schmidli et al., 2007), months (Kleinn et al., 2005) have been investigated.

Meenu et al (2012) have used HEC-HMS hydrological model to assess hydrologic impacts of climate change on daily maximum, minimum temperature and precipitation in the four sub-basins of the study area in Tunga–Bhadra river basin, India. They found out that HEC-HMS can be used for hydrological modelling in the river basin. The monthly flows are better simulated than daily flows. However, under

prediction of high flows was estimated during calibration and validation of hydrological modelling.

The use of hydrological models in climate change studies ranges from simple lumped models (Massari et al., 2013; Driessen et al., 2010) to complex distributed models (Mascaro et al., 2013; Guo et al., 2009) to assess the streamflow and peak flow variation.

Maurer et al (2010) have used two hydrology models: the Sacramento Soil Moisture Accounting model and the variable infiltration capacity model to project changes of streamflows for three Sierra Nevada rivers using Statistical Downscaling Model. They found out that the two hydrological models produced significantly different simulations of current and future daily and seasonal extreme flow. However, the changes in monthly streamflows generally did not differ.

Petheram et al (2012) have studies the estimation of the impact climate change on runoff across the tropical region in Australia using conceptual rainfall-runoff models (RRMs). 115 streamflow gauging stations were calibrated in PRMs model. They revealed that there will be an increase in mean annual runoff to 29% and a decrease to 26%. However, they commented that for extreme runoff events and low flows, improvements are required in both GCMs and rainfall-runoff modelling.

Many investigations have been conducted to estimate rainfall intensity considering the climate change impacts to reveal the probability of extreme precipitation in the future (e.g., Nguyen et al., 2007; Prodanovic and Simonovic, 2007; Simonovic and Peck, 2009; Onof and Arnbjeg-Nielsen, 2009; Mirhosseini et al., 2012; Zhu et al., 2012). Mirhosseini et al (2012) have studied the impact of climate change on rainfall IDF curves in Alabama, using 3-hourly precipitation data simulated by six combinations of global and regional climate models. They found out that there will be expected to change toward less intense rainfalls for short duration events. However, due to employing six climate change models, a large uncertainty existed on projected rainfall intensity.

Simonovic and Peck (2009) have investigated the impact of climate change on rainfall intensity for the city of London for 2050s under CCSR/NIES-GCM model to estimate rainfall intensity using daily rainfall data. The results revealed that there will be approximately from 11% to 35% changes in rainfall intensity information for 2050s.

Many studies have shown the role of the evapotranspiration into hydrological modelling (Zhao et al., 2013; Meenue et al., 2012; Milly et al., 2011). The methods to calculate the ET include Gridded Priestly Taylor, Priestly Taylor and Monthly Average methods. The Gridded Priestly Taylor and Priestly Taylor equations require some data such as solar radiation, crop factors and dryness factor and that make them difficult to use in hydrological models. Several studies have evaluated Hargreaves' method and found out that the method has a good result in various climates (Das et al., 2012; Temesgen, et al., 2005). Since Hargreaves' method just depends on the air temperature, so it is well-known in evapotranspiration calculation enormously. Temesgen et al. (2005) have evaluated the performance of FAO-P&M with Hargreaves. They found that Hargreaves' equation can compensate the lack of data required in Penman and Penman- Monteith Methods.

Hargreaves and Allen (2003) have shown that the Hargreaves' results were close to FAO-P&M's results due to the study conducted on more than 3,000 stations worldwide. They have shown that there is no substantial problem using Hargreaves' equation at low latitudes in equatorial zones. Saghravani et al. (2009) have evaluated the performance of the three ET equations (Hargreaves, FAO-P&M and P&M) in one station at Klang watershed. They found that there is a different between the results obtained from three different methods. However, the differences did not reject the results given by Hargreaves and Allen (2003) as the difference between Hargreaves and FAO-P&M may reach a maximum of one mm/d in the tropical regions. This method was used due to its simplicity and modest data requirement, which made it attractive for the hydrology modelling.

### 1-2-5- Previous Work on Related Topic

The Malaysian Meteorological Department (2009) has studied the global analysis of the impacts of climate change in Malaysia using nine different AOGCMs to investigate an ensemble projection for the climate data (temperature and rainfall) to the 2100 year. The results of all nine models showed an increase in temperature with the ensemble mean of 2.6$^{o}$ C for the peninsular. However, there was no clear trend of precipitation due to the high variability in the precipitation which indicates an increase of 6 – 10% over west coast, a decrease of 4 – 6 % over central Pahang and coastal Kelantan compared to 1990-1999. Figure 2 shows the ensemble mean of nine GCMs models used for precipitation projection in the Malaysia boundary.

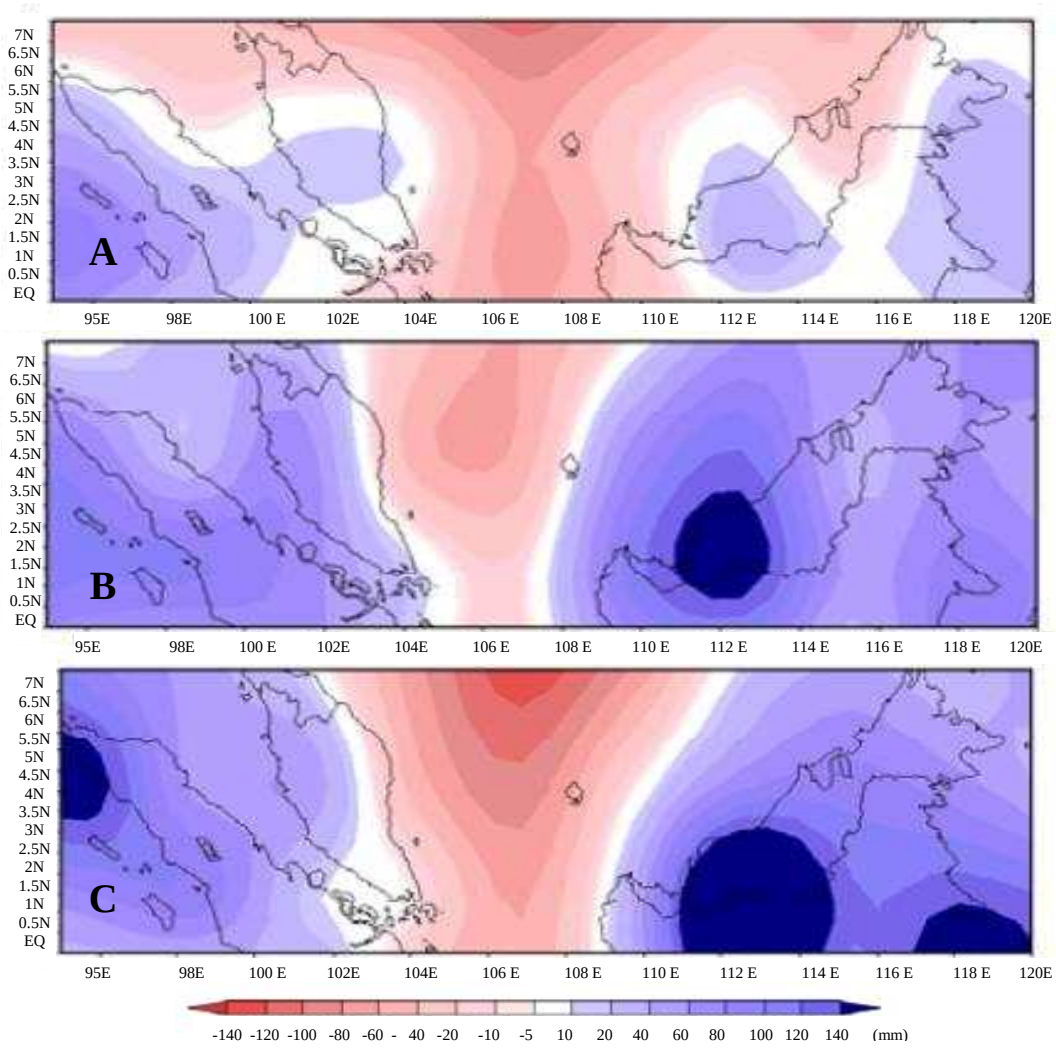


Figure 2 A GCM map of precipitation projection for the future in three time slices: Ensemble precipitation projection for the period: (**A**) 2020-2029, (**B**) 2050-2059 and (**C**) 2090-2099
*(Source: Malaysia's Meteorological Department, 2009)*

Besides, the application of the nine Global scale models used to define the climate change scenarios for Malaysia, a RCM was applied by using Regional Climates for Impacts Studies (PRECIS) model developed at the Hadley Centre, United Kingdom Met Office to project the regional scale (50 km) climate change scenarios for the Malaysia. HadCM3 model was used in regional climate model simulation. It assumed A2 and B2 scenarios. The dynamical RCM simulation was run for the periods 1960-2100. However, the baseline period for comparison of simulation output was assumed as 1961-1990. The RCM simulation results for Malaysia in the future are illustrated in Figures (3 and 4). Figure 3 shows that there will be an increasing mean temperature in the southern of Peninsular ranging from 1.4 $^{o}$C to 3.2 $^{o}$C for the future (2020-2100). Figure 4 indicates that rainfall amount that seems to be decreasing towards the middle the century but it will be increased through 2080s about 15 % relative to 1990-1999.

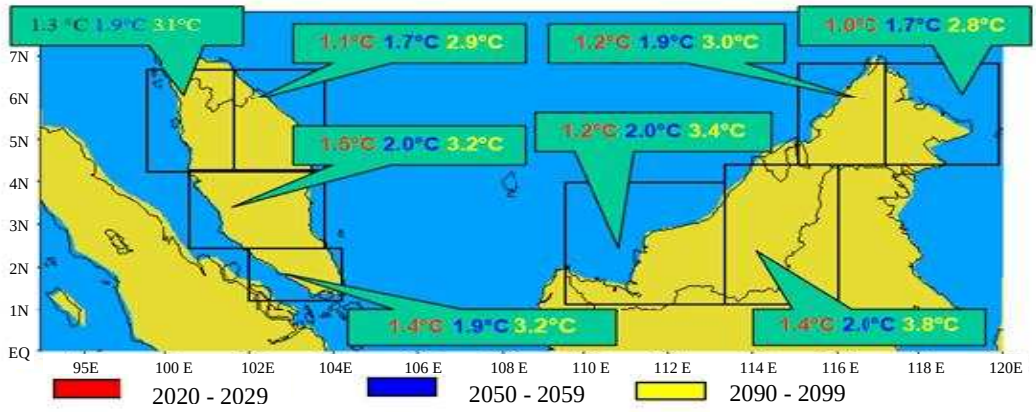


Figure 3 The RCM map of temperature anomaly ($^{o}$C) for the future in three time slices (Malaysia Meteorological Department, 2009)

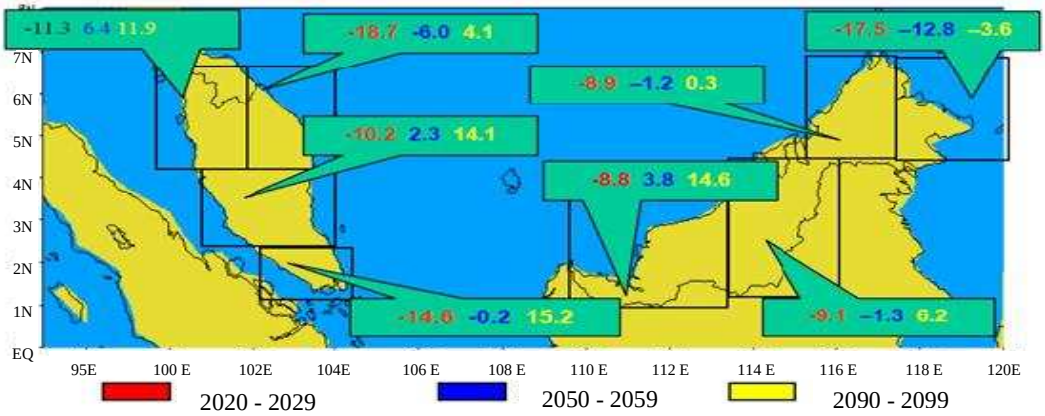


Figure 4 The RCM map of precipitation anomaly (%) for the future in three time slices (Source: Malaysia Meteorological Department, 2009)

Kavvas et al. (2006) have investigated the impact of climate change on the hydrologic regime for Peninsular Malaysia. They have developed the hydrologic-atmospheric model, RegHCM-PM, which is an integration model of MM5 atmospheric model of US National Centre for Atmospheric Research and IRSHAM Integrated Regional Scale Hydrologic-Atmospheric hydrology model. The large scale CGCM1 (410km) model was downscaled to a fine grid resolution (9 km) to assess the climate change impacts on the hydrological regime in Peninsular Malaysia. The projection was run for the middle future of 2050s to assess the monthly streamflows at some stream gauges. They found that there was a higher discharge peak through the flood season and a lower streamflow in the dry season in Klang watershed in 2050s comparing to the observed data.

### 1-2-6- Summary of Literature Review

Some points are presented to highlight the shortcomings in the literatures. In this study, it has been attempted to fill the gaps of literatures for estimation of future runoff and peak flow as follow:

The majority of previous investigations have failed to account for the watershed scale spatially, which generates an average value of downscaled variables over the watershed scale. To address shortcomings of previous investigations, the work undertaken in this study implements **Spatially Statistical Downscaling Model** to downscale the predictand variables and evaluates the impact of climate changes on the future discharge and peak flow.

In the various climate change studies (Duffy et al., 2006; Maurer and Hidalgo, 2008), RCM model has been used as a dynamic downscale model. The simulations did not predict the nature of the complicated process in the watershed scale and consequently, projected over/under prediction of the runoff and flood levels. As a result, the RCM model could not represent the precipitation variables of a fine scale, in comparison to the Statistical Downscaling Models.

Statistical Downscaling Model (SDSM) generates different scenarios for the individual raingauge station at point scale by projecting the possible climate in future

(Meenu et al., 2012; Fiseha et al., 2012). SDSM projects the future patterns for each raingauge station individually and does not represent the overall pattern of the rainfall variables over the watershed. To fill the gap, the **Multi Rainfall** is used to robust the precipitation downscaling over Klang watershed. The Geospatial interpolation technique in GIS is used to generate the areal maps by making spatial average to estimate the mean value of precipitation over the watershed.

In the studies that have been conducted by (Yang et al., 2012; Nguyen et al., 2007; Prodanovic and Simonovic, 2007; Simonovic and Peck, 2009; Onof and Arnbjeg-Nielsen, 2009; Mirhosseini et al., 2012; Zhu et al., 2012), the impact of climate change on the occurrence of extreme precipitation events has been estimated for single raingauge station. It makes it difficult to estimate the mean extreme precipitation events for entire the watershed. To fill the gap, rainfall intensity is evaluated by spatial mapping in GIS using the appropriate distribution equation for estimation of rainfall quantiles for all the raingauge stations in Klang watershed.

### 1-3- Significance of the Study

One of the most important consequences of climate change impacts in South Asian regions is the lack of water resources due to the adverse impact on water demand and quality. Drying of wetlands and severe degradation of ecosystems has resulted in delta regions of South Asian countries due to precipitation decline and droughts (IPCC, 2007). According to IPCC (2007), Malaysia is a developing country which will be vulnerable to climate change. Because of the less flexibility to adjust the economical structure and being largely dependent on agriculture, the impact of climate change has far reach implication in Malaysia.

Klang watershed which is located in Kuala Lumpur city terrestrial has been chosen as a study area for this project. This site has been contributed to the environmental damages especially in land degradation and also soil erosion which will potentially produce more extent area affected by intensified flood events in the watershed. In this area, most flooding events are originated from convectional storms which caused intensive and localised rainfall. The watershed has been facing often flash floods,

rising out of an intense rainfall in a short time. The area has experienced 16 major flood events. Table 1 show that there is an increase in the flooding events which is being more frequently through the last decade nine events of flooding were recorded since 1996 until now.

Table 1 Flood events in Kuala Lumpur

| Year | No. of Major Flood | Year | No. of Major Flood |
|---|---|---|---|
| 1926 | 1 | 1997 | 1 |
| 1971 | 1 | 2000-Apr | 1 |
| 1982 | 1 | 2001-Apr and Oct | 2 |
| 1986 | 1 | 2002-Jun | 1 |
| 1988 | 1 | 2003-Jun | 1 |
| 1993 | 1 | 2004-Jun | 1 |
| 1995 | 1 | 2007-Jun | 1 |
| 1996 | 1 | | |

The hydrological regime of Klang watershed is highly influenced by accumulated water of upstream. Although, Klang watershed is on the urbanisation process, but its conditions under future climatic change has not been investigated at the local scale. Projecting the regime of the streamflow using climate change and hydrological model seems to be important. Since precipitation is the main component in runoff modelling which specify the discharge behaviour along with the river, this study has accomplished the modelling of surface runoff of Klang watershed. It demonstrates the flooding caused by peak flow when an extreme rainfall occurs corresponding to the climate change scenarios in the future.

Moreover, the frequency analysis of extreme hydrological events need to be estimated based on climate change scenarios for the urbanised Klang watershed where will expect to be faced by extreme rainfall events (Kavvas et al., 2006; Malaysia Meteorological Department, 2009).

## 1-4- Objectives of the Study

The aim of the study is to assess the impact of climate change on future runoff and peak flow over Klang watershed. The other purpose of the research is to specify Klang watershed's characteristics pertaining to possible climatic changes in the

future. The result of the hydrological model is generation of the runoff hydrograph by a spatially distributed rainfall over the watershed in the future (2100 year). The detailed objectives of this research are as follow:

- To generate fine resolution climate change scenarios using Statistical Downscaling Model in the watershed scale,

- To project the variability in temperature, precipitation and evaporation for the three time slices, 2020s, 2050s and 2080s, based on A2 and B2 scenarios,

- To calibrate and validate hydrological model using historical observed flow data to verify the performance of hydrological model,

- To evaluate the impact of climate changes on the future discharge and future peak flow for three timeslices 2020s, 2050s and 2080s.

Thus, to meet the objectives in this study, projection of the future climate based on climate change scenarios from IPCC in the study area can be considered as the most important component throughout the research. Therefore, the assessment on the quality and adequacy of the hydro-climatological data must be estimated to ensure the reliability of model output.

## 1-5- Scope of the Research

The study focuses on the impact of climate change on runoff and peak flow by downscaling the Climate Change Scenarios at a watershed scale. The criteria for selecting appropriate IPCC scenarios are based on the physically consistency at a fine scale. The A2 (Medium-High emissions scenario) and B2 (Medium-Low emissions scenario) scenarios reveal the reliable projection of a plausible future climate condition at the regional scale while other scenarios represent at the global scale. Thus, applicability of A2 and B2 scenarios in estimating impacts of climate change at the watershed scale is more realistic compared to other scenarios which were constructed at global scale. Hence, A2 and B2 scenarios have been used to generate

the local climate change scenarios using statistical downscaling model in the watershed scale.

## 1-6- Limitations of the Study

The lack of data on streamflow does not allow the calibration and validation of hydrological modelling for each sub-basin. The only streamflow station (Jambatan Sulaiman) is situated at the outlet of Upper Klang watershed and the hydrological modelling uses it for calibration and validation to simulate runoff. Furthermore, the lack of updated land use, soil and topography data have forced the study to consider it as an assumption with no change during the time.

## 1-7- Thesis Outline

This thesis comprises seven chapters, which are briefly outlined below. The study has three main steps:

- Study of physical characteristics and history of the watershed which includes a review on hydro-climate trends to prepare all the required data for the hydrological modelling.

- Making Climate Change Downscaling Model and linking between climate change downscaled output and hydrological model in providing the potential impacts of climate change on flow through Klang watershed.

- Runoff and peak flow modelling have been developed using HEC-HMS model for all sub-watersheds in Klang watershed.

**Chapter 1** explores the climate changes and its future scenarios. It describes impacts of climate change on precipitation, run off and flooding events. It is also presents the objectives, scope and importance of the study on Klang watershed. The chapter also describes some literatures on Climate Change Downscaling Model, hydrology models and climate change impacts on runoff and peak flow studies.

**Chapter 2** describes the methods used to make various modelling in this study. The models used in this study are as follow: Climate Change Downscaling Model, Hydrological (Watershed Management, Surface Runoff) and Peak flow modelling.

**Chapter 3** consists of two parts. The first part of the chapter introduces the case study, Klang watershed, and describes the environmental-physical features such as terrain, river network, geology, landuse and soil obtained from various sources in this study. The second part of the chapter is to describe the climate pattern and hydrological characteristics of study area. It also describes the baseline hydro-climatology for Klang watershed using a long term series of climate data to reflect the observed trend n the hydro-climate data such as precipitation, temperature and streamflow. Furthermore, data preparation and quality control on the historic data are conducted using graphical, statistical and spatial methods.

**Chapter 4** presents the implementation of the Climate Change Downscaling Model using SDSM tool. SDSM uses NCEP-Predictor variables to make a linear regression to the local predictand data from Klang watershed. The output of downscaled climate parameters is used as an input to the hydrology modelling in **Chapter 5**.

**Chapter 5** presents the implementation of hydrological modelling using Hec-Geo-HMS, a GIS module. The algorithm is used to delineate the sub-watersheds which distribute over whole Klang watershed. It can extract the necessary parameters required in hydrological modelling. Then, it attempts to implement HEC-HMS to generate the runoff hydrographs for each sub-watershed.

**Chapter 6** describes the findings and results of the research. It demonstrates the climate change scenarios over the watershed's meteorological parameters such as precipitation, temperature and evaporation and its trends in the future. The discussion is based on the plausible changes of the future climate and runoff corresponding to the A2 and B2 scenarios at the watershed scale.

**Chapter 7** conclusion arrived through the study for future research is presented. It includes conclusion on the climate change impacts on the mean and maximum

streamflow regime and the frequency of extreme flood events with regard to the climate change scenarios.

# 2- METHODOLOGY

This chapter is divided into four sub-sections consists of Climate Change Downscaling Model (SDSM), Watershed Modelling, Runoff simulation and Flood Frequency Analysis (FFA). Statistical downscaling model is used to produce the local climate change scenarios at the local scale. The climate change downscaling results are used as input into rainfall-runoff HEC-HMS modelling to forecast the future surface runoff at the discharge station. Watershed Modelling is carried out using Hec-Geo-HMS in GIS system to derive physiographic parameters of the watershed which need to be used in hydrological modelling. Thus, runoff processes are simulated on each sub-watershed system from the upstream to the watershed outlet throughout the streamflow network.

## 2-1- Overall Framework of the Research

This research involves connecting hydrology modelling to climate change downscaled output by GIS system. The study initiates to enhance the understanding of the impact of climate change scenarios by quantifying the potential changes including hydro-climatological data. It provides the variety in future rainfall based on areal rainfall for Klang watershed instead of relying just on some raingauge stations independently.

GIS system plays a pivotal role in these analyses because of various data representation and running different modelling such as climate change and hydrology modelling to estimate the hydrological parameters in Klang watershed. The study also provides forecast on hydrology data for the future development in Klang watershed. The scenarios would be downscaled in the watershed scale to employ in the hydrologic models.

Flood management plans for the watershed should consider climate change scenarios in addition to landuse change and urbanisation. Regarding the linking climate change to flooding, a major focus has been given to extremes such as peak runoff, frequency and intensity of heavy rainfall. However, there are an uncertainty according to landuse changes and its impact on streamflows. Figure 5 illustrates the conceptualised

framework of the study which consists of two steps: 1) Climate change downscaling and 2) hydrology modelling.

Studies on climate change trend have been conducted in Malaysia using General Circulation Models (GCMs) and Regional Climate Models (RCMs) to determine the specific future scenarios at the country and at state scales respectively. Therefore, in this study it has been attempted to generate climate change scenarios at the local scale. Downscaling technique is applied at a watershed scale to generate the future climatic scenarios in Klang watershed. This technique has been employed to fill up the gap existing between the large scale GCM and local scale variables.

The output from statistical downscaling is used as input into HEC-HMS model to project the discharge of Klang River. The hydrological model output will then be used to determine the future streamflow and peak flow in the watershed.

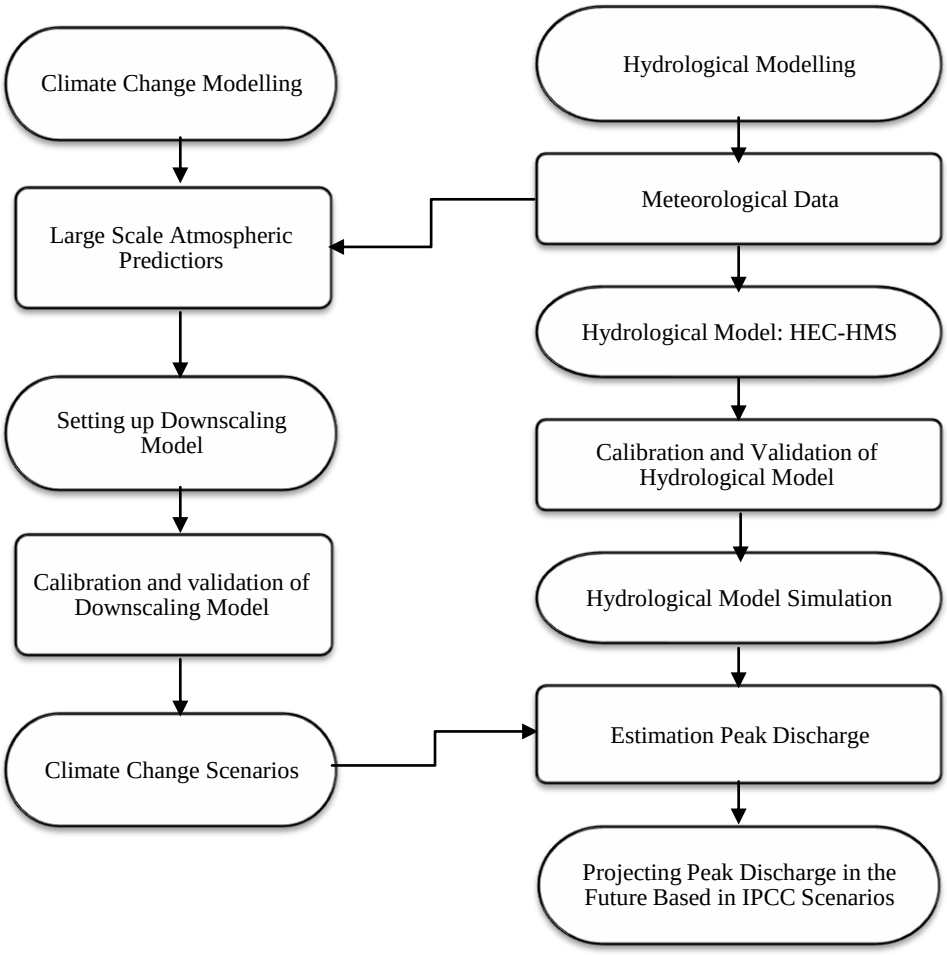


Figure 5 Conceptual framework for the study

## 2-2- Climate Change Downscale Modelling

The methods of climate change downscaling, the IPCC scenarios and climate change models are summarised. In the following section, the IPCC scenarios are described to highlight their applications into climate change downscaling at the watershed scale. Furthermore, the advantages of using statistical downscaling technique compared to the dynamical downscaling for hydrology modelling are described.

### 2-2-1- Climate Change Scenarios

According to the IPCC (2007), a scenario is a coherent, internally consistent and plausible description of a possible future state of the world. A set of four main groups of emission scenarios namely A1, A2, B1 and B2 were released by IPCC in 2000 and are published in Special Report on Emissions Scenarios (SRES). The SRES were constructed by considering the economical, technological, demographic and environmental developments, which reflect the possible future developments in the world pertaining to the production of greenhouse gas emissions. The scenarios are neither predictions nor forecasts. However, it was developed based on realistic future emission scenarios over the world representing the complex and interrelated dynamics of demographic development, socio-economic development and technological change.

The scenarios are the only sources to implement a projection of future, which reflect the condition of demography, society, economy, technology, emissions and climate. A1 and B1 scenarios form the world homogeneously with an increasing in population by mid century and a decreasing afterwards, but an economy focus in A1 and an environmentally focus in B1. A2 scenario is a scenario with higher rates of greenhouse gas emissions in combination with higher sulphate and other aerosol emissions while B2 scenario is a lower rate of emissions that assumes the world is more committed to solving global and local environmental (IPCC, 2007). The four main groups of emission scenarios are explained as below.

**A1 scenario** is constructed based on the homogeneous world. It describes the world of very rapid economic growth, global population and the rapid introduction of efficient technologies. Major focuses are convergence among regions, capacity building, and increased cultural and social interactions, with a substantial reduction in regional differences in per capita income (IPCC, 2007). A1 scenario is developed into three groups that describe alternative directions of technological change in the energy system. A1 scenario family develops into three groups: fossil intensive (A1FI), non-fossil energy sources (A1T), or a balance across all sources (A1B). In A1 scenario, population will be increasing to 8.7 billion in 2050 and declining toward 7 billion people by end of the century (IPCC, 2007).

**A2 scenario** (Medium-High Emissions scenario) is a scenario with higher rates of greenhouse gas emissions in combination with higher sulphate and other aerosol emissions. It represents a differentiated world and describes the world in a various economic regions in which the income gap between developed and developing countries is not narrow. The rate of technology growth is more rapid than average in some regions and slower in others and dependent on industry adjusts to local resource. Regions with abundant energy and mineral resources evolve more resource-intensive economies. In this scenario, global environmental concerns are relatively weak but regional and local pollutions are planned to mitigate. A2 scenario is constructed based on the different economy growth rate and efficiency of technology dependent on the regional scale in which population reaches to 15 billion people in year 2100 and will be increased after 2100 (IPCC, 2007).

**B1 scenario** describes a future based on the high level of environmental approach and a balanced economic development. It is similar to A1 scenario into fast-changing and convergent world but the priorities differ**.** In fact, A1 focuses on global investments by further economic growth and benefits from increased productivity while, B1 scenario focuses on global environmental protection and gains in improved efficiency of resource use. The best measures are taken to reduce material wastage by maximising recycling and enhancing energy saving lead to reductions in pollution. B1 scenario has a major push toward post-fossil technologies. Population is the same as A1 scenario but a slower rate (IPCC, 2007).

**B2 scenario** (Medium-Low Emissions scenario) is a lower rate of emissions that assumes the world is more committed to solving global and local environmental (IPCC, 2007). It is designed based on the world emphasises on local solutions to economic, social, and environmental sustainability. Increasing in population is assumed at a lower rate than A2 scenario. B2 Scenario focuses on intermediate levels of economic development, less rapid technological development compared to B1 and A1 scenarios. However, it focuses toward environmental protection and social equity at the local and regional scale. In B2 scenario, population reaches to 10 billion in 2100 and increasing with slower development rate of technology compared to A1 or B1 scenarios.

GHG and aerosols are the two main groups of atmospheric concentrations to construct the climate change scenarios. Sulphate is the major aerosol component plays a cooling effect role in the lower atmosphere by scattering back sunlight. Figure 6 shows the Annual Global mean temperature to 2100 according to the IPCC Scenarios. It is found out that global warming rates will strongly be seen after 2050 to 2100 ranges from 1.9°C for the B1 to 4.0°C for the A1FI emission scenario, as minimal using fossil fuel in B1 to a total reliance on fossil fuel in A1FI scenarios. The diverging of the temperature in the middle of century can be described as being highly influenced by the past emissions, particularly sulphate aerosols and GHG in the world. IPCC (2007) has stated that according to the scenarios, the respond of the climate system will likely be in the land areas of the equatorial belt to the least warming.

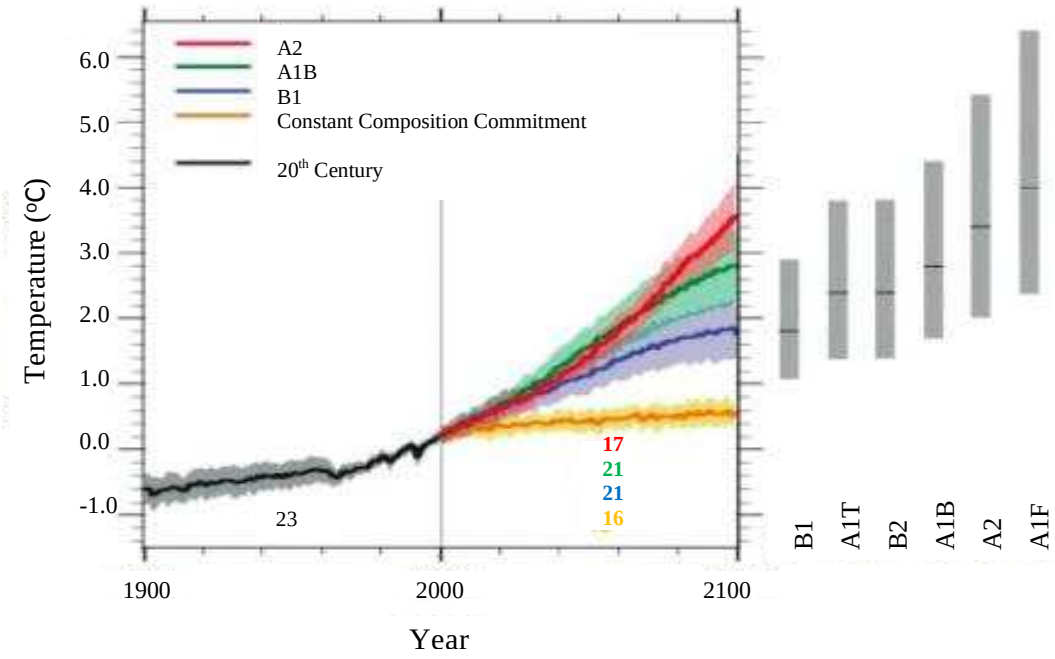


Figure 6 Annual Global Average Surface Air Temperature ($^{o}$C**)** by end of the century for various SRES (IPCC 2007)

**A1:** Is categorised into three groups (A1FI, A1T and A1B) which describe alternative directions of technological change in the energy system.
**B1:** Similar to A1 scenario but with rapid changes in economic structures and the introduction of clean and resource-efficient technologies.
**A2**: Intensive fossil fuel, continuously increasing population and regionally oriented economic development
**B2:** Continuously increasing population, but at a slower rate than in A2, less rapid and more fragmented technological change than in A1 and B1.
**A1F1**: Fossil fuel intensive
**A1B**: Balanced between fossil fuel and non-fossil fuel consumption
**A1T**: Predominantly non-fossil fuel

### 2-2-2- Large Scale Predictor NCEP/NCAR Re-Analysis Data

National Centre for Environmental Prediction (NCEP) is a joint product with the National Centre for Atmospheric Research (NCAR). It has all the gridded predictor variables to use in calibration and validation in SDSM. The horizontal grid resolution in NCEP atmospheric predictors is 2.5°, 2.5°. NCEP/NCAR provided a 40-year record of global analysis of atmospheric predictors. The 26 predictor variables are produced by state-of-art assimilation of all available observed weather data into a global climate forecasting model that produces interpolated grid output of many weather variables (Saha et al., 2010). Figure 7 illustrates the NCEP grid data for Asia and Table 2 shows the large atmospheric variable predictors in NCEP. The data can be obtained from http://www.cics.uvic.ca/scenarios/index.cgi.

Table 2 Large scale predictor variable NCEP Re-Analysis available in SDSM (Wilby and Dawson, 2007)

| No | Predictor variable | Predictor description |
|---|---|---|
| 1 | mslpas | Mean Sea Level pressure |
| 2 | fas | Surface airflow strength |
| 3 | uas | Surface zonal velocity |
| 4 | vas | Surface meridional velocity |
| 5 | zas | Surface velocity |
| 6 | thas | Surface wind direction |
| 7 | zhas | Surface divergence |
| 8 | 5fas | 500 hpa airflow strength |
| 9 | 5uas | 500 hpa zonal velocity |
| 10 | 5vas | 500 hpa a medridional velocity |
| 11 | 5zas | 500 hpa vorticity |
| 12 | 500as | 500 hpa geopotential height |
| 13 | 5thas | 500 hpa wind direction |
| 14 | 5zhas | 500 hpa divergence |
| 15 | 8-fas | 850hpa airflow strength |
| 16 | 8-uas | 850hpa zonal velocity |
| 17 | 8-vas | 850 hpa meridional velocity |
| 18 | 8zas | 850 hpa vorticity |
| 19 | 850as | 850hpa geopotential height |
| 20 | 8thas | 850hpa wind direction |
| 21 | 8zhas | 850hpa divergence |
| 22 | r500as | Relative humidity at 500 hpa |
| 23 | r850as | Relative humidity at 850 hpa |
| 24 | rhumas | Near surface relative humidity |
| 25 | shumas | Surface specific humidity |
| 26 | tempas | Mean temperature at 2m |

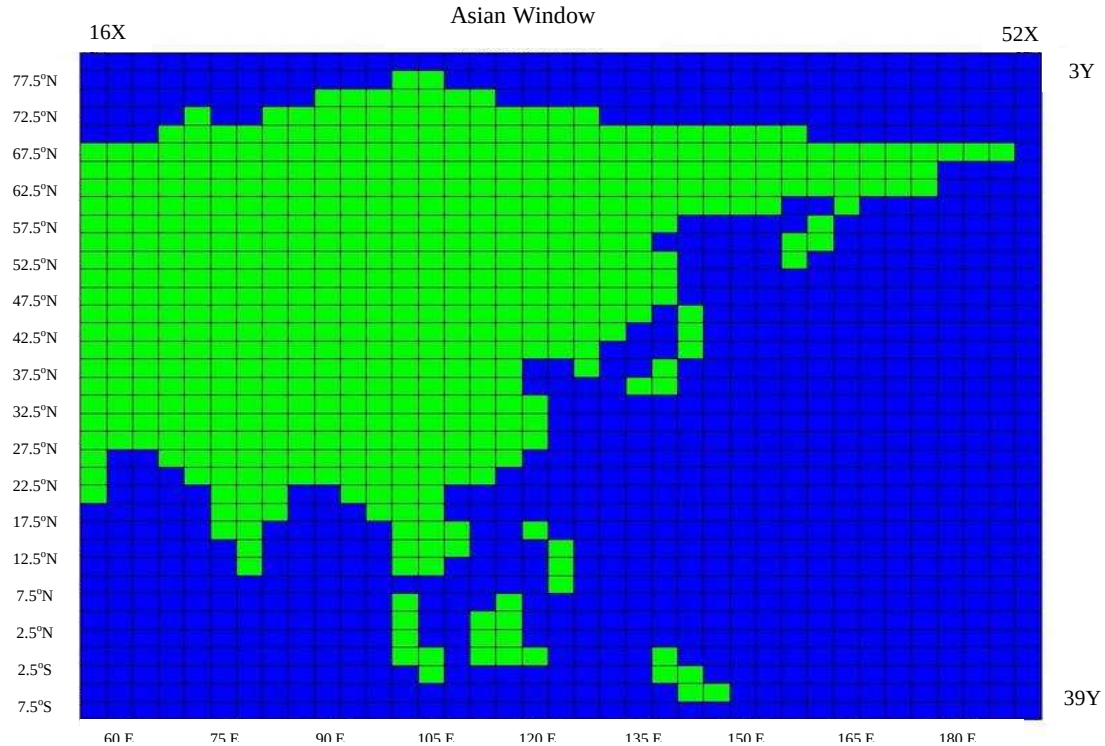


Figure 7 Large Scale Predictor NCEP/NCAR Re-Analysis Data for Asia
(Source: www.cics.uvic.ca/scenarios/index.cgi)

### 2-2-3- Global Climate Change - HadCM3 Model

Climate change models are highly complex because of contributing the couple atmosphere and oceanic components in it. Therefore, there can be uncertainties for projections of scenarios particularly in a local scale. In this study, the Hadley Centre Couple Model, Ver. 3.0 (HadCM3) Model is used for the GCM downscaling, which is a coupled oceanic - atmospheric general circulation model. Wilby and Dawson (2007) stated that the SDSM model is a hybrid of stochastic weather generators and regression based techniques and HadCM3 model is a coupled atmosphere-ocean general circulation model (AOGCM) which is composed of the atmospheric model, HadAM3, and the ocean model, HadOM3.

The horizontal resolution of atmospheric component is 2.5 by 3.75 degrees while the oceanic component's resolution is 1.25 by 1.25. The simulation of HadCM3 assumes the year length in 360 – day calendar which 30 days per month. The model was developed in 1999 and was the first coupled atmosphere-ocean which did not require flux adjustments (IPCC, 2009). The adjustments have to be done artificially by the

other climate change models to prevent them from drifting into unrealistic climate states.

The high quality of current climate simulation using HadCM3 model, made it one of the most efficient and reliable model in climate change studies. It still ranks highly compared to other models in this respect (Reichler and Kim, 2008). HadCM3 was used extensively in IPCC through the Third and Fourth Assessments. It also has the capability to capture the time-dependent fingerprint of historical climate change in response to natural and anthropogenic forcing (Stott et al., 2000) which has made it a particularly useful tool in studies concerning the detection and attribution of past climate changes. The Figure 8 illustrates the resolution of HadCM3 Model- GCM.

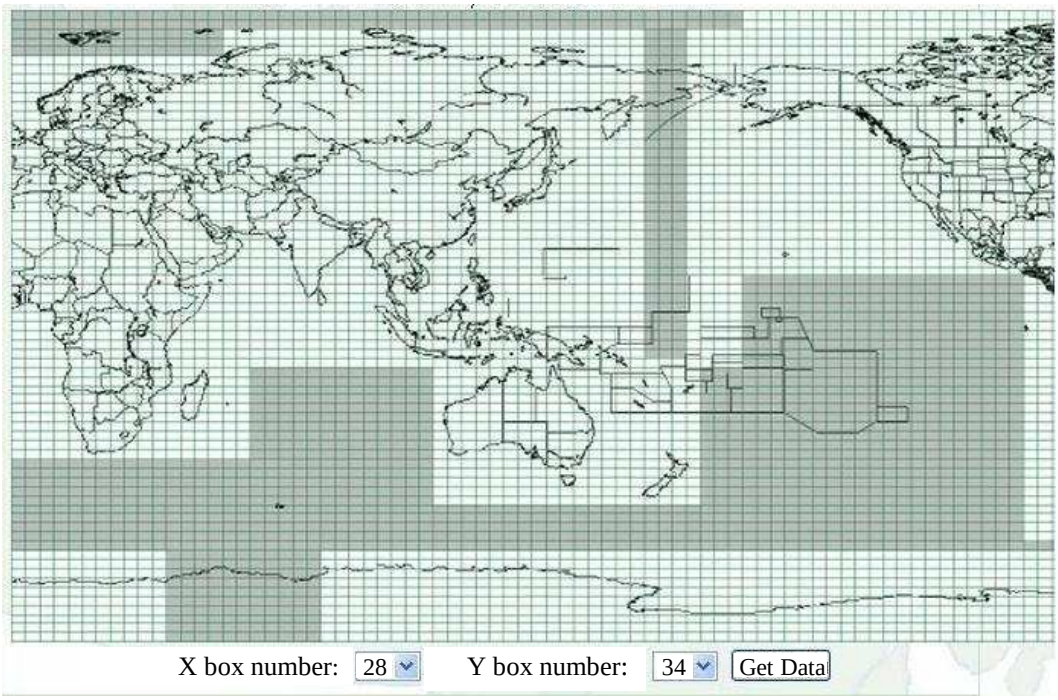


Figure 8 The fine resolution of the HadCM3 Model- GCM (Source: www.cccsn.ec.gc.ca)

The horizontal atmosphere resolution produces a total grid of 96 x 73 grid cells for the whole world which the surface resolution varies from 417 km x 278 km at the Equator to 295 km x 278 km at 45 degrees of latitude. The HadCM3 data can be downloaded from IPCC and also the Canadian Climate Impact Scenarios and CCIS provides all the NCEP and HadCM3 data in the grid box based on the entering of

latitude/longitude of the study area and the grid box provides a zip file contains three directories: NCEP-1961-2001, H3A2a-1961-2099 and H3B2a-1961-2099.

### 2-2-3-1- NCEP-1961-2001

It contains all the observed predictors data produced from NCEP/NCAR. Since there is a difference in the resolution in grid cells of NCEP and HadCM3, all the 41 years of daily observed predictor data were interpolated to the same grid as HadCM3 and then the data were normalised.

### 2-2-3-2- H3A2a-1961-2099

It contains 139 years of daily GCM predictor data assuming a characteristic of scenarios with higher rates of GHG emissions in combination with higher sulphate and other aerosol emissions. H3A2a was normalised over the 1961-1990 period.

### 2-2-3-3- H3B2a-1961-2099

It contains 139 years of daily GCM predictor data assuming a characteristic of scenarios with higher rates of GHG emissions in combination with lower rate of sulphate and other aerosol emissions. H3B2a data was normalised over the 1961-1990 period.

The normalisation was done by dividing each time slice of future (2011-2040, 2041-2070 and 2071-2099) to the current period (1961-1990). This method is described by NCEP and makes an appropriate method to construct the comparable future scenarios to the base period which are in the same number years.

### 2-2-4- Statistical Downscaling Model (SDSM)

The SDSM is a tool to downscale the climate variables to fine scale in climate change studies. SDSM is the best described as a hybrid of the stochastic weather generator and regression-based downscaling methods. This is because large-scale circulation

patterns and atmospheric moisture variables are used to linearly condition local-scale weather generate parameters (Wilby et al., 2004). There are many studies which used SDMS in climate change impact assessments (Wilby and Dawson, 2012; Meenu et al., 2012; Fiseha et al., 2012; Yang et al., 2012).

The version 4.2 of SDSM was used in this research obtained from Canadian Institute for Climate Studies (CICS), (https://co-public.lboro.ac.uk/cocwd/SDSM/). The software involves of several tasks as follows: quality control, data transformation; predictor variable screening; model calibration; weather generation; statistical analyses; graphing model output; and scenario generation. Figure 9 illustrates the structure of SDSM which has been developed by Wilby and Dawson, 2007.

Advantages of using SDSM in downscaling climate parameters

- It has been widely used in many watershed scales over a range of different climatic condition in the world by producing reliable results.

- It is user friendly and freely available software which can be downloaded from https://co-public.lboor.ac.uk/cocwd/SDSM/

- It generates ensembles which enable the user to implement uncertainty analyses.

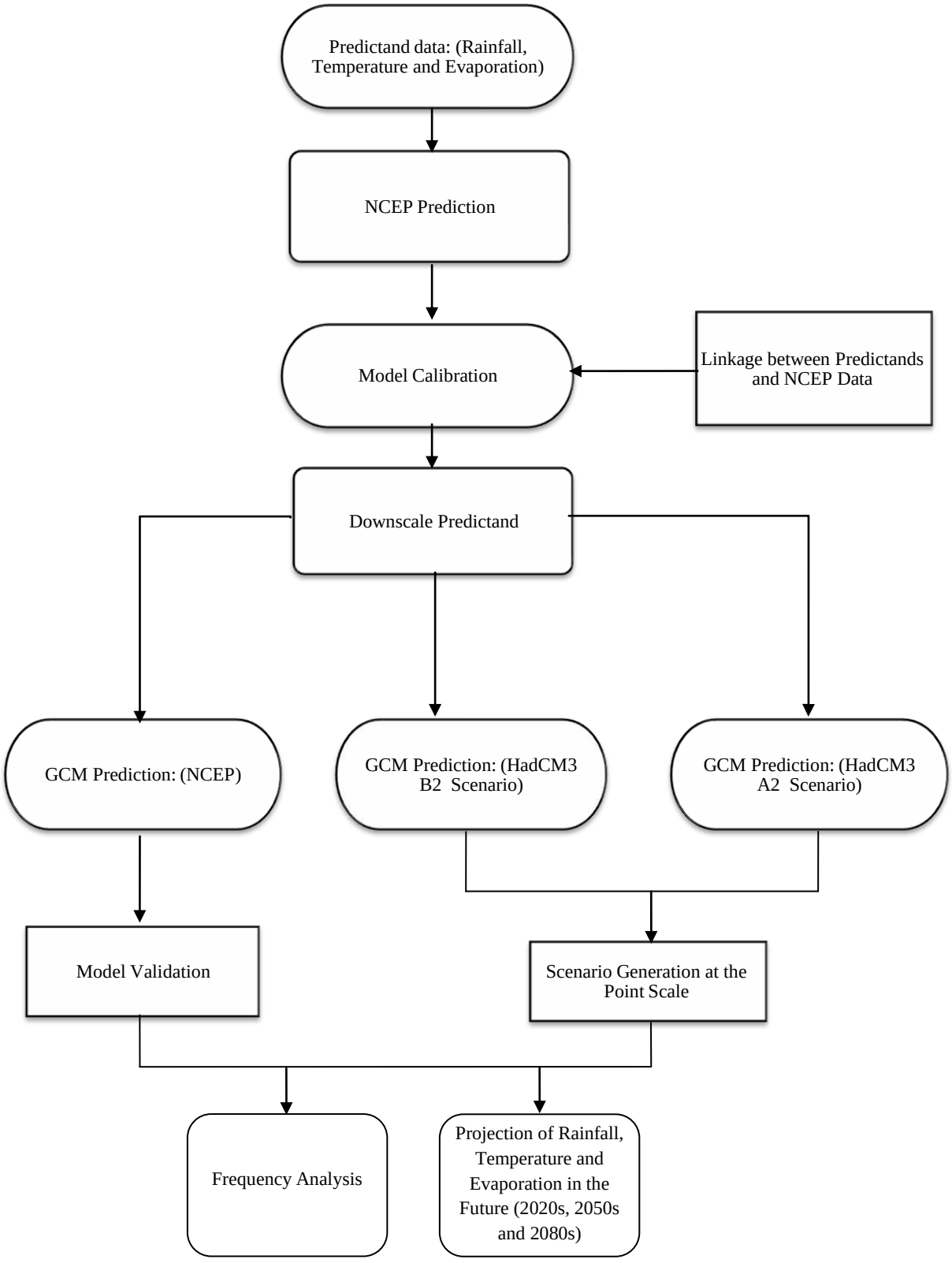


Figure 9 The structure of Statistical Downscaling Model (Wilby and Dawson, 200)

### 2-2-4-1- Conditional Probability

Generally, statistical downscaling implements a quantitative relationship between large scale atmospheric variable (predictors) and local surface variable (predictands). Full technical details are provided by Wilby et al. (1999 and 2002). Equation 1 is the most general form of a downscaling model as defined by Wilby et al., 1999.

$$R_t = F(X_T) \qquad F(X_T) \text{ for } T \leq t \qquad \text{Equation 1}$$

Where, $R_t$ is the local scale predictand at single or multiple sites at time t, $X_T$ is the predictor data of large-scale atmospheric variables and F is the techniques used to quantify the relationship between two disparate spatial scales.

The conditional method in precipitation and evaporation downscaling has been described by Wilby et al., 1999. It consists of two steps: the first step is the probability of occurrence and the second is to estimate the amount of climatologic parameters. Probability of precipitation is modelled as Equation 2 (Wilby et al., 1999).

$$\omega_i = \alpha_o + \sum_{j=1}^{n} \alpha_j \mu_i^j \qquad \text{Equation 2}$$

Where, $\omega_i$ is the conditional probability of precipitation occurrence on particular day i, $\mu_i^j$ is the normalised predictor of the daily predictor data, j on particular day i. $\alpha_j$ is regression coefficients estimated for each month using least squares regression. $\alpha_o$ is $\omega_i$ - intercept.

Wet/dry spell length are estimated stochastically by comparing $\omega_i$ with the output of a linear random-number generator, $r_i$, the occurrence of precipitation occurs if $\omega i$ takes equal or less to $r_i$.

The predictand (precipitation) amount at the site on the large-scale atmospheric circulation is modelled as Equation 3 (Wilby et al., 1999).

$$Z_i = \beta_o + \sum_{j=1}^{n} \beta_j \mu_i^j + \varepsilon \qquad \text{Equation 3}$$

Where, $Z_i$ is the z-score for day i, $\beta_j$ is the estimated regression coefficients for each month using Least-Squares regression, $\beta_o$ is $Z_i$ -intercept and $\varepsilon$ is a normally distributed stochastic error term which is modelled using a series of serially independent Gaussian numbers.

$$Z_i = \emptyset^{-1}\left[F(y_i)\right] \qquad \text{Equation 4}$$

Where, $\emptyset$ is the normal cumulative distribution function, $F(y_i)$ is the empirical distribution function of $y_i$, the daily precipitation amounts (Charles et al., 1999).

### 2-2-4-2- Selection of Predictor Variables for Downscaling

Selection of predictor variables is the most important steps in the statistical downscaling processes because it largely affects the character of the generated scenarios. The predictor variables were selected based on the criteria such as physically related to the predictand, produce the highest explained variance ($r^2$) and the lowest standard error (SE) (Wilby and Wigley, 2000). Obviously, the high correlation values indicate a strong relationship of two data series (predictand and predictors) of all the twelve months.

The significant test explained variance ($r^2$) is given in Equation 5. The explained variance identified the variance of predictand explained by the predictor and can be written as following Equation (Douglas and Runger, 2003).

$$r^2 = 1 - \sum_{i=1}^{n} (p_i - s_i)^2 \,/\, \sum_{i=1}^{n} (p_i - \bar{p}) \qquad \text{Equation 5}$$

Where, $p_i$ is the observed rainfall occurrence at day i, $\bar{p}$ is the average $p_i$ of the values of wet-days, $s_i$ is the estimated rainfall probability for day i and, n is the number of days in the record.

The Standard Error (SE) measure the index of the difference between the predictand and the actual value of the criterion variable. It is defined as Equation 6 (Douglas and Runger, 2003).

$$SE = \tilde{s} \sqrt{\left[\frac{n-1}{n-2}\right]} \left[1-r^2\right] \qquad \text{Equation 6}$$

Where, $\tilde{s}$ is the adjusted standard error of estimate values and n is the number of data.

Finally, the correlation coefficient (linear correlation and scatter plots) is used to assess how well the linear model fits the data that has been obtained through Pearson Product-Moment Correlation Equation (Wilby et al., 2002). It is sometimes referred to Pearson product moment correlation coefficient in honour of its developer Karl Pearson (Douglas and Runger, 2003).

$$P_c = \sum_{i=1}^{n} \frac{(x_i - \bar{x})(y_i - \bar{y})}{(n-1)(s_x s_y)} \qquad \text{Equation 7}$$

Where, $s_x$ and $s_y$ are the standard deviations. The correlation falls between – 1 and +1, the zero corresponds to the situation where there is no linear association.

The correlation analysis is carried out to screen all the 26 predictor variables (NCEP Re-Analysis) for predictand data. A monthly regression analysis is performed. A correlation matrix and explained variance are the output of the monthly regression. Significance Level of $p < 0.05$ (5%) is defined to find the most correlated predictor variables with the predictand. Then, the values of less than significance level indicate the high correlation of the data fit. Once the predictand has been identified the screen variable operation assists in the selection of the required downscaling predictor variables based on correlation between predictand and predictors.

### 2-2-4-3- Model Evaluation and Validation

SDSM employs Ranked Probability Scores (RPS) technique to evaluate forecasts as used by Jolliffe and Stephenson, 2003. RPS classifies a random variable X with k greater than two as thresholds, x1<x2<…xk, that defines the events Ak= {X≤xk} for k=1, 2, …, K with the forecast probabilities (p1,p2,...,pk). The binary indicator variable for the Kth event is denoted as ok= 1 if Ak occurs and 0 otherwise. Ranked Probability Scores (RPS) (Obled et al., 2002) of precipitation and Continuous Ranked Probability Scores (CRPS) (Hersch, 2000) are given as Equations 8 and 9, respectively.

$$RPS = {}^{1}/_{N}\, {}^{1}/_{K} \sum_{n=1}^{n} \sum_{k=1}^{k} (p_k - o_k)^2 \qquad \text{Equation 8}$$

$$CRPS = {}^{1}/_{N} \sum_{n=1}^{n} \int_{-\infty}^{\infty} \left[ f_{(x)} - H\left(x - x_o\right)^2 \right] dx \qquad \text{Equation 9}$$

Where, N is the number of forecast and $x_o$ is observed value. CPRS is the continuous extensions of RPS where F(x) is the Cumulative Distribution Function (C.D.F), F(x) = p ($X \leq x$) and H($x - x_0$) is the Heaviside function that has the value 0, when ($x - x_0$) < 0 and 1, otherwise.

In order to quantify the performance of the probability score, the skill score (SS) (Wilks, 1995) is calculated as Equation 10:

$$SS(C)RPS = 1 - \frac{(C)RPS_{FP}}{(C)RPS_{RP}} \qquad \text{Equation 10}$$

Where, $(C)RPS_{FP}$ denotes the forecast score and $(C)RPS_{RP}$ is the score of a reference forecast of the same predictand.

The SS(C)RPS is the validation tool that compares how the distribution of an ensemble of forecasts predicts the observed value, and it is sensitive to bias as well as variability in the forecasted values. A skill score SS(C)RPS close to one means a successful simulation; if the skill score is negative, the method is performing worser

than the reference forecast.

### 2-2-4-4- Optimisation

The classifications are evaluated using measures of their ability to classify Patterns with large differences in precipitation structure. These measures are designed for precipitation occurrence $I_1$ and amount $I_2$ for a specific pattern. The optimisation derives circulation patterns that explain precipitation patterns (dry and wet conditions) and this is achieved by maximising two objective functions developed by Bardossy et al., 2001:

$$I_1 = \frac{1}{T}\sum_{t=1}^{T}\sqrt{p(CP_t - \bar{p})^2} \qquad \text{Equation 11}$$

$$I_2 = \frac{1}{T}\sum_{t=1}^{T}\left|\ln\left(\frac{z[CP_T]}{z}\right)\right| \qquad \text{Equation 12}$$

Where, T is the number of classified days, $p(CP_t)$ is the probability of the precipitation on day t, z is the mean precipitation amount in day t with classification CP and p is the probability of precipitation for all days.

## 2-3- Model Error

The Large Scale Predictor NCEP is the most reliable source to check the performance of downscaling model for the predictand variables. Error analysis in climate change downscaling is conducted by comparison with mean and variance between historical and downscaled output. There are some studies to implement the model error analysis in statistical climate change downscaling (Ebrahim et al., 2012; Buytaert et al., 2010; Raje and Mujumdar, 2010).

The techniques such as Wilcoxon Test (Conover, 1980) and Leven's Test (Levene, 1960) are used to indicate the model errors. These techniques have been employed to investigate the model error in statistical climate change downscaling by (Khan et al., 2005; Ebrahim et al., 2012; khan and Coulibaly, 2010).

These two tests are used to construct a hypothesis test p-value to estimate variability of two population means. The p-value is the level of significance for which observed test statistic lies on the boundary between acceptance and rejection of the null hypothesis. The p-value great than 0.05 (95% significant level) indicates the similarity of two observed and modelled data.

Rainfall dataset does not follow normal distribution, a non-parametric analysis is applied on it. On the other hand, temperature and evaporation dataset can be considered as normal variables. The parametric analysis is used to estimate the model error.

## 2-4- Hydrological Modelling

This section describes the hydrology model that has been used for the research. It contains an explanation of method and functions (Loss model, Hydrographical transformation, Channel routing and Reservoir flood routing) have been employed in HEC-HMS. The detailed method of hydrology modelling in HEC-HMS can be found in (Ford et al., 2008) and (Scharffenberg and Fleming, 2008).

### 2-4-1- Watershed Delineation

Watershed delineation generates the hydrology parameters needed for the hydrology modelling. These hydrological parameters are driven automatically by GIS system using Hec-Geo-HMS for the watershed. The automatic watershed delineation in GIS is described as below. Figure 10 illustrates the processes for automatic watershed delineation in GIS system. The detailed method of the watershed delineation using Hec-Geo-HMS can be found in (Fleming and Doan, 2010).

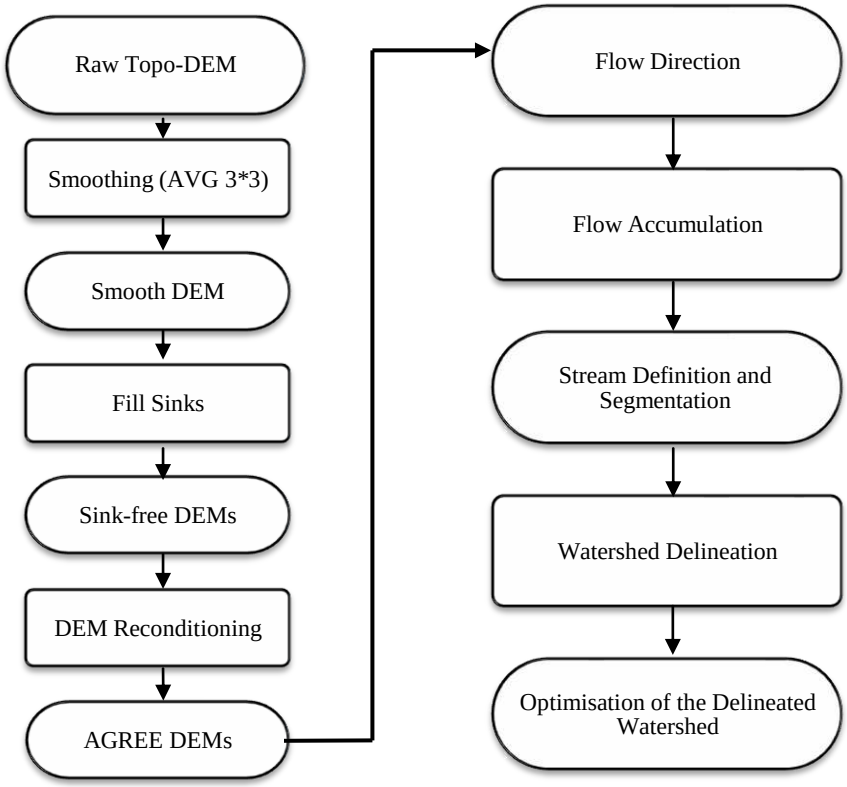


Figure 10 Generating watershed delineation from a raw elevation map in GIS

### 2-4-2- Loss Model

Loss model estimates the rainfall losses infiltrated by the ground. HEC-HMS provides various methods to calculate the loss rate in the watershed/sub-watershed such as deficit and constant, exponential loss, Green-Ampt, SCS Curve Number, initial and constant.

The HSGs consists of four categories A, B, C, and D, which A and D are the highest and the lowest infiltration rate respectively. In this study, based on the range infiltration rate of various soil units in Klang watershed, Hydrological Soil Groups (HSGs) has been identified as Table 23 in Chapter 5.

The SCS-CN loss method is used in runoff estimation to specify the amount of infiltration rates of soils. The method uses an integration of landuse and soil data to determine CN values of the watershed. In this study the CN values were adopted from Technical Release 55, United States Department of Agriculture- Natural Resources Conservation Service (USDA-NRCS, 2000). To develop the CN map, the soil data of Klang watershed has been categorised into hydrologic soil groups (HSGs) and then have been combined with landuse data. CN map indicates the integrated landuse-soil of Klang watershed. The relevant equations developed by Natural Resources Conservation Service (USDA-NRCS, 2000) are as follows:

$$S = \frac{25400}{CN} - 254 \qquad \text{Equation 13}$$

$$Q = \frac{(P-0.2S)^2}{P+0.8S} \qquad \text{Equation 14}$$

Where, Q is direct runoff (mm), P is accumulated rainfall (mm), S is potential maximum soil retention (mm) and CN is Curve Number.

### 2-4-3- Time of Concentration

The time of concentration is defined as the length of time between the ending of excess precipitation and the first milestone on descending hydrograph while the standard lag time is defined as the length of time between the centroid of precipitation mass and the peak flow of the hydrograph.

In this study, SCS dimensionless hydrograph was used to generate hydrograph for a long time daily rainfall over Klang watershed. The parameters of the method are: time of concentration, lag time, duration of the excess rainfall, time to peak flow, peak flow. The relevant equations developed by Natural Resources Conservation Service (USDA-NRCS, 2000) are defined as:

$$T_p = 0.6T_c + \sqrt{T_c} \qquad \text{Equation 15}$$

$$T_c = \frac{L^{0.8}\left(\frac{1000}{CN} - 9\right)^{0.7}}{1140S^{0.5}} \qquad \text{Equation 16}$$

$$q_p = \frac{2.083QA}{t_p} \qquad \text{Equation 17}$$

Where, $T_p$ is time to peak (min), $T_c$ is time of concentration (hr), L is hydraulic length of watershed (ft), S is average land slope of the watershed (percent), $q_p$ is peak flow ($m^3/s$), Q is direct runoff (cm), A is area of watershed ($km^2$) and $T_p$ is time to peak (hr.)

### 2-4-4- Channel Routing

In this study, Muskingum method was used to calculate the hydrologic river routing in Klang watershed. The method is well known and has been extensively used in hydrologic modelling (Nawarathna et al., 2005; Shrestha et al., 2011). Muskingum method in HEC-HMS was used due to its simplicity and modest data requirement which make it practical method for Klang watershed while other methods require

complex data. The general equation of Muskingum was developed by McCarthy (1938) which is based on Storage Equation. Details of the Muskingum Equation can be found in (Birkhead and James, 2002; Al-Humoud and Esen, 2006). The Muskingum Equation represents a relationship between storage, inflow, and outflow of the reach to calculate changes in flow hydrograph when a flood wave passes downstream. The Discharge-Storage Equation of Muskingum in the routing reach developed by McCarthy in the 1930s cited by (Chin, 2000).

$$S = xkQi^{0.6} + (1-x)\,kQo^{0.6} \qquad \text{Equation 18}$$

Where, S is the amount of storage ($m^3$), $Q_i$ and $Q_o$ is inflow and outflow ($m^3/s$).

X is a weighting factor defines the effect of the amount of discharge on the storage having a range of $0 \leq X \leq 0.5$ and K is storage coefficient and defines the ratio of storage to the discharge which can be calculated by the travel time through a reach.

### 2-4-5- Stage-Storage-Discharge Relationship

The Stage-Storage- Discharge be analysed for the structures in the watershed as they contribute into the flow of a flood. It determines the relationship between the depth of water and the relevant storage volume in the structure. Hydrological Storage Equation is referred to as Water-Balance Equation. There are two main methods to specify the storage relation, Elevation-Storage and Elevation-Area in HEC-HMS for the watershed system. Many studies have conducted the Stage-Storage-Discharge behaviour in hydrological modelling (e.g. Aksoy and Wittenberg, 2011; Wang, 2011; McGuire and McDonnell, 2010). . More details on the storage-discharge method can be found in (Das and Saikia, 2009).

## 2-5- Flood Frequency Analysis

Flood Frequency Analysis (FFA) is performed by selecting the Annual Maximum Series (AMS) over long years, at least 10 years. The AMS are ranked and fitted to the frequency distribution model. Bulletin 17B proposes to gather the time series of annual maximum floods at the discharge station to determine flood flow frequency.

Many studies have evaluated the climate change impact on precipitation and flood frequency (Samiran and Simonovic, 2012; Raff et al., 2009; Sivapalan and Samuel, 2009; Hamlet and Lettenmaier, 2007; Hirabayashi et al., 2008).

The distribution can be carried out by some statistical analysis such as Normal Distribution, Log-normal Distribution, Gumbel Distribution and Log-Pearson Type III Distribution to fit the probability of occurrence of flood series. Frequency factor equation for Pearson Type III Distribution can be written in terms of discharge as Equation 19 (Helsel and Hirsch, 2010).

$$Log_{Qt} = \sum_{i=1}^{n} \frac{\log Qi}{n} + K_T(T, Gs) \left[ \sqrt{\sum_{i=1}^{n} \frac{\log Qi - \sum_{i=1}^{n} \frac{\log Qi}{n}}{n-1}} \right] \qquad \text{Equation 19}$$

Where, $Q_t$: The discharge for the T-year return period, $Q_i$: Any recorded discharge for a river with the n record length, and $K_t$: The frequency factor.

The frequency factor is dependent on the return period, T and the coefficient of skewness, Gs. When Gs =0,

$$KT = z \qquad \text{Equation 20}$$

Where, z: the standard normal variable. Kite (1977), suggested the frequency factor value when the G is not zero,

$$K_T(T, Gs) = Z + \left(Z^2 - 1\right)K + \frac{1}{3}\left(Z^3 - 6Z\right)K^2 - \left(Z^2 - 1\right)K^3 + ZK^4 + \frac{1}{3}K^5 \qquad \text{Equation 21}$$

K can be determined as follows (Mays, 2001):

$$K = Gs/6 \qquad \text{Equation 22}$$

# 3- CLIMATE BASE AND HYDRO-METEOROLOGICAL ANALYSIS

This chapter consists of two parts. The first part of the chapter focuses on the characteristics of the study area, Klang watershed in Kuala Lumpur. It presents a description of the watershed by determining the environmental-physical aspects such as topography, geology, soil and landuse. The second part of the chapter describes the climate pattern and hydrological characteristics of study area. A study on interpretation on flow and flood through the watershed conducted by Flood Frequency Analysis (FFA) and Flow Duration Curve (FDC) techniques to reflect the behaviour of flow regime. Furthermore, data preparation and quality control on the historic data are conducted using graphical, statistical and spatial methods.

## 3-1- Study Area

### 3-1-1- Watershed Description

Klang watershed is located at the West Coast of Peninsular Malaysia. The watershed consists of Kuala Lumpur in the state of Selangor in Malaysia, a country in the South East of Asia; between 101°.30´ to 101°.55´ E longitudes and 3° to 3°.30´ N latitude.

Klang River originates from the main range at an elevation of 1400 metres above mean sea level around the East and North-East of Selangor. It is 120 km in length and the area of watershed is 674 km² approximately. Klang River traverses through the two states, Selangor and Wilayah Persekutuan and finally discharges into the straits of Malacca to the west. The upstream of the river comprises of mountainous terrains which are steeper. Most parts of the watershed are intact, underdeveloped and covered by a thick canopy of tropical jungle. Klang River has 11 major tributaries, these include Gombak River, Batu River, Kerayong River, Damansara River, Keruh River, Kuyoh River, Penchala River and Ampang River. Figure 11 shows the geographical location of the study area chosen.

### 3-1-2- Geology

The geology of the watershed is one of the layers used in hydrological modelling to specify different soil characteristics such as texture, structure, organic matter content, and soil depth required by the model. These parameters influence the surface runoff (Stadler et al., 2013). The soils formed from rocks are eroded and deposited at some parts of the river during flooding. Metamorphism and erosion of the rocks in the area produces a huge amount of sediments mostly made up of medium to fine washing into the straits of Malacca. Sands and clays are predominantly the results of weathering and erosion of quartz and granite bedrock in the watershed.

Gobbet and Hutchison (1973) conducted a detail study on the geology of Peninsular Malaysia. Yin (1976) studied on geology of Kuala Lumpur. Table 3 summarises the stratiography and major rock formation in the study area. The area is underlain by an extensive limestone bedrock formation. The different geology unit of Klang watershed is illustrated in Figure 12. The Kenny Hill formation comprises of quartzite and phyllite is dominating the geologic formation in the study area.

Table 3 Geological units of Klang watershed (Sasekumar and Chong, 2006)

| **Geologic age** | **Formation** |
|---|---|
| Carboniferous to Permian (286 to 360 Ma) | Kenny Hill Formation |
| Middle to Upper Silurian (408 to 421 Ma) | Quartzite/Phyllite |
| Ordovican to Silurian (408 to 505 Ma) | Kuala Lumpur Limestone |
| Pre-Silurian (older than 438 Ma) probably Cambrian (505 to 590 Ma) | Hawthornden Schist |
| | Dinding Schist |

### 3-1-3- Soil

The rock, soil types and their properties are capable to change the hydrological model results of infiltration, time of concentration. Therefore it is necessary to determine the soil units of Klang watershed to use in hydrological modelling. In Malaysia, two types

of soil classifications are used to integrate the soil maps which are Soil Texture Classification and Soil Taxonomy Classification (Soil Survey Staff, 1975). Figure 13 shows the soil map of Klang watershed in terms of Great Soil Groups (GSG) in the Soil Taxonomy Classification System. It categorises the soil units based on soil properties such as soil structure, porosity, permeability, water holding capacity, and etc. However, the Food and Agriculture Organization of the United Nations (FAO) soil data classification system is used to fill some gaps of soil data from the Department of Agriculture (DOA). FAO soil categorisations comprise of dominant soil units, their texture and slope information. It consists of 4930 different soil units for the global soil types at a scale of 1:5, 000, 000 (Kavvas et al., 2006).

In this study, in order to estimate soil properties in Klang watershed, the soil units are converted to US. Department of Agriculture (USDA) classification using a lookup table which was developed by Rawls, et al. (1982) and McCuen et al. (1981). It relates the Brooks and Corey's soil hydraulic parameters to the 11 USDA soil texture classes. The relation between the soil series and its components along with great soil groups was created in Table 4 for Klang watershed.

Table 4 Soil units of Klang watershed

| **Soil Series** | **Area ($km^2$)** | **Great Soil Groups (GSG)** | **Area ($km^2$)** |
|---|---|---|---|
| Mined Land | 22.67 | Hapludox-Hapludults | 11.79 |
| Munchong-Seremban | 11.79 | Mined Land | 22.67 |
| Rengam-Jerangau | 58.30 | Palehumults | 149.85 |
| Serdang-Bungor-Munchong | 31.00 | Paleudults-Hapludox | 89.00 |
| Serdang-Kedah | 44.81 | Paleudults-Hapludults | 44.81 |
| Steepland | 149.85 | Tropopsamments-Fluvaquents | 9.14 |
| Telemong-Akob-Local Alluvium | 9.14 | Urban Land | 334.82 |
| Urban Land | 334.82 | water | 11.97 |
| Water | 11.97 | | |

### 3-1-4- Landuse

Landuse data is essential in runoff estimation. It affects infiltration rate resulting in changes on surface runoff. Landuse such as roads, pavements, parking lots and

buildings obviously do not allow infiltration and consequently increase surface runoff. On the other hand, land covered by plants, vegetates and forests cause infiltration rate high resulting in decreasing surface runoff (e.g. Barnes et al., 2002; Liu et al., 2006).

Urbanisation and industrial growth in Klang watershed in a high rate have increased pressure on the flow capacities of the main rivers and its tributaries. There are two dams in Klang River System namely Batu and Klang Gate dam which play a crucial role for the region to control flooding and for water supply (DID, 2010; NAHRIM, 2010). The middle part of Klang watershed has a high proportion of impervious urban area (about 50%), and much of it is perched on susceptible land to flooding. The flat plain grounds have mostly been used for agriculture and commercial planting such as oil palm, orchard, rubber and scrub. Although a rapid grow in converting the agriculture landuse to new residential area construction is observed (Verburg and Overmars, 2007). The matching between Malaysian and USGS landuse units in Klang watershed are listed in Table 5. Figure 14 shows the landuse map for Klang watershed.

Table 5 Malaysian and USGS Landuse/cover matching in Klang watershed

| Malaysia Classification | USGS Classification |
|---|---|
| Agricultural station | Agriculture |
| Agricultural station (cattle farm) | Agriculture |
| Agricultural station (diversified crops) | Agriculture |
| Agricultural station (oil palm) | Agriculture |
| Agricultural station (orchards) | Agriculture |
| Aquaculture | Agriculture |
| Cemetery | Urban |
| Estate building and associated areas | Urban |
| Ex-tin mining areas | Mining |
| Forest | Forest |
| Main road and highway | Urban |
| Market gardening | Agriculture |
| mixed horticulture | Agriculture |
| mixed horticulture, neglected grassland | Agriculture |
| mixed horticulture, rubber | Agriculture |
| Neglected grassland | Pasture |
| Neglected grassland (main road and highway) | Pasture |
| Neglected grassland/orchards | Pasture |
| Neglected grassland, scrubs | Pasture |
| Neglected grassland, scrubs (recreational areas) | Pasture |
| Newly cleared land | Newly cleared land |
| Newly cleared land (urban and associated areas) | Newly cleared land |
| Oil palm | Agriculture |
| Orchards | Agriculture |
| Orchards/rubber | Agriculture |
| Orchards/scrubs | Agriculture |
| Orchards, neglected grassland | Agriculture |
| Orchards, scrubs | Agriculture |
| Other mining areas | Mining |
| Other mining areas, neglected grassland | Mining |
| Pond/lake | Water body |
| Poultry/ducks | Agriculture |
| Power lines | Urban |
| Railway | Urban |
| Recreational areas | Urban |
| Reforested | Forest |
| Rubber | Agriculture |
| Scrubs/orchards | Agriculture |
| Scrubs, orchards | Agriculture |
| Swamps | Swamps |
| Swamps/orchards | Swamps |
| Swamps, scrubs | Swamps |
| Tin mining areas | Mining |
| Urban and associated areas | Urban |

### 3-1-5- Topography

Topographic data is one of the basic data in terrain analysis. It is used as the base data to specify sub-watersheds boundary through the delineation of watershed and drainage network. Then, the quality and scale of topography data affect on surface runoff modelling in hydrological simulations. Some useful data are extracted from topography such as slope and aspect, length, surface roughness, flow convergence or divergence which influence the runoff estimation (Jain and Singh, 2005).

There are various sources to obtain the elevation data. One of the famous sources is SRTM-DEM which has a potential application and has been used in many studies (Durga et al., 2011; Ali et al., 2011). The coarse spatial resolution of SRTM-DEM may influence the hydrology modelling as mentioned by many studies to investigate the runoff and flooding regime (e.g., Ludwig and Schneider, 2006). SRTM-DEM is useful to delineate and derive the hydrological parameters in the US boundary, as 30 metres in cell size. Besides that, SRTM-DEM provides approximately 3 arc-second data in Malaysia which is about 90 metres at the equator.

Akbari et al. (2010) carried out a study to specify the practical use of SRTM-DEM in Klang watershed to watershed modelling using Hec-Geo-HMS extension in GIS. They found a good agreement of SRTM-DEM elevation data as compared to the topography sheet data of watershed particularly in the hilly area but not the flat terrain such as Kuala Lumpur, an urban area. The coarse resolution of SRTM-DEM may provide an inaccurate representation of terrain. In this study, it was not used for Klang watershed to avoid any uncertainty of the raw elevation data with 90m resolution.

Another source of elevation data is LIDAR (Light Detection And Ranging) which is a remote sensing product. The usage of this source for Klang watershed involves a very high cost which is approximately Rm 150 000 at 10 metre resolution (AAMhatch , 2007). In spite of its high quality and the most reliable source, this type of elevation data for hydrological modelling is expensive (Wheater et al., 2008). The high cost of LIDAR data was the restriction not to use it in this study.

In this study the topography sheets obtained from JUPEM are used in the hydrological modelling. Klang watershed consists of nine digital sheets at the scale of 1:25,000.The topography of Klang watershed is characterised by steep mountainous terrain with elevations ranging from approximately 5m around the southwest to 1400 m on top of the surrounding mountains toward Northeast of area. The elevations gradually decrease between 30 and 60 metres above mean sea level through the middle and west part of the watershed. Mean elevation is around 194 m.

In Figure 15 A, there is a data gap in sheet 3757b. Therefore, it was attempted to fill the gap in elevation data by using 24 digital topography sheets at a scale of 10,000 to create the Digital Elevation Model as shown in Figure 16.

### 3-1-6- Slope

The mean slope of the study area is about 11.7 percent. It reaches high about 85 percent in hill tops and ridges and decrease through the middle and South-West of the watershed from zero to three percent. Figure 17 shows the slope of Klang watershed in terms of percentage.

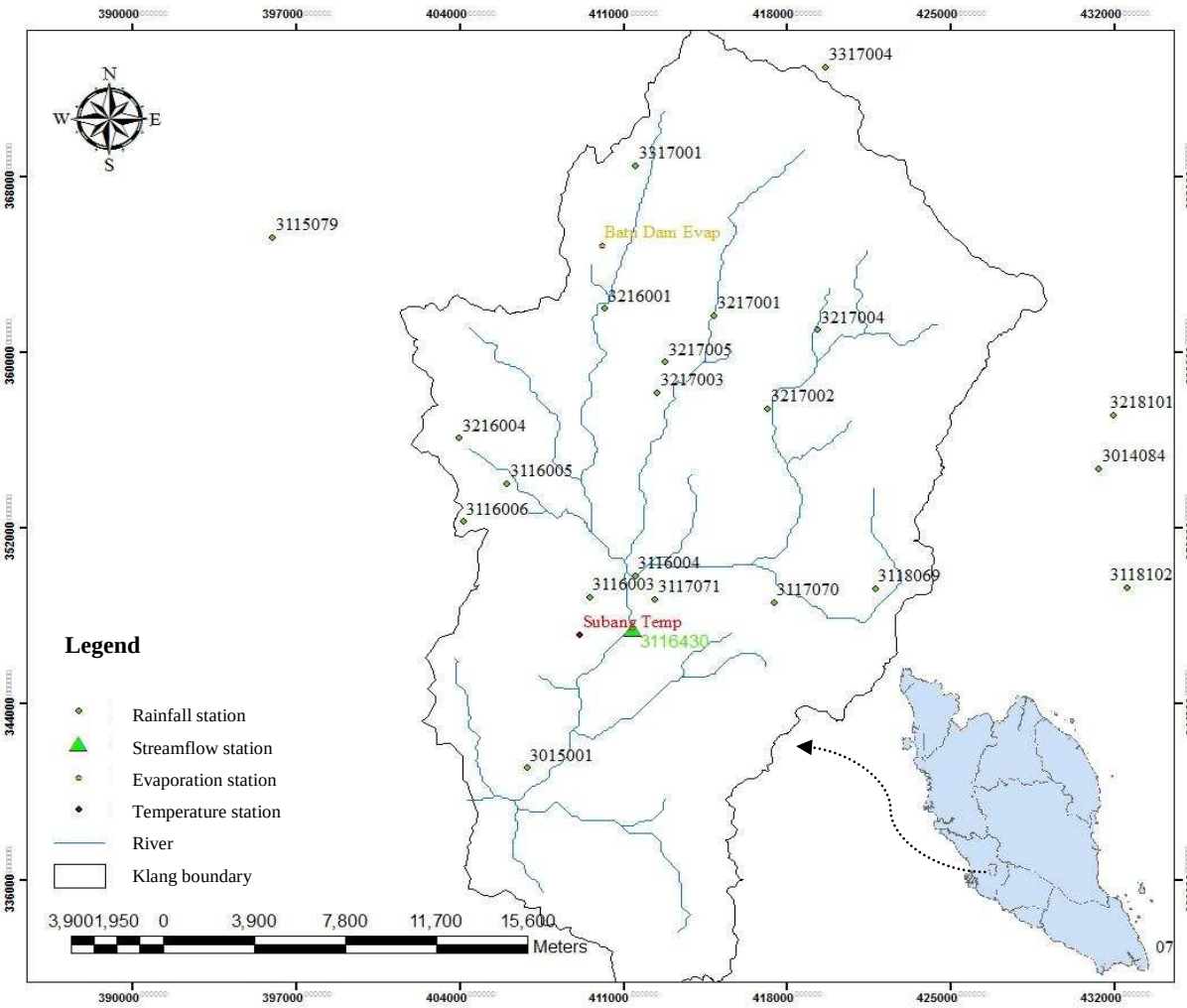


Figure 11 Location of the hydro-meteorological gauging stations in Klang watershed

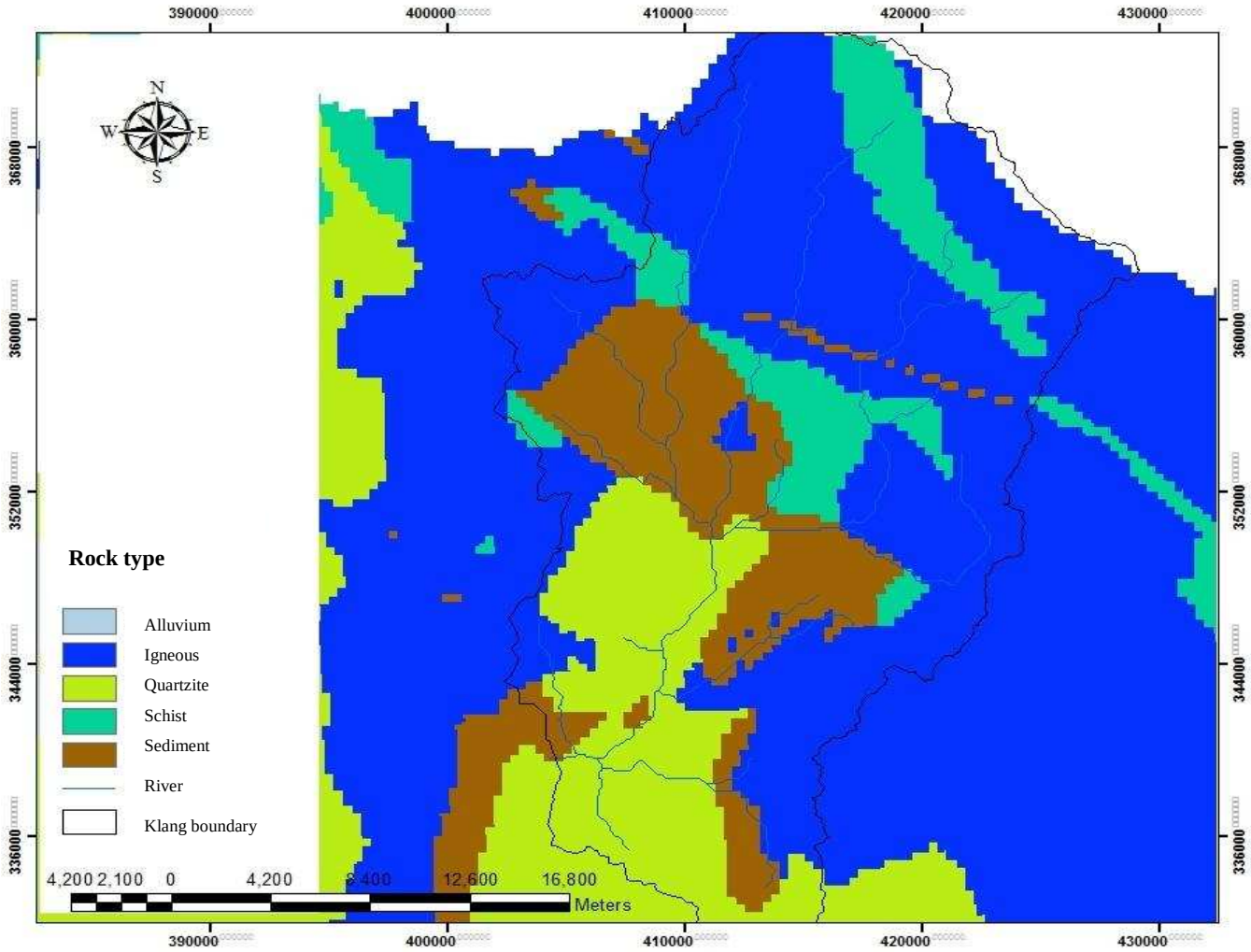


Figure 12 Geology map of Klang watershed

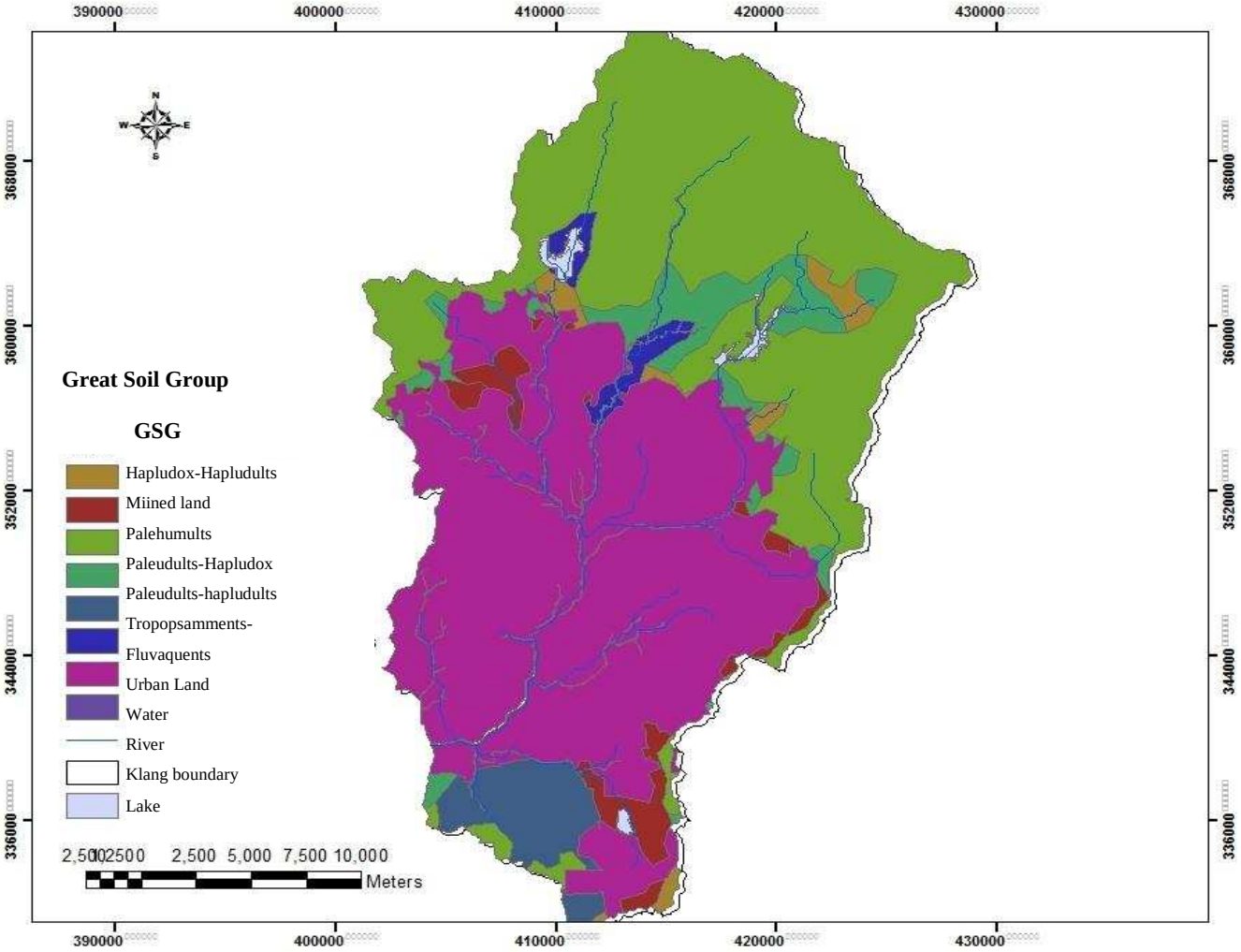


Figure 13 Soil map of Klang watershed

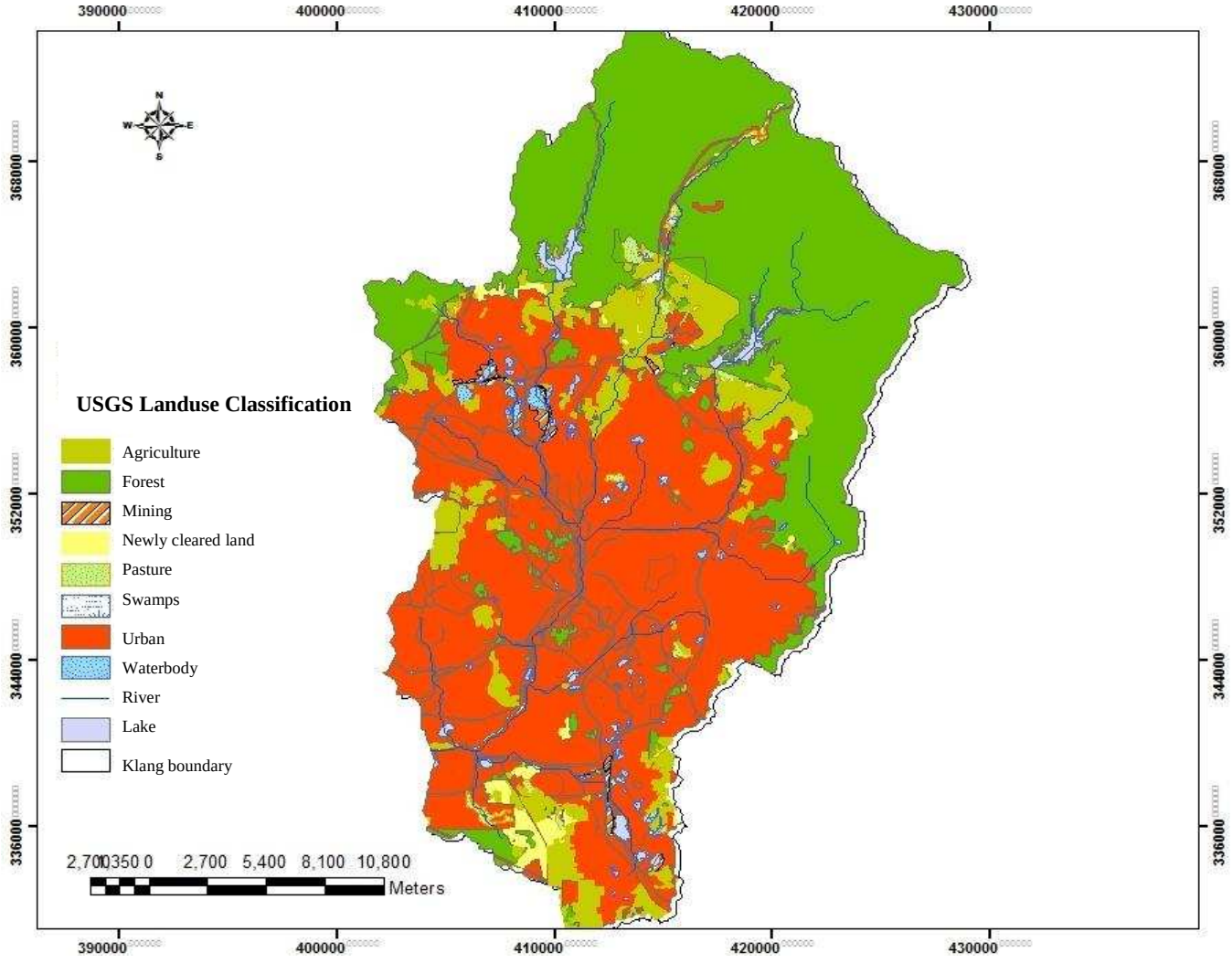


Figure 14 Landuse map of Klang watershed

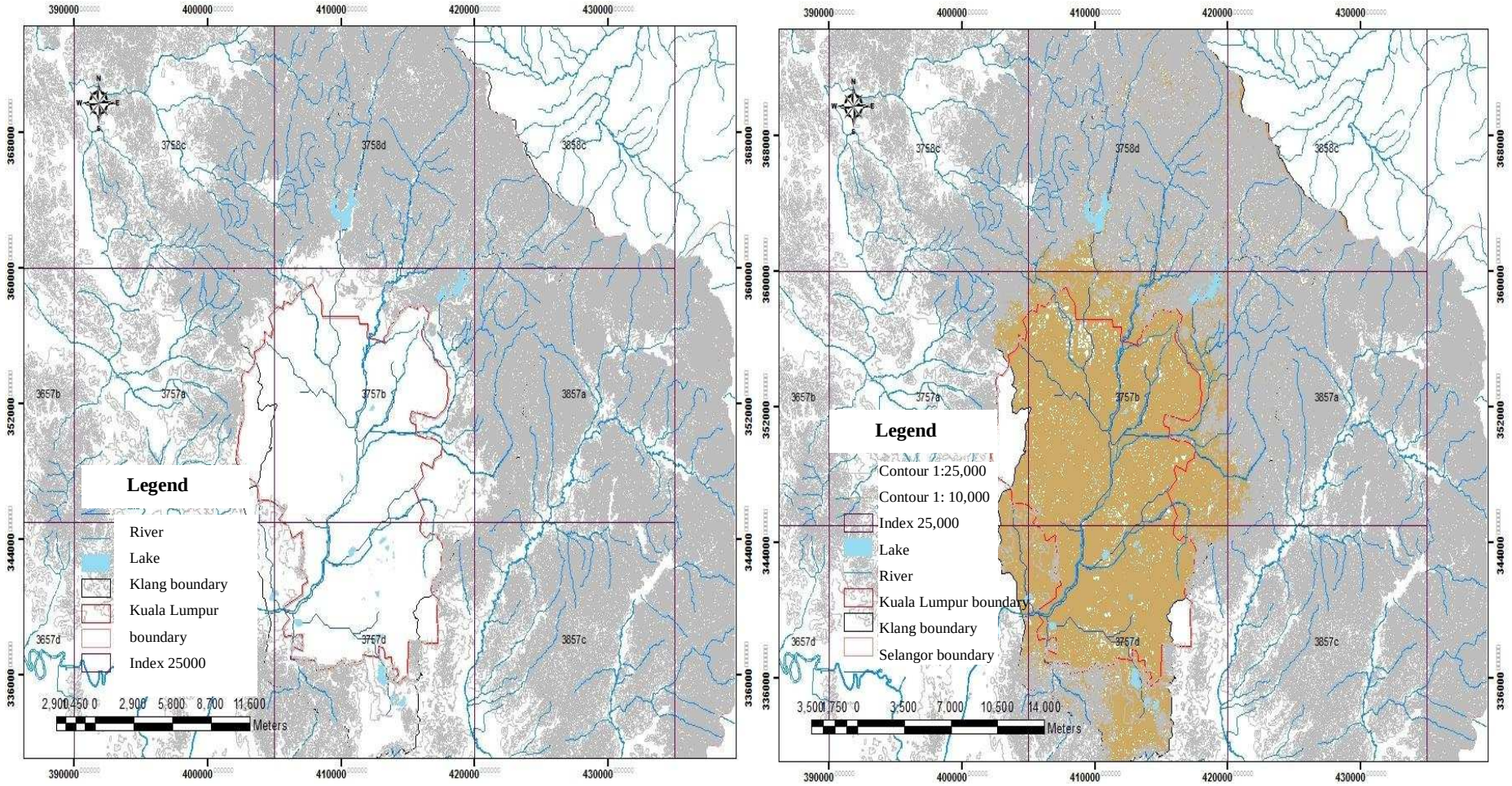


**A-** **B-**

Figure 15 The topographic map of Klang watershed (**A:** Gap data seen at scale of 1:25000, **B:** filled the gap by topo at 1:10000)

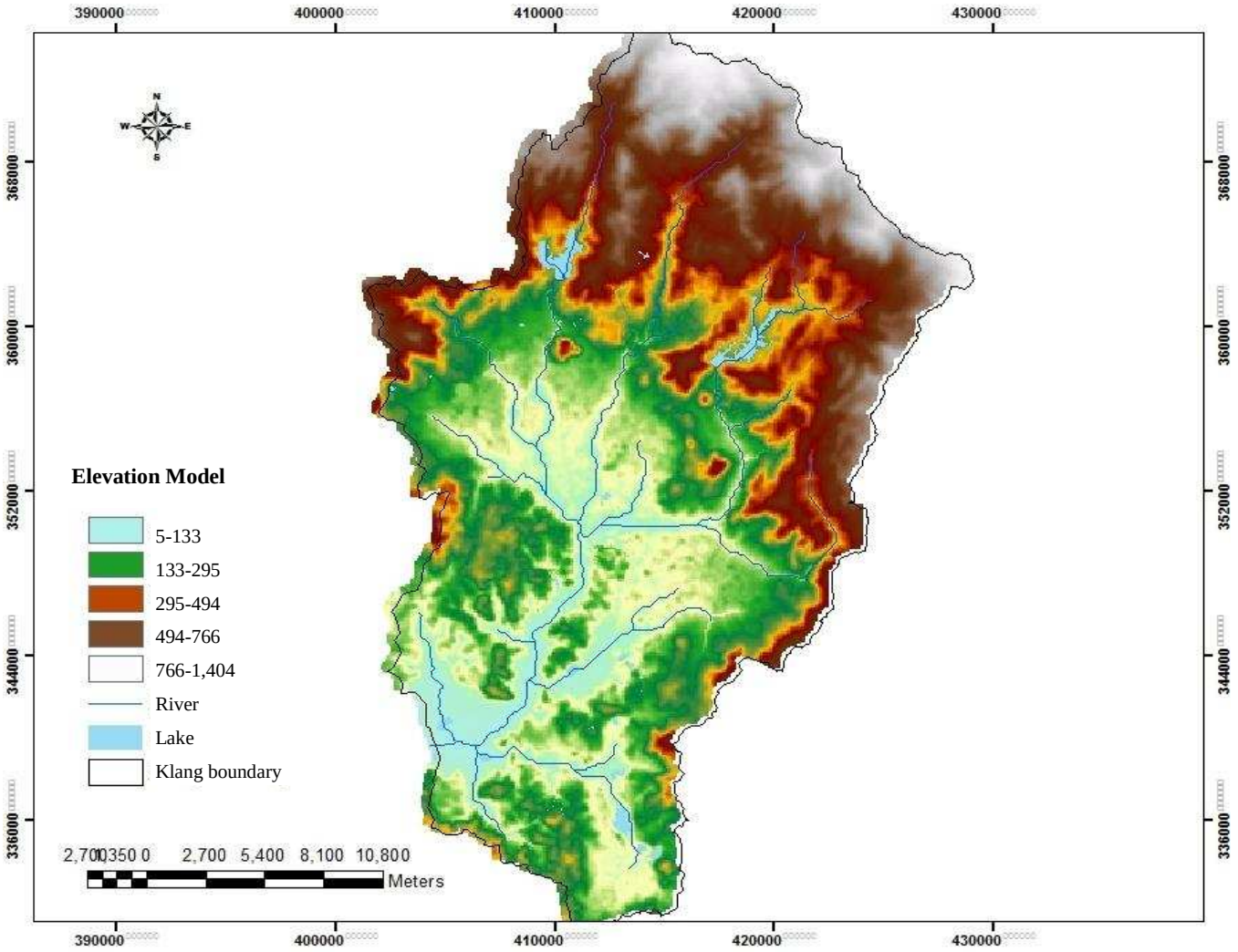


Figure 16 Elevation classification for Klang watershed

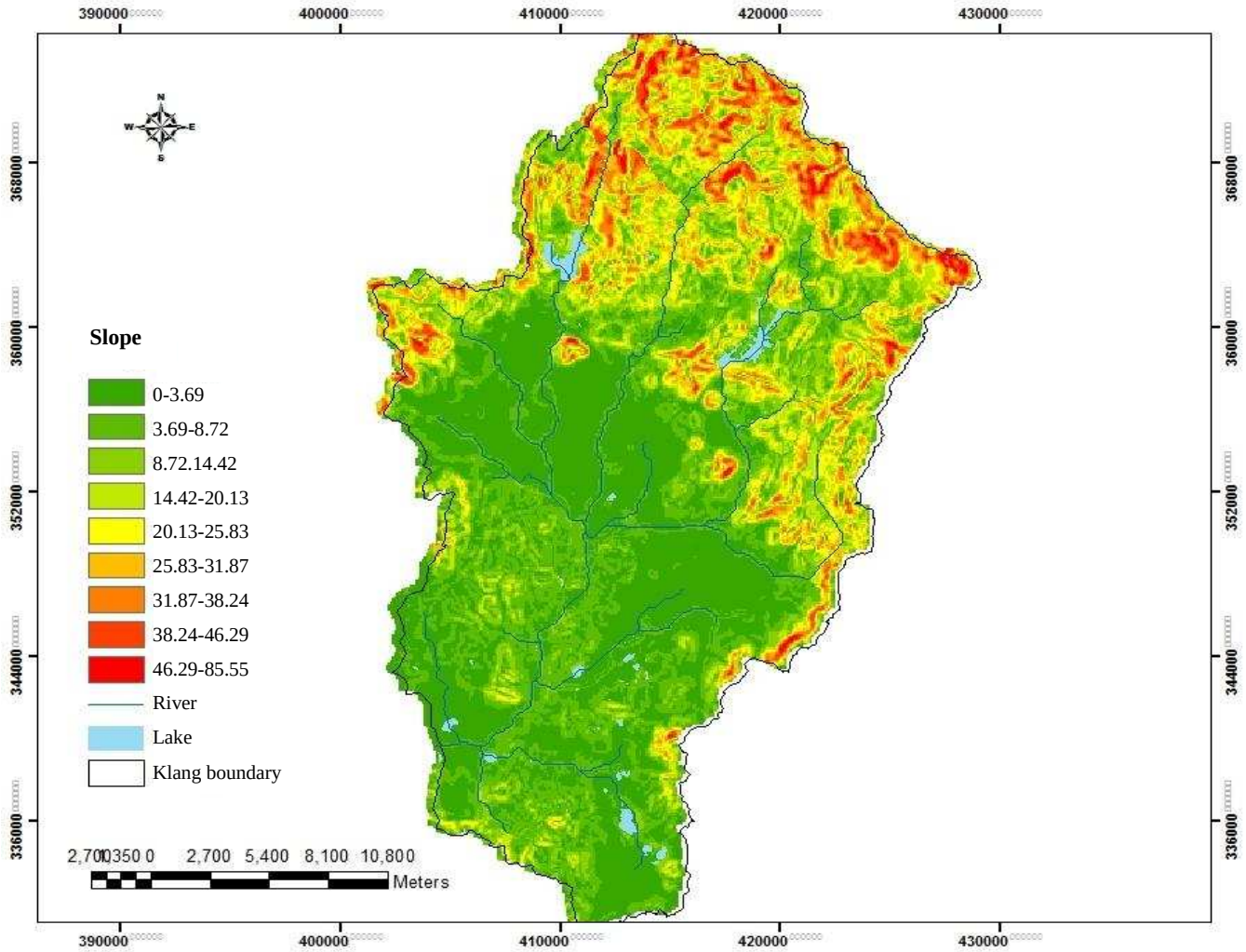


Figure 17 Slope classification for Klang watershed

## 3-2- Data Preparation

### 3-2-1- Data Sources

In this research, the data has been obtained from various sources. The Landuse, Geology and Soil data are obtained from Department of Agriculture, (DOA). Malaysia. Klang's index map in digital topo-sheets at a scale of 1:25,000 are obtained from the Department of Surveying and Mapping, Malaysia which also known as JUPEM. Historic climate data records such as rainfall, temperature, evaporation and other hydrometric data have been acquired from the Department of Irrigation and Drainage (DID), Malaysia.

### 3-2-2- Rainfall Data

In this study 23 raingauges have been selected to cover Klang watershed which is shown in Table 6. It represents the geographical coordination, station name, Id number, the year and mean rainfall over the year for every gauge station in the study area.

Table 6 The characterisations of the meteorological stations

| Id | Station name | Station no. | Longitude (degree) | Latitude (degree) | Mean rainfall (mm/year) | Period (year) |
|---|---|---|---|---|---|---|
| 1 | Pejabat jps. Klang | 3014084 | 101.88 | 3.21 | 2162.60 | 1972-2006 |
| 2 | Ldg. Bkt. Rajah | 3014089 | 101.44 | 3.09 | 1946.61 | 1972-2006 |
| 3 | Puchong drop | 3015001 | 101.66 | 3.08 | 2109.42 | 1982-2002 |
| 4 | Ldg. Dominion | 3018107 | 101.88 | 3.00 | 2486.12 | 1972-2006 |
| 5 | Pusat penyel. Getah | 3115079 | 101.56 | 3.30 | 2311.35 | 1972-2006 |
| 6 | I/pejabat | 3116003 | 101.68 | 3.15 | 2829.65 | 1993-2006 |
| 7 | Wilayah persekutu | 3116004 | 101.70 | 3.16 | 2232.58 | 1975-1992 |
| 8 | Taman maluri | 3116005 | 101.65 | 3.20 | 2388.95 | 1977-2000 |
| 9 | Edinburgh | 3116006 | 101.63 | 3.18 | 2312.54 | 1982-2002 |
| 10 | Pusat penyelidekan | 3117070 | 101.75 | 3.15 | 2474.94 | 1972-2006 |
| 11 | Loji air bkt.,weld | 3117071 | 101.71 | 3.15 | 2403.33 | 1972-1985 |
| 12 | Pemasokan ampang | 3118069 | 101.79 | 3.16 | 2577.54 | 1972-2006 |
| 13 | Sek.keb. Kg.lui | 3118102 | 101.89 | 3.16 | 2171.70 | 1974-2006 |
| 14 | Kg. Sg. Tua | 3216001 | 101.69 | 3.27 | 2324.68 | 1972-2006 |
| 15 | Keb kepong | 3216004 | 101.63 | 3.22 | 2319.50 | 1982-2003 |
| 16 | Ibu bekalan km | 3217001 | 101.73 | 3.27 | 2388.61 | 1973-2006 |
| 17 | Empangan genting kelang | 3217002 | 101.75 | 3.23 | 2305.83 | 1977-2006 |
| 18 | Ibu bekalan km | 3217003 | 101.71 | 3.24 | 2242.52 | 1975-2006 |
| 19 | Kg.kuala sleh | 3217004 | 101.77 | 3.26 | 2320.47 | 1980-2006 |
| 20 | Gombak Damsite | 3217005 | 101.71 | 3.25 | 1834.93 | 1982-2000 |
| 21 | Jenaletrik lln | 3218101 | 101.88 | 3.23 | 2230.42 | 1972-2006 |
| 22 | Terjun sg.batu | 3317001 | 101.70 | 3.33 | 2301.52 | 1975-2006 |
| 23 | Genting sempah | 3317004 | 101.77 | 3.37 | 2329.41 | 1975-2006 |

### 3-2-3- Hydro-Meteorological Data

There are three stream gauging stations in Klang watershed namely Sentul at W. Persekutuan (3116434), Gombak at Jln. Tun Razak (3116433) and SG. Klang at Jambatan Sulaiman (3116430). Table 7 shows the geographical coordinate and length of data collected from DID for the study.

The maximum average monthly flow has occurred in November, 1975 and April 2007 at Sulaiman streamflow station are 62.77 $m^3/s$ and 57.31 $m^3/s$ and the minimum value observed are 9.46 $m^3/s$ and 9.53 $m^3/s$ in February and August respectively.

Table 7 Geographical coordinates and length of years for hydro-meteorological data

| Station name | Station no. | River name | Longitude (degree) | Latitude (degree) | Mean flow ($m^3/s$) | Period (year) |
|---|---|---|---|---|---|---|
| Jambatan Sulaiman | 3116430 | Sg. Klang | 101.69 | 3.16 | 20.02 | 1975-2007 |
| Tun Razak | 3116433 | Sg. Gombak | 101.69 | 3.17 | 4.94 | 1960-2007 |
| Batu Sentul | 3116434 | Sg. Batu | 101.68 | 3.17 | 8.21 | 1960-2007 |

### 3-2-4- Data Quality Control

Rainfall and streamflow data have been collected from various sources are tested for its errors, gaps, accuracy and quality of data. Then, analysis on the data can be reliable for climate studies and hydrological modelling.

#### 3-2-4-1- Meteorological Data Screening

In this research, the data screening procedure was carried out to check the homogeneity, consistency and stationary of the observed data by the following techniques: Homogeneity analysis, Visual examination and Double-Mass curve

##### 3-2-4-1-1- Homogeneity Analysis

Homogeneity analysis describes the statistical properties of the time series. An inconsistency and non-homogeneity in hydrological data may be caused by some gaps

or exaggerations in data through the use of different instruments, methods of observation and human error. Figure 18 indicates the evaluation of homogeneity of 23 selected raingauge stations over Klang watershed using non-dimensionalising the month's rainfall. The non-dimensionalising of the month's value is carried out by using the following Equation 23 (Potter, 1981):

$$P_i = \frac{\bar{P}_i}{\bar{P}} * 100\% \qquad \text{Equation 23}$$

Where, $P_i$ is non-dimensional value of rainfall for month i, $\bar{P}_i$ is averaged monthly rainfall at the station i and, $\bar{P}$ is the average yearly rainfall of the station.

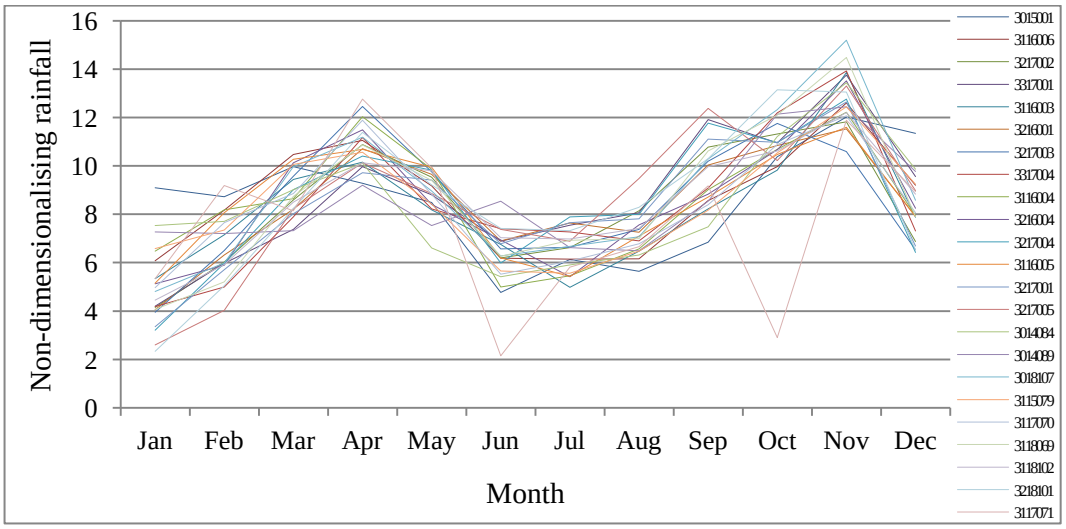


Figure 18 Non-dimensionalised analysis for 23 raingauge stations for Klang watershed

### 3-2-4-1-2- Visual Examination

Figure 19 indicates visual examination by plotting the time series data. It is a simple method to estimate discontinuities in data.

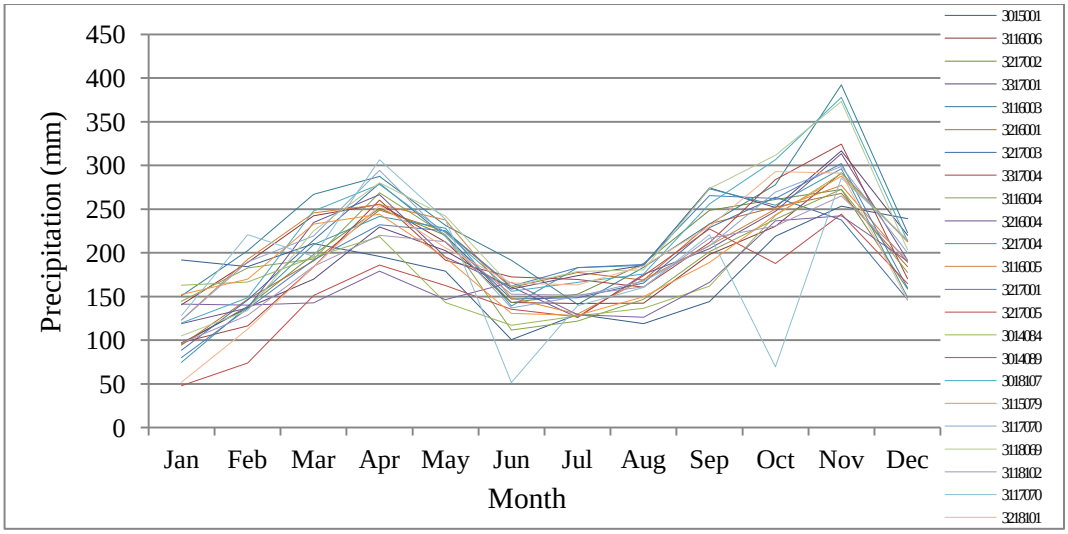


Figure 19 Monthly rainfall over 23 raingauge stations for Klang watershed [mm/month]

### 3-2-4-1-3- Double-Mass Curve

The double-mass analysis is used to estimate proportionality properties of the data which it reveals consistency and homogeneity of the data. The double-mass technique plots the accumulated rainfall data against the mean value of all neighbourhood stations. Figure 20 illustrates the double mass curve of the station 3217003. The other 22 double mass curves are available in Appendix B.

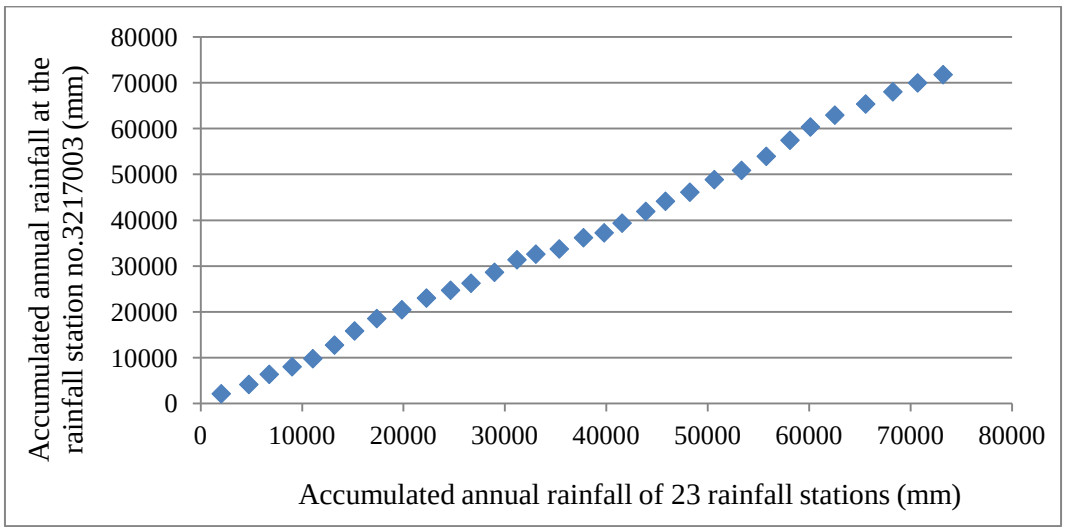


Figure 20 Double Mass Curve at station 3217003

Raingauge stations located in Klang watershed show that the data are consistence and homogenous and have the same trend of precipitation over the time series chosen for the study (Figures: 18 and 19). There is a homogeneous nature of the stations in Klang

watershed. The Figures reveal that all the stations in the study area have the same pattern of rainfall and indicate one distinct climatic. The maximum rainfall occurs between October to December and the minimum rainfall occurs between June to August and January to February.

### 3-2-4-2- Raingauge Network Analysis

The pattern of rainfall in Klang watershed is different in spatial and temporal scales. The daily precipitation data from 23 stations are used in the study area. To study the spatial network analysis of rainfall, two methods by GIS have been used including: Spatial Homogeneity and Spatial Raingauge Network Analysis.

#### 3-2-4-2-1- Spatial Homogeneity

Testing data for regional homogeneity is important particularly in frequency analysis (Dinpashoh, 2004). Spatial rainfall homogeneity was conducted to estimate correlation with respect to distance between adjacent stations (e.g. Aksara and Kenji, 2012; Yusof and Kane, 2013). A Geostatistical function was used by GIS to analyze the spatial variability of rainfall at all the available stations in the study area. It makes a correlation between each pairs of stations that provides a quantitative measure of the rainfall variability according to the distance among the raingauges. Then, it produces a surface map which is interpolated on the base of distance and correlation of raingauge stations. The correlation values range from -1 to +1. A value of -1 implies a perfectly negative correlation and a value of +1 implies a perfectly positive correlation whereas a value of 0 reflects no relationship between two variables.

The Semivariogram/Covariance was employed to show the empirical semivariogram for all pairs of raingauge stations to examine spatial correlation. The red dot in Figure 21 shows the difference squared plotted relative to the distance of a pair of raingauge station in Klang watershed. The spatial correlation between two stations and for time series “t” of rainfall is calculated by Semivariogram function (Journel and Huijbregts, 1978).

$$\gamma^{h,\alpha} = \frac{1}{2n(h,\alpha)} \sum_{i=1}^{N(h)} \left\{ Z_{x_i} - z_{(x_i+h)} \right\}^2 \qquad \text{Equation 24}$$

Where, $\gamma^{h,\alpha}$ is a semivariance as a function of both the magnitude of the lag distance or separation vector h and its direction α; N(h) is the number of observation pairs separated by h used in each summation; $Z_{x_i}$ is the random variable at location, $x_i$.

In Klang watershed the correlation value of all 23 meteorological stations considering pairs correlation reveals the resemblance of the observed values at the station. Spatial correlation in Figure 21 shows a constant straight line correlation. The correlation value as zero is not being affected with respect to distance between stations. It indicates that the spatial variability of rainfall is not distance dependence in Klang watershed.

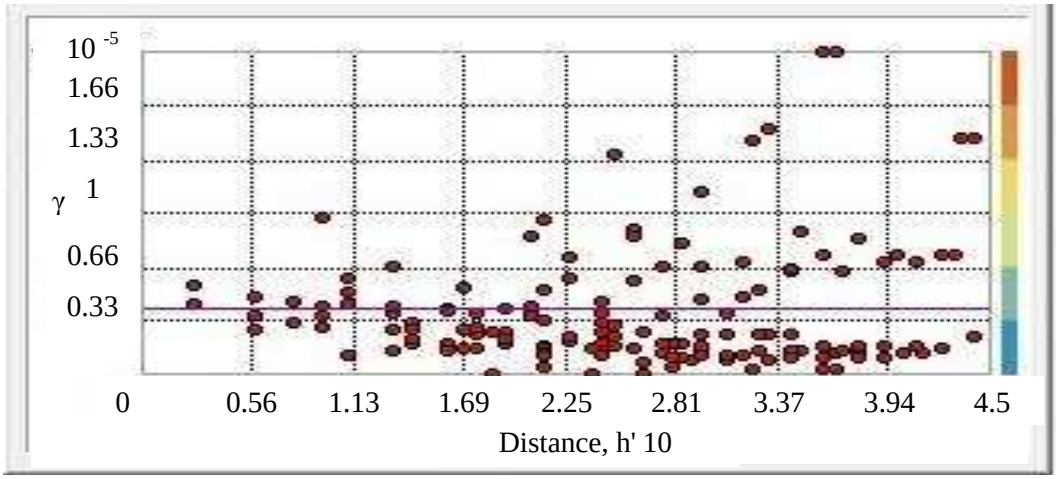


Figure 21 Spatial Correlation of the rainfall data for 23 Meteorological stations with respect to inter-station distance.

### 3-2-4-2-2- Spatial Raingauge Network Analysis

The total number of raingauge stations in Malaysia is 1038 by an average density of 310 km² of stations but the raingauges in the city of Kuala Lumpur is dense, 24 km² per raingauge (Desa and Niemczynowicz, 1996). According to the past report, the total cost for flood mitigation projects in Kuala Lumpur in ten years is about Rm 466 million which is equal to an average cost of raingauge, (13 raingauges) Rm 36 million.

A missing data leads to inappropriate estimation of the hydrological modelling which will result in the misjudgement of study. Thus, obtaining the high quality rainfall data is crucial to make an accurate spatial and temporal analysis particularly over a long time series.

The estimation of the spatial rainfall distribution depends on an optimal network of raingauge stations. The usage of Geostatistical functions in GIS helps the estimation of optimal distribution of the network. Raingauge network was estimated based on the proximity and the homogeneity of the rainfall distribution. The World Meteorological Organization (1986) guidelines for determining the minimum densities of precipitation networks has suggested the ideal densities of precipitation networks which is 1 station per 600–900 km² for flat, per 100–250 km² for mountainous regions. In this research, 23 raingauges in the study area is much more than the gauge density suggested by Army Corps of Engineers (USACE) in 1996 as following Equation:

$$n = 2.5\ (A)^{0.33} \qquad \text{Equation 25}$$

Where, n is the number of raingauge and A is the area of the watershed in terms of $Km^2$.

However, Vieux (2004) has recommended the raingauge density which can be exceed one gauge per 10 to 20 km². The main reason for selection of 23 raingauge stations is, based on the spatial distribution covering the watershed under study and minimising the gap in the observed data.

Figure 22 shows the proximity maps over the study area. Proximity function in GIS creates polygon of rainfall point stations which divide the space and allocate it to the nearest raingauge station. Another spatial network analysis of the raingauge network was conducted by the distance function which generates a map containing the measured distance from every cell to the nearest raingauge station based on the Euclidean distance. Figure 23 shows the distance map of raingauge stations used in this study in terms of metre.

### 3-2-4-3- Flow/Discharge Data Screening

Hydro meteorological data is one of the most important data in water resources studies. Thus it is required to estimate the quality of the data before using it for the hydrological system simulation. Figure 24 (A, B and C) illustrates visual scan of the monthly time series for three streamflow stations in Klang watershed to show the gap, detect the gross errors and missed recordings.

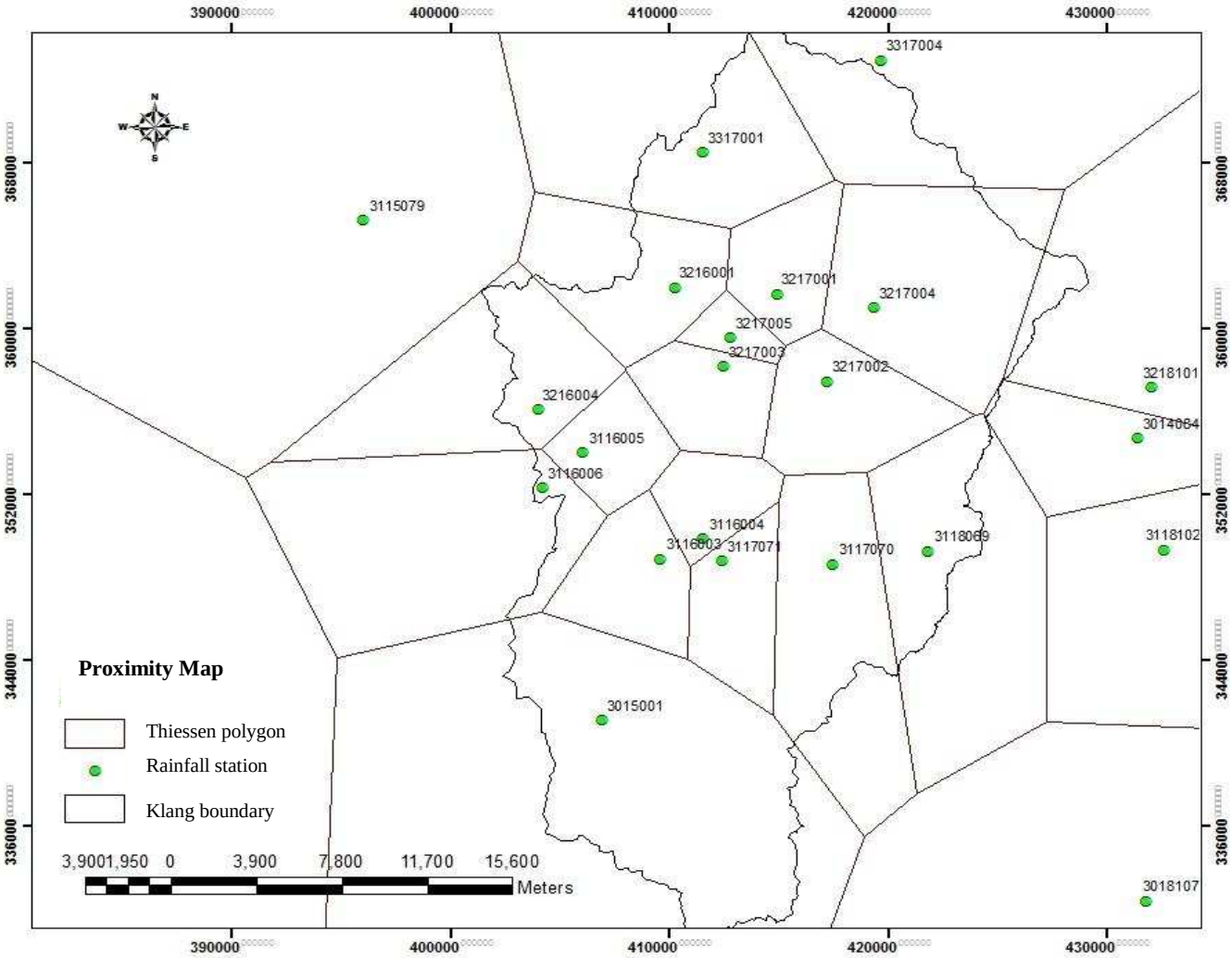


Figure 22 Proximity map of raingauge stations in Klang watershed

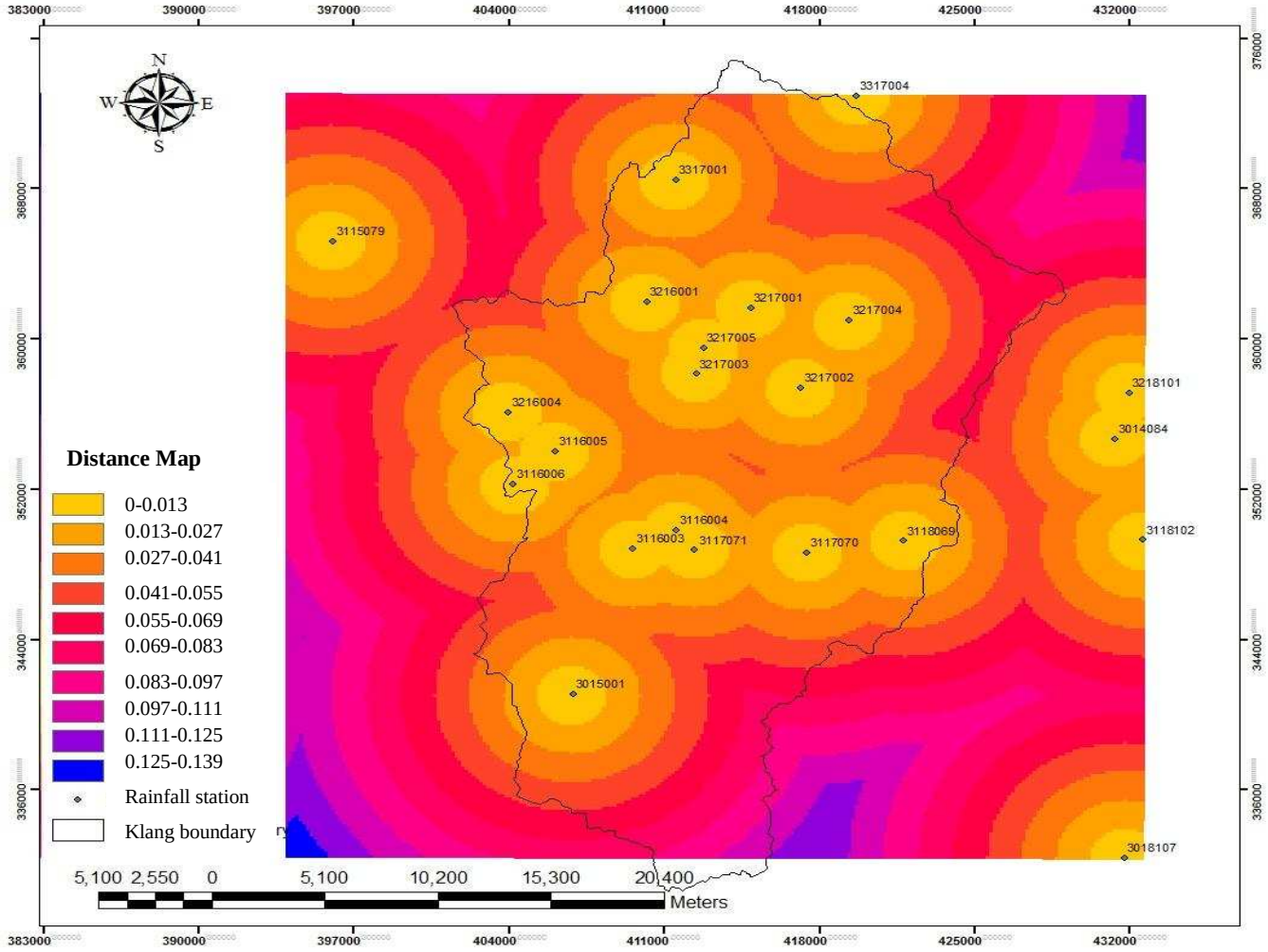


Figure 23 Distance map of raingauge stations in Klang watershed

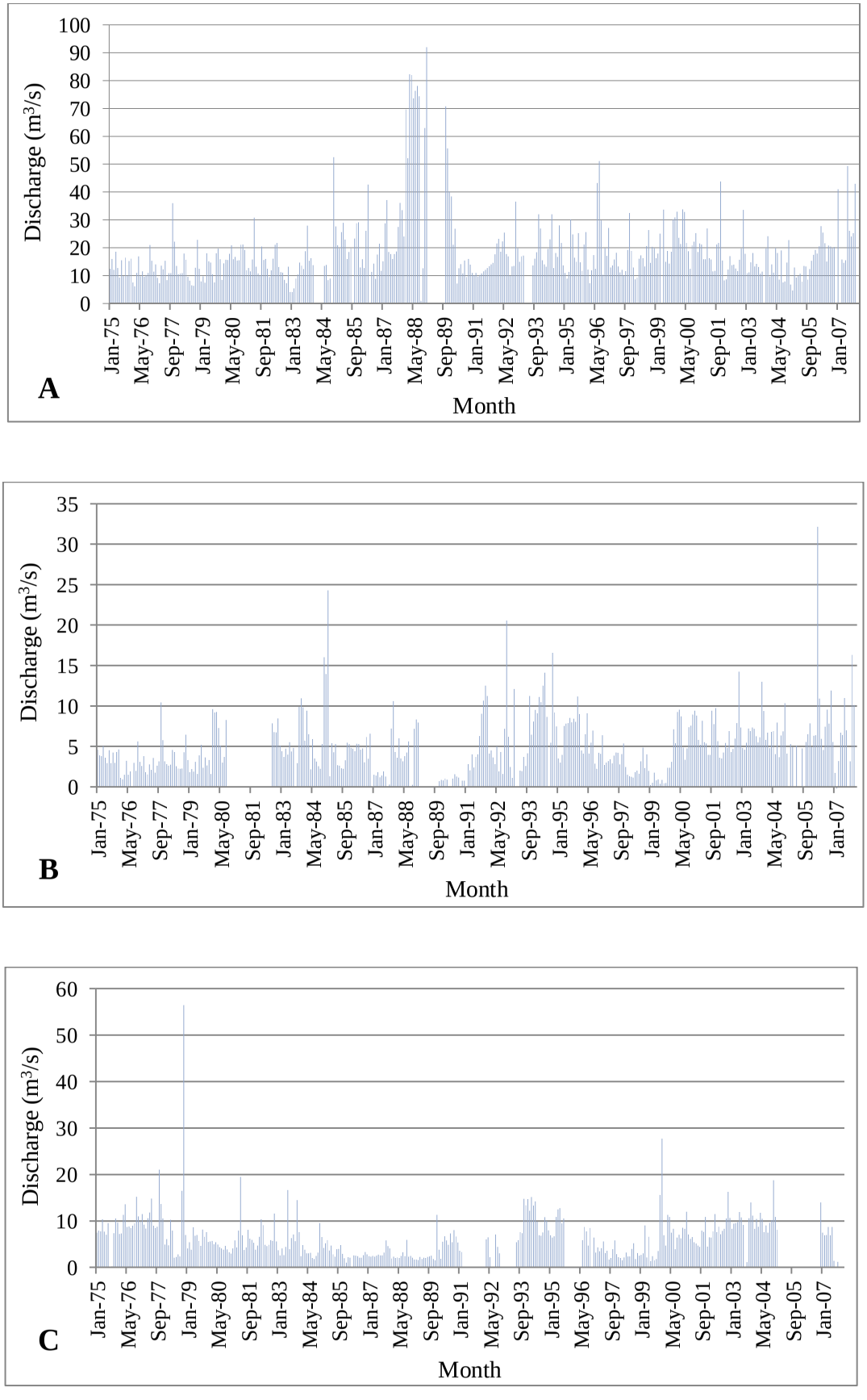


Figure 24 Observed streamflow from three streamflow stations, Jambatan Sulaiman **(A)**, Jln. Tun Razak **(B)** and Batu Sentul **(C)** in Klang watershed.

### 3-2-4-4- Filling Missing Data

There are various methods such as Arithmetic Mean method and Normal Ratio method (Chow et al., 1988) to fill in the missing data. Homogeneity analysis and double mass curve techniques are used to fill the gap of monthly and yearly rainfall data.

#### 3-2-4-4-1- Filling Rainfall Data

Linear interpolation regression was used to fill up the gaps of long series daily rainfall data. The method is applied due to a large number of daily data of the multiple raingauge stations. To run the regression, the correlations among the daily rainfall data are ranked and then the missing data is estimated using a linear regression with the station that has the highest correlation through the common period. The linear regression is expressed by the following formula (Helsel and Hirsch, 2010):

$$P_X = b_0 + b_1 p_1 + b_2 p_2 + \ldots + b_n p_n \qquad \text{Equation 26}$$

Where, $P_X$ is the missing precipitation value for station x, $P_1$, $P_2$, … $P_n$ are precipitation values at the neighbouring stations for the current period, $b_0$,… $b_n$ are coefficients calculated by least-squares methods and n is the number of nearby gauges.

The correlation coefficient of ten raingauge stations used for the climate change downscaling in SDSM was determined to fill the gaps of daily rainfall data in the study area which have the high correlation with the other neighbouring stations. Ten raingauge stations were selected based on the high quality, with no gap in daily time series and spatially distributed in the study area covering the whole watershed. Table 8 illustrates the correlation coefficient among the raingauge stations used for downscaling purpose. The higher correlation between a raingauge station and corresponding stations are used to fill up gaps between them. Appendix C illustrates the correlation coefficient between the raingauge stations.

Table 8 The Correlation coefficient of ten raingauge stations with daily rainfall series for the period years according to Table (13)

| Station no. | 3216001 | 3217001 | 3317004 | 3217002 | 3217003 | 3217004 | 3116005 | 3116006 | 3117070 | 3118069 |
|---|---|---|---|---|---|---|---|---|---|---|
| **3216001** | 1.000 | 0.365 | 0.053 | 0.235 | 0.280 | 0.231 | 0.122 | 0.000 | 0.050 | 0.025 |
| **3217001** | **0.365** | 1.000 | **0.055** | **0.402** | 0.368 | 0.320 | 0.097 | 0.000 | 0.056 | 0.026 |
| **3317004** | 0.053 | 0.055 | 1.000 | 0.051 | 0.042 | 0.020 | 0.023 | 0.000 | 0.022 | 0.010 |
| **3217002** | 0.235 | **0.402** | 0.051 | 1.000 | 0.389 | 0.289 | 0.100 | 0.000 | 0.075 | 0.044 |
| **3217003** | 0.280 | 0.368 | 0.042 | 0.389 | 1.000 | **0.412** | **0.135** | 0.000 | 0.074 | 0.031 |
| **3217004** | 0.231 | 0.320 | 0.020 | 0.289 | **0.412** | 1.000 | 0.101 | **0.001** | 0.041 | 0.026 |
| **3116005** | 0.122 | 0.097 | 0.023 | 0.100 | 0.135 | 0.101 | 1.000 | **0.001** | 0.039 | 0.008 |
| **3116006** | 0.000 | 0.000 | 0.000 | 0.000 | 0.000 | 0.001 | 0.001 | 1.000 | 0.000 | 0.001 |
| **3117070** | 0.050 | 0.056 | 0.022 | 0.075 | 0.074 | 0.041 | 0.039 | 0.000 | 1.000 | **0.134** |
| **3118069** | 0.025 | 0.026 | 0.010 | 0.044 | 0.031 | 0.026 | 0.008 | **0.001** | **0.134** | 1.000 |

### 3-2-4-4-2- Filling Discharge Data

The outliers in the daily discharge data have been removed to determine the accurate correlation between the discharge stations. Result shows that there is no high correlation between Sulaiman streamflow station to other stations in developing the Regression Equation. Therefore, there is no reliable source to fill up the gaps of streamflow data at Sulaiman streamflow station. The figures are available in Appendix D.

### 3-3- Climate Base Analysis

Climate pattern is specified spatially and temporally by mean monthly, mean annual, Probable Maximum Precipitation (PMP) and Frequency Analysis techniques for rainfall data of the watershed.

### 3-3-1- Temperature Trend

In the study area, mean annual temperatures vary between 26 $^{o}$C and 28.6 $^{o}$C, maximum temperatures vary between 30.9 $^{o}$C and 33.8 $^{o}$C and minimum temperature range from 22.3 $^{o}$C to 24.8 $^{o}$C. The estimation over a long term period (1961-2011) at the Subang temperature station, located as the nearest temperature station to Klang watershed indicates a general trend of an increase in temperature over the last 40 years. Figure 25 illustrates the absolute values of annual average, maximum and minimum temperatures. Figures (26: A, B and C) show the year to year variation of annual average, maximum and minimum temperatures in terms of normalised temperature anomalies averaged over 1961 to 2011.

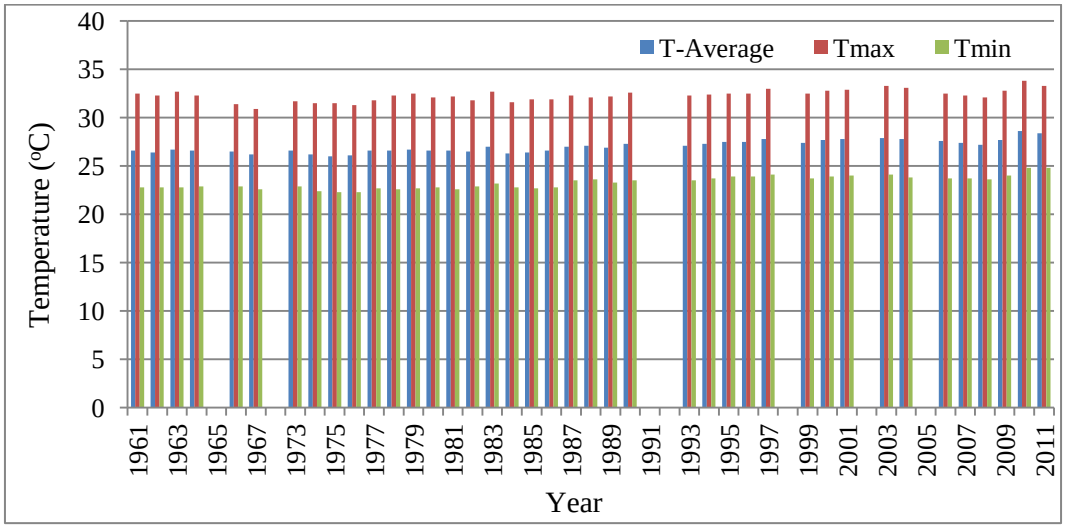


Figure 25 Absolute Maximum, Mean and Minimum temperature values of Subang temperature Station

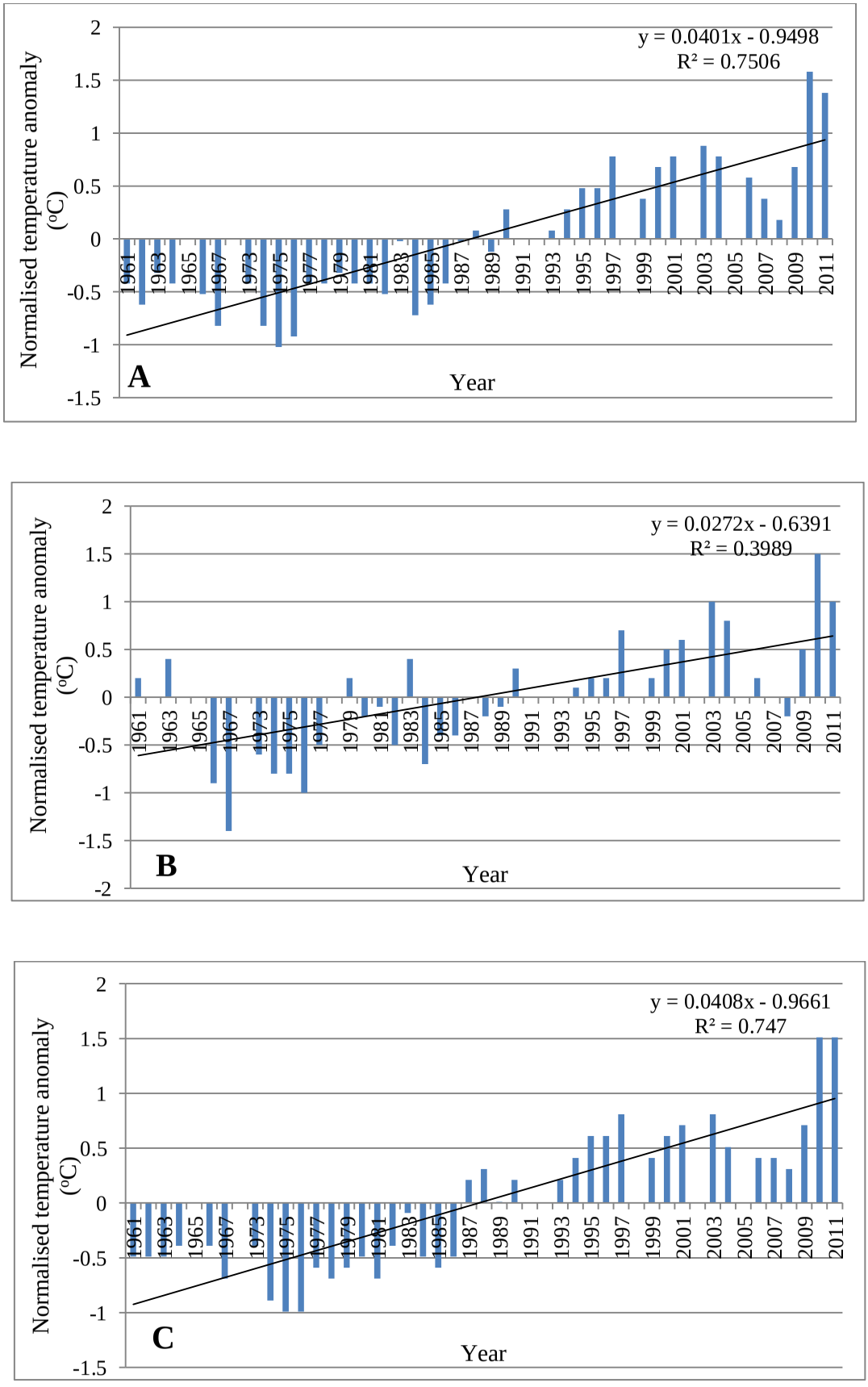


Figure 26 Annual variability of temperature over Klang watershed (**A:** Average temperature, **B:** Maximum Temperature and **C:** Minimum temperature)

### 3-3-2- Rainfall Trend

The region experiences heavy precipitation due to the location at equatorial zone particularly during the Northeast monsoon which is from November to March and Southwest monsoon which from late May to September (Sayang et al., 2010). Obviously, climate of the study area is warm with a high percentage of humidity throughout the year. The most significant heavy precipitation has been observed during the months of October, November and December (Chen et al., 2013; Ahmad et al., 2012).

In the study area, duration of the rainfall events is short which occurs only in a small part of region whose average annual rainfall is about 2300 mm. To investigate the variations of mean monthly rainfall distributions, four raingauge stations (3317004, 3116004, 3117070 and 3015001) are considered as representatives of the watershed. In all the stations the maximum rainfall is observed in November during the north eastern monsoon season. Figure 27 (A,B,C and D) show the maximum average monthly rainfall of the watershed at the raingauge stations 3317004, 3116004, 3117070 and 3015001 are 324.3, 272.9, 253.5 and 298.7 mm in November, respectively. The values indicate the high proportion of North-East monsoon precipitation in Klang watershed which is 83, 77.8, 79.3 and 71.5 percent, respectively. Mean monthly rainfall for other raingauge stations can be seen in Appendix E.

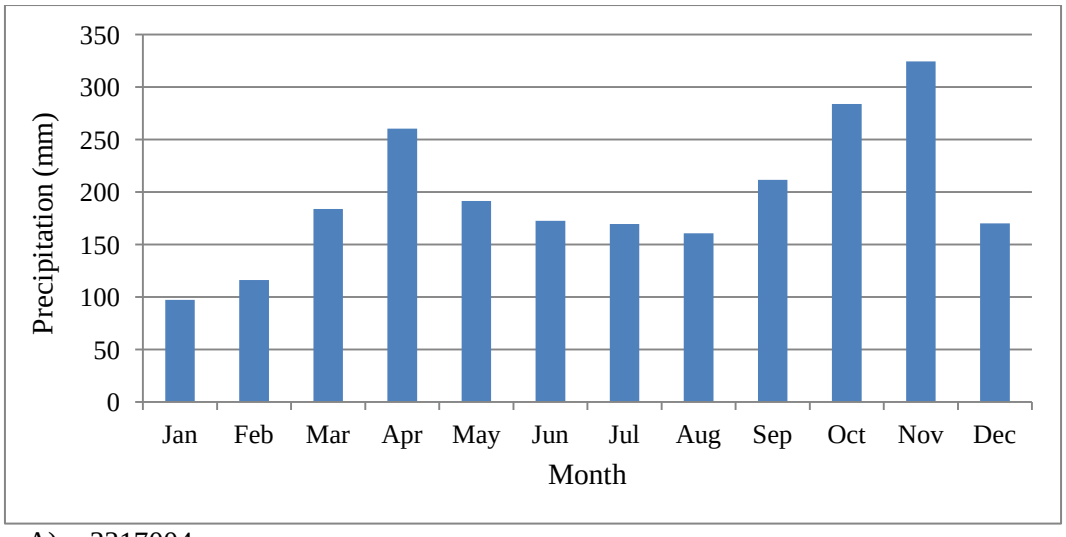


A) 3317004

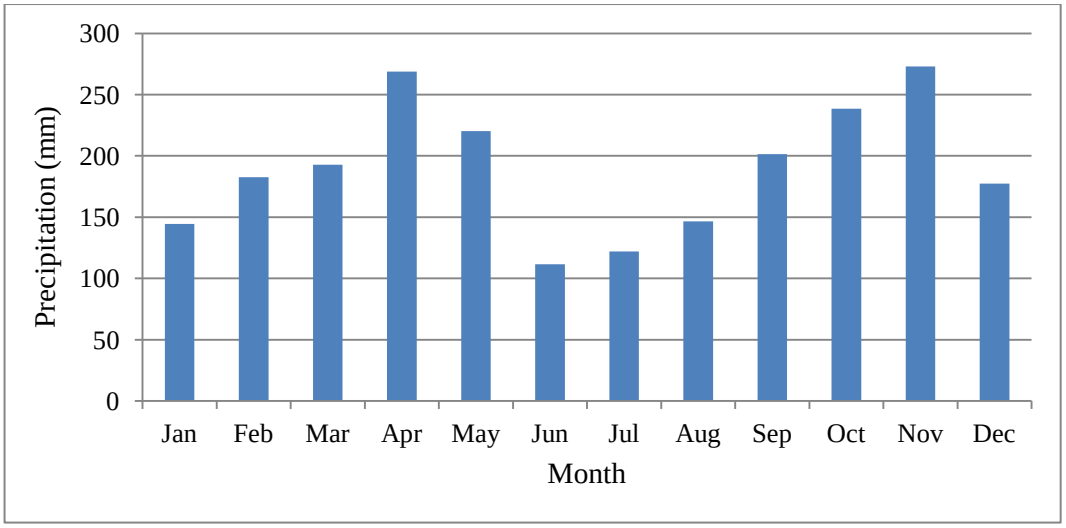


B) 3116004

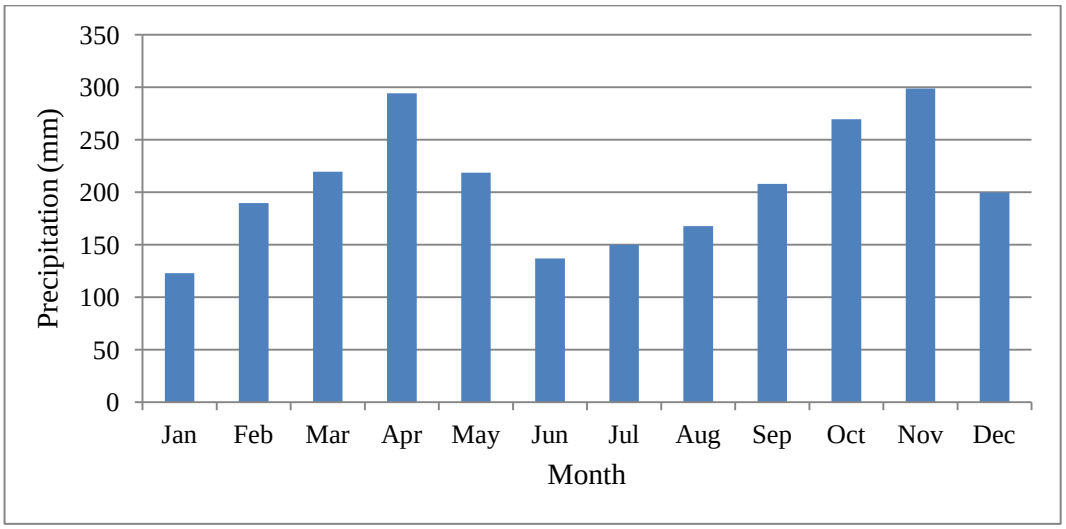


C) 3117070

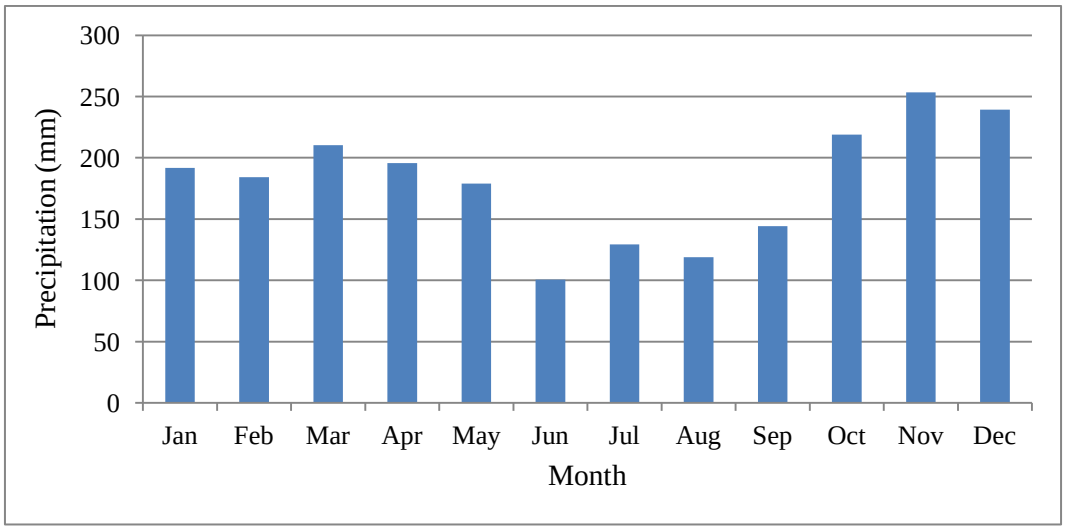


D) 3015001

Figure 27 Mean monthly rainfall from four raingauge stations in Klang watershed.

### 3-3-3- Spatial Annual Mean Rainfall

The simplest method to make the spatial mean of data was provided by Thiessen (1911). But it does not reflect all the physical aspects particularly topography data as it amounts at drawing around each gauge, a polygon of influence with the boundaries at a distance of halfway between gauge pairs.

The Isohyetal method (McCuen, 1998) is used to estimate the non-sample location by interpolation within the isohyets. However, the main limitation of isohyetal is an extensive gauge network is required to draw isohyets accurately. Kriging is the most famous Geostatistical method used in ArcGIS to produce the spatial map from the certain points. However, there are known limitations with Kriging, especially its numerical instability for large samples and/or dimensions (Cressie and Johannesson, 2008).

To estimate rainfall trend over Klang watershed it was attempted to establish a spatial rainfall analysis over 23 selected raingauge stations using GIS system. Mean annual rainfall is about 2400 mm and mean monthly rainfall ranges from 200 to 400 mm (Tick and Samah, 2004).

Inverse Distance weighting (IDW), developed by U.S. National Weather Service in 1972, is based on the distance weighting. Many studies have used this method for a long range of precipitation data (Segond et al., 2007; Lu and Wong, 2008; Wu et al., 2010). Hsieh et al., (2006) studied spatial interpolation of daily rainfall record from 20 raingauges in 11 year period. They found out that IDW has a good performance for interpolation of rainfall in Shih-Men watershed in Taiwan.

In this study, the interpolation processes employed the IDW method to estimate spatial mean precipitation as the available data of distributed raingauges in Klang watershed and also with long time series. The amount of rainfall at the non-sampling location is then estimated by interpolation with IDW. The IDW formula defined by Morrison (1971) is given below:

$$R_p = \sum_{i=1}^{n} \left( \frac{d_i^{-\alpha}}{\sum_{i=1}^{n} d_i^{-\alpha}} \right) R_i \qquad \text{Equation 27}$$

Where, $R_p$ is the unknown rainfall data (mm), $R_i$ is the rainfall value at the known location (mm), $d_i$ is the distance from each raingauge station to unknown site, n is the number of raingauge station and $\alpha$ is the coefficient, which is assumed equal to 2 (Lin and Yu, 2008).

The watershed has an average annual rainfall of 2282 mm, the largest portion of the rainfall occurs in October, November and December. As it is observed from Figure 28, the spatial variability of rainfall in the watershed indicates that the mean annual rainfall is high on the central area of the scope at the centre and West where two of the main rivers, Klang and Batu river are connected near to the coastal line.

### 3-3-4- Probable Maximum Precipitation (PMP)

PMP is defined as the greatest depth of precipitation for a given duration that is physically or meteorologically possible over a given station or area at a particular geographical location at a certain time of the year (WMO, 1986). PMP is calculated at a point site and for preparing a spatial map of PMP which needs to be interpolated by GIS to a surface map for the whole watershed. Obviously, using long time period of data gives an accurate value of PMP for each raingauge.

In this study, the Harshfield method (WMO, 1986) is used to calculate the probable maximum precipitation because of statistical approach which uses annual maximum rainfall series in the study area. The Harshfield Equation is given as:

$$PMP = X_n + K\delta \qquad \text{Equation 28}$$

PMP is Probable maximum precipitation, $X_n$ is mean of the series of annual maximum daily rainfall, K is frequency factor, $\delta$ is Standard deviation of the series of annual maximum daily rainfall.

Hydrologic frequency factor, K, is a location dependant and it is a primarily function of the recurrence interval for a particular probability distribution. Desa et al. (2001) have suggested frequency factor, k, equals to 8.7 employing the Harshfield method to analyse the frequency factor for the Peninsula Malaysia using annual daily maximum series rainfall.

Table 9 gives PMP values of 1, 3 and 7 day and Figures (from 29 to 31) show spatial PMP maps using annual daily maximum rainfall series in Klang watershed. The Figures reveal that the mountain parts particularly in east and north-east have the highest value of PMP and on the other hand the inland area of Klang watershed has the lowest values. It can be concluded that the trend of PMP in the watershed is dependent on the influence of northeast monsoon winds although the mountains can play an obstruction in the area.

Table 9 The Maximum precipitation and Probable Maximum Precipitation (PMP) for 23 raingauge stations in Klang watershed

| Id | Station no. | 1 Day Max(mm) | 3 Day Max(mm) | 7 Day Max(mm) | PMP 1 Day(mm) | PMP 3 Day(mm) | PMP 7 Day(mm) |
|---|---|---|---|---|---|---|---|
| 1 | 3014084 | 84.4 | 101.6 | 132.6 | 291.1 | 390.7 | 629.5 |
| 2 | 3014089 | 96.6 | 106.7 | 127.5 | 347.9 | 362.8 | 523.2 |
| 3 | 3015001 | 97.5 | 113.7 | 150.9 | 263.7 | 254.6 | 423.8 |
| 4 | 3018107 | 95.4 | 132.3 | 171.4 | 257.5 | 551.4 | 720.3 |
| 5 | 3115079 | 96.0 | 109.5 | 139.2 | 308.3 | 363.7 | 475.5 |
| 6 | 3116003 | 103.8 | 127.4 | 162.8 | 307.3 | 455.9 | 555.1 |
| 7 | 3116004 | 93.2 | 118.8 | 161.2 | 293.9 | 507.9 | 652.1 |
| 8 | 3116005 | 104.6 | 138.3 | 174.1 | 377.1 | 599.7 | 678.5 |
| 9 | 3116006 | 98.2 | 119.7 | 149.8 | 361.5 | 467.4 | 603.3 |
| 10 | 3117070 | 104.0 | 123.8 | 159.2 | 306.7 | 396.2 | 642.7 |
| 11 | 3117071 | 101.4 | 114.6 | 158.1 | 264.2 | 342.9 | 621.7 |
| 12 | 3118069 | 100.6 | 116.1 | 148.7 | 322.1 | 365.1 | 518.8 |
| 13 | 3118102 | 124.1 | 134.7 | 161.4 | 668.7 | 719.3 | 814.7 |
| 14 | 3216001 | 93.5 | 108.3 | 133.8 | 292.2 | 384.7 | 504.4 |
| 15 | 3216004 | 100.7 | 120.7 | 155.9 | 317.1 | 413.7 | 563.9 |
| 16 | 3217001 | 97.4 | 117.6 | 146.8 | 282.2 | 325.6 | 443.1 |
| 17 | 3217002 | 95.4 | 115.7 | 146.9 | 294.0 | 413.1 | 522.5 |
| 18 | 3217003 | 93.7 | 120.5 | 153.5 | 289.3 | 494.8 | 678.9 |
| 19 | 3217004 | 93.1 | 124.1 | 157.3 | 286.8 | 396.2 | 584.9 |
| 20 | 3217005 | 86.6 | 117.2 | 139.8 | 285.9 | 480.8 | 593.6 |
| 21 | 3218101 | 109.3 | 122.5 | 147.1 | 592.8 | 594.1 | 619.8 |
| 22 | 3317001 | 97.1 | 111.4 | 148.1 | 264.8 | 459.6 | 552.1 |
| 23 | 3317004 | 104.6 | 125.2 | 150.6 | 1231.4 | 1256.7 | 1296.3 |

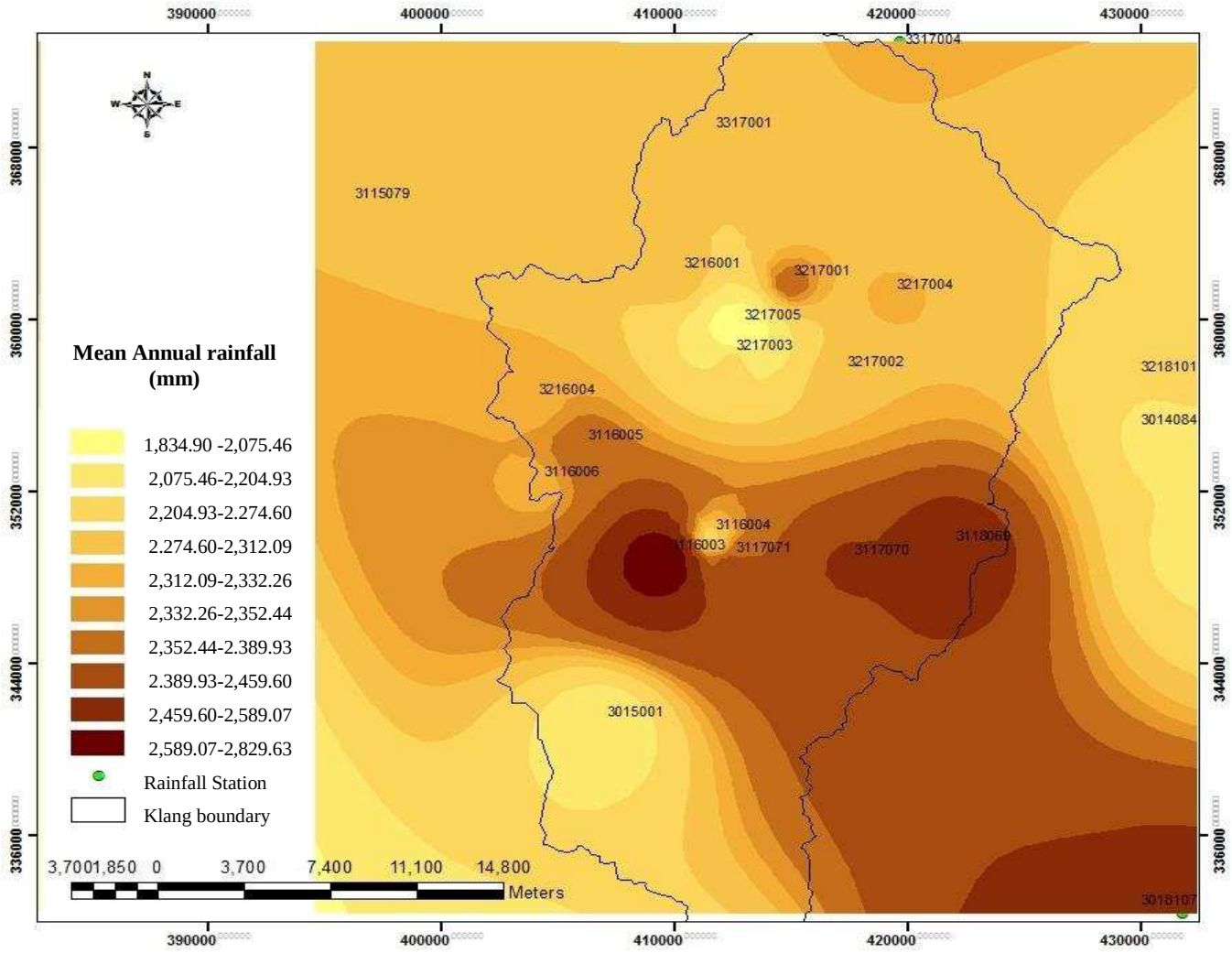


Figure 28 Mean annual rainfall distribution in Klang watershed

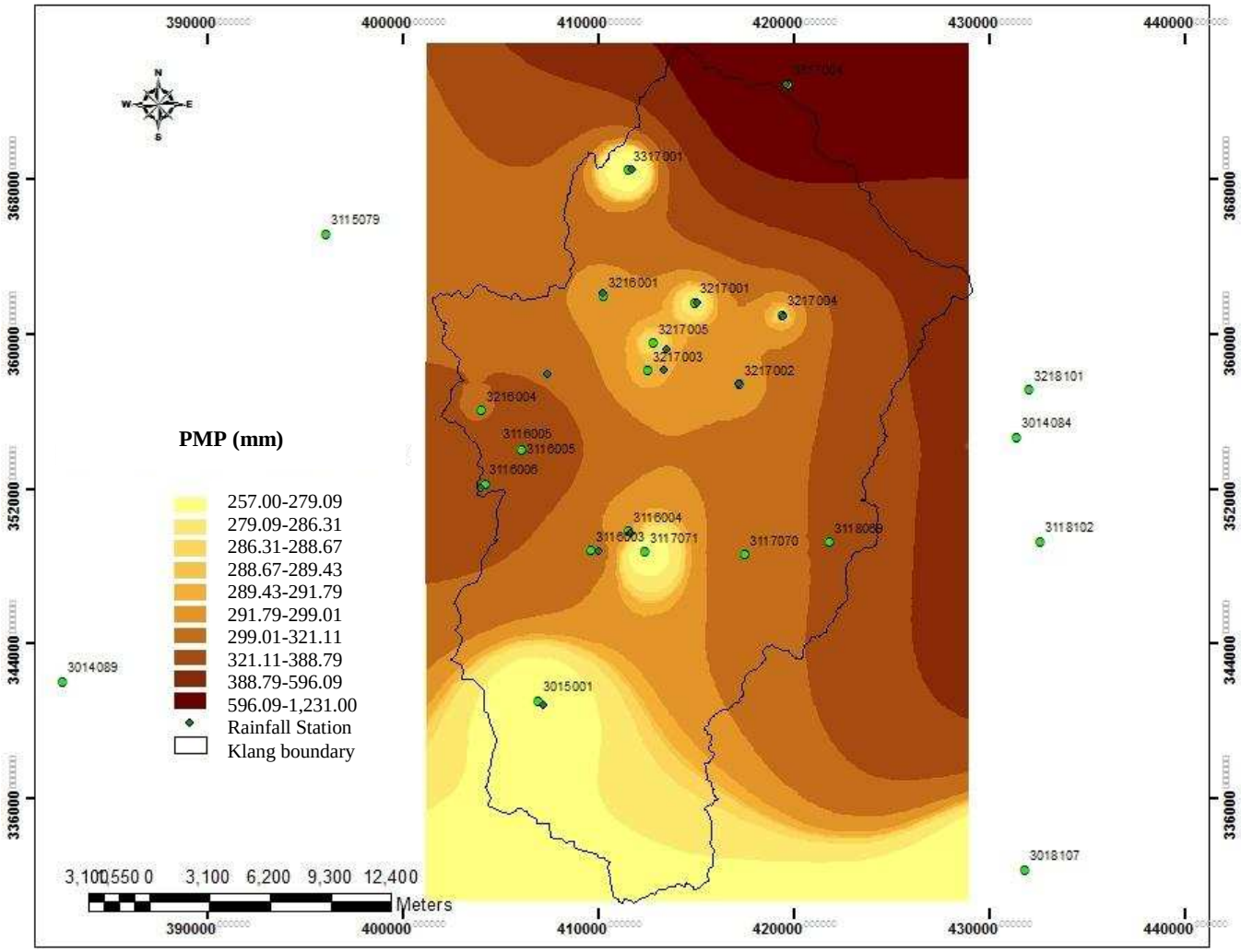


Figure 29 Probable Maximum Precipitation of one day rainfall

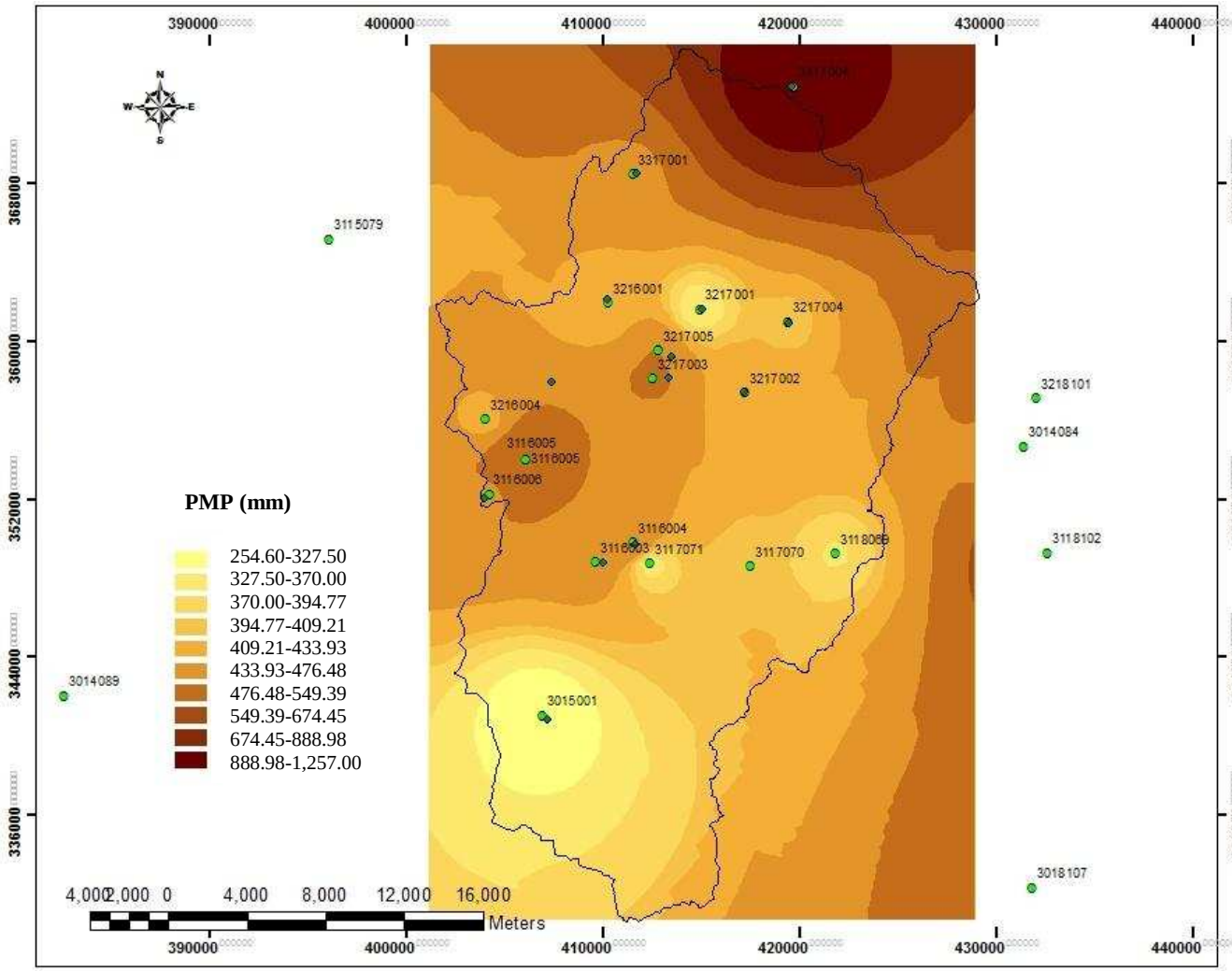


Figure 30 Probable Maximum Precipitation of three day rainfall

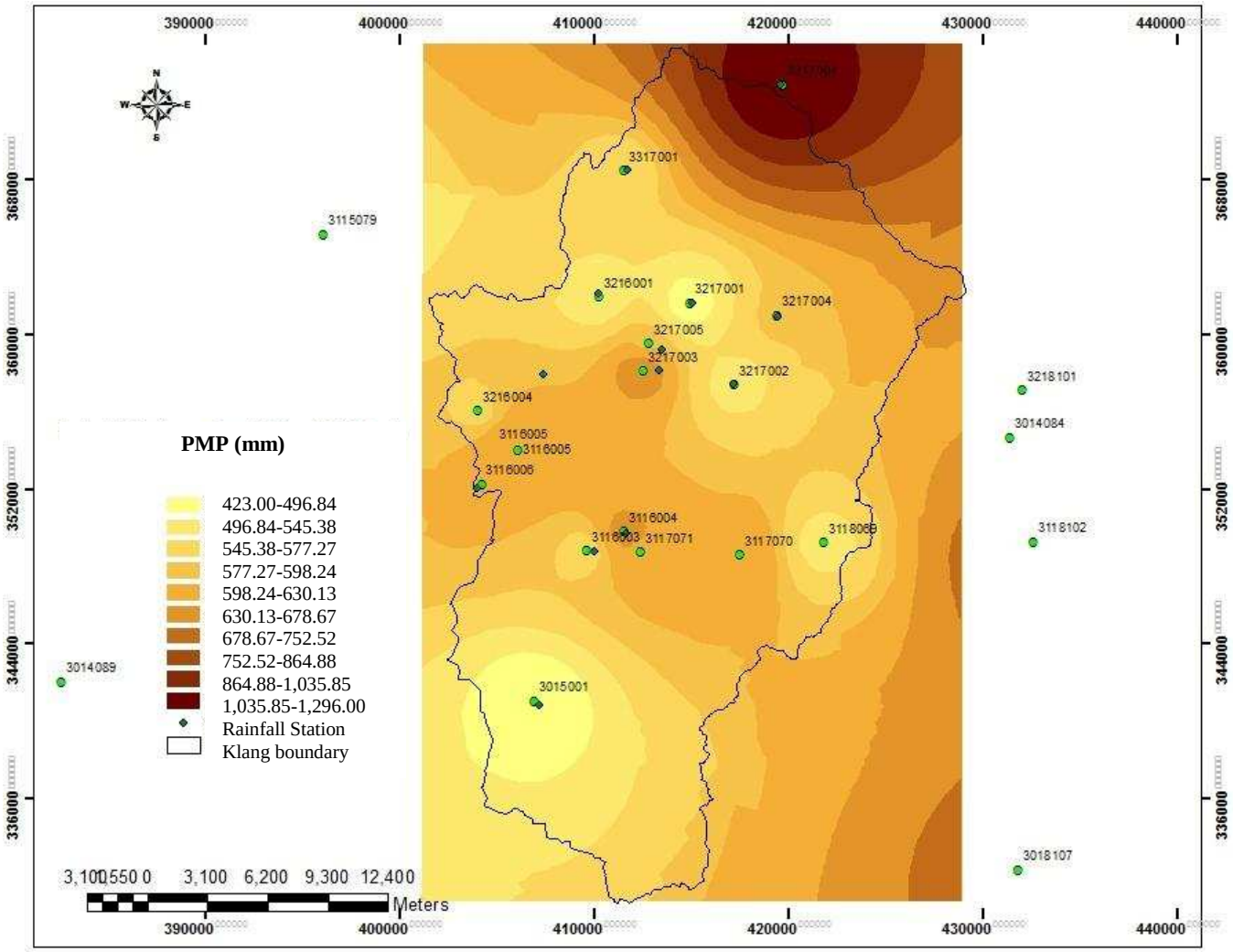


Figure 31 Probable Maximum Precipitation of seven day rainfall

### 3-3-5- Frequency Analysis

Frequency analysis is a technique of fitting a probability distribution to a series of observations to define the probabilities of future occurrences of some events of interest. In this study, the daily rainfall is used. The duration of rainfall is one, three, seven, ten and fifteen day for 5, 10, 25, 50 and 100 years of recurrence interval. Gumbel Extremal Type I as a distribution analysis was employed to estimate extreme precipitation intensity. The data are used to calculate intensities using SMADA software as shown in Table 10. Figures (from 32 to 35) show the maps of extreme precipitation intensity of 23 raingauge stations for one day duration rainfall for the years of recurrence interval. SMADA fits a Gumbel Type 1 distribution to the data using the annual maximum series (Helsel and Hirsch, 2010).

$$F(x)= 1-e^{-e^{-(x-\mu)/\sigma}} \qquad \text{Equation 29}$$

Where, x is the maximum daily rainfall, μ and σ are the mean and variance of maximum daily rainfall, respectively.

The annual maximum for a return period of T-years can be calculated from:

$$Q_T= \bar{Q}+ K(T)S_Q \qquad \text{Equation 30}$$

$$K(T)= -\sqrt{6}/\pi\ (\gamma+\text{Ln Ln}\left[\frac{T(x)}{T}\ (X)- 1\right]) \qquad \text{Equation 31}$$

Which, Q is the mean annual maximums, $S_Q$ is the standard deviation of the maximums, $K(T)$ is a frequency factor, $T_{(X)}$ is the return period in years, and $\gamma$ is a constant equal to 0.5772.

Table 10 Extreme precipitation intensities of 23 raingauge stations for 5, 10, 25, 50 and 100 years of recurrence interval using Gumbel Extremal Type I

| Id | Station no. | Extreme Precipitation Intensities (mm/day) | | | | |
|---|---|---|---|---|---|---|
| | | 5 year | 10 year | 25 year | 50 year | 100 year |
| 1 | 3014084 | 102.7 | 118.8 | 139.2 | 154.4 | 169.4 |
| 2 | 3014089 | 118.5 | 137.9 | 162.3 | 180.4 | 198.4 |
| 3 | 3015001 | 112.1 | 125.3 | 141.4 | 153.6 | 165.6 |
| 4 | 3018107 | 109.4 | 120.4 | 134.2 | 144.5 | 154.6 |
| 5 | 3115079 | 115.2 | 134.5 | 158.9 | 177.8 | 194.9 |
| 6 | 3116003 | 125.1 | 143.5 | 166.6 | 183.8 | 200.8 |
| 7 | 3116004 | 113.4 | 129.0 | 148.6 | 163.1 | 177.6 |
| 8 | 3116005 | 130.3 | 150.2 | 175.4 | 194.3 | 212.6 |
| 9 | 3116006 | 121.8 | 142.8 | 169.5 | 189.2 | 208.8 |
| 10 | 3117070 | 121.5 | 135.3 | 152.6 | 165.5 | 178.3 |
| 11 | 3117071 | 119.5 | 133.3 | 150.7 | 163.7 | 176.5 |
| 12 | 3118069 | 12.3 | 143.3 | 178.1 | 203.8 | 229.5 |
| 13 | 3118102 | 170.1 | 209.4 | 258.1 | 294.6 | 330.8 |
| 14 | 3216001 | 110.7 | 124.2 | 141.2 | 153.8 | 166.3 |
| 15 | 3216004 | 121.6 | 137.8 | 158.1 | 173.3 | 188.3 |
| 16 | 3217001 | 113.2 | 125.8 | 141.7 | 153.5 | 165.3 |
| 17 | 3217002 | 112.9 | 126.6 | 143.9 | 156.7 | 169.4 |
| 18 | 3217003 | 111.1 | 124.4 | 141.4 | 154.1 | 166.6 |
| 19 | 3217004 | 112.4 | 132.7 | 158.3 | 177.4 | 196.3 |
| 20 | 3217005 | 108.2 | 128.3 | 153.7 | 172.5 | 191.2 |
| 21 | 3218101 | 291.1 | 183.3 | 227.8 | 260.8 | 293.6 |
| 22 | 3317001 | 113.3 | 125.8 | 141.6 | 153.3 | 165.2 |
| 23 | 3317004 | 204.2 | 281.6 | 379.6 | 452.3 | 524.5 |
| **Average** | | **124.8** | **144.1** | **170.5** | **190.2** | **209.7** |

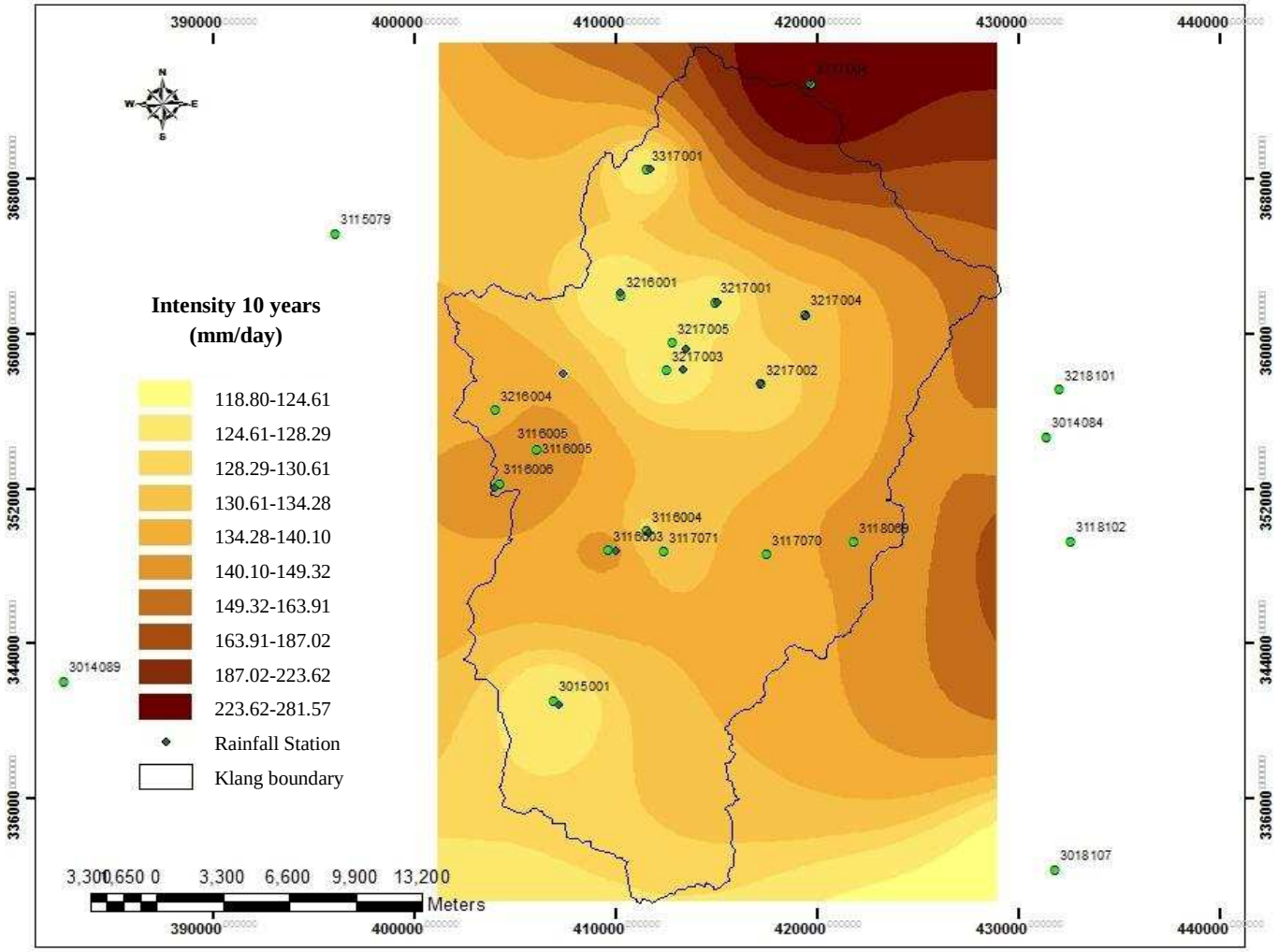


Figure 32 Extreme Precipitation Intensity of 23 raingauge stations for one day duration rainfall in Klang watershed, for 10 years of recurrence interval.

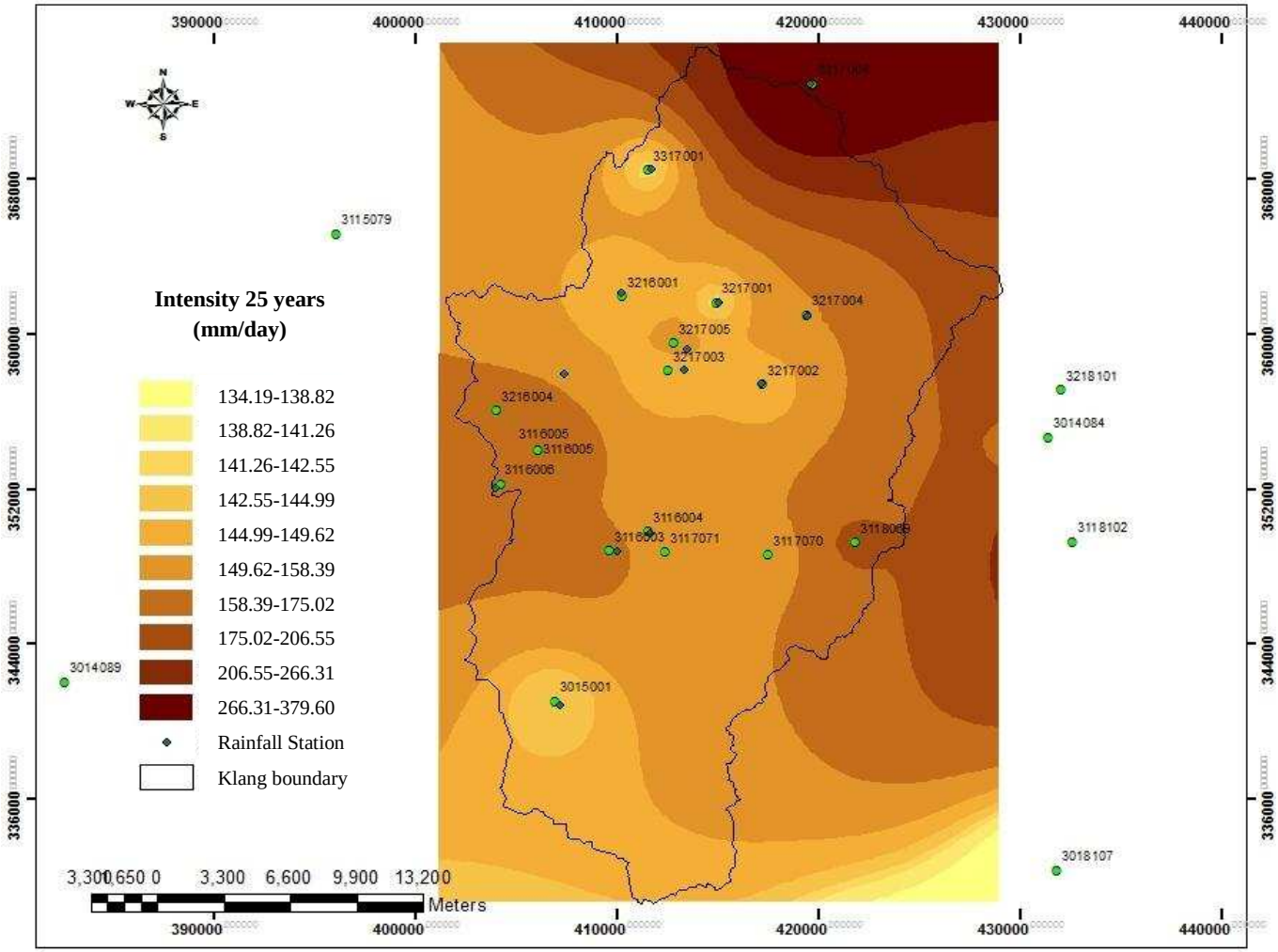


Figure 33 Extreme Precipitation Intensity of 23 raingauge stations for one day duration rainfall in Klang watershed, for 25 years of recurrence interval.

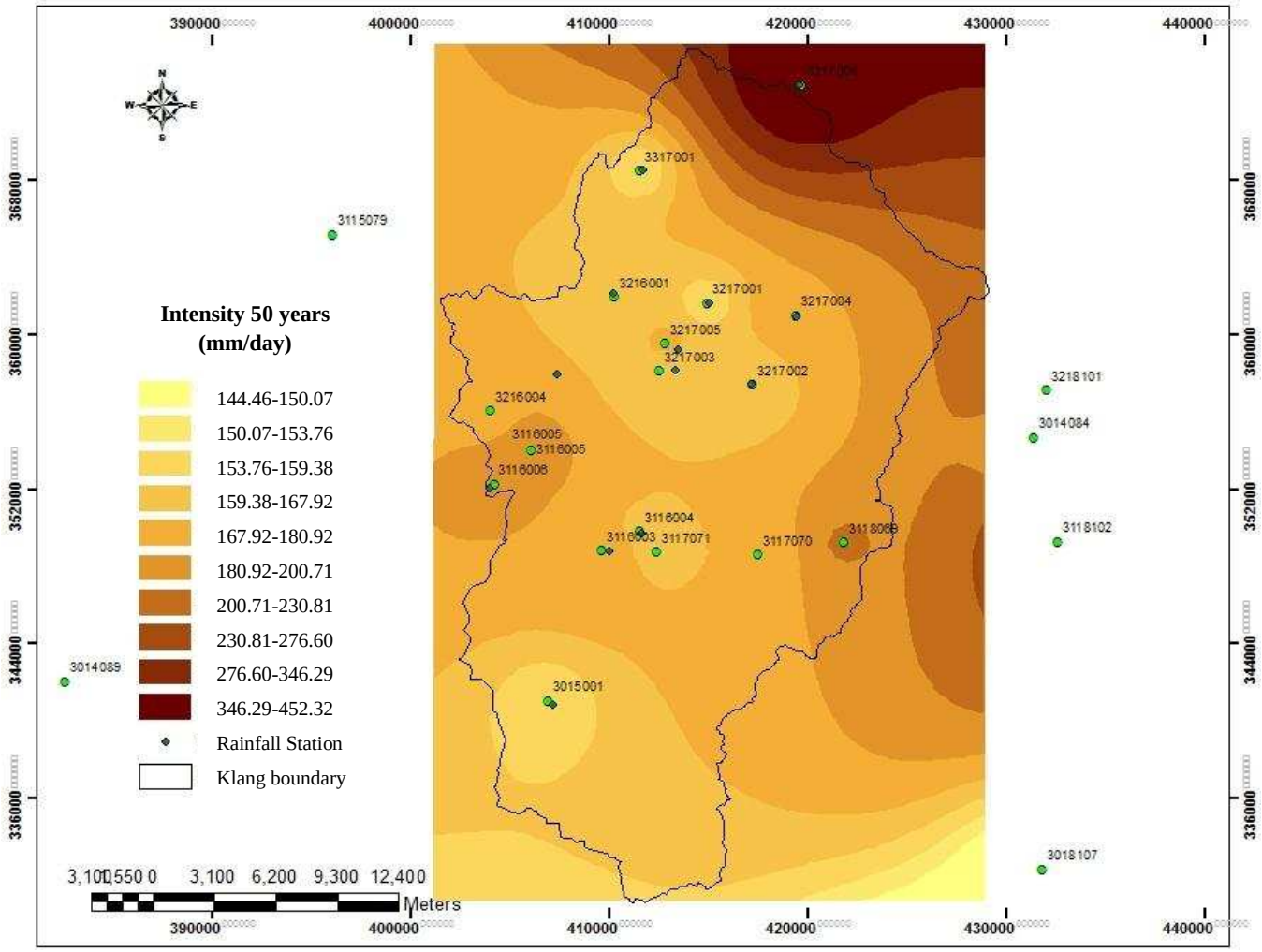


Figure 34 Extreme Precipitation Intensity of 23 raingauge stations for one day duration rainfall in Klang watershed, for 50 years of recurrence interval.

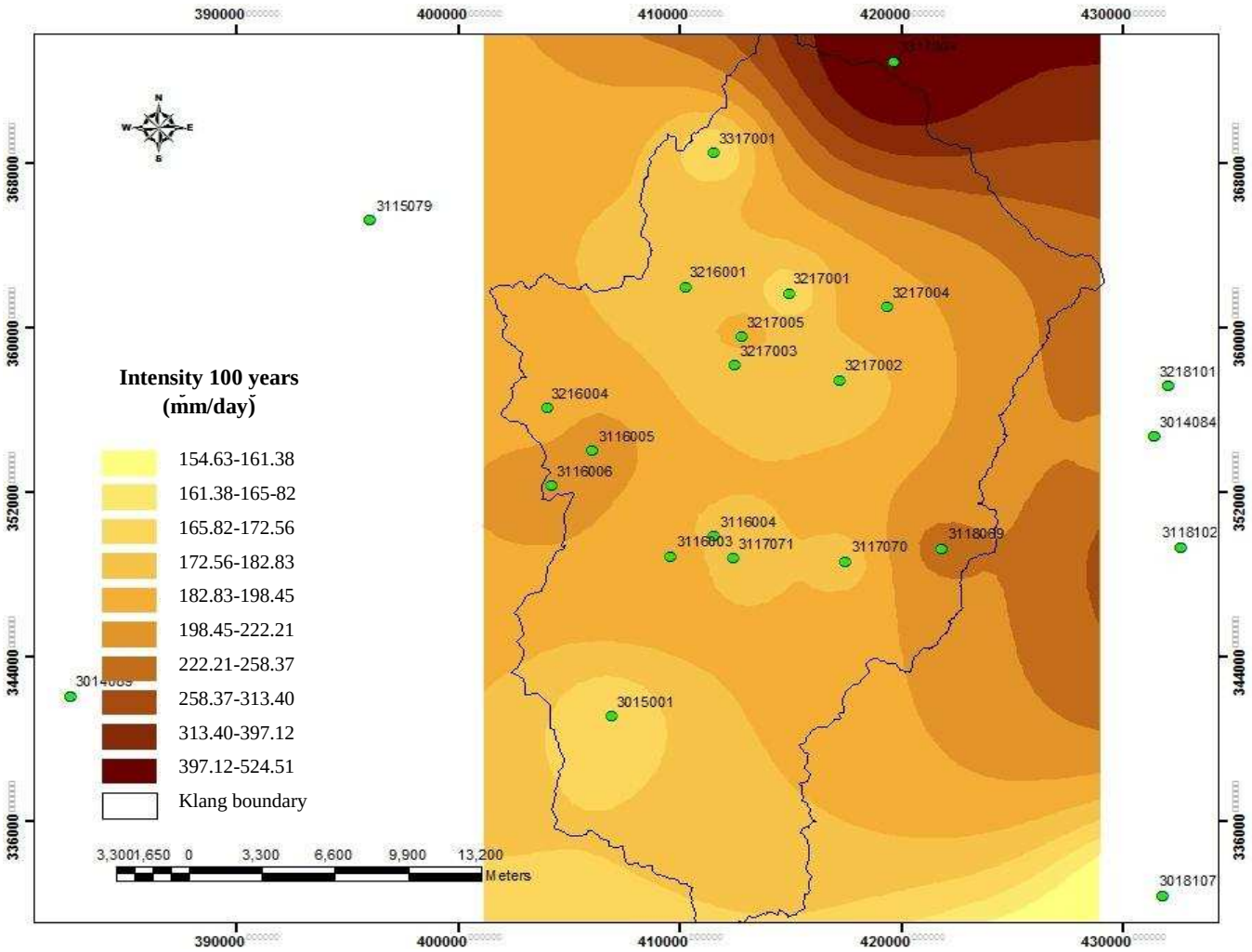


Figure 35 Extreme Precipitation Intensity of 23 raingauge stations for one day duration rainfall in Klang watershed, for 100 years of recurrence interval.

## 3-4- River Discharge Analysis

River discharge is the volume of water moving across a vertical section of water flow in a time unit. It is usually measured in cubic metre per second for rivers. There are parameters such as topography, landuse and soil affect the behaviour of the streamflow by altering the rainfall-runoff relationship. For example, changing landuse toward increasing area of impervious surfaces would increase peak discharges by not allowing the water to infiltrate into the ground.

In this study, daily river discharge data over 33 years (1975-2007) are used to analysis the monthly and annual variation of the streamflow. It reveals the historic pattern of streamflow and the frequency of extreme flow events occurrence to show the expected trend of future streamflow and also yearly flow duration relations.

The trend analysis of the discharge at Sulaiman streamflow station in Klang River can help reveal the streamflow behaviour. Since Sulaiman streamflow station is situated along the main Klang river at the outlet of Upper Klang watershed, the hydrological modelling uses this discharge station for calibration and validation of modelled runoff.

### 3-4-1- Mean Monthly River Discharge

Figure 36 is the plot of the mean monthly discharge of the river for the period of 1975 to 2007 at the Jambatan Sulaiman streamflow station. The Figure reveals the highest river discharge records between October to December and also through April and May. The streamflow is the lowest between June to September and January to March.

The flow data of Klang River at Sulaiman streamflow station reveals that the flow regime mainly depends on the North-East monsoon which is from November to March contributes around 41 percent compared to the South-West monsoon equals to 31 percent of the annual streamflow as Table 11. The mean monthly river discharge for the period of 1960 -2007 for the Tun Razak and Batu Sentul streamflow stations are available in Appendix F.

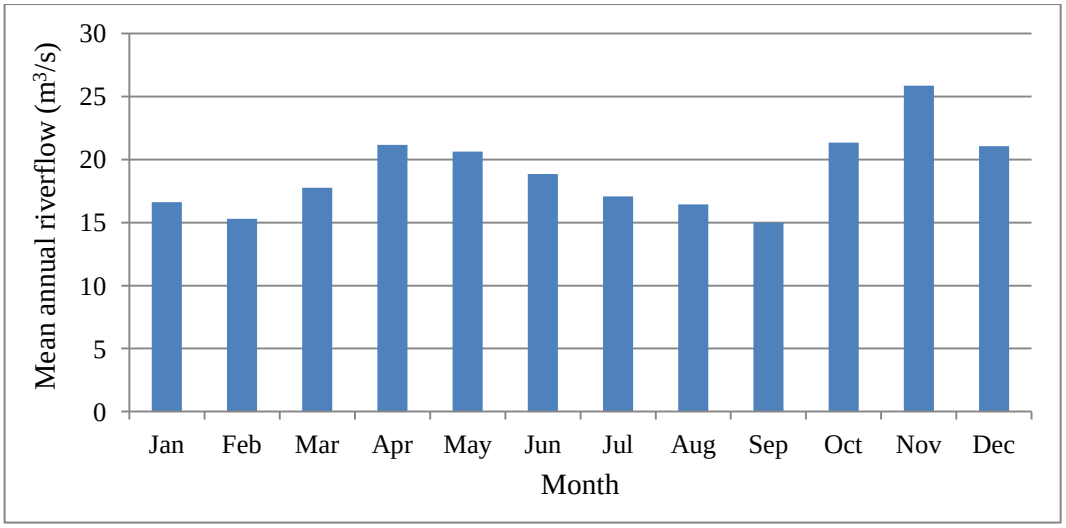


Figure 36 Mean monthly flow of River at Jln. Sulaiman streamflow station

Table 11 Mean and percent monthly flow of River at Jln. Sulaiman streamflow station

| Month | Mean ($m^3/s$) | Percent |
|---|---|---|
| Jan | 15.8 | 7.0 |
| Feb | 15.3 | 6.7 |
| Mar | 17.7 | 7.8 |
| Apr | 21.1 | 9.3 |
| May | 20.4 | 9.0 |
| Jun | 17.6 | 7.8 |
| Jul | 18.5 | 8.1 |
| Aug | 18.9 | 8.3 |
| Sep | 16.1 | 7.1 |
| Oct | 20.6 | 9.0 |
| Nov | 24.7 | 10.9 |
| Dec | 20.6 | 9.1 |

### 3-4-2- Annual River Discharge Analysis

The mean annual river discharge and also the anomalies on mean annual flow of Klang River for a period of 1975-2007 at Sulaiman streamflow station is shown in Figures (37 and 38) respectively. The anomalies of mean annual discharge indicate that there has been consecutive decrease over the years 1975-1983 and an increase in 1988 and 1989. The Figures of mean annual flow and anomaly of mean at two other stations are in Appendix G.

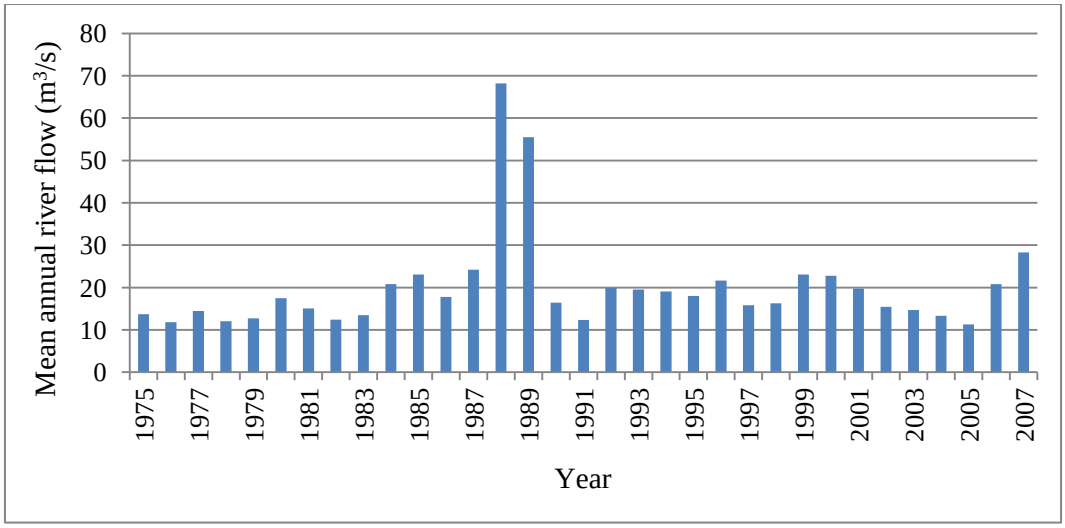


Figure 37 Mean annual flow of River Klang at Sulaiman streamflow station

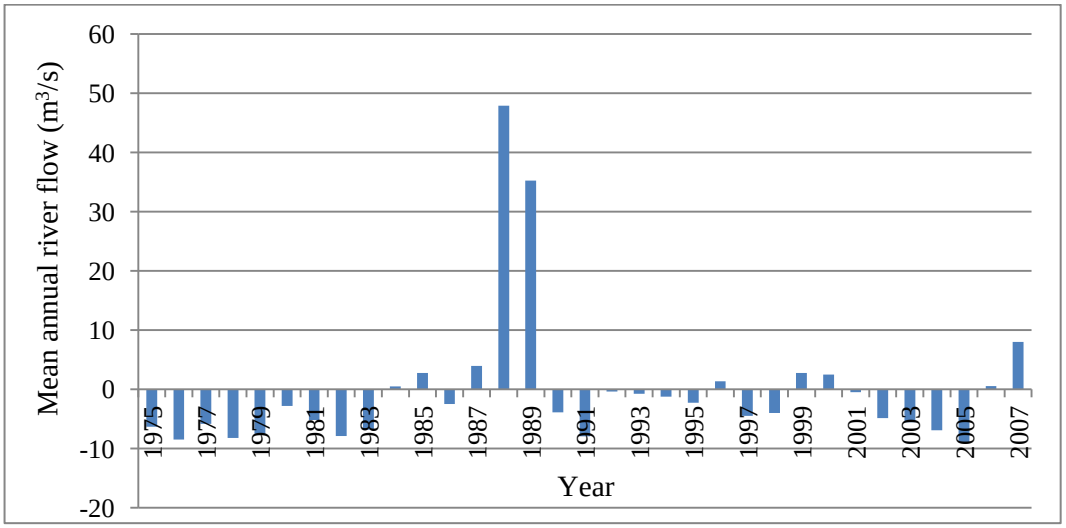


Figure 38 Annual variability of mean annual discharge of River Klang at Sulaiman streamflow station

### 3-4-3- Flood Frequency Analysis

For the flood frequency analysis of Klang River, Log-Pearson type III method has been used. It has been used in US for flood frequency analysis and the detail of the log-Pearson type III can be found in Bulletin 17B-IACWD (1982). Flood frequency was carried out for Klang River at Sulaiman streamflow station to determine design floods amount of discharge for the return periods 2, 5, 10, 25, 50, 100 and 200 years. The advantage of this method is that extrapolation can be made of the values for events with return periods well beyond the observed flood events. The probabilities of floods of various sizes can be extracted from the curve. Table 12 and Figure 39 show

the results of Log-Pearson type III distribution design flood at Sulaiman streamflow station. The other plots of streamflow stations can be seen in Appendix H.

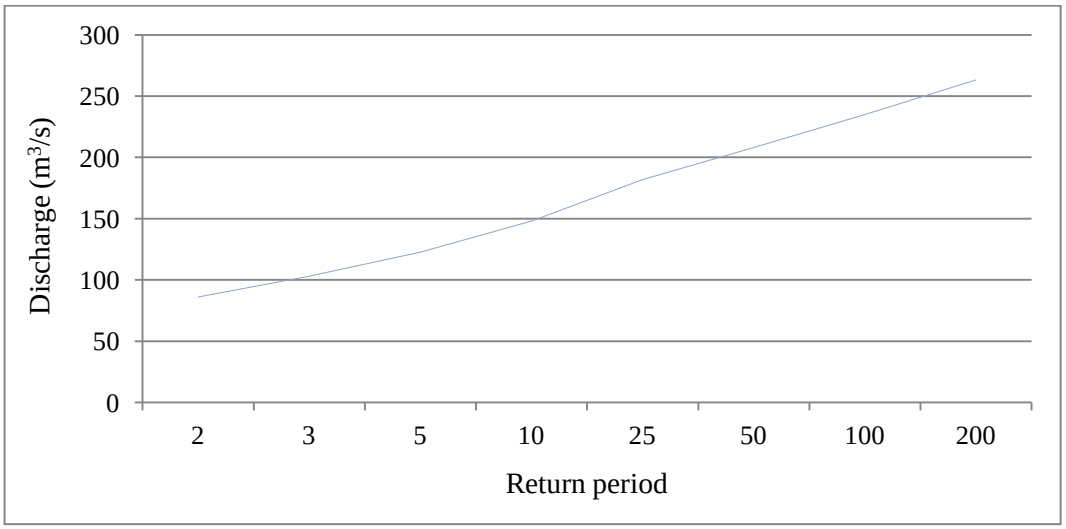


Figure 39 The Flood frequency curve of Sulaiman streamflow station using log-Pearson type III using average daily maximum streamflow data (1975-2007)

Table 12 The results of Log-Pearson type III distribution design flood in SMADA

| **Return period (Year)** | **Probability** | **Discharge ($m^3/s$)** | **Standard deviation** |
|---|---|---|---|
| 200 | 0.99 | 263.24 | 64.16 |
| 100 | 0.99 | 235.12 | 48.50 |
| 50 | 0.98 | 208.06 | 35.59 |
| 25 | 0.96 | 181.88 | 25.29 |
| 10 | 0.90 | 148.12 | 15.44 |
| 5 | 0.80 | 122.57 | 10.64 |
| 3 | 0.66 | 103.03 | 8.25 |
| 2 | 0.50 | 86.09 | 6.70 |

### 3-4-4- Flow Duration Curve

The flow duration curve represents information about the percentage of time that a particular streamflow is exceeded over some historical period. Flow duration curve indicates the hydrologic responses of watershed. However, it can be employed to validate the hydrologic model output. The shape of flow duration curve reveals the hydro geological characteristics of a watershed (Smakhtin, 2001).

The upper-flow region in the curve indicates that the flow regime faced flooding and inversely the lower-flow region represents the flow regime characterisation which maintains low flows during dry spell. The median-flows of the curve which is obtained from coincidence of percent of time in X axis and discharge in Y axis represent the baseflow condition. Having a low slope on the median point suggests a continuous discharge to the river whereas, steep slope for the base-flow indicates that the stream is not fed highly from natural storage like groundwater. Therefore, it is more likely to expect the flow to cease to flow after relatively long period. Figure 40 illustrates flow duration curve for Klang River at Sulaiman streamflow station. The median flow is equal to 36.5 $m^3/s$ with continuous discharge to the stream. The other two flow duration curves are available in Appendix I.

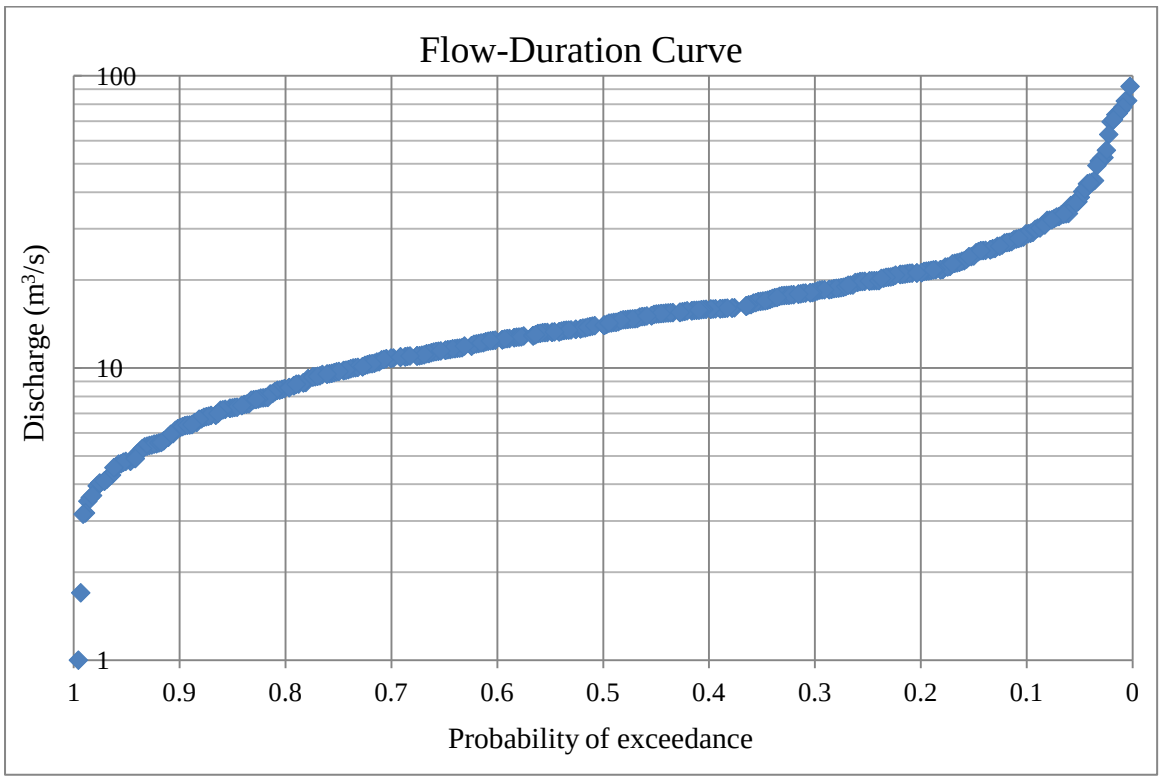


Figure 40 Flow duration curve at Sulaiman streamflow station

# 4- CLIMATE CHANGE DOWNSCALING

This chapter presents the climatic variable downscaling which is based on the statistical downscaling method. The ten raingauge stations have been selected to make a spatial downscaling and also one temperature and evaporation station have been downscaled in Klang watershed. Daily time series data are used for all the variables to run the statistical downscaling in Statistical Downscaling Model (SDSM). SDSM uses a multi-regression method to link large scale climate variables (predictors) as provided by Global Climate Models (GCMs) simulations with daily climatic data at local site (predictands) using the popular SDSM.

## 4-1- Data used in SDSM

The data used for the climate change downscaling contain: daily climatic parameters (Rainfall, temperature and evaporation) as predictand variables at a local scale of Klang watershed. The predictor variables contain the historical NCEP data with the specific scenarios (H3A2a and H3B2a) inside the spatial grid cell of the large scale climate change GCM-HadCM3 model.

### 4-1-1- Predictand Data

In this research predictand data includes rainfall, temperature and evaporation collected over Klang watershed. As gap in data may affect SDSM results and it is important to run statistical downscaling with reliable results and minimum uncertainties. Ten raingauge stations were selected based on the high quality with no gap, daily time series which are spatially distributed over the whole watershed.

The Subang temperature station as the nearest temperature station to Klang watershed was used to downscale maximum and minimum daily temperature by using the SDSM downscaling. Daily temperature of years (1975-2001) was analysed. The evaporation station is located next to Batu dam. Daily evaporation from (1985-2001) are acquired from DID. The selected stations for downscaling are listed in Table 13.

Table 13 The climatological stations used for downscaling in Klang watershed

| Id | Station name | Station no. | Longitude (degree) | Latitude (degree) | Period (year) |
|---|---|---|---|---|---|
| 1 | Taman maluri | 3116005 | 101.65 | 3.20 | 1977-2001 |
| 2 | Edinburgh | 3116006 | 101.63 | 3.18 | 1977-2001 |
| 3 | Pusat penyelidekan | 3117070 | 101.75 | 3.15 | 1972-2001 |
| 4 | Pemasokan ampang | 3118069 | 101.79 | 3.16 | 1972-2001 |
| 5 | Kg. Sg. Tua | 3216001 | 101.69 | 3.27 | 1973-2001 |
| 6 | Ibu bekalan km | 3217001 | 101.73 | 3.27 | 1975-2001 |
| 7 | Empangan genting klang | 3217002 | 101.75 | 3.23 | 1975-2001 |
| 8 | Ibu bekalan km | 3217003 | 101.71 | 3.24 | 1975-2001 |
| 9 | Kg.kuala sleh | 3217004 | 101.77 | 3.26 | 1975-2001 |
| 10 | Genting sempah | 3317004 | 101.77 | 3.37 | 1975-2001 |
| 11 | Subang (Temperature) | 486470 | 101.55 | 3.11 | 1975-2001 |
| 12 | Batu dam (Evaporation) | - | 101.68 | 3.27 | 1985-2001 |

### 4-1-2- Predictor Data

Observed large scale NCEP reanalysis data are prepared by the Canadian Institute for climate studies under Canadian Climate Impact Scenarios (CCIS) project. NCEP data is composed of 26 daily atmospheric variables which are extracted from the grid box covering the predictands. It consists of the grid box (28X, 34Y) of large scale predictor (NCEP, H3A2a and H3B2a) of the study area. Figure 41 shows the grid box of NCEP predictor data for the chosen area.

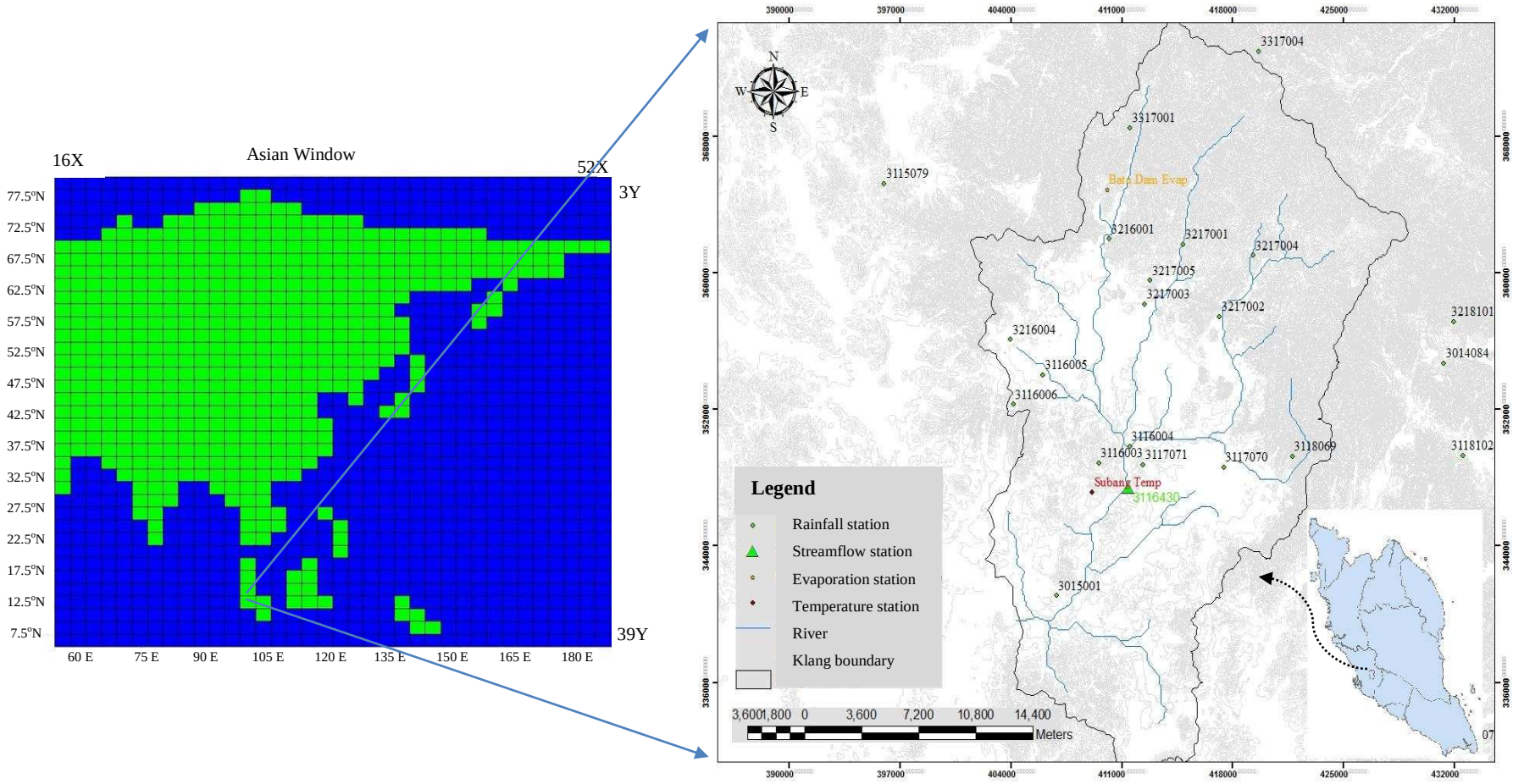


Figure 41 Grid box (28X, 34Y) of large scale predictor (NCEP, H3A2a and H3B2a) of the study area

## 4-2- Statistical Downscaling Model (SDSM) for Daily Precipitation, Temperature and Evaporation

SDSM 4.2 was developed by Wilby and Dawson (2007). In this study, SDSM version 4.2 was used to construct climate change scenarios for the watershed of Klang/ Selangor in West Malaysia. SDSM uses the grid resolution of GCM output from the HadCM3 experiments.

SDSM was adopted as a statistical tool due to several advantages such as low cost and user friendly of over dynamical models such as RCMs. SDSM combines a stochastic weather generator and transfer function method to relate large scale GCM output (the predictors) to local variables such as precipitation (the predictands) (Wilby and Dawson, 2007; Wilby et al., 1999).

The daily climatic data in the study area are used in SDSM. These stations are chosen based on temporal and spatial covering along with completeness and quality of data as shown in Figure 42.

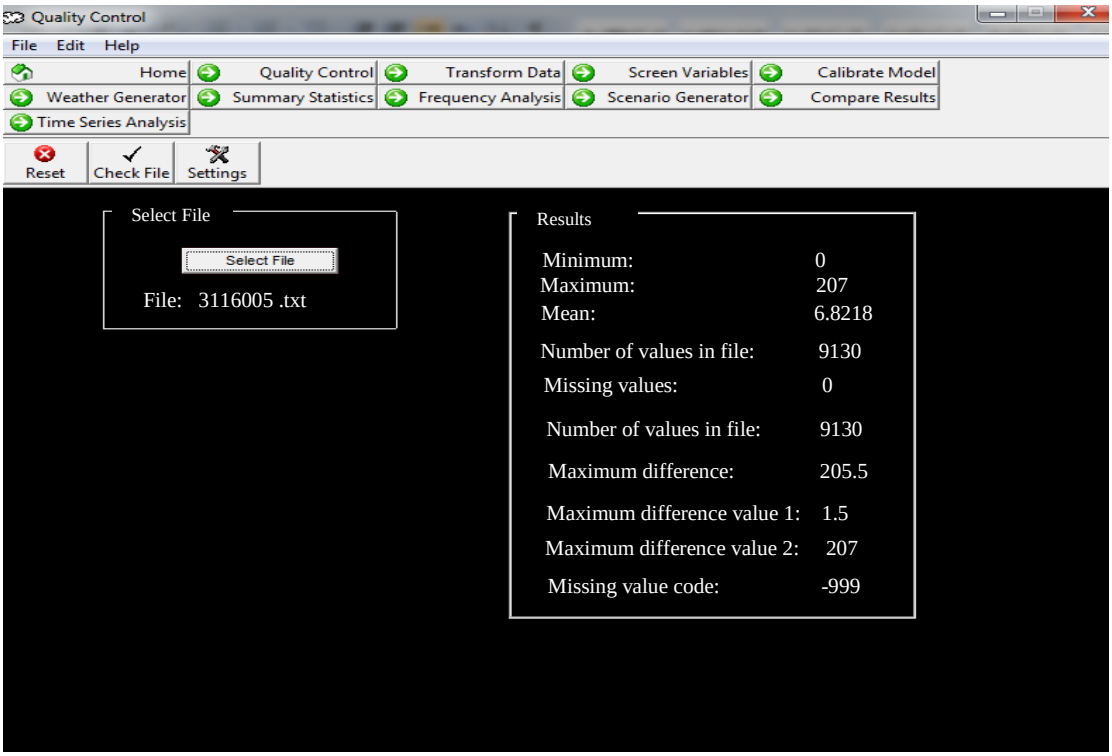


Figure 42 Graphical user interface of SDSM version 4.2

### 4-2-1- SDSM for Klang Watershed

In this study, precipitation, maximum and minimum temperatures and evaporation as predictand data are downscaled for the study area. According to Wilby et al. (2001) SDSM needs to set up for the various predictands to get a reliable result. This task runs quality control checks of the observed daily climate data to identify the gross data error and missing data. It also transforms a fourth root model function to normalise the distribution and make it less skewed to low precipitation values. The fourth root transformation is used as distribution of data is skewed in a conditional process (Khan et al., 2005). Setting up of SDSM involves following steps:

- Adjusting a 366 days as the year length for the predictand and NCEP data,

- Adjusting a 360 days as the year length for HadCM3-GCM model where, each month is 30 days,

- To set the value of 0.3 mm per day as threshold value in precipitation data (Khan et al., 2005) and a zero value for temperature: Specifying the threshold value which is useful to trace the rainy days in calibration and validation in SDSM,

- Defining the conditional model for precipitation and evaporation in downscaling,

- Defining the non-conditional model for temperature in downscaling,

- Defining the fourth root transformation for transformation of precipitation and evaporation data. However, no transformation function was used for temperature data.

- Setting variance inflation value of 12 as default for all the predictands data. (The variance inflation controls the range of variation of downscaled daily predictands) and

- Setting bias correction to 1, for all the predictands. It means the process will be run without any bias correction. The bias correction is able to moderate for any tendency to over or underestimate the mean of conditional processes by the downscaling model.

### 4-2-2- Exploratory Data Analysis

SDSM is a useful tool to provide a series of statistic functions including both generic and conditional statistics such as: monthly/seasonal/annual means, measures of dispersion (variance), serial correlation, frequencies of extremes, spell lengths etc. It shows the comprehensive statistical characteristics of all daily predictands used for downscaling. Table 14 shows the statistical characteristics of all the predictands and Figures (from 43 to 46) show the exploratory data analysis of rainfall, temperature and evaporation data. Other Figures for the exploratory data analysis are available in the Appendix J.

Table 14 The statistical characteristics of 10 daily raingauge stations, Subang temperature and Batu dam evaporation station

| Predictor / Predictand | No. of observation | Minimum | Maximum | 1st Quartile | Median | 3rd Quartile | Mean | Variance | Standard deviation |
|---|---|---|---|---|---|---|---|---|---|
| 3116005 (mm) | 8948 | 0.0 | 207.2 | 0.0 | 0.0 | 6.5 | 6.9 | 208.2 | 14.4 |
| 3116006 (mm) | 10957 | 0.0 | 205.1 | 0.0 | 0.5 | 7.0 | 7.1 | 211.5 | 14.5 |
| 3117070 (mm) | 12784 | 0.0 | 166.8 | 0.0 | 0.0 | 6.5 | 6.8 | 206.8 | 14.4 |
| 3118069 (mm) | 12784 | 0.0 | 170.6 | 0.0 | 0.0 | 8.0 | 7.5 | 231.2 | 15.2 |
| 3216001 (mm) | 12776 | 0.0 | 169.0 | 0.0 | 0.5 | 6.5 | 6.6 | 180.8 | 13.4 |
| 3217001 (mm) | 12776 | 0.0 | 199.0 | 0.0 | 0.5 | 7.0 | 6.7 | 183.1 | 13.5 |
| 3217002 (mm) | 11688 | 0.0 | 142.1 | 0.0 | 0.5 | 6.5 | 6.4 | 177.6 | 13.3 |
| 3217003 (mm) | 11688 | 0.0 | 140.4 | 0.0 | 0.0 | 6.0 | 6.5 | 190.8 | 13.8 |
| 3217004 (mm) | 11688 | 0.0 | 141.7 | 0.0 | 0.0 | 6.5 | 6.6 | 178.5 | 14.5 |
| 3317004 (mm) | 11688 | 0.0 | 802.4 | 0.0 | 1.0 | 7.5 | 6.8 | 353.2 | 18.8 |
| $T_{ma}$ | 9862 | 31.0 | 36.0 | 31.8 | 32.2 | 32.9 | 32.9 | 0.6 | 0.7 |
| $T_{min}$ | 9862 | 22.0 | 25.0 | 22.6 | 23.0 | 23.5 | 23.1 | 0.3 | 0.6 |
| Evaporation(mm) | 6209 | 0.4 | 10.0 | 4.7 | 5.6 | 6.7 | 5.7 | 1.8 | 135.0 |

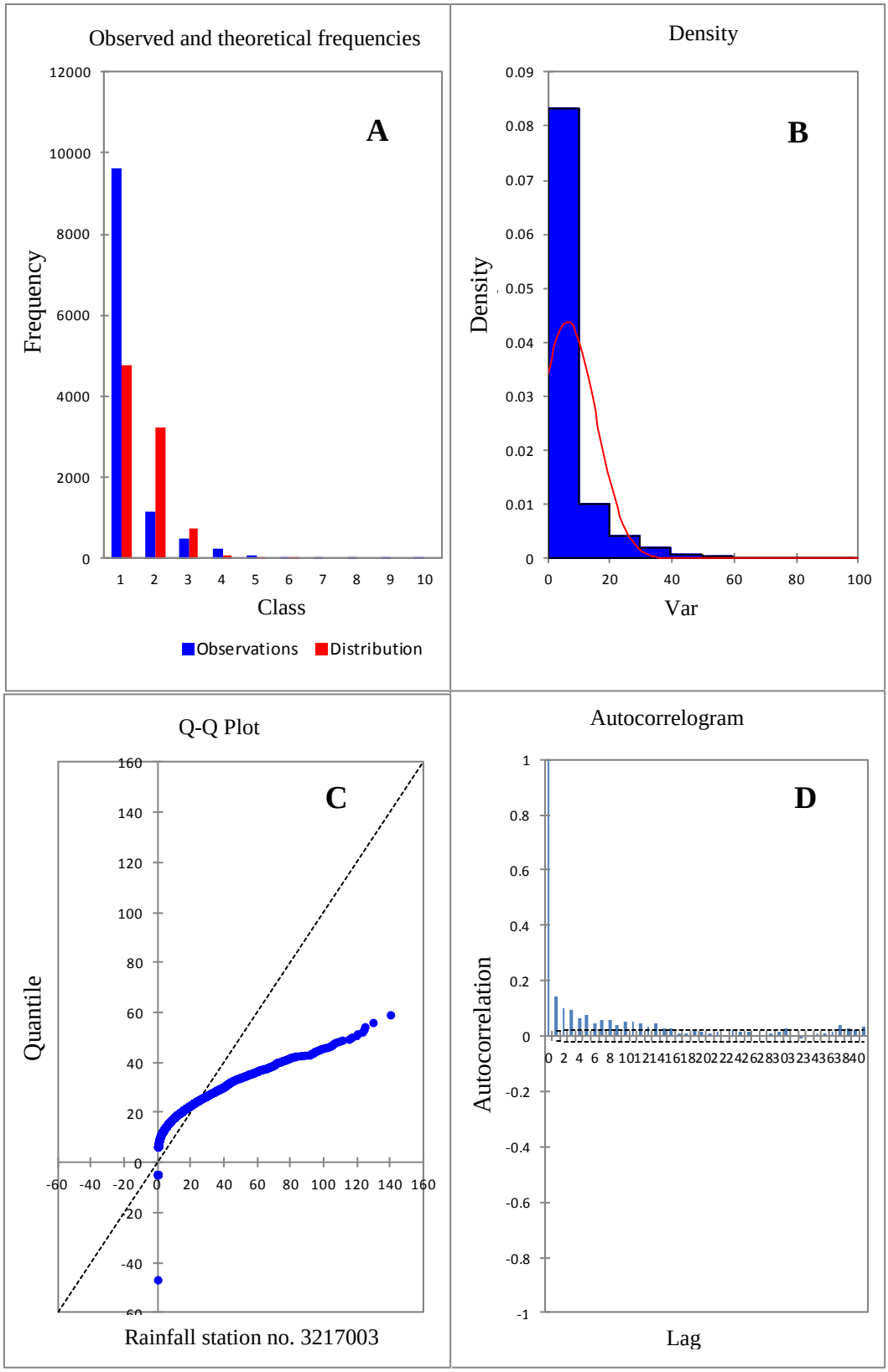


Figure 43 The exploratory analysis plots (**A:** frequency, **B:** density, **C:** Q-Q and **D:** ACF plot) of observed daily precipitation, at station no.3217003

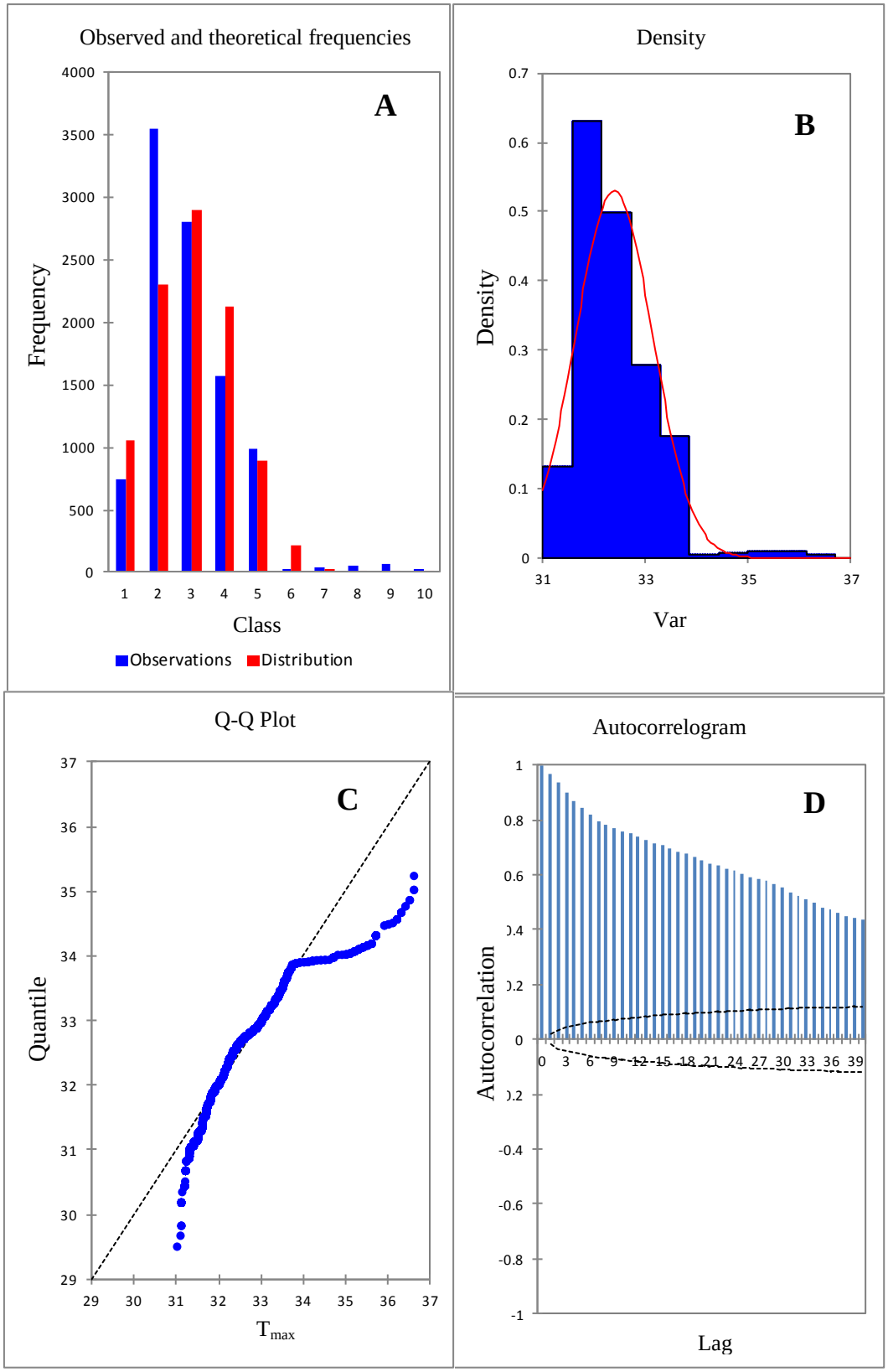


Figure 44 The exploratory analysis plots (**A:** frequency, **B:** density, **C:** Q-Q and **D:** ACF plot) of observed daily $T_{max}$ at Subang Station

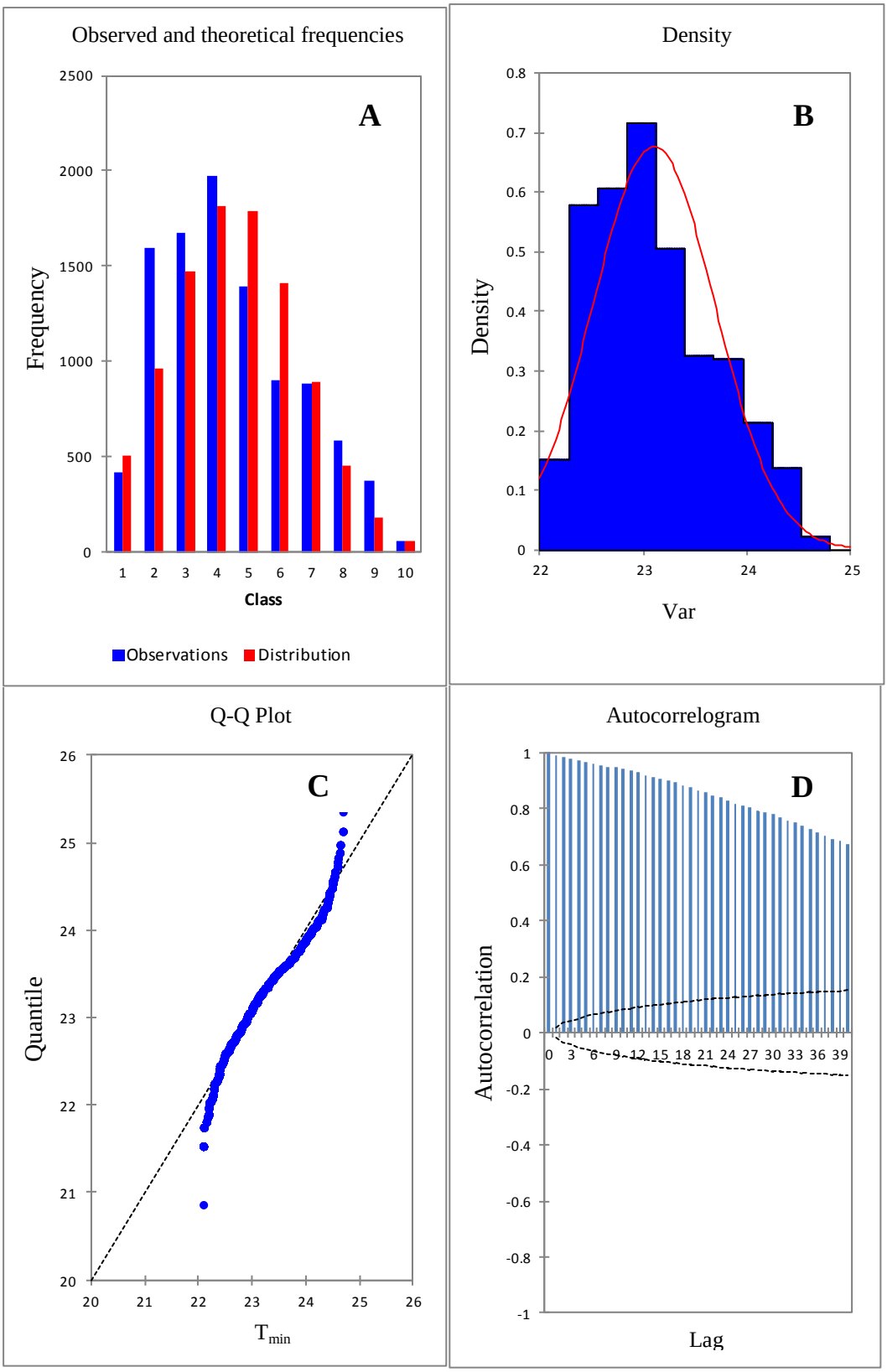


Figure 45 The exploratory analysis plots (**A:** frequency, **B:** density, **C:** Q-Q and **D:** ACF plot) of observed daily $T_{min}$ at Subang station

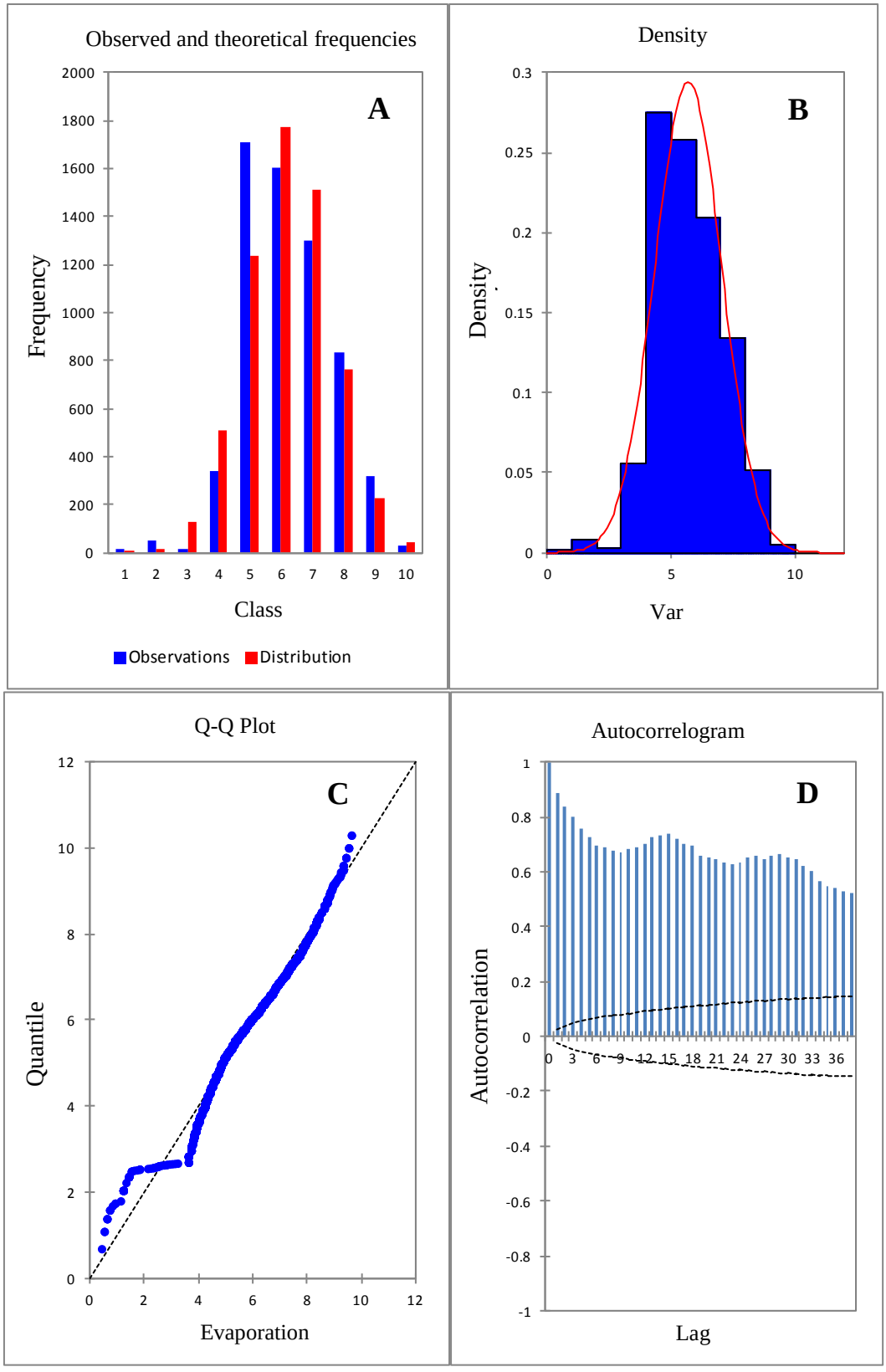


Figure 46 The exploratory analysis plots (**A**: frequency, **B**: density, **C**: Q-Q and **D**: ACF plot) of observed daily evaporation at Batu dam station

Exploratory Data Analysis (EDA) techniques such as Frequency, Density, Q-Q- and ACF plots were used for the observed daily rainfall, maximum and minimum temperature and evaporation. EDA plots are used to indicate the statistical states of the predictands. The EDA results suggest application of the parametric/non-parametric approaches in the uncertainty assessment of downscaled daily precipitation, daily maximum and minimum temperatures and evaporation.

Figure 43 illustrates the distribution characterisation of the rainfall data. It reveals that the daily rainfall for the period (1975-2001) is non-normal with the skew distribution towards the left, as shown in histogram and density plots. Also, the Q-Q plot is not straight which exhibit the presence of outliers in the daily rainfall data. Auto Correlation Function (ACF) for the daily rainfall suggests no significant serial correlation as most often ACF values are within 95% confidence bands. It means there is no good correlation among the daily rainfall data.

On the other hand, the daily maximum and minimum temperatures as in (Figures: 44 and 45) at the Subang station for the period, 1975-2001 and daily evaporation (Figure 46) at Batu dam station for the period, 1985-2001 show that the data are normal. The histogram and density plots are clearly presenting the normality states and the Q-Q plots do not exhibit outliers in the data. The ACF plots for these data indicate a high correlation among the data.

The results show that all the precipitation data are non-normal and on the contrary, the maximum and minimum temperature and evaporation data have normal distribution.

### 4-2-3- Selection of Predictors

A Multiple Linear Regression Equation is constructed via an optimisation algorithm (dual simplex/ordinary least squares) between predictands and the predictors that are determined through screening variables step. Screening variables in SDSM shows a linear regression between gridded predictors and predictands which is the most significant phase to the statistical downscaling method to choose appropriate downscaling predictor variables which largely affects the generated scenarios. SDSM

generates a correlation matrix and explained variance reveals the correlations between the predictand and predictors. The correlation of each predictand data to the 26 Re-Analysis NCEP predictor variables as listed in SDSM are obtained (Saha et al., 2010). The predictors are which high correlated with the predictand ($p < 5\%$) have been chosen for the future prediction. The selected large scale predictors for all the local predictands are listed in Table 15. Table 16 shows the calculated P-Value for the correlation of the NCEP and predictands.

For precipitation, mean sea level pressure, 850 hPa Geopotential height, 500 hPa Geopotential height, Near surface relative humidity, Surface specific humidity and Mean temperature at 2m were chosen as predictors to provide a good correlation to the observed data. For the temperature, Surface specific humidity, mean temperature at 2m and 500 hPa Geopotential height are selected. For the evaporation, the surface specific humidity and mean temperature at 2m were chosen to represent the best correlation of the daily evaporation to the large scale predictors NCEP-reanalysis data.

Table 15 Large scale predictor variables selected for predicting daily precipitation, maximum and minimum temperature and evaporation

| **Predictor** / **Predictand** | **Mean sea level pressure (ncepmslpas)** | **850 hpa Geopotential height (ncepp850as)** | **500 hpa Geopotential height (ncepp500as)** | **Near surface relative humidity (nceprhumas)** | **Surface specific humidity (ncepshumas)** | **Mean temperature (nceptempas)** |
|---|---|---|---|---|---|---|
| 3116005 | * | * | | | | * |
| 3116006 | * | * | | * | | * |
| 3117070 | * | * | * | * | * | * |
| 3118069 | * | * | * | * | * | * |
| 3217001 | * | * | * | * | * | * |
| 3216001 | * | * | * | * | * | * |
| 3217002 | * | | * | * | * | |
| 3217003 | * | * | * | * | | |
| 3217004 | | * | | * | * | * |
| 3317004 | * | | * | * | * | * |
| $T_{max}$ | | | | | * | * |
| $T_{min}$ | | | * | | * | * |
| Evaporation | | | | | * | * |

Table 16 P-Value of correlation of large scale predictor variables and predictands

| Predictor / Predictand | Mean sea level pressure (ncepmslpas) | 850 hpa Geopotential height (ncepp850as) | 500 hpa Geopotential height (ncepp500as) | Near surface relative humidity (nceprhumas) | Surface specific humidity (ncepshumas) | Mean temperature (nceptempas) |
|---|---|---|---|---|---|---|
| 3116005 | 0.521 | 0.210 | 0.030 | 0.010 | 0.041 | 0.240 |
| 3116006 | 0.564 | 0.010 | 0.510 | 0.330 | 0.082 | 0.110 |
| 3117070 | 0.419 | 0.560 | 0.450 | 0.450 | 0.391 | 0.440 |
| 3118069 | 0.542 | 0.240 | 0.500 | 0.370 | 0.562 | 0.210 |
| 3217001 | 0.146 | 0.270 | 0.110 | 0.520 | 0.542 | 0.460 |
| 3216001 | 0.343 | 0.560 | 0.310 | 0.560 | 0.516 | 0.560 |
| 3217002 | 0.497 | 0.040 | 0.290 | 0.140 | 0.457 | 0.020 |
| 3217003 | 0.353 | 0.410 | 0.560 | 0.220 | 0.012 | 0.020 |
| 3217004 | 0.045 | 0.220 | 0.050 | 0.320 | 0.172 | 0.120 |
| 3317004 | 0.099 | 0.030 | 0.560 | 0.430 | 0.161 | 0.250 |
| $T_{max}$ | 0.000 | 0.000 | 0.000 | 0.000 | 0.160 | 0.320 |
| $T_{min}$ | 0.000 | 0.000 | 0.310 | 0.060 | 0.450 | 0.000 |
| Evaporation | 0.040 | 0.000 | 0.020 | 0.000 | 0.172 | 0.320 |

### 4-2-4- Model Calibration

SDSM presents two kinds of model calibration based on the nature of climate data which are categorised into conditional and unconditional processes. A conditional process is defined for the precipitation and evaporation data as dependent on the regional scale predictors. There is an indirect link assumed between the data and predictors, whereas an unconditional process can be established for the temperature data as a direct link to the predictors assumed. Therefore, in conditional process some local parameters of precipitation would estimate such as wet/dry-day occurrences.

In order to run the calibration in SDSM, the NCEP-Re-analysis data set is used in compliance with the specified year period for each predictand (as Table 13) to identify the empirical linear regression of the large scale predictors with the local sites. The historical data of predictands are split into two parts: the first part is used for calibration and the second part of the data is used for validation as an independent dataset. A best performed calibration results are obtained with correlation and standard errors for every month. The results reveal that the calibration can preserve the basic statistical properties and there is no significant variation in mean and variance of observed and calibrated precipitation.

Table 17 shows the calibration and validation period lengths for variety of predictands used in SDSM. Figures (from 47 to 54) illustrate the calibration results at the raingauge station (3217003), Subang temperature and Batu dam evaporation stations. Table 18 gives the accuracy of the calibrated data. Other figures related to calibration can be seen in Appendix K.

Table 17 Time series for calibration and validation in SDSM downscaling

| Id | Station name | Station no. | Period (year) | Calibrated period (year) | Validated period (year) |
|---|---|---|---|---|---|
| 1 | Taman maluri | 3116005 | 1977-2001 | 1977-1990 | 1991-2001 |
| 2 | Edinburgh | 3116006 | 1977-2001 | 1977-1990 | 1991-2001 |
| 3 | Pusat Penyelidekan | 3117070 | 1972-2001 | 1972-1990 | 1991-2001 |
| 4 | Pemasokan Ampang | 3118069 | 1972-2001 | 1972-1990 | 1991-2001 |
| 5 | Kg. Sg. Tua | 3216001 | 1973-2001 | 1973-1990 | 1991-2001 |
| 6 | Ibu Bekalan km | 3217001 | 1975-2001 | 1975-1990 | 1991-2001 |
| 7 | Empangan Genting Kelang | 3217002 | 1975-2001 | 1975-1990 | 1991-2001 |
| 8 | Ibu Bekalan km | 3217003 | 1975-2001 | 1975-1990 | 1991-2001 |
| 9 | Kg.kuala Sleh | 3217004 | 1975-2001 | 1975-1990 | 1991-2001 |
| 10 | Genting Sempah | 3317004 | 1975-2001 | 1975-1990 | 1991-2001 |
| 11 | Subang (Temperature) | 486470 | 1975-2001 | 1975-1990 | 1991-2001 |
| 12 | Batu dam (Evaporation) | - | 1985-2001 | 1985-1990 | 1991-2001 |

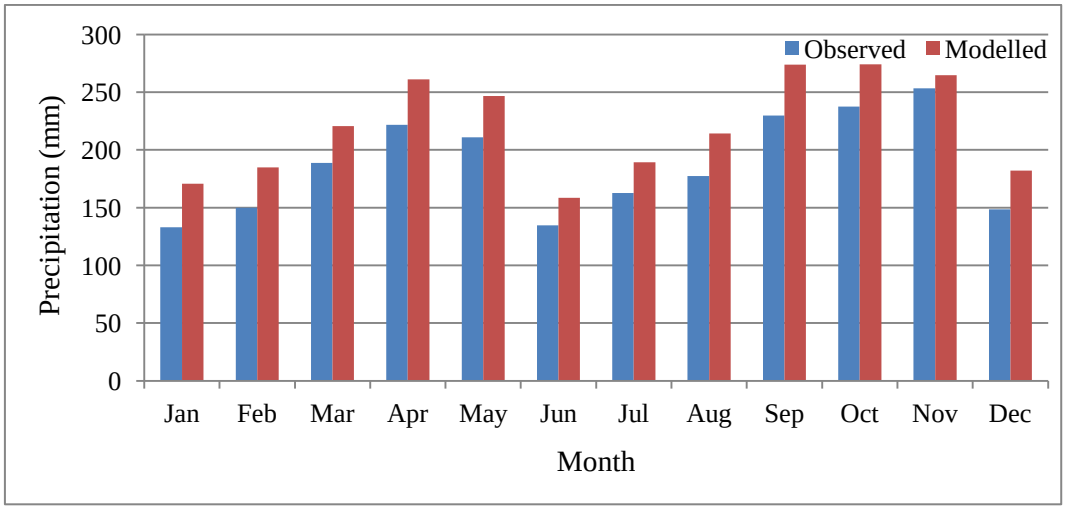


Figure 47 Daily mean precipitation between observed and calibrated at 3217003

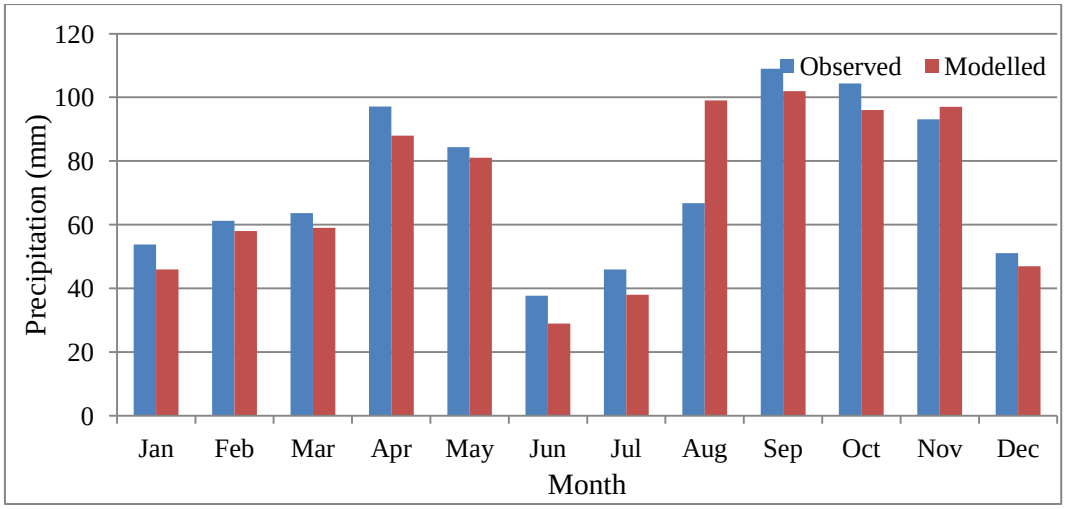

Figure 48 Daily mean precipitation distribution between observed and calibrated at 3217003

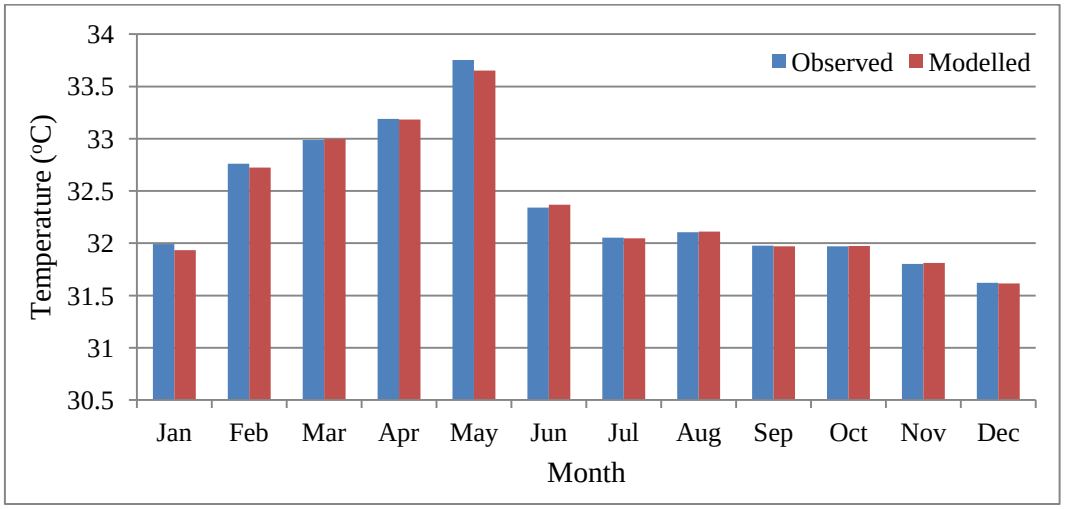

Figure 49 Mean daily maximum temperature between observed and calibrated at Subang station

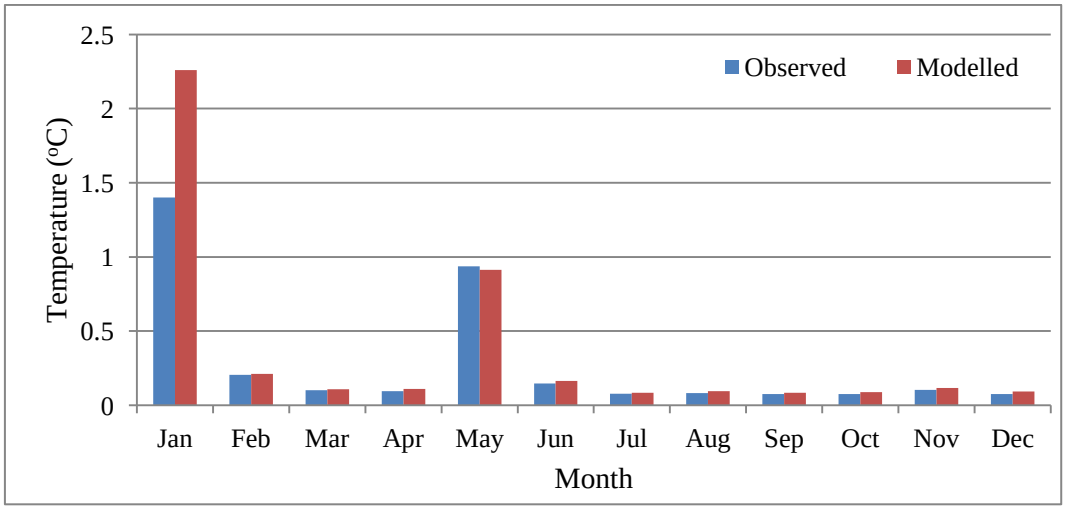

Figure 50 Daily mean maximum distribution between observed and calibrated at Subang station

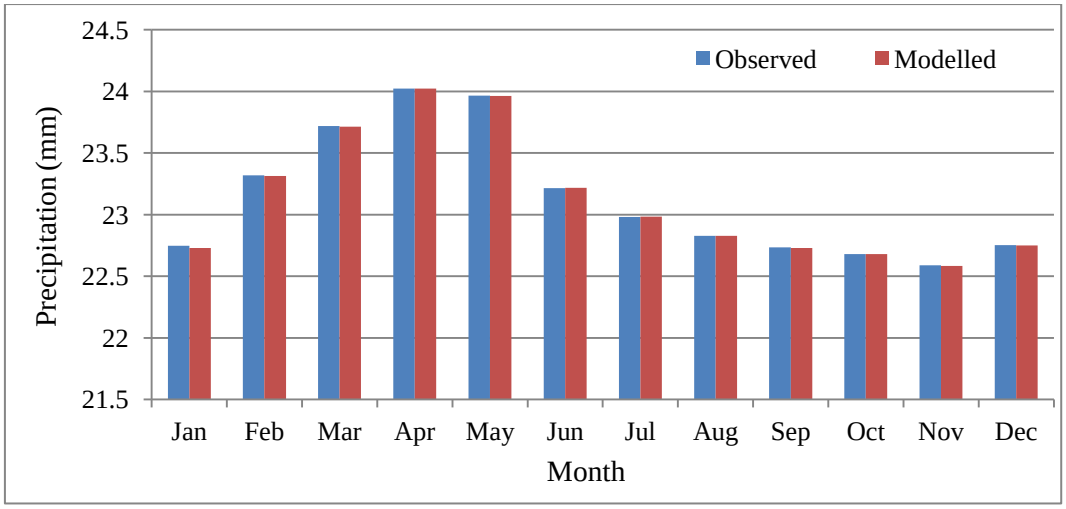


Figure 51 Mean daily minimum temperature between observed and calibrated at Subang station

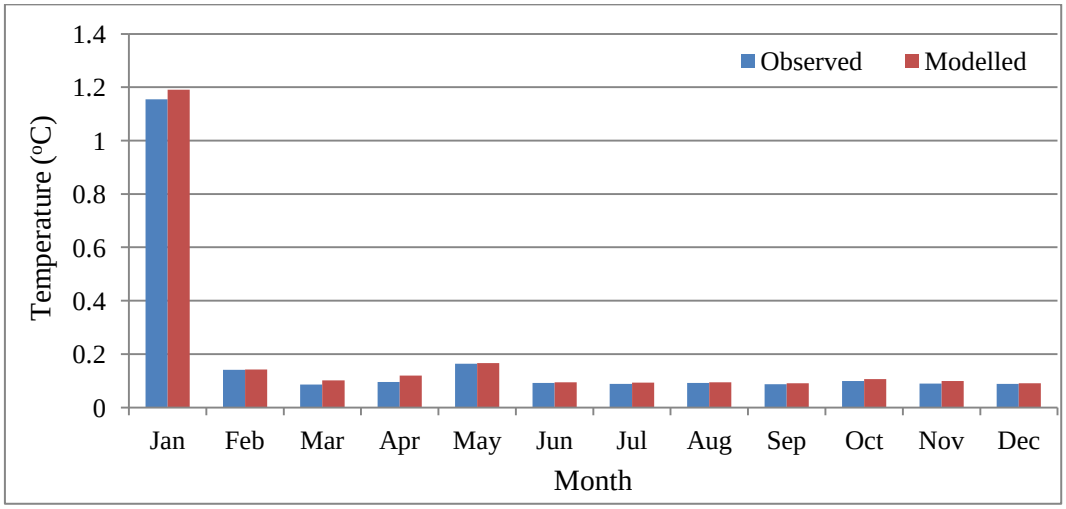


Figure 52 Daily mean minimum temperature distribution between observed and calibrated at Subang station

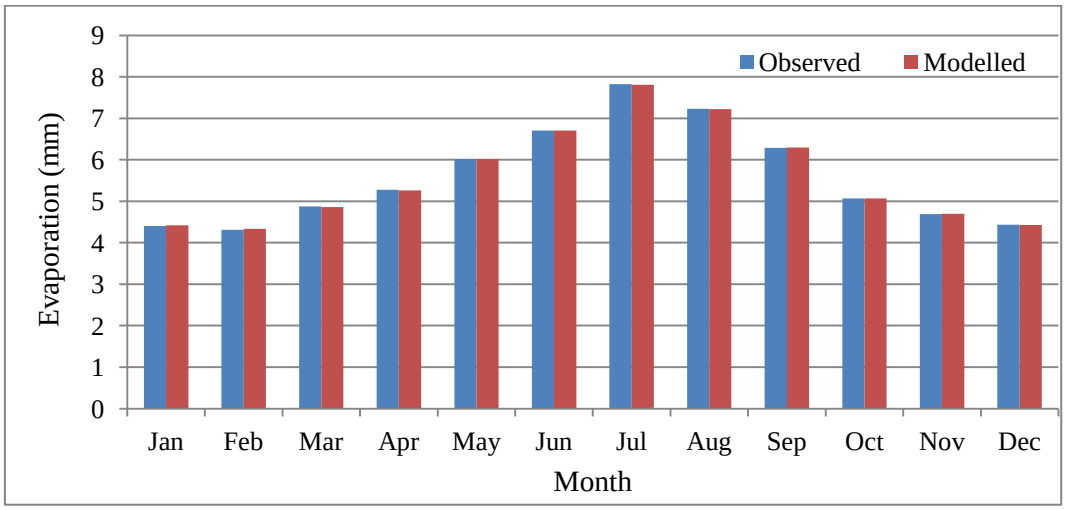


Figure 53 Daily mean evaporation between observed and calibrated at Batu dam station

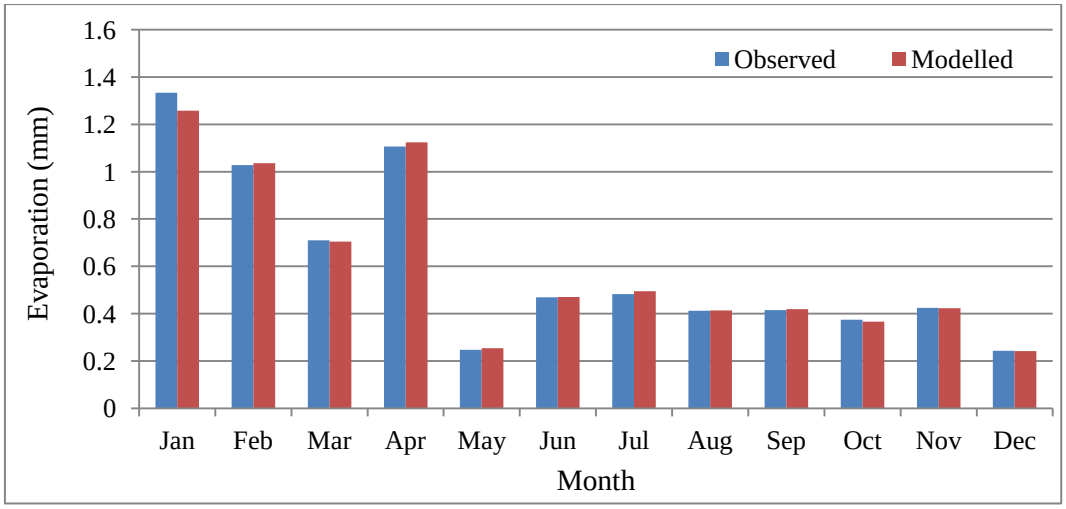


Figure 54 Daily mean evaporation distribution between observed and calibrated at Batu dam station

Table 18 Coefficient of Determination of the calibration test

| Predictand variables | Mean | Maximum | Variance |
|---|---|---|---|
| 3116006 | 0.966 | 0.689 | 0.802 |
| 3117070 | 0.884 | 0.121 | 0.907 |
| 3118069 | 0.968 | 0.236 | 0.992 |
| 3216001 | 0.990 | 0.120 | 0.993 |
| 3217001 | 0.998 | 0.114 | 0.918 |
| 3217002 | 0.996 | 0.780 | 0.914 |
| 3217003 | 0.960 | 0.232 | 0.814 |
| 3217004 | 0.920 | 0.632 | 0.853 |
| 3317004 | 0.990 | 0.990 | 0.892 |
| $T_{max}$ | 0.990 | 0.560 | 0.950 |
| $T_{min}$ | 0.990 | 0.585 | 0.990 |
| Evaporation | 0.990 | 0.885 | 0.990 |

### 4-2-5- Model Validation

Weather generator syntheses the predictand to validate the independent data. It produces synthesis of artificial time series for present climate condition. Validation test is conducted after getting an agreeable result of calibration test. Validation test is run to identify the accuracy of the model which is likely to downscale for the future projections.

During validation, mean and variance of downscaled daily predictands are adjusted by bias correction and variance inflation factor to force the model to replicate the

observed data. Bias correction compensates any tendency to over or under estimates the mean of downscaled variables.

To evaluate the validation output of precipitation (as conditional variable), Dry spell and Wet spell length, the observed and validated were compared in Table 19. Figures (from 55 to 62) compare output from the validated model against known data from NCEP re-analysis normalised period (as specified in Table 13). The results indicate that the model run is satisfactorily validated and it can be seen that there is a remarkable skill of simulation data compared to the observed data. The validation results can be seen in Appendix L.

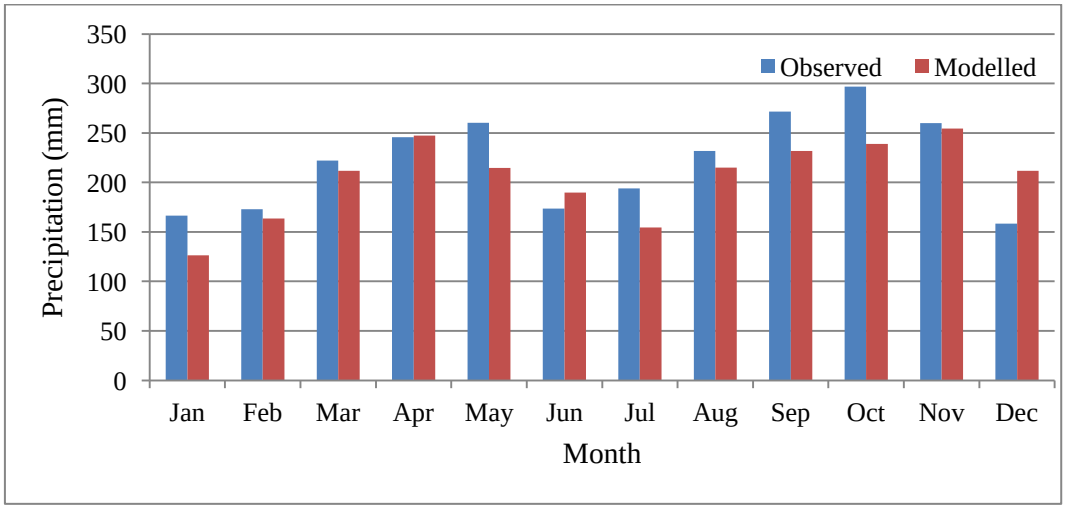


Figure 55 Daily mean precipitation between observed and validated at 3217003

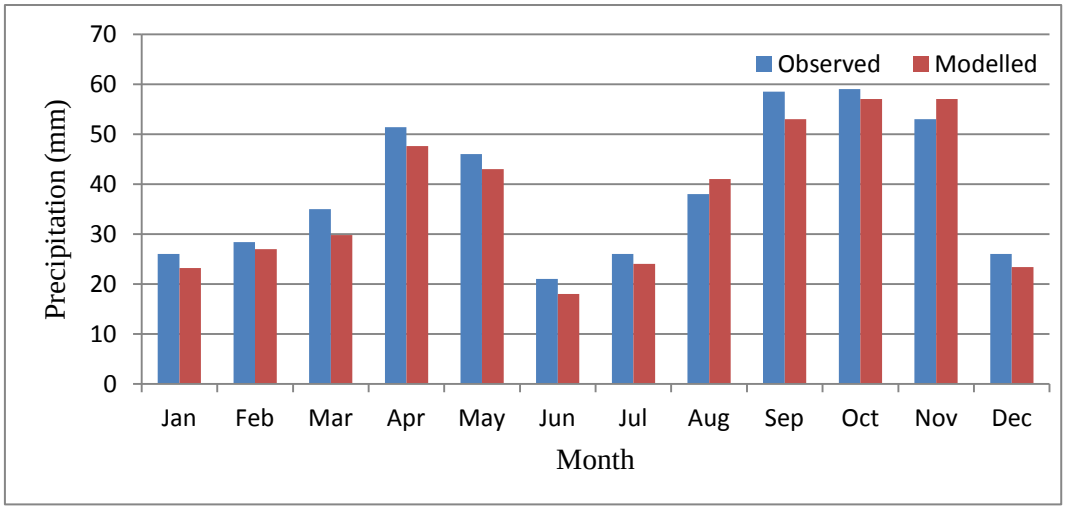


Figure 56 Daily mean precipitation distribution between observed and validated at 3217003

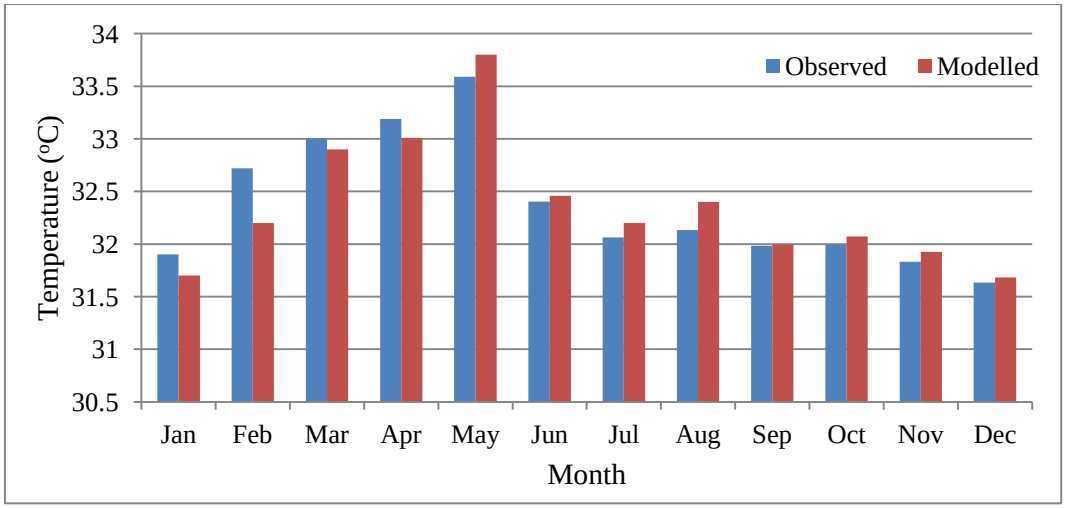


Figure 57 Mean daily maximum temperature between observed and validated at Subang station

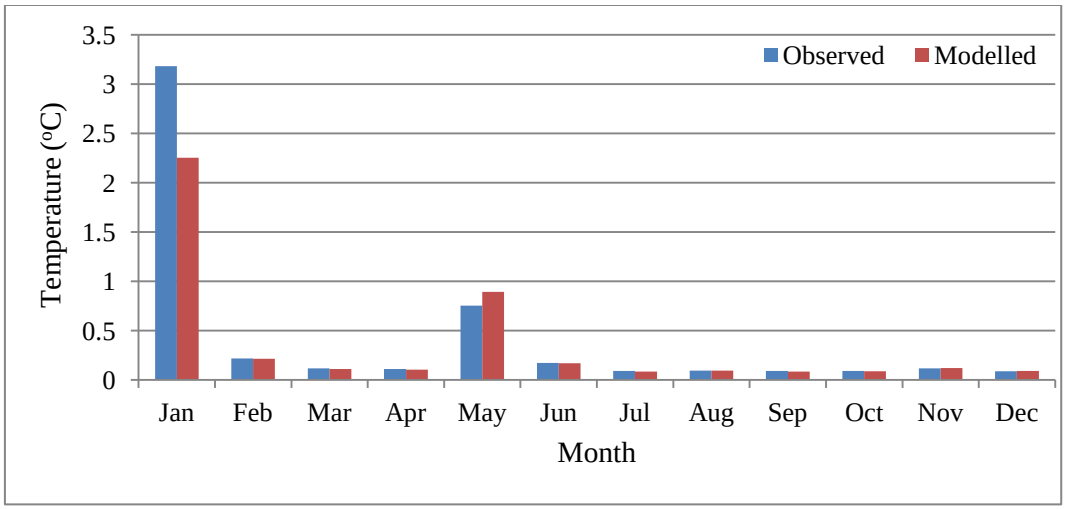


Figure 58 Daily mean maximum distribution between observed and validated at Subang station

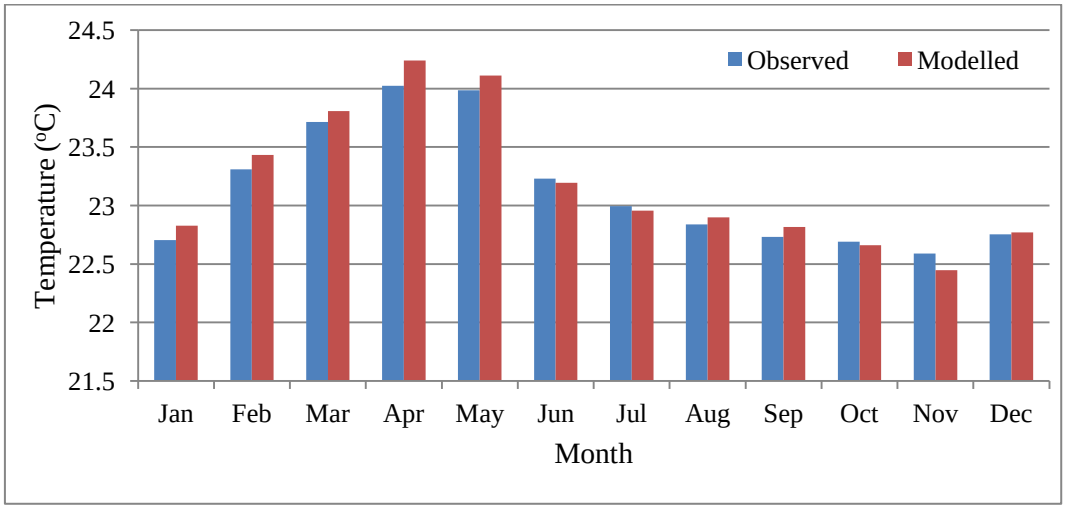


Figure 59 Mean daily minimum temperature between observed and validated at Subang station

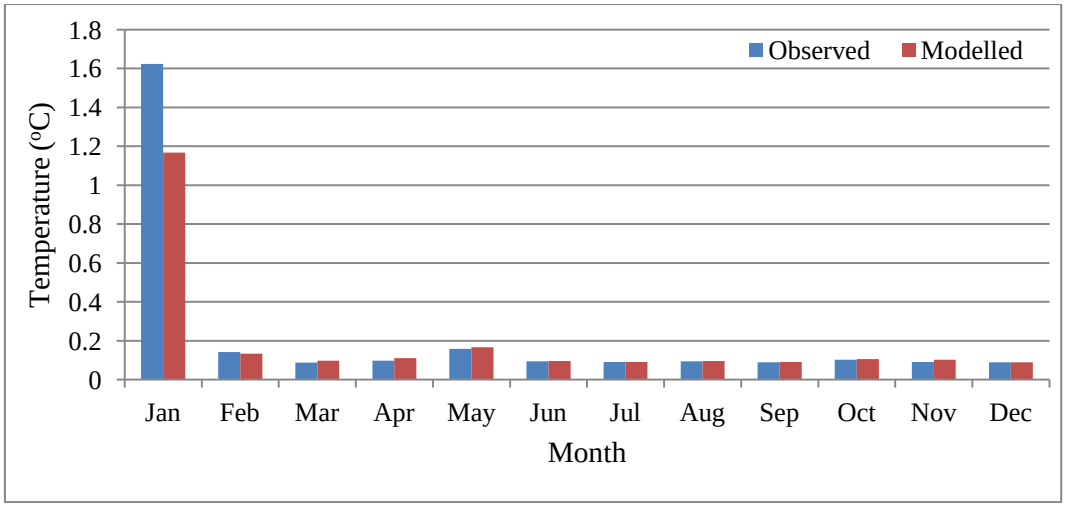


Figure 60 Daily mean minimum distribution between observed and validated at Subang station

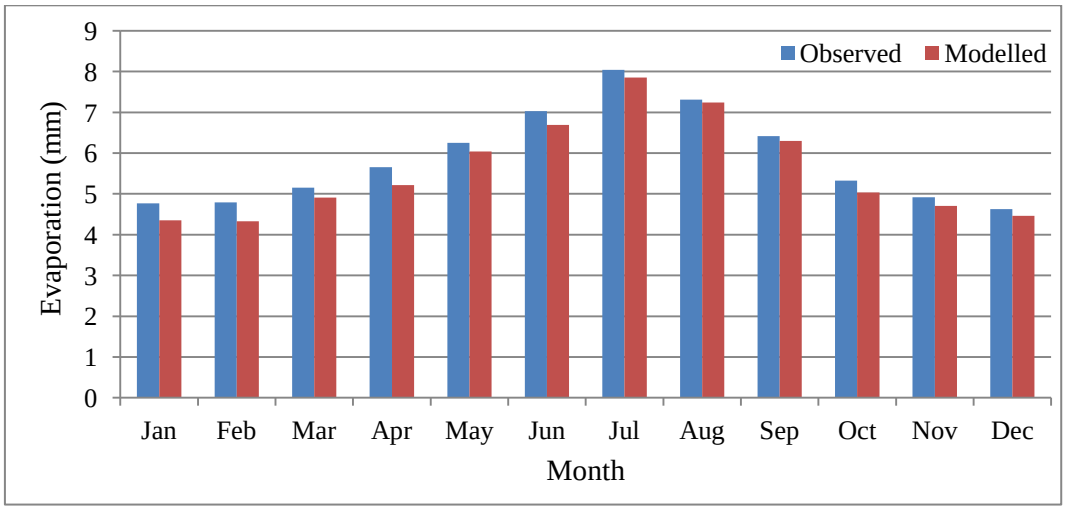


Figure 61 Daily mean evaporation between observed and validated Batu dam station

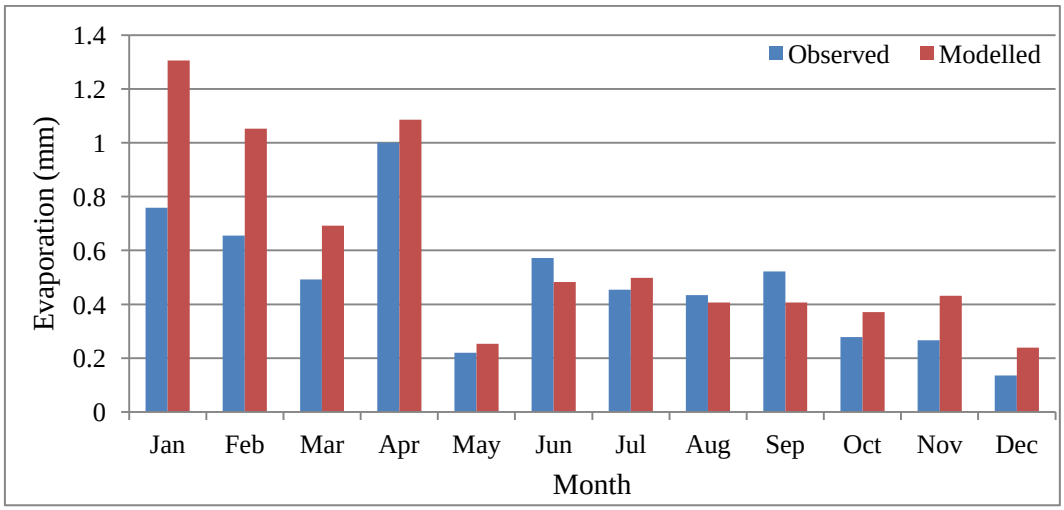


Figure 62 Daily mean evaporation distribution between observed and validated at Batu dam station

Table 19 Pearson Correlation results of the validation

| Predictand | Mean | Maximum | Variance | Dry Spell | Wet Spell |
|---|---|---|---|---|---|
| 3116005 | 0.47 | 0.27 | 0.62 | 0.65 | 0.41 |
| 3116006 | 0.49 | 0.22 | 0.35 | 0.67 | 0.72 |
| 3117070 | 0.87 | 0.54 | 0.72 | 0.78 | 0.69 |
| 3118069 | 0.50 | 0.30 | 0.62 | 0.53 | 0.44 |
| 3216001 | 0.68 | 0.16 | 0.05 | 0.64 | 0.48 |
| 3217001 | 0.51 | 0.32 | 0.40 | 0.82 | 0.54 |
| 3217002 | 0.20 | 0.11 | 0.40 | 0.75 | 0.56 |
| 3217003 | 0.80 | 0.45 | 0.82 | - | 0.19 |
| 3217004 | 0.72 | 0.35 | 0.43 | 0.51 | 0.67 |
| 3317004 | 0.33 | 0.14 | 0.10 | 0.46 | 0.75 |
| $T_{max}$ | 0.88 | 0.54 | 0.98 | - | - |
| $T_{min}$ | 0.98 | 0.43 | 1.00 | - | - |
| Evaporation | 0.99 | 0.93 | 0.73 | - | - |

### 4-2-6- Scenario Generator

Hadley Centre Couple Model is used as the GCM downscaling to produce the local scenario at the watershed. It contains all the observed predictors data produced from NCEP/NCAR and IPCC A2 and B2 scenarios. More explanations of the IPCC scenarios are available in Chapter 2 (Section: 2-2-1).

The scenario generator in SDSM produces ensembles of synthetic daily weather series for the current and future climate using NCEP re-analysis and GCM. The simulation of HadCM3-GCM model using A2 and B2 scenarios are run in SDSM to project the trend of future climate change variables at watershed scale. To evaluate the future climate change, the long time period of projection to 2100 is divided to three parts (2020s, 2050s and 2080s) to compare the observed precipitation, temperature and evaporation. The generated climate change scenarios for the raingauge stations are found in the Appendix M.

The criteria used for selecting the appropriate IPCC scenarios to assess the climate change impacts are explained as below:

- **Consistency at the fine scale:** A2 and B2 scenarios reveal the reliable projection of a plausible future climate condition in regional scale, while scenarios

A1 and B1 form the world homogeneously A1 and B1 represent at global scale. According to IPCC (2007), Malaysia is a developing country which will be vulnerable to climate change and has less flexibility to adjust the economical structure and being largely dependent on agriculture. Likewise, Malaysia is expected to a high rate of population growth which affects on the future social, economic and technological state of the region. These characteristics of the region possibly cause a high rate of GHG emissions in the future.

- **Applicability in impact assessments in hydrological modelling:** Scenarios should describe changes in a sufficient number of climate variables on a spatial and temporal scale that allows for impact assessment (Nigel, 2004). Hydrology modelling at watershed scale is restricted to the climate change impact to the streamflow. Then, the resolution of climate change downscaling may affect on the local scenarios over the watershed scale. In this regard, A2 and B2 scenarios as the finest IPCC scenarios meet the requirements of the climate change data in hydrology modelling. Thus, the applicability of A2 and B2 scenarios in estimating impacts of climate change at a watershed scale is more realistic compared to other scenarios, which were constructed at a global scale.

- **Representativeness:** The scenarios should be representative of the potential range of future Using a single climate change scenario is not recommended for an environmental investigation. Then, two scenarios were selected, HadCM3-A2, and HadCM3-B2. A2 scenario (Medium-High Emissions scenario) is a scenario with higher rates of greenhouse gas emissions in combination with higher sulphate and other aerosol emissions while B2 scenario (Medium-Low Emissions scenario) is a lower rate of emissions that assumes the world is more committed to solving global and local environmental (IPCC, 2007).

- **Compatibility with HadCM3-GCM model:** HadCM3 model in SDSM involves A2 and B2 scenarios. The predictor variables are supplied on a grid box. It provides a zip file contains three directories: NCEP-1961-2001, H3A2a-1961-2099 and H3B2a-1961-2099.

- **Uncertainty:** It brings to the question that to what would be the effect of IPCC different scenarios in downscaling and to what extent they would affect the local hydrology processes. The main reason in selection of multiple climate change scenarios is to build a realistic picture of the range of climate and reveal impact response to changes in atmospheric composition. However, the main source of uncertainty of climate change impact studies in humid climates stems from the choice of Climate Change Models rather than IPCC scenarios (Prudhomme and Davies, 2009). HadCM3 model assumes IPCC different A2 and B2 scenarios as a higher and lower rate of emissions respectively to project the future climate. Hence, A2 and B2 scenarios have been used to generate a range of local climate change scenarios using statistical downscaling model in the watershed scale.

As a result, A2 and B2 IPCC scenarios are the currently most reliable scenarios to assess climate change at fine scale but A1 and B1 scenarios do not meet the needed resolution to assess the climate change at local scale which is required for hydrological modelling. Thus, applicability of A2 and B2 scenarios in estimating impacts of climate change at a watershed scale is more realistic compared to other scenarios, which were constructed at a global scale.

# 5- HYDROLOGICAL MODELLING

This chapter focuses on formulating a hydrological model in Klang watershed. GIS system facilitates driving hydrologic parameters required for the watershed and hydrologic modelling to simulate surface runoff. Hec-Geo-HMS extension is used to derive and transfer the hydrological parameters into HEC-HMS to implement further analysis of the hydrological modelling of Klang watershed. A rainfall-runoff model was used to simulate the impact of climate change on runoff value. It was made by linking to the climate change output to describe the streamflow regime in the future based on the climate change scenarios. It was performed by making a linkage between large scale climate variables as provided by GCM- HadCM3 model and daily precipitation, temperature and evaporation at the local site using the SDSM tool. The effects of climate change were estimated by considering the proportions of the downscaled mean and maximum precipitation output by SDSM as described in the Chapter 4.

## 5-1- Hydrologic Modelling for Klang Watershed

In this study, two steps have been conducted as given in Figure 63, to simulate the hydrologic modelling using HEC-HMS in Klang watershed. Initially, the watershed was divided into homogeneous sub-watersheds using Hec-Geo-HMS to get the sub-watershed geometric data. Then, the hydrological modelling was developed in HEC-HMS for the watershed using all the parameters obtained from the previous step. The rainfall-runoff (USACE-HEC, 2000) hydrologic model was used to predict runoff in the watershed. The rainfall-runoff model takes into account the influences of physical parameters of the watershed such as climatic, topography, landuse, soil data and boundary condition over the watershed to simulate runoff. The hydrological soil type was derived from soil data and combined with landuse data to generate the SCS-CN loss rate. The current (observed) and future rainfall, temperature and evapotranspiration downscaled by SDSM (Chapter 4) are used as input into the Meteorological modelling in HEC-HMS.

Finally, the flow hydrographs was produced to determine the streamflow regime for the future corresponding to the IPCC scenarios. Figure 63 illustrates a diagram representing the flow diagram of runoff and peak flow estimation and prediction for the future in Klang watershed.

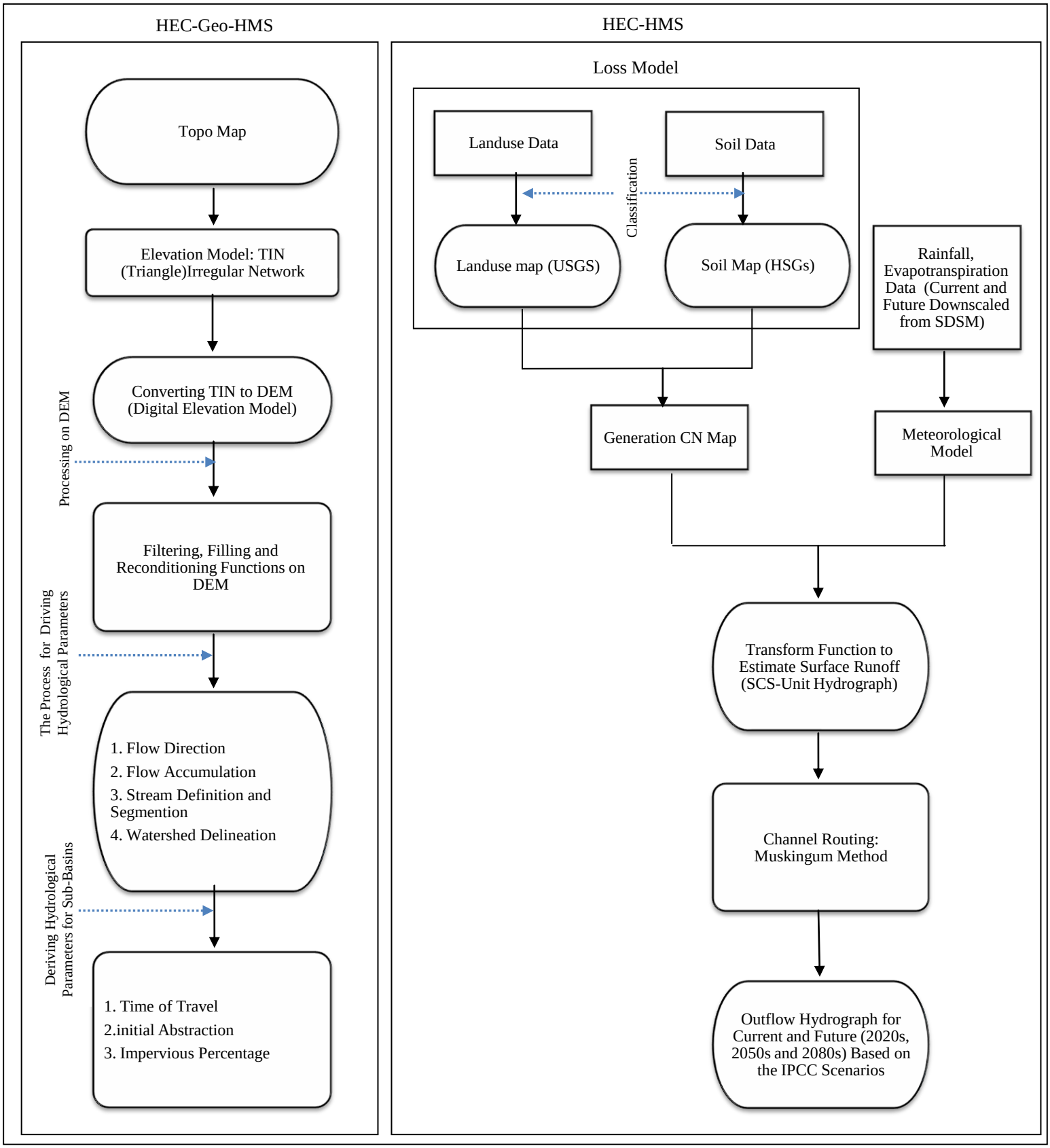


Figure 63 Flow diagram of runoff and peak flow modelling using HEC-HMS

## 5-2- Watershed Modelling

The hydrological parameters needed in the rainfall-runoff modelling were generated using Hec-Geo-HMS. The data layers have been driven from the watershed physical characteristics including watershed area, perimeter, length of the river, mean elevation, slope, runoff coefficient, lag time, landuse and soil unites. These hydrological parameters could be generated automatically by GIS system using Hec-Geo-HMS for each sub-watershed of Klang. Thus, runoff values are estimated on each sub-watershed system from the upstream to the watershed outlet throughout the streamflow network.

### 5-2-1- Building a Digital Elevation Model of Klang Watershed Using TIN (Triangular Irregular Network)

To build the TIN of Klang watershed, the topo maps (at scale of 1:25000 and 1:10000) and also spot heights were used. The topo maps have Malaysia's coordinate system (Rectified Skewed Orthomorphic-RSO projection). The highest and lowest elevations of the elevation points are 5 and 1404, respectively. Figure 64 illustrates the elevation model of the watershed developed in ArcGIS. Hec-Geo-HMS requires the DEM format as the basic input for the watershed delineation. Therefore, the TIN of Klang watershed was converted to the DEM format. One of the most important concerns in building DEM is to determine its cell size. Maidment (2002) has proposed a holistic DEM cell size in terms of their application. It has been represented by a 30 m cell size of DEM in urban watershed.

In this study, the DEM was developed at 30 metre cell size which seems to be efficient for a scale of 1:25000 (Hengl, 2006). Nine series of topo maps at 1:25000 scale were used to make the elevation map of Klang watershed. The data were acquired from the Malaysian department of surveying and mapping (JUPEM). However, the digital topography at the scale of 1:25000 does not cover the urban area of Klang watershed. Then the topo maps in the scale of 1:10000 used to fill the gap of elevation data.

### 5-2-2- DEM Optimisation

Topography is the base data to determine the flow direction of streamflow across a watershed. This data is considered as the most significant data which affects the hydrological models. Consequently, any uncertainty in the topographic models is propagated into the output of hydrologic model prediction, causing inaccuracies (Wua et al., 2008). The spot heights (Figure 65) was used to combine to the topo maps to promote the accuracy of the developed DEM, as the spot heights are often point elevations of the ridges and peaks of Klang watershed.

### 5-2-3- Delineation of watershed Boundary, Outlet and Stream Network Layers

As mentioned before, the initial DEM of Klang watershed was built from topo maps. At first, raw DEM was smoothed by filtering in GIS to smooth the sharp ridges and pits. Then, the fill function in GIS was run on it to remove the pits to delineate the stream network. Burn-DEM method was run using AGREE-DEM algorithm in Hec-Geo-HMS extension to extract the more accurate stream network from the DEM. Smoothing, filling depressions/sinks and reconditioning functions were run on the DEM of Klang watershed for automatic delineation which will be preceded through the flow direction, flow accumulation, stream definition, stream segmentation and watershed delineation.

#### 5-2-3-1- DEM Smoothing

Filtering is a spatial analysis tool in GIS for smoothing the sharp ridges and pits exists in the created DEM. GIS involves two kinds of filtering which are Low Pass (smoothes the DEM) and high pass (enhances the edges and boundaries of DEM), processing on focal functions with a weighted kernel neighbours. Low filter option in GIS as an averaging filter was run to assign the value of cells in the 3*3 window. The centre is assigned by the sum of the products of the cell value and its direct neighbours which are 8 adjacent pixels in a 3 x 3 filter. In low filter all 9 cells have an equal weight to determine the value of the centre cell. The sum of all 9 specified weights in the low filtering is equal to 1 as not changing the general elevation after

processing. It increases the elevation values at pit cells and decreases at peak cells. Table 20 shows the changes of the DEM characterisations by low filter. Figure 66 shows the smoothed DEM

Table 20 The smoothing statistics of DEM

| DEM statistics | Min | Max | Mean | Standard deviation |
|---|---|---|---|---|
| After Filtering | 10.48 | 1398.00 | 198.01 | 221.67 |
| Before Filtering | 5.12 | 1404.00 | 193.56 | 216.88 |

### 5-2-3-2- Filling Depressions / Sinks

Hec-Geo-HMS is an extension in GIS that provides pre-processing of the DEM to remove sinks, pits and null data. The pits and depressions have to be filled to allow water to flow across the landscape. The depressionless DEM was developed by fill function through the Arc Hydro tool in GIS to fill the pits by increasing its elevation to the level of the surrounding terrain.

### 5-2-3-3- DEM Reconditioning

AGREE algorithm developed by Hellweger and Maidment (1997) was used to modify the DEM by imposing the stream network on it. The river vector map was burnt into the DEM. Table 21 gives the specified stream buffer, smooth and sharp drop for the segments of the drainage network of Klang watershed. Figure 67 illustrates the DEM reconditioning map for Klang watershed.

Table 21 Changing the parameters of DEM reconditioning for stream segments of the drainage network of Klang watershed

| Stream/Segment | Stream Buffer (no of cell) | Smooth drop/raise | Sharp drop raise |
|---|---|---|---|
| Jinjang | 20 | 1 | 1 |
| Gombak | 20 | 1 | 1 |
| Bunus | 20 | 1 | 1 |
| Ampang | 40 | 2 | 2 |
| Klang | 40 | 2 | 2 |
| Kerayong | 40 | 2 | 2 |

### 5-2-3-4- Flow Direction

The flow direction of Klang DEM was created based on D8 algorithm (Jenson and Domingue, 1988). The direction of flow is determined based on the lowest cell's slope than its neighbour. As Archydro extension was used, the maximum drop was assumed for each cell to specify the flow direction. The maximum drop is calculated by the most changing in elevation corresponding to the distance between two cells centre. Figure 68 shows the Flow Direction of Klang watershed.

### 5-2-3-5- Flow Accumulation

Flow direction grid is used as input to create flow accumulation of Klang DEM. Flow accumulation is produced by taking the total number of cells of flow direction grid which flows into each cell. The cells with high accumulation are designated as stream network. Figure 69 shows the flow accumulation for Klang DEM.

### 5-2-3-6- Stream Definition and Stream Segmentation

This function provides a threshold value to compute the stream grid. It assigns a value of 1 to all the cells in the flow direction grid which have the value greater than the given threshold. A threshold value in this function can be defined based on number of cells or area. Then, it affects on dense of the stream network which will result the number of sub-watersheds delineated. Tarboton and Mohammed (2010) have developed TauDEM software for watershed delineation. They provided threshold value to delineate the watershed according to geomorphological river network properties. The threshold value of 8 $km^2$ for Klang watershed was assumed for stream definition function. In stream segmentation function, a unique value was given to each segment of the stream network. In Klang watershed 39 separated segments were identified in which each segment composed of cells with a same grid code. Figure 70 illustrates the stream segmentation of Klang watershed.

### 5-2-3-7- Watershed Delineation

Once the stream segmentation grid has been prepared, the watershed delineation can be run to delineate the sub-watersheds that belong to the stream segment. Delineation is performed for a grid in which each cell allocates a specific value based on the stream segments in the whole of DEM. Since 39 streams were produced by stream segmentation function with the same number, 39 sub-watersheds were generated indicating to which sub-watershed the segment stream belongs. Figure 71 illustrates the automatic watershed delineation of Klang watershed.

### 5-2-3-8- Optimisation of the Delineated Watershed

To optimise the final watershed map, some useful points and objects located in Klang watershed were identified in compliance with reality of the sub-watershed boundaries. The benchmark points have been found in the area distributed on the watershed map. Hec-Geo-HMS has useful tools such as watershed merge, delineate batch point and split watershed at confluences to amend the boundaries and outlets. Finally, 33 sub-watersheds were generated. Figure 72 shows the benchmarks used to conduct optimisation of Klang watershed.

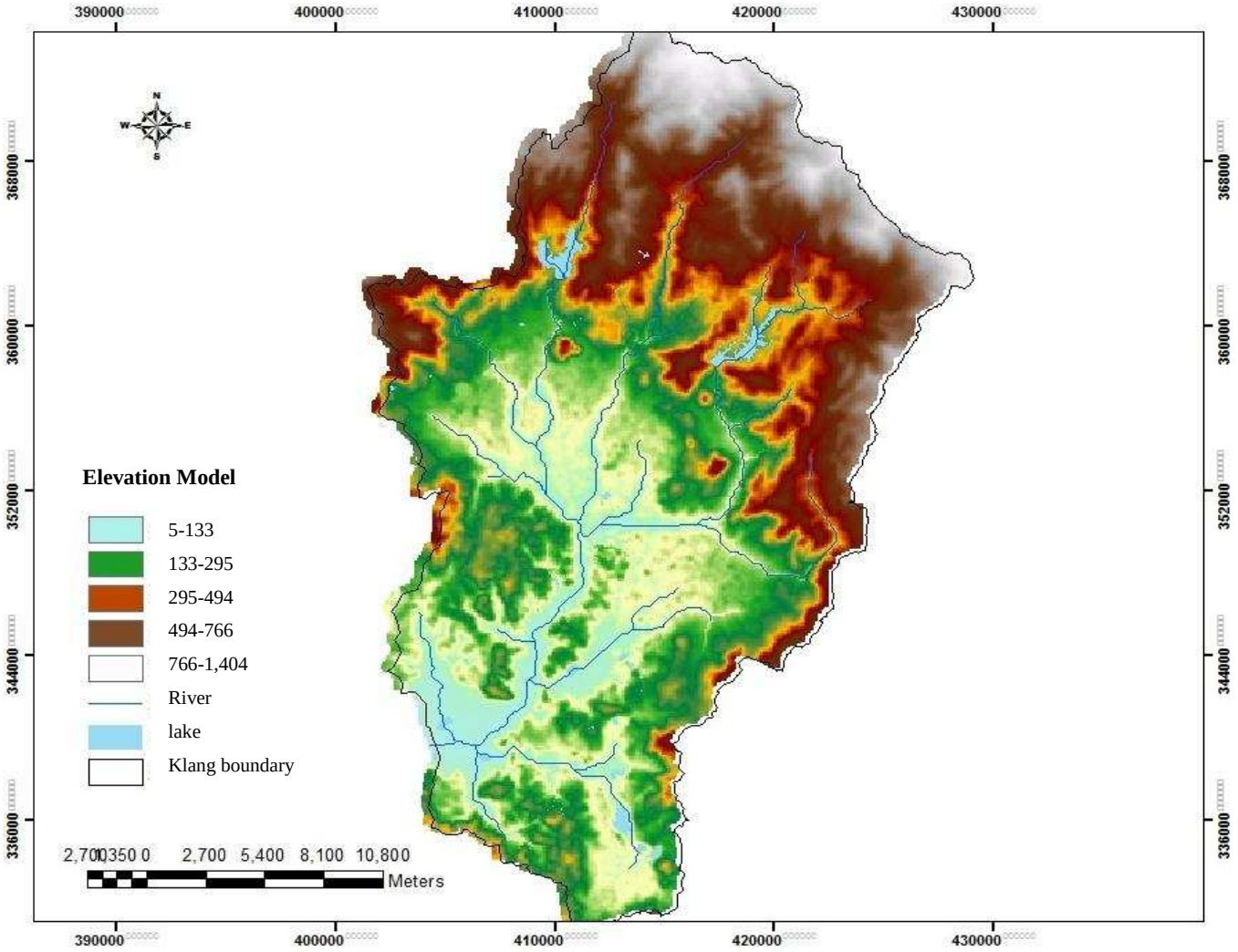


Figure 64 Digital Elevation Model of Klang watershed (DEM format)

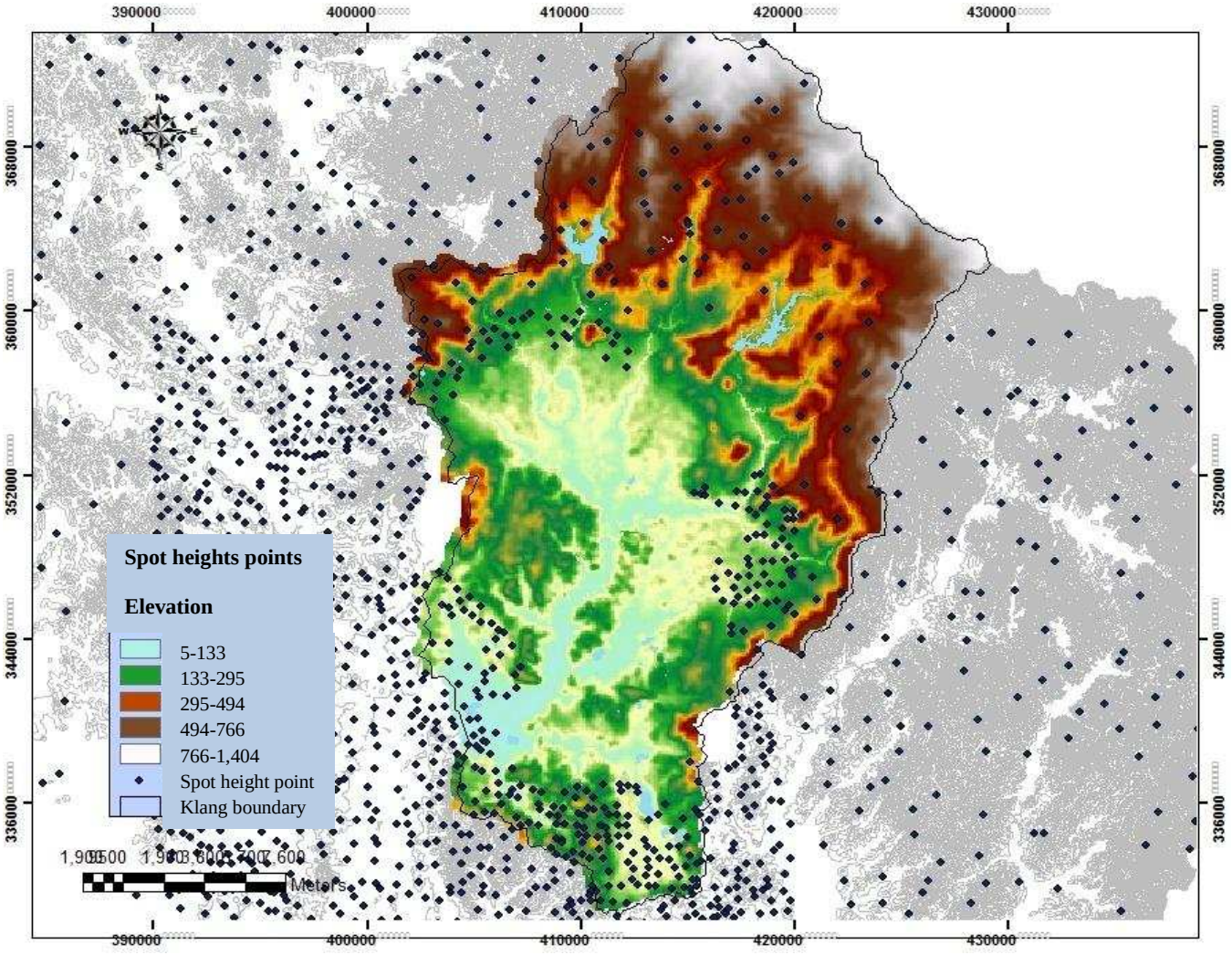


Figure 65 Spot heights for DEM optimisation

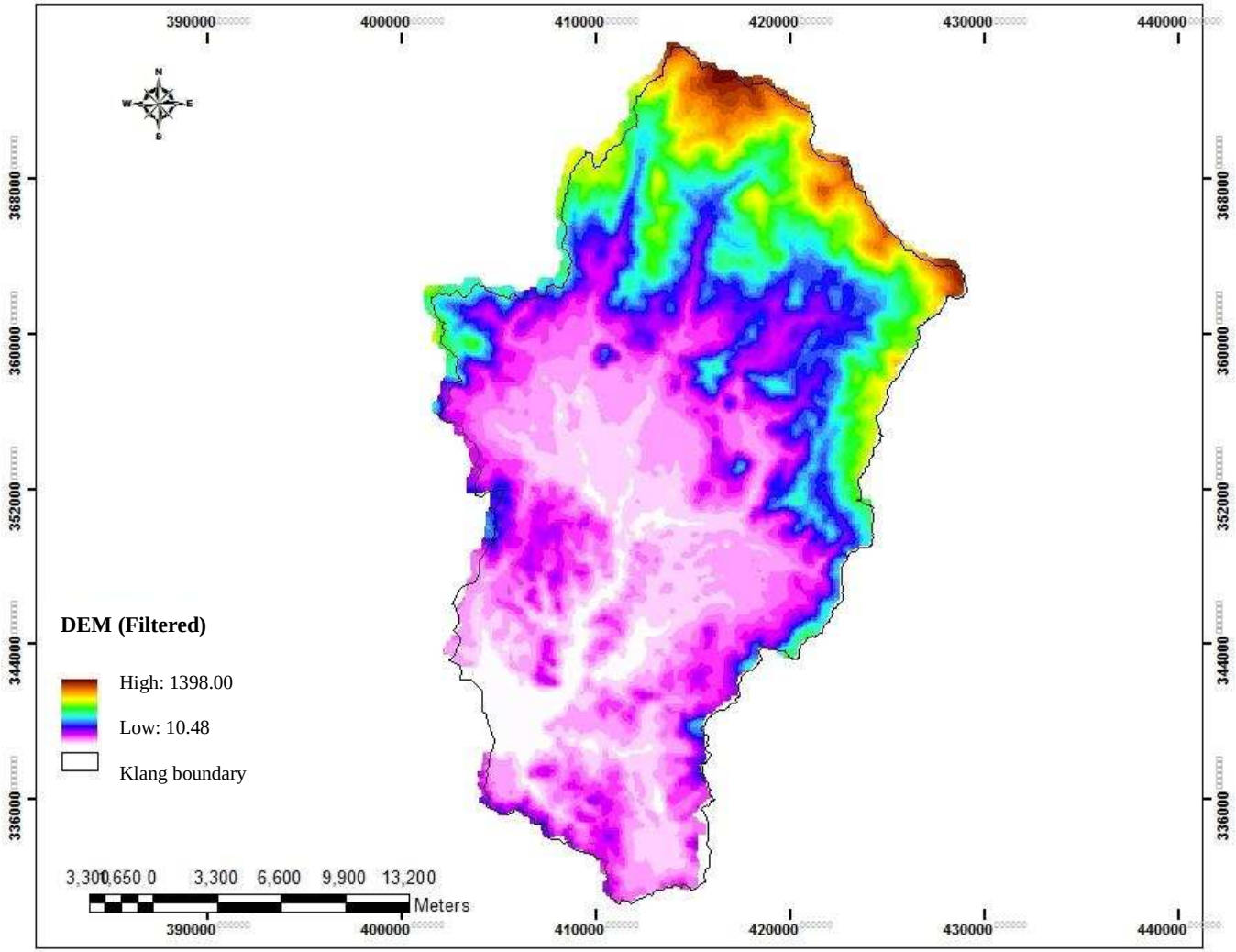


Figure 66 Smoothed DEM of Klang watershed

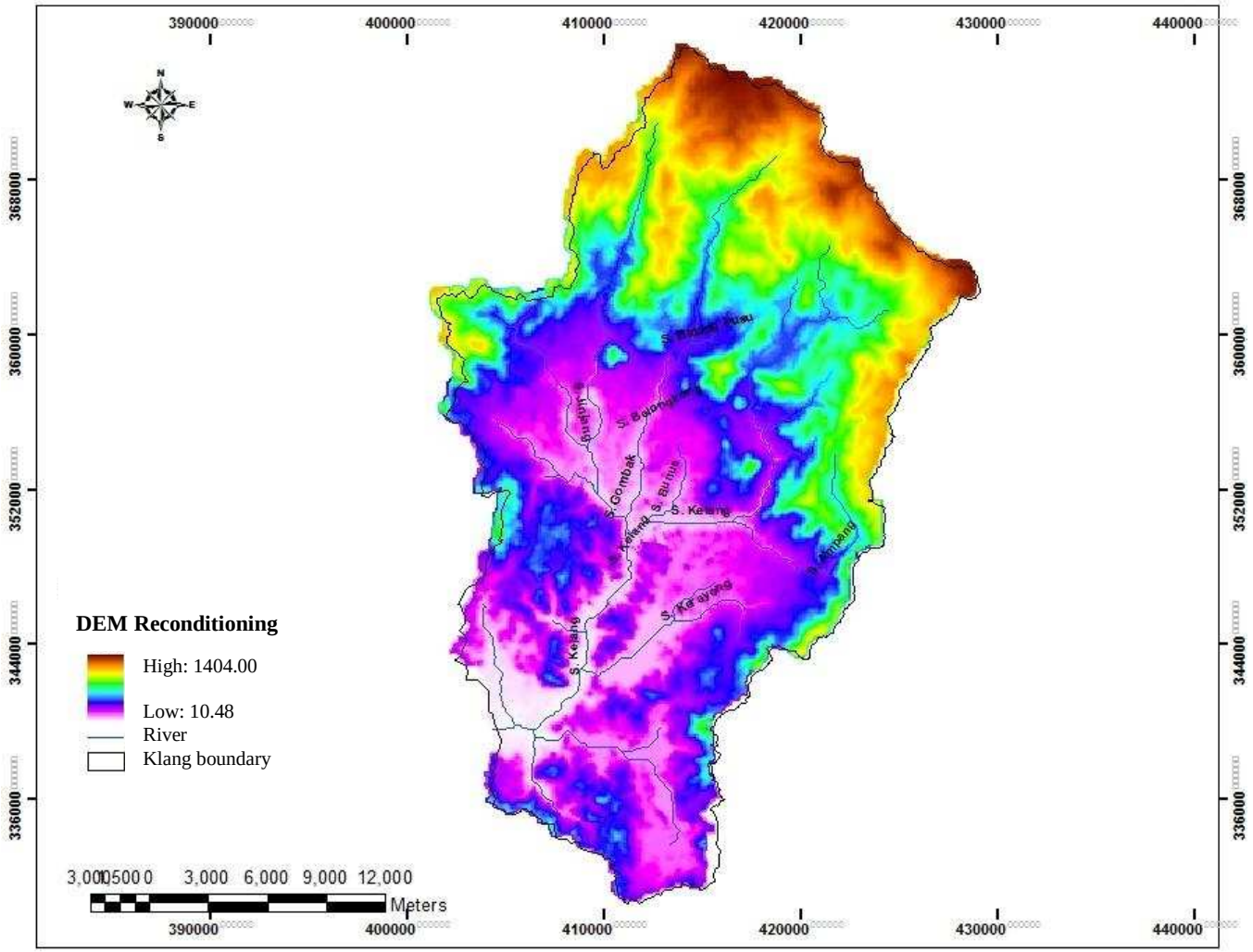


Figure 67 DEM Reconditioning for Klang watershed

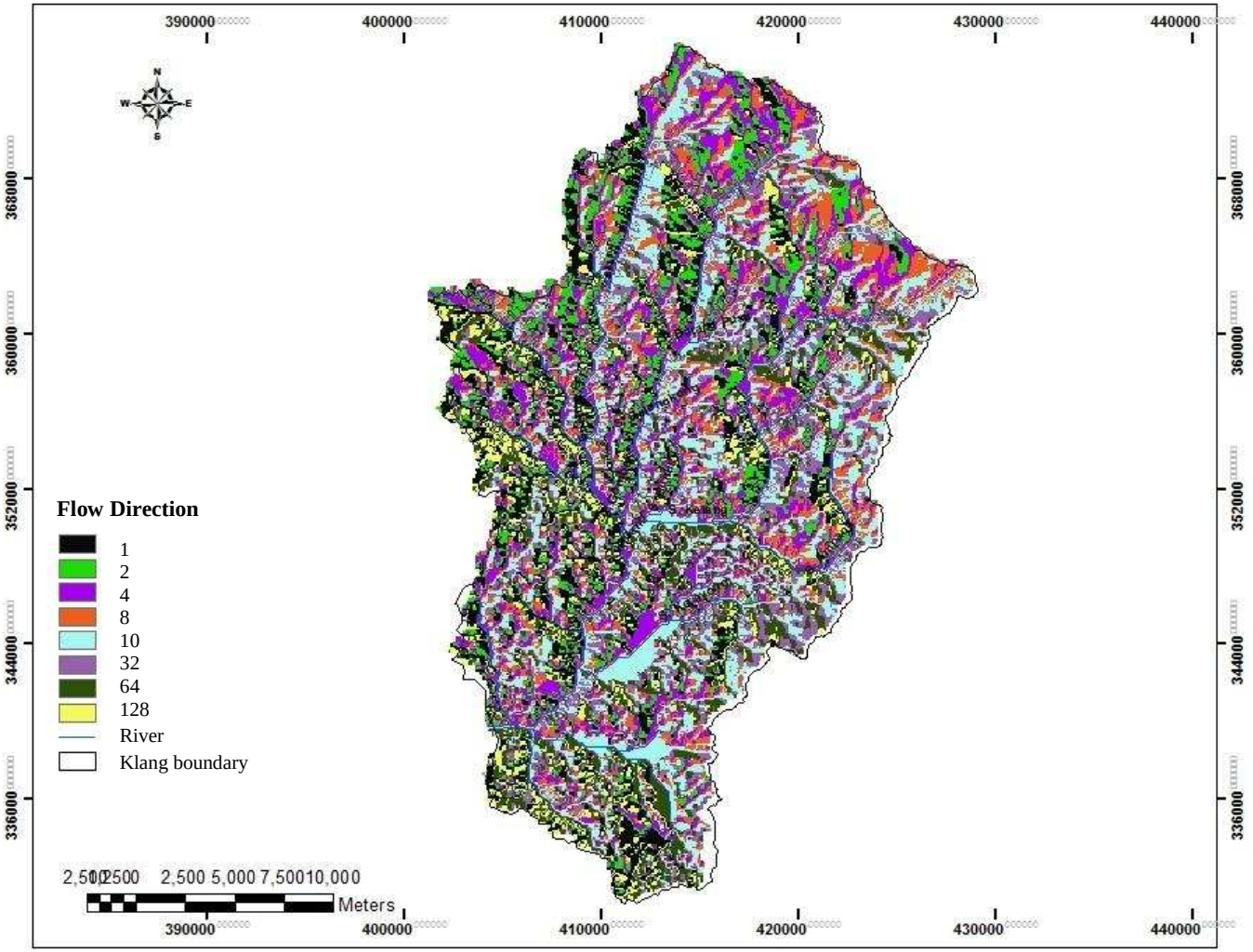


Figure 68 Flow direction map for Klang watershed

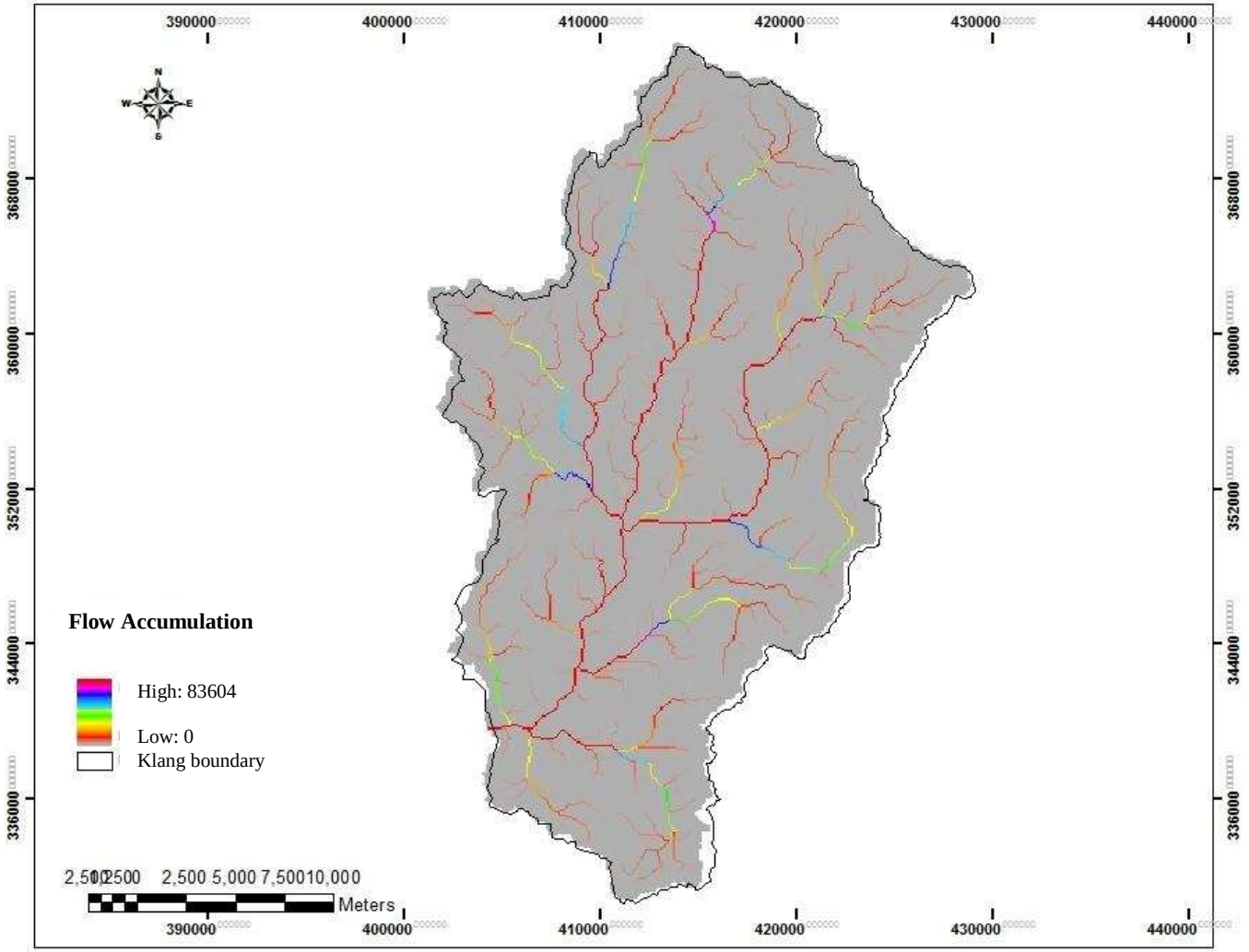


Figure 69 Flow accumulation map for Klang watershed

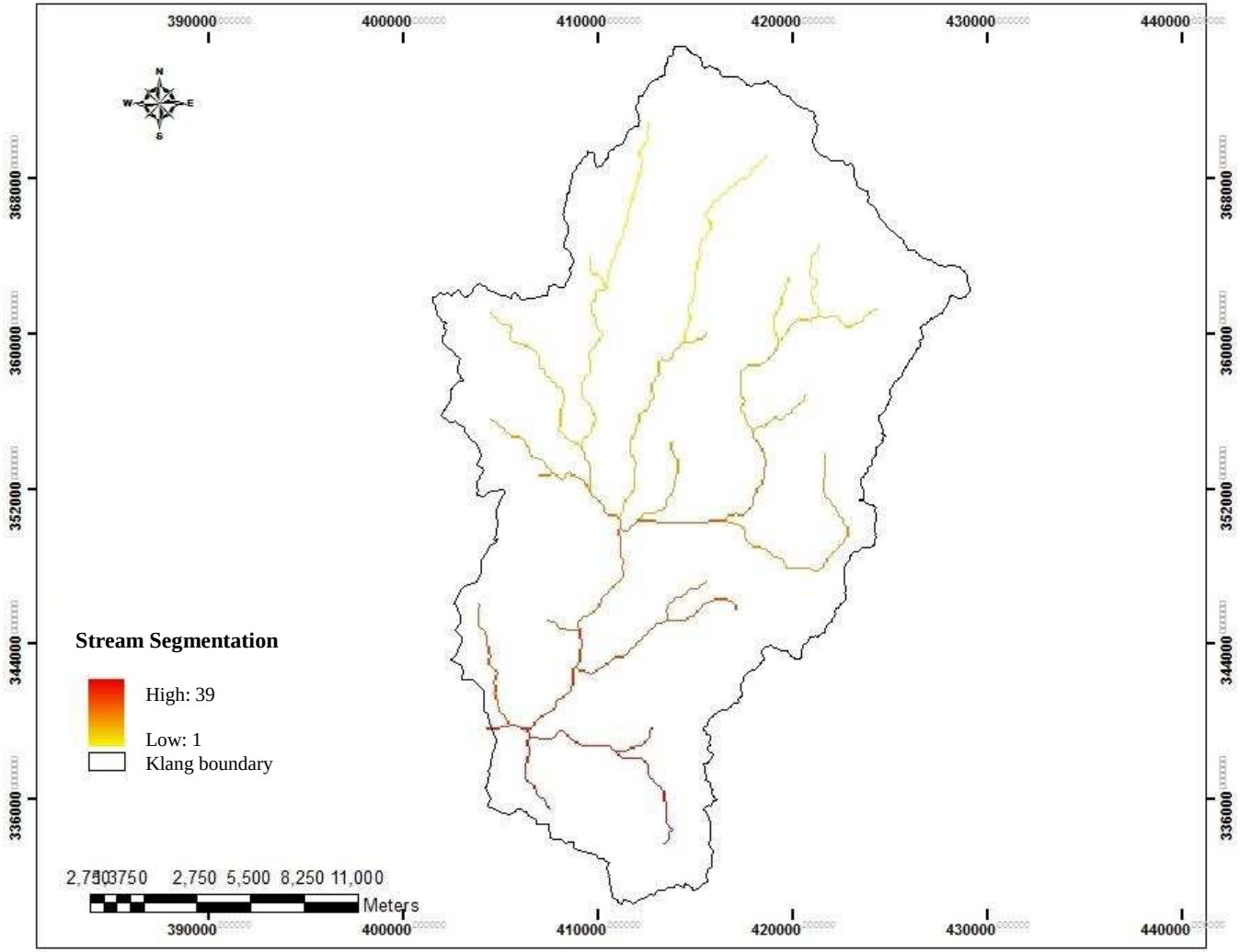


Figure 70 Stream segmentation map for Klang watershed

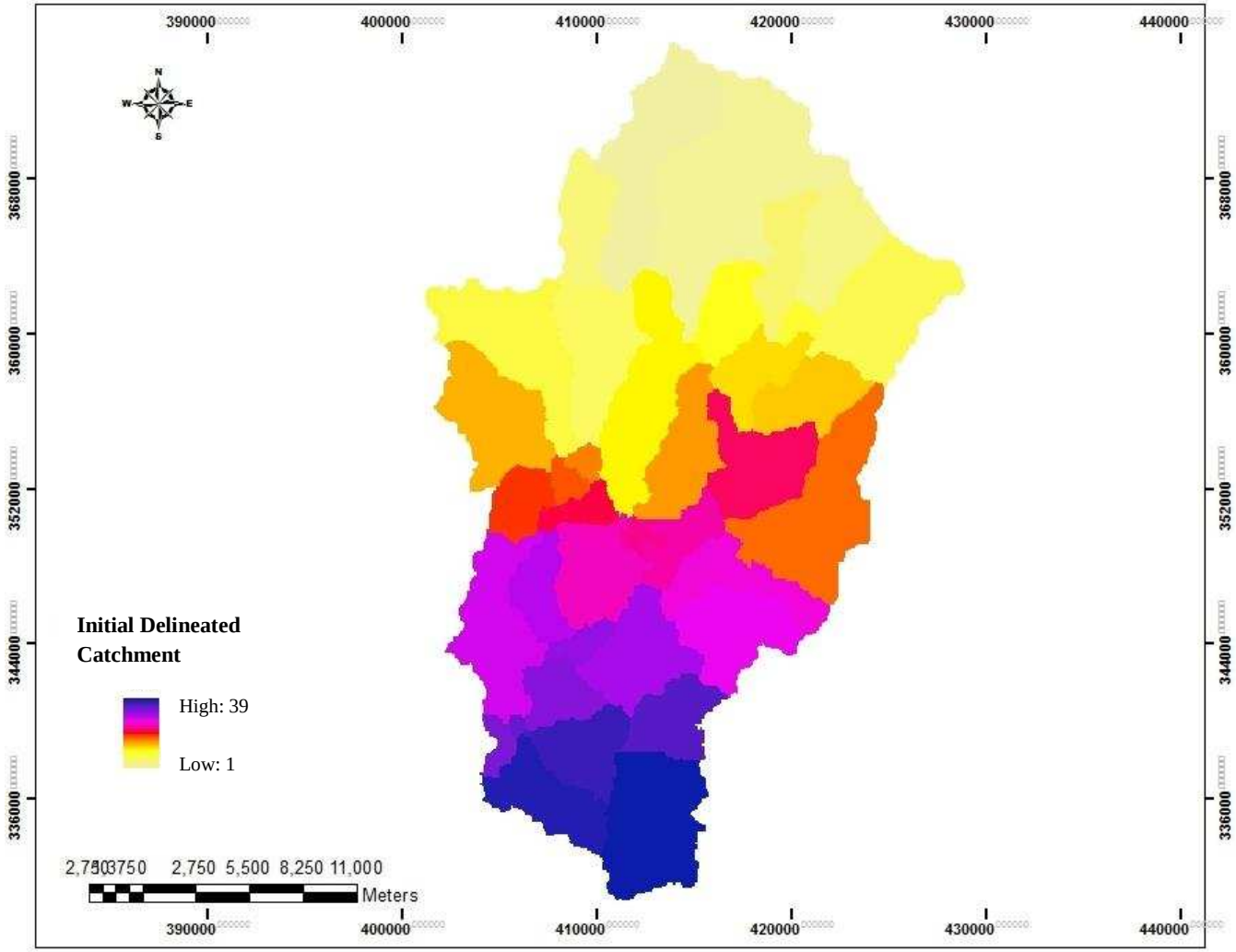


Figure 71 Automatic watershed delineation of raw elevation map in GIS system for Klang watershed

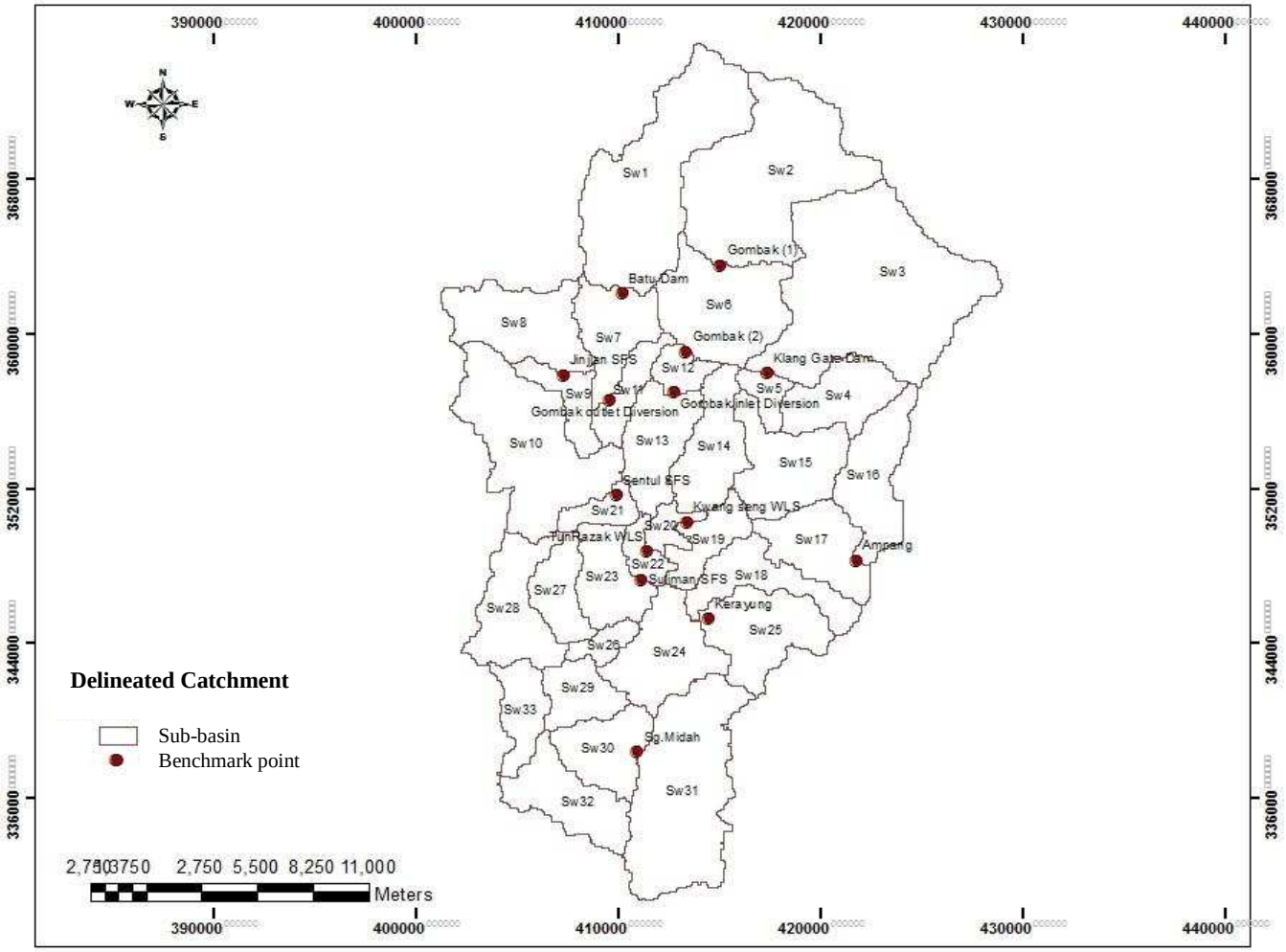


Figure 72 Benchmark points used for optimisation of delineated sub-watershed

## 5-3- The Runoff Simulation

HEC-HMS is software to simulate the rainfall-runoff relations of a watershed system which can be obtained from the Hydrologic Engineering Centre's home page at: http://www.wrc-hec.usace.army.mil/.

The main reason for using rainfall-runoff is to account for the influences of physical parameters of the watershed representing the boundary condition over the watershed to simulate runoff. HEC-HMS provides various methods suitable for a long period continuous simulation which are necessary in this research. The steps involved in hydrology modelling for Klang watershed can be divided into five categories: Estimation of Rainfall loss rate, Hydrographical Transformation, Channel routing, Reservoir flood routing and Meteorological modelling.

The overall framework of HEC-HMS is described as follows, Watershed delineations have been driven for Klang watershed to extract hydrological parameters which was used as an input into HEC-HMS hydrology model. The SCS-CN loss method in HEC-HMS needs the data such as CN, initial abstraction, potential soil storage and imperviousness. These data have been developed using GIS spatially. Figure 73 shows the Hec-Geo-HMS model for Klang watershed. The physical watershed characteristics such as watershed area, perimeter, watershed length and slope were automatically calculated in Hec-Geo-HMS (Table 22).

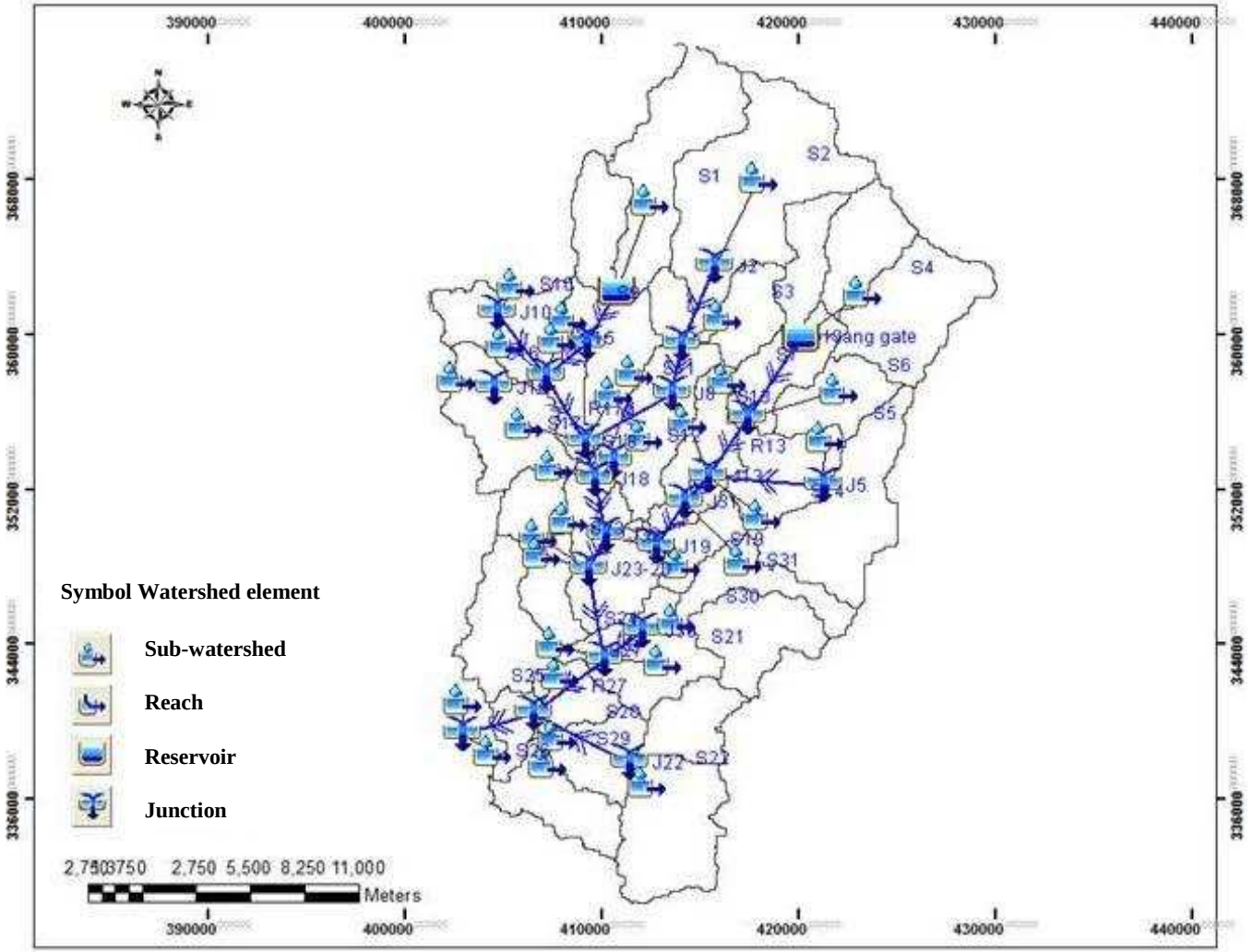


Figure 73 Klang watershed model using Hec-Geo-HMS

Table 22 Physical characteristics of Klang watershed

| Sub-watershed | Area ($km^2$) | Mean Elevation (m) | Watershed Slope (%) | River Slope (%) | Longest Flow Length (km) |
|---|---|---|---|---|---|
| 1 | 53.77 | 457.53 | 23.25 | 0.05 | 15.24 |
| 2 | 56.06 | 517.27 | 23.95 | 0.00 | 13.95 |
| 3 | 76.23 | 379.32 | 19.82 | 0.03 | 15.14 |
| 4 | 16.18 | 213.12 | 16.21 | 0.02 | 8.95 |
| 5 | 4.88 | 122.97 | 15.35 | 0.01 | 3.39 |
| 6 | 29.92 | 181.15 | 13.46 | 0.04 | 5.70 |
| 7 | 16.41 | 100.58 | 9.12 | 0.00 | 8.27 |
| 8 | 23.72 | 183.13 | 15.15 | 0.01 | 8.92 |
| 9 | 8.48 | 56.41 | 2.89 | 0.05 | 4.84 |
| 10 | 42.33 | 92.19 | 7.12 | 0.01 | 13.45 |
| 11 | 8.16 | 64.67 | 5.05 | 0.08 | 7.93 |
| 12 | 5.65 | 74.06 | 5.85 | 0.00 | 2.54 |
| 13 | 17.57 | 46.07 | 1.83 | 0.01 | 7.25 |
| 14 | 18.16 | 73.29 | 5.49 | 0.00 | 9.76 |
| 15 | 22.53 | 111.78 | 12.21 | 0.05 | 6.16 |
| 16 | 20.48 | 323.05 | 18.60 | 0.01 | 11.75 |
| 17 | 17.89 | 107.55 | 11.02 | 0.01 | 7.03 |
| 18 | 16.33 | 75.57 | 4.45 | 0.00 | 11.53 |
| 19 | 10.31 | 47.33 | 2.85 | 0.04 | 3.52 |
| 20 | 4.09 | 40.44 | 3.79 | 0.01 | 2.20 |
| 21 | 5.66 | 64.89 | 5.35 | 0.04 | 2.13 |
| 22 | 5.10 | 48.43 | 4.73 | 0.08 | 3.64 |
| 23 | 14.61 | 59.71 | 5.79 | 0.00 | 3.59 |
| 24 | 21.49 | 50.20 | 3.98 | 0.01 | 5.90 |
| 25 | 22.28 | 90.89 | 7.06 | 0.00 | 9.75 |
| 26 | 4.58 | 48.65 | 5.75 | 0.01 | 2.01 |
| 27 | 11.08 | 71.80 | 7.19 | 0.00 | 7.01 |
| 28 | 20.52 | 60.56 | 4.75 | 0.01 | 9.10 |
| 29 | 10.69 | 41.90 | 5.59 | 0.01 | 4.50 |
| 30 | 15.49 | 54.18 | 4.52 | 0.01 | 5.09 |
| 31 | 47.51 | 66.56 | 5.20 | 0.01 | 12.09 |
| 32 | 18.25 | 68.86 | 7.69 | 0.00 | 9.58 |
| 33 | 10.78 | 28.37 | 2.20 | 0.01 | 4.72 |

### 5-3-1- Loss Model

Five loss models in the Urban Stormwater Management Manual for Malaysia (MSMA) were proposed by the Department of Irrigation and Drainage (DID) in 2004. In this study, SCS Curve Number (CN) was used as loss model to estimate rainfall loss in the watershed. The applicability of CN loss model for Klang watershed has been investigated by Kabiri et al., 2013 and Akbari et al., 2012. The loss model is highly dependent on the Curve Number which is a function of the physical parameters of the watershed such as types of soil and landuse units, antecedent moisture condition to estimate amount of infiltration rates of soils. The advantages of using CN loss model for Klang watershed are explained as below:

- It is a simple conceptual method in distributed rainfall-runoff model to estimate the surface runoff amount from a storm rainfall amount which is well supported by empirical data (Shrestha et al., 2011). Then, Curve Number can be used as loss model in Klang watershed to estimate rainfall loss infiltrated by ground using empirical daily rainfall (26 years). The long period daily rainfall data were used for calibration and validation of HEC-HMS simulation for Klang watershed. The numbers of 16 years (from 1975- 1990) and the 11 year lengths from 1991- 2001 were selected for calibration and validation, respectively.

- It was not developed to consider the complexity of a small urban watershed with many different land-covers (USDA-NRCS, 2000). The area of klang watershed is 674 km² which is a fairly large watershed. Thus, applicability of CN loss model in estimating rainfall loss at Klang watershed scale is more realistic compared to other methods in HEC system.

- It is believed to be relatively accurate for larger scale watersheds include the storage ponds and flood control facility (Ramakrishnan et al., 2009). There are two major reservoirs in Klang watershed which are Batu dam and Klang Gate dam which play a crucial role for the region to control flooding and for water supply (DID, 2010; NAHRIM, 2010). HEC system provides various methods to conduct flow routing which is compatible with SCS-CN loss model.

- It has difficulty accurately to determine runoff for small precipitation events (less than 3") (Peters, 2010) while, Klang watershed often experiences the extreme precipitation events. Then, the method is believed to be more accurate for the watershed where extreme precipitation events occur.

- Curve Number loss model can be employed in the urbanised watershed with a long-term hydrologic simulation (Mishra and Singh, 2004). Urbanisation in Klang watershed has highly been increasing which reduces the infiltration rate, consequently. Therefore, the impervious area contributes as a significant data, demonstrating various infiltration rates in the watershed.

- It contributes directly vegetation cover type and density to runoff while, other methods such as Green-Ampt loss model was developed based on bare soil and does not directly consider the effects of landuse and vegetation cover which cause a high infiltration rate resulting in decreasing surface runoff (e.g. Barnes et al., 2002; Liu et al., 2006).

- Modified CN value is constructed by changing the value of two parameters (CN and Initial abstraction) to determine their effects on peak discharge. Optimisation is performed in amount of initial abstraction ratio ($\lambda$= 0.2) into ($\lambda$ = 0.05) for Klang watershed and consequently changing the curve number values for all the sub-watersheds (Akbari wt al., 2012). Woodward et al. (2003) developed the equation to convert $CN_{0.2}$ to $CN_{0.05}$. The values of two parameters (CN and Initial abstraction) are changed to determine their effects on peak discharge of flood. Results revealed that initial abstraction ($\lambda$=0.05) and $CN_{0.05}$ of daily rainfall by percent error in peak have given no significant difference rather than initial abstraction with 0.2 value and $CN_{0.2}$. The relation between $CN_{0.2}$ and $CN_{0.05}$ values are given in Table 26. The equation assumes the potential soil storage equivalent to initial abstraction ($\lambda$=0.05) as in Equation 32 (Woodward et al., 2003).

$$S_{0.05}=1.33(S_{0.20})^{1.15} \qquad \text{Equation 32}$$

Where, S is the potential soil storage (mm).

### 5-3-1-1- Determining Curve Number

The main objective of this section is to estimate the rainfall loss rate in the watershed using Curve Number Infiltration Method. According to the available data of Klang watershed, the SCS-CN Loss Method was used to estimate precipitation losses. In order to determine the Curve Number for Klang watershed, the landuse and soil maps are categorised based on the SCS-CN method and then are integrated to generate the CN map. The details are given below.

#### 5-3-1-1-1- Soil Categorisation

Soil type as one of the significant layers affects the rate of rainfall loss was classified based on the Hydrological Soil Group system (HSGs). In order to estimate soil properties in Klang watershed, the soil type was matched with US. Department of Agriculture (USDA) classification using a lookup table which was developed by Rawls et al. (1982) and McCuen et al. (1981). It relates the Brooks and Corey's soil hydraulic parameters to the 11 USDA soil texture classes. The relation between the soil units and SCS soil classification groups (HSGs) was created in Table 23 for Klang watershed. The hydraulic maps of Klang watershed are available in Appendix N.

Table 23 The relation between the soil units and Hydrological Soil Groups for Klang watershed

| **Soil series** | **Great Soil Groups (GSG)** | **Porosity (%)** | **Initial moisture (Volume ratio)** | **Hydraulic conductivity (mm/h)** | **Saturate water content (Volume ratio)** | **$HSG_S$** |
|---|---|---|---|---|---|---|
| Munchong-Seremban | Hapludox-Hapludults | 50.22 | 0.31 | 29.91 | 0.44 | A |
| Rengam-Jerangau | Paleudults-Hapludox | 51.49 | 0.31 | 29.91 | 0.44 | A |
| Serdang-Kedah | Paleudults-Hapludults | 47.67 | 0.25 | 10.90 | 0.45 | A |
| Telemong-Akob-Local Alluvium | Tropopsamments-Fluvaquents | 49.32 | 0.31 | 29.90 | 0.44 | A |
| Steepland | Palehumults | 0.00 | 0.17 | 6.52 | 0.50 | B |
| Mined Land | Mined Land | 0.00 | 0.17 | 6.52 | 0.50 | B |
| Water | Water | 0.00 | 0.00 | 0.00 | 0.00 | Water |

### 5-3-1-1-2- Landuse Categorisation

As explained in Chapter 3 (Section: 3-1-4), the landuse data, acquired from Department of Agriculture (DOA) is composed of the Malaysian landuse classes. USGS landuse classification of Klang watershed was then developed. The USGS codes were added to the landuse's attribute in GIS. Table 24 presents the USGS landuse classification in Klang watershed.

Table 24 Landuse classes present in Klang watershed

| Landuse | Area ($km^2$) | Percent of total area |
|---|---|---|
| Agriculture | 59.45 | 8.82 |
| Forest | 248.28 | 36.83 |
| Mining | 4.10 | 0.61 |
| Newly cleared land | 8.58 | 1.27 |
| Pasture | 6.23 | 0.92 |
| Swamps | 0.64 | 0.09 |
| Urban | 334.82 | 49.67 |
| Water body | 11.97 | 1.78 |
| Total area | 674.00 | 100.00 |

### 5-3-1-1-3- Overlaying the Landuse and Soil maps

USACE-HEC (2000) hydrologic model was used to predict runoff in the watershed. It provides the Curve Number (CN) value for the different landuse considering the four soil groups. In order to construct the CN value of Klang watershed, two landuse and soil layer in GIS were overlaid. Table 25 presents the CN values for the different landuse units along with the HSG soil group in Klang watershed and Figures 74 illustrates the overlaid map of the landuse and soil layers indicating CN values. To calculate the average value of the hydrologic parameters for each sub-watershed, the Cross function in Hec-Geo-HMS was used. Weighted average CN value is driven for each sub-watershed using Equation 33 (Fleming and Doan, 2010):

$$Hpv_{sub} = \frac{\sum A_i \ Hpv_i}{\sum A_i} \qquad \text{Equation 33}$$

Where, $Hpv_{sub}$ is weighted average of the hydrologic parameter for sub-watershed; $Hpv_i$ is the parameter value and $A_i$ is area inside the specified sub-watershed.

Table 25 Linking landuse, soil unit and CN of Klang watershed

| Landuse | $HSG_S$ | $CN_{0.2}$ | Landuse | $HSG_S$ | $CN_{0.2}$ |
|---|---|---|---|---|---|
| Agricultural station | A | 77 | Orchards | B | 65 |
| Agricultural station | B | 67 | Orchards | A | 43 |
| Agricultural station (cattle farm) | A | 76 | Orchards / rubber | B | 65 |
| Agricultural station (cattle farm) | B | 85 | Orchards / rubber | A | 44 |
| Agricultural station (diversified crops) | A | 67 | Orchards, neglected grassland | A | 58 |
| Agricultural station (diversified crops) | B | 77 | Orchards, scrubs | B | 43 |
| Agricultural station (oil palm) | A | 66 | Other mining areas | A | 76 |
| Agricultural station (oil palm) | B | 45 | Other mining areas, neglected grassland | A | 85 |
| Agricultural station (orchards) | A | 43 | Pond/lake | A | 100 |
| Agricultural station (orchards) | B | 65 | Poultry/ducks | B | 77 |
| Aquaculture | B | 100 | Poultry/ducks | A | 67 |
| Cemetery | B | 79 | Power lines | B | 98 |
| Estate building & associated areas | A | 92 | Power lines | A | 98 |
| Ex-tin mining areas | B | 85 | Railway | B | 98 |
| Forest | B | 55 | Railway | A | 98 |
| Forest | A | 43 | Recreational areas | B | 85 |
| Main road & highway | B | 98 | Recreational areas | A | 76 |
| Main road & highway | A | 98 | Reforested | B | 55 |
| Market gardening | B | 77 | Reforested | A | 43 |
| mixed horticulture | B | 77 | Rubber | B | 66 |
| mixed horticulture | A | 67 | Rubber | A | 45 |
| mixed horticulture, neglected grassland | B | 68 | Rubber/orchards | B | 77 |
| mixed horticulture, neglected grassland | A | 48 | Rubber/orchards | A | 77 |
| mixed horticulture, rubber | B | 71 | Rubber/scrubs | B | 77 |
| mixed horticulture, rubber | A | 66 | Rubber/scrubs | A | 77 |
| Neglected grassland | B | 58 | Rubbish disposal areas | B | 92 |
| Neglected grassland (main road and highway) | B | 98 | Scrubs | B | 43 |
| Neglected grassland / orchards | B | 61 | Scrubs/orchards | B | 65 |
| Neglected grassland, scrubs | B | 79 | Scrubs/orchards | A | 43 |
| Neglected grassland, scrubs | A | 42 | Swamps | B | 100 |
| Newly cleared land | B | 86 | Swamps/orchards | A | 100 |
| Newly cleared land | A | 77 | Swamps, scrubs | A | 100 |
| Newly cleared land (urban and associated areas) | B | 92 | Tin mining areas | B | 85 |
| Newly cleared land / urban and associated areas | A | 89 | Tin mining areas | A | 76 |
| Oil palm | B | 66 | Urban and associated areas | B | 92 |
| Oil palm | A | 45 | Urban and associated areas | A | 92 |

Table 26 The relation between $CN_{0.2}$ and $CN_{0.05}$ values for each sub-watershed in Klang watershed

| **Sub-watershed** | **$CN_{0.2}$** | **$CN_{0.05}$** |
|---|---|---|
| 1 | 46 | 20 |
| 2 | 46 | 18 |
| 3 | 45 | 35 |
| 4 | 54 | 21 |
| 5 | 72 | 18 |
| 6 | 58 | 23 |
| 7 | 78 | 46 |
| 8 | 73 | 65 |
| 9 | 91 | 57 |
| 10 | 85 | 35 |
| 11 | 89 | 74 |
| 12 | 81 | 73 |
| 13 | 90 | 63 |
| 14 | 87 | 57 |
| 15 | 85 | 84 |
| 16 | 43 | 65 |
| 17 | 82 | 73 |
| 18 | 89 | 73 |
| 19 | 92 | 78 |
| 20 | 92 | 71 |
| 21 | 89 | 74 |
| 22 | 90 | 74 |
| 23 | 87 | 76 |
| 24 | 91 | 78 |
| 25 | 89 | 78 |
| 26 | 89 | 76 |
| 27 | 88 | 65 |
| 28 | 89 | 71 |
| 29 | 90 | 55 |
| 30 | 81 | 69 |
| 31 | 86 | 78 |
| 32 | 76 | 78 |
| 33 | 92 | 80 |

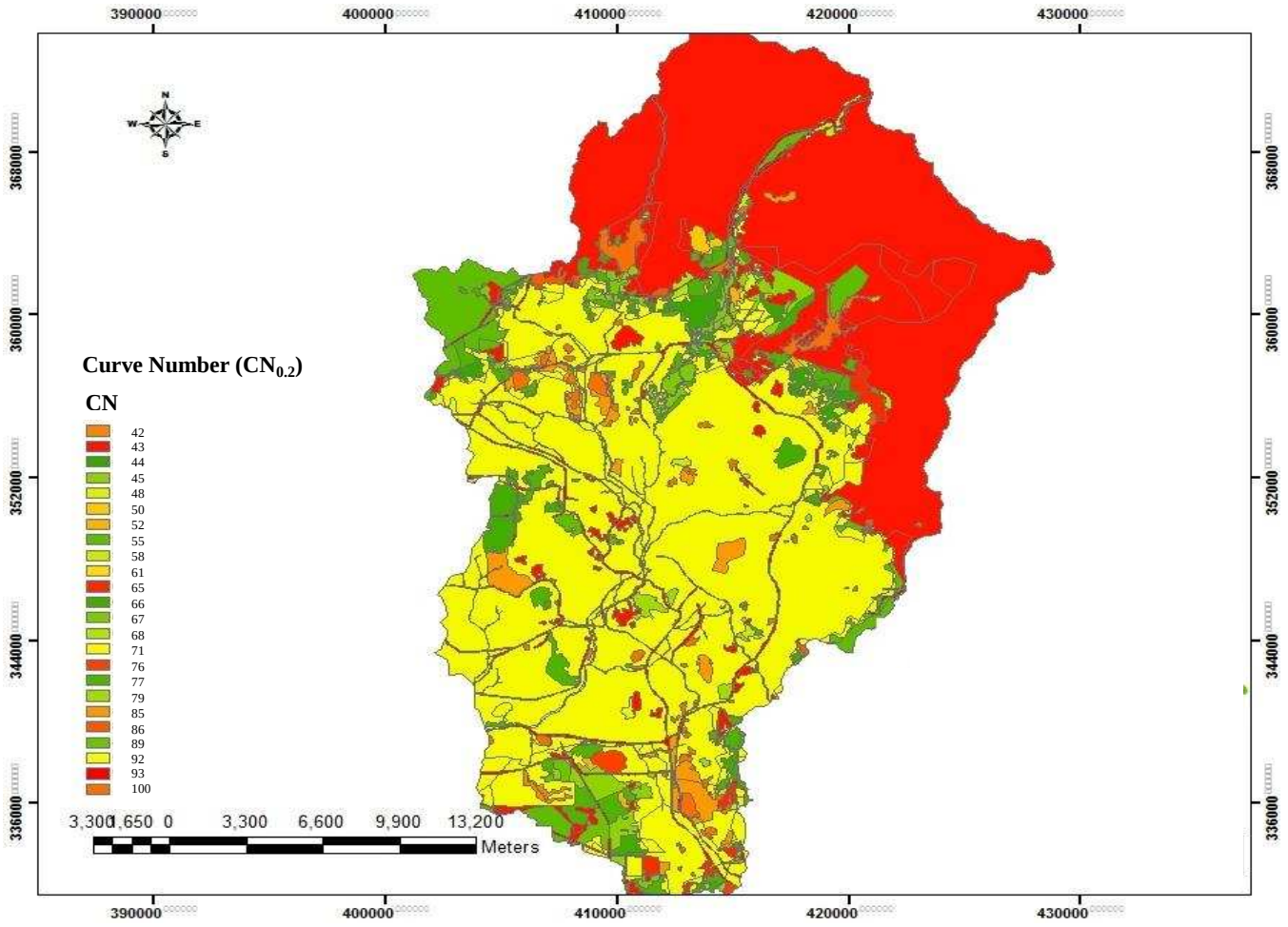


Figure 74 Curve Number ($CN_{0.2}$) map of Klang watershed

### 5-3-2- SCS Unit Hydrograph Transform

SCS Soil Conservation Service Unit Hydrograph (SCS UH) model in HEC-HMS requires watershed lag time and impervious percentage .The standard shape was employed in HEC-HMS to define the shape of the unit hydrograph. In this method the standard lag is defined as the length of time between the centroid of precipitation mass and the peak flow of the resulting hydrograph. Watershed lag is considered as 0.6 times the time of concentration of the flow. Table 27 gives the lag time, potential soil storage and initial abstraction calculated for each sub-watershed of Klang watershed.

Table 27 Hydrologic parameters of Klang watershed

| Sub-watershed | $CN_{0.2}$ | Lag Time (0.2) (hr) | Potential soil storage (0.2) (mm) | Initial abstraction (0.2) (mm) | $CN_{0.05}$ | Lag Time (0.05) (hr) | Potential soil storage (0.05) (mm) | Initial abstraction (0.05) (mm) |
|---|---|---|---|---|---|---|---|---|
| 1 | 46 | 3.72 | 298.17 | 59.63 | 20 | 80.22 | 1022.90 | 16.16 |
| 2 | 46 | 3.42 | 298.17 | 59.63 | 18 | 78.66 | 1123.60 | 17.54 |
| 3 | 45 | 4.12 | 310.44 | 62.09 | 35 | 49.71 | 463.44 | 8.12 |
| 4 | 54 | 2.37 | 216.37 | 43.27 | 21 | 58.82 | 932.15 | 14.91 |
| 5 | 72 | 0.71 | 99.17 | 19.83 | 18 | 32.75 | 1178.10 | 18.28 |
| 6 | 58 | 1.62 | 180.54 | 36.11 | 23 | 42.18 | 849.95 | 13.76 |
| 7 | 78 | 1.57 | 72.03 | 14.41 | 46 | 32.77 | 292.58 | 5.44 |
| 8 | 73 | 1.50 | 94.18 | 18.84 | 65 | 15.81 | 135.56 | 2.79 |
| 9 | 91 | 1.16 | 26.05 | 5.21 | 57 | 28.40 | 193.17 | 3.79 |
| 10 | 85 | 2.09 | 44.82 | 8.96 | 35 | 75.42 | 463.44 | 8.12 |
| 11 | 89 | 1.40 | 31.41 | 6.28 | 74 | 18.34 | 87.09 | 1.90 |
| 12 | 81 | 0.69 | 58.31 | 11.66 | 73 | 7.34 | 96.12 | 2.07 |
| 13 | 90 | 2.08 | 28.22 | 5.64 | 63 | 40.58 | 146.29 | 2.98 |
| 14 | 87 | 1.73 | 38.79 | 7.76 | 57 | 36.09 | 193.17 | 3.79 |
| 15 | 85 | 0.86 | 45.98 | 9.20 | 84 | 6.27 | 46.74 | 1.10 |
| 16 | 43 | 3.66 | 336.70 | 67.34 | 65 | 17.78 | 135.56 | 2.79 |
| 17 | 82 | 1.10 | 55.03 | 11.01 | 73 | 12.07 | 96.12 | 2.07 |
| 18 | 89 | 2.00 | 30.73 | 6.15 | 73 | 28.20 | 96.12 | 2.07 |
| 19 | 92 | 0.87 | 23.08 | 4.62 | 78 | 10.96 | 70.01 | 1.57 |
| 20 | 92 | 0.51 | 21.98 | 4.40 | 71 | 8.67 | 105.45 | 2.24 |
| 21 | 89 | 0.48 | 32.45 | 6.49 | 74 | 6.22 | 87.09 | 1.90 |
| 22 | 90 | 0.74 | 27.28 | 5.46 | 74 | 10.16 | 87.09 | 1.90 |
| 23 | 87 | 0.75 | 38.16 | 7.63 | 76 | 8.45 | 78.41 | 1.73 |
| 24 | 91 | 1.16 | 26.23 | 5.25 | 78 | 14.02 | 70.01 | 1.57 |
| 25 | 89 | 1.41 | 32.39 | 6.48 | 78 | 15.73 | 70.01 | 1.57 |
| 26 | 89 | 0.44 | 32.66 | 6.53 | 76 | 5.33 | 78.41 | 1.73 |
| 27 | 88 | 1.11 | 34.59 | 6.92 | 65 | 18.92 | 135.56 | 2.79 |
| 28 | 89 | 1.59 | 30.29 | 6.06 | 71 | 24.09 | 105.45 | 2.24 |
| 29 | 90 | 0.81 | 28.22 | 5.64 | 55 | 20.13 | 205.93 | 4.01 |
| 30 | 81 | 1.37 | 59.07 | 11.81 | 69 | 16.50 | 115.14 | 2.42 |
| 31 | 86 | 2.19 | 42.44 | 8.49 | 78 | 21.77 | 70.01 | 1.57 |
| 32 | 76 | 2.07 | 82.21 | 16.44 | 78 | 14.86 | 70.01 | 1.57 |
| 33 | 92 | 1.24 | 22.16 | 4.43 | 80 | 14.50 | 61.94 | 1.41 |

### 5-3-3- Impervious Surface

Impervious percentage for each sub-watershed must be entered in HEC-HMS. Impervious surfaces are the area covered by impenetrable material. It impedes the infiltration process in hydrology cycle and does not allow water being absorbed by soil. Therefore, loss calculation is not performed on the impervious surfaces. To do the SCS-CN runoff simulation in HEC-HMS, an impervious area in terms of percentage is needed. To determine the impervious area in Klang watershed the topo sheets at 1:25000 scale were used. The building blocks were extracted from the topo sheets and the impervious area for each sub-watershed was driven using cross function in Hec-Geo-HMS. Table 28 shows impervious area for Klang watershed.

Table 28 Impervious area for each sub-watershed in Klang watershed

| Sub-watershed | Impervious ($m^2$) | Impervious (%) |
|---|---|---|
| 1 | 2250.00 | 0.55 |
| 2 | 318.87 | 0.77 |
| 3 | 0.00 | 0.00 |
| 4 | 543.77 | 1.32 |
| 5 | 829.56 | 2.01 |
| 6 | 391.44 | 0.95 |
| 7 | 1176.10 | 2.85 |
| 8 | 1390.42 | 3.37 |
| 9 | 1115.73 | 2.71 |
| 10 | 1086.92 | 2.64 |
| 11 | 890.82 | 2.16 |
| 12 | 687.48 | 1.67 |
| 13 | 885.50 | 2.15 |
| 14 | 828.23 | 2.01 |
| 15 | 1291.42 | 3.13 |
| 16 | 653.72 | 1.59 |
| 17 | 991.24 | 2.40 |
| 18 | 1440.21 | 3.49 |
| 19 | 1430.75 | 3.47 |
| 20 | 3352.57 | 8.13 |
| 21 | 3936.02 | 9.55 |
| 22 | 3387.14 | 8.22 |
| 23 | 1194.32 | 2.90 |
| 24 | 1456.68 | 3.53 |
| 25 | 1175.86 | 2.85 |
| 26 | 697.86 | 1.69 |
| 27 | 1049.89 | 2.55 |
| 28 | 1526.25 | 3.70 |
| 29 | 979.82 | 2.38 |
| 30 | 1095.66 | 2.66 |
| 31 | 1786.28 | 4.33 |
| 32 | 1052.52 | 2.55 |
| 33 | 2354.57 | 5.71 |

### 5-3-4- Streamflow (Channel) Routing

HEC-HMS provides various methods to conduct flow routing in reach element which needs a different level of details. In this study, Muskingum method was used to calculate the hydrologic river routing in Klang watershed. Muskingum method in HEC-HMS was used due to its simplicity and modest data requirement which make it practical to be used for Klang watershed while other methods require complex data to use in HEC-HMS. The value of K can be calculated by length of reach divided by the average flow velocity and the value of X is between 0.0 and 0.5. A value of 0.0 represents maximum attenuation from the procedure and 0.5 provides the minimum attenuation. However, in natural channels X ranges from 0.1 to 0.3 (Raghunath, 2006). To assign the value of X in the Muskingum method in Klang watershed, a value of 0.4 was used in a landuse map of the watershed. This reveals the drainage system has been strongly urbanised and the natural channel in the area has been transformed into concreted channels. According to the channel properties, a high value of 0.4 was assumed.

### 5-3-5- Reservoir Flood Routing

There are two major reservoirs in Klang watershed which are Batu dam and Klang Gate dam. Routing methods are used to simulate the storage of reservoir. In this regard, HEC-HMS provides three methods namely storage-outflow relationships, specified release and the method based on individual components of the outlet works. With the available data from reservoirs (Appendix O), the Storage-Discharge Method was used for both dams. Figures 75 and 76 illustrate Storage-Discharge relationships of Klang Gate dam and Batu dam as derived in HEC-HMS, respectively.

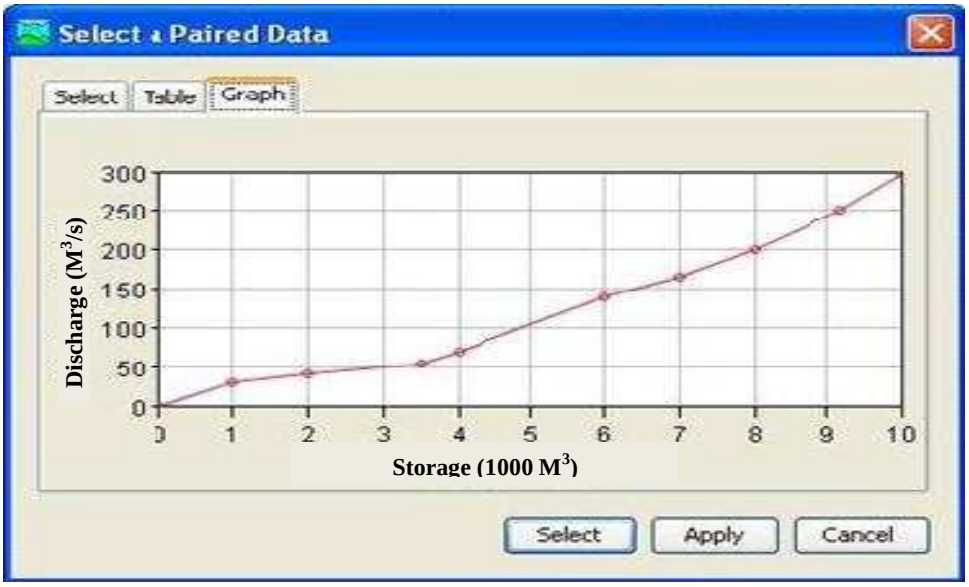


Figure 75 Storage-discharge relationship of Klang Gate dam (output of HEC-HMS)

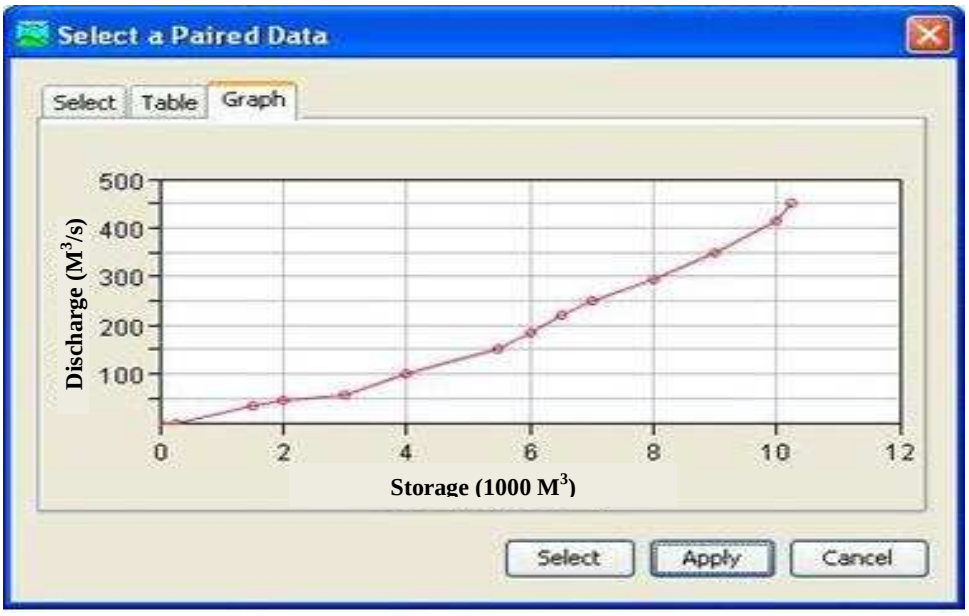


Figure 76 Storage-discharge relationship of Batu dam (output of HEC-HMS)

### 5-3-6- Meteorological Model

To define the meteorological model in HEC-HMS for Klang watershed, the Gauge Weight Method was used to allocate the climatic parameters for each sub-watershed (Meenu et al., 2012). The daily time-series of the 23 raingauges were entered into the meteorological model to develop hydrograph at the sub-watersheds. The meteorological model used monthly average evapotranspiration (ET) for the rainfall-runoff simulation. The daily evaporation from Batu dam station for the period (1985-2001) was used. The empirical Hargreaves method (Salazar et al., 1984) was used to calculate the ET. It is based on the air temperature and requires the maximum and minimum air temperature to calculate ET. The Hargreaves and Samani (1985) Equation 34 is described as below:

$$E_t=0.0023R_a\ (T_{mean}+17.8)\sqrt{T_{max}-T_{min}} \qquad \text{Equation 34}$$

Where, $T_{mean}$ is daily mean air temperature ($^oC$), it is equivalent to ($T_{max}+T_{min}/2$), $T_{max}$ is daily maximum air temperature ($^oC$), $T_{min}$: Daily minimum air temperature ($^oC$), $R_a$ is extraterrestrial radiation in equivalent evaporation in mm/day. The mean air temperature in the Hargreaves' equation is calculated as an average of $T_{max}$ and $T_{min}$.

Table 29 shows the daily and monthly ET calculated for the Batu dam for the observed data.

Table 29 Calculation of the daily and monthly evapotranspiration values for the year 1985-2001

| Month | Evaporation (mm) | $T_{max}$ ($^oC$) | $T_{min}$ ($^oC$) | Daily Evapotranspiration (mm) | Monthly Evapotranspiration (mm) |
|---|---|---|---|---|---|
| Jan | 4.5 | 32.0 | 22.7 | 1.4 | 44.4 |
| Feb | 4.5 | 32.8 | 23.3 | 1.4 | 40.7 |
| Mar | 5.0 | 33.0 | 23.7 | 1.6 | 49.9 |
| Apr | 5.4 | 33.2 | 24.0 | 1.7 | 52.5 |
| May | 6.1 | 33.8 | 23.9 | 2.0 | 63.7 |
| Jun | 6.8 | 32.3 | 23.2 | 2.7 | 64.9 |
| Jul | 7.9 | 32.1 | 22.9 | 2.5 | 77.0 |
| Aug | 7.3 | 32.1 | 22.8 | 2.3 | 71.4 |
| Sep | 6.3 | 32.0 | 22.7 | 2.0 | 60.0 |
| Oct | 5.2 | 32.0 | 22.6 | 1.6 | 50.7 |
| Nov | 4.8 | 31.8 | 22.6 | 1.5 | 45.0 |
| Dec | 4.5 | 31.6 | 22.7 | 1.4 | 43.1 |

### 5-3-7- Model Calibration and Validation

The characteristics of the hydrological parameters of the watershed used are assumed to be constant throughout the simulation period. The Curve Number, needed for the SCS-CN loss method and the sub-watershed lag time parameter in SCS unit hydrograph transform method are used in the rainfall-runoff simulation.

The daily rainfall data from the 23 raingauges over a long period were used for calibration and validation of HEC-HMS simulation of Klang watershed. Time series of 16 years data (from 1975- 1990) were selected for calibration and 11 years from 1991- 2001 for validation of model developed in HEC-HMS. The same period of calibration and validation are used in rainfall downscaling in SDSM.

Some statistical efficiency criteria are used to perform evaluation of the calibration and validation results between model output and observed data. Root Mean Square Error (RMSE), Coefficient of Determination ($r^2$) and Correlation Coefficient (r) are used to indicate the best fit between simulated and observed data. The Equations are described below.

**Root Mean Square Error** (Douglas and Runger, 2003) is a measure of the average error and indicates the average magnitude of the model errors with no direction of it. RMSE ranges from 0 to infinity, value of 0 represents a perfect score.

$$RMSE = \sqrt{\frac{\sum_{i=1}^{n} (Q_{o,i}-Q_{m,i})^2}{n}} \qquad \text{Equation 35}$$

**Coefficient of Determination** (Douglas and Runger, 2003) is a measure of a regression line describes how good it fits a set of data. It ranges from 0 (unacceptable) to 1 (best fit).

$$r^2 = \frac{\sum_{i=1}^{n}\left((Q_o)_i-\bar{Q}_o\right)\left((Q_m)_i-\bar{Q}_m\right)}{\sqrt{\sum_{i=1}^{n}\left((Q_o)_i-\bar{Q}_o\right)^2 \sum_{i=1}^{n}\left((Q_m)_i-\bar{Q}_m\right)^2}} \qquad \text{Equation 36}$$

**Correlation Coefficient (**Douglas and Runger, 2003) is a measure of the strength and direction of the linear relationship between observed and modelled data. It ranges from -1(strong negative correlation) to +1(strong positive correlation) and a value of 0 implies no correlation between two data.

$$r = \frac{n\sum_{i=1}^{n} Q_o Q_m - \left(\sum_{i=1}^{n} Q_o\right)\left(\sum_{i=1}^{n} Q_m\right)}{\sqrt{n\left(\sum_{i=1}^{n}(Q_o)^2\right)-\left(\sum_{i=1}^{n} Q_o\right)^2}\ \sqrt{n\left(\sum_{i=1}^{n} Q_m\right)-\left(\sum_{i=1}^{n} Q_m\right)^2}} \qquad \text{Equation 37}$$

Where, $Q_m$ is the modelled discharge, $Q_o$ is the observed discharge, $\bar{Q}_o$ is the average observed discharge and, $\bar{Q}_m$ is the average modelled discharge.

The calibration of the rainfall-runoff model in HEC-HMS for Klang watershed is performed by comparing the modelled daily streamflows with the observed flow at Sulaiman streamflow station. Table 30 gives the statistics of the daily and monthly observed and modelled streamflow at Sulaiman streamflow station for the calibration and validation period. The maximum and mean values of daily flows are underestimated during calibration and validation periods as found in Table 30. The statistics of lengthy daily data and monthly flow modelling which are illustrated in Figures (from 77 to 82) indicate that flows are well simulated. However, most of the

daily high flows in the calibration and validation periods are underpredicted. However, the discrepancy of daily flow modelling at Sulaiman streamflow station has already been commented by Kavvas et al. (2006).

Table 31 gives the performance assessment for the daily and monthly discharges in the calibration and validation periods. It is noteworthy that due to many gaps of daily discharge data at Sulaiman streamflow station, a high correlation between observed and modelled could not be obtained. It wouldn't be able to get a good fit particularly for the maximum discharges. The lack of updated landuse data has forced the study to assume with no change during the time. The relevant scatter plots are found in Appendix P.

Sensitivity analysis in HEC-HMS was run to estimate the magnitude of underprediction of high flows and to address the uncertainty involved in the HEC-HMS modelling. In this study, sensitivity analysis was performed to estimate the accuracy of calibration and validation results of hydrological model. Many studies have been conducted on sensitivity analysis of HEC-HMS to tackle the calibration error. Sensitivity analysis is performed to determine the effective parameters for calibration of the loss model to achieve better results. The daily and monthly simulations in HEC-HMS are run using sensitivity parameters of CN model to create optimal results for calibration period in HEC-HMS. The analysis is optimised according to objective function of peak weighted root mean square. The simulated flows are underestimated compared to observed discharges equal to 23.6% and 13.49% for calibration and validation periods respectively.

The model is reliable for mean simulation. However, the peak flow simulation hasn't been employed for the further process in modelling runoff estimation. Thus, it can be concluded that HEC-HMS model responds well particularly in monthly mean simulation of the hydrological processes at Klang watershed.

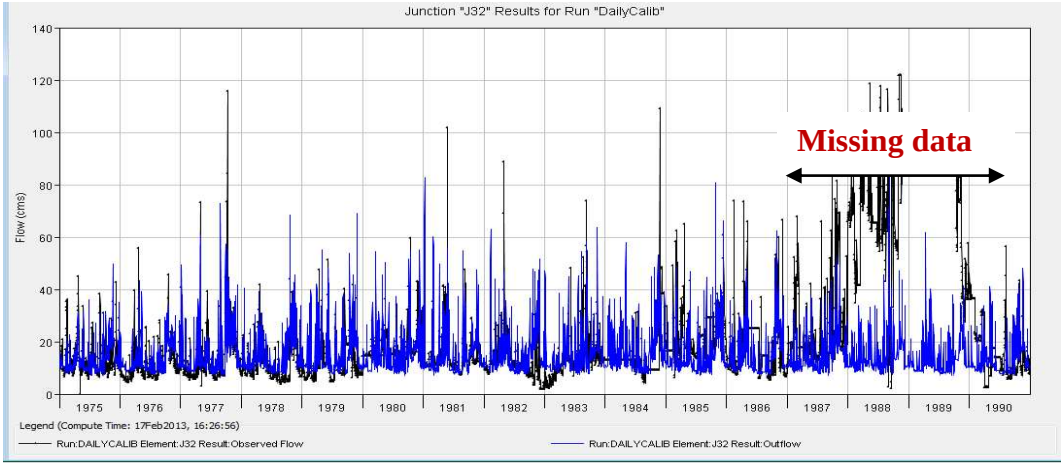


Figure 77 Calibration result of observed and simulated daily discharge at Sulaiman streamflow station during the calibration period (1975–1990)

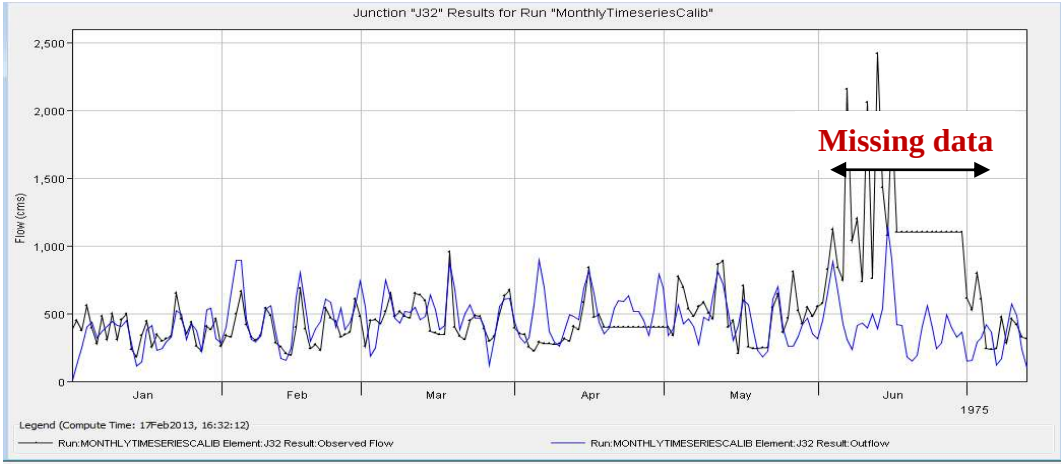


Figure 78 Calibration result of observed and simulated monthly discharge at Sulaiman streamflow station during the calibration period (1975–1990)

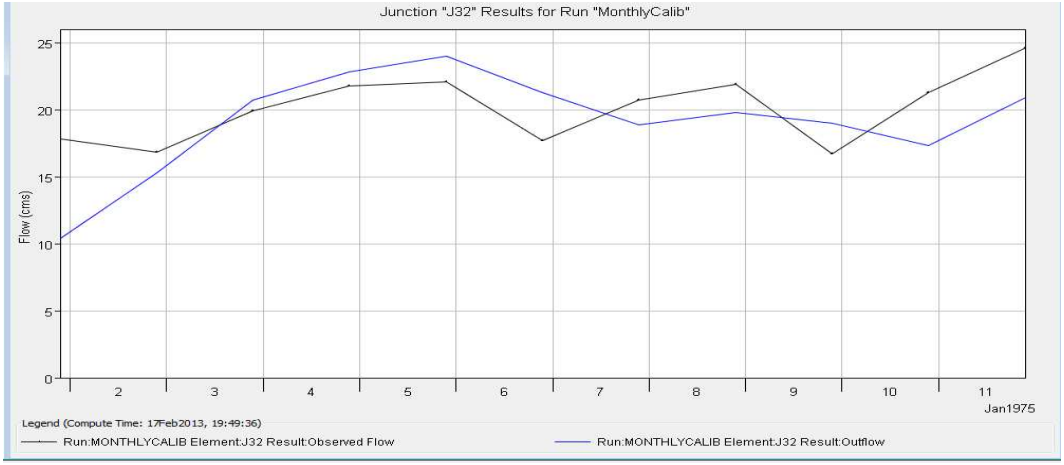


Figure 79 Calibration result of observed and simulated average monthly discharge at the gauging streamflow during the calibration period (1975–1990)

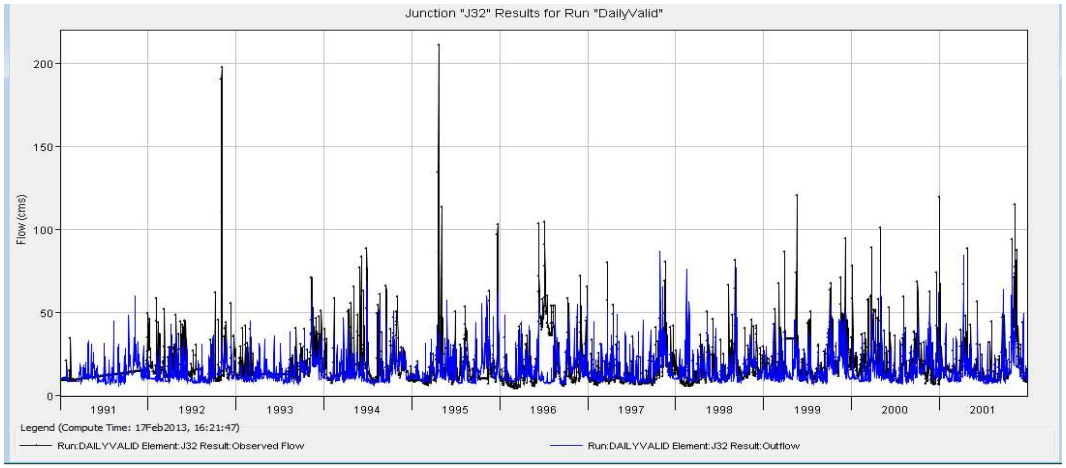


Figure 80 Validation result of observed and simulated daily discharge at Sulaiman streamflow station during the calibration period (1990–2001)

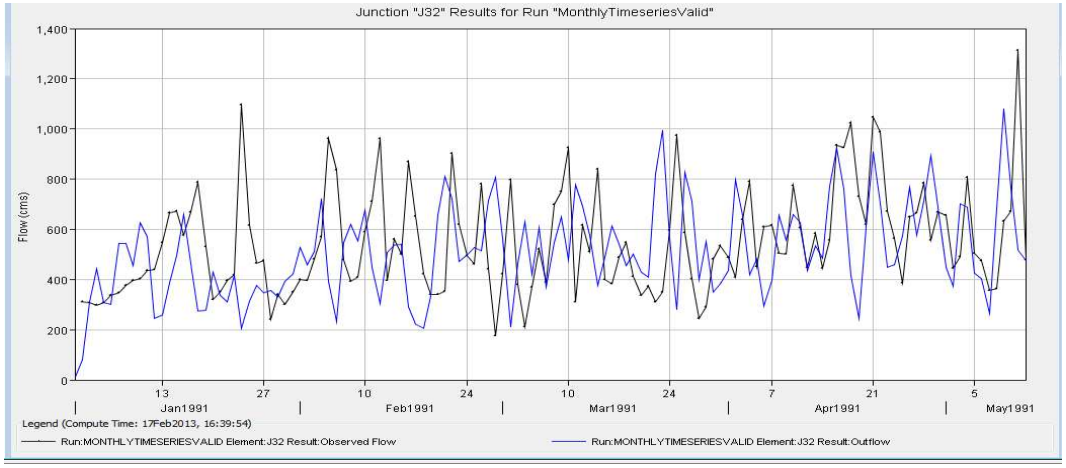


Figure 81 Validation result of observed and simulated monthly discharge at Sulaiman streamflow station during the calibration period (1990–2001)

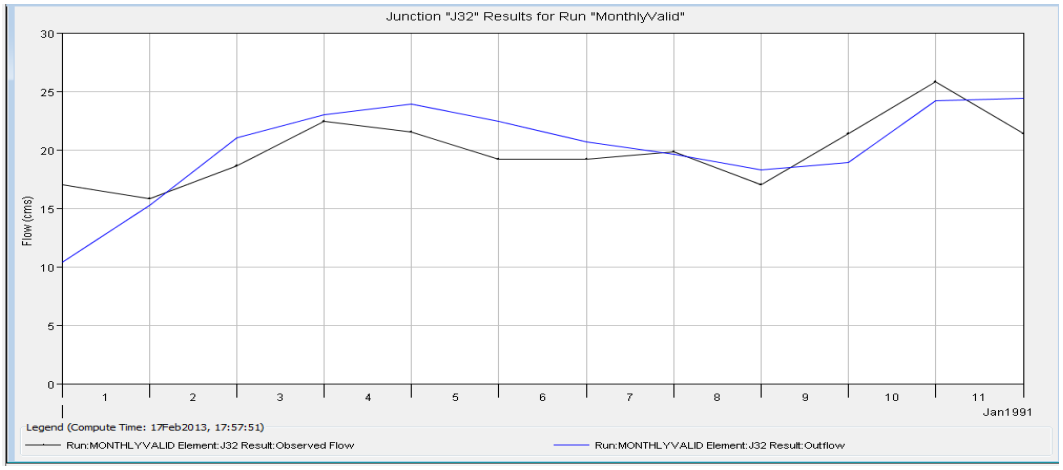


Figure 82 Validation result of observed and simulated average monthly discharge at the gauging streamflow during the calibration period (1990–2001)

Table 30 Statistics of the observed and simulated daily flows at Sulaiman streamflow station during calibration and validation

| | **Calibration (1975-1990)** | | **Validation (1991-2001)** | |
|---|---|---|---|---|
| | **Simulated** | **Observed** | **Simulated** | **Observed** |
| | **($m^3/s$)** | **($m^3/s$)** | **($m^3/s$)** | **($m^3/s$)** |
| **Max** | 93.80 | 121.57 | 87.10 | 211.00 |
| **Mean** | 15.49 | 18.61 | 16.25 | 18.79 |
| **SD** | 8.76 | 16.51 | 9.50 | 13.96 |

Table 31 Performance assessment of hydrological model at Sulaiman streamflow station during calibration and validation

| | **Calibration and Validation (Daily)** | | **Calibration and Validation (Monthly)** | |
|---|---|---|---|---|
| | **Calibrated** | **Validated** | **Calibrated** | **Validated** |
| **RMSE** | 0.08 | 0.02 | 9.34 | 3.83 |
| **$r^2$** | 0.06 | 0.22 | 0.03 | 0.07 |
| **r** | 0.28 | 0.46 | 0.18 | 0.27 |

# 6- RESULTS AND DISCUSSION

This section represents the climate change downscale scenarios which are generated by SDSM and also describes the impacts of climate change using the hydrological model. It simulates the streamflow behaviour corresponding to the current and future climate condition. The future climate was projected using SDSM as presented in Chapter 4.

## 6-1- Changes in Temperature

The output generated by the HadCM3 GCM model has projected an increase in both maximum and minimum temperature for Klang watershed. The maximum and minimum temperatures increased towards the end of the century by 2.7 $^{o}$C and 0.8 $^{o}$C, respectively compared to the current observed temperature at Subang temperature station. The maximum daily temperature under A2 scenario increased the most in May by 1.6 $^{o}$C, 2.2 $^{o}$C and 2.7 $^{o}$C for 2020s, 2050s and 2080s, respectively which is a considerable increase in daily temperature through the year. The trend under B2 scenario is similar in May which is 1.4 $^{o}$C, 1.5 $^{o}$C and 2.4 $^{o}$C. The minimum daily temperature decreased in months (October, November and December) and increased in months from January to May, August and September, with no significant vary through June and July under A2 and B2 scenarios. Tables (32 and 33) show the monthly analysis in three time slices to show the temperature pattern based on IPCC scenarios. Figures (from 83 to 86) illustrate projected changes in maximum and minimum daily temperature at Subang station.

The graphs reveal a continually increasing temperature of Subang station at Klang watershed as per A2 simulation which is generally higher than B2 scenario simulation. Because A2 includes the highest concentration of $CO_2$ equal to 850 ppm (IPCC, 2000). Scenario A2 is a Medium-High emission scenario assumes the higher usage of fossil fuel while Medium-Low emissions scenario B2 is a lower rate of emissions which is based on least using fossil fuel and taking environmental approaches at local scale.

The result shows that differences between A2 and B2 scenarios are minor at Klang watershed. Since Malaysia is a developing country with an increasing in population and economy development, a high usage of fossil fuel has formed the climate change scenarios with no focus on environmental improvement. It leads to rather similarity of two A2 and B2 scenarios in the region. Hence, B2 scenario in Malaysia does not describe quite differently to A2 scenario. However, IPCC (2007) has stated that the response of climate system in the land areas of the equatorial belt will likely be least warming.

Table 32 SDSM results on mean monthly maximum temperature at Subang temperature station (in $^{o}$C**)**

| Month | Observed | A2 | | | B2 | | |
|---|---|---|---|---|---|---|---|
| | | 2020s | 2050s | 2080s | 2020s | 2050s | 2080s |
| **Jan** | 31.90 | 33.20 | 33.50 | 34.00 | 33.00 | 33.10 | 33.80 |
| **Feb** | 32.75 | 34.21 | 34.18 | 34.26 | 34.11 | 34.00 | 34.21 |
| **Mar** | 32.98 | 34.01 | 34.03 | 33.96 | 34.00 | 34.02 | 33.50 |
| **Apr** | 33.16 | 34.49 | 34.60 | 34.84 | 34.00 | 34.30 | 34.74 |
| **May** | 33.62 | 35.20 | 35.80 | 36.30 | 35.00 | 35.10 | 36.00 |
| **Jun** | 32.38 | 33.77 | 33.82 | 33.85 | 33.20 | 33.20 | 33.25 |
| **Jul** | 32.05 | 32.94 | 33.02 | 33.04 | 32.20 | 33.00 | 32.85 |
| **Aug** | 32.15 | 33.13 | 33.17 | 33.15 | 33.00 | 32.90 | 33.00 |
| **Sep** | 31.98 | 32.95 | 32.99 | 33.08 | 32.60 | 32.40 | 32.60 |
| **Oct** | 32.00 | 33.05 | 33.16 | 33.37 | 33.01 | 33.00 | 33.10 |
| **Nov** | 31.82 | 33.04 | 33.27 | 33.59 | 33.02 | 33.00 | 33.37 |
| **Dec** | 31.64 | 32.68 | 32.89 | 33.12 | 32.50 | 32.10 | 32.70 |
| **Annual** | 32.37 | 33.56 | 33.70 | 33.88 | 33.30 | 33.34 | 33.59 |

Table 33 SDSM results on mean monthly minimum temperature at Subang temperature station (in $^{o}$C**)**

| Month | Observed | A2 | | | B2 | | |
|---|---|---|---|---|---|---|---|
| | | 2020s | 2050s | 2080s | 2020s | 2050s | 2080s |
| **Jan** | 22.78 | 22.85 | 22.90 | 22.95 | 22.84 | 22.87 | 22.90 |
| **Feb** | 23.35 | 23.44 | 23.52 | 23.63 | 23.43 | 23.51 | 23.56 |
| **Mar** | 23.75 | 23.83 | 23.85 | 23.82 | 23.79 | 23.79 | 23.81 |
| **Apr** | 24.03 | 24.32 | 24.45 | 24.81 | 24.29 | 24.44 | 24.65 |
| **May** | 23.97 | 24.09 | 24.23 | 24.43 | 24.09 | 24.19 | 24.35 |
| **Jun** | 23.22 | 23.23 | 23.21 | 23.21 | 23.22 | 23.21 | 23.22 |
| **Jul** | 22.96 | 22.96 | 22.97 | 22.96 | 22.96 | 22.97 | 22.96 |
| **Aug** | 22.85 | 22.93 | 23.00 | 23.14 | 22.92 | 22.99 | 23.07 |
| **Sep** | 22.76 | 22.85 | 22.96 | 23.10 | 22.87 | 22.93 | 23.01 |
| **Oct** | 22.64 | 22.62 | 22.58 | 22.55 | 22.60 | 22.56 | 22.49 |
| **Nov** | 22.50 | 22.36 | 22.26 | 22.16 | 22.36 | 22.23 | 22.03 |
| **Dec** | 22.75 | 22.73 | 22.70 | 22.68 | 22.71 | 22.69 | 22.67 |
| **Annual** | 23.13 | 23.18 | 23.22 | 23.29 | 23.17 | 23.20 | 23.23 |

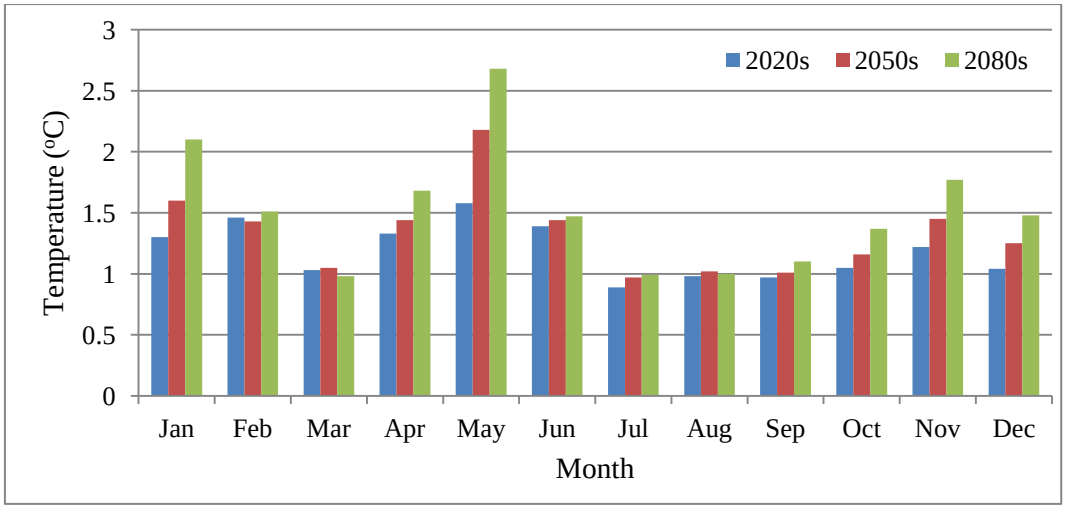


Figure 83 Projected changes in maximum daily temperature at Subang station to A2 scenario

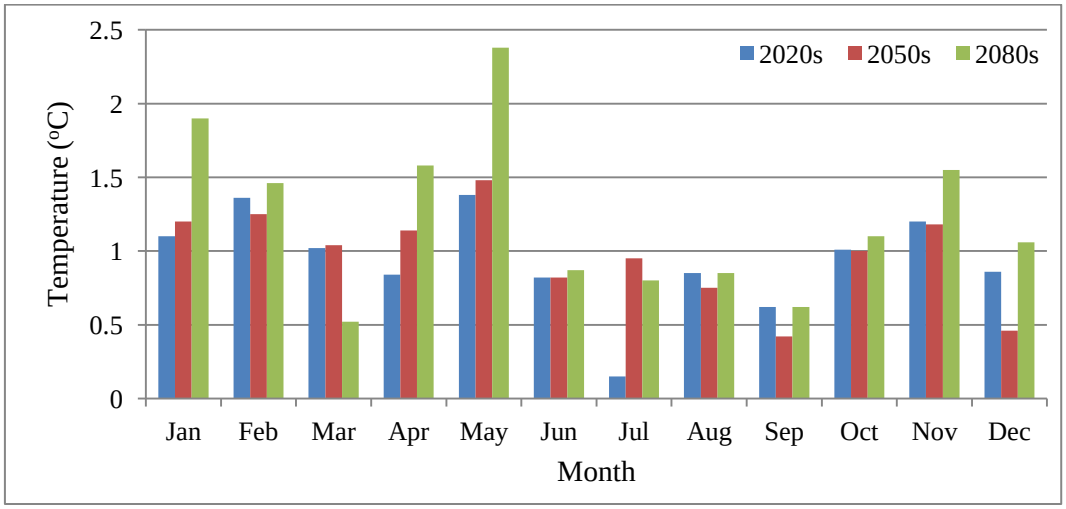


Figure 84 Projected changes in maximum daily temperature at Subang station to B2 scenario

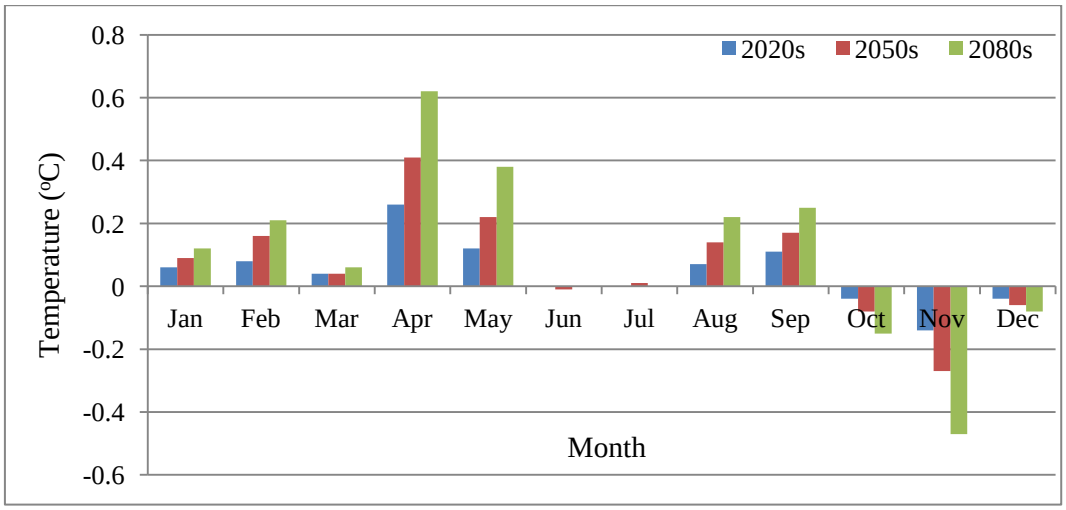


Figure 85 Projected changes in minimum daily temperature at Subang station to A2 scenario

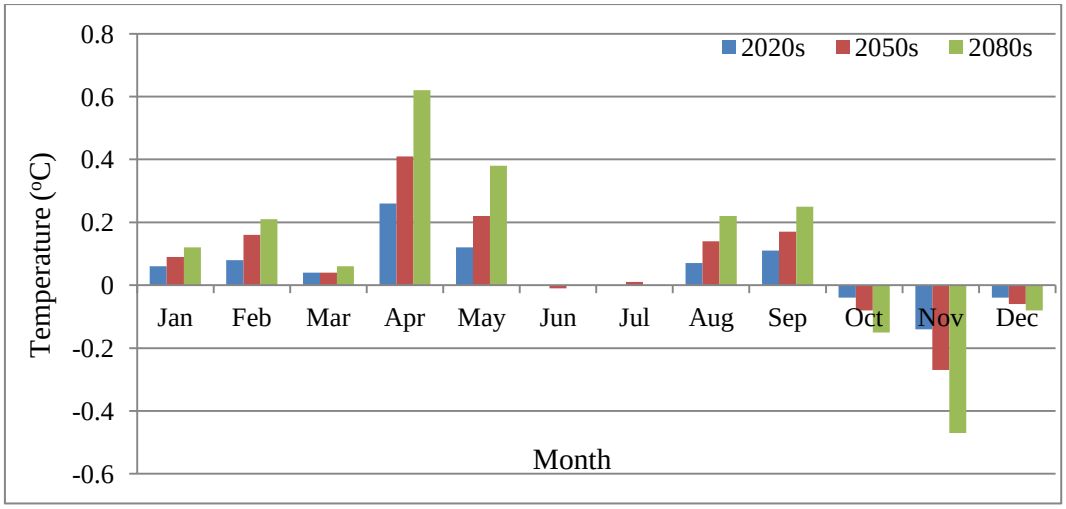


Figure 86 Projected changes in minimum daily temperature at Subang station toB2scenario

## 6-2- Change in Evaporation

An examination on Table 34 shows that there is a little to no change in the evaporation value over observed value at Batu dam evaporation station. The changes are expected to decrease about 0.6%, 1.4% and 2.6% for the 2020s, 2050s and 2080s under A2 scenario, respectively. Similar trend is observed for the projected evaporation values under B2 scenario which are expected a decreasing about 0.5%, 1.2% and 2%.

Table 34 SDSM results on mean daily evaporation relative at Batu dam evaporation station (in mm)

| Month | Observed | A2 | | | B2 | | |
|---|---|---|---|---|---|---|---|
| | | 2020s | 2050s | 2080s | 2020s | 2050s | 2080s |
| **Jan** | 4.42 | 4.32 | 4.19 | 3.99 | 4.32 | 4.18 | 4.08 |
| **Feb** | 4.29 | 4.29 | 4.30 | 4.31 | 4.29 | 4.30 | 4.31 |
| **Mar** | 4.77 | 4.72 | 4.62 | 4.42 | 4.70 | 4.62 | 4.51 |
| **Apr** | 5.22 | 5.08 | 4.94 | 4.73 | 5.07 | 4.97 | 4.83 |
| **May** | 6.04 | 5.96 | 5.85 | 5.67 | 5.95 | 5.85 | 5.74 |
| **Jun** | 6.69 | 6.65 | 6.61 | 6.59 | 6.65 | 6.63 | 6.57 |
| **Jul** | 7.80 | 7.87 | 7.96 | 8.10 | 7.88 | 7.96 | 8.04 |
| **Aug** | 7.21 | 7.19 | 7.19 | 7.18 | 7.19 | 7.19 | 7.18 |
| **Sep** | 6.29 | 6.26 | 6.24 | 6.19 | 6.26 | 6.25 | 6.22 |
| **Oct** | 5.05 | 5.00 | 4.93 | 4.83 | 4.99 | 4.95 | 4.88 |
| **Nov** | 4.69 | 4.72 | 4.75 | 4.79 | 4.74 | 4.77 | 4.78 |
| **Dec** | 4.46 | 4.48 | 4.52 | 4.54 | 4.48 | 4.51 | 4.53 |

## 6-3- Change in Evapotranspiration

The future Evapotranspiration (ET) was calculated for the three time horizons (2020s, 2050s and 2080s) based on the climate change scenarios using Hargreaves' equation. The $T_{max}$, $T_{min}$ and evaporation data are used to calculate ET. The future ET is shown in Table 35. Figures (87 and 88) illustrate projected changes in mean monthly ET corresponding to A2 and B2 scenarios, respectively. It shows the simulated ET by Hargreaves' method for both A2 and B2 scenarios for the baseline period (1985-2001) and for three future time slices (2020s, 2050s and 2080s). The projected mean ET value increase by 4.3% in the 2020s and 2050s, 3.8% in 2080s, under A2 scenario. The trend for B2 scenario is likely be a decrease to 1.5% for 2020s and an increase by 2.2% and 2.7% for 2050s and 2080s respectively.

The results reveal that there is no a significant change of future ET to the observed for Klang watershed. The most ET value is expected in July for the future demonstrates dependency on the amount of evaporation and temperature in Hargreaves ET equation. There is an increase in mean monthly ET throughout the year except March, April and a slightly decreasing in January affected by a decrease in evaporation in these months for the future period under A2 and B2 scenarios.

Table 35 Projected changes in the monthly evapotranspiration values (in mm)

| Month | Observed | A2 | | | B2 | | |
|---|---|---|---|---|---|---|---|
| | | 2020s | 2050s | 2080s | 2020s | 2050s | 2080s |
| **Jan** | 44.4 | 45.5 | 44.8 | 43.8 | 44.9 | 43.7 | 44.4 |
| **Feb** | 40.7 | 42.3 | 42.1 | 42.3 | 42.0 | 41.8 | 42.2 |
| **Mar** | 49.9 | 50.2 | 49.3 | 46.9 | 49.9 | 49.1 | 46.4 |
| **Apr** | 52.5 | 52.8 | 51.4 | 49.3 | 51.2 | 50.8 | 50.3 |
| **May** | 63.7 | 67.2 | 67.9 | 67.1 | 66.4 | 65.3 | 67.0 |
| **Jun** | 64.9 | 69.0 | 68.8 | 68.7 | 66.7 | 66.5 | 66.1 |
| **Jul** | 77.0 | 81.1 | 82.4 | 84.0 | 77.5 | 82.3 | 82.4 |
| **Aug** | 71.4 | 75.1 | 75.1 | 74.4 | 74.4 | 73.8 | 73.9 |
| **Sep** | 60.0 | 62.7 | 62.4 | 61.9 | 61.4 | 60.3 | 60.6 |
| **Oct** | 50.7 | 52.5 | 52.2 | 52.0 | 52.3 | 52.0 | 51.6 |
| **Nov** | 45.0 | 48.5 | 49.6 | 51.3 | 48.6 | 49.0 | 50.4 |
| **Dec** | 43.1 | 45.8 | 46.9 | 47.8 | 45.4 | 44.5 | 46.6 |

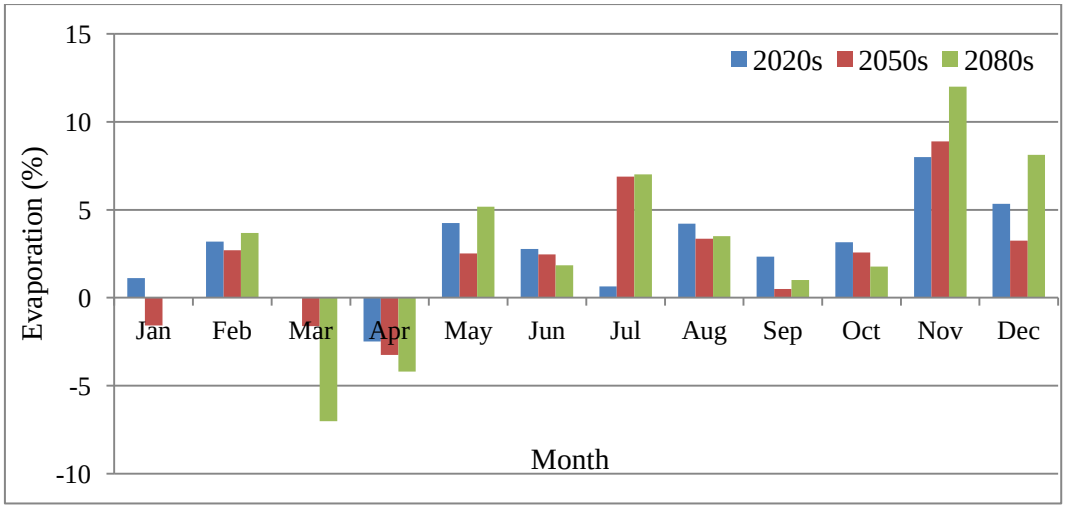


Figure 87 Projected changes in mean monthly evapotranspiration to A2 scenario

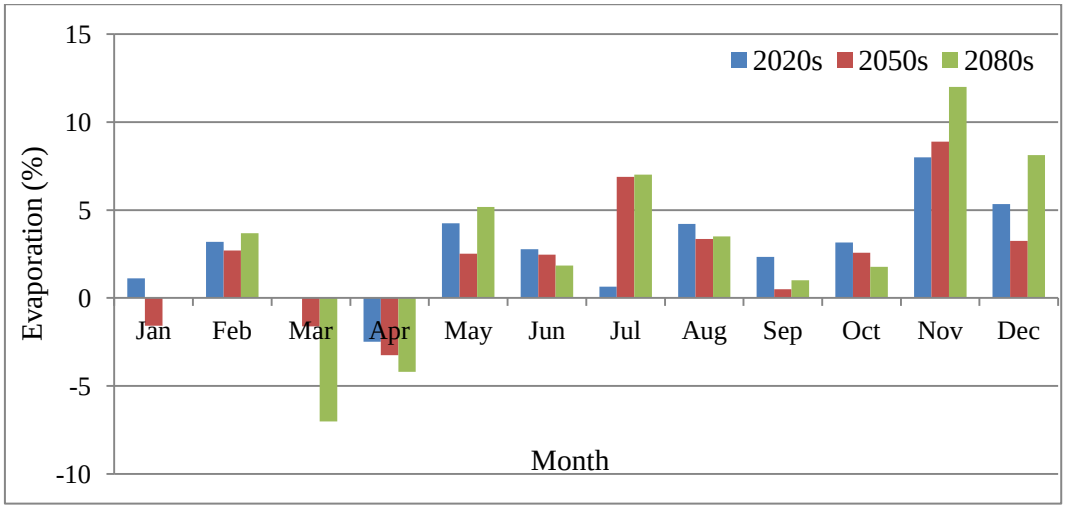


Figure 88 Projected changes in mean monthly evapotranspiration to B2 scenario

## 6-4- Change in Rainfall Variables

The rainfall variables are Mean, Max, Wet-day, Dry Spell and Wet Spell which need to be estimated to reveal future climate pattern. The wet spell length indicates the number of consecutive days with non zero precipitation whereas, dry spell length reveals the number of consecutive days without precipitation. In this study a value of 0.3 (Khan et al., 2005) was used in SDSM to define the wet spell length as conditional precipitation variable. SDSM has generated the different scenarios of the precipitation by projecting the possible climate in the future in three time slices via 2020s, 2050s and 2080s.

A single raingauge station for the watershed scale does not represent the reliable trend of rainfall. Then, monthly mean rainfall was estimated based on the multi raingauge stations downscaled in the watershed. Geostatistical function in GIS system generated monthly map of mean rainfall of ten raingauge stations to determine the accurate pattern of rainfall. The results are more important for the maximum amount of rainfall to the mean rainfall because estimation of maximum rainfall at the point scale represents a higher uncertainty.

After all the precipitation data have been downscaled by SDSM, the spatial analysis was conducted to achieve the average precipitation for the entire Klang watershed. The interpolation produced monthly plot by assuming the current and future downscaled data. This method is applied for 20's, 50's and 80's corresponding to A2 and B2 scenarios. A number of 480 maps were produced for A2 Scenario. The same numbers of maps were produced for B2 scenario. To interpolate and plot the maps, the spatial mean value is used. GIS is able to estimate a mean value of each map as an average of all the point data values distributed over the whole watershed.

Table 36 (from A to G) shows the monthly mean of mean, max, Wet-day, Dry Spell and Wet Spell for the current and 2020s, 2050s and 2080s corresponding to A2 and B2 scenarios, as an average value of precipitation variables for whole the watershed. Tables (37 and 38) show the mean changes in rainfall values for the three time slices (2020s, 2050s and 2080s)

The watershed seems to experience increased rainfall by 2080s. However, the analysis indicates that there will likely be a negative trend of mean rainfall in 2020s and with no difference in 2050s according A2 scenario. The highest rainfall increase was simulated for 2080s, which corresponds to the highest temperature variation for the same time. The results reveal that the precipitation trend for both A2 and B2 scenarios modelled show an equal or decreasing trend from June to August, December to January and an increasing trend from February to May (except march) and September to November. Precipitation will likely be increased over Klang watershed in the months that already have much precipitation, while it might decrease in already dry months.

Mean annual precipitations are projected to increase in the future for A2 compared to B2 scenario. The precipitation experiences a mean annual decrease by 7.9%, 0.6% for A2 scenario in 2020s, 2050s respectively and an increase by 12.4% in 2080s under A2 scenario. The change for B2 scenario is projected to decrease 11.5% in the 2020s, 6.6% in 2050s and increase 2.6% in 2080s.

The precipitation in month February, April and September in all the three time slices of future increased under A2 and B2 scenarios. In 2080s, 26.4%, 30% and 88% increase in February, April and September are projected under A2 scenario, while the increase for B2 scenario are projected 21.5%, 19.7% and 65.2% in these months.

A decrease of 50% of mean wet spell length was projected for the future, an increasing of mean dry spell length probably will reach to 10% compared to the current condition by 2080s while there will expect to decrease in consecutive days without rainfall approximately 10% and 15.5% for A2 scenario in 2020s and 2050s, respectively.

It can be concluded that the probability of flood happening are higher due to increasing rainfall intensity. Hence, the days with heavy precipitation will be expected to occur very frequently during the year.

The analysis indicates that there will be an increase in mean monthly precipitation but with a decrease in the number of consecutive wet-days which can be concluded as a possibility of more precipitation amount in fewer days.

The results is agreement with the dynamical climate change downscaling model (RCM) conducted by Meteorological Dep. Malaysia (2009). However, RCM model used nine GCM models to project the rainfall trend in Malaysia. The results of RCM model demonstrated no clear trend of rainfall due to high variability in the rainfall-modulating factor for Klang area. However, the weakness of a number of 32 GCM models to predict monsoon rainfall over Southeast Asia has been examined by Vitart in 2004.

Table 36 Average monthly precipitation observed and projected for Klang watershed

**A) Observed**

| Precipitation statistics | Jan | Feb | Mar | Apr | May | Jun | Jul | Aug | Sep | Oct | Nov | Dec |
|---|---|---|---|---|---|---|---|---|---|---|---|---|
| Mean (mm) | 108.66 | 152.08 | 208.34 | 259.14 | 455.91 | 160.23 | 161.40 | 183.10 | 234.68 | 259.98 | 274.86 | 184.89 |
| Max (mm) | 140.16 | 194.44 | 256.84 | 297.22 | 201.36 | 181.51 | 184.68 | 199.41 | 252.28 | 285.58 | 329.55 | 218.27 |
| Wet Spell (day) | 5.27 | 4.92 | 5.06 | 5.61 | 5.21 | 4.68 | 4.81 | 4.77 | 5.12 | 5.98 | 6.41 | 6.13 |
| Wet Day (%) | 0.45 | 0.50 | 0.56 | 0.66 | 0.61 | 0.50 | 0.52 | 0.53 | 0.63 | 0.69 | 0.74 | 0.59 |
| Dry Spell(day) | 3.73 | 3.07 | 2.64 | 2.10 | 2.48 | 2.92 | 2.69 | 2.72 | 2.12 | 2.17 | 2.17 | 2.52 |

**B) 2020s (A2 Scenario)**

| Precipitation statistics | Jan | Feb | Mar | Apr | May | Jun | Jul | Aug | Sep | Oct | Nov | Dec |
|---|---|---|---|---|---|---|---|---|---|---|---|---|
| Mean (mm) | 94.37 | 168.92 | 186.62 | 277.87 | 346.25 | 116.95 | 159.11 | 159.43 | 291.31 | 234.04 | 265.48 | 135.43 |
| Max (mm) | 149.54 | 217.06 | 203.69 | 369.45 | 739.82 | 202.96 | 192.52 | 192.16 | 357.16 | 344.46 | 336.62 | 152.81 |
| Wet Spell (day) | 1.77 | 2.03 | 2.42 | 2.62 | 2.90 | 1.82 | 2.05 | 1.88 | 2.85 | 2.89 | 3.52 | 2.08 |
| Wet Day (%) | 0.40 | 0.49 | 0.59 | 0.63 | 0.65 | 0.39 | 0.49 | 0.44 | 0.66 | 0.65 | 0.71 | 0.50 |
| Dry Spell(day) | 2.63 | 2.08 | 1.70 | 1.57 | 1.58 | 2.96 | 2.08 | 2.31 | 1.49 | 1.55 | 1.55 | 2.05 |

**C) 2050s (A2 Scenario)**

| Precipitation statistics | Jan | Feb | Mar | Apr | May | Jun | Jul | Aug | Sep | Oct | Nov | Dec |
|---|---|---|---|---|---|---|---|---|---|---|---|---|
| Mean (mm) | 88.14 | 179.07 | 191.34 | 299.64 | 437.62 | 105.33 | 164.98 | 151.84 | 337.08 | 259.99 | 286.77 | 125.53 |
| Max (mm) | 156.31 | 235.59 | 222.16 | 418.52 | 770.36 | 264.06 | 206.84 | 198.07 | 457.80 | 398.04 | 395.86 | 156.51 |
| Wet Spell (day) | 1.80 | 2.17 | 2.62 | 2.64 | 3.74 | 1.80 | 2.08 | 1.83 | 3.07 | 2.98 | 3.83 | 2.03 |
| Wet Day (%) | 0.39 | 0.52 | 0.62 | 0.63 | 0.73 | 0.34 | 0.49 | 0.41 | 0.68 | 0.66 | 0.72 | 0.47 |
| Dry Spell(day) | 2.91 | 2.00 | 1.61 | 1.58 | 1.44 | 5.23 | 2.16 | 2.55 | 1.47 | 1.56 | 1.44 | 2.52 |

**D) 2080s (A2 Scenario)**

| Precipitation statistics | Jan | Feb | Mar | Apr | May | Jun | Jul | Aug | Sep | Oct | Nov | Dec |
|---|---|---|---|---|---|---|---|---|---|---|---|---|
| Mean (mm) | 81.93 | 192.27 | 196.49 | 336.86 | 601.70 | 110.19 | 169.75 | 135.42 | 441.34 | 270.53 | 321.68 | 111.92 |
| Max (mm) | 162.29 | 301.72 | 234.76 | 469.58 | 893.68 | 395.48 | 224.97 | 211.77 | 678.35 | 520.59 | 471.84 | 166.13 |
| Wet Spell (day) | 1.90 | 2.42 | 3.01 | 2.59 | 5.96 | 1.81 | 2.17 | 1.77 | 3.81 | 3.04 | 4.55 | 1.92 |
| Wet Day (%) | 0.38 | 0.56 | 0.67 | 0.62 | 0.81 | 0.31 | 0.47 | 0.36 | 0.72 | 0.65 | 0.72 | 0.47 |
| Dry Spell(day) | 3.41 | 1.92 | 1.49 | 1.60 | 1.33 | 10.25 | 2.52 | 3.15 | 1.41 | 1.60 | 1.55 | 4.18 |

**E) 2020s (B2 Scenario)**

| Precipitation statistics | Jan | Feb | Mar | Apr | May | Jun | Jul | Aug | Sep | Oct | Nov | Dec |
|---|---|---|---|---|---|---|---|---|---|---|---|---|
| Mean (mm) | 88.36 | 158.49 | 179.94 | 265.42 | 321.55 | 110.96 | 152.59 | 152.42 | 284.29 | 246.23 | 251.80 | 126.86 |
| Max (mm) | 144.53 | 210.06 | 202.14 | 343.00 | 723.81 | 198.95 | 185.05 | 190.36 | 348.41 | 328.73 | 316.56 | 146.39 |
| Wet Spell (day) | 1.82 | 2.06 | 2.06 | 2.66 | 2.92 | 1.88 | 2.09 | 1.94 | 2.87 | 2.87 | 2.90 | 2.14 |
| Wet Day (%) | 0.41 | 0.50 | 0.59 | 0.63 | 0.66 | 0.40 | 0.50 | 0.44 | 0.67 | 0.65 | 0.71 | 0.51 |
| Dry Spell(day) | 2.60 | 2.05 | 1.68 | 1.56 | 1.56 | 2.87 | 2.04 | 2.33 | 1.48 | 1.55 | 1.42 | 2.06 |

**F) 2050s (B2 Scenario)**

| Precipitation statistics | Jan | Feb | Mar | Apr | May | Jun | Jul | Aug | Sep | Oct | Nov | Dec |
|---|---|---|---|---|---|---|---|---|---|---|---|---|
| Mean (mm) | 84.10 | 168.85 | 183.70 | 283.46 | 388.08 | 98.56 | 156.69 | 146.49 | 320.67 | 247.23 | 269.19 | 121.30 |
| Max (mm) | 159.79 | 227.76 | 217.82 | 401.50 | 714.93 | 254.04 | 203.55 | 196.76 | 437.77 | 397.56 | 381.97 | 155.32 |
| Wet Spell (day) | 1.86 | 2.15 | 2.55 | 2.64 | 3.53 | 1.82 | 2.10 | 1.87 | 3.01 | 2.92 | 3.67 | 2.07 |
| Wet Day (%) | 0.40 | 0.52 | 0.61 | 0.63 | 0.72 | 0.35 | 0.49 | 0.42 | 0.68 | 0.65 | 0.72 | 0.48 |
| Dry Spell(day) | 2.79 | 1.97 | 1.61 | 1.58 | 1.45 | 4.50 | 2.13 | 2.49 | 1.47 | 1.57 | 1.43 | 2.32 |

**G) 2080s (B2 Scenario)**

| Precipitation statistics | Jan | Feb | Mar | Apr | May | Jun | Jul | Aug | Sep | Oct | Nov | Dec |
|---|---|---|---|---|---|---|---|---|---|---|---|---|
| Mean (mm) | 79.16 | 184.89 | 186.94 | 310.35 | 509.95 | 102.04 | 161.94 | 134.98 | 387.75 | 252.38 | 292.23 | 109.59 |
| Max (mm) | 159.57 | 265.17 | 227.78 | 439.55 | 752.81 | 388.44 | 209.53 | 197.26 | 655.73 | 460.68 | 438.86 | 151.90 |
| Wet Spell (day) | 1.87 | 2.37 | 2.84 | 2.62 | 5.37 | 1.79 | 2.15 | 1.82 | 3.37 | 2.92 | 4.18 | 1.99 |
| Wet Day (%) | 0.39 | 0.56 | 0.65 | 0.63 | 0.79 | 0.31 | 0.48 | 0.39 | 0.70 | 0.64 | 0.72 | 0.46 |
| Dry Spell(day) | 3.09 | 1.89 | 1.54 | 1.59 | 1.34 | 9.55 | 2.30 | 2.78 | 1.43 | 1.60 | 1.49 | 3.21 |

Table 37 Changes in precipitation variables in Klang watershed under A2 scenario

| Precipitation Variable | 2020s | 2050s | 2080s | Observed | Change in 2020s | Change in 2050s | Change in 2080s |
|---|---|---|---|---|---|---|---|
| Mean precipitation (mm) | 202.81 | 218.94 | 247.50 | 220.27 | -17.46 | -1.33 | 27.23 |
| Wet Spell (day) | 2.40 | 2.55 | 2.91 | 5.33 | -2.93 | -2.78 | -2.42 |
| Wet Day (%) | 0.55 | 0.55 | 0.56 | 0.58 | -0.03 | -0.03 | -0.02 |
| Max precipitation (mm) | 291.04 | 323.34 | 394.30 | 228.4 | 62.64 | 94.94 | 165.9 |
| Dry Spell (day) | 1.96 | 2.21 | 2.87 | 2.61 | -0.65 | -0.4 | 0.26 |

Table 38 Changes in precipitation variables in Klang watershed under B2 scenario

| Precipitation Variable | 2020s | 2050s | 2080s | Observed | Change in 2020s | Change in 2050s | Change in 2080s |
|---|---|---|---|---|---|---|---|
| Mean precipitation (mm) | 194.91 | 205.69 | 226.02 | 220.27 | -25.36 | -14.58 | 5.75 |
| Wet Spell (day) | 2.35 | 2.52 | 2.77 | 5.33 | -2.98 | -2.81 | -2.56 |
| Wet Day (%) | 0.56 | 0.56 | 0.56 | 0.58 | -0.02 | -0.02 | -0.02 |
| Max precipitation (mm) | 278.17 | 312.04 | 362.27 | 228.40 | 49.77 | 83.64 | 133.87 |
| Dry Spell (day) | 1.93 | 2.11 | 2.65 | 2.61 | -0.68 | -0.5 | 0.04 |

## 6-5- Assessment of Climate Change Impact on the Mean and Maximum River Discharge

The present and future streamflow were compared to reveal the possible changes of runoff behaviour for the future based on the climate change scenarios. HEC-HMS hydrological model in Klang watershed was found skilful through the long time series streamflow record. It handles geospatial data and distributed grid-based precipitation data for the multi raingauge stations. Using appropriate hydrological model to predict the future streamflow depends on its ability to model the current scenarios (Dibike and Coulibaly, 2007).

Tables (39 and 40) show the projected changes for the mean and maximum monthly discharge for three time slices of future corresponding to A2 and B2 scenarios with respect to the baseline discharge at Sulaiman streamflow station. Figures (from 89 to 100) illustrate the projected changes in the mean and maximum monthly river hydrograph for three time slices period (2020s, 2050s and 2080s).

The assessment of climate change impacts on the river discharge at Sulaiman streamflow station has been performed to estimate mean and maximum monthly river hydrograph for the future. The downscaled baseline and future precipitation, temperature and evaporation obtained from SDSM are entered into HEC-HMS model to simulate the baseline and future streamflows. Downscaled temperature data to calculate ET using Hargreaves' method, are also entered into HEC-HMS for discharge simulation. The validated HEC-HMS model is used to simulate the runoff at Sulaiman streamflow station located at the outlet of the watershed.

The lack of updated landuse, soil and topography data have forced the study to consider it as an assumption with no change during the time. Neither change in soil nor landuse cover is considered to project future streamflow which makes it assure that the streamflow projections for future are solely dependent on the climate change scenarios.

Results of HEC-HMS model indicate that the discharge patterns will change for the future. It is seen that the downscaled mean and maximum precipitation may produce a

wide range of changes in the hydrology of Klang watershed. Sulaiman streamflow station in Klang River is identified by a typical hydrograph includes two main discharge peaks which are in April and November for the period 1975-2001,whereas February and September is attributed as the least amount of discharge of Sulaiman streamflow station. It reveals that the wet season is from April to June and October to December, while the dry season is from January to March and July to September.

It is obvious from the results that predicted annual mean discharge for future periods are decreasing except the period 2080s is increasing according to A2 scenario. The projected mean discharge indicated a decline in months from January to April and also from July to August in all the three time slices periods for A2 and B2 scenarios. There is an increasing trend in the discharge of June, September and October in all the three future periods under A2 scenario. However, peak flow of mean runoff in May and June did not change much for 2020s and 2050s. Obviously, the magnitude of increasing is higher in A2 than in B2 scenario.

In the three future time slices predicted, the annual mean discharge is predicted a decrease by 9.4%, 4.9% and an increase of 3.4% for A2 while a decrease about 17.3%, 14.3% and 6.2% for B2 scenario. The average annual maximum discharge is projected a decrease of 7.7% in 2020s and an increase of 4.2% and 29% in A2 scenario for 2050s and 2080s respectively, while there will most likely be a decrease as the maximum discharge for all the future under B2 scenario. It is projected a decrease of 32.4%, 19.5% and 2.1% for 2020s, 2050s and 2080s, respectively.

The maximum absolute increase in the mean peak runoff was projected in May and October for 2080s under A2 scenario, with a difference of 7.6 $m^3/s$ (29.7 $m^3/s$ as compare to 21.9 $m^3/s$ in May) and 7.6 $m^3/s$ (28.9 $m^3/s$ as compare to 21.3 $m^3/s$ in October). On the other hand, the maximum absolute increase in the maximum peak runoff was projected in May and October for 2080s under A2 scenario, with a difference of 36.8 $m^3/s$ (90.3 $m^3/s$ as compare to 53.5 $m^3/s$ in May) and 53.4 $m^3/s$ (105.3 $m^3/s$ as compare to 51.9 $m^3/s$ in October).

Absolute increase of mean precipitation in months of May, September and November are 145.8 mm, 206.7 mm and 46.8 mm in 2080s under A2 scenario. The changes in

mean precipitation in these months (32% in May, 88% in September, 17% in November) result in the increase of mean runoff by 34%, 52% and 4%., respectively. The highest increase in evapotranspiration and rather increase in maximum temperature in November, cause the changes of mean runoff by 4% in this month. Mean precipitation is expected to a rather increase in July by 5% but an increase in evapotranspiration in this month causes a reduction in mean runoff.

A reduction of precipitation by 24.6% and 5.7% in January and March in 2080s under A2 scenario, result a reduction of runoff by 52% and 17%, respectively. However, there is a reduction of precipitation in June by 31%, the runoff is affected by the high volume of precipitation in May (455.9 mm). It can produce a large amount of baseflow or delayed runoff in the watershed. The baseflow or delayed runoff affects the part of runoff occurs after the end of the flood which produces the continuous high flow rates in the hydrograph.

Absolute increase of maximum precipitation in months of September, October and November are 426 mm, 235 mm and 142.3 mm in 2080s under A2 scenario. The changes in mean precipitation in these months (168.9% in September, 82% in October, and 43.2% in November) result in the increase of maximum runoff by 122.5%, 102.9% and 28.8%., respectively. There is an increase in maximum precipitation by 118% in June, which causes an increase in maximum discharge by 93%. It was affected by the delayed runoff of month May. Maximum precipitation is quite high in May which is 893.7 mm in 2080s. However, a reduction of runoff by 30.6% is observed, which is highly affected by baseflow runoff in March. A reduction of maximum precipitation by 8.6% in March causes a decrease in runoff by 22%.

Results of comparison between the projected changes for monthly mean streamflows at Sulaiman streamflow station indicate small difference between the two IPCC scenarios. This difference ranges between 8.7%, 10.3% and 9.5% for 2020s, 2050s and 2080s, respectively. The most significant heavy precipitation has been observed during the months of October, November and December as the watershed experiences the north-eastern monsoon season in those months (Chen et al., 2013; Ahmad et al., 2012). The flow data of Klang River at Sulaiman streamflow station reveals that the flow regime mainly depends on the northeast monsoon which is from November to

March as Table 39. The contribution of the northeast monsoon is expected to 83.4 $m^3/s$, 84.6 $m^3/s$ and 87.4 $m^3/s$ under A2 scenario in 2020s, 2050s and 2080s respectively while the value are estimated to 76.9 $m^3/s$ in 2020s, 77.5 $m^3/s$ .in 2050s and 81.9 $m^3/s$ in 2080s corresponding B2 scenario.

Appendix Q lists the spatial maps of rainfall intensity for the future corresponding to A2 and B2 scenarios estimates for a return period of 10 to 100 year will expect an increase in precipitation around north and south of the watershed. It reveals that the mountain parts particularly in north have the highest value of rainfall intensities and on the other hand the inland area of Klang watershed has the lowest values. It can be concluded that the trend of rainfall intensity in Klang watershed is dependent on the influence of northeast monsoon winds although the mountains can play an obstruction in the area. It indicates clearly that the projected storms during northeast monsoon produces higher peak discharge and lower flood volume particularly in 2080s compared with that induced from the storms through southwest monsoon due to the high rainfall intensity and low antecedent soil moisture.

The results represent the trend of simulated runoff of Klang watershed and the importance of soil moisture in controlling the surface runoff production which is because of the maximum flood is expected to occur mostly in October in 2020s and 2050s while in May in 2080s. The reduction in the runoff is due to the reduction in base flow during periods of no rain or less rainfall. It is not due to the reduction in direct surface runoff during storm events.

The large relative increase in the wet season runoff is associated with the seasonal variability of precipitation in Klang watershed. However, it was predicted an uneven reduction in runoff in dry season, which is explained by the shift during the period of flows from the months.

The modelled runoff and its peak flow vary based on the spatial distribution of the raingauge stations over Klang watershed. The Gauge Weight Method allocates the climatic parameters for each sub-watershed in Klang watershed. The results reveal that runoff and its peak flow are highly dependent on the spatial variability of precipitation. Downscaled climate variables and the spatial pattern cause to shift in

the runoff hydrographs and its peak flow. However, most of the peak flows at Sulaiman streamflow station are caused by convective precipitation events. Overall, a higher streamflow during the flood season and a lower streamflow during the dry season are estimated in mean runoff for the future periods.

One of the factors may affect the predictions of future runoff is the uncertainty of the GCM projection. The interface between the GCM and local streamflow simulations is a great simplification may strongly affect in the hydrograph. GCM outputs demonstrate a range of projected future precipitation amounts, while local precipitation and ET have a significant role in runoff generation. Surface runoff simulation in Klang watershed which is located in the Southeast Asia, a monsoon region, is the result of downscaled climate data. Then, the discrepancy between current runoff in the watershed and simulated runoff resulted from the GCM-HadCM3 model is expected. However, none of the current climate change models are able to simulate perfectly the monsoon conditions over Southeast Asia (Webster et al., 1998). The main concern is the accuracy of the rainfall-runoff model, particularly in maximum runoff and peak flow. It can be affected by a large volume of detention storage in Klang watershed on the initial loss model.

Table 39 Projected changes for monthly mean streamflows at Sulaiman streamflow station under A2 and B2 scenarios (in $m^3/s$)

| Month | A2 | | | B2 | | |
|---|---|---|---|---|---|---|
| | 2020s | 2050s | 2080s | 2020s | 2050s | 2080s |
| Jan | 10.4 | 9.2 | 8.51 | 10.2 | 8.8 | 8.1 |
| Feb | 13.6 | 13.8 | 14.0 | 13.1 | 13.4 | 14.2 |
| Mar | 16.0 | 16.3 | 16.5 | 15.1 | 15.4 | 16.9 |
| Apr | 17.9 | 18.4 | 19.3 | 16.6 | 17.0 | 18.4 |
| May | 21.9 | 24.6 | 29.7 | 19.6 | 21.8 | 26.2 |
| Jun | 18.1 | 19.4 | 22.7 | 16.4 | 17.5 | 20.4 |
| Jul | 16.2 | 16.2 | 16.5 | 15.0 | 15.0 | 15.3 |
| Aug | 17.9 | 18.3 | 18.9 | 16.2 | 16.6 | 17.2 |
| Sep | 21.1 | 22.4 | 25.5 | 18.8 | 19.8 | 22.5 |
| Oct | 23.1 | 25.4 | 28.9 | 20.4 | 22.2 | 25.2 |
| Nov | 22.7 | 23.9 | 25.6 | 20.1 | 21.1 | 22.5 |
| Dec | 20.7 | 21.4 | 22.8 | 18.4 | 18.8 | 20.2 |
| Annual | 18.3 | 19.1 | 20.7 | 16.7 | 17.3 | 18.9 |

Table 40 Projected changes for monthly maximum streamflows at Sulaiman streamflow station under A2 and B2 scenarios (in $m^3/s$)

| Month | A2 | | | B2 | | |
|---|---|---|---|---|---|---|
| | 2020s | 2050s | 2080s | 2020s | 2050s | 2080s |
| Jan | 19.2 | 21.1 | 27.7 | 17.8 | 19.8 | 20.1 |
| Feb | 18.7 | 25.4 | 25.1 | 18.3 | 21.3 | 19.3 |
| Mar | 24.4 | 29.2 | 28.8 | 20.0 | 27.4 | 23.9 |
| Apr | 34.3 | 37.2 | 42.6 | 25.7 | 29.9 | 33.1 |
| May | 71.0 | 76.5 | 90.3 | 49.2 | 57.1 | 67.0 |
| Jun | 55.9 | 62.9 | 81.3 | 39.3 | 47.3 | 60.3 |
| Jul | 31.9 | 36.9 | 47.0 | 24.3 | 29.2 | 36.0 |
| Aug | 39.1 | 40.8 | 45.2 | 28.8 | 31.8 | 34.4 |
| Sep | 46.7 | 57.3 | 81.9 | 33.6 | 43.2 | 60.2 |
| Oct | 61.3 | 74.3 | 105.3 | 42.4 | 54.4 | 76.0 |
| Nov | 58.9 | 69.6 | 84.1 | 40.3 | 51.0 | 61.3 |
| Dec | 47.5 | 54.6 | 62.4 | 33.0 | 40.7 | 46.5 |
| Annual | 42.4 | 48.8 | 60.1 | 31.1 | 37.8 | 44.8 |

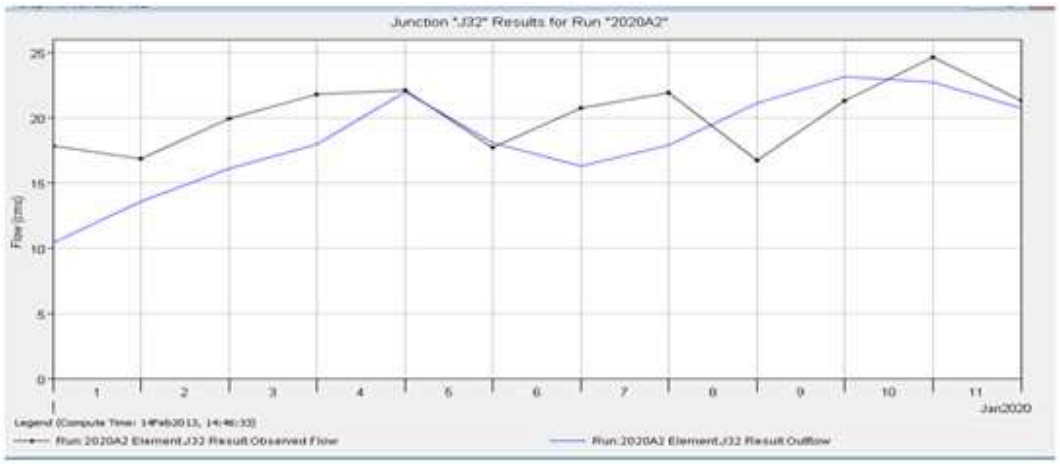


Figure 89 Comparison between the observed and 2020s average monthly streamflows simulated at Sulaiman streamflow station under A2 scenario

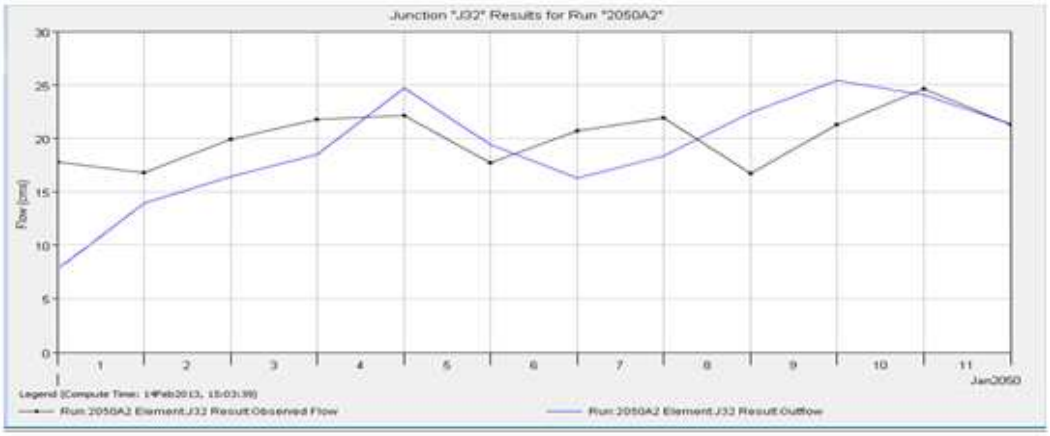


Figure 90 Comparison between the observed and 2050s average monthly streamflows simulated at Sulaiman streamflow station under A2 scenario

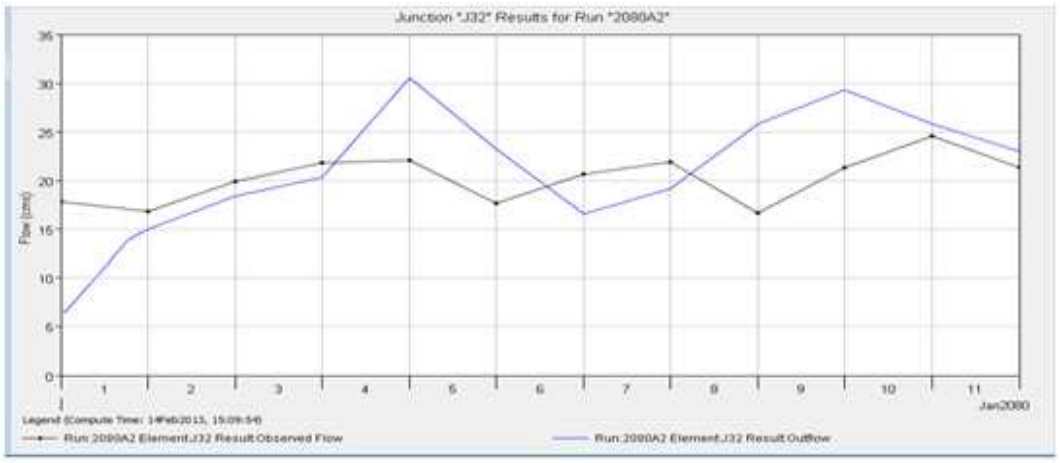


Figure 91 Comparison between the observed and 2080s average monthly streamflows simulated at Sulaiman streamflow station under A2 scenario

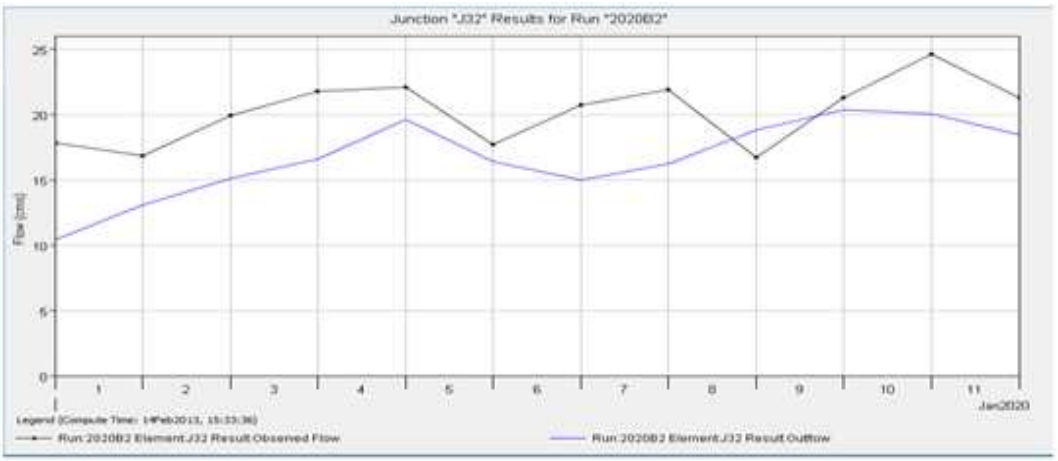


Figure 92 Comparison between the observed and 2020s average monthly streamflows simulated at Sulaiman streamflow station under B2 scenario

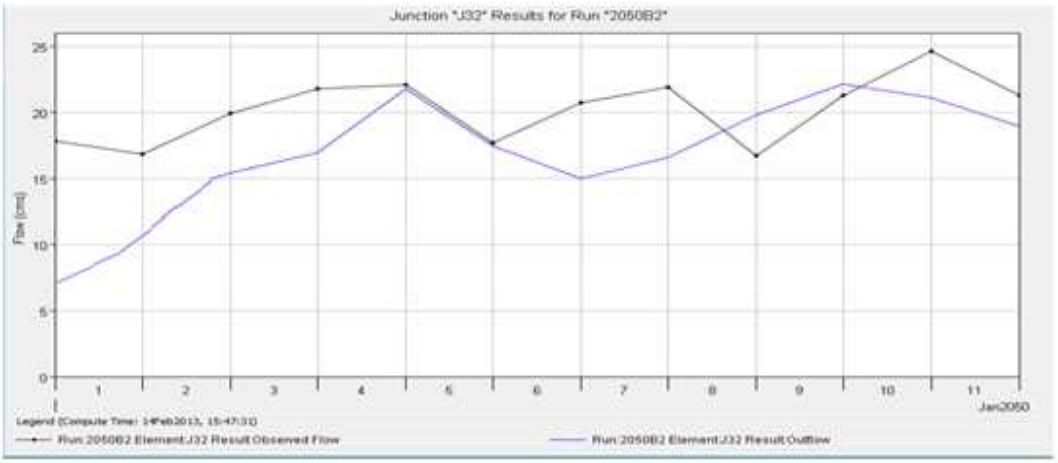


Figure 93 Comparison between the observed and 2050s average monthly streamflows simulated at Sulaiman streamflow station under B2 scenario


Figure 94 Comparison between the observed and 2080s average monthly streamflows simulated at Sulaiman streamflow station under B2 scenario

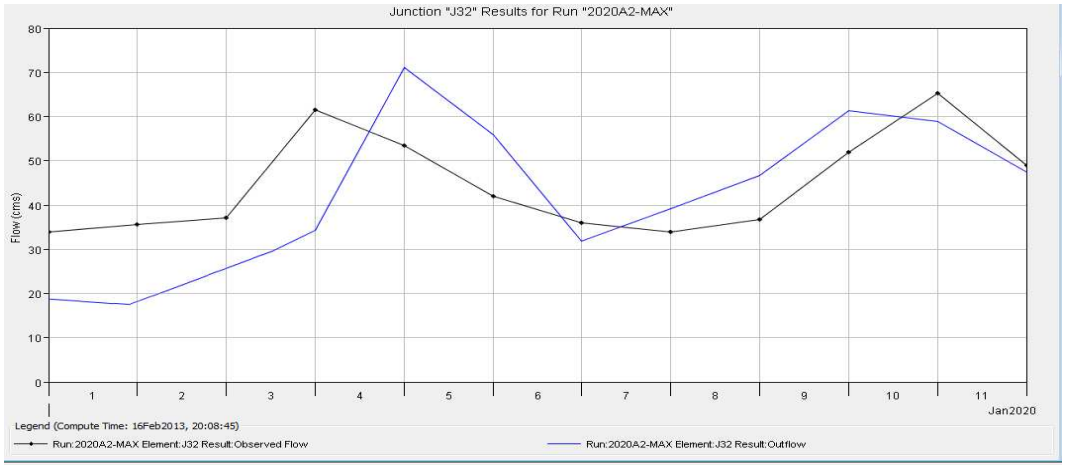


Figure 95 Comparison between the observed and 2020s maximum monthly streamflows simulated at Sulaiman streamflow station under A2 scenario

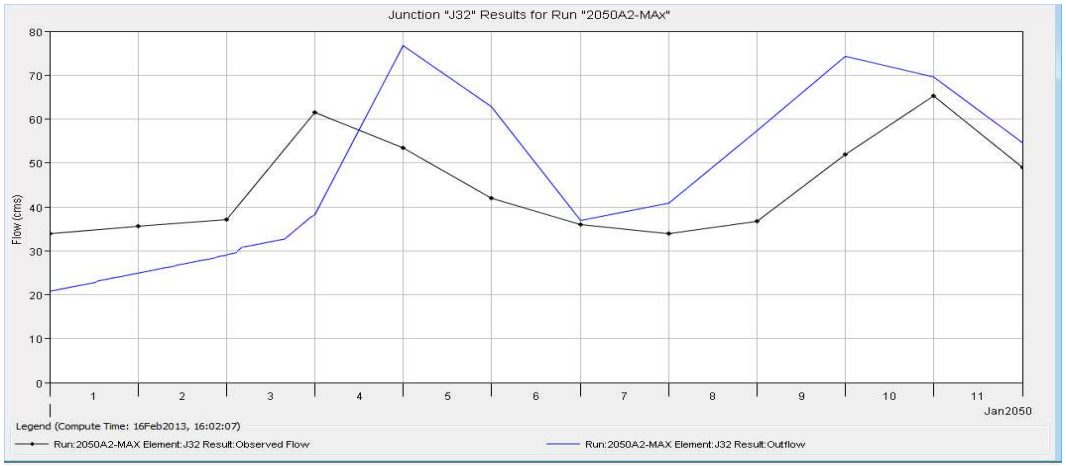


Figure 96 Comparison between the observed and 2050s maximum monthly streamflows simulated at Sulaiman streamflow station under A2 scenario

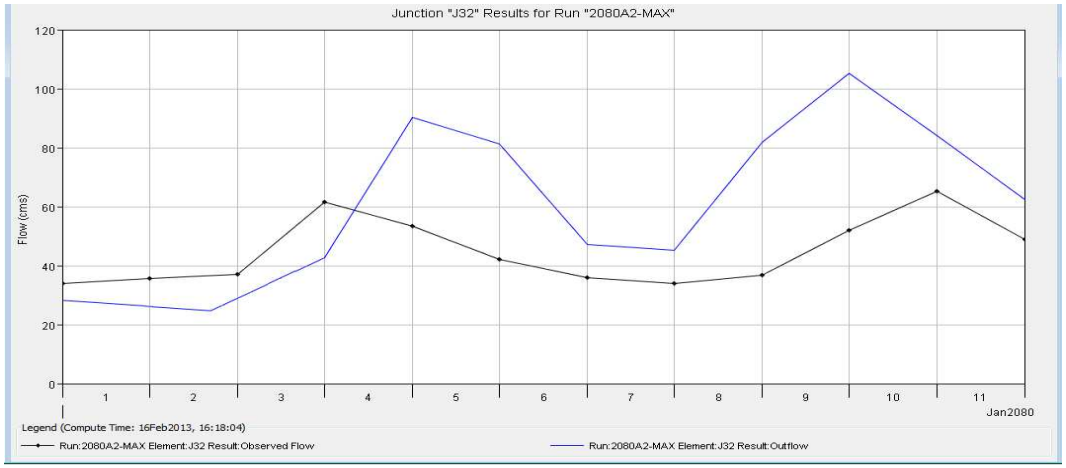


Figure 97 Comparison between the observed and 2080s maximum monthly streamflows simulated at Sulaiman streamflow station under A2 scenario

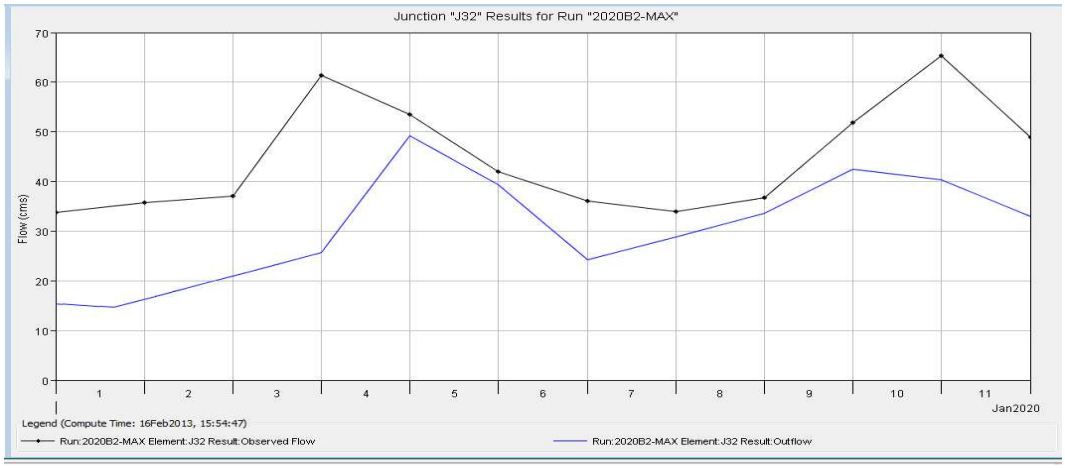


Figure 98 Comparison between the observed and 2020s maximum monthly streamflows simulated at Sulaiman streamflow station under B2 scenario

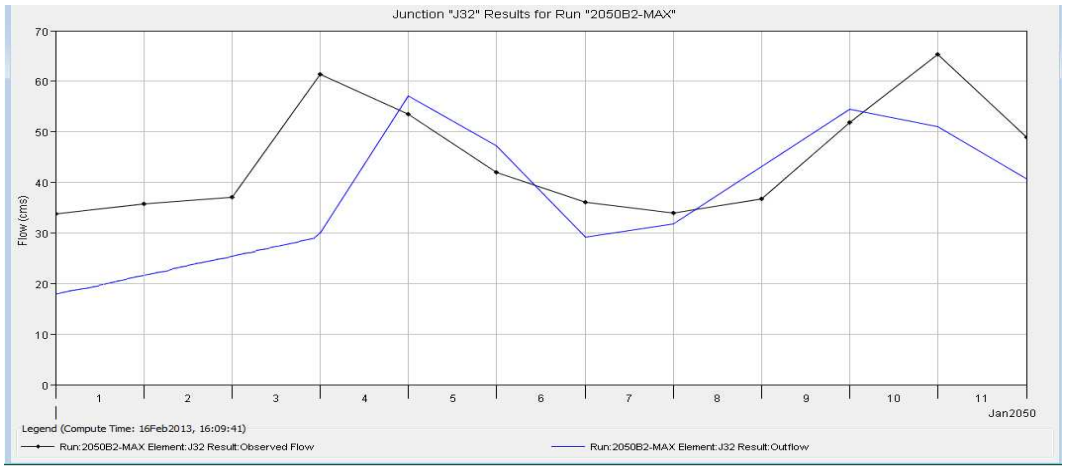


Figure 99 Comparison between the observed and 2050s maximum monthly streamflows simulated at Sulaiman streamflow station under B2 scenario

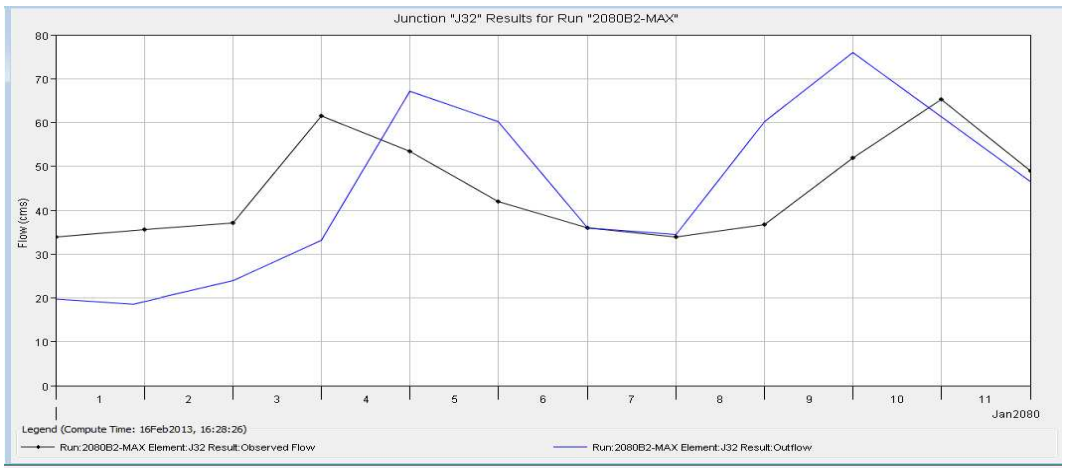


Figure 100 Comparison between the observed and 2080s maximum monthly streamflows simulated at Sulaiman streamflow station under B2 scenario

## 6-6- Assessment of Climate Change Impact on the Flood Frequency

The analysis was done for assessment of climate change impacts on the occurrence of extreme precipitation events at 10 raingauge stations and also on the discharge station to determine the amount of discharge for the return periods 5, 10, 25, 50 and100 years for three time slices (2020s, 2050s and 2080s) corresponding to A2 and B2 scenarios.

### 6-6-1- Assessment of Climate Change Impact on the Occurrence of Extreme Precipitation Events

The impact of climate change on the occurrence of precipitation events was evaluated by spatial mapping in GIS (Appendix Q). The Gumbel Distribution was run for estimation of extreme precipitation events at 10 raingauge stations over Klang watershed. Tables (from 41 to 46) show the maximum precipitation downscaled for the future which is used as input into Gumbel Distribution function. Tables (from 47 to 53) and Figures (101 and 102) show results for 5, 10.20,50 and 100 year return periods according to current and future depths.

Maximum precipitation intensity for return period of 5 year is estimated to 146.97 mm in 2020s, 150.11 mm in 2050s and 164.45 mm in 2080s corresponding A2 scenario. It is found an increase about 22.18 mm, 25.32 mm and 39.66 mm for 2020s, 2050s and 2080s respectively compared to the observed extreme precipitation. B2 scenario for return period of 5 year is projected lower values than A2 scenario. A decrease of 7.78 mm in 2020s, 7.35 mm in 2050s and increase of 10.22 mm in 2080s are estimated for B2 scenario.

There is an increase of extreme precipitation intensity for return period of 5 to 100 years range between 146.97 mm to 281.05 mm in 2020s, 150.11 mm to 288.93 mm in 2050s and 164.45 mm to 340.45 mm in 2080s. This trend for B2 scenario was estimated to a range from 139.10 mm to 263.79 mm in 2020s, 142.76 mm to 271.56 mm in 2050s and 154.23 mm to 311.85 mm in 2080s.

The minimum increase of extreme precipitation intensity is observed in 2020s under A2 scenario for the return period of 5 year by 22.18 mm and the maximum increase of

intensity in this time slice will likely be expected by 71.25 mm for return period of 100 year. The minimum increase of extreme precipitation intensity in 2050s is observed by 25.32 mm and the maximum increase of 79.17 mm for return periods of 5 and 100, respectively. The trend in this time slice under B2 scenario was estimated to 17.97 mm and 61.76 mm for the relevant return period respectively.

The highest increase in maximum precipitation intensity will be expected in 2080s for both A2 and B2 scenarios. The minimum and maximum increase ranges between 39.66 mm and 130.65 mm for return period of 5 and 100 year, respectively. The values under B2 scenario range between 29.44 mm and 102.05 mm for the relevant return period respectively.

The frequency curve of predicted peak precipitation events for A2 scenario is higher than the peak events of B2 scenario in all the tree time slices for the return periods. The frequency analysis results of the extreme precipitation indicated that the increasing extreme precipitation will occur according to the A2 and B2 scenarios in Klang watershed. The highest increase in maximum precipitation intensity is in 2080s under A2 scenario. The increase in the magnitude of 100 year is found about 88% greater than observed. The analysis reveals that overall increasing trend of three time slices' future flood frequency is a linear trend. It is obvious that occurrence of extreme precipitation events are compliance with downscaled precipitation output from SDSM. The downscaled precipitation indicated an increase in precipitation with a decrease in the number of consecutive wet-days in the future. It causes a probability of flooding due to increasing of rainfall intensity.

It can be concluded that the probability of flood happening are higher due to increasing rainfall intensity. Hence, the days with heavy precipitation will be expected to occur more frequently during the year. Climate change will likely result in an increase in the intensity and frequency of extreme precipitation events in the future.

Table 41 Projected maximum precipitation for 2020s under A2 scenario

| Month | 3116005 | 3116006 | 3117070 | 3118069 | 3216001 | 3217001 | 3217002 | 3217003 | 3217004 | 3317004 |
|---|---|---|---|---|---|---|---|---|---|---|
| **Jan** | 57.84 | 66.07 | 101.34 | 42.14 | 66.62 | 59.98 | 104.63 | 27.22 | 87.29 | 66.90 |
| **Feb** | 96.46 | 116.07 | 150.75 | 57.38 | 104.04 | 122.71 | 96.09 | 28.77 | 158.50 | 81.23 |
| **Mar** | 90.14 | 110.98 | 103.49 | 61.96 | 109.11 | 124.51 | 107.72 | 31.12 | 99.31 | 86.79 |
| **Apr** | 128.95 | 140.45 | 173.32 | 56.79 | 159.24 | 137.55 | 143.78 | 36.70 | 166.86 | 117.04 |
| **May** | 81.88 | 98.19 | 173.69 | 61.27 | 168.24 | 144.36 | 130.81 | 35.98 | 119.08 | 844.54 |
| **Jun** | 69.58 | 81.15 | 142.48 | 37.31 | 103.13 | 108.86 | 78.56 | 24.17 | 88.69 | 88.49 |
| **Jul** | 61.13 | 75.62 | 95.29 | 52.90 | 126.68 | 107.59 | 88.47 | 26.81 | 96.97 | 98.01 |
| **Aug** | 71.00 | 63.34 | 121.03 | 56.24 | 138.68 | 112.78 | 101.42 | 32.00 | 97.98 | 122.49 |
| **Sep** | 99.30 | 95.20 | 152.52 | 65.65 | 172.79 | 134.73 | 149.43 | 40.57 | 106.94 | 122.91 |
| **Oct** | 86.35 | 82.57 | 166.94 | 79.17 | 106.14 | 142.82 | 165.12 | 42.32 | 121.22 | 122.42 |
| **Nov** | 91.38 | 129.38 | 101.50 | 88.19 | 144.99 | 125.97 | 109.67 | 37.36 | 112.40 | 114.71 |
| **Dec** | 92.91 | 94.13 | 106.71 | 46.00 | 104.26 | 100.95 | 99.23 | 27.43 | 99.94 | 77.29 |
| **Annual** | **85.58** | **96.10** | **132.42** | **58.75** | **125.33** | **118.57** | **114.58** | **32.54** | **112.93** | **161.90** |

Table 42 Projected maximum precipitation for 2050s under A2 scenario

| Month | 3116005 | 3116006 | 3117070 | 3118069 | 3216001 | 3217001 | 3217002 | 3217003 | 3217004 | 3317004 |
|---|---|---|---|---|---|---|---|---|---|---|
| **Jan** | 62.01 | 64.11 | 94.27 | 42.57 | 62.03 | 59.11 | 102.80 | 26.75 | 93.58 | 65.53 |
| **Feb** | 89.16 | 104.77 | 154.30 | 55.59 | 123.22 | 134.90 | 107.81 | 29.58 | 146.50 | 85.16 |
| **Mar** | 96.61 | 102.37 | 91.25 | 67.70 | 119.64 | 116.19 | 110.71 | 31.91 | 106.43 | 73.09 |
| **Apr** | 128.22 | 158.24 | 182.10 | 52.93 | 187.17 | 148.97 | 133.19 | 36.34 | 165.91 | 116.08 |
| **May** | 92.78 | 96.91 | 185.20 | 63.39 | 221.72 | 140.26 | 127.90 | 35.73 | 134.92 | 739.35 |
| **Jun** | 72.25 | 88.07 | 166.70 | 37.46 | 94.66 | 95.59 | 84.09 | 25.65 | 92.09 | 95.52 |
| **Jul** | 57.84 | 72.62 | 94.13 | 52.79 | 158.82 | 104.28 | 98.93 | 26.85 | 91.74 | 103.76 |
| **Aug** | 74.43 | 58.66 | 105.87 | 58.67 | 158.26 | 97.49 | 96.02 | 30.73 | 102.71 | 113.80 |
| **Sep** | 94.30 | 98.48 | 194.54 | 69.82 | 209.65 | 150.05 | 141.46 | 40.31 | 101.55 | 111.92 |
| **Oct** | 93.57 | 64.53 | 166.35 | 80.59 | 111.72 | 153.23 | 188.35 | 41.59 | 131.34 | 116.68 |
| **Nov** | 101.96 | 130.04 | 74.20 | 90.01 | 143.66 | 161.20 | 109.31 | 36.48 | 125.42 | 128.56 |
| **Dec** | 100.23 | 91.39 | 87.30 | 45.80 | 102.55 | 88.97 | 96.63 | 26.53 | 107.81 | 73.50 |
| **Annual** | **88.61** | **94.18** | **133.02** | **59.78** | **141.09** | **120.85** | **116.43** | **32.37** | **116.67** | **151.91** |

Table 43 Projected maximum precipitation for 2080s under A2 scenario

| Month | 3116005 | 3116006 | 3117070 | 3118069 | 3216001 | 3217001 | 3217002 | 3217003 | 3217004 | 3317004 |
|---|---|---|---|---|---|---|---|---|---|---|
| **Jan** | 66.11 | 67.37 | 77.97 | 45.19 | 56.78 | 36.71 | 115.50 | 26.14 | 99.77 | 64.37 |
| **Feb** | 90.57 | 121.88 | 136.44 | 59.60 | 139.24 | 139.02 | 100.92 | 29.13 | 148.82 | 74.51 |
| **Mar** | 98.98 | 98.37 | 98.77 | 69.46 | 106.38 | 117.25 | 107.72 | 30.88 | 109.05 | 89.50 |
| **Apr** | 126.45 | 155.52 | 222.01 | 52.12 | 199.23 | 152.30 | 126.83 | 37.68 | 163.62 | 117.24 |
| **May** | 90.43 | 121.41 | 282.35 | 62.05 | 277.06 | 169.64 | 150.56 | 35.70 | 131.50 | 847.87 |
| **Jun** | 64.40 | 93.36 | 206.24 | 37.81 | 25.18 | 98.63 | 82.15 | 24.69 | 82.08 | 108.53 |
| **Jul** | 46.83 | 67.98 | 85.79 | 46.34 | 173.20 | 87.24 | 95.34 | 26.22 | 74.28 | 102.69 |
| **Aug** | 71.46 | 41.27 | 120.11 | 55.72 | 146.53 | 87.35 | 87.38 | 32.47 | 98.61 | 122.73 |
| **Sep** | 95.05 | 95.55 | 209.76 | 75.79 | 240.73 | 162.32 | 160.49 | 40.70 | 102.36 | 108.82 |
| **Oct** | 102.95 | 60.64 | 187.39 | 81.20 | 98.02 | 167.96 | 207.96 | 40.78 | 144.52 | 110.66 |
| **Nov** | 96.26 | 118.61 | 52.92 | 83.93 | 189.50 | 158.45 | 111.85 | 38.25 | 118.40 | 112.45 |
| **Dec** | 87.12 | 74.19 | 51.94 | 43.88 | 96.99 | 99.81 | 80.43 | 25.95 | 93.71 | 80.84 |
| **Annual** | **86.38** | **93.01** | **144.31** | **59.43** | **145.74** | **123.06** | **118.93** | **32.38** | **113.89** | **161.68** |

Table 44 Projected maximum precipitation for 2020s under B2 scenario

| Month | 3116005 | 3116006 | 3117070 | 3118069 | 3216001 | 3217001 | 3217002 | 3217003 | 3217004 | 3317004 |
|---|---|---|---|---|---|---|---|---|---|---|
| **Jan** | 52.58 | 65.57 | 95.50 | 39.71 | 66.45 | 63.39 | 99.32 | 27.38 | 67.15 | 61.04 |
| **Feb** | 87.69 | 110.59 | 158.02 | 60.14 | 115.37 | 134.23 | 102.56 | 29.93 | 121.92 | 72.75 |
| **Mar** | 81.95 | 95.31 | 105.52 | 63.17 | 118.42 | 120.87 | 111.30 | 31.31 | 76.39 | 79.07 |
| **Apr** | 117.23 | 162.97 | 162.46 | 53.23 | 156.39 | 134.21 | 132.56 | 37.40 | 128.35 | 113.09 |
| **May** | 74.44 | 99.98 | 158.60 | 55.94 | 173.07 | 134.24 | 124.91 | 35.91 | 91.60 | 766.11 |
| **Jun** | 63.26 | 81.49 | 137.77 | 36.08 | 97.69 | 103.29 | 84.60 | 25.10 | 68.22 | 94.50 |
| **Jul** | 55.57 | 66.89 | 100.51 | 55.80 | 123.05 | 101.39 | 89.96 | 26.48 | 74.59 | 98.49 |
| **Aug** | 64.55 | 72.10 | 120.45 | 55.97 | 129.33 | 111.75 | 122.58 | 32.12 | 75.37 | 123.63 |
| **Sep** | 90.27 | 97.64 | 170.81 | 73.52 | 167.23 | 133.84 | 137.34 | 40.28 | 82.26 | 119.52 |
| **Oct** | 78.50 | 82.68 | 156.84 | 74.38 | 118.85 | 140.16 | 179.11 | 40.62 | 93.24 | 115.05 |
| **Nov** | 83.07 | 117.81 | 92.84 | 80.67 | 126.02 | 138.60 | 108.39 | 36.16 | 86.46 | 120.32 |
| **Dec** | 84.46 | 91.76 | 98.48 | 42.46 | 104.82 | 95.58 | 81.28 | 26.27 | 76.88 | 78.37 |
| **Annual** | **77.80** | **95.40** | **129.82** | **57.59** | **124.72** | **117.63** | **114.49** | **32.41** | **86.87** | **153.50** |

Table 45 Projected maximum precipitation for 2050s under B2 scenario

| Month | 3116005 | 3116006 | 3117070 | 3118069 | 3216001 | 3217001 | 3217002 | 3217003 | 3217004 | 3317004 |
|---|---|---|---|---|---|---|---|---|---|---|
| **Jan** | 55.81 | 69.23 | 90.58 | 42.25 | 66.96 | 53.62 | 117.68 | 25.70 | 82.35 | 58.14 |
| **Feb** | 80.24 | 111.90 | 151.57 | 56.26 | 143.71 | 137.33 | 99.21 | 29.25 | 128.92 | 78.82 |
| **Mar** | 86.95 | 102.25 | 88.85 | 65.65 | 113.79 | 113.20 | 99.93 | 31.07 | 93.66 | 85.07 |
| **Apr** | 115.40 | 147.73 | 180.48 | 54.00 | 164.17 | 134.88 | 122.37 | 38.08 | 146.00 | 120.59 |
| **May** | 83.50 | 106.25 | 183.92 | 60.42 | 200.42 | 148.99 | 130.45 | 35.54 | 118.73 | 714.49 |
| **Jun** | 65.03 | 79.53 | 153.38 | 34.49 | 97.52 | 98.94 | 82.60 | 23.95 | 81.04 | 88.48 |
| **Jul** | 52.05 | 65.33 | 93.87 | 48.27 | 145.38 | 108.19 | 100.72 | 26.78 | 80.73 | 94.46 |
| **Aug** | 66.99 | 64.64 | 111.30 | 58.21 | 160.29 | 101.98 | 98.31 | 32.31 | 90.38 | 127.88 |
| **Sep** | 84.87 | 100.12 | 190.06 | 74.95 | 184.48 | 149.81 | 133.89 | 39.38 | 89.37 | 117.73 |
| **Oct** | 84.21 | 69.46 | 161.54 | 82.95 | 107.06 | 132.09 | 172.42 | 40.39 | 115.58 | 117.91 |
| **Nov** | 91.77 | 118.46 | 77.36 | 83.68 | 135.14 | 151.87 | 100.96 | 38.20 | 110.37 | 116.95 |
| **Dec** | 90.20 | 93.77 | 83.78 | 45.45 | 105.59 | 87.30 | 93.14 | 26.09 | 94.87 | 71.59 |
| **Annual** | **79.75** | **94.06** | **130.56** | **58.88** | **135.38** | **118.18** | **112.64** | **32.23** | **102.67** | **149.34** |

Table 46 Projected maximum precipitation for 2080s under B2 scenario

| Month | 3116005 | 3116006 | 3117070 | 3118069 | 3216001 | 3217001 | 3217002 | 3217003 | 3217004 | 3317004 |
|---|---|---|---|---|---|---|---|---|---|---|
| **Jan** | 58.84 | 73.76 | 73.35 | 45.39 | 58.80 | 47.01 | 99.54 | 26.81 | 90.79 | 60.55 |
| **Feb** | 80.60 | 106.12 | 139.33 | 56.47 | 137.80 | 119.83 | 103.10 | 28.60 | 135.42 | 76.08 |
| **Mar** | 88.09 | 88.23 | 89.79 | 69.37 | 113.40 | 123.60 | 106.26 | 30.26 | 99.23 | 81.36 |
| **Apr** | 112.54 | 156.37 | 200.49 | 52.19 | 191.51 | 148.46 | 124.55 | 37.97 | 148.90 | 105.88 |
| **May** | 80.48 | 107.90 | 249.75 | 61.78 | 245.75 | 174.04 | 135.24 | 36.82 | 119.67 | 749.96 |
| **Jun** | 57.32 | 80.04 | 209.26 | 33.39 | 68.25 | 87.30 | 78.74 | 24.66 | 74.69 | 110.12 |
| **Jul** | 41.68 | 63.05 | 86.23 | 42.74 | 155.47 | 97.78 | 102.08 | 26.55 | 67.59 | 103.22 |
| **Aug** | 63.60 | 52.86 | 126.84 | 56.33 | 154.78 | 90.93 | 81.18 | 32.80 | 89.73 | 129.61 |
| **Sep** | 84.60 | 87.81 | 224.30 | 70.38 | 230.67 | 160.28 | 152.34 | 38.99 | 93.15 | 116.36 |
| **Oct** | 91.63 | 61.88 | 196.23 | 88.67 | 99.36 | 148.61 | 221.60 | 40.66 | 131.51 | 115.88 |
| **Nov** | 85.67 | 111.58 | 57.13 | 84.97 | 156.44 | 147.18 | 107.54 | 37.17 | 107.74 | 121.39 |
| **Dec** | 77.54 | 78.72 | 49.02 | 39.81 | 93.54 | 98.54 | 94.34 | 26.59 | 85.28 | 76.29 |
| **Annual** | **76.88** | **89.03** | **141.81** | **58.46** | **142.15** | **120.3** | **117.21** | **32.32** | **103.64** | **153.89** |

Table 47 Return periods at 10 raingauge stations for 2020s under A2 scenario

| Id | Station no. | Extreme Precipitation Intensities (mm/day) | | | | |
|---|---|---|---|---|---|---|
| | | 5 year | 10 year | 25 year | 50 year | 100 year |
| 1 | 3116005 | 105.59 | 120.65 | 139.69 | 153.82 | 167.84 |
| 2 | 3116006 | 121.16 | 140.03 | 163.88 | 181.57 | 199.14 |
| 3 | 3117070 | 164.02 | 187.81 | 217.87 | 240.18 | 262.32 |
| 4 | 3118069 | 73.63 | 84.83 | 98.99 | 109.49 | 119.92 |
| 5 | 3216001 | 158.33 | 183.18 | 214.58 | 237.88 | 261.01 |
| 6 | 3217001 | 142.58 | 160.67 | 183.53 | 200.48 | 217.31 |
| 7 | 3217002 | 142.00 | 162.64 | 188.73 | 208.09 | 227.30 |
| 8 | 3217003 | 38.65 | 43.25 | 49.06 | 53.37 | 57.65 |
| 9 | 3217004 | 139.31 | 159.17 | 184.27 | 202.89 | 221.38 |
| 10 | 3317004 | 384.40 | 551.97 | 763.69 | 920.76 | 1076.66 |
| **Average** | | **146.97** | **179.42** | **220.43** | **250.85** | **281.05** |

Table 48 Return periods at 10 raingauge stations for 2050s under A2 scenario

| Id | Station no. | Extreme Precipitation Intensities (mm/day) | | | | |
|---|---|---|---|---|---|---|
| | | 5 year | 10 year | 25 year | 50 year | 100 year |
| 1 | 3116005 | 108.62 | 123.68 | 142.72 | 156.84 | 170.86 |
| 2 | 3116006 | 123.91 | 146.29 | 174.58 | 195.56 | 216.39 |
| 3 | 3117070 | 179.80 | 215.02 | 259.54 | 292.56 | 325.34 |
| 4 | 3118069 | 75.71 | 87.70 | 102.86 | 114.11 | 125.27 |
| 5 | 3216001 | 190.69 | 228.04 | 275.24 | 310.25 | 345.00 |
| 6 | 3217001 | 153.74 | 178.51 | 209.81 | 233.03 | 256.07 |
| 7 | 3217002 | 145.44 | 167.29 | 194.90 | 215.38 | 235.71 |
| 8 | 3217003 | 38.13 | 42.47 | 47.96 | 52.03 | 56.07 |
| 9 | 3217004 | 141.34 | 159.92 | 183.40 | 200.82 | 218.11 |
| 10 | 3317004 | 343.72 | 488.17 | 670.68 | 806.08 | 940.48 |
| **Average** | | **150.11** | **183.71** | **226.17** | **257.66** | **288.93** |

Table 49 Return periods at 10 raingauge stations for 2080s under A2 scenario

| Id | Station no. | Extreme Precipitation Intensities (mm/day) | | | | |
|---|---|---|---|---|---|---|
| | | 5 year | 10 year | 25 year | 50 year | 100 year |
| 1 | 3116005 | 108.20 | 124.62 | 145.38 | 160.78 | 176.06 |
| 2 | 3116006 | 126.48 | 151.69 | 183.54 | 207.17 | 230.62 |
| 3 | 3117070 | 221.99 | 280.50 | 354.42 | 409.26 | 463.70 |
| 4 | 3118069 | 75.27 | 87.20 | 102.28 | 113.46 | 124.57 |
| 5 | 3216001 | 222.17 | 279.73 | 352.45 | 406.41 | 459.96 |
| 6 | 3217001 | 166.20 | 198.69 | 239.74 | 270.20 | 300.43 |
| 7 | 3217002 | 157.76 | 187.00 | 223.95 | 251.37 | 278.58 |
| 8 | 3217003 | 38.62 | 43.33 | 49.27 | 53.67 | 58.05 |
| 9 | 3217004 | 142.61 | 164.23 | 191.56 | 211.83 | 231.95 |
| 10 | 3317004 | 385.18 | 553.50 | 766.17 | 923.95 | 1080.55 |
| **Average** | | **164.45** | **207.05** | **260.87** | **300.81** | **340.45** |

Table 50 Return periods at 10 raingauge stations for 2020s under B2 scenario

| Id | Station no. | Extreme Precipitation Intensities (mm/day) | | | | |
|---|---|---|---|---|---|---|
| | | 5 year | 10 year | 25 year | 50 year | 100 year |
| 1 | 3116005 | 95.99 | 109.69 | 126.99 | 139.84 | 152.58 |
| 2 | 3116006 | 123.09 | 143.94 | 170.28 | 189.83 | 209.23 |
| 3 | 3117070 | 161.24 | 184.91 | 214.81 | 237.00 | 259.02 |
| 4 | 3118069 | 71.98 | 82.82 | 96.51 | 106.67 | 116.76 |
| 5 | 3216001 | 155.58 | 178.81 | 208.17 | 229.95 | 251.57 |
| 6 | 3217001 | 141.66 | 159.75 | 182.62 | 199.58 | 216.42 |
| 7 | 3217002 | 142.66 | 163.87 | 190.68 | 210.56 | 230.30 |
| 8 | 3217003 | 38.14 | 42.45 | 47.90 | 51.94 | 55.96 |
| 9 | 3217004 | 107.16 | 122.44 | 141.74 | 156.07 | 170.28 |
| 10 | 3317004 | 353.52 | 504.15 | 694.48 | 835.68 | 975.83 |
| **Average** | | **139.10** | **169.28** | **207.42** | **235.71** | **263.79** |

Table 51 Return periods at 10 raingauge stations for 2050s under B2 scenario

| Id | Station no. | Extreme Precipitation Intensities (mm/day) | | | | |
|---|---|---|---|---|---|---|
| | | 5 year | 10 year | 25 year | 50 year | 100 year |
| 1 | 3116005 | 97.76 | 111.31 | 128.45 | 141.16 | 153.77 |
| 2 | 3116006 | 120.37 | 140.19 | 165.23 | 183.80 | 202.24 |
| 3 | 3117070 | 175.46 | 209.27 | 251.99 | 283.69 | 315.15 |
| 4 | 3118069 | 75.02 | 87.17 | 102.52 | 113.92 | 125.22 |
| 5 | 3216001 | 175.33 | 205.42 | 243.43 | 271.64 | 299.63 |
| 6 | 3217001 | 148.95 | 172.12 | 201.40 | 223.12 | 244.67 |
| 7 | 3217002 | 137.83 | 156.80 | 180.77 | 198.55 | 216.20 |
| 8 | 3217003 | 38.34 | 42.95 | 48.77 | 53.09 | 57.37 |
| 9 | 3217004 | 124.38 | 140.73 | 161.39 | 176.72 | 191.94 |
| 10 | 3317004 | 334.21 | 473.43 | 649.33 | 779.83 | 909.37 |
| **Average** | | **142.76** | **173.94** | **213.33** | **242.55** | **271.55** |

Table 52 Return periods at 10 raingauge stations for 2080s under B2 scenario

| Id | Station no. | Extreme Precipitation Intensities (mm/day) | | | | |
|---|---|---|---|---|---|---|
| | | 5 year | 10 year | 25 year | 50 year | 100 year |
| 1 | 3116005 | 96.29 | 110.91 | 129.39 | 143.09 | 156.69 |
| 2 | 3116006 | 118.23 | 140.23 | 168.02 | 188.64 | 209.11 |
| 3 | 3117070 | 215.28 | 270.62 | 340.53 | 392.40 | 443.88 |
| 4 | 3118069 | 76.39 | 89.89 | 106.96 | 119.61 | 132.18 |
| 5 | 3216001 | 203.51 | 249.72 | 308.11 | 351.43 | 394.43 |
| 6 | 3217001 | 158.51 | 187.28 | 223.64 | 250.61 | 277.38 |
| 7 | 3217002 | 157.45 | 187.75 | 226.03 | 254.44 | 282.63 |
| 8 | 3217003 | 38.25 | 42.71 | 48.34 | 52.52 | 56.67 |
| 9 | 3217004 | 129.77 | 149.45 | 174.32 | 192.77 | 211.08 |
| 10 | 3317004 | 348.61 | 495.25 | 680.54 | 817.99 | 954.43 |
| **Average** | | **154.23** | **192.38** | **240.59** | **276.35** | **311.85** |

Table 53 Comparison between the baseline and future Extreme Precipitation Intensities based on average maximum precipitation events for whole Klang watershed under A2 and B2 scenarios

| Return period (Year) | Extreme Precipitation Intensities (mm/day) | | | | | | |
|---|---|---|---|---|---|---|---|
| | Observed | A2 | | | B2 | | |
| | | 2020s | 2050s | 2080s | 2020s | 2050s | 2080s |
| **5** | 124.79 | 146.97 | 150.11 | 164.45 | 139.10 | 142.76 | 154.23 |
| **10** | 144.06 | 179.42 | 183.71 | 207.05 | 169.28 | 173.94 | 192.38 |
| **25** | 170.56 | 220.43 | 226.17 | 260.87 | 207.42 | 213.33 | 240.59 |
| **50** | 190.22 | 250.83 | 257.66 | 300.81 | 235.71 | 242.55 | 276.35 |
| **100** | 209.80 | 281.05 | 288.93 | 340.45 | 263.79 | 271.56 | 311.85 |

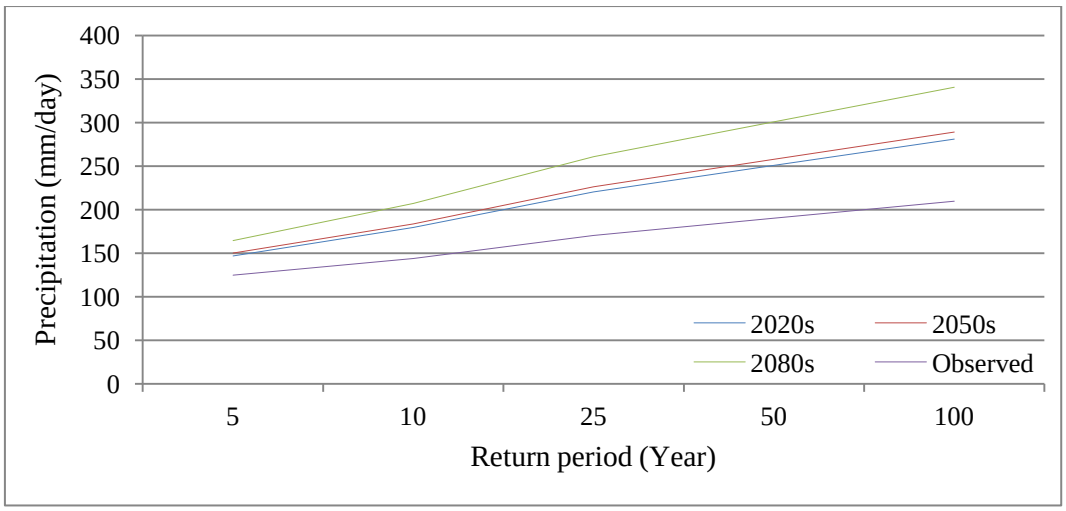


Figure 101 Comparison between the baseline and future extreme precipitation events based on average maximum precipitation events for whole Klang watershed under A2 scenario

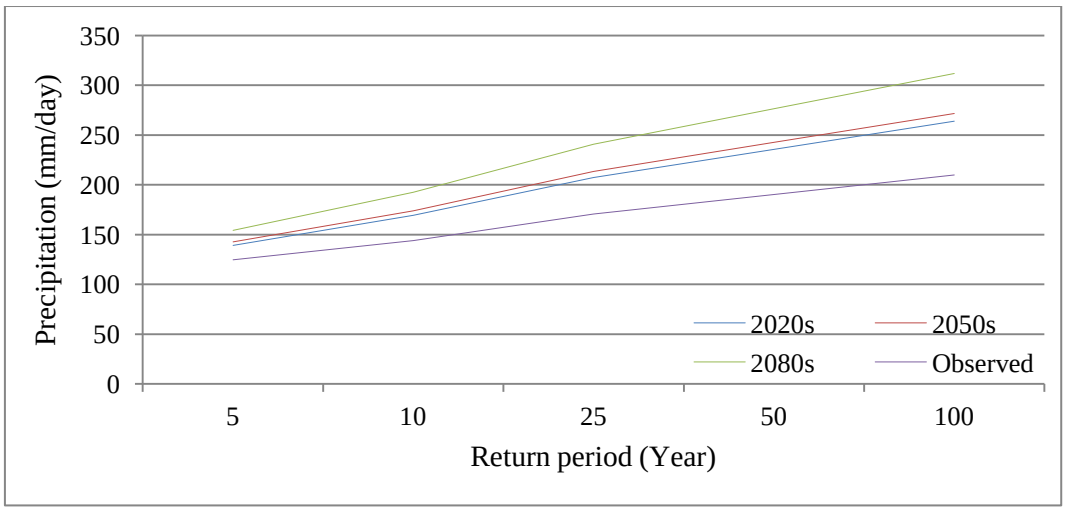


Figure 102 Comparison between the baseline and future extreme precipitation events based on average maximum precipitation events for whole Klang watershed under B2 scenario

### 6-6-2- Assessment of Climate Change Impacts on the Frequency of Mean and Extreme Flood Events at the Discharge Station

This section represents the potential impacts of possible consequences of climate change on average and maximum future flood flows according to the predicted runoff under A2 and B2 scenarios. Log-Pearson type III method, Bulletin 17B-IACWD (1982), was used to fit the frequency distributions for the downscaled discharge. The historic annual maximum floods (1975-1990) at Sulaiman streamflow station as the current potential and the downscaled discharges for the future are used to estimate flood frequency. The mean and maximum discharge simulation output made by HEC-HMS hydrology model is the basis input data to assess the flood frequency. The analysis was done for Klang River at Sulaiman streamflow station to provide amount of discharge for the return periods of 5, 10, 25, 50 and100 years for three time slices (2020s, 2050s and 2080s) corresponding A2 and B2 scenarios.

The percentage change in mean flood flows for Sulaiman streamflow station under the A2 and B2 scenarios is shown in Table 54. Figures (103 and 104) show the results of flood frequency curves for mean flood events. Table (55) and. Figures (105 and 106) show the results of flood frequency analysis of extreme flood events at Sulaiman streamflow station.

The greatest mean floods predicted for return period of 5 year are estimated to 21.9 $m^3/s$, 23.9 $m^3/s$ and 27.2 $m^3/s$ for 2020s, 2050s and 2080s corresponding A2 scenario. It is found a decrease of 2.62 % in 2020s and an increase of 5.15% and 20.95 % in 2050s and 2080s, respectively compared to the observed mean flood at Sulaiman streamflow station**.** The trend of mean flood prediction for B2 scenario is expected to a decrease of 13.49% in 2020s and 7.5 % in 2050s and an increase of 4.79% in 2080s.

The greatest osf mean floods predicted at Sulaiman streamflow station are expected to 21.90 $m^3/s$ in May, 23.1 $m^3/s$ in October and 22.7 $m^3/s$ in November for 2020s, 24.6 $m^3/s$ in May, 22.4 $m^3/s$ in September, 25.4 $m^3/s$ in October and 23.9 $m^3/s$ in November for 2050s, 29.7 $m^3/s$ in May, 25.5 $m^3/s$ in September, 28.9 $m^3/s$ in October and 25.6 $m^3/s$ in November for 2080s under A2 scenario. On the other hand, the greatest of mean floods are expected with a maximum discharge of 19.6 $m^3/s$, 20.4

$m^3/s$ and 20.1 m3/s for 2020s, 21.8 $m^3/s$, 19.8 $m^3/s$, 22.2 $m^3/s$ and 22.1 $m^3/s$ for 2050s, 26.2 $m^3/s$, 22.5 $m^3/s$, 24.4 $m^3/s$ and 22.5 $m^3/s$ for 2080 in those months under B2 scenario.

There is a decreasing trend of greatest mean floods of return period years from 5 to 100 years range between 21.9 $m^3/s$ to 23.85 $m^3/s$ in 2020s while, this increasing trend of the mean flood prediction at the streamflow station range from 23.6 $m^3/s$ to 27.2 $m^3/s$ in 2050s and 27.2 $m^3/s$ to 32.6 $m^3/s$ in 2080s corresponding A2 scenario. The minimum increase of mean flood predicted as compared to the observed data, is observed in 2050s under A2 scenario for the return period of 100 year by 27.2 $m^3/s$ and the maximum increase of intensity in this time slice will likely be expected for return period of 10 year by 25.1 $m^3/s$. The trend in this time slice under B2 scenario is estimated about 21.9 $m^3/s$ and 23.6 $m^3/s$ for return period of 10 and 100 year, respectively.

The greatest maximum floods predicted for return period of 5 year are projected to 60.5 $m^3/s$, 69.9 $m^3/s$ and 89.8 $m^3/s$ for 2020s, 2050s and 2080s respectively corresponding A2 scenario. It is found an increase of 13.71% in 2020s, 31.55% in 2050s and 68.96% in 2080s compared to the observed maximum flood at Sulaiman streamflow station. The trend of maximum flood prediction for B2 scenario is expected to a decrease of 21.41% in 2020s and 3.4% in 2050s and an increase of 23.06% in 2080s which is based on the maximum discharge estimated for those years in the future runoff simulation. The increasing trend of the greatest maximum floods is expected for all the return period years range between 60.7 $m^3/s$ to 75.5 $m^3/s$ in 2020s, 69.9 $m^3/s$ to 87.2 $m^3/s$ in 2050s and 89.8 $m^3/s$ to 117.7 $m^3/s$ in 2080s. The trend under B2 scenario is expected the range between 41.7 $m^3/s$ to 52.7 $m^3/s$, 51.5 $m^3/s$ to 65.5 $m^3/s$ and 65.4 $m^3/s$ to 88.5 $m^3/s$.

The discharge reduction drops below from 1.3% in return period of 25 year to 18.8% in return period of 100 year for 2020s, 6.3% in return period of 100 year for 2050s under A2 scenario. On the other hand, all the predicted maximum discharges in 2020s and 2050s, is lower than the observed under B2 scenario. The frequency curve of maximum observed peak discharge events is higher than the peak discharge in 2020s for the return periods greater than 25 year and in 2050s for the return periods greater

than 50 year under A2 scenario. However, the maximum observed discharge is greater than the peak discharge of all the return period in 2020s and 2050s in B2 scenario.

The highest increase in maximum flood frequency at Sulaiman streamflow station is in 2080s under A2 scenario. The increase in the magnitude of 100 year is found 26.54% greater than the peak discharge of the maximum observed for 2080s under A2 scenario. A 100 year flood may have a discharge of $m^3/s$ in 2080s for A2 scenarios. It is evident that A2 scenario is more critical for 2080s with an increase of the maximum discharge by 26.5% greater than the peak discharge of the maximum observed.

The results indicated quite different changes for future as compared to the current condition. The high flows are expected to occur more frequent and severe at Sulaiman streamflow station. In particular, for Klang river the flood forecast corresponding A2 scenario is characterised by a high increase of discharge by end of century. It indicates increasing annual flood risks in the future, which mostly are related to increasing peak flows at Sulaiman streamflow station. It can be inferred that the extreme flood events will be magnified significantly in the future in Klang watershed with the maximum discharge in magnitude is expected 105.3 $m^3/s$ in October for 2080s under A2 scenario.

Table 54 Changes in percentage for mean flood magnitudes between current and future at Sulaiman discharge station under A2 and B2 scenarios (in %)

| Return period (Year) | A2 | | | B2 | | |
|---|---|---|---|---|---|---|
| | 2020s | 2050s | 2080s | 2020s | 2050s | 2080s |
| 5 | -2.62 | 5.15 | 20.95 | -13.49 | -7.50 | 4.79 |
| 10 | -3.54 | 6.03 | 24.00 | -14.72 | -7.34 | 6.71 |
| 25 | -5.81 | 5.45 | 25.14 | -16.88 | -8.26 | 7.34 |
| 50 | -7.78 | 4.35 | 24.84 | -18.62 | -9.33 | 7.04 |
| 100 | -9.69 | 3.03 | 24.04 | -20.30 | -10.53 | 6.36 |

Table 55 Changes in percentage for maximum flood magnitudes between current and future at Sulaiman streamflow station under A2 and B2 scenarios (in %)

| Return period (Year) | A2 | | | B2 | | |
|---|---|---|---|---|---|---|
| | 2020s | 2050s | 2080s | 2020s | 2050s | 2080s |
| 5 | 13.71 | 31.55 | 68.96 | -21.41 | -3.04 | 23.06 |
| 10 | 9.20 | 26.64 | 66.07 | -24.91 | -6.95 | 21.37 |
| 25 | -1.33 | 14.35 | 52.38 | -31.93 | -15.64 | 12.53 |
| 50 | -10.21 | 3.93 | 39.58 | -37.62 | -22.96 | 4.01 |
| 100 | -18.82 | -6.27 | 26.54 | -43.24 | -30.14 | -4.82 |

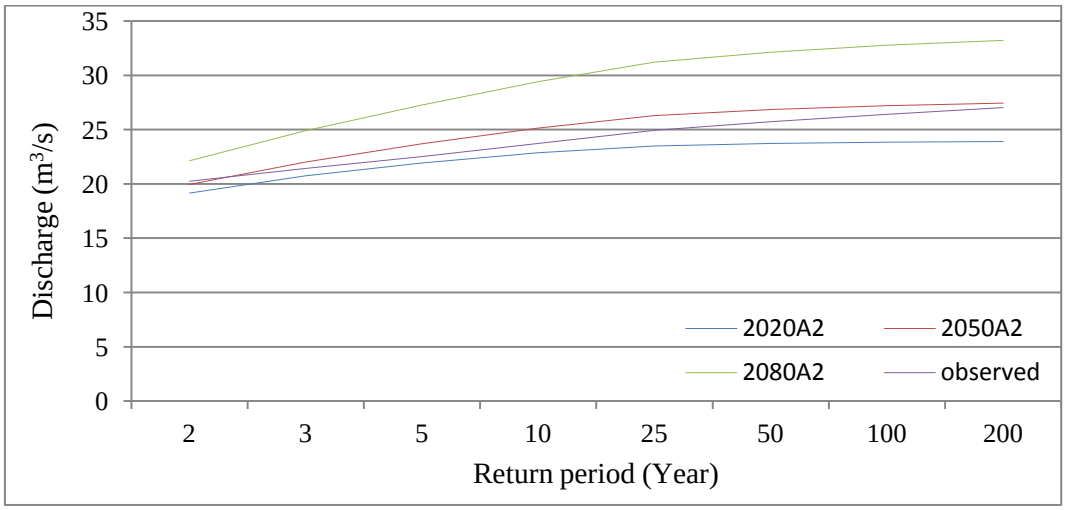


Figure 103 Comparison between the baseline and future flood frequency curve based on mean flood events calculated at Sulaiman streamflow station under A2 scenario (in $m^3/s$)

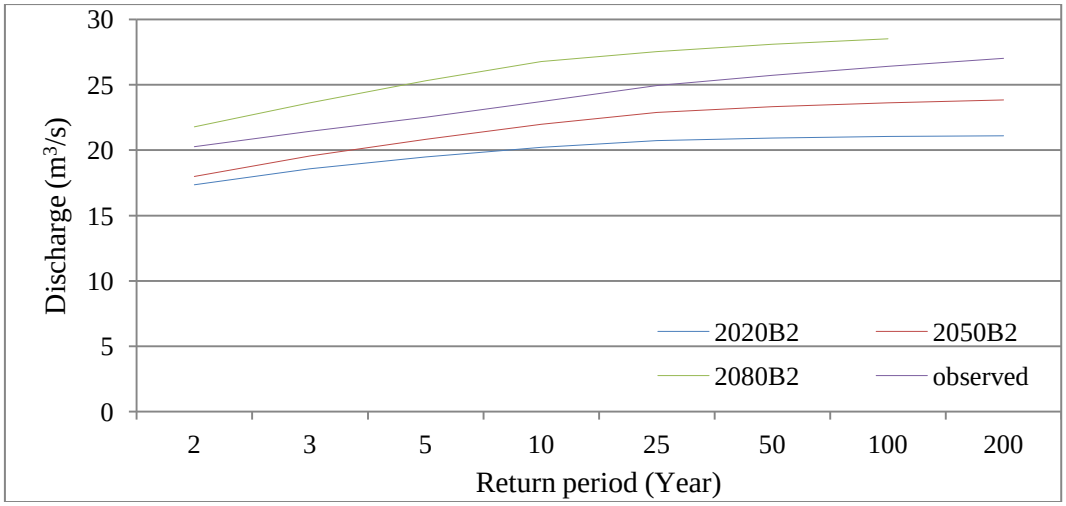


Figure 104 Comparison between the baseline and future flood frequency curve based on mean flood events calculated at Sulaiman streamflow station under B2 scenario (in $m^3/s$)

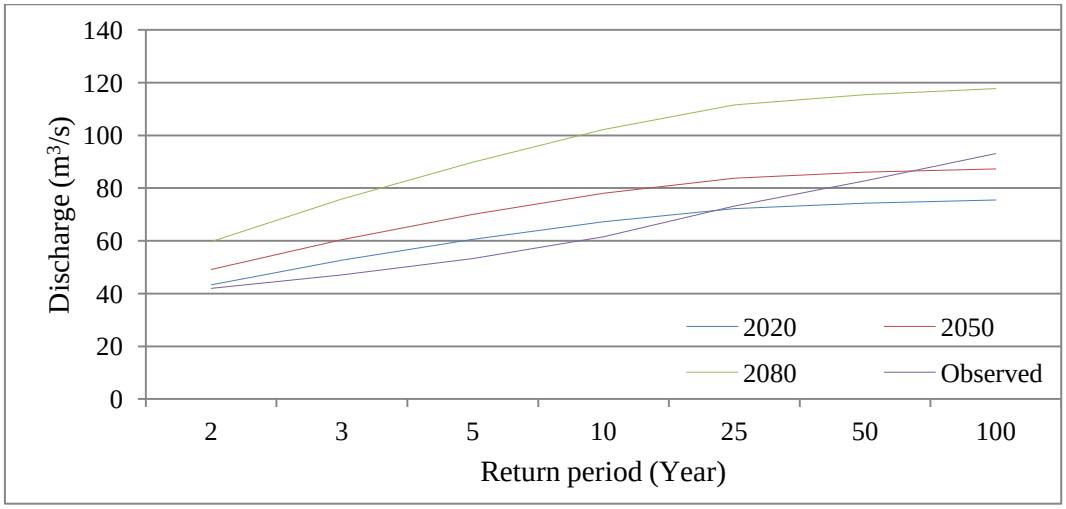


Figure 105 Comparison between the baseline and future flood frequency curve based on extreme flood events calculated at Sulaiman streamflow station under A2 scenario (in $m^3/s$)

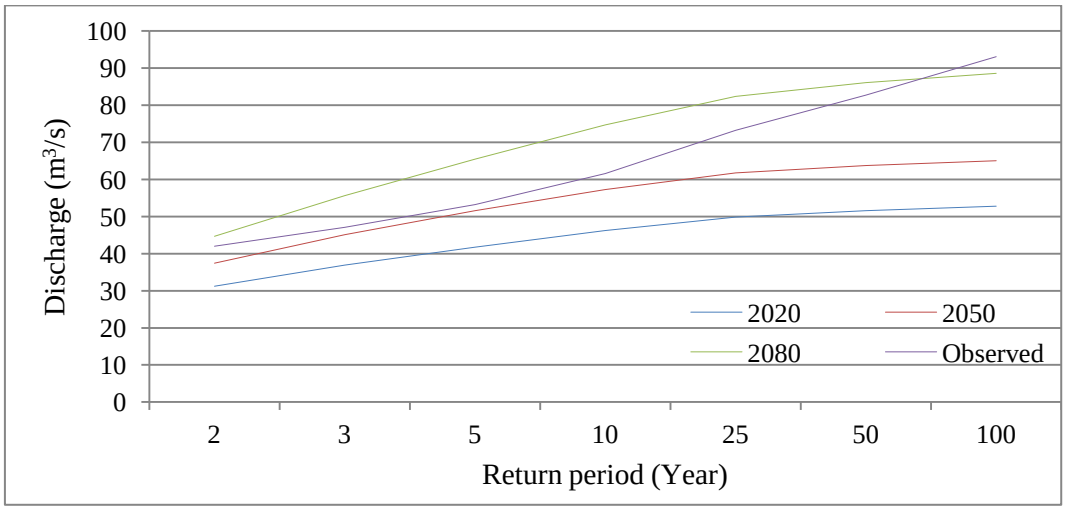


Figure 106 Comparison between the baseline and future flood frequency curve based on extreme flood events calculated at Sulaiman streamflow station under B2 scenario (in $m^3/s$)

## 6-7- Error Analysis of Downscaling output

### 6-7-1- Model Error in the Estimates of Mean and Variance

Although calibration and validation test have been run for the historical dataset a comparison for the observed to the simulated output to indicate the model error, but in this section it was attempted to perform a further error assessment using parametric/non-parametric confidence intervals to estimate mean and variance differences of observed and downscaled output.

The error analysis was conducted on daily rainfall downscaled at 10 raingauge stations, maximum and minimum temperature downscaled at Subang temperature station and evaporation downscaled at Batu dam station with SDSM. The assessment was done on the downscaling output using Large Scale Predictor Re-analysis NCEP and Had-CM3 GCM model. Error assessment in climate change downscaling is conducted by comparison with mean and variance between observed/historical and downscaled output. The Sigma XL extension in Microsoft Excel which is a statistical package was used for the model error. The evaluation was conducted to estimate the model error in terms of differences between the mean values of observed and downscaled output. The historical NCEP Large Scale Re-analysis data over 1975-2001 was used as observed data in error model.

Figures (from 107 to 114) show the differences between observed and modelled for the data. It seems that SDSM can preserve downscaling model in the study area. As Figures (from 115 to 122) indicate the model error in the SDSM with the p-value higher than 0.05 which presents the similarity of two observed and simulated output. In fact, SDSM does not produce significant error of the rainfall, maximum and minimum temperature and evaporation for all the months over the year. However, there can be seen a slight error in the December at raingauge station (3217003). P-values are found greater than the significance level alpha = 0.05, which cannot reject the null hypothesis H0.

The confidence interval at 5% significant level was run to estimate the variance variability of observed and modelled. The p-values are found greater than 0.05

indicate that the observed and modelled variances are close together and can be considered as one group. All the model error calculated for other raingauge stations are in the Appendix R.

In daily precipitation, temperature and evaporation downscaling at all the stations in Klang watershed, the statistical downscaling model errors are insignificant in all the months as p-values at 5% significance level are found above 0.05 which means the model errors are insignificant at 95% confidence level.

Regarding to the maximum temperature, the performance of the SDSM model was less satisfactory than extreme precipitation. It has found that the skill of SDSM to reproduce the maximum temperature is limited. However, the error of maximum temperature is less significant in this study because the maximum temperature downscaling output are used for calculating evapotranspiration while the precipitation downscaling output are mainly employed for the rainfall-runoff hydrological modelling in HEC-HMS.

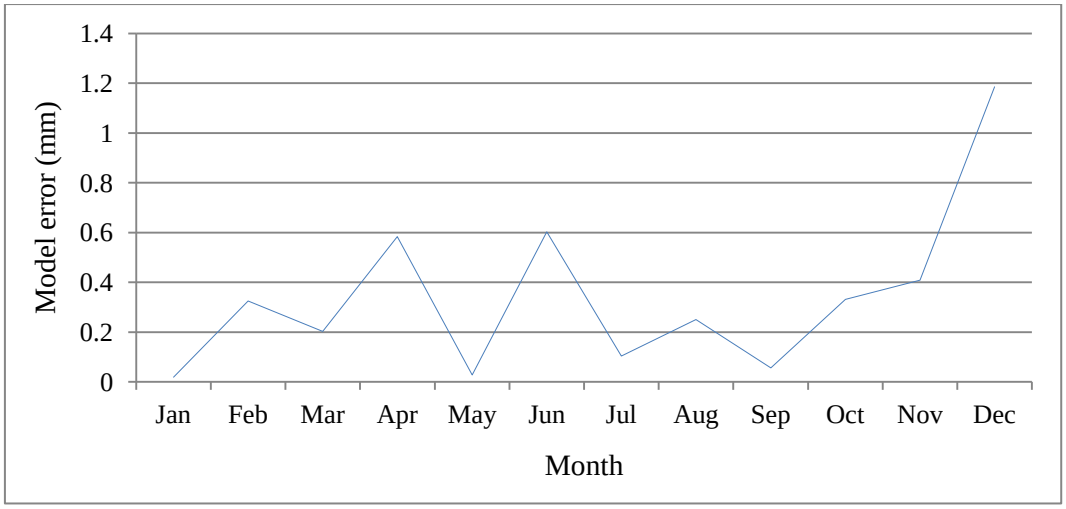


Figure 107 Model errors in downscaled mean daily precipitation with NCEP at the raingauge station: 3217003, (1975-2001)

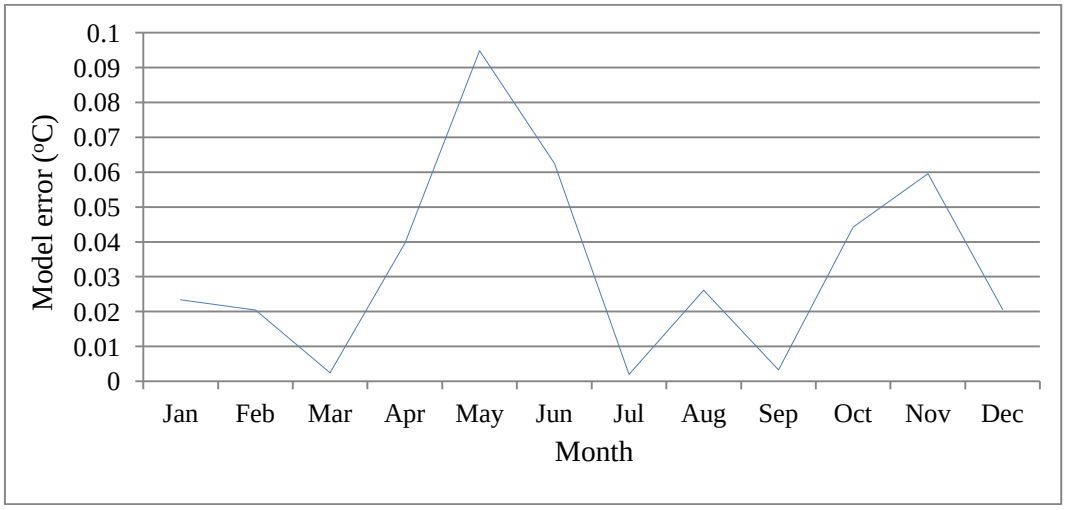


Figure 108 Model error in downscaled maximum temperature with NCEP at Subang station (1975-2001)

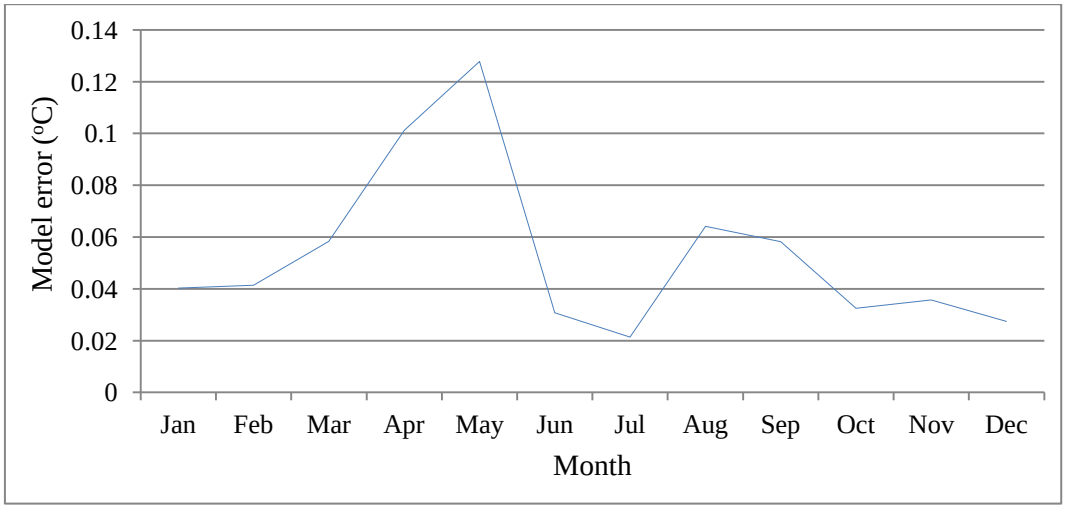


Figure 109 Model error in downscaled minimum temperature with NCEP at Subang station (1975-2001)

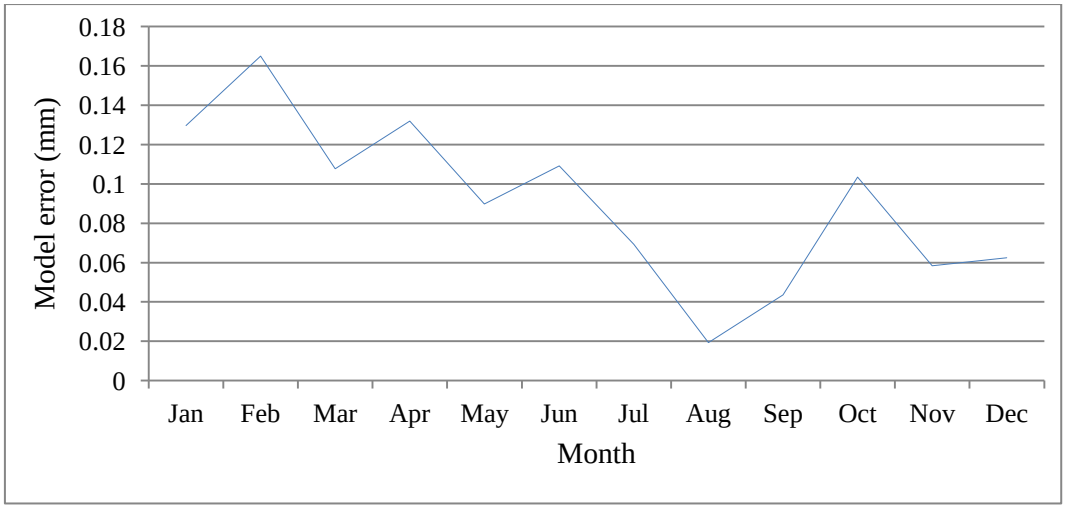


Figure 110 Model error in downscaled evaporation with NCEP at Batu dam station (1985-2001)

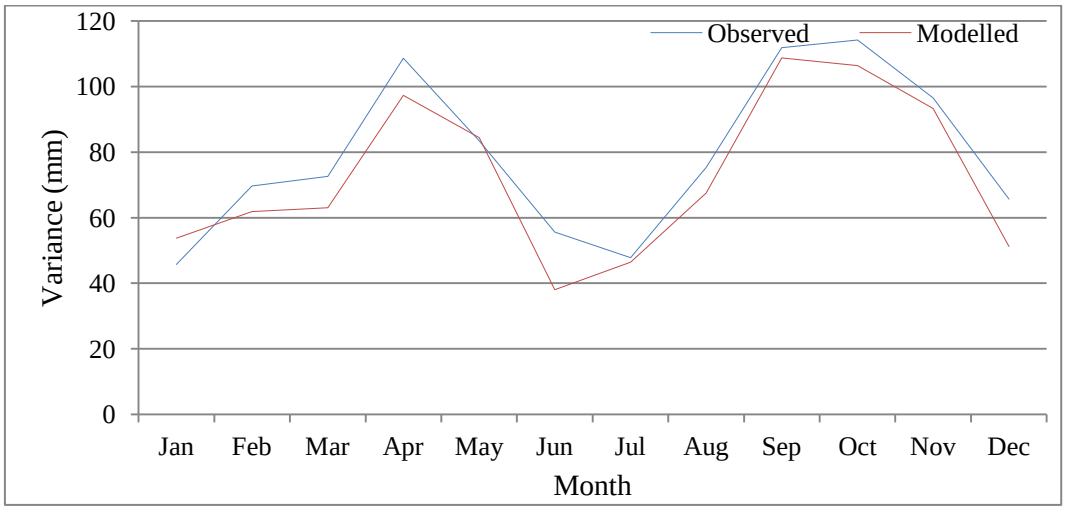


Figure 111 Comparison Variances plots of the downscaled daily mean precipitation with NCEP at the raingauge station: 3217003, (1975-2001)

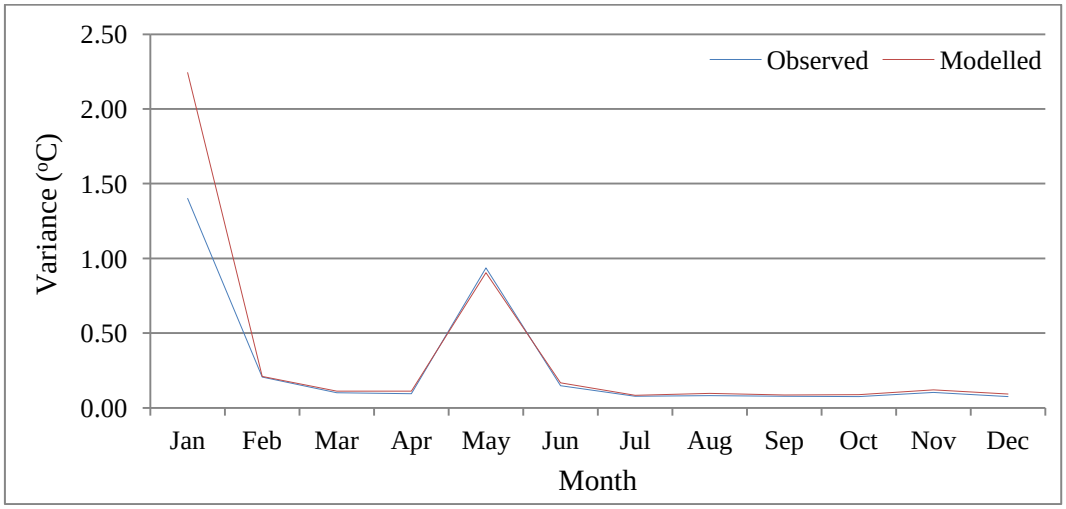


Figure 112 Comparison Variances plots of the downscaled maximum temperature with NCEP at Subang station (1975-2001)

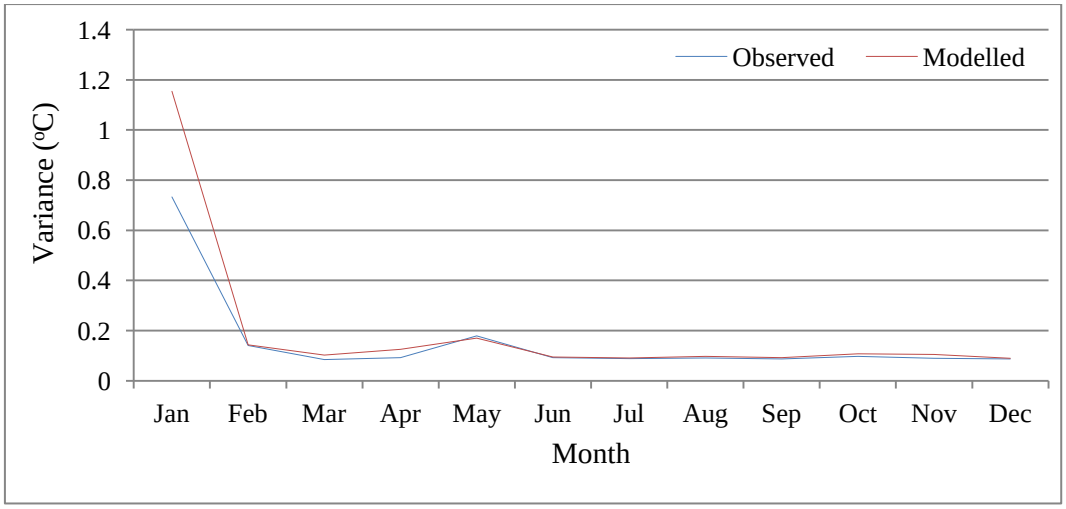


Figure 113 Comparison Variances plots of the downscaled minimum temperature with NCEP at Subang station (1975-2001)

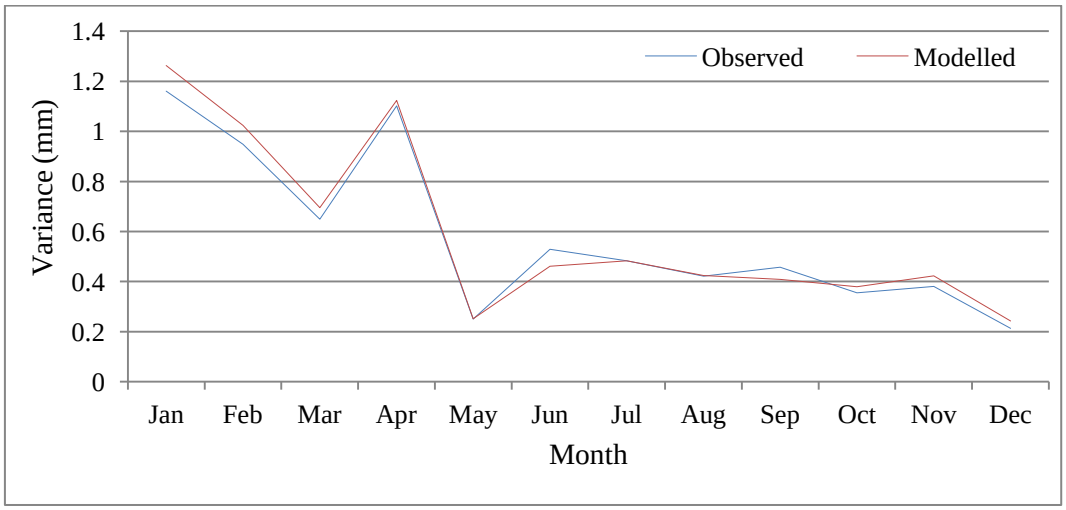


Figure 114 Comparison Variances plots of the downscaled evaporation with NCEP at Batu dam station (1985-2001)

### 6-7-2- Error Evaluation in Estimates of Means and Variances

In this section, it was attempted to apply the parametric Wilicoxon test and non-parametric statistical levene‘s test to estimate the equality of mean and variances between observed and downscaled data at 95% confidence level, respectively. Figures (from 115 to 122) present that SDSM could produce a reliable downscaling model in Klang watershed as the mean and variances of observed and downscaled of all the data are close together and the calculated P-values are above 0.05 at 5% significant level which means the SDSM model errors are insignificant at 95% confidence level. Table 56 illustrates the results of statistical tests Wilcoxon and leven’s tests. Other figures are available in Appendix S.

All the results reveal that the observed data in the watershed considered as predictands are in a good regression to the large scale re-analysis NCEP in statistical downscaling model using SDSM software which simulates the related predictands with 95% confidence level.

Table 56- P-value of the Wilcoxon and leven’s tests for the difference of means and variances of the observed and downscaled daily rainfall, $t_{max}$ and $t_{min}$ and evaporation at 95% confidence level

| Predictand Variable | Wilcoxon test | Levene's test |
|---|---|---|
| 3116005 | 0.421 | 0.712 |
| 3116006 | 0.327 | 0.678 |
| 3117070 | 0.327 | 0.773 |
| 3118069 | 1.000 | 0.053 |
| 3217001 | 0.456 | 0.644 |
| 3216001 | 0.969 | 0.644 |
| 3217002 | 0.170 | 0.571 |
| 3217003 | 0.055 | 0.983 |
| 3217004 | 0.051 | 0.925 |
| 3317004 | 0.055 | 0.735 |
| $T_{max}$ | 0.472 | 0.508 |
| $T_{min}$ | 0.767 | 0.494 |
| Evaporation | 0.863 | 0.703 |

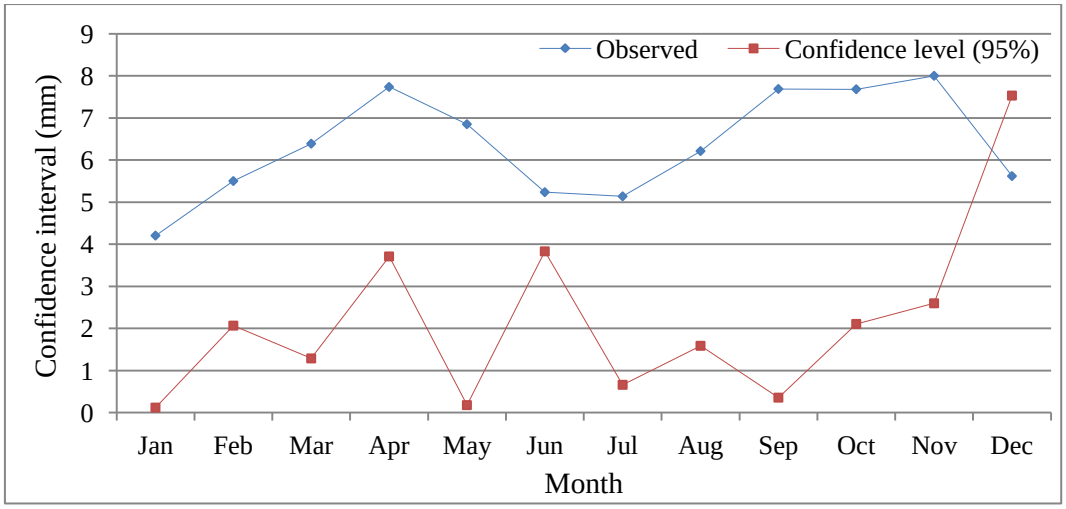


Figure 115 Non-parametric 95% confidence intervals for the estimation of mean daily precipitation downscaled with NCEP at raingauge station: 3217003 (1975-2001)

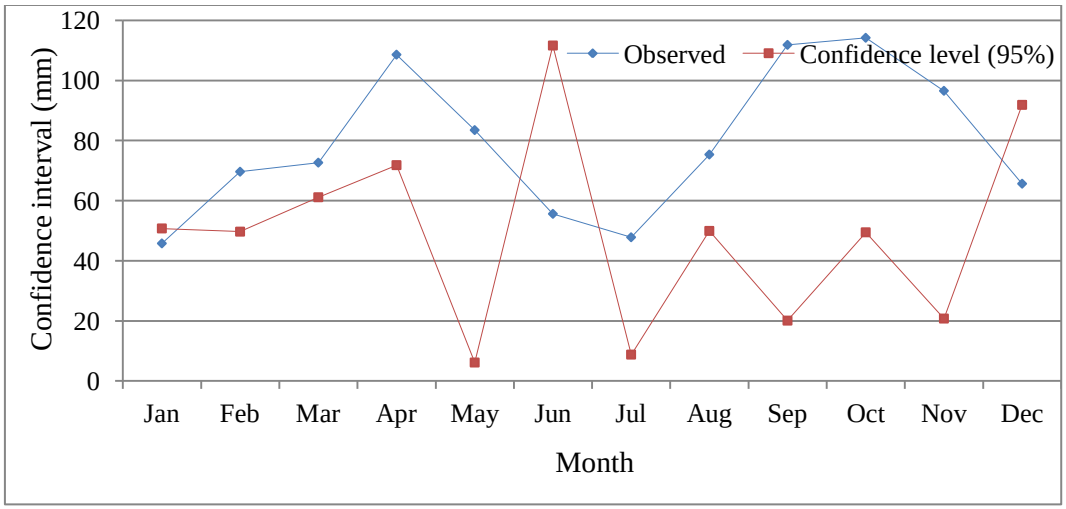


Figure 116 Non-parametric 95% confidence intervals for the estimation of variance daily precipitation downscaled with NCEP at raingauge station: 3217003 (1975-2001)

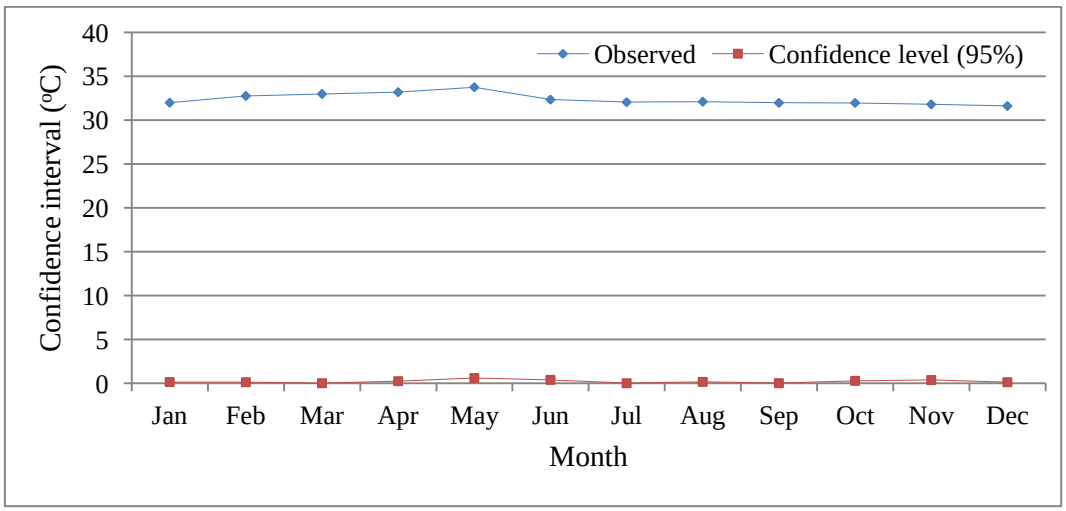


Figure 117 Non-parametric 95% confidence intervals for the estimation of mean daily $T_{max}$ downscaled with NCEP at Subang station (1975-2001)

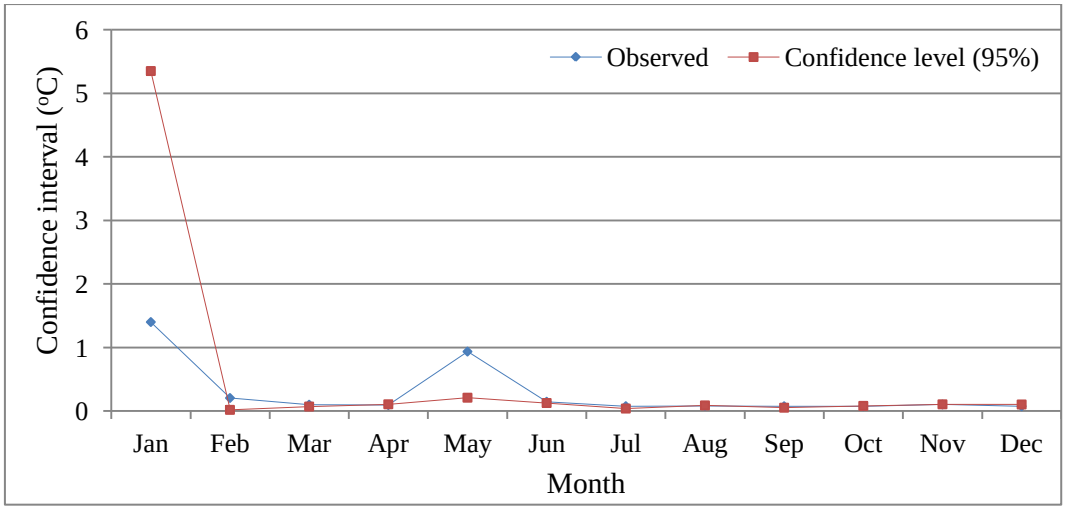


Figure 118 Non-parametric 95% confidence intervals for the estimation of variance daily $T_{max}$ downscaled with NCEP at Subang station (1975-2001)

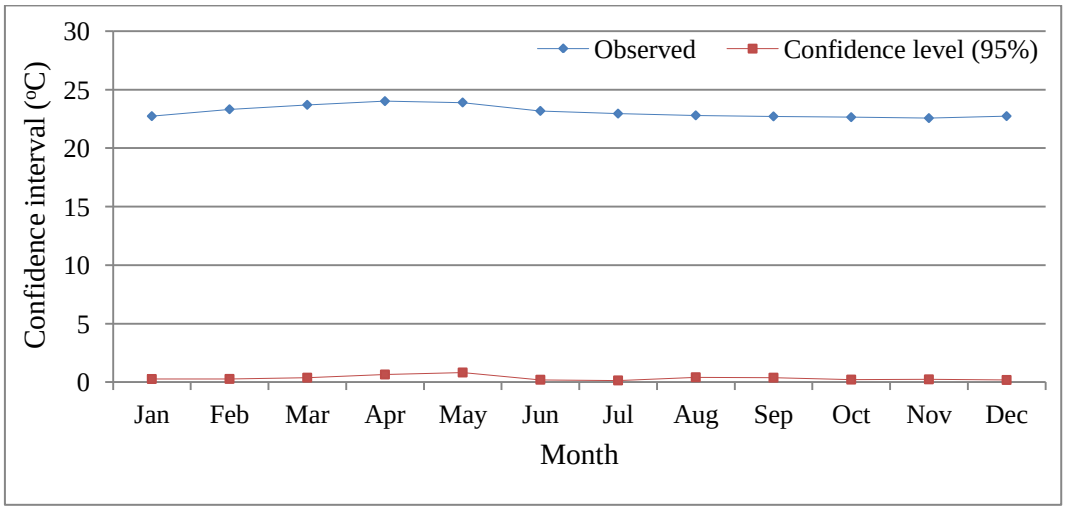


Figure 119 Non-parametric 95% confidence intervals for the estimation of mean daily $T_{min}$ downscaled with NCEP at Subang station (1975-2001)

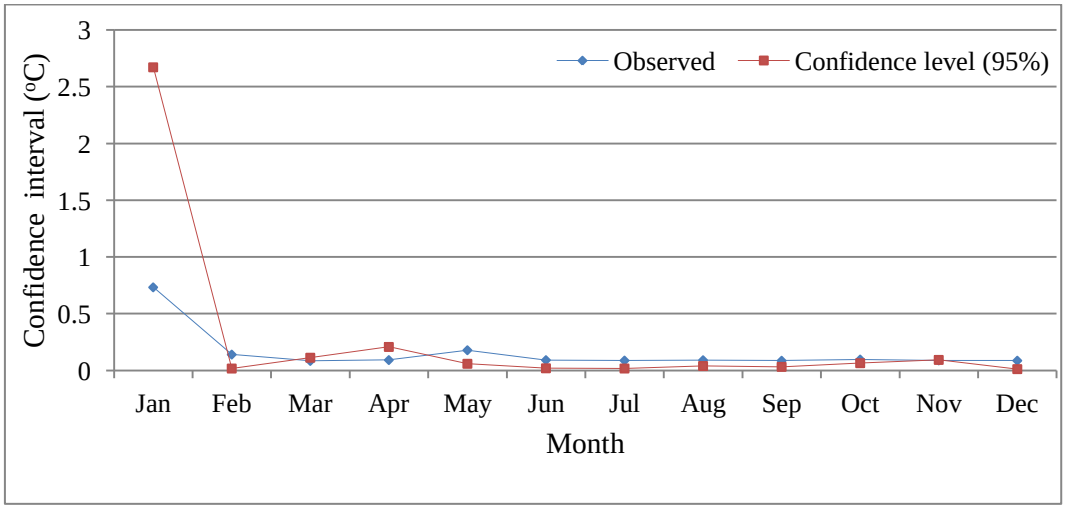


Figure 120 Non-parametric 95% confidence intervals for the estimation of variance daily $T_{min}$ downscaled with NCEP at Subang station (1975-2001)

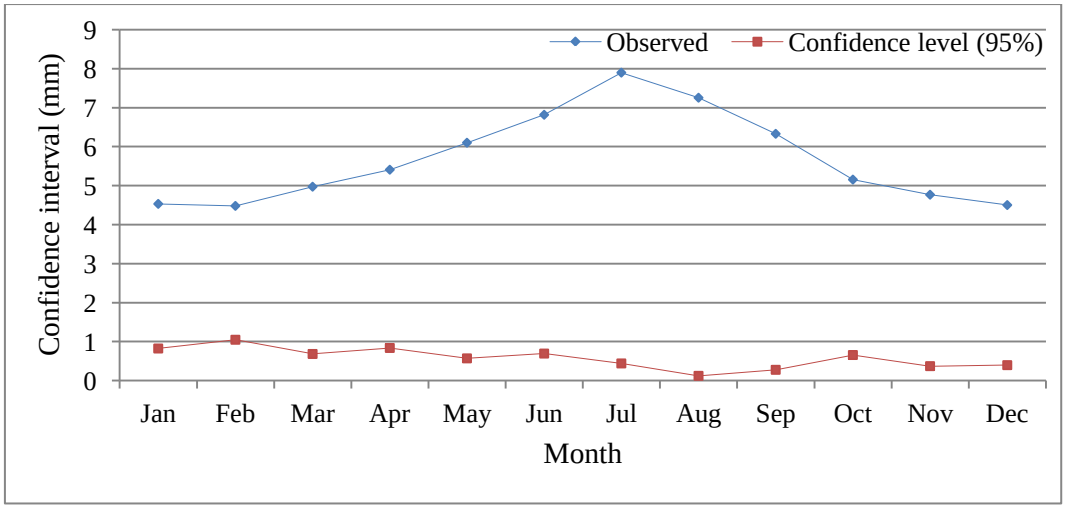


Figure 121 Non-parametric 95% confidence intervals for the estimation of mean daily evaporation downscaled with NCEP at Batu dam station (1975-2001)

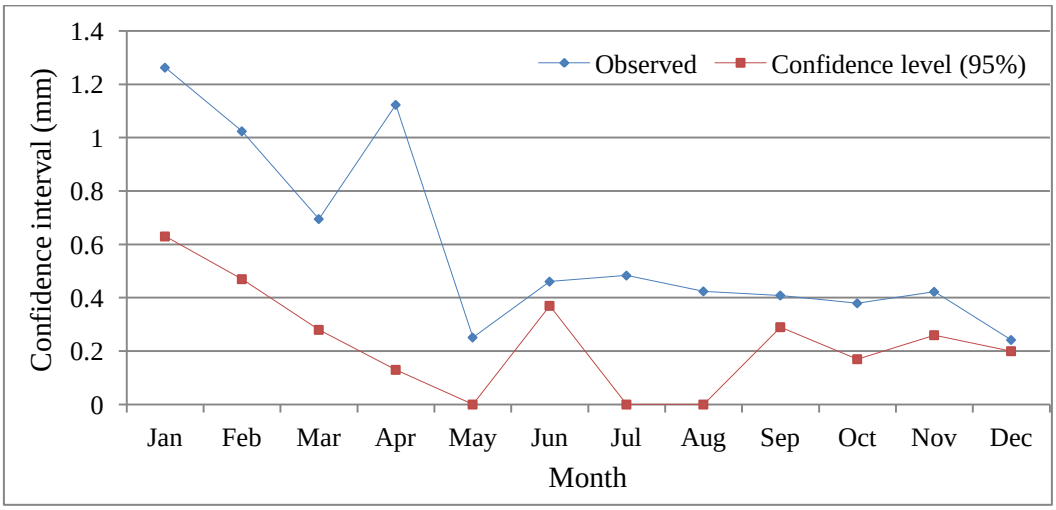


Figure 122 Non-parametric 95% confidence intervals for the estimation of variance daily evaporation downscaled with NCEP at Batu dam station (1975-2001)

# 7- CONCLUSION

This chapter presents conclusions on the climate change impact on streamflow regime and frequency of extreme flood events according to the climate change scenarios.

Linear regression-based Statistical Downscaling Model version 4.2 (SDSM 4.2) was used to downscale the daily precipitation, maximum and minimum temperature and evaporation at local scale. The A2 and B2 scenarios obtained from the Hadley Centre Coupled Model version 3 (HadCM3) were used to project the local scenario at the watershed scale. The calibration and testing of the downscaling procedure reveal that statistical downscaling model can be used as reliable downscaling tool in Klang watershed. It has been ascertained that SDSM resolves the local climate change scenarios of the precipitation, temperature and evaporation in Klang watershed by generating accurate results and in good agreement with observed.

The Hydrologic Modelling System version 3.5 (HEC-HMS 3.5), a physically based semi-distributed model was employed for the hydrological modelling using SCS-CN loss method in runoff estimation to determine the amount of infiltration rates of soil for the urbanised Klang watershed.

A linkage between the downscaling output and hydrological model has been made to project the streamflow regime for the three future periods (2011–2040, 2041–2070, and 2071–2099). It was conducted by incorporating the future climate variables into the HEC-HMS hydrology model.

## 7-1- Assessment of Climate Change Impact on Climate Variables

The maximum and minimum temperature are likely to be increased toward the end of the century by more than approximately 2.7$^{o}$C and 0.8$^{o}$C, respectively compared to the observed temperature at Subang temperature station. However, as per IPCC 2004, there is no significant difference between A2 and B2 scenarios in the area that lies in the equatorial region (IPCC, 2004). The A2 (Medium-High Emissions scenario) scenario implies focus on economic growth and increasing population, while the B2

(Medium-Low Emissions scenario) scenario focuses on environmental sustainability. Since Malaysia is a developing country with an increasing in population and economy development, a high usage of fossil fuel has formed the climate change scenarios with no focus on environmental improvement. It leads to rather similarity of two A2 and B2 scenarios in the region. Hence, B2 scenario in Malaysia does not describe quite differently to A2 scenario.

Mean yearly downscaled precipitation variables were determined to indicate mean, maximum, wet spell and dry spell. Precipitation will likely be increased over Klang watershed in the months that already have much precipitation, while it might decrease in already dry months.

The watershed seems to experience increased rainfall towards the end of the century. However, the analysis indicates that there will likely be a negative trend of mean precipitation in 2020s and with no difference in 2050s according A2 scenario. According to the RCM result investigated by Meteorological Dep. Malaysia (2009), the change in rainfall shows no clear trend by all of the nine models due to the high variability in the precipitation-modulating factor.

The results show that mean annual precipitation amount are projected to increase in the future for A2 as compare to B2 scenario. The precipitation experiences a mean annual decrease by 7.9%, 0.6% for A2 scenario in 2020s and 2050s respectively and an increase by 12.4% in 2080s.

Among three time slice years, highest rainfall reduction is obtained for 2020s, which corresponds to the lowest temperature variation being simulated for annual temperature anomaly. In contrast, the highest rainfall increase is obtained for 2080s, which corresponds to the highest temperature variation for the same time.

It is projected a decreasing of average wet spell length for the future, approximately 50%, an increasing of average dry spell length to 10% as compared to the current condition by 2080s. There will decrease in consecutive days without rainfall approximately 10% and 15.5% for A2 scenario in 2020s and 2050s, respectively.

It can be concluded that the probability of flood happening are higher due to increasing rainfall intensity. Hence, the days with heavy precipitation will be expected to be occurred very frequently during the year.

The analysis indicates that there will be an increase in mean monthly precipitation but with a decrease in the number of consecutive wet-days which can be concluded as a possibility of more precipitation amount in fewer days.

The study shows that differences between the IPCC scenarios (A2 and B2) results are minor in Klang watershed and are mainly major for maximum precipitation. As the climate forcing is smaller in B2 case and the climate response correspondingly is weaker and so some differences of this nature are expected.

### 7-2- Assessment of Climate Change Impact on the River Discharge

In the future time slices predicted, the average annual mean discharge is predicted to be decreasing by 9.4%, 4.9%, and an increase of 3.4 % for the A2 and a decrease about 17.3% and 14.3% and 6.2% for the B2 scenario, respectively. The average annual maximum discharge is projected to decrease by 7.7% in 2020s, and an increase by 4.2% and 29% in A2 scenario for 2050s and 2080s, respectively. But there will most likely be a decrease in the maximum discharge for all the future under B2 scenario. It is projected a decrease of 32.4%, 19.5% and 2.1% for 2020s, 2050s and 2080s, respectively.

The projected discharge indicates a decline in the months from January to April and also from July to August in all the three future periods for A2 and B2 scenarios. There is an increasing trend in the discharge of September and October in the 2020s according to the A2 and B2 scenarios.

There are two peak flows in the hydrograph in 2050s, May-June for the first peak and September-October for the second peak. Finally, it is found out that there is an increase in the discharge regime in 2080s from September to December and also from

May to June. Obviously, the magnitude of increasing is higher in the A2 than in the B2 scenario.

The changes in runoff values considering the control period will be expected according to both scenarios. It can be concluded that days with heavy precipitation will occur more frequently causing a higher frequency of peak river flow events.

### 7-3- Assessment of Climate Change Impact on the Flood Frequency

The impact of climate change on the occurrence of precipitation events was evaluated by spatial mapping in GIS. The frequency analysis of the extreme precipitation indicated that the increasing extreme precipitation will occur according to the A2 and B2 scenarios in Klang watershed. The highest increase in maximum rainfall intensity is in 2080s under A2 scenario. The increase in the magnitude of 100 year is found about 88% greater than observed. The analysis reveals that overall increasing trend of three time slices' future flood frequency is a linear trend. It is obvious those extreme precipitation events are compliance with downscaled precipitation output from SDSM. The downscaled precipitation indicated an increase in precipitation with a decrease in the number of consecutive wet-days in the future which causes a probability of flooding due to increasing of rainfall intensity.

It can be concluded that the probability of flood happening are higher due to increasing rainfall intensity. Hence, the days with heavy precipitation will be expected to occur more frequently during the year. Climate change will likely result in an increase in the intensity and frequency of extreme precipitation events in the future.

The analysis was done for Klang river at Sulaiman streamflow station to provide amount of discharge for the return periods of 5, 10, 25, 50 and100 years for three time slices (2020s, 2050s and 2080s) corresponding A2 and B2 scenarios. The results indicated quite different changes for future as compared to the current condition. The high flows are expected to occur more frequent and severe at Sulaiman streamflow discharge. The frequency curve of observed peak discharge events is higher than the peak discharge in 2020s and 2050s under A2 scenario, for the return periods greater

than 25 year. However, the maximum observed discharge is greater than the peak discharge of the return period in 2020s and 2050s. The highest increase in flood frequency at Sulaiman streamflow station is in 2080s under A2 scenario. The increase in the magnitude of 100 year is found about 26.5% greater than the peak discharge of the maximum observed.

It indicates increasing annual flood risks in the future, which mostly are related to increasing peak flows at Sulaiman streamflow station. It can be inferred that the extreme flood events will be magnified significantly in the future in Klang watershed.

## 7-4- Recommendation for Future Research

This study has significantly contributed to the research on the hydrology of Klang watershed and its environmental management in the future. However, some critical questions still remain unanswered. For example, the landuse and soil were assumed constant and the impacts of the changes in these parameters were not taken into account in the investigation. These data and also uncertainty due to climate change scenarios developed by IPCC can interact with hydrological cycle in many ways by changing the climatic and discharge behaviour.

In light of these findings, the study can be extended to cover other factors in order to establish better understanding of climate change impact on environment. It can also find the mitigation measures and to manage the environmental costs for the watershed system.

An Environmental Impact Assessment (EIA) using climate change approach for the existing dams in Klang watershed can be considered to demonstrate the future supply and demand of water body of the watershed. This would investigate the changes in all hydrogeology variables. Detailed investigations on the watershed system should be implemented using both physical and biological parameters to establish a series of indicators encompassing the effects of climate change on the watershed scale.

In addition, flood zone mapping of the river can also be investigated including the 3D maps of floods along with streamflow demonstrating the potential impacts of climate change on the flood zones. The generated scenarios and flood maps can be developed as a Decision Support System (DSS) to be used for operational purposes by policy makers and environmental managers.

# REFERENCES


Abood M., A.M., Thamer, A.H. Ghazali, A. R. Mahmud & L.M. Sidek, 2012. Impact of Infiltration Methods on the Accuracy of Rainfall-Runoff Simulation. Research Journal of Applied Sciences Engineering and Technology,4 (12), pp.1708-1713.

Ahmad, K., W. Tahir, A.B.S. Hamid & W.W. Maisarah, 2012. Statistical verification of two numerical weather prediction models for quantitative precipitation forecast, International Sustainability and Civil Engineering Journal, 1(1).pp. 16-24.

Ahmad, S., I.H. Khan & B.P., Parida, 2001. Performance of stochastic approaches for forecasting river water quality. Water Research, 35, 18, pp. 4261-4266.

Akbari, A., A. Samah & F. Othman, 2012. Practical use of SRTM digital elevation dataset in the urban-watershed modelling, Journal of Spatial Hydrology, V.10 (2). doi:10.5194/hessd-9-4747.

Aksara P. & T. Kenji, 2012. Optimal Raingauge Network Design and Spatial Precipitation Mapping Based on Geostatistical Analysis from Colocated Elevation and Humidity Data, International Journal of Environmental Science and Development, 3(2), pp. 124-129

Aksoy, H. & H. Wittenberg, 2011. Nonlinear baseflow recession analysis in watersheds with intermittent streamflow. Hydrological Sciences Journal, 56(2), pp.226 -237.

Al-Humoud, J. M. & I. Esen, 2006. Approximate method for the estimation of Muskingum flood routing parameters. Water Resources Management, 20, pp.979-990.

Ali, M., S. Khan, I. slam & Z. Khan, 2011. Simulation of the impacts of land-use change on surface runoff of Lai Nullah Watershed in Islamabad, Pakistan. Landscape and Urban Planning, 102, pp. 271-279.

Anandhi A, A., Frei, D.C., Pierson, E.M., Schneiderman, M.S., Zion, D., Lounsbury, & A.H., Matonse, 2011. Examination of change factor methodologies for climate change impact assessment. Water Resources Research, 47, W03501, doi: 10.1029/2010WR009104.

Arnell, N. & C., Liu, 2001. Hydrology and water resources. In Climate Change: Impacts, Adaptation, and Vulnerability. Contribution of Working Group II to the Third Assessment Report of the Intergovernmental Panel on Climate Change, by McCarthy J.J., O.F. Canziani, N.A. Leary, D.J., Dokken and K.S. White (eds.). Cambridge University Press, Cambridge.

Arnold, J. G., & N. Fohrer. 2005. SWAT2000: Current capabilities and research opportunities in applied watershed modeling. Hydrological Processes. 19 (3), pp. 563-572.

Arnold, J. G., R. Srinivasan, R. S. Muttiah, & J. R. Williams, 1998. Large-area hydrologic modeling and assessment: Part I. Model development. Journal of the American Water Resources Association, 34 (1), pp. 73-89.

Bardossy, A., I., Bogardi & I., Matyasovszky, 2005. Fuzzy Rule-Based Downscaling of precipitation. The oreticaland Applied Climatology, 82, pp. 119-129.

Bardossy, A., J. Stehlik, & H.J. Caspary, 2001. Generating of areal precipitation series in the Upper Neckar Catchment, Journal of Physics and Chemistry of the Earth, 26, pp. 683-687.

Barnes, K. B., J. M. Morgan & M . C. Roberge, 2002. Impervious surfaces and the quality of natural and built environments. Publication. Department of Geography and Environmental Planning, Towson University.

Bergström, S., 1995. The HBV model. In: Singh, V.P. (Ed.) Computer Models of Watershed Hydrology. Water Resources Publications, Highlands Ranch, CO., pp. 443-476.

Beven, K. J. & M.J. Kirkby,1979. A physically based variable contributing area model of catchment hydrology. Hydrological Sciences Bulletin, 24, pp. 43-69.

Beven, K., 2012. Hydrological Similarity, Distribution Functions and Semi-Distributed Rainfall-Runoff Models, in Rainfall-Runoff Modelling: The Primer, Second Edition, John Wiley & Sons, Ltd, Chichester, UK. doi: 10.1002/9781119951001.ch6

Beven, k.J., 2001. How far can we go in distributed hydrological modelling?, Hydrology and Earth System Sciences, 5, pp. 1-12.

Beven, K.J., A. Calver & A.M. Morris, 1987. The institute of hydrology distributed mode, Institute of hydrology: Report 98, Wallingford, UK.

Birkhead, A.L., C.S. James, 2002. Muskingum river routing with dynamic bank storage. Journal of Hydrology, 264, pp.113-132.

Bolle, H.J., M. Menenti & I. Rasool, 2008. Assessment of climate change for the Baltic Sea watershed. Regional Climate Studies. Springer-Verlag, Berlin/Heidelberg.

Bormann H., L. Breuer, S. Giertz, J.A. Huisman & N. R. Viney, 2009. Spatially explicit versus lumped models in catchment hydrology – experiences from two case studies. Uncertainties in Environmental Modelling and Consequences for Policy Making, pp.3-26

Bosshard, T., S. Kotlarski, T. Ewen & C. Schar, 2011. Spectral representation of the annual cycle in the climate change signal, Hydrological Sciences Journal, 15, pp. 777-2788. doi:10.5194/hess-15-2777-2011

Brian, H. H., M. Callaway, J. Smith & P. Karshen, 2004. Climatic change and U.S. water resources: From modelled watershed, Journal of the American Water Resources Association, 40, pp. 129-148.

Bronstert, A., V. Kolokotronis, D. Schwandt & H. Straub, 2007. Comparison and evaluation of regional climate scenarios for hydrological impact analysis: General scheme and application example. International Journal of Climatology, 27(12), pp.1579-1594.

Brown, A. E., L. Zhang, T. A. McMahon, A. W. Westen & R. A. Vertessy. 2005. A review of paired catchment studies for determining changes in water yield resulting from alterations in vegetation. Journal of Hydrology. 310, pp. 28-61.

Burnash, R.J.C., 1995. The NWS River Forecast System - Catchment Modeling, Computer Models of Watershed Hydrology, Singh, V.P., ed., pp. 311-366.

Buytaert, W., M. Vuille, A. Dewulf, R. Urrutia, A. Karmalkar & R. Célleri, 2010. Uncertainties in climate change projections and regional downscaling in the tropical Andes: Implications for water resources management. Hydrology and Earth System Sciences, 14, pp.1247-1258.

Carpenter, T.M. & K.P. Georgakakos, 2006. Discretisation scale dependencies of the ensemble flow range versus catchment area relationship in distributed hydrologic modelling. Journal of hydrology, 328, pp. 242-257.

Chang, H., B. M. Evans & D. R. Easterling, 2001. The effects of climate change on stream flow and nutrient loading, Journal of the American Water Resources Association. 37, pp. 973-985

Charles, S.P., B.C. Bates & J.P. Hughes, 1999. A spatio-temporal model for downscaling precipitation occurrence and amounts. Geophysical Research, 104, pp. 31657-31669.

Chen H., C. Xu & S. Guo, 2012. Comparison and evaluation of multiple GCMs, statistical downscaling and hydrological models in the study of climate change impacts on runoff. Journal of Hydrology, 434-435, PP. 36-45, doi:10.1016/j.jhydrol.2012.02.040.

Chen, T.S., J.D. Tsay, M.C., Yen & J. Matsumoto, 2013. Interannual Variation of the Winter Rainfall in Malaysia Caused by the Activity of Rain-Producing Disturbances. Journal of Climate, 26, pp. 4630-4648. doi: http://dx.doi.org/10.1175/JCLI-D-12-00367.1

Chin, D., 2000. Water Resources Engineering, New Jersey: Prentice Hall.

Chow V.T., D.R. Maidment & L.W. Mays, 1988. Applied Hydrology. Mc Graw Hill Book Company, ISBN 0-07-010810-2.

Collins, M. 2007. Ensembles and probabilities: a new era in the prediction of climate change, Philosophical Transaction of the Royal Society, 365, pp. 1957-1970, doi:10.1098/rsta.2007.2068

Collischonn, W., D. Allasia, B. C. DA Silva & C. E. M. Tucci, 2007. The MGB-IPH model for large-scale rainfall-runoff modelling. Hydrological Sciences, 5 (5), pp. 878-895

Conover, W.J., 1980. Practical Nonparametric Statistics. Second ed. Wiley, New York.

Crawford, N.H. & R.K. Linsley, 1966. Digital Simulation in Hydrology: Stanford Watershed Model IV. Stanford University, Dept. Civ. Eng. Tech. Rep. 39

Cressie, N. & G. Johannesson, 2008. Fixed rank Kriging for very large data sets. Journal of the Royal Statistical Society, B, 70, pp. 209-226.

Cunderlik, M.J., 2003. Hydrologic model selection for the CFCAS project: Assessment of water resources risk and vulnerability to changing climatic conditions, project Report I. university of Western Ontario, Canada.

Cuo L., D.P. Lettenmaier, B.V. Mattheussen, P. Storck, M. Wiley, 2008. Hydrologic prediction for urban watersheds with the Distributed Hydrology-Soil-Vegetation Model. Hydrological Processes. 22, pp. 4205-4213.

Dankers, R., O.B., Christensen, L., Feyen, M., Kalas & A., de Roo, 2007. Evaluation of very highresolution climate model data for simulating flood hazards in the Upper Danube Watershed. Journal of Hydrology, 347, pp.319-331

Das, L., J. D. Annan, J. C. Hargreaves1, S. Emori, 2012. Improvements over three generations of climate model simulations for eastern India, Journal of climate research, 51, pp. 201-216. doi: 10.3354/cr01064.

Das, M.M & M.S. Saikia, 2009. Hydrology. Delhi, India. ISBN 978-81-203-3707-7

Day C.A, 2013. Statistically Downscaled Climate Change Projections for the Animas River Watershed, Colorado, USA. Mountain Research and Development, 33 (1), pp.75-84. doi: http://dx.doi.org/10.1659/MRD-JOURNAL-D-12-00067.1.

Desa M.M.N., A.B. Noriah & P.R. Rakhecha, 2001. Probable Maximum Precipitation for 24 hrs Duration Over Southeast Asian Monsoon Region-Selangor, Malaysia. Atmospheric Research Journal, 58, pp. 41-54.

Desa, M.N., J. Niemczynowicz, 1996. Spatial variability of rainfall in Kuala Lumpur Malaysia: long and short term characteristics. Hydrological. Sciences Journal, 41, pp. 345-362.

Descheemaeker, K., J. Posen, L. Borselli, J. Nyssen, D. Raes, M. Haile, B. Muys & J. Deckers, 2008. Runoff curve numbers for steep hillslopes with natural vegetation in semi-arid tropical highland, Northern Ethiopia, Journal of Hydrological Processes, 22. pp. 4097-4105.

DHI, 2000. MIKE: A modelling system for rivers and channels. DHI Water and Environment, 82 p.

Diallo, I., M. B. Sylla, F. Giorgi, A. T. Gaye & M. Camara, 2012. Multimodel GCM-RCM Ensemble-Based Projections of Temperature and Precipitation over West Africa for the Early 21st Century. International Journal of Geophysics. doi:10.1155/2012/972896

Dibike & P. Coulibaly, 2007. Validation of hydrologic models for climate scenario simulation: The case of Saguenay watershed in Quebec. Hydrological Processes, 21(23), pp. 3123-31235.

Dibike, Y. B., & P. Coulibaly, 2005. Hydrologic impact of climate change in the Saguenay watershed, comparison of downscaling methods and hydrologic models. Hydrology, 307(1-4), pp. 145-163.

Dibike, Y.B. & P. Coulibaly, 2007.Validation of hydrologic models for climate scenario simulation: The case of Saguenay watershed in Quebec. Hydrological Processes, 21(23), pp.3123-3135.

Dickinson, R., R. Errico, F. Giorgi & G. Bates, 1989. A regional climate model for the Western Unites States. Journal of Climate Change, 15 (3), pp. 383-422.

DID: Department of Irrigation and Drainage, 2010. Processed Data of Batu dam from 1989 up to 2010. Manual report , Dam Measurement Office.

Dinpashoh, Y., et al., 2004. Selection of variables for the purpose of regionalization climate using multivariate methods. Journal of Hydrology, 297, pp.109-123. doi: http://dx.doi.org/10.1175/2009JHM1160.1.

Douglas C. M & G. C. Runger, 2003. Applied Statistics and Probability for Engineers, 3rd edition, Wiley and sons.

Driessen, T. L. A., R. T. W. L. Hurkmans, W. Terink, P. Hazenberg, P. J. J. F. Torfs, & R. Uijlenhoet, 2010. The hydrological response of the Ourthe catchment to climate change as modelled by the HBV model. Hydrology and Earth System Sciences, 14, pp. 651-665.

Duffy P.B., R.W. Arritt, J. Coquar, W. Gutowski, J. Han, J. Iorio, J. Kim, L.R. Leung, J. Roads & E. Zeledon, 2006. Simulations of present and future climates in the Western United States with four nested Regional Climate Models. Journal of Climate,19, pp.873-895. doi:10.1175/ JCLI3669.1.

Ebrahim, G.Y., A. Jonoski, A.Griensven & G.D. Baldassarre, 2012. Downscaling technique uncertainty in assessing hydrological impact of climate change in

the Upper Beles River Watershed, Ethiopia. Hydrology Research, 44, 2, pp.377-398.

Fiseha, B.M., A.M. Melesse., E . Romano., Volpi. and E. A. Fiori, 2012. Statistical Downscaling of Precipitation and Temperature for the Upper Tiber Watershed in Central Italy. International Journal of Water Sciences. 1, pp.14, doi: 10.5772/52890

Fleming, M.J. & J.H. Doan, 2010. HEC-GEOHMS: Geospatial Hydrologic Modelling Extension, User's Manual. Davis, CA: U.S. Army Corps of Engineers. Hydrologic Engineering Centre, HEC.

Ford, D., N. Pingel, & J. J. Devries, 2008. Hydrologic Modelling System HEC-HMS ,Applications Guid. Davis, CA: U.S. Army Corps of Engineers. Hydrologic Engineering Centre, HEC.

Fowler, H.J., S. Blenkinsop & C. Tebaldi, 2007. Linking climate change modelling to impacts studies: recent advances in downscaling techniques for hydrological modelling. Climatology, 27, pp.1547-1578.

Fu, G.B., S. P. Charles & F. H. S. Chiew, 2007. A two-parameter climate elasticity of streamflow index to assess climate change effects on annual streamflow. Water Resoures Research., 43, W11419, doi:10.1029/2007WR005890.

Fu, S., G. Zhang; N. Wang & L. Luo, 2011. Initial abstraction ratio in the SCS-CN method in the Loess Plateau of China, Trans. ASABE, 54, pp.163-169.

Ghavidelfar, S., S.R. Alvankar & A. Razmkhah, 2011. Comparison of the Lumped and Quasi-distributed Clark Runoff Models in Simulating Flood Hydrographs on a Semi-arid Watershed. Water Resources Management, 25 (6), pp.1775-1790

Giorgio, F., M. Marinucci & G. Visconti, 1990. Use of a limited- area model nested in a General-Circulation model for regional climate simulation over Euroupe. Journal of Geophysical Research Atmospheres, 95, D11, pp. 18411-18431.

Gobbett, D.J. & C.S. Hutchison, 1973. Geology of the Malay Peninsula: West Malaysia and Singapore. John Wiley-Interscience, New York, 438 p.

Graham, L.P., S. Hagemann, S. Jaun & M. Beniston, 2007. On interpreting hydrological change from regional climate models, Climatic Change, 81, pp. 97-122, doi:10.1007/s10584-006-9217-0

Grayson, R. & G. Blöschl, 2001. Spatial Patterns in Catchment Hydrology: observation and modelling. Cambridge University Press, 416, ISBN 0-521-63316-8

Grayson, R.B., I.D. Moore & T.A. Mcmahon, 1992. Physically-based hydrologic modelling. A terrain-based model for investigative purposes. Water resources research, 28 (10), pp. 2639-2658.

Guilyardi, E., & Coauthors, 2004: Representing El Niño in Coupled Ocean–Atmosphere GCMs: The Dominant Role of the Atmospheric Component. Journal of Climate, 17, pp. 4623-4629. doi: http://dx.doi.org/10.1175/JCLI-3260.1

Guo, S.L., J. Guo, J. Zhang & H. Chen, 2009. VIC distributed hydrological model to predict climate change impact in the Hanjiang basin. Science in China Series E: Technological Sciences, 52 (11), pp. 3234-3239

Gutmann, E.D., R.M. Rasmussen, C. Liu, K. Ikeda, D. J. Gochis, M P. Clark, J. Dudhia & G. Thompson, 2012.A Comparison of Statistical and Dynamical Downscaling of Winter Precipitation over Complex Terrain. Journal of Climate, 25, pp.262-281. doi: http://dx.doi.org/10.1175/2011JCLI4109.1

Hamlet, A.F. & D.P. Lettenmaier, 2007. Effects of 20th century warming and climate variability on flood risk in the western US. Water Resources Research, 43, W06427.

Hansen, J. W. & T. Mavromatis, 2001. Correcting low-frequency variability bias in stochastic weather generators. Agricultural and Forest Meteorology, 109 (4), pp. 297-310

Hargreaves, G.H. & R.G. Allen, 2003. History and evaluation of Hargreaves evapo-transpiration equation. Journal of Irrigation and Drainage. Eng., ASCE, 129(1), pp.53-63.

Hargreaves, G.H. & Z.A. Samani, 1985. Reference crop evapo-transpiration from temperature. Applied Engineering in Agriculture, 1(2), pp.96-99.

Hassan, Z. & S., Haroun, 2012. Application of statistical downscaling model for long lead rainfall prediction in Kurau river catchment of Malaysia. Malaysian Journal of Civil Engineering, 24 (1), pp. 1-12.

Hegerl, G. C. & Coauthors, 2007. Understanding and attributing climate change. Climate Change 2007: The Physical Science Basis. Contribution of Working Group I to the Fourth Assessment Report of the Inter-governmental Panel on Climate Change, S. Solomon et al., Eds., Cambridge University Press, pp.663–745.

Hellweger, F. & D. Maidment, 1997. AGREE - DEM Surface Reconditioning System. http://www.crwr.utexas.edu/gis/gishyd98/quality/agree/agree.htm

Helsel, D.R. & R. M. Hirsch, 2010. Statistical Methods in Water Resources Techniques of Water Resources Investigations. Book 4, Chapter A3. U.S. Geological Survey. 522 pp

Hengl, T. 2006. Finding the right pixel size. Journal of Computer & Geosciences, 32, pp.1283-1298.

Hersch, H., 2000. Decomposition of the continuous ranked probability score for ensemble prediction systems, Weather Forecasting, 15, pp. 559-570.

Hirabayashi,Y., S. Kanae , S. Emori, T. Oki & M. Kimoto, 2008. Global projections of changing risks of floods and droughts in a changing climate. Hydrological Science Journal, 53(4), pp.754-773.

Hsieh H.H., S.J., Cheng, J.Y., Liou, S.C., Chou & B.R., Siao, 2006. Characterisation of spatially distributed summer daily rainfall. Agricultural and Biological Engineering, 52(1). pp.47-55

Huang, M. B., J. Gallichand, C. Y. Dong, Wang, Z. L., & M. A. Shao, 2007. Use of moisture data and curve number method for estimating runoff in the Loess Plateau of China, Journal of Hydrological Processes, 21, pp.1471-1481.

Huber, W.C. & R.E. Dickinson, 1988. Storm Water Mangement Model, version 4, user's manual , EPA, 600/3-88-001a, U.S. Environmental Protection Agency, Athens, GA.

Huth, R., 2000, A circulation classification scheme applicable in GCM studies. Theoretical and Applied Climatology, 67, pp.1-18

Interagency Advisory Committee on Water Data (IACWD), 1982. Guidelines for determining flood flow frequency, Bulletin 17B, U.S. Department of the Interior, Geological Survey, Office of Water Data Collection, Reston, VA.

IPCC, 2001. Climate Change: The Scientific Basis. Contribution of Working Group I to the Third Assessment Report of the Intergovernmental Panel on Climate Change. J.T. Houghton, Y. Ding, D.J. Griggs, M. Noguer, P.J. van der Linden, X. Dai, K. Maskell and C.A. Johnson (eds.). Intergovernmental Panel on Climate Change. Cambridge University Press, 881pp.

IPCC, 2007. Regional Climate Projections. In: Climate Change 2007: The Physical Science Basis. Contribution of Working Group I to the Fourth Assessment Report of the Intergovernmental Panel on Climate Change. Cambridge University Press. Cambridge, United Kingdom and New York, NY, USA.

Ivanov, V.Y., R. L. Bras & D. C. Curtis, 2007. A weather generator for hydrological, ecological, and agricultural applications. Journal of Water Resources Research, 43 (10), doi. 10.1029/2006WR005364

Jain, M.K. & V.P. Singh, 2005. DEM Based Modelling of Surface Runoff using Diffusion Wave equation. Journal of Hydrology, Elsevier Science, 302, 1-4, pp.107-126.

Jakeman, A.J. & G.M. Hornberger, 1993. How Much Complexity Is Warranted in a Rainfall-Runoff Model?. Water Resources Research 29, 8, pp. 2637-49.

Jakeman, A.J., I.G. Littlewood, P.G. Whitehead, 1990. Computation of the instantaneous unit hydrograph and identifiable component flows with application to two small upland catchments. Journal of Hydrology, 117, (1-4), pp.275-300.

Jasper, K., P. Calanca, D. Gaylistras & J. Fuhrer, 2004. Differential impacts of climate change on the hydrology of two alpine river basins, Climate Research, 26, pp.113-129,

Jenson, S. K. & J. O. Domingue, 1988. Extracting Topographic Structure from Digital Elevation Data for Geographic Information System Analysis. Photogrammetric Engineering and Remote Sensing, 54**,** pp. 1593-1600.

Journel, A.G. & C.J., Huijbregts, 1978. Mining Geostatistics. Academic Press Inc, London, UK, 600pp.

Kabat, P., R.E.Schulze, M.E.Hellmuth & J.A. Veraart, 2002. Coping with Impacts of Climate Variability and Climate Change in Water Management: A Scoping Paper. DWC-Report no. DWCSSO-01(2002), International Secretariat of the Dialogue on Water and Climate, Wageningen.

Kabiri, R., A. Chan & Ramani Bai.V., 2013. Comparison of SCS and Green-Ampt Methods in Surface Runoff-Flooding Simulation for Klang Watershed in Malaysia. Open Journal of Modern Hydrology, 3(3), pp. 102-114. doi: 10.4236/ojmh.2013.33014

Kavvas, M. L., Z.Q. Chen, & N. Ohara, 2006. Study of the Impact of Climate Change on the Hydrologic Regime And Water Resources of Peninsular Malaysia. California Hydrologic Research Laboratory 526 Isla Place, Davis, California 95616 U.S.A.

Khan, M.S. & P. Coulibaly, 2010. Assessing Hydrologic Impact of Climate Change with Uncertainty Estimates: Bayesian Neural Network Approach. American Meteorological Society., 11, pp.482-495.

Khan, M.S., P. Coulibaly & Y. Dibike, 2005. Uncertainty analysis of statistical downscaling methods, Journal of Hydrology, 319, pp. 357-382.

Khazaei M.R, B. Zahabiyoun, B. Saghafian, 2012. Assessment of climate change impact on floods using weather generator and continuous rainfall-runoff model. International Journal of Climatology, 32 (13), pp. 1997-2006. doi: 10.1002/joc.2416.

Kite, G. M., 1977. Frequency and Risk Analysis in Hydrology. Water Resources Publications, Fort Collins, N.Y.

Kleinn, I., C. Frei, J. Gurtz, D. Luthi, P.L. Vidale & C. Schar, 2005. Hydrologic simulations in the Rhine basin driven by a regional climate model, Journal of Geophysical Research, 110, D04102, doi:10.1029/2004JD005143, 2005

Knudsen, J., A. Thomsen, & J.C. Refsgaard, 1986. WATBAL - A semi-distributed physically based hydrological modeling system. NORDIC HYDROLOGY. 17, pp. 415

Korada, H et al., 2011. A distributed model for real-time flood forecasting in the Godavari Watershed using space inputs. International Journal of Disaster Risk Science, 2(3), pp. 31-40.

Kouwen, N. 2001. WATFLOOD/SPL9 Hydrological Model & Flood Forecasting System. University of Waterloo, 192 p

Levene, H., 1960. Contributions to Probability and Statistics. Stanford University Press.

Liang, X.Z., L. Li, A. Dai & K. E. Kunkel, 2004. Regional climate model simulation of summer precipitation diurnal cycle over the United States. Geophysical Research Letters., 31(24). doi: 10.1029/2004GL021054

Lin, X.S & Q. Yu, 2008. Study on the spatial interpolation of agroclimatic resources in Chongqing. Journal of Anhui Agriculture science, 36(30), pp.13431–13463

Linsley R.k., M.A. Kohler & J. Paulus, 1982. Hydrology for Engineers. McGraw-Hill New York, USA.

Liu, Y. B., S. Gebremeskel, F. De. Smedt, L. Hoffmann & L. Pfister, 2006. Predicting storm runoff from different land-use classes using a geographical information system-based distributed model. Journal of Hydrological Processes, 20, pp. 533-548. doi: 10.1002/hyp.5920

Liu, Z., Z.., Xu, S.P., Charles, Fu, G., & L., Liu, 2011, Evaluation of two statistical downscaling models for daily precipitation over an arid watershed in China. International Journal of Climatology, 31, pp. 2006-2020.

Lorraine E.F., & L.F. Alan, 2012. Downscaling future climate scenarios to fine scales for hydrologic and ecological modelling and analysis. Ecological Processes, 1(2), doi: 10.1186/2192-1709-1-2.

Lu, G.Y., and D.W. Wong, 2008. An adaptive inverse-distance weighting spatial interpolation technique. Computers & Geosciences, 34 (9), pp.1044–1055

Ludwig, R. & P. Schneider, 2006. Validation of digital elevation models from SRTM X-SAR for applications in hydrologic modelling. ISPRS Journal of Photogrammetry & Remote Sensing, 60, pp.339-358.

Maidment, D. R., 2002. Arc Hydro: GIS for Water Resources, ESRI Press, Redlands, Ca.

Malaysian Meteorological Department, 2009. Climate change scenarios for Malaysia 2001- 2099.

Mascaro, G., M. Piras, R. Deidda & E.R. Vivoni, 2013. Distributed hydrologic modeling of a sparsely monitored basin in Sardinia, Italy, through hydrometeorological downscaling, Hydrology and Earth System Science, 17, pp. 4143-4158, doi:10.5194/hess-17-4143-2013

Massari, C., L. Brocca, S. Barbetta, C. Papathanasiou, M. Mimikou & T. Moramarco, 2013. Using globally available soil moisture indicators for flood modelling in Mediterranean catchments. Hydrology and Earth System Sciences, 10, pp.10997-11033. doi:10.5194/hessd-10-10997-2013

Maurer E. P., L. D. Brekke, & T. Pruitt, 2010. Contrasting Lumped and Distributed Hydrology Models for Estimating Climate Change Impacts on California Watersheds. Journal of the American Water Resources Association, 46 (5), pp.1024-1035. doi: 10.1111/j.1752-1688.2010.00473.x

Maurer, E. P. & H. G. Hidalgo, 2008. Utility of daily vs. monthly large-scale climate data: An intercomparison of two statistical downscaling methods. Hydrology and Earth System Sciences, 12, pp. 551-563, doi: 10.5194hess-12-551-2008.

Mccarthy, G.T., 1938. The unit hydrograph and flood routing, Conference of North Atlantic Division. US Army Corps of Engineers, New London, CT. US Engineering.

McCuen, R. H., W.J. Rawls & D.L. Brakensiek, 1981. Statistical analysis of the Brooks-Corey and the Green-Ampt parameters across soil textures. Water Resources Research, 2(4), pp.1005-1013.

McCuen, R.H., 1998. Hydrologic Analysis and Design. 2nd ed, Prentice Hall, Englewood Cliffs, NJ.

McGuire, K. & J. McDonnell, 2010. Hydrological connectivity of hillslope and stream: Characteristic timescales and non-linearities. Journal of Water Resources Research, 46, W10543. doi:10.1029/2010WR009341.

Mearns L. O., I. Bogardi, F. Giorgi, I. Matyasovszky , M. Palecki, 2012. Comparison of climate change scenarios generated from regional climate model experiments and statistical downscaling. Journal of Geophysical Research: Atmospheres , 104, pp. 6603-6621, doi: 10.1029/1998JD200042.

Mearns, L.O., M. Hulme, T.R. Carter, R. Leemans, M. Lal & P. Whetton, 2001. Climate scenario development. In: Climate Change 2001: The Scientific Basis. Contribution of Working Group I to the Third Assessment Report of the Intergovernmental Panel on Climate Change, J.T. Houghton, Y. Ding, D.J. Griggs, M. Noguer, P.J. van der Linden, X. Dai, K. Maskell & C.A. Johnson (Eds.), Cambridge University Press, Cambridge, UK and New York, NY, pp.

739-768. Available for download from: http://www.ipcc.ch (Chapter 13 of the IPCC WG1 Assessment).

Meenu, R., S. Rehan, & P. P. Mujumdar, 2012. Assessment of hydrologic impacts of climate change in Tunga–Bhadra river watershed, India with HEC-HMS and SDSM. Hydrological Processes, pp. 1085-1099, doi: 10.1002/hyp.9220.

Miller, J.R. & G. L. Russell, 2012. The impact of global warming on river runoff. Journal of Geophysical Research, 97, D3, pp.2757-2764. doi: 10.1029/91JD01700

Milly, P. C. D., Krista A. Dunne, 2011: On the Hydrologic Adjustment of Climate-Model Projections: The Potential Pitfall of Potential Evapo-Transpiration. Earth Interactions. 15, pp. 1-14.

Mirhosseini, G., P. Srivastava & L. Stefanova, 2012. The impact of climate change on rainfall Intensity–Duration–Frequency (IDF) curves in Alabama. Regional Environmental Change, doi: 10.1007/s10113-012-0375-5

Mishra, S. K. & V. P. Singh, 2004. Long-term hydrological simulation based on the Soil Conservation Service curve number, Journal of Hydrological Process, 18, pp. 1291-1313.

Mishra, S., R. Sahu, T. Eldho & M. Jain, 2006. An improved Ia–S relation incorporating antecedent moisture in SCS-CN methodology. Water Resources Management, 20 (5), pp. 643–660.

Morin, G., 2002. CEQUEAU hydrological model. In: V.P. Singh et D.K. Frevert (Editors), MAthematical models of large watershed hydrology. Journal of Water Resource, Publ. Highlands Ranch, Colorado, pp. 507-576.

Morrison, J.L., 1971. Method- Produced Error in Isarithmic Mapping, American Congress on Surveying and Mapping, Cartography Division. Technical Monograph No. CA -5.

Music, B. & D. Caya, 2000. Evaluation of the hydrological cycle over the Mississippi River Watershed as simulated by the Canadian Regional Climate Model (CRCM), Journal of Hydrometeorology. 8, pp. 969-988.

NAHRIM: National Hydraulic Research Institute of Malaysia, 2010. Urbanisation and water quality control for the source of water in Kuala Lumpur city, Ministry of Natural Resources and Environment, Malaysia.

Nawarathna, N., Y. Tachikawa & K. Takara, 2005. Water resources distribution of the lower Mekong region: distributed hydrological modelling approach, Role of Water Sciences in Transboundary River Watershed Management. Thailand, pp.43-48, http://www.mekongnet.org/images/b/bf/Bandara.pdf.

Neitsch, S.L., J.G. Arnold, J.R. Kiniry & J.R. Williams, 2005. Soil and water assessment tool, input/output file documentation. Version 2005, Grassland, Soil and water Research Laboratory, USDA ARS/blackland Research Centre, Temple, Texas Agricultural Experiment Station, Texas. Available at: http://swat.tamu.edu/media/1291/swat2005io.pdf (Accessed 14 Jan 20140).

Nguyen, T.D., V.T., Nguyen & P. Gachon, 2007. A spatial-temporal downscaling approach for construction of intensity-duration-frequency curves in consideration of GCMbased climate change scenarios. Advances in Geosciences, 6, pp. 11-21.

Nigel W. A, 2004. Climate change and global water resources: SRES emissions and socio-economic scenarios. journal of Global Environmental Change., 14, pp. 31-52

Nor, N.I.A., S. Harun & A.H.M. Kassim, 2007. Radial basis function modeling of hourly streamflow hydrograph. Journal of Hydrologic Engineering, 12, pp. 113-123.

Obled, C., G. Bontron, & R. Garcon, 2002. Quantitative precipitation forecasts: A statistical adaptation of model outputs through an analogues sorting approach, Journal of Atmospheric Research, 63, pp. 303-324.

Ogden, F.L., 1998. CASC2D Reference Manual. Department of Civil and Environmental Engineering, U-37, University of Connecticut, 83 p

Onof, C. & K., Arnbjerg-Nielsen, 2009. Quantification of anticipated future changes in high resolution design rainfall for urban areas. Atmospheric Research, 92,pp.350-363. doi:10.1016/j.atmosres.2009.01.014.

Parry, M.L., J.A. Lowe, C. Hanson, 2009.Overshoot, adapt and recover. Nature. 258 (7242), pp.1102-1103.

Peters, E G., 2010. Improving the Practice of Modelling Urban Hydrology, Stormwater. Journal of Surface Water Quality professionals. Accessed on 30-Aug-2012, (online) Available: http://www.stormh2o.com/marchapril-2012/improving-practice-modeling.aspx

Petheram, C. et al., 2012: Estimating the Impact of Projected Climate Change on Runoff across the Tropical Savannas and Semiarid Rangelands of Northern Australia. Journal of Hydrometeorology, 13, pp. 483-503.doi: http://dx.doi.org/10.1175/JHM-D-11-062.1

Petrosellia, A., S. Grimaldib & N. Romanoe, 2013. Curve-Number/Green-Ampt Mixed Procedure for Net Rainfall Estimation: A Case Study of the Mignone Watershed, IT, Procedia Environmental Sciences, 19, pp. 113-121

Piechota, T.C., J.D. Garbrecht & J.M. Schneider, 2006. Climate variability and climate change. In: Garbrecht, J.D., T.C. Piechota, (Eds.), Climate Variations, Climate Change, and Water Resources Engineering. ASCE.

Pielke S.r., R.A. Marland, G. Betts, R.A. Chase, T.N. Eastman, J.L. Niles & J.O. Niyogi, 2002. The influence of land-use change and landscape dynamics on the climate system-relevance to climate change policy beyond the radiative effect of greenhouse gases. Philos. Trans, A 1797, pp.1705-1719.

Potter, K.W., 1981. Illustration of a new test for detecting a shift in mean in precipitation series, Monthly Weather Review., 109, pp. 2040-2045.

Praskievicz, S. & H., C. hang, 2009. A review of hydrological modelling of basin scale climate change & urban development impacts. Progress in Physical Geography, 33 (5), pp. 650-671. doi: 10.1177/0309133309348098

Prentice, C., G. Farquhar, M. Fasham, M. Goulden, M. Heimann, V. Jaramillo, H. Kheshgi, C. L. Quere, R. Scholes, & D. Wallace, 2001. The carbon cycle and atmospheric CO2, in Climate Change 2001: The Scientific Basis: Contribution of WGI to the Third Assessment Report of the IPCC, edited by J. T. Houghton et al., pp. 183-237, Cambridge Univ. Press, New York.

Prodanovic,P. & S.P. Simonovic, 2007. Development of Rainfall Intensity Duration Frequency Curves for the City of London Under the Changing Climate. Water Resources Research Report no. 058, Facility for Intelligent Decision Support, Department of Civil and Environmental Engineering, London, Ontario, Canada, 51 pages.

Prudhomme, C., H. Davies, 2009. Assessing uncertainties in climate change impact analyses on the river flow regimes in the UK. Part 2: future climate. Journal of Climatic Change, 93, pp. 197-222.

Prudhomme, C., N., Renard, & S., Crooks, 2002. Downscaling of global climate models for flood frequency analysis: where we are now? Journal of Hydrological Processes, 16, pp. 1137-1150

Qi, S., G. Sun, Y. Wang, S. G. McNulty & J. A. Moore Myers, 2009. Streamflow response to climate and landuse changes in a coastal watershed in North Carolina. American Society of Agricultural and Biological Engineers, 52 (3) pp. 739-749. doi: 10.13031/2013.27395

Racsko, P., L. Szeidl & M.A. Semenov,1991. A serial approach to local stochastic weather models. Ecological Modelling, 57, pp. 27-41.

Raff, D. A., T. Pruitt & L. D. Brekke, 2009. A framework for assessing flood frequency based on climate projection information. Hydrology and Earth System Sciences, 13, pp. 2119-2136.

Raghunath, H. M., 2006. Hydrology: Principles, Analysis and Design. New Delhi, New Age International.

Raje, D., & P.P. Mujumdar, 2010. Constraining uncertainty in regional hydrologic impacts of climate change: Nonstationarity in downscaling. Water Resources Research, 46, W07543.

Ramakrishnan, D., A. Bandyopadhyay & K.N. Kusuma, 2009. SCS-CN and GIS-based approach for identifying potential water harvesting sites in the Kali Watershed, Mahi River Basin, India. Journal of Hydrology and earth system science, 118 (4), pp. 355-368.

Randin C.F., R.Engler, S. Normand, M. Zappa, N.E. Zimmermann, P.B. Pearman, P. Vittoz, W. Thuiller & A. Guisan, 2009. Climate change and plant distribution: local models predict high elevation persistence. Global Change Biology, 15, pp. 1557-1569.

Rango, A. 1995. The snowmelt runoff model SRM in: Singh, V., (ed): Computer Models of Watershed Hydrology, Water Resources Publications. pp. 477-520

Rawls, W.J., D.L. Brakensiek, & K.E. Saxton, 1982. Estimation of Soil Water Properties. Transactions of the ASCE, pp.1316-1320.

Reichler, T., & J. Kim, 2008. How Well Do Coupled Models Simulate Today's Climate? American Meteorological Society, 89, pp. 303-311.

Richardson, C.W. & D.A. Wright, 1984. WGEN: a model for generating daily weather variables. US Department of Agriculture. Agricultural Research Service, ARS-8, pp. 83.

Richardson, C.W., 1981. Stochastic simulation of daily precipitation, temperature and solar radiation. Water Resources Research, 17: 182-190.

Rose, S., & N. E. Peters, 2001. Effects of urbanization on streamflow in the Atlanta area (Georgia, USA): A comparative hydrological approach. Hydrology Process, 15 (8), pp.1441-1457

Saghravani S. R., S. Mustapha, S. Ibrahim & E. Randjbaran, 2009. Comparison of Daily and Monthly Results of Three Evapo-transpiration Models in Tropical Zone: A Case Study. American Journal of Environmental Sciences, 5(6), pp. 698-705.

Saha, S., & Coauthors, 2010. The NCEP climate forecast system reanalysis. Bulletin of the American Meteorological Society, 91(8), pp. 1015-1057. doi: http://dx.doi.org/10.1175/2010BAMS3001.1

Sahu, R. K., S. K. Mishra & T. I., Eldho, 2010. An improved AMC-Coupled runoff curve number model, Journal of Hydrological Processes, 24, pp. 2834-2839.

Salarpour, M., N.A. Rahman & Z. Yusop, 2011. Simulation of flood extent mapping by InfoWorks RS-case study for tropical catchment. Journal of Software Engineering, 5, pp. 127-135.

Salazar, L., G.H. Hargreaves, R.K. Stutler & J. Garcia, 1984. Irrigation scheduling manual. Irrigation Centre. Utah State University, Logan UT.

Samadi, S., G. J. Carbone, M. Mahdavi, F. Sharifi, & M. R. Bihamta, 2012. Statistical downscaling of climate data to estimate streamflow in a semi-arid catchment. Hydrology and Earth System Sciences Discussion, 9, pp. 4869-4918.

Samiran Das & S.P. Simonovic, 2012. Guidelines for Flood Frequency Estimation under Climate Change. Water Resources Research Report no. 082, Facility for Intelligent Decision Support, Department of Civil and Environmental Engineering, London, Ontario, Canada, pp.44.

Sasekumar A., & V.C. Chong, 2006. Ecology of Klang Strait. University of Malaya Press, University of Malaya, Kuala Lumpur, p.269. ISBN: 983-100-304-7

Sayang M. D., A.A. Jemain & I. Kamarulzaman, 2010. The best probability models for dry and wet spells in Peninsular Malaysia during monsoon seasons, International Journal of Climatology, 30 (8), pp.1194-1205.

Scharffenberg, W. A. & M. J. Fleming, 2008. Hydrologic Modelling System HEC-HMS; User's Manual. Davis, California: US Army Corps of Engineers. Institute for Water Resources, Hydrologic Engineering Centre.

Schmidli, J., C.M. Goodess, C. Frei, M.R. Haylock, M. R. Hundecha, Y. Ribalaygua, & T. Schmith, 2007. Statistical and dynamical downscaling of precipitation: An evaluation and comparison of scenarios for the European Alps, Journal of Geophysical Research Atmosphere, 112, D04105, doi:10.1029/2005JD007026.

Schneider, S.H., 2009. The worst-case scenario. Nature, 458 (7242) pp. 1104-1105.

Schroeter et al.., 1996. GAWSER: Guelph All-Weather Sequential-Events Runoff Model, Version 6.5, Training Guide and Reference Manual. Ontario Ministry of Natural Resources and the Grand River Conservation Authority

Segond M.L., N. Neokleous, C. Makropoulos & C. Maksimovic, 2007. Simulation and spatio-temporal disaggregation of multisite rainfall data for urban drainage applications. Journal of Hydrology Science, 52 (5), pp.917-935

Semenov, M.A., R.J. Brooks, E.M. Barrow & C.W. Richardson, 1998. Comparison of WGEN and LARS-WG stochastic weather generators for diverse climates. Climate Research, 10, pp. 95-107.

Sharma, A., A. Das Gupta, & M. S. Babel, 2007. Spatial disaggregation of bias-corrected GCM precipitation for improved hydrologic simulation: Ping River Watershed, Thailand. Hydrology and Earth System Sciences, 11, pp. 1373-1390.

Shi, Z. H., L. D. Chen, N. F. Fang, D. F. Qin & C. F. Cai, 2009. Research on the SCS-CN initial abstraction ratio using rainfall-runoff event analysis in the Three Gorges Area, China, CATENA, 77(1), pp.1-7.

Shrestha, R.R., Y.B. Dibike & T.D. Prowse, 2011. Modelling of climate-induced hydrologic changes in the Lake Winnipeg watershed. Journal Great Lakes Research, doi:10.1016/j.jglr.2011.02.004.

Simonovic S.P & A. Peck, 2009. Updated Rainfall Intensity Duration Frequency Curves for the City of London under Changing Climate. Water Resources Research Report no. 065, Facility for Intelligent Decision Support, Department of Civil and Environmental Engineering, London, Ontario, Canada, 64pages. ISBN: (print) 978-0-7714-2819-7; (online) 987-0-7714-2820-3.

Singh, V.P. & D.K. Frevert, 2002. Mathematical Models of Large Watershed Hydrology. Water Resource Publications, Highlands Ranch, Colorado, USA., ISBN: 9781887201346, pp. 891.

Singh, V.P. & D.K. Frevert, 2002. Mathematical Models of Small Watershed Hydrology and Applications. Water Research Publication, USA, ISBN-13: 9781887201353, pp. 950.

Sivapalan, M. & J.M. Samuel, 2009. Transcending lmitations of stationarity and the return period: process-based approach to flood estimation and risk assessment. Hydrological Process. 23, pp. 1671-1675, doi:10.1002/hyp.7292, 2009.

Soil Survey Staff, 1975. Soil taxonomy: A basic system of soil classification for making and interpreting soil surveys. U.S. Soil Conservation Service Agricultural Handbook No. 436 (U.S. Department of Agriculture), Washington, D.C. 754 pp.

Solomon, S. et al., 2007, Technical Summary, Climate Change 2007: The Physical Science Basis, Contribution of Working Group 1 to the Fourth Assessment Report of the Intergovernmental Panel on Climate Change, S. Solomon et al. (eds.), Cambridge University Press, Cambridge, United Kingdom and New York, http://www.ipcc.ch/

Stadler, H., C. Reszler, J. Komma, W. Poltnig, E. Strobl, & G. Blöschl, 2013. Hydrogeological Mapping and Hydrological Process Modelling for *understanding the interaction of surface runoff and infiltration in a karstic* catchment, Geophysical Research Abstracts,15, EGU2013-7857-1

USDA/NRC (1986) Urban Hydrology for Small Watersheds TR-55, Technical Release 55. Washington DC. pp. 132-139.

Stott, P.A., M.R. Allen & G.S. Jones, 2000. Estimating signal amplitudes in optimal fingerprinting II: Application to general circulation models. Hadley Centre Tech Note 20, Hadley Centre for Climate Prediction and Response. Meteorological Office, RG12, 2SY, UK.

Sun, S., & J.E. Hansen, 2003. Climate simulations for 1951-2050 with a coupled atmosphere-ocean model. Journal of Climate, 16, pp. 2807-2826.

Tague, C., G. Grant, M. Farrell, J. Choate & A. Jefferson, 2008. Deep groundwater mediates streamflow response to climate warming in the Oregon Cascades, Climatic Change, 86, pp. 189-210.

Tan, K.S., H. S. Chiew & R. B. Grayson, 2008. Stochastic Event-Based Approach to Generate Concurrent Hourly Mean Sea Level Pressure and Wind Sequences for Estuarine Flood Risk Assessment. Journal of Hydrologic Engineering, 13 (6), pp. 449-460.

Tarboton, D.G., & I.N. Mohammed, 2010. Terrain analysis using digital elevation models. TauDEM, version 5.0. Available from: http://hydrology.usu.edu/taudem/taudem5.0/

Temesgen, B., S. Eching, B. Davidoff & K. Frame, 2005. Comparison of some reference evapo-transpiration equations for California.Journal of Irrigation and Drainage, Eng., ASCE, 131(1), pp.73-84.

Teng, J., F. H. S. Chiew, J. Vaze, S. Marvanek & D. G. C. Kirono, 2012: Estimation of Climate Change Impact on Mean Annual Runoff across Continental Australia Using Budyko and Fu Equations and Hydrological Models. Journal of Hydrometeorology, 13, pp.1094-1106. doi: http://dx.doi.org/10.1175/JHM-D-11-097.1

Teng, J., F. H. S. Chiew, J. Vaze, S. Marvanek & D. G. C. Kirono, 2012. Estimation of Climate Change Impact on Mean Annual Runoff across Continental Australia Using Budyko and Fu equations and Hydrological Models. Hydrometeor, 13, pp.1094-1106. doi: http://dx.doi.org/10.1175/JHM-D-11-097.1

Thiessen, A.H., 1911. Precipitation averages for large areas. Monthly Weather Reveiw, 39 (7), pp.1082-1084.

Tick, L.J. & A.A. Samah, 2004. Weather and Climate of Malaysia. 1st Edn., University Malaya Perss, Kuala Lumpur, ISBN: 9831001761.

U.S. Dept. Agric., Soil Conservation Service, 2000. Urban Hydrology for small watersheds SCS Technical release 55. U.S. Government Printing Office, Washington, D.C.

Urban Stormwater Management Manual for Malaysia, MSMA, 2004. Flow estimation and Routing, Chapter 14.

USACE, 2000. Hydrologic Aspects of Flood Warning-Preparedness Programs, in: Engineers, Technical Letter, edited by: U. S. A. C. O., U.S. Army Corps of Engineers, Washington, DC.

USGS-NPD, 1991. SSARR Model Streamflow Synthesis and Reservoir Regulation, 426 p

Vaze, J. & J. Teng, 2011. Future climate and runoff projections across New South Wales, Australia: results and practical applications. Hydrological Process, 25(1), pp. 18-35.

Verburg, P.H., & K.P. Overmars, 2007. Dynamic simulation of landuse change trajectories with the CLUES model. In: Koomen E, Stillwell J, Bakema A, and Scholten HJ (eds.). Modelling Landuse Change. Progress and applications. The GeoJournal Library, 90. Springer. pp.321-338

Viessman, J.R.W. & G.L. Lewis, 2003. Introduction to Hydrology. Prentice Hall, Englewood Cliffs, New Jersey

Vieux, B. E, 2004. Distributed Hdyrologic Modelling Using GIS. Kluwer Academic Publishers.

Vitart.F., 2004. Dynamical seasonal forecasts of tropical storm statistics. In Hurricanes and Typhoons: Past, Present and Future, ed. by Murnane, R.J. and K.-B. Liu, Columbia Univ. Press.

Vrac, M. & P., Naveau, 2007. Stochastic downscaling of precipitation: From dry events to heavy rainfalls, Journal of Water Resource Research, 43, W07402, doi:10.1029/2006WR005308.

Wang, D. 2011. On the base flow recession at the Panola Mountain Research Watershed, Georgia, United States. Journal of Water Resources Research, 47, W03527. doi:10.1029/2010WR009910.

Webster,P.J., V.O.Magana, T.N.Palmer, J.Shukla, R.A.Tomas, M.Yanai, & T.Yasunari, 1998. Monsoons: Processes, predictability, and the prospects for prediction. Journal of Geophysics Research. 103(C7), pp. 14451-14510

Wheater, H., S. Sorooshian, K. Sharma & E. Corporation, 2008. Hydrological modelling in arid and semi-arid areas. Cambridge University Press.

Wigmosta, M.S., L. Vail, & D.P. Lettenmaier, 1994. A distributed hydrology-vegetation model for complex terrain, Water Resource and Research, 30, pp. 1665-1679, doi: 10.1029/94WR00436

Wilby R.L & C.W. Dawson, 2007. SDSM (4.2) - A decision support tool for the assessment of regional climate impacts, User Manual. King's College London.

Wilby, R. L. & C. W. Dawson, 2012, The Statistical DownScaling Model: insights from one decade of application. International Journal of Climatology, pp. 1097-0088.

Wilby, R.L., & T.M.L. Wigley, 1997. Downscaling general circulation model output: a review of methods and limitations. Progress in Physical Geography, 21, pp. 530–548.

Wilby, R.L., & T.M.L. Wigley, 2000. Precipitation predictors for downscaling observed and general circulation model relationships. Journal of Climatology, 20(6): pp. 641-661.

Wilby, R.L., C.W. Dawson & E.M. Barrow, 2002. SDSM - a decision support tool for the assessment of climate change impacts. Environmental Modelling and Software, 17, pp. 147–159.

Wilby, R.L., L.E. Hay & G.H. Leavesley, 1999. A comparison of downscaled and raw GCM output: implications for climate change scenarios in the San Juan River Watershed, Colorado. Journal of Hydrology, 225, pp.67–91.

Wilby, R.L., S.P. Charles, E. Zorita, B. Timbal, P. Whetton & L.O. Mearns, 2004. The guidelines for use of climate scenarios developed from statistical downscaling methods. Supporting material of the Intergovernmental Panel on Climate Change (IPCC), prepared on behalf of Task Group on Data and Scenario Support for Impacts and Climate Analysis.

Wilby,R.L., J. Troni, Y. Biot, L. Tedd, B. C. Hewitson, D. M. Smithe & R. T. Suttonf, 2009. Review a review of climate risk information for adaptation and development planning, International Journal Of Climatology, 29, pp.1193–1215, doi: 10.1002/joc.1839.

Wilks D.S & R.L. Wilby, 1999. The weather generator game: a review of stochastic weather models. Progress in Physical Geography. 23, pp.29-357

Wilks D.S., 2012. Stochastic weather generators for climate change downscaling, part II: multivariable and spatially coherent multisite downscaling. Journal of Wiley Interdisciplinary Reviews: Climate Change, 3 (3). doi: 10.1002/wcc.167

Wilks, D. S., 1995. Statistical Methods in the Atmospheric Sciences. International Geophysics Series, 59, Academic Press, 467 pp.

Woodward, D. E., R.H. Hawkins, R. Jiang, A.T. Hjelmfelt, J.A. Van Mullem & D.Q. Quan, 2003. Runoff Curve Number Method: Examination of the Initial Abstraction Ratio. World Water and Environmental Resources. Congress 2003 and Related Symposia EWRI, ASCE, 23-26 June, 2003, Philadelphia, Pennsylvania, USA, doi:10.1061/40685(2003)308.

World Meteorological Organization (WMO), 1986. Manual for Estimation of Probable Maximum Precipitation. Operational Hydrological Report No 1; second edition; Geneva; p. 96.

Wu L., Wu X.J., Xiao & C. Tian, 2010. On temporal and spatial error distribution of five precipitation interpolation models. Journal of Geographical Information Science, 26(3), pp.19-24.

Wua, S., J. Lib & G.H. Huang, 2008. A study on DEM-derived primary topographic attributes for hydrologic applications: Sensitivity to elevation data resolution. Applied Geography,28, pp. 210–223.

Wurbs, R.A., R.S. Muttiah, F. Felden, 2005. Incorporation of climate change in water avaibility modelling. Journal of hydrologic Engineering, 10 (5), pp. 375-385.

Xu, C.Y. & V.P. Singh, 1998. A review on monthly water balance models for water resources investigations. Journal of Water Resources Management, 12, pp. 31-50.

Yang, L. Huihui, W. Weiguang , X. Chong-Yu, Y. Zhongbo, 2012.Statistical downscaling of extreme daily precipitation, evaporation, and temperature and construction of future scenarios. Hydrological Processes, 26(23), pp. 3510–3523. doi: 10.1002/hyp.8427.

Yarnal, B., A.C., Comrie, B., Frakes & D.P., Brown, 2001. Developments and prospects in synoptic climatology. International Journal of Climatology, 21, pp. 1923-1950.

Yin, E.H. 1976. Geologic Map of Selangor. Jabatan Penyiasatan Kajibumi Malaysia.

Yoon, J.H., M.O. Kingtse & E.F. Wood, 2012. Dynamic-Model-Based Seasonal Prediction of Meteorological Drought over the Contiguous United States. Journal of Hydrometeor, 13, pp. 463-482 doi: http://dx.doi.org/10.1175/JHM-D-11-038.1

Yusof, F. & I. L. Kane, 2013. Volatility modeling of rainfall time series. Journal of Theoretical and Applied Climatology, doi: 10.1007/s00704-012-0778-8.

Zhang, Y., & F. Chiew, 2009. Evaluation of regionalisation methods for predicting runoff in ungauged catchments in southeast Australia. In: Anderssen, R., Braddock, R., and Newham, L. (eds), 18th World IMACS Congress and MODSIM09 International Congress on Modelling and Simulation, July 2009, Cairns: Modelling and Simulation Society of Australian and New Zealand and International Association for Mathematics and Computers in Simulation. pp. 3442-3448. http://www.mssanz.org.au/modsim09/I7/zhang_yq.pdf

Zhao, L., J. Xia, C. Xu, Z. Wang & L. Sobkowiak, 2013. Cangrui Long Evapo-transpiration estimation methods in hydrological models, Journal of Geographical Sciences, 23 (2), pp. 359-369.

Zhu, J., C. M. Stone & W. Forsee, 2012. Analysis of potential impacts of climate change on intensity-duration-frequency (IDF) relationships for six regions in the United States. Journal of Water and Climate Change, 3 (3), pp. 185-196.

# APPENDICES

## Appendix A- Climate Change Models

| Model | Institution | Atmospheric prognostic variables | Oceanic prognostic variables | Atmospheric resolution | Oceanic resolution |
|---|---|---|---|---|---|
| **CNCM3** | Meteorological Research Institute, France | temperature<br>northward and eastward wind components<br>specific humidity<br>ozone concentration<br>surface pressure | temperature<br>salinity<br>vertical eddy viscosity<br>meridional and vertical velocity components | 2.8 degrees x 2.8 | 182 degree (longitude) x 152 degree |
| **MRCGCM** | Meteorological Research Institute, Japan Meteorological Agency | velocity potential<br>stream function<br>temperature<br>specific humidity | velocities (eastward and northward)<br>temperature<br>salinity | 2.8 degrees x 2.8 | 2.5 degree x 2.0 degree |
| **FGOALS** | LASG, Institute of Atmospheric Physics, Chinese Academy of Sciences, China | temperature<br>northward and eastward wind<br>surface pressure<br>specific humidity<br>ice water<br>liquid water | Sea surface height<br>temperature<br>salinity<br>horizontal velocity | 2.8 degree x 2.8 | 1 degree x1 |
| **GFCM20** | Geophysical Fluid Dynamics Laboratory, NOAA | Zonal and meridional wind components<br>surface pressure<br>temperature<br>specific humidity of water vapor<br>cloud liquid<br>cloud ice<br>and cloud fraction | u<br>v<br>free surface height<br>temperature and salinity | 2.5 degrees x 2.0 degrees | 1 degree longitudinal, 1 degree latitudinal with enhanced tropical resolution (1/3 on equator) |
| **MPEH5** | Max Planck Institute for Meteorology, Germany | Vorticity<br>divergence<br>temperature<br>log surface pressure<br>water vapor<br>cloud liquid water<br>cloud ice | U<br>v<br>w<br>t<br>s<br>surface elevation | 1.8 degrees x 1.8 | 1.5 deg x 1.5 |
| **NCPCM** | National Centre for Atmospheric Research (NCAR), NASA, and NOAA | Vorticity<br>Divergence<br>Temperature<br>Specific humidity<br>Surface pressure<br>Grid box averaged liquid condensate amount<br>Grid box averaged ice condensate amount | grid-oriented zonal and meridional velocity components<br>vertical velocity<br>pressure<br>density<br>potential temperature<br>salinity<br>ideal age | 2.8 degrees x 2.8 | 320x384 horizontal grid |

## Climate Change Models (Continued)

| Model | Institution | Atmospheric prognostic variables | Oceanic prognostic variables | Atmospheric resolution | Oceanic resolution |
|---|---|---|---|---|---|
| **CSMK3** | CSIRO, Australia | Temperature<br>Vorticity<br>Divergence<br>Surface Pressure<br>Atmospheric moisture<br>(vapour<br>liquid<br>and ice) | Velocities U and V<br>Temperature and<br>Salinity | 2.8 degrees x<br>2.8 | 1.875 EW<br>x 0.84 NS |
| **CGMR** | Canadian Centre for Climate Modelling and Analysis (CCCma) | velocity potential<br>temperature<br>specific humidityl | velocities (eastward and northward)<br>temperature<br>salinity | 3.75 degrees x<br>3.75 | 1.8 degree<br>x 1.8 |
| **MIROC** | CCSR/NIES/FRCGC, Japan | temperature<br>northward and eastward<br>wind components<br>surface pressure<br>specific | zonal and meridional<br>velocity<br>temperature<br>salinity<br>sea surface height | 3.75 degrees x<br>2.5 | 1.4 degree<br>x 1.4 |
| **CCSR/NIES** | Centre for Climate System Research, University of Tokyo, Japan | temperature<br>northward and eastward<br>wind components<br>surface pressure<br>specific | zonal and meridional<br>velocity<br>temperature<br>salinity<br>sea surface height | 5.6 degrees x<br>5.6 | 2.8 degree<br>x<br>2.8 |
| **CSIRO- MK2** | CSIRO Atmospheric Research<br>Australia | Temperature<br>Vorticity<br>Divergence<br>Surface Pressure<br>Atmospheric moisture<br>(vapour<br>liquid<br>and ice) | Velocities U and V<br>Temperature and<br>Salinity | 5.6 degrees x<br>3.2 | 4.3 degrees<br>x 4.3 |
| **ECHAM** | National Centre for Atmospheric Research (NCAR), NASA, and NOAA | Vorticity<br>divergence<br>temperature<br>log surface pressure<br>water vapor<br>cloud liquid water<br>cloud ice | u<br>v<br>w<br>t<br>s<br>surface elevation | 2.8 degrees x<br>2.8 | 1.5<br>degree x<br>1.5 |

## Appendix B – Double-Mass Curve

Station no. 3014084

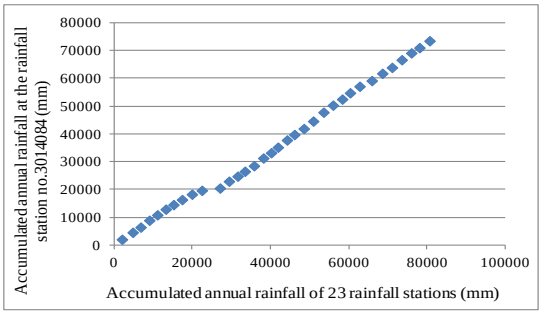


Station no. 3014089

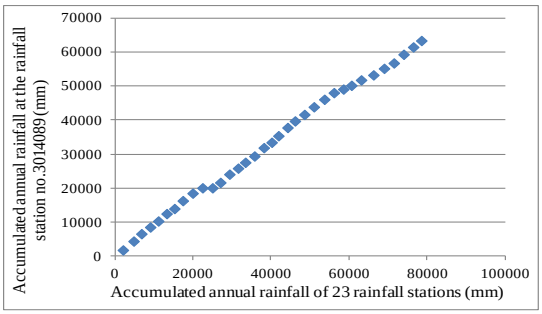


Station no. 3015001

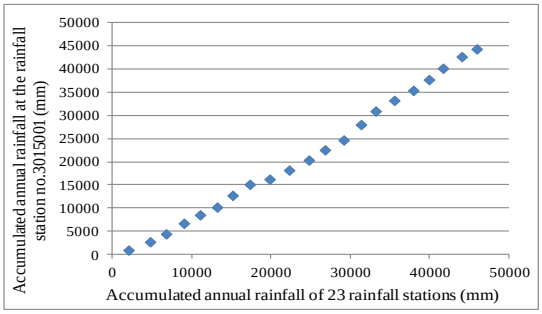


Station no. 3018107

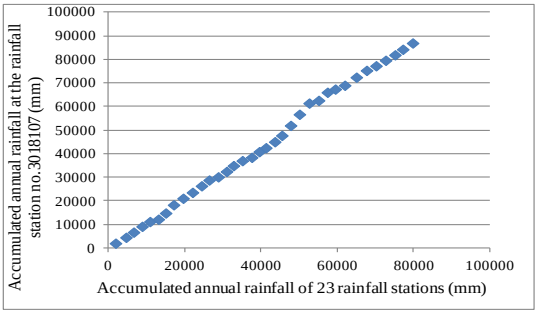


Station no. 3115079

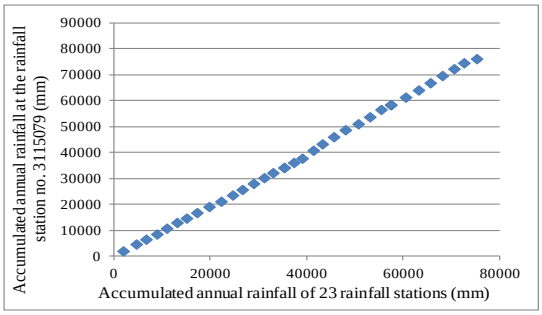


Station no. 3116003

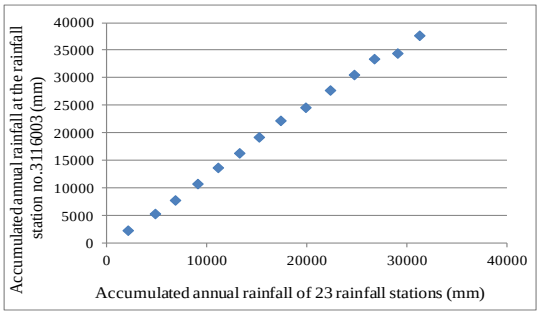


Station no.3116004

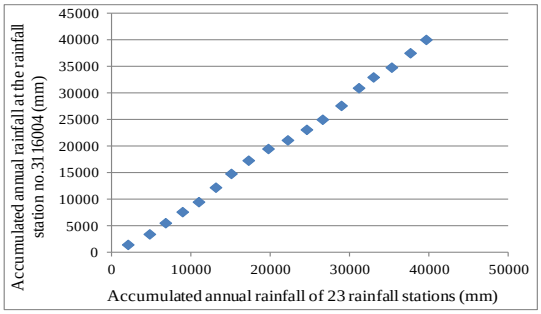


Station no. 3116005

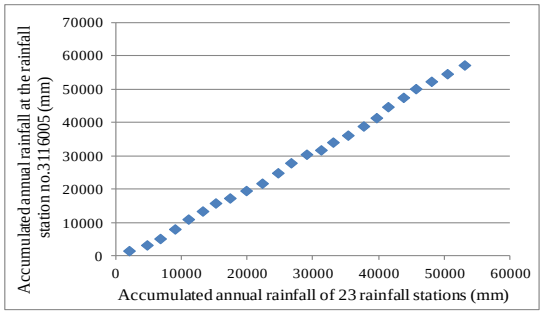

Station no. 3116006

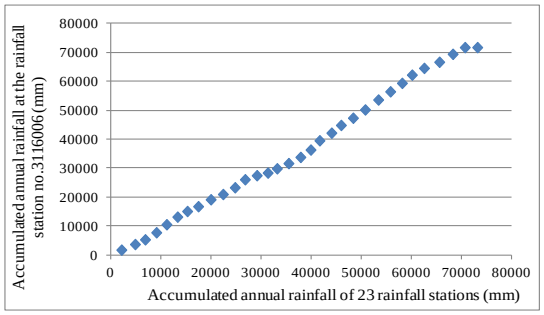


Station no. 3117070

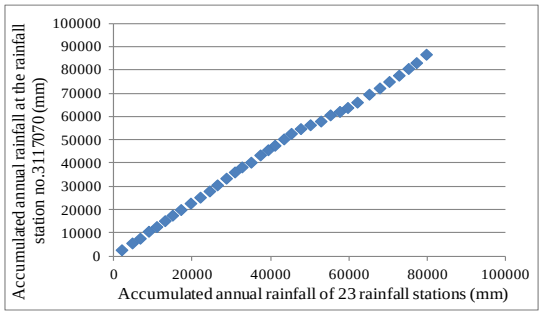


Station no. 3117071

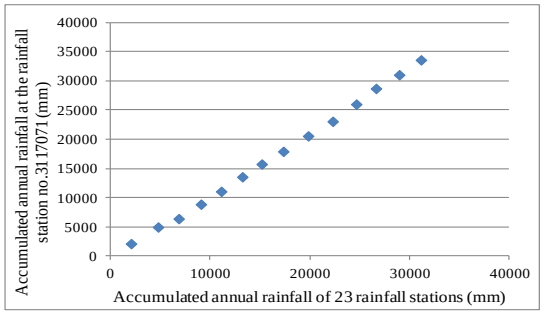


Station no. 3118069

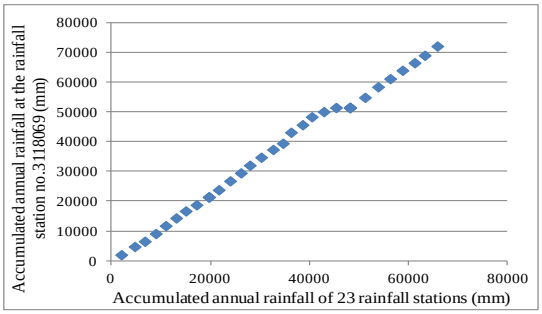


Station no. 3118102

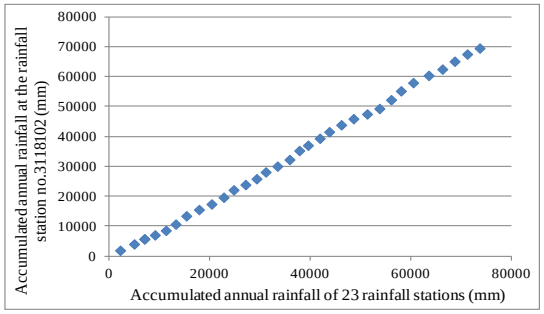


Station no. 3216001

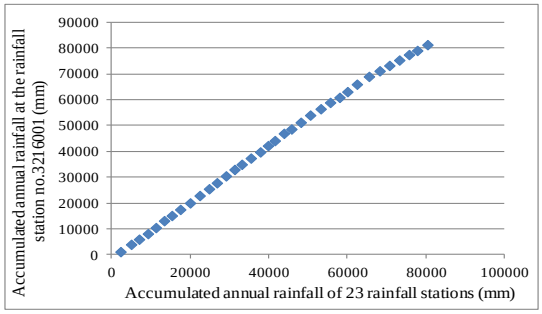


Station no. 3216004

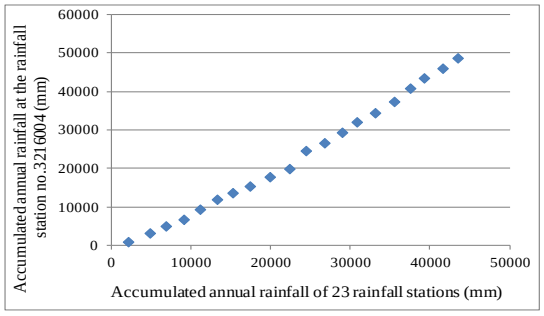


Station no. 3217001

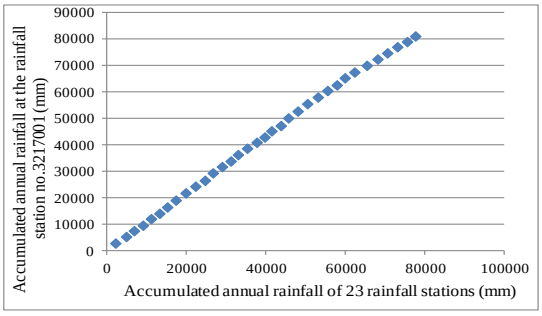

Station no. 3217002

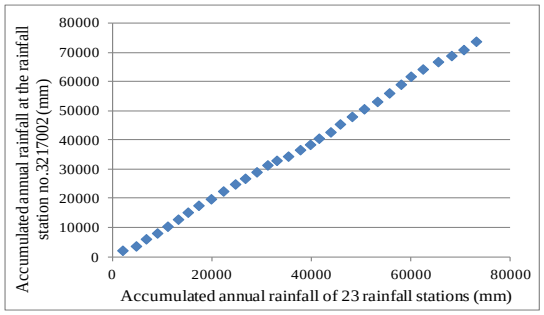


Station no. 3217004

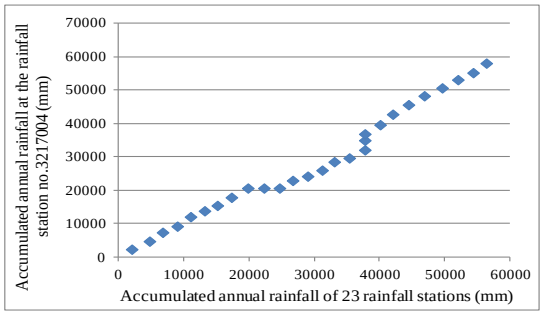


Station no. 3217005

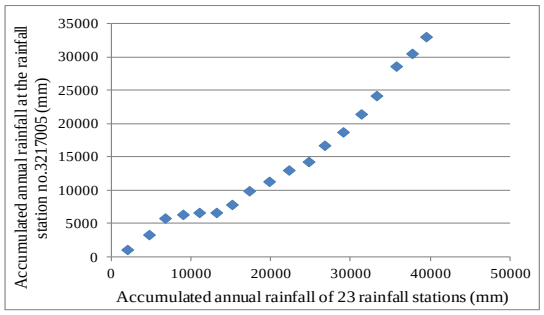


Station no. 3218101

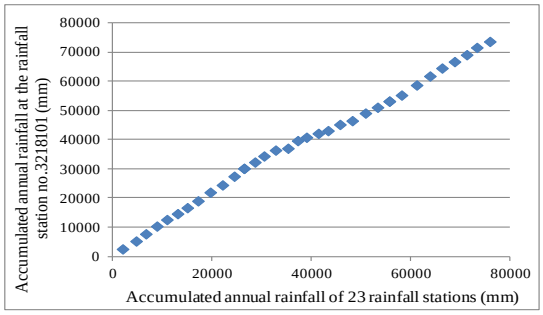


Station no. 3317001

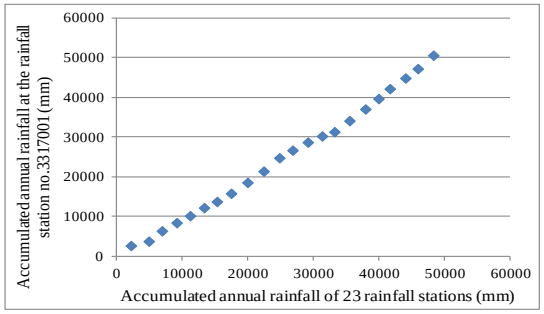


Station no. 3317004

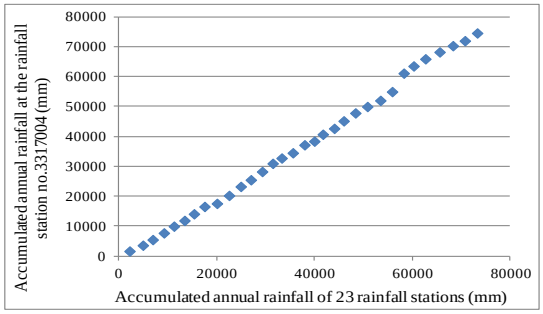

## Appendix C– Correlation between Raingauge Stations of Daily Rainfall Data

Station no. (3216001 and 3217001)

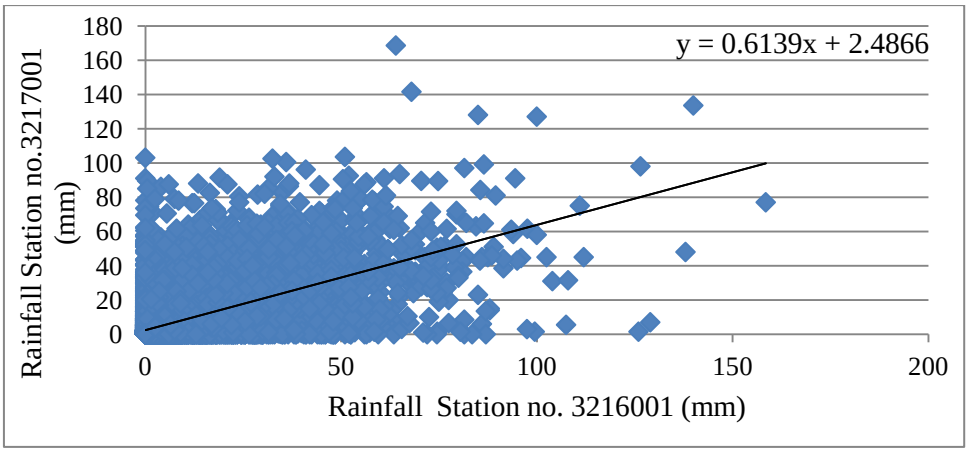


Station no. (3217003 and 3217004)

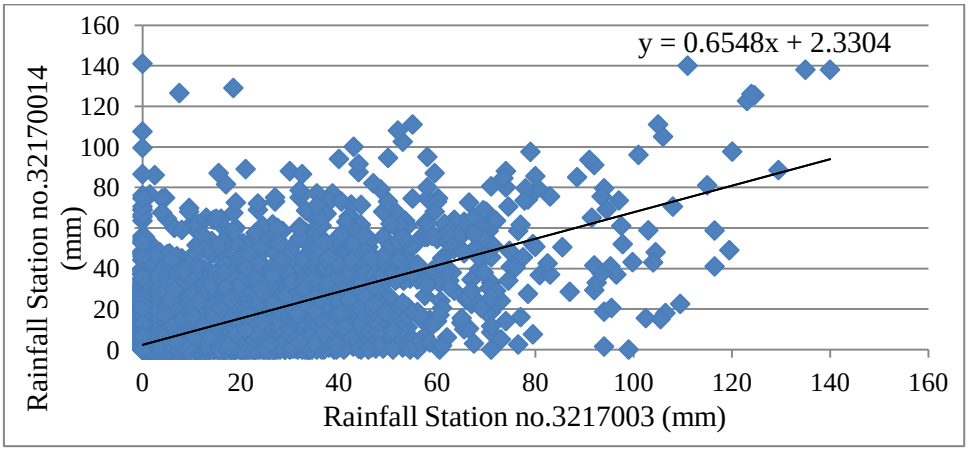


Station no. (3117070 and 3118069)

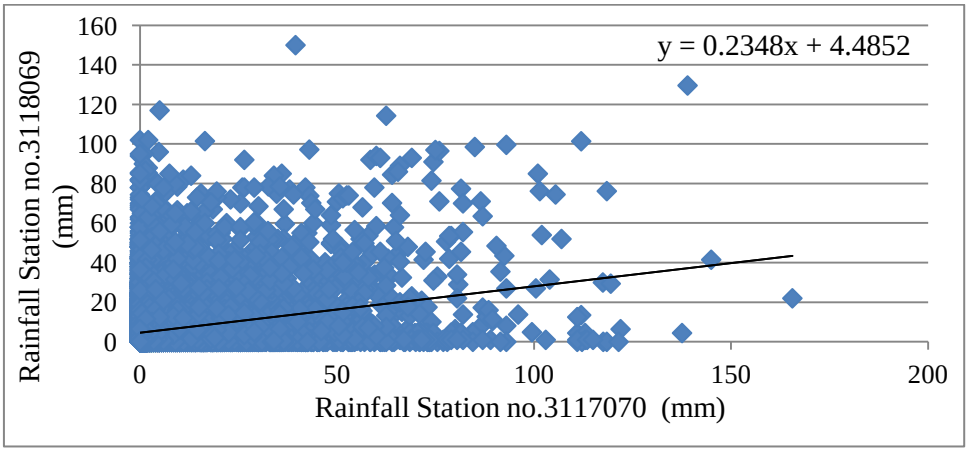

Station no. (3217001 and 3217002)

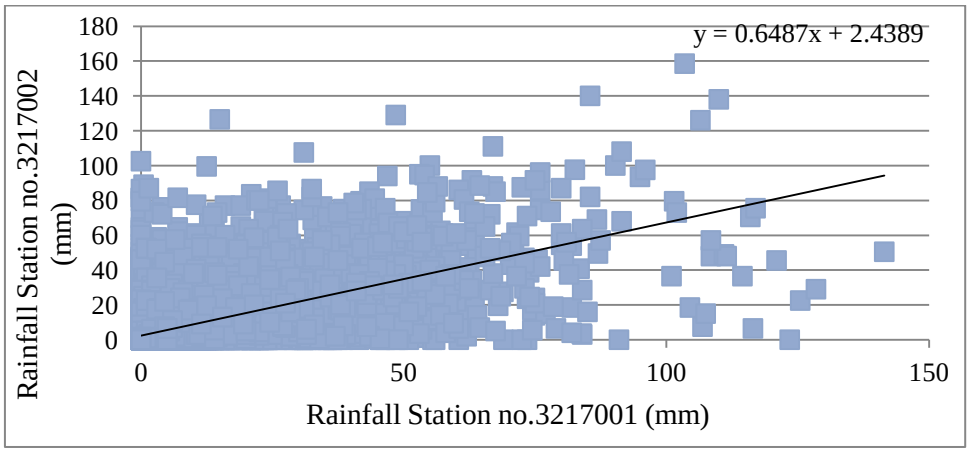


Station no. (3217070 and 3118069)

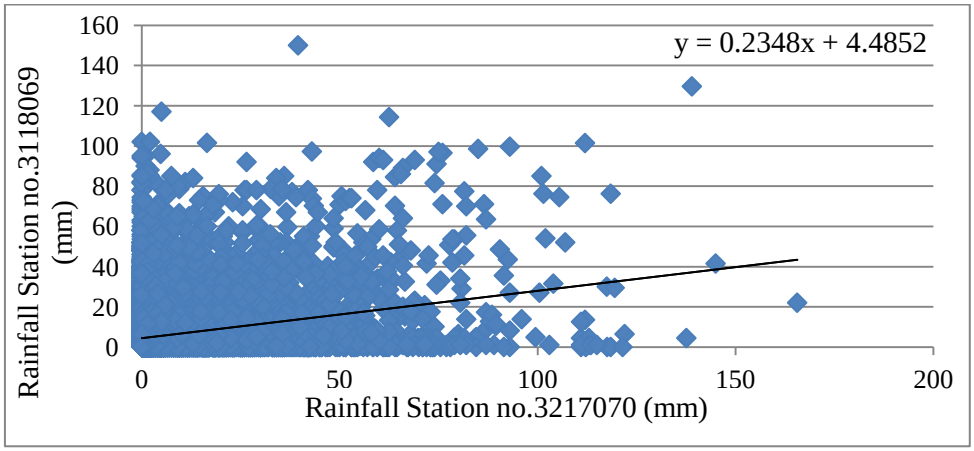


Station no. (3217003 and 3116005)

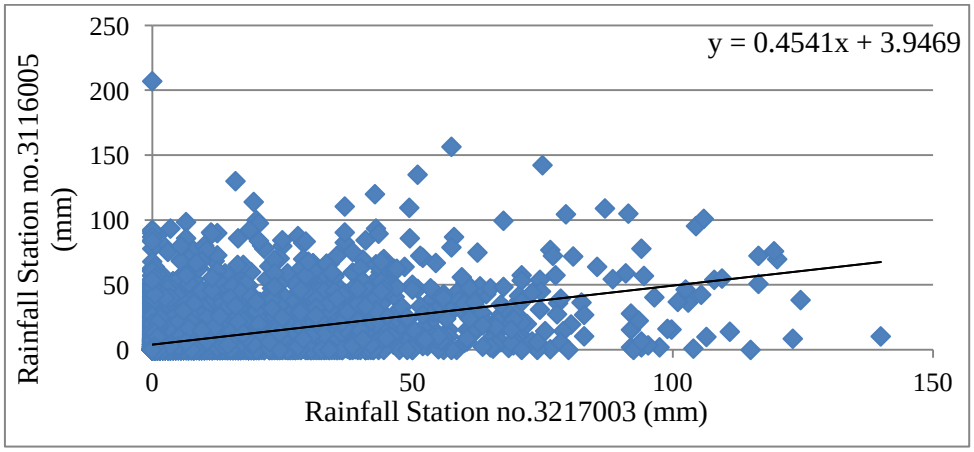

Station no. (3317004 and 3217001)

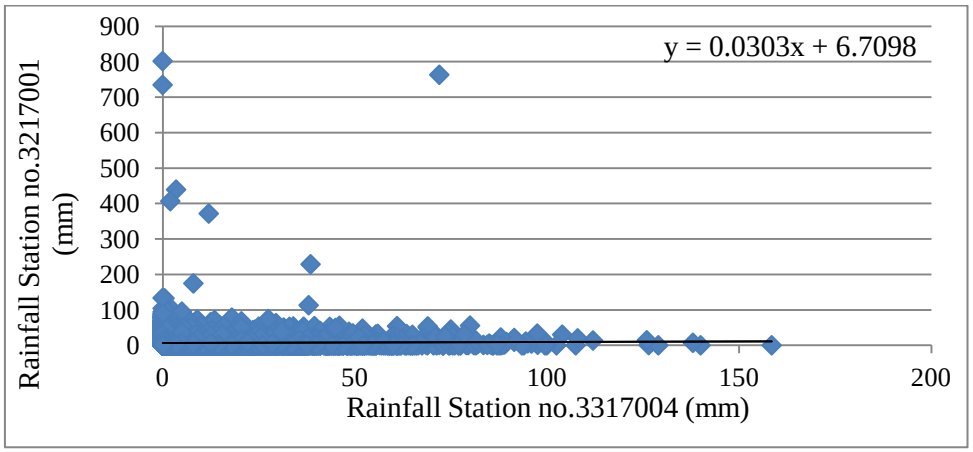


**Appendix D- The Correlation of Daily Discharge Data between the Discharge Stations in Klang Watershed**

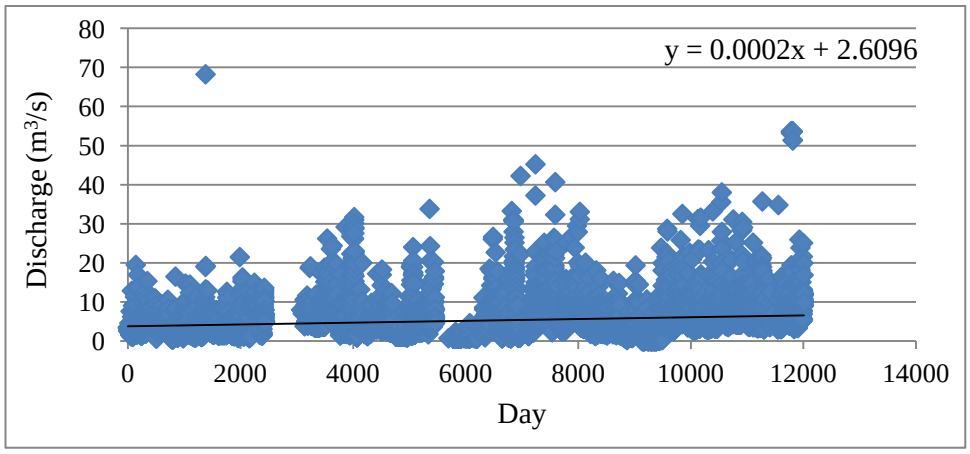


The correlation of daily discharge data between Sulaiman and, JLN. Tun Razak streamflow stations in Klang watershed

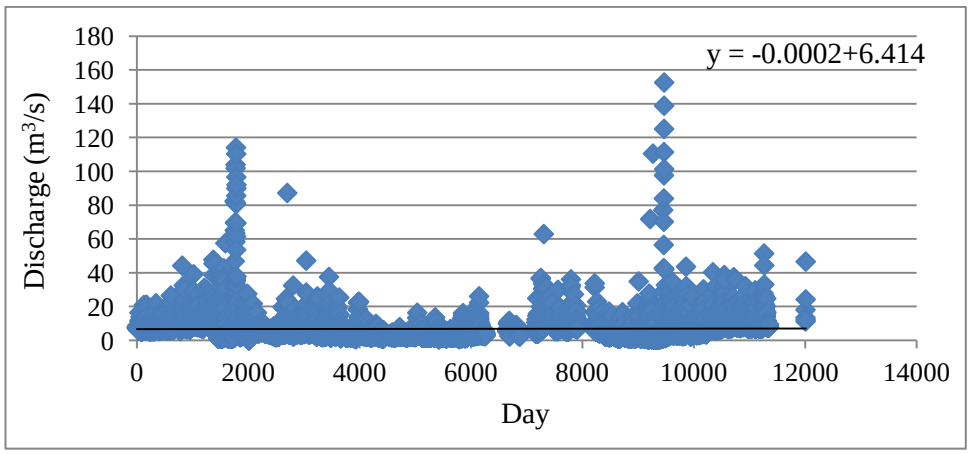


The correlation of daily discharge data between Sulaiman and Batu Sentul streamflow stations in Klang watershed

## Appendix E- Mean Monthly Rainfall for All the Raingauge Stations

Station no. 3014084

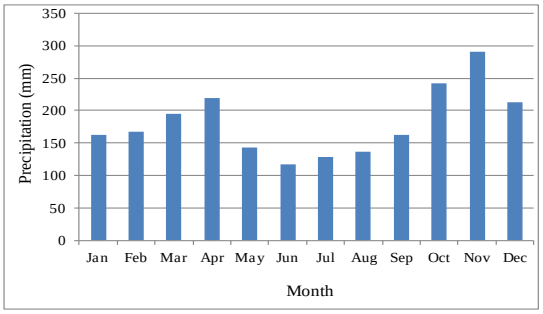


Station no. 3014089

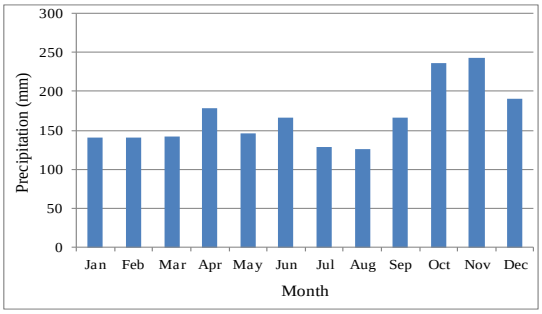


Station no.3018107

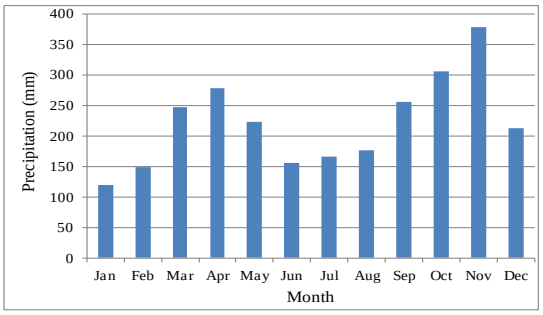


Station no. 3115079

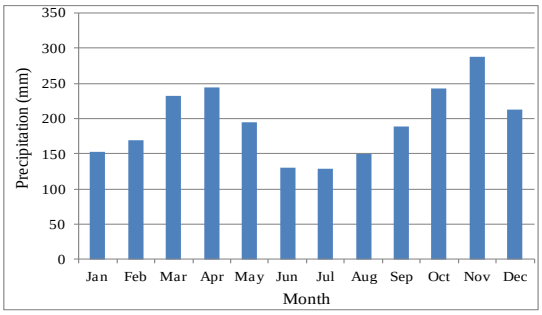


Station no. 3116005

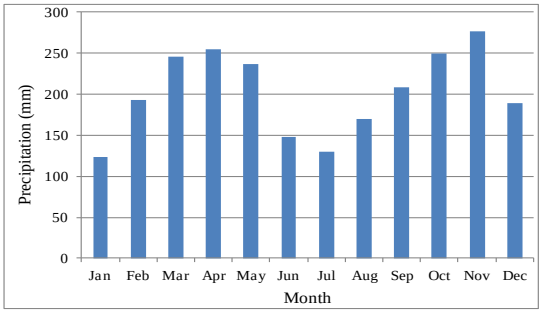


Station no. 3116006

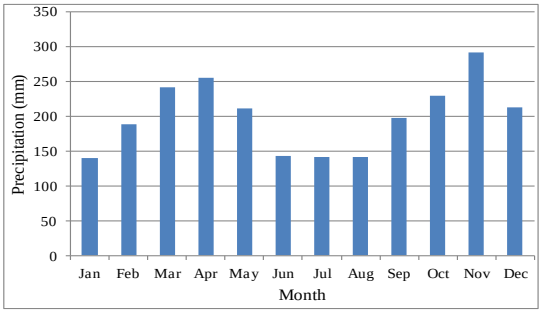


Station no. 3117071

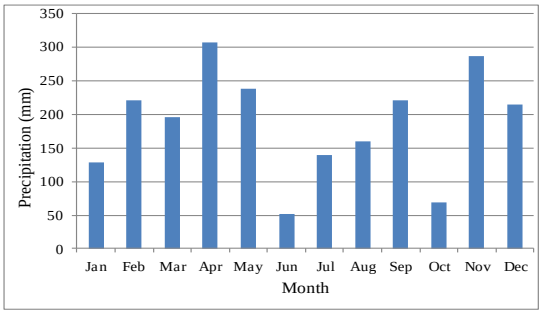


Station no. 3118069

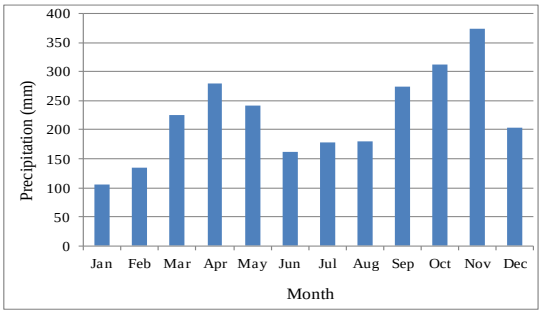

Station no. 3118102

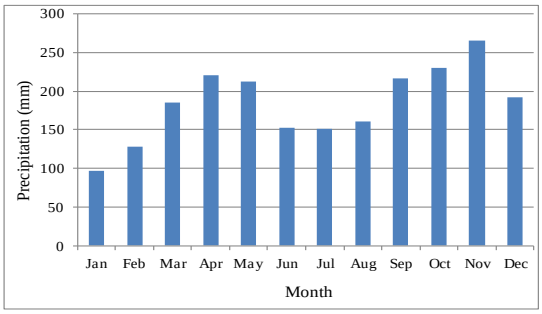


Station no. 3119001

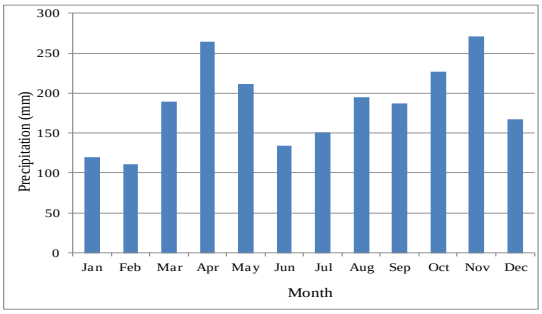


Station no. 3216001

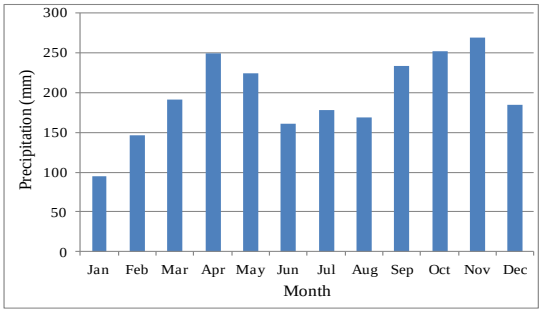


Station no.3216004

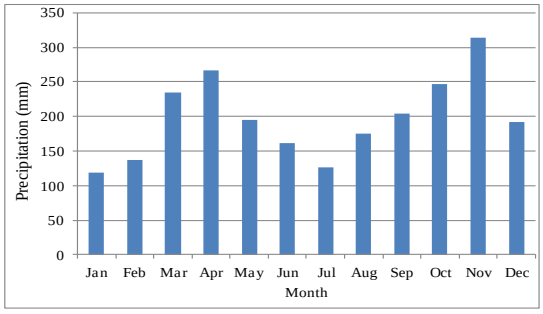


Station no. 3217001

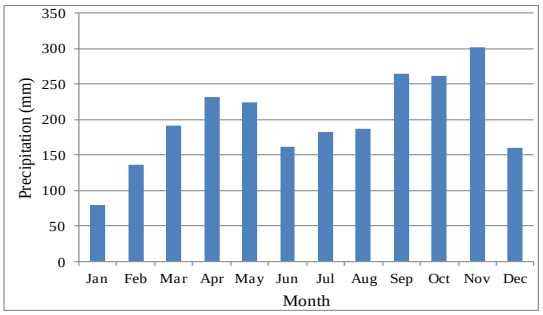


Station no.3217002

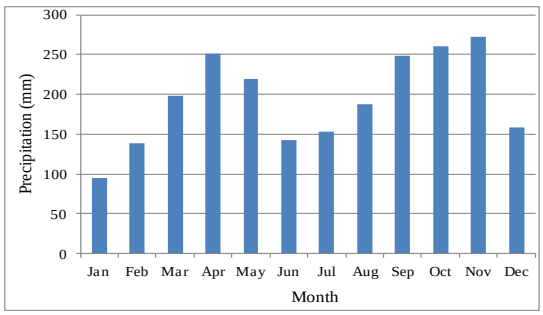


Station no.3217003

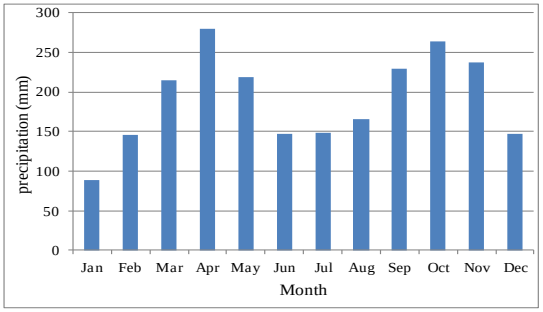


Station no.3217004

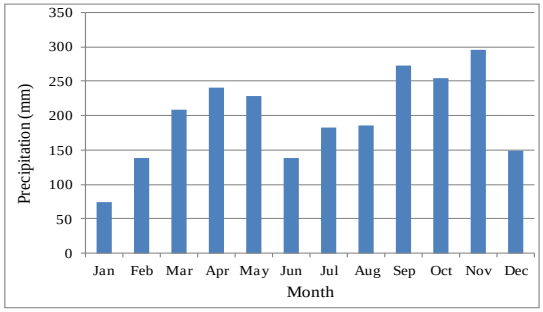

Station no. 3217005

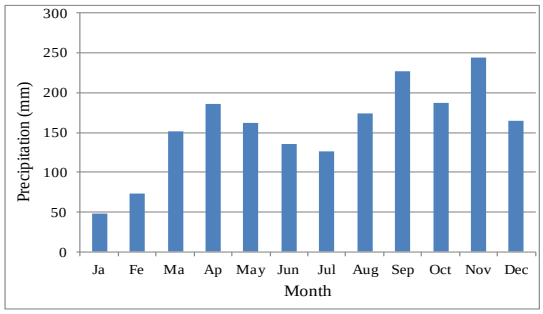


Station no.3218101

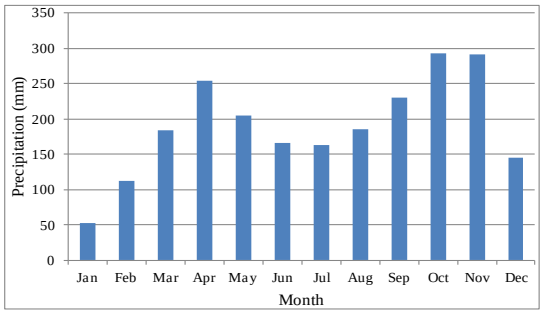


Station no. 3317001

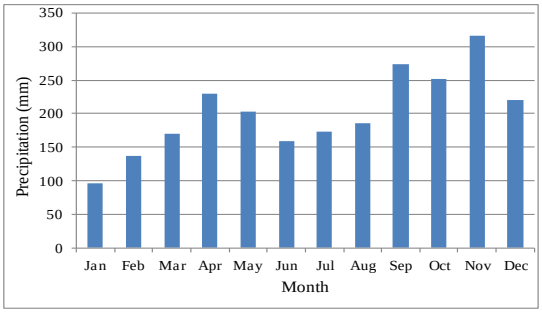

## Appendix F- Mean Monthly River Discharge

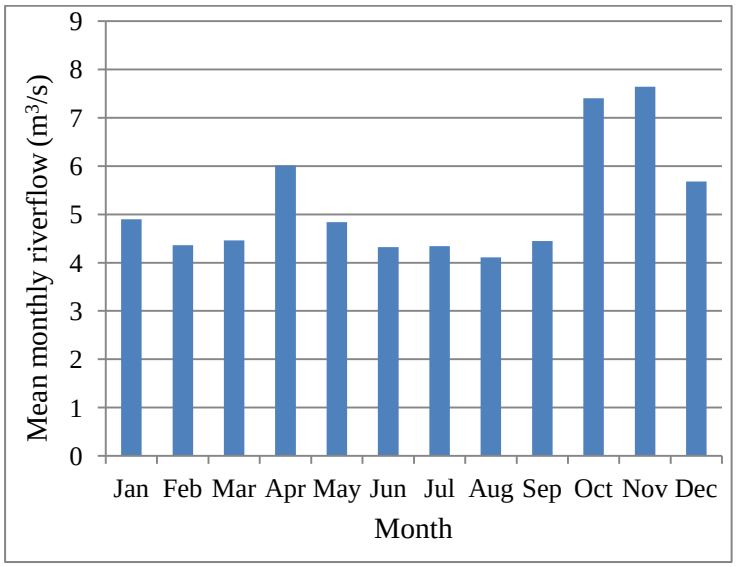


| Month | Mean ($m^3/s$) | Percent |
|---|---|---|
| Jan | 4.90 | 7.84 |
| Feb | 4.36 | 6.97 |
| Mar | 4.46 | 7.13 |
| Apr | 6.01 | 9.62 |
| May | 4.84 | 7.74 |
| Jun | 4.32 | 6.91 |
| Jul | 4.34 | 6.94 |
| Aug | 4.11 | 6.58 |
| Sep | 4.45 | 7.12 |
| Oct | 7.40 | 11.85 |
| Nov | 7.64 | 12.22 |
| Dec | 5.68 | 9.08 |

Mean monthly flow of River at Tun Razak streamflow station

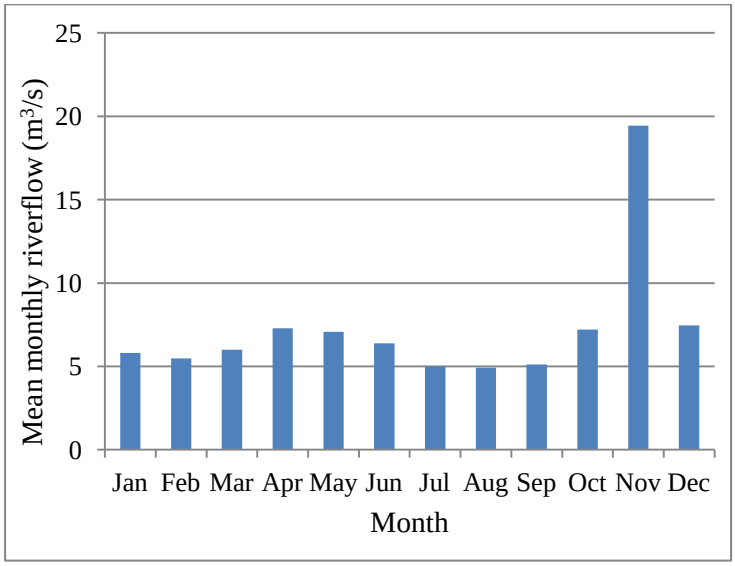


| Month | Mean ($m^3/s$) | Percent |
|---|---|---|
| Jan | 5.80 | 6.66 |
| Feb | 5.47 | 6.27 |
| Mar | 6.00 | 6.89 |
| Apr | 7.29 | 8.36 |
| May | 7.08 | 8.12 |
| Jun | 6.38 | 7.32 |
| Jul | 5.00 | 5.74 |
| Aug | 4.92 | 5.65 |
| Sep | 5.12 | 5.88 |
| Oct | 7.20 | 8.26 |
| Nov | 19.44 | 22.31 |
| Dec | 7.46 | 8.56 |

Mean monthly flow of River at Batu Sentul streamflow station

**Appendix G- Annual River Discharge Analysis: Mean Annual Flow and Anomaly of Mean at Discharge Stations**

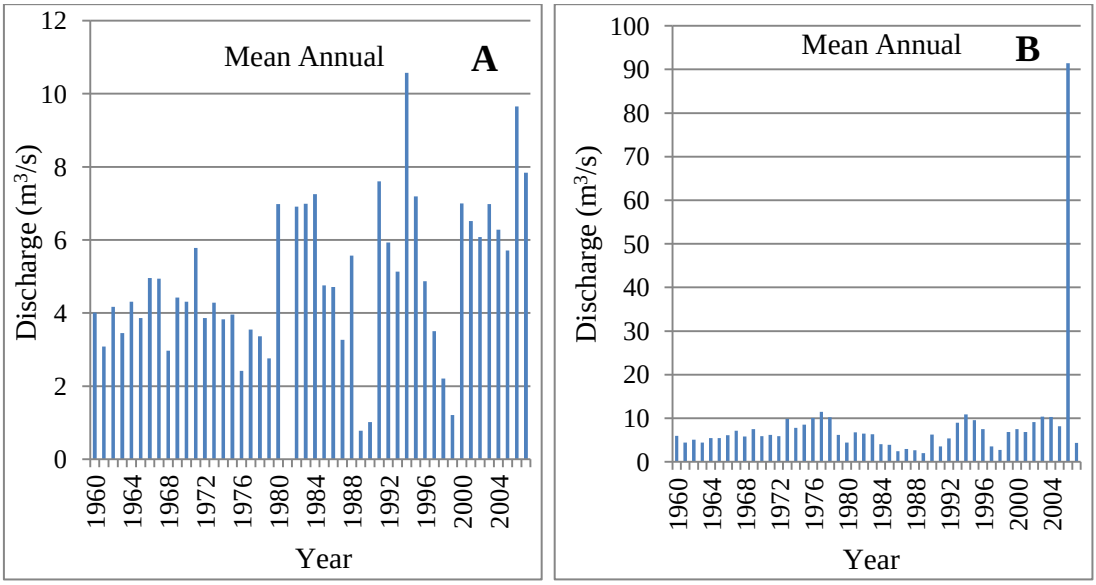


Mean annual flow of River Klang at Tun Razak **(A)** and Batu Sentul **(B)** streamflow station

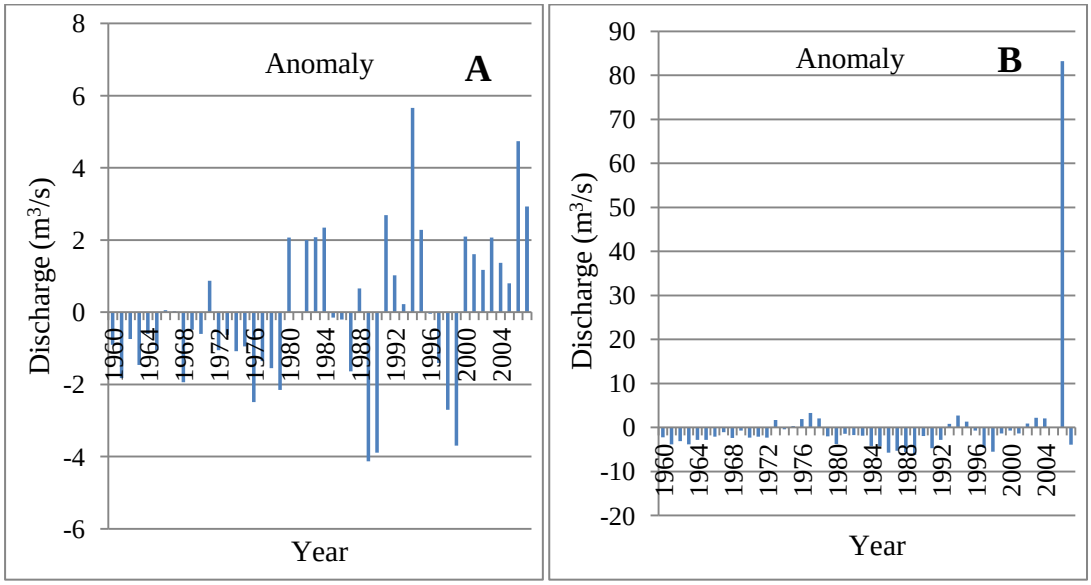


Annual variability of mean annual discharge of River Klang at Tun Razak **(A)** and Batu Sentul **(B)** streamflow station

## Appendix H- Flood Frequency Curve at Discharge Stations

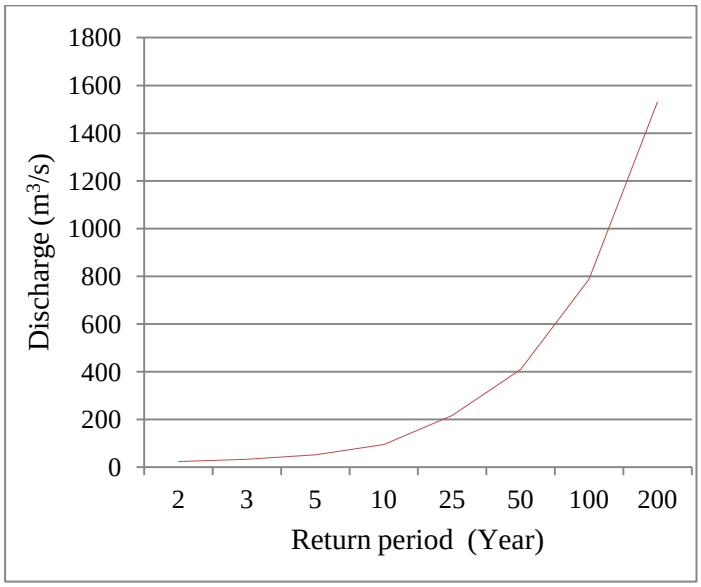


| Return period (Year) | Prediction ($m^3/s$) | Standard Deviation |
|---|---|---|
| 200 | 1530.6 | 3267.9 |
| 100 | 786.8 | 1099.2 |
| 50 | 419.7 | 371.1 |
| 25 | 216.1 | 123.9 |
| 10 | 94.7 | 30.9 |
| 5 | 51.5 | 13.8 |

The Flood frequency curve of Tun Razak streamflow station using log-Pearson type III using average daily maximum streamflow data

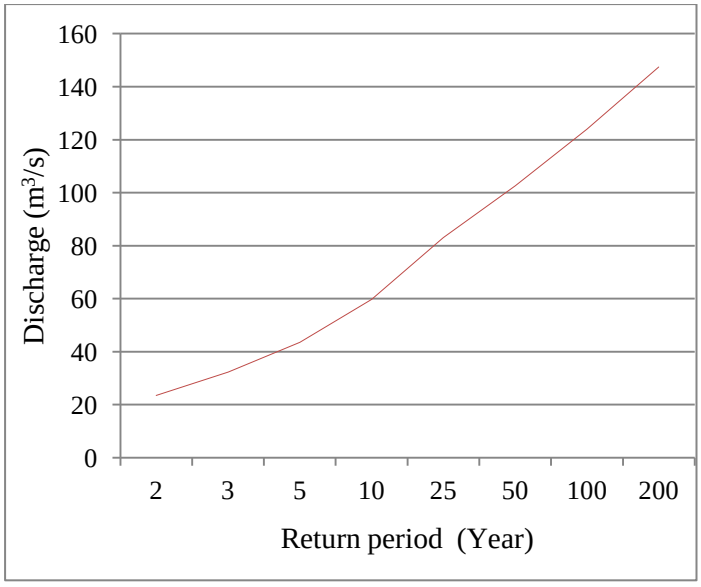


| Return period (Year) | Prediction ($m^3/s$) | Standard Deviation |
|---|---|---|
| 200 | 147.4 | 88.0 |
| 100 | 124.0 | 55.5 |
| 50 | 103.6 | 31.4 |
| 25 | 83.0 | 16.7 |
| 10 | 59.7 | 13.4 |
| 5 | 43.6 | 13.6 |

The Flood frequency curve of Batu Sentul streamflow station using log-Pearson type III using average daily maximum streamflow data

## Appendix I- Flow Duration Curves at Discharge Stations

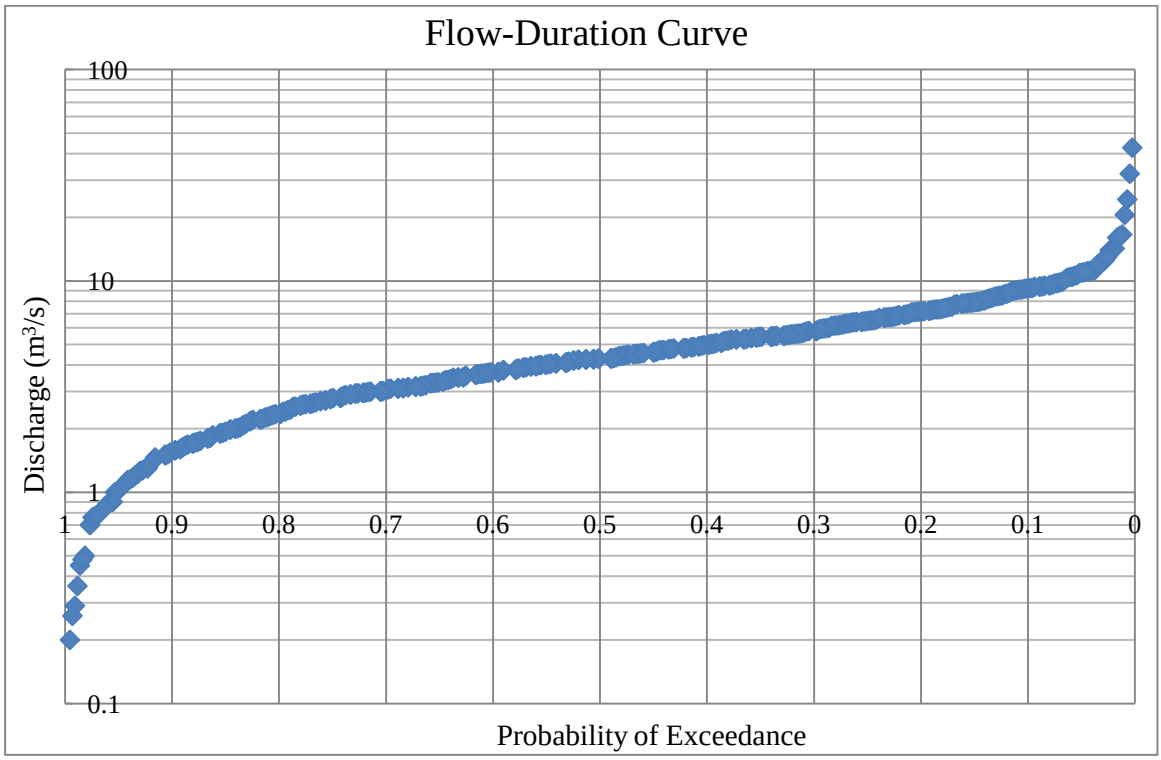


Flow duration curve at Tun Razak streamflow station

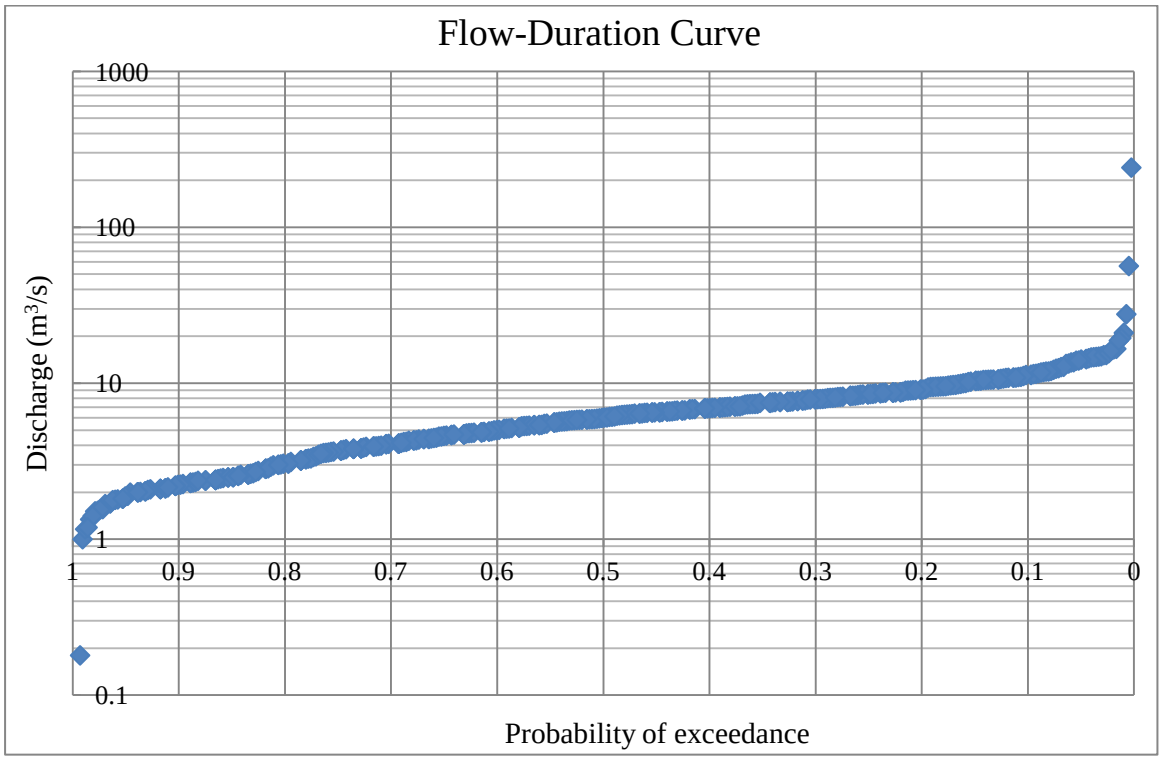


Flow duration curve at Batu Sentul streamflow station

## Appendix J- Exploratory Data Analysis at All the Raingauge Stations Used for Downscaling

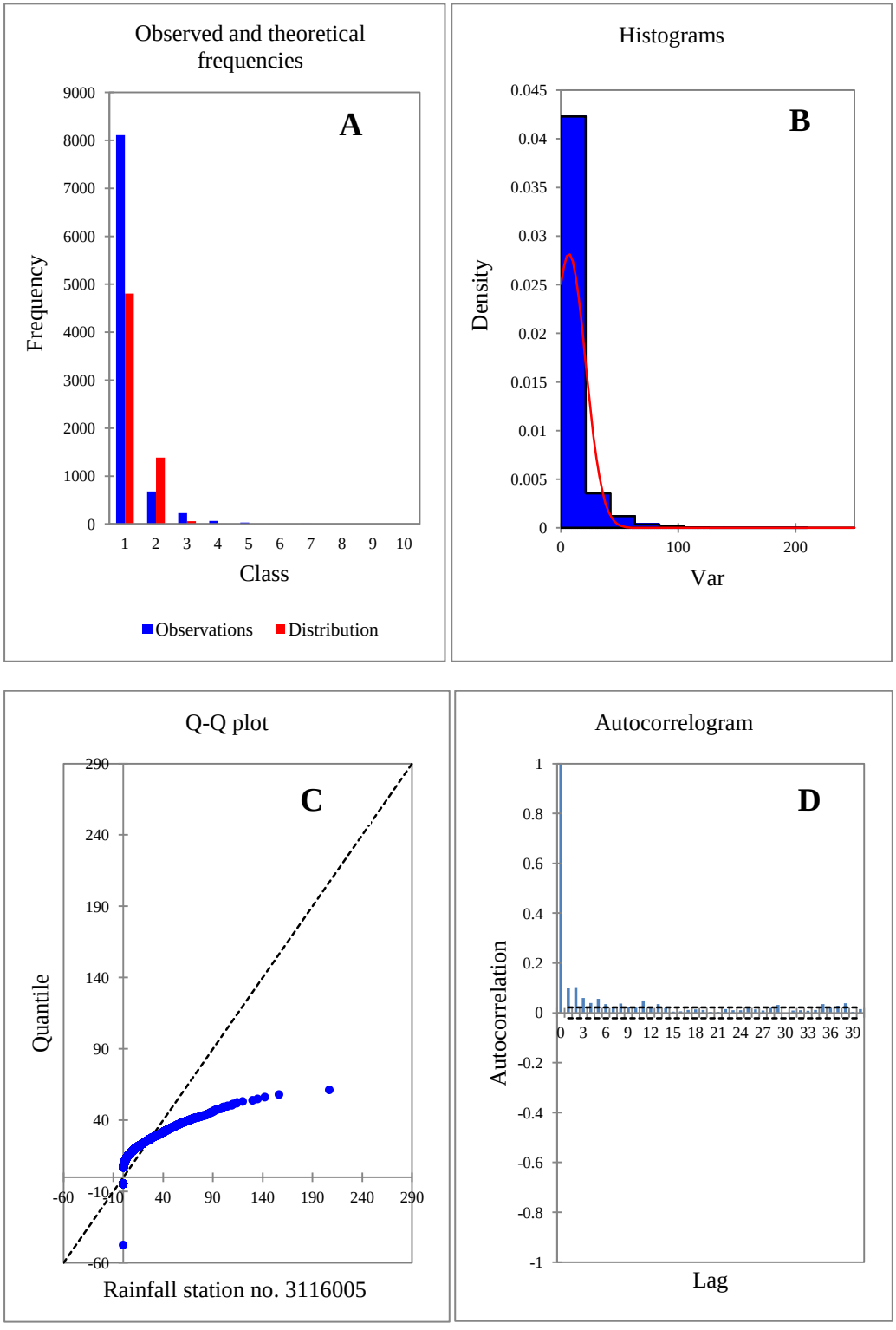


The exploratory analysis plots (A: frequency, B: density, C: Q-Q and D: ACF plot) of observed daily precipitation, at station no.3116005

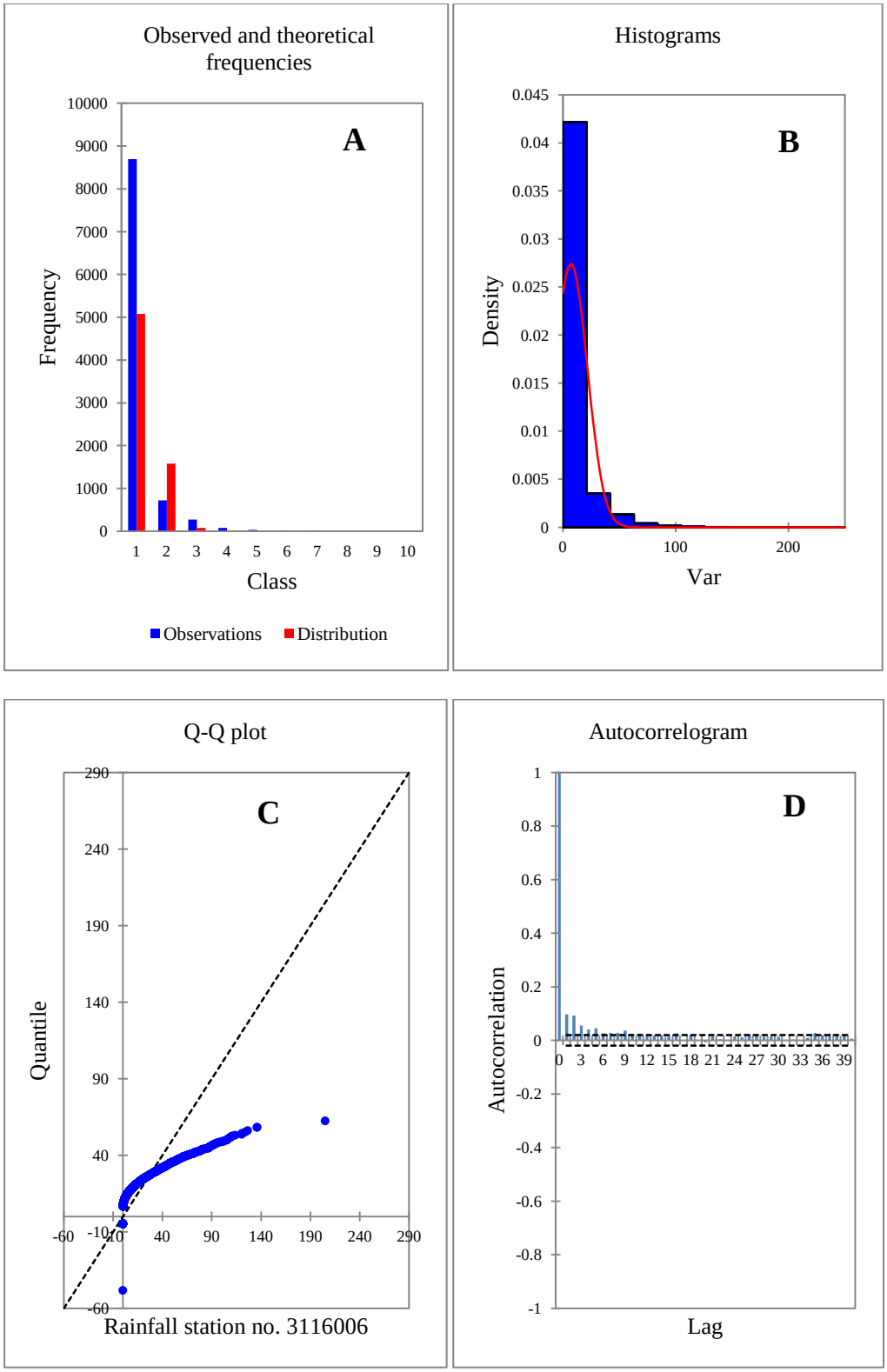


The exploratory analysis plots (A: frequency, B: density, C: Q-Q and D: ACF plot) of observed daily precipitation, at station no. 3116006

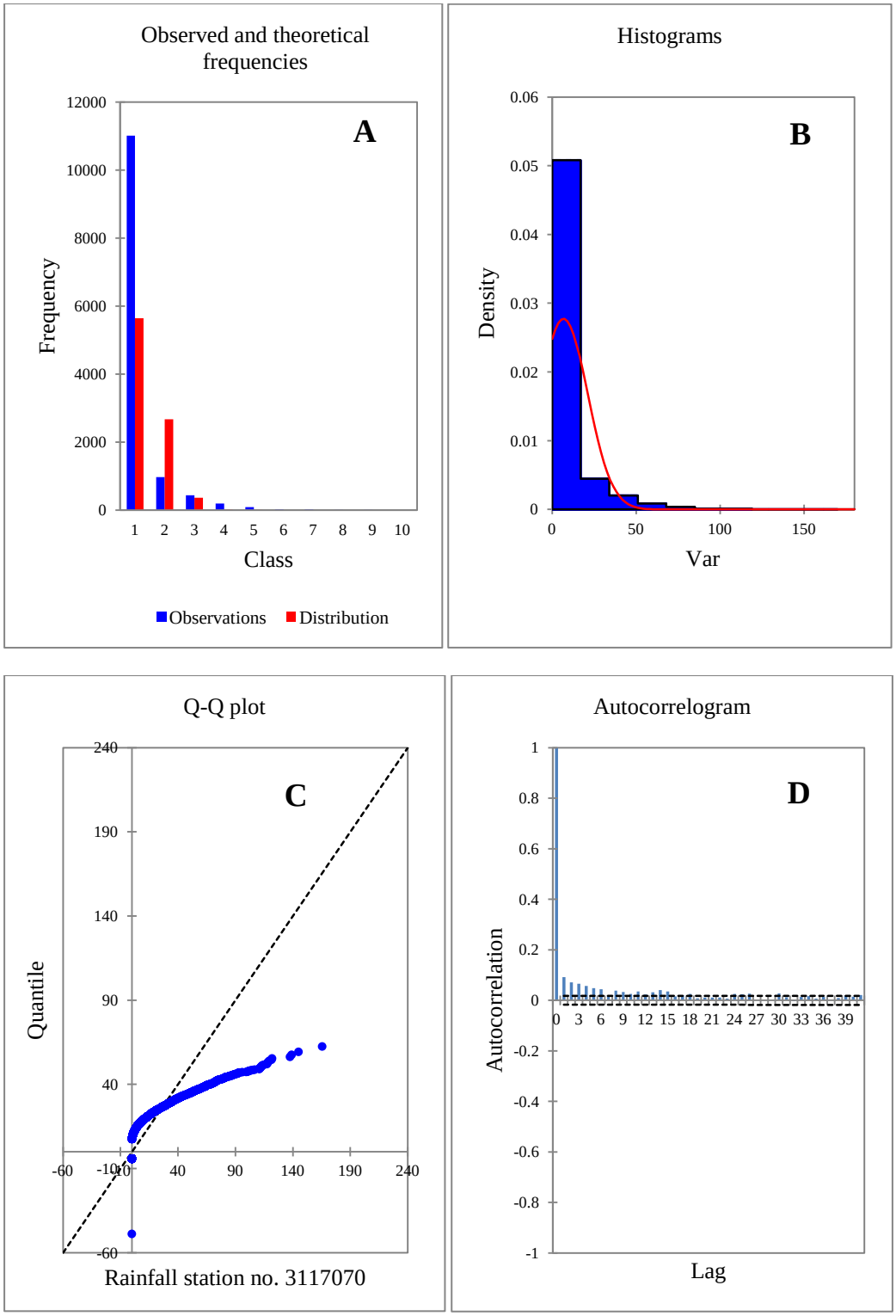


The exploratory analysis plots (A: frequency, B: density, C: Q-Q and D: ACF plot) of observed daily precipitation, at station no. 3117070

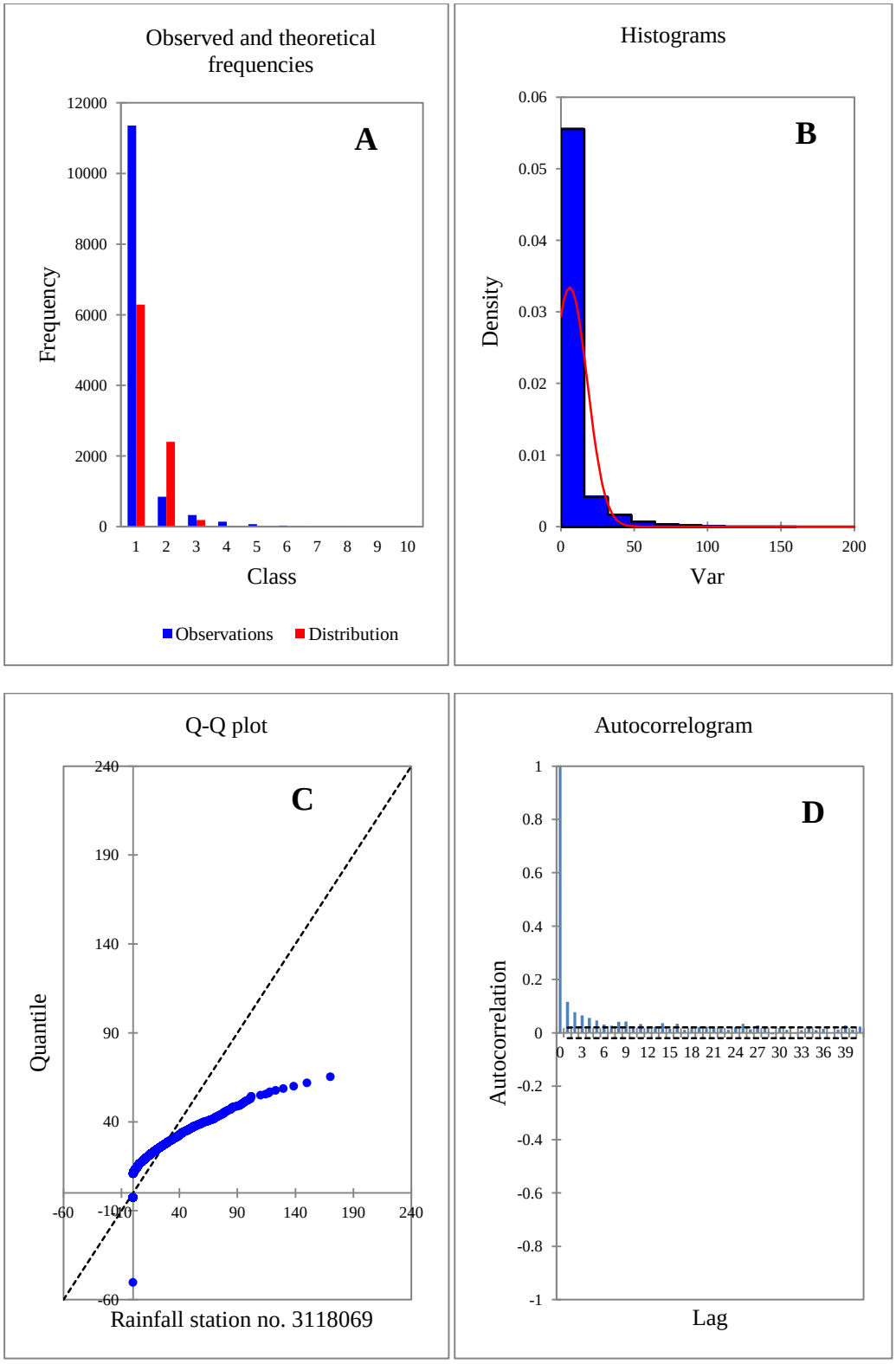


The exploratory analysis plots (A: frequency, B: density, C: Q-Q and D: ACF plot) of observed daily precipitation, at station no. 3118069

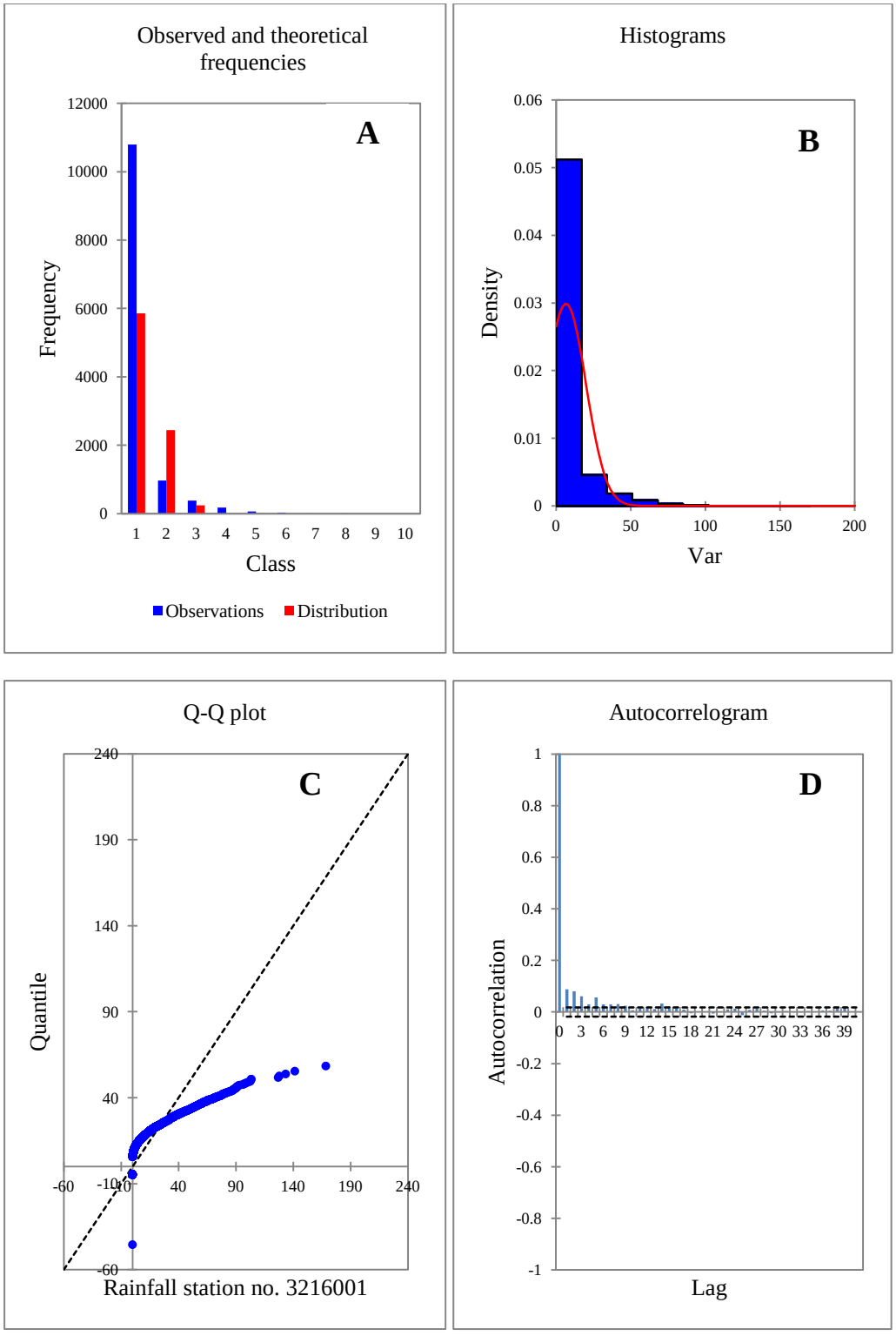


The exploratory analysis plots (A: frequency, B: density, C: Q-Q and D: ACF plot) of observed daily precipitation, at station no. 3216001

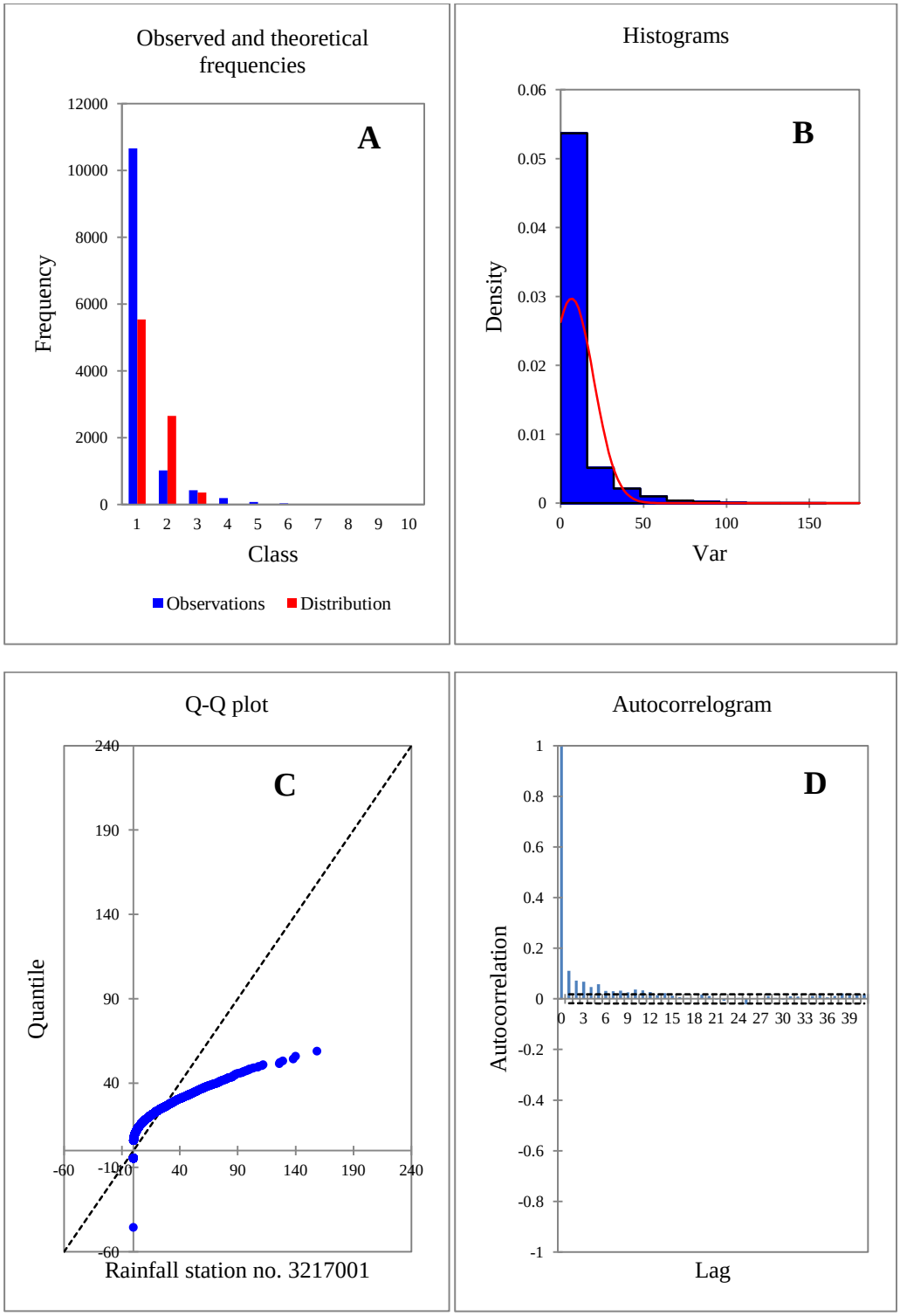


The exploratory analysis plots (A: frequency, B: density, C: Q-Q and D: ACF plot) of observed daily precipitation, at station no. 3217001

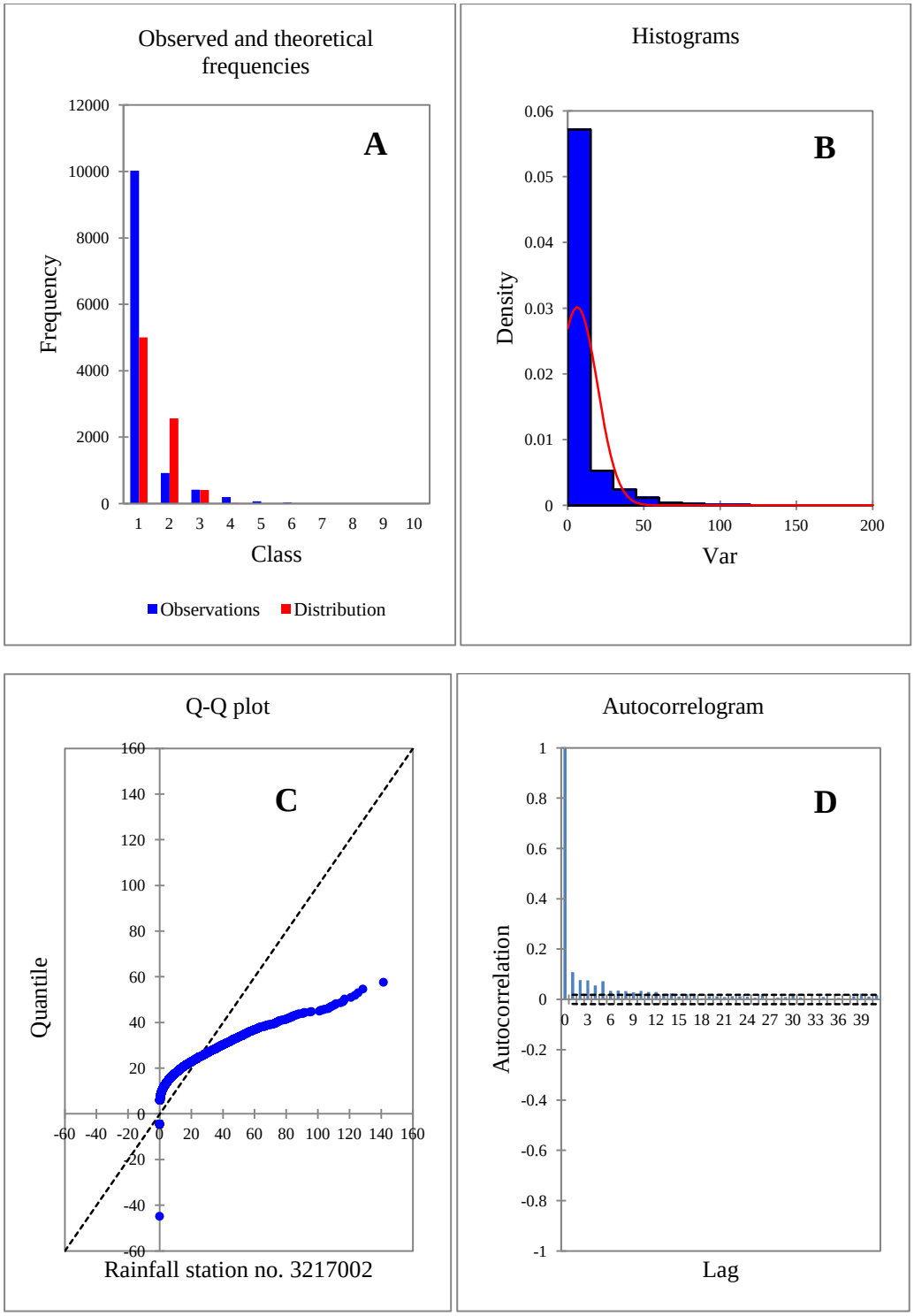


The exploratory analysis plots (A: frequency, B: density, C: Q-Q and D: ACF plot) of observed daily precipitation, at station no. 3217002

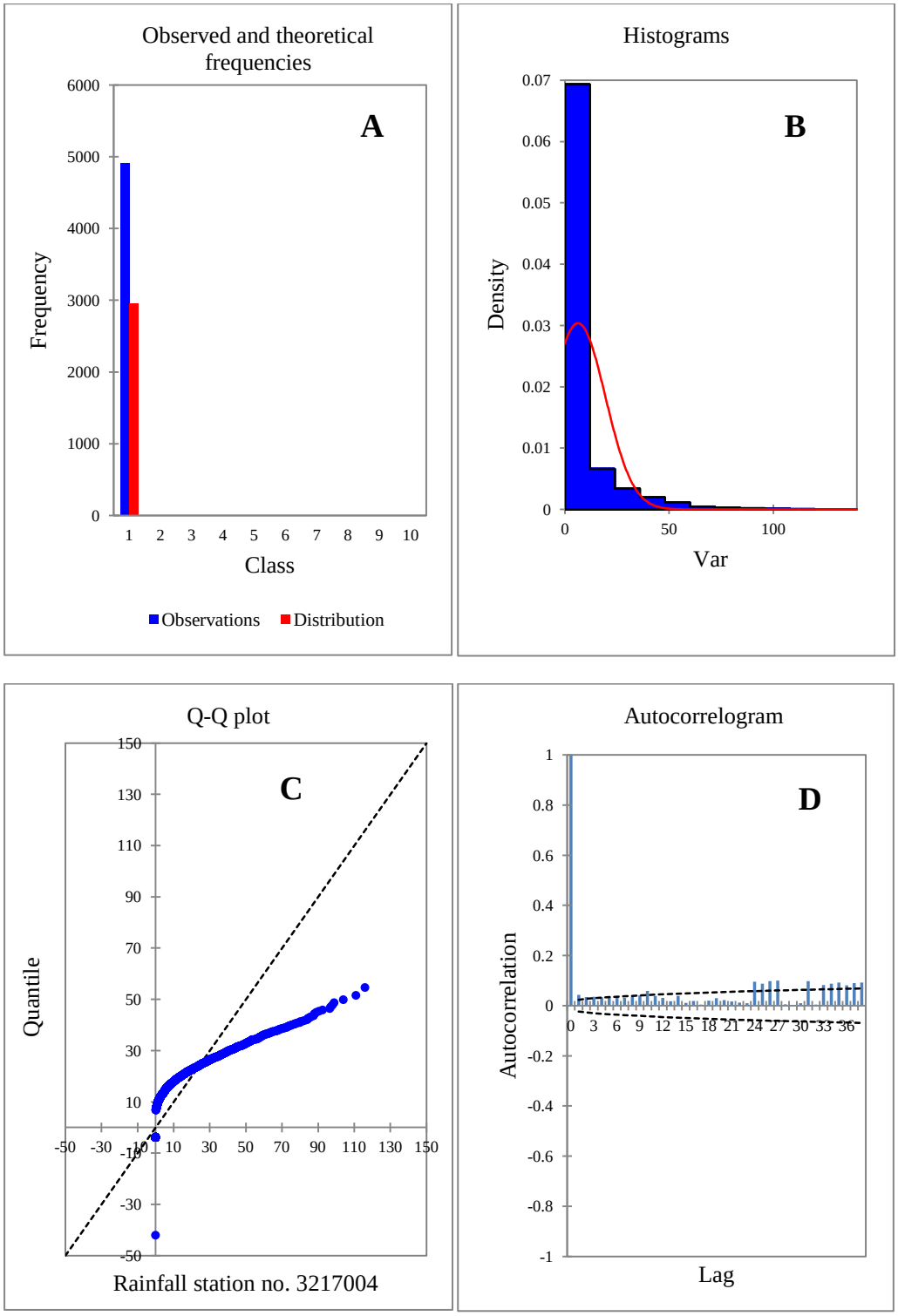


The exploratory analysis plots (A: frequency, B: density, C: Q-Q and D: ACF plot) of observed daily precipitation, at station no. 3217004

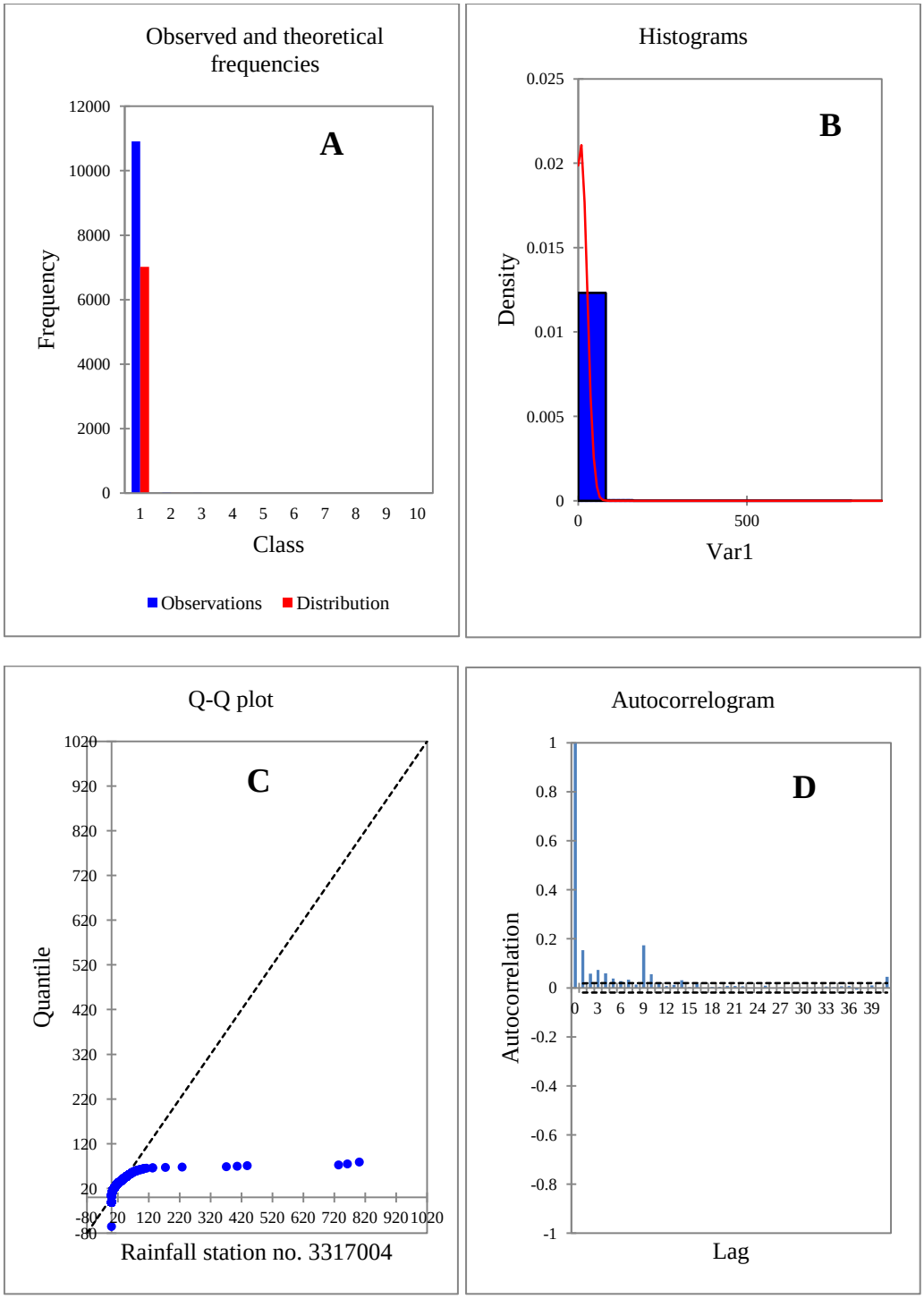


The exploratory analysis plots (A: frequency, B: density, C: Q-Q and D: ACF plot) of observed daily precipitation, at station no. 3317004

## Appendix K- Comparison between observed and calibrated of mean and variance precipitation (mm)

### A- Comparison between observed and calibrated of mean precipitation

Station no. 3116005

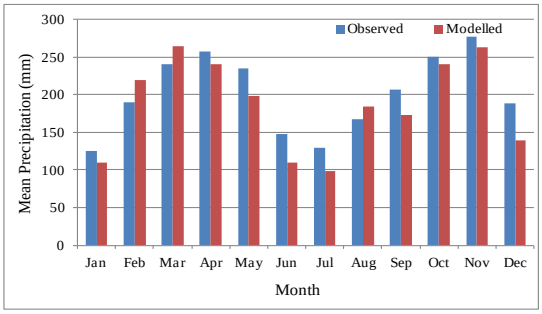


Station no. 3116006

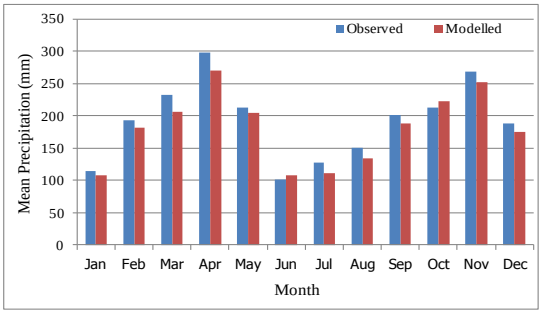


Station no. 3117070

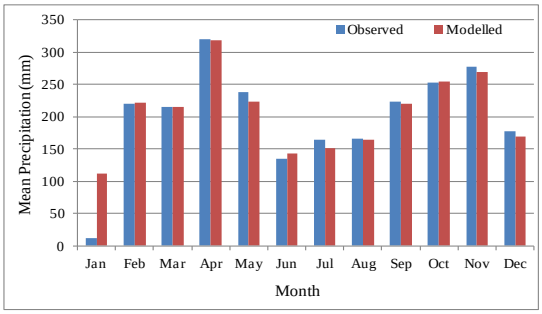


Station no. 3118069

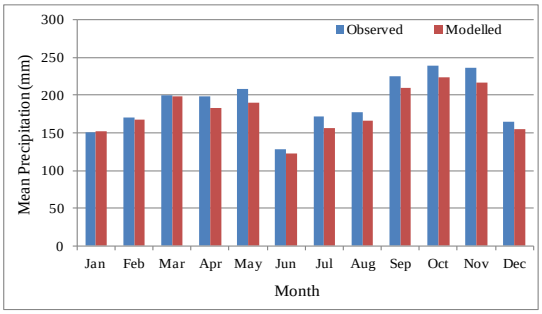


Station no. 3216001

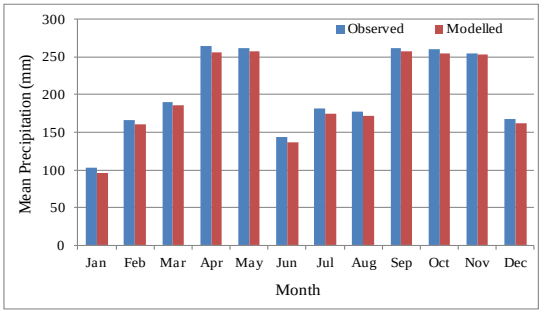


Station no. 3217001

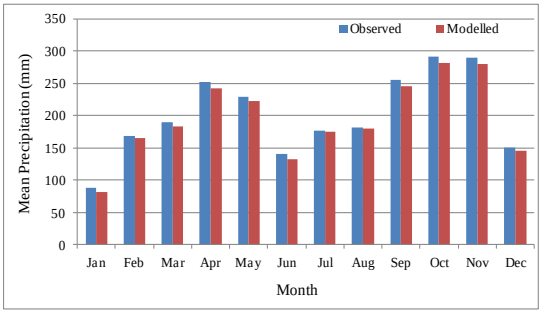


Station no. 3217002

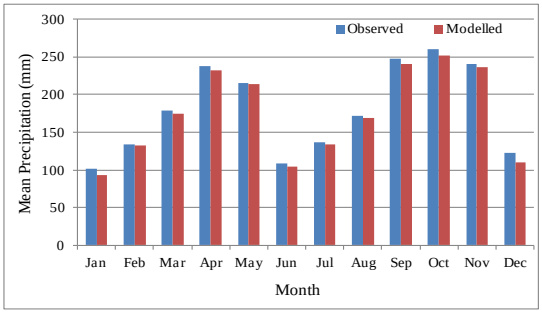


Station no. 3217004

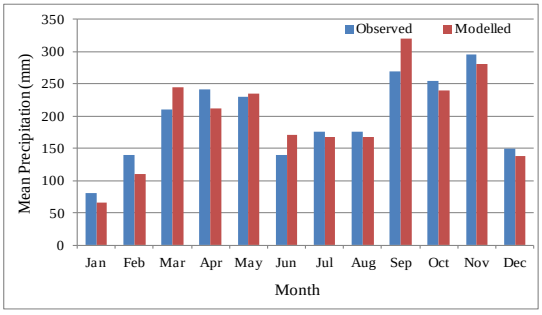

Station no. 3317004

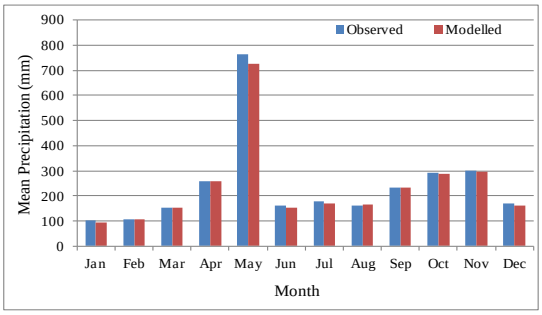


## B- Comparison between observed and calibrated of variance precipitation

Station no. 3116005

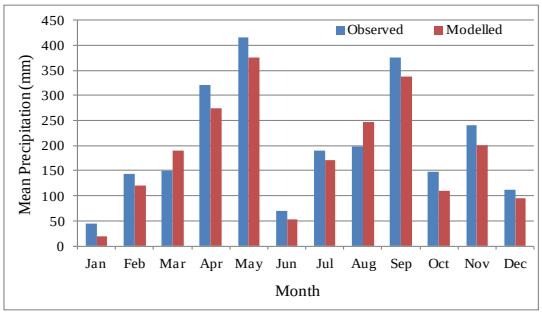


Station no. 3116006

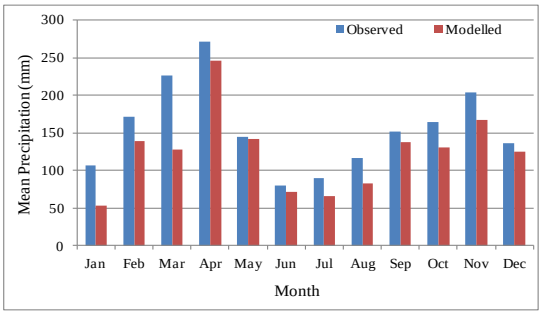


Station no. 3117070

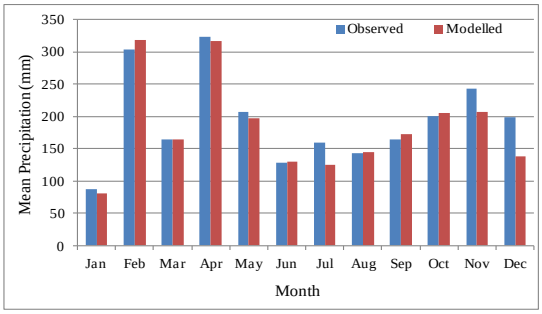


Station no. 3118069

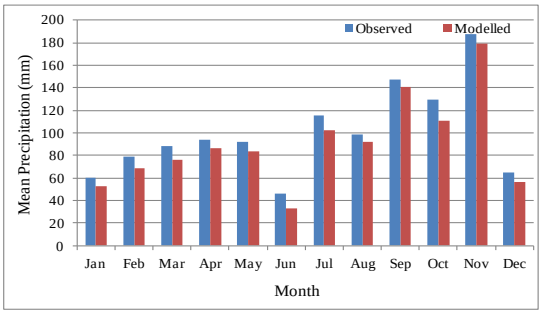


Station no. 3216001

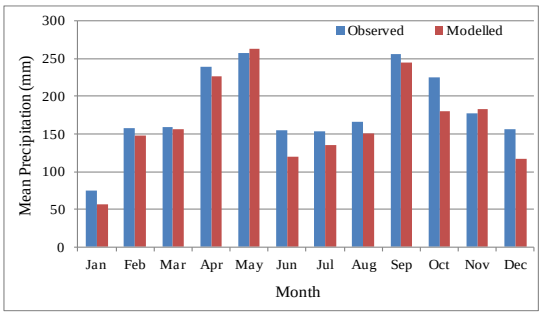


Station no. 3217001

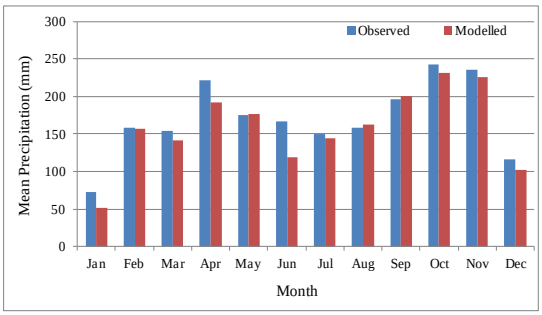

Station no. 3217002

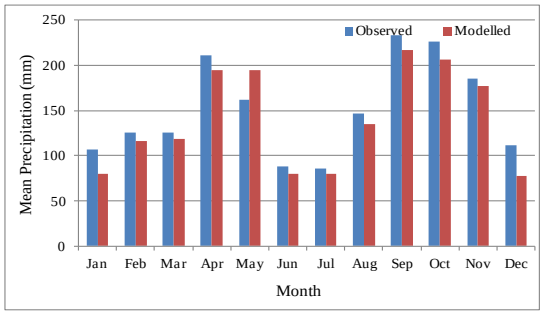


Station no. 3217004

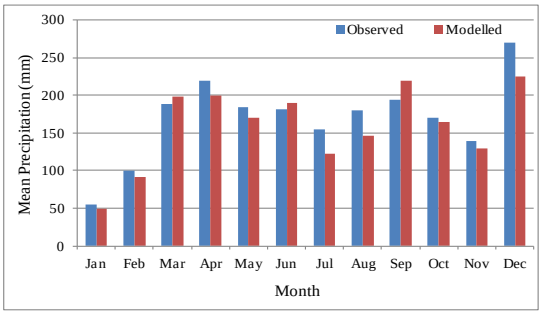


Station no.3317004

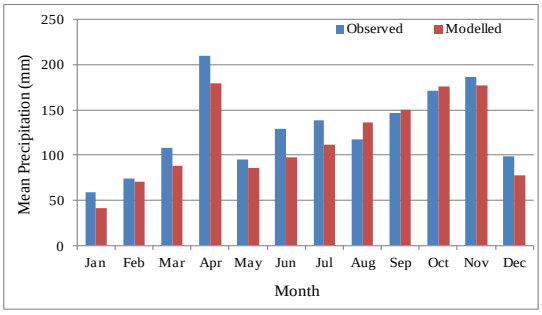

## Appendix L- SDSM Output: Summary of Statistics for Observed and Validated Data

### A- Summary of statistics for observed precipitation at rainfall gauge stations

3116005 (Observed)

| Month | Mean (mm) | Maximum (mm) | Variance (mm) | Dry-Spell (day) | Wet-Spell (day) | Standard dev. Wet-Spell | Standard dev. Dry-Spell |
|---|---|---|---|---|---|---|---|
| January | 4.10 | 64.20 | 39.06 | 1.35 | 2.09 | 1.38 | 1.20 |
| February | 6.42 | 68.30 | 138.42 | 2.04 | 1.82 | 1.08 | 1.97 |
| March | 8.18 | 72.30 | 145.73 | 0.95 | 2.54 | 1.85 | 0.89 |
| April | 8.51 | 95.48 | 315.22 | 0.67 | 3.23 | 2.58 | 0.51 |
| May | 7.92 | 79.40 | 412.79 | 0.66 | 3.46 | 2.75 | 0.56 |
| June | 4.94 | 62.54 | 72.85 | 0.98 | 2.37 | 1.64 | 0.81 |
| July | 4.32 | 61.46 | 189.52 | 0.96 | 2.38 | 1.61 | 0.84 |
| August | 5.65 | 87.23 | 196.27 | 1.80 | 1.88 | 1.15 | 1.73 |
| September | 6.94 | 95.94 | 373.01 | 0.60 | 3.37 | 2.66 | 0.40 |
| October | 8.34 | 98.50 | 142.82 | 0.46 | 4.38 | 3.59 | 0.24 |
| November | 9.24 | 97.40 | 232.46 | 0.36 | 6.40 | 5.48 | 0.09 |
| December | 6.29 | 73.40 | 106.00 | 0.78 | 2.88 | 2.06 | 0.63 |

Station no. 3116006 (Observed)

| Month | Mean (mm) | Maximum (mm) | Variance (mm) | Dry-Spell (day) | Wet-Spell (day) | Standard dev. Wet-Spell | Standard dev. Dry-Spell |
|---|---|---|---|---|---|---|---|
| January | 11.91 | 136.00 | 312.92 | 2.92 | 2.53 | 2.27 | 2.56 |
| February | 10.91 | 87.00 | 202.81 | 2.33 | 2.86 | 3.94 | 1.67 |
| March | 16.29 | 113.80 | 387.90 | 2.18 | 2.68 | 2.73 | 1.50 |
| April | 14.40 | 124.00 | 393.98 | 2.09 | 3.41 | 3.44 | 1.90 |
| May | 15.39 | 205.00 | 508.39 | 2.55 | 2.94 | 3.65 | 2.20 |
| June | 12.50 | 90.50 | 277.79 | 2.47 | 1.93 | 1.30 | 2.38 |
| July | 11.66 | 81.00 | 233.51 | 2.92 | 1.93 | 1.26 | 2.99 |
| August | 11.75 | 82.50 | 267.34 | 2.42 | 2.39 | 2.28 | 2.03 |
| September | 13.83 | 87.50 | 239.01 | 2.57 | 2.88 | 2.93 | 2.31 |
| October | 12.98 | 87.50 | 280.87 | 1.90 | 3.63 | 3.91 | 1.54 |
| November | 14.91 | 89.50 | 299.26 | 1.71 | 4.64 | 5.02 | 1.20 |
| December | 13.37 | 120.50 | 304.14 | 2.47 | 3.98 | 3.48 | 2.13 |

Station no. 3117070 (Observed)

| Month | Mean (mm) | Maximum (mm) | Variance (mm) | Dry-Spell (day) | Wet-Spell (day) | Standard dev. Wet-Spell | Standard dev. Dry-Spell |
|---|---|---|---|---|---|---|---|
| January | 10.05 | 63.50 | 170.96 | 3.69 | 1.93 | 1.17 | 4.90 |
| February | 15.80 | 86.50 | 358.49 | 3.25 | 2.09 | 1.38 | 2.95 |
| March | 13.48 | 60.00 | 204.12 | 2.77 | 2.47 | 1.98 | 2.76 |
| April | 15.34 | 117.50 | 343.37 | 2.05 | 3.11 | 2.43 | 1.39 |
| May | 14.49 | 121.50 | 371.72 | 2.65 | 2.37 | 1.59 | 2.30 |
| June | 12.83 | 82.00 | 268.30 | 3.09 | 1.72 | 1.14 | 3.43 |
| July | 12.59 | 93.00 | 347.67 | 3.52 | 1.84 | 1.23 | 3.23 |
| August | 12.53 | 78.00 | 263.36 | 2.89 | 2.47 | 1.99 | 3.31 |
| September | 12.87 | 78.50 | 216.87 | 2.80 | 2.80 | 2.51 | 2.38 |
| October | 14.99 | 87.00 | 298.57 | 2.20 | 2.75 | 2.34 | 1.90 |
| November | 11.74 | 111.00 | 223.49 | 2.34 | 3.18 | 2.77 | 1.89 |
| December | 12.68 | 102.00 | 271.75 | 3.14 | 2.89 | 2.32 | 2.77 |

Station no. 3118069 (Observed)

| Month | Mean (mm) | Maximum (mm) | Variance (mm) | Dry-Spell (day) | Wet-Spell (day) | Standard dev. Wet-Spell | Standard dev. Dry-Spell |
|---|---|---|---|---|---|---|---|
| January | 5.02 | 90.00 | 107.64 | 5.15 | 5.03 | 9.58 | 4.67 |
| February | 9.08 | 71.00 | 232.24 | 3.63 | 3.13 | 6.61 | 2.65 |
| March | 11.25 | 72.00 | 233.66 | 3.02 | 3.29 | 6.76 | 2.60 |
| April | 12.22 | 78.00 | 208.44 | 2.65 | 3.23 | 5.33 | 2.43 |
| May | 14.39 | 150.00 | 416.18 | 3.10 | 2.78 | 5.48 | 2.66 |
| June | 10.52 | 78.00 | 212.03 | 4.98 | 2.69 | 5.95 | 5.22 |
| July | 10.61 | 92.00 | 249.89 | 4.78 | 2.81 | 6.27 | 5.17 |
| August | 9.58 | 102.00 | 238.06 | 3.35 | 3.21 | 6.94 | 3.30 |
| September | 13.39 | 95.00 | 314.58 | 2.62 | 3.67 | 6.79 | 2.52 |
| October | 13.95 | 93.00 | 381.94 | 3.00 | 4.02 | 7.25 | 2.32 |
| November | 14.14 | 94.00 | 361.89 | 3.17 | 3.68 | 6.80 | 2.86 |
| December | 12.57 | 91.00 | 368.64 | 3.48 | 3.63 | 7.18 | 3.59 |

Station no. 3216001 (Observed)

| Month | Mean (mm) | Maximum (mm) | Variance (mm) | Dry-Spell (day) | Wet-Spell (day) | Standard dev. Wet-Spell | Standard dev. Dry-Spell |
|---|---|---|---|---|---|---|---|
| January | 8.02 | 87.50 | 170.15 | 3.55 | 2.09 | 1.73 | 3.08 |
| February | 12.28 | 71.30 | 261.48 | 2.98 | 2.19 | 1.72 | 2.42 |
| March | 12.96 | 78.50 | 265.47 | 2.75 | 2.38 | 1.86 | 2.70 |
| April | 13.51 | 82.00 | 266.25 | 1.88 | 2.51 | 1.77 | 1.44 |
| May | 12.35 | 79.00 | 215.96 | 2.13 | 2.32 | 1.90 | 1.98 |
| June | 15.20 | 128.00 | 374.17 | 2.90 | 2.30 | 1.68 | 3.44 |
| July | 13.62 | 99.10 | 275.59 | 2.88 | 2.24 | 1.53 | 2.73 |
| August | 14.05 | 93.50 | 288.30 | 2.42 | 2.52 | 1.94 | 1.88 |
| September | 14.91 | 73.80 | 218.61 | 2.64 | 3.00 | 2.76 | 3.04 |
| October | 12.53 | 76.00 | 185.07 | 2.16 | 3.52 | 2.66 | 2.25 |
| November | 12.79 | 91.00 | 242.90 | 2.23 | 3.75 | 3.50 | 2.69 |
| December | 11.33 | 141.50 | 376.33 | 2.53 | 3.52 | 4.08 | 2.35 |

Station no. 3217001 (Observed)

| Month | Mean (mm) | Maximum (mm) | Variance (mm) | Dry-Spell (day) | Wet-Spell (day) | Standard dev. Wet-Spell | Standard dev. Dry-Spell |
|---|---|---|---|---|---|---|---|
| January | 7.41 | 63.00 | 116.47 | 4.05 | 2.04 | 1.41 | 3.87 |
| February | 10.91 | 86.00 | 229.57 | 3.21 | 2.38 | 1.97 | 2.61 |
| March | 13.73 | 75.50 | 294.95 | 2.83 | 3.00 | 2.59 | 2.56 |
| April | 13.20 | 138.00 | 307.40 | 1.91 | 2.83 | 1.99 | 1.39 |
| May | 13.75 | 107.50 | 337.34 | 2.22 | 2.70 | 2.23 | 1.64 |
| June | 14.55 | 158.50 | 415.68 | 2.64 | 2.37 | 2.38 | 2.67 |
| July | 12.51 | 102.50 | 354.67 | 2.66 | 2.55 | 2.10 | 2.37 |
| August | 13.81 | 93.50 | 293.61 | 2.04 | 2.51 | 1.99 | 2.10 |
| September | 15.74 | 87.00 | 249.76 | 2.01 | 2.47 | 1.93 | 1.57 |
| October | 12.38 | 91.50 | 183.99 | 2.29 | 3.71 | 2.74 | 2.23 |
| November | 11.83 | 108.00 | 243.92 | 1.65 | 3.03 | 3.46 | 1.26 |
| December | 9.93 | 100.00 | 199.18 | 2.63 | 3.15 | 3.10 | 2.67 |

Station no. 3217002 (Observed)

| Month | Mean (mm) | Maximum (mm) | Variance (mm) | Dry-Spell (day) | Wet-Spell (day) | Standard dev. Wet-Spell | Standard dev. Dry-Spell |
|---|---|---|---|---|---|---|---|
| January | 7.60 | 75.00 | 156.75 | 3.92 | 2.00 | 1.61 | 3.52 |
| February | 12.29 | 91.00 | 337.60 | 3.39 | 2.33 | 1.72 | 4.11 |
| March | 13.88 | 80.00 | 260.24 | 2.97 | 2.67 | 2.32 | 3.62 |
| April | 13.09 | 110.00 | 297.51 | 2.01 | 2.63 | 1.77 | 1.82 |
| May | 13.02 | 73.50 | 258.72 | 2.23 | 3.00 | 2.72 | 2.01 |
| June | 12.08 | 103.50 | 253.73 | 2.62 | 2.26 | 1.68 | 2.84 |
| July | 9.81 | 57.50 | 183.54 | 3.12 | 2.06 | 1.53 | 4.09 |
| August | 12.74 | 95.00 | 261.65 | 2.56 | 2.87 | 3.11 | 2.36 |
| September | 12.85 | 125.50 | 308.75 | 2.16 | 2.98 | 2.63 | 1.44 |
| October | 10.73 | 87.00 | 261.52 | 2.04 | 4.09 | 4.16 | 1.36 |
| November | 13.44 | 101.00 | 269.85 | 1.66 | 3.19 | 3.00 | 1.09 |
| December | 10.14 | 90.30 | 185.89 | 2.76 | 3.43 | 3.13 | 2.80 |

Station no. 3217003 (Observed)

| Month | Mean (mm) | Maximum (mm) | Variance (mm) | Dry-Spell (day) | Wet-Spell (day) | Standard dev. Wet-Spell | Standard dev. Dry-Spell |
|---|---|---|---|---|---|---|---|
| January | 3.77 | 52.90 | 29.07 | 0.00 | 31.00 | 0.00 | 0.00 |
| February | 5.35 | 63.70 | 76.83 | 0.00 | 28.27 | 0.45 | 0.00 |
| March | 6.53 | 56.30 | 78.14 | 0.00 | 31.00 | 0.00 | 0.00 |
| April | 7.20 | 76.60 | 97.48 | 0.00 | 30.00 | 0.00 | 0.00 |
| May | 7.24 | 51.90 | 87.97 | 0.00 | 31.00 | 0.00 | 0.00 |
| June | 5.81 | 72.20 | 69.24 | 0.00 | 30.00 | 0.00 | 0.00 |
| July | 4.69 | 41.10 | 43.17 | 0.00 | 31.00 | 0.00 | 0.00 |
| August | 6.47 | 66.50 | 79.26 | 0.00 | 31.00 | 0.00 | 0.00 |
| September | 7.23 | 87.10 | 101.73 | 0.00 | 30.00 | 0.00 | 0.00 |
| October | 6.95 | 61.00 | 92.67 | 0.00 | 31.00 | 0.00 | 0.00 |
| November | 8.11 | 70.50 | 100.13 | 0.00 | 30.00 | 0.00 | 0.00 |
| December | 5.98 | 63.30 | 59.81 | 0.00 | 31.00 | 0.00 | 0.00 |

3217004 (Observed)

| Month | Mean (mm) | Maximum (mm) | Variance (mm) | Dry-Spell (day) | Wet-Spell (day) | Standard dev. Wet-Spell | Standard dev. Dry-Spell |
|---|---|---|---|---|---|---|---|
| **January** | 2.25 | 41.40 | 52.25 | 1.75 | 2.66 | 1.69 | 2.95 |
| **February** | 3.55 | 76.40 | 100.84 | 2.44 | 2.28 | 2.13 | 2.08 |
| **March** | 7.95 | 102.90 | 183.22 | 1.35 | 3.42 | 3.81 | 2.20 |
| **April** | 8.68 | 102.90 | 222.95 | 1.07 | 3.24 | 3.06 | 1.36 |
| **May** | 7.76 | 111.40 | 182.50 | 1.06 | 3.29 | 2.80 | 1.16 |
| **June** | 5.41 | 105.40 | 173.04 | 1.38 | 3.75 | 4.84 | 0.87 |
| **July** | 4.35 | 86.40 | 156.47 | 1.36 | 3.02 | 4.48 | 2.24 |
| **August** | 6.58 | 90.40 | 178.39 | 2.20 | 3.41 | 3.74 | 1.76 |
| **September** | 7.78 | 84.40 | 187.81 | 1.00 | 3.05 | 3.22 | 0.90 |
| **October** | 7.76 | 87.90 | 171.86 | 0.86 | 4.80 | 4.42 | 0.78 |
| **November** | 8.61 | 88.40 | 135.75 | 0.76 | 5.04 | 5.38 | 0.52 |
| **December** | 5.07 | 182.90 | 268.78 | 1.18 | 4.50 | 5.17 | 3.68 |

Station no. 3317004 (Observed)

| Month | Mean (mm) | Maximum (mm) | Variance (mm) | Dry-Spell (day) | Wet-Spell (day) | Standard dev. Wet-Spell | Standard dev. Dry-Spell |
|---|---|---|---|---|---|---|---|
| January | 5.66 | 33.00 | 53.65 | 3.12 | 2.86 | 1.89 | 3.15 |
| February | 8.19 | 68.00 | 103.34 | 2.54 | 2.48 | 2.33 | 2.28 |
| March | 12.09 | 94.50 | 185.02 | 2.68 | 3.62 | 4.01 | 2.40 |
| April | 11.53 | 94.50 | 226.15 | 1.98 | 3.44 | 3.26 | 1.56 |
| May | 10.60 | 103.00 | 184.60 | 1.78 | 3.49 | 3.00 | 1.36 |
| June | 9.61 | 97.00 | 175.64 | 1.84 | 3.95 | 5.04 | 1.07 |
| July | 9.20 | 78.00 | 157.77 | 2.75 | 3.22 | 4.68 | 2.44 |
| August | 11.17 | 82.00 | 179.79 | 2.03 | 3.61 | 3.94 | 1.96 |
| September | 10.54 | 76.00 | 189.61 | 1.63 | 3.25 | 3.42 | 1.10 |
| October | 11.47 | 79.50 | 173.76 | 1.65 | 5.00 | 4.62 | 0.98 |
| November | 10.68 | 80.00 | 137.85 | 1.43 | 5.24 | 5.58 | 0.72 |
| December | 9.82 | 174.50 | 269.98 | 3.05 | 4.70 | 5.37 | 3.88 |

## B- Summary of Statistics for Validated precipitation at rainfall gauge stations

3116005 (Validated)

| Month | Mean (mm) | Maximum (mm) | Variance (mm) | Dry-Spell (day) | Wet-Spell (day) | Standard dev. Wet-Spell | Standard dev. Dry-Spell |
|---|---|---|---|---|---|---|---|
| January | 4.41 | 65.00 | 30.00 | 1.55 | 1.29 | 0.88 | 1.10 |
| February | 4.97 | 77.00 | 124.02 | 2.24 | 1.02 | 0.58 | 1.87 |
| March | 8.26 | 82.00 | 193.00 | 1.15 | 1.74 | 1.35 | 0.79 |
| April | 8.02 | 100.88 | 283.00 | 0.87 | 2.43 | 2.08 | 0.41 |
| May | 8.88 | 87.00 | 383.00 | 0.86 | 2.66 | 2.25 | 0.46 |
| June | 5.90 | 74.74 | 58.45 | 1.18 | 1.57 | 1.14 | 0.71 |
| July | 5.15 | 71.66 | 175.12 | 1.16 | 1.58 | 1.11 | 0.74 |
| August | 6.89 | 96.93 | 250.00 | 2.00 | 1.08 | 0.65 | 1.63 |
| September | 7.11 | 101.34 | 339.00 | 0.80 | 2.57 | 2.16 | 0.30 |
| October | 8.97 | 108.00 | 116.00 | 0.66 | 3.58 | 3.09 | 0.14 |
| November | 9.94 | 112.00 | 205.00 | 0.56 | 5.60 | 4.98 | -0.01 |
| December | 6.76 | 81.00 | 95.00 | 0.98 | 2.08 | 1.56 | 0.53 |

Station no. 3116006 (Validated)

| Month | Mean (mm) | Maximum (mm) | Variance (mm) | Dry-Spell (day) | Wet-Spell (day) | Standard dev. Wet-Spell | Standard dev. Dry-Spell |
|---|---|---|---|---|---|---|---|
| **January** | 6.64 | 58.97 | 73.76 | 2.01 | 1.95 | 1.35 | 1.48 |
| **February** | 11.06 | 79.27 | 179.56 | 1.66 | 2.47 | 1.99 | 1.04 |
| **March** | 10.22 | 85.21 | 169.92 | 1.46 | 2.81 | 2.22 | 0.80 |
| **April** | 15.55 | 125.88 | 356.26 | 1.63 | 2.54 | 1.99 | 0.99 |
| **May** | 10.48 | 85.13 | 172.39 | 1.73 | 2.26 | 1.68 | 1.11 |
| **June** | 9.31 | 67.52 | 124.84 | 2.44 | 1.61 | 1.04 | 1.84 |
| **July** | 7.93 | 59.77 | 102.77 | 2.75 | 1.57 | 0.95 | 2.24 |
| **August** | 8.87 | 56.86 | 110.20 | 2.32 | 1.72 | 1.08 | 1.70 |
| **September** | 10.71 | 84.62 | 170.83 | 1.50 | 2.92 | 2.36 | 0.87 |
| **October** | 8.76 | 79.33 | 125.63 | 1.57 | 2.70 | 2.07 | 0.93 |
| **November** | 13.20 | 99.08 | 247.09 | 1.35 | 3.32 | 2.62 | 0.68 |
| **December** | 10.23 | 83.78 | 162.61 | 1.92 | 2.08 | 1.48 | 1.29 |

Station No.3117070 (Validated)

| Month | Mean (mm) | Maximum (mm) | Variance (mm) | Dry-Spell (day) | Wet-Spell (day) | Standard dev. Wet-Spell | Standard dev. Dry-Spell |
|---|---|---|---|---|---|---|---|
| January | 9.99 | 74.85 | 159.16 | 2.38 | 1.73 | 1.13 | 1.91 |
| February | 17.03 | 125.20 | 471.07 | 2.08 | 1.80 | 1.18 | 1.48 |
| March | 12.87 | 93.60 | 219.67 | 1.82 | 2.06 | 1.42 | 1.20 |
| April | 19.75 | 128.92 | 493.13 | 1.73 | 2.29 | 1.68 | 1.10 |
| May | 15.28 | 122.15 | 341.22 | 1.84 | 2.06 | 1.49 | 1.19 |
| June | 13.67 | 100.01 | 269.34 | 2.43 | 1.62 | 0.99 | 1.84 |
| July | 10.72 | 91.60 | 219.31 | 2.34 | 1.62 | 0.98 | 1.67 |
| August | 14.09 | 95.42 | 272.60 | 2.43 | 1.67 | 1.10 | 1.89 |
| September | 14.10 | 94.28 | 254.43 | 1.75 | 2.24 | 1.70 | 1.16 |
| October | 15.23 | 109.22 | 290.78 | 1.69 | 2.35 | 1.72 | 1.02 |
| November | 11.69 | 90.26 | 208.52 | 1.67 | 2.34 | 1.85 | 1.06 |
| December | 12.22 | 86.36 | 210.19 | 2.53 | 1.56 | 0.91 | 1.89 |

Station no.3118069 (Validated)

| Month | Mean (mm) | Maximum (mm) | Variance (mm) | Dry-Spell (day) | Wet-Spell (day) | Standard dev. Wet-Spell | Standard dev. Dry-Spell |
|---|---|---|---|---|---|---|---|
| January | 6.95 | 35.36 | 33.74 | 1.47 | 2.98 | 2.47 | 0.82 |
| February | 8.67 | 48.14 | 62.10 | 1.50 | 2.78 | 2.23 | 0.89 |
| March | 9.40 | 50.68 | 67.46 | 1.49 | 2.92 | 2.45 | 0.87 |
| April | 7.95 | 45.57 | 54.28 | 1.43 | 3.09 | 2.45 | 0.78 |
| May | 9.22 | 55.80 | 71.30 | 1.46 | 3.28 | 2.79 | 0.81 |
| June | 5.67 | 31.45 | 26.65 | 1.57 | 2.53 | 2.01 | 0.92 |
| July | 6.62 | 48.51 | 53.05 | 1.54 | 2.56 | 2.00 | 0.91 |
| August | 7.38 | 43.92 | 53.32 | 1.61 | 2.50 | 1.93 | 1.00 |
| September | 8.88 | 56.19 | 84.80 | 1.37 | 3.51 | 2.99 | 0.70 |
| October | 9.59 | 66.99 | 99.11 | 1.32 | 4.06 | 3.41 | 0.68 |
| November | 9.31 | 62.22 | 101.65 | 1.42 | 3.51 | 2.91 | 0.75 |
| December | 6.35 | 39.85 | 36.36 | 1.48 | 3.13 | 2.56 | 0.84 |

Station no.3216001 (Validated)

| Month | Mean (mm) | Maximum (mm) | Variance (mm) | Dry-Spell (day) | Wet-Spell (day) | Standard dev. Wet-Spell | Standard dev. Dry-Spell |
|---|---|---|---|---|---|---|---|
| January | 7.99 | 47.79 | 84.72 | 2.96 | 1.48 | 0.85 | 2.37 |
| February | 11.11 | 77.57 | 179.87 | 2.11 | 1.86 | 1.25 | 1.53 |
| March | 10.95 | 90.80 | 193.94 | 1.81 | 2.05 | 1.43 | 1.17 |
| April | 15.91 | 122.85 | 348.05 | 1.54 | 2.58 | 1.91 | 0.87 |
| May | 18.04 | 140.94 | 470.90 | 1.41 | 3.27 | 2.73 | 0.73 |
| June | 13.92 | 104.25 | 343.77 | 4.05 | 1.35 | 0.69 | 3.81 |
| July | 13.92 | 112.47 | 284.05 | 2.20 | 1.72 | 1.08 | 1.59 |
| August | 13.79 | 96.07 | 268.25 | 2.52 | 1.64 | 0.99 | 1.97 |
| September | 16.52 | 138.19 | 410.08 | 1.69 | 2.33 | 1.72 | 1.09 |
| October | 11.76 | 87.71 | 206.85 | 1.65 | 2.41 | 1.79 | 1.03 |
| November | 13.62 | 98.48 | 264.91 | 1.41 | 3.37 | 2.84 | 0.75 |
| December | 9.79 | 83.00 | 168.39 | 2.04 | 1.91 | 1.33 | 1.47 |

Station no.3217001 (Validated)

| Month | Mean (mm) | Maximum (mm) | Variance (mm) | Dry-Spell (day) | Wet-Spell (day) | Standard dev. Wet-Spell | Standard dev. Dry-Spell |
|---|---|---|---|---|---|---|---|
| January | 7.16 | 50.06 | 83.17 | 3.54 | 1.34 | 0.64 | 2.86 |
| February | 15.42 | 102.55 | 331.83 | 2.29 | 1.70 | 1.09 | 1.71 |
| March | 12.35 | 95.29 | 231.08 | 1.87 | 2.02 | 1.40 | 1.24 |
| April | 14.60 | 107.50 | 303.36 | 1.63 | 2.47 | 1.84 | 1.04 |
| May | 13.14 | 112.91 | 258.62 | 1.40 | 3.11 | 2.48 | 0.75 |
| June | 10.96 | 85.59 | 216.58 | 2.79 | 1.52 | 0.87 | 2.13 |
| July | 11.13 | 91.88 | 207.47 | 1.93 | 2.00 | 1.42 | 1.26 |
| August | 12.43 | 104.06 | 267.48 | 2.24 | 1.65 | 1.01 | 1.62 |
| September | 13.11 | 98.65 | 248.73 | 1.63 | 2.43 | 1.81 | 0.96 |
| October | 12.62 | 97.75 | 226.74 | 1.56 | 2.57 | 1.97 | 0.91 |
| November | 14.33 | 108.73 | 281.48 | 1.34 | 3.64 | 3.10 | 0.66 |
| December | 9.95 | 72.92 | 151.35 | 1.98 | 2.02 | 1.32 | 1.36 |

Station no.3217002 (Validated)

| Month | Mean (mm) | Maximum (mm) | Variance (mm) | Dry-Spell (day) | Wet-Spell (day) | Standard dev. Wet-Spell | Standard dev. Dry-Spell |
|---|---|---|---|---|---|---|---|
| January | 10.09 | 75.51 | 168.94 | 2.65 | 1.49 | 0.84 | 2.09 |
| February | 12.03 | 83.61 | 211.90 | 2.71 | 1.55 | 0.93 | 2.07 |
| March | 11.24 | 88.45 | 184.21 | 1.79 | 2.11 | 1.54 | 1.19 |
| April | 12.46 | 94.05 | 237.80 | 1.61 | 2.36 | 1.88 | 0.97 |
| May | 13.27 | 119.05 | 298.27 | 1.49 | 2.68 | 2.10 | 0.84 |
| June | 9.43 | 69.93 | 147.22 | 2.65 | 1.60 | 0.95 | 2.02 |
| July | 11.44 | 79.97 | 175.86 | 2.25 | 1.77 | 1.13 | 1.63 |
| August | 11.28 | 88.93 | 200.25 | 2.03 | 1.88 | 1.26 | 1.41 |
| September | 13.94 | 113.02 | 294.58 | 1.49 | 2.64 | 2.02 | 0.82 |
| October | 17.41 | 141.25 | 439.78 | 1.57 | 2.58 | 1.95 | 0.94 |
| November | 11.51 | 88.89 | 191.99 | 1.59 | 2.61 | 2.12 | 0.97 |
| December | 8.52 | 65.06 | 122.73 | 2.82 | 1.47 | 0.83 | 2.24 |

Station no.3217003 (Validated)

| Month | Mean (mm) | Maximum (mm) | Variance (mm) | Dry-Spell (day) | Wet-Spell (day) | Standard dev. Wet-Spell | Standard dev. Dry-Spell |
|---|---|---|---|---|---|---|---|
| January | 7.73 | 24.77 | 25.85 | 1.45 | 3.08 | 2.52 | 0.78 |
| February | 8.50 | 27.30 | 30.27 | 1.38 | 3.29 | 2.69 | 0.69 |
| March | 9.35 | 29.07 | 34.16 | 1.27 | 3.83 | 3.08 | 0.59 |
| April | 11.03 | 34.34 | 50.81 | 1.33 | 3.59 | 2.91 | 0.63 |
| May | 10.99 | 32.64 | 47.27 | 1.29 | 3.83 | 3.19 | 0.60 |
| June | 7.41 | 22.30 | 20.84 | 1.25 | 4.00 | 3.30 | 0.54 |
| July | 8.13 | 25.06 | 26.21 | 1.31 | 4.00 | 3.24 | 0.65 |
| August | 9.72 | 29.90 | 37.58 | 1.27 | 3.87 | 3.17 | 0.56 |
| September | 12.02 | 37.85 | 59.33 | 1.34 | 3.76 | 3.12 | 0.66 |
| October | 12.27 | 37.66 | 59.08 | 1.27 | 4.15 | 3.40 | 0.57 |
| November | 11.39 | 34.28 | 52.77 | 1.31 | 3.85 | 3.36 | 0.63 |
| December | 7.43 | 23.44 | 23.39 | 1.45 | 3.03 | 2.40 | 0.78 |

3217004 (Validated)

| Month | Mean (mm) | Maximum (mm) | Variance (mm) | Dry-Spell (day) | Wet-Spell (day) | Standard dev. Wet-Spell | Standard dev. Dry-Spell |
|---|---|---|---|---|---|---|---|
| January | 3.45 | 47.90 | 56.55 | 2.25 | 2.16 | 1.19 | 2.15 |
| February | 4.07 | 78.90 | 104.14 | 2.74 | 1.38 | 1.23 | 1.78 |
| March | 8.75 | 108.30 | 188.72 | 2.05 | 3.12 | 3.51 | 1.70 |
| April | 8.88 | 107.30 | 226.75 | 1.37 | 2.64 | 2.46 | 0.76 |
| May | 8.36 | 114.20 | 186.90 | 1.86 | 3.09 | 2.60 | 0.66 |
| June | 6.31 | 112.00 | 178.74 | 2.58 | 3.05 | 4.14 | -0.03 |
| July | 4.76 | 90.70 | 158.77 | 1.56 | 2.02 | 3.48 | 0.84 |
| August | 6.88 | 96.70 | 180.49 | 2.80 | 2.11 | 2.44 | 0.26 |
| September | 8.39 | 86.60 | 190.31 | 1.50 | 2.35 | 2.52 | 0.50 |
| October | 8.46 | 95.60 | 172.96 | 1.56 | 4.30 | 3.92 | 0.08 |
| November | 8.81 | 92.70 | 136.45 | 0.96 | 4.44 | 4.78 | -0.08 |
| December | 6.27 | 187.80 | 269.98 | 1.48 | 3.70 | 4.37 | 2.88 |

Station no.3317004 (Validated)

| Month | Mean (mm) | Maximum (mm) | Variance (mm) | Dry-Spell (day) | Wet-Spell (day) | Standard dev. Wet-Spell | Standard dev. Dry-Spell |
|---|---|---|---|---|---|---|---|
| January | 8.01 | 56.15 | 82.53 | 2.15 | 1.79 | 1.18 | 1.50 |
| February | 9.26 | 55.50 | 117.85 | 2.84 | 1.52 | 0.88 | 2.27 |
| March | 9.22 | 72.66 | 123.47 | 1.75 | 2.24 | 1.65 | 1.19 |
| April | 11.79 | 100.88 | 197.65 | 1.47 | 2.93 | 2.38 | 0.81 |
| May | 27.27 | 460.41 | 3388.85 | 1.46 | 3.16 | 2.55 | 0.86 |
| June | 9.93 | 74.74 | 132.11 | 1.78 | 2.07 | 1.44 | 1.11 |
| July | 9.98 | 71.66 | 152.10 | 1.76 | 2.08 | 1.41 | 1.14 |
| August | 14.99 | 96.93 | 285.18 | 2.60 | 1.58 | 0.95 | 2.03 |
| September | 11.73 | 101.34 | 193.93 | 1.40 | 3.07 | 2.46 | 0.70 |
| October | 12.87 | 91.21 | 196.58 | 1.26 | 4.08 | 3.39 | 0.54 |
| November | 12.05 | 106.81 | 212.07 | 1.16 | 6.10 | 5.28 | 0.39 |
| December | 8.18 | 66.23 | 97.12 | 1.58 | 2.58 | 1.86 | 0.93 |

**Appendix M- Statistical Summary of Statistics for Simulated Precipitation for Future Period: Summary of Statistics for Observed and Validated Data 2011-2040 (2020s); 2041-2070 (2050s) and 2071-2099 (2080s) corresponding to A2 and B2 Scenarios**

### A- Projected rainfall for 2020s - A2 scenario

Station no.3116005

| Month | Mean Daily (mm) | Maximum (mm) | Variance (mm) | Mean Monthly (mm) | Wet-days (%) | Dry-Spell (day) | Wet-Spell (day) | Standard dev. Wet-Spell (day) | Standard dev. Dry-Spell (day) |
|---|---|---|---|---|---|---|---|---|---|
| January | 2.61 | 57.84 | 42.66 | 72.56 | 0.28 | 3.29 | 1.38 | 0.78 | 2.52 |
| February | 5.90 | 96.46 | 142.02 | 171.35 | 0.46 | 2.21 | 1.86 | 1.37 | 1.44 |
| March | 6.58 | 90.14 | 149.33 | 191.50 | 0.54 | 1.96 | 2.18 | 1.68 | 1.16 |
| April | 10.69 | 128.95 | 318.82 | 314.95 | 0.58 | 1.82 | 2.37 | 1.86 | 1.01 |
| May | 12.95 | 81.88 | 416.39 | 382.60 | 0.66 | 1.82 | 3.14 | 3.08 | 1.10 |
| June | 2.78 | 69.58 | 76.45 | 77.73 | 0.19 | 4.76 | 1.31 | 0.74 | 4.73 |
| July | 6.62 | 61.13 | 193.12 | 192.73 | 0.41 | 2.46 | 1.70 | 1.15 | 1.66 |
| August | 6.25 | 71.00 | 199.87 | 181.74 | 0.36 | 2.78 | 1.57 | 1.02 | 2.07 |
| September | 12.11 | 99.30 | 376.61 | 357.37 | 0.62 | 1.74 | 2.61 | 2.13 | 0.93 |
| October | 6.98 | 86.35 | 146.42 | 203.47 | 0.55 | 1.94 | 2.26 | 1.80 | 1.15 |
| November | 9.81 | 91.38 | 236.06 | 288.59 | 0.69 | 1.62 | 3.14 | 2.68 | 0.78 |
| December | 5.11 | 92.91 | 109.60 | 147.51 | 0.47 | 2.22 | 1.88 | 1.35 | 1.43 |

Station no.3116006

| Month | Mean Daily (mm) | Maximum (mm) | Variance (mm) | Mean Monthly (mm) | Wet-days (%) | Dry-Spell (day) | Wet-Spell (day) | Standard dev. Wet-Spell (day) | Standard dev. Dry-Spell (day) |
|---|---|---|---|---|---|---|---|---|---|
| January | 3.43 | 66.07 | 49.78 | 103.01 | 0.45 | 2.16 | 1.79 | 1.20 | 1.58 |
| February | 6.66 | 116.07 | 140.06 | 199.73 | 0.59 | 1.69 | 2.40 | 1.88 | 1.09 |
| March | 6.70 | 110.98 | 130.89 | 201.10 | 0.67 | 1.46 | 2.81 | 2.29 | 0.83 |
| April | 9.54 | 140.45 | 296.52 | 286.29 | 0.60 | 1.65 | 2.40 | 1.85 | 1.02 |
| May | 5.61 | 98.19 | 114.28 | 168.18 | 0.57 | 1.70 | 2.24 | 1.64 | 1.12 |
| June | 3.67 | 81.15 | 70.44 | 110.01 | 0.38 | 2.50 | 1.60 | 1.00 | 1.87 |
| July | 2.46 | 75.62 | 42.66 | 73.86 | 0.32 | 2.95 | 1.48 | 0.87 | 2.46 |
| August | 2.85 | 63.34 | 48.13 | 85.35 | 0.36 | 2.62 | 1.56 | 0.92 | 2.07 |
| September | 6.93 | 95.20 | 129.42 | 207.78 | 0.71 | 1.42 | 3.19 | 2.64 | 0.78 |
| October | 5.02 | 82.57 | 83.33 | 150.52 | 0.63 | 1.63 | 2.64 | 2.18 | 1.05 |
| November | 9.24 | 129.38 | 208.49 | 277.34 | 0.71 | 1.39 | 3.24 | 2.67 | 0.73 |
| December | 4.55 | 94.13 | 102.61 | 136.57 | 0.44 | 2.27 | 1.81 | 1.23 | 1.72 |

Station no.3117070

| Month | Mean Daily (mm) | Maximum (mm) | Variance (mm) | Mean Monthly (mm) | Wet-days (%) | Dry-Spell (day) | Wet-Spell (day) | Standard dev. Wet-Spell (day) | Standard dev. Dry-Spell (day) |
|---|---|---|---|---|---|---|---|---|---|
| January | 4.65 | 101.34 | 99.03 | 139.40 | 0.47 | 2.08 | 1.84 | 1.23 | 1.56 |
| February | 7.24 | 150.75 | 268.72 | 217.07 | 0.45 | 2.17 | 1.82 | 1.23 | 1.61 |
| March | 6.43 | 103.49 | 138.47 | 192.89 | 0.55 | 1.79 | 2.18 | 1.62 | 1.18 |
| April | 12.32 | 173.32 | 392.70 | 369.45 | 0.61 | 1.62 | 2.49 | 1.94 | 0.98 |
| May | 11.38 | 173.69 | 353.36 | 341.53 | 0.60 | 1.67 | 2.43 | 1.93 | 1.05 |
| June | 6.77 | 142.48 | 220.18 | 202.97 | 0.40 | 2.37 | 1.63 | 1.00 | 1.79 |
| July | 4.19 | 95.29 | 95.80 | 125.68 | 0.41 | 2.30 | 1.67 | 1.05 | 1.76 |
| August | 5.31 | 121.03 | 151.43 | 159.42 | 0.38 | 2.50 | 1.57 | 0.95 | 1.94 |
| September | 11.38 | 152.52 | 368.45 | 341.30 | 0.56 | 1.78 | 2.20 | 1.66 | 1.17 |
| October | 10.87 | 166.94 | 334.63 | 326.07 | 0.58 | 1.68 | 2.27 | 1.66 | 1.05 |
| November | 4.26 | 101.50 | 80.16 | 127.81 | 0.54 | 1.87 | 2.14 | 1.60 | 1.32 |
| December | 3.00 | 106.71 | 78.70 | 89.88 | 0.30 | 3.22 | 1.44 | 0.82 | 2.80 |

Station no.3118069

| Month | Mean Daily (mm) | Maximum (mm) | Variance (mm) | Mean Monthly (mm) | Wet-days (%) | Dry-Spell (day) | Wet-Spell (day) | Standard dev. Wet-Spell (day) | Standard dev. Dry-Spell (day) |
|---|---|---|---|---|---|---|---|---|---|
| January | 4.98 | 42.14 | 33.18 | 149.54 | 0.72 | 1.43 | 3.39 | 2.93 | 0.80 |
| February | 5.75 | 57.38 | 59.36 | 172.49 | 0.67 | 1.52 | 2.96 | 2.55 | 0.90 |
| March | 6.79 | 61.96 | 71.35 | 203.69 | 0.72 | 1.38 | 3.27 | 2.71 | 0.73 |
| April | 6.05 | 56.79 | 56.26 | 181.59 | 0.72 | 1.39 | 3.36 | 2.95 | 0.74 |
| May | 5.96 | 61.27 | 58.68 | 178.77 | 0.70 | 1.46 | 3.22 | 2.72 | 0.86 |
| June | 3.56 | 37.31 | 23.35 | 106.94 | 0.62 | 1.59 | 2.53 | 1.97 | 0.96 |
| July | 4.02 | 52.90 | 40.78 | 120.48 | 0.63 | 1.58 | 2.55 | 1.98 | 0.96 |
| August | 4.56 | 56.24 | 50.95 | 136.93 | 0.57 | 1.77 | 2.33 | 1.85 | 1.20 |
| September | 6.38 | 65.65 | 79.45 | 191.30 | 0.72 | 1.41 | 3.40 | 2.92 | 0.76 |
| October | 7.44 | 79.17 | 94.69 | 223.30 | 0.76 | 1.32 | 3.82 | 3.34 | 0.64 |
| November | 6.98 | 88.19 | 101.32 | 209.38 | 0.70 | 1.45 | 3.22 | 2.73 | 0.81 |
| December | 4.68 | 46.00 | 33.66 | 140.44 | 0.72 | 1.41 | 3.48 | 3.03 | 0.80 |

Station no.3216001

| Month | Mean Daily (mm) | Maximum (mm) | Variance (mm) | Mean Monthly (mm) | Wet-days (%) | Dry-Spell (day) | Wet-Spell (day) | Standard dev. Wet-Spell (day) | Standard dev. Dry-Spell (day) |
|---|---|---|---|---|---|---|---|---|---|
| January | 2.41 | 66.62 | 42.46 | 72.35 | 0.30 | 3.08 | 1.41 | 0.74 | 2.50 |
| February | 5.70 | 104.04 | 141.82 | 171.14 | 0.48 | 2.00 | 1.89 | 1.33 | 1.42 |
| March | 6.38 | 109.11 | 149.13 | 191.29 | 0.56 | 1.75 | 2.21 | 1.64 | 1.14 |
| April | 10.49 | 159.24 | 318.62 | 314.74 | 0.60 | 1.61 | 2.40 | 1.82 | 0.99 |
| May | 12.75 | 168.24 | 416.19 | 382.39 | 0.68 | 1.61 | 3.17 | 3.04 | 1.08 |
| June | 2.58 | 103.13 | 76.25 | 77.52 | 0.21 | 4.55 | 1.34 | 0.70 | 4.71 |
| July | 6.42 | 126.68 | 192.92 | 192.52 | 0.43 | 2.25 | 1.73 | 1.11 | 1.64 |
| August | 6.05 | 138.68 | 199.67 | 181.53 | 0.38 | 2.57 | 1.60 | 0.98 | 2.05 |
| September | 11.91 | 172.79 | 376.41 | 357.16 | 0.64 | 1.53 | 2.64 | 2.09 | 0.91 |
| October | 6.78 | 106.14 | 146.22 | 203.26 | 0.57 | 1.73 | 2.29 | 1.76 | 1.13 |
| November | 9.61 | 144.99 | 235.86 | 288.38 | 0.71 | 1.41 | 3.17 | 2.64 | 0.76 |
| December | 4.91 | 104.26 | 109.40 | 147.30 | 0.49 | 2.01 | 1.91 | 1.31 | 1.41 |

Station no.3217001

| Month | Mean Daily (mm) | Maximum (mm) | Variance (mm) | Mean Monthly (mm) | Wet-days (%) | Dry-Spell (day) | Wet-Spell (day) | Standard dev. Wet-Spell (day) | Standard dev. Dry-Spell (day) |
|---|---|---|---|---|---|---|---|---|---|
| January | 1.55 | 59.98 | 26.76 | 46.46 | 0.23 | 3.97 | 1.31 | 0.64 | 3.45 |
| February | 6.79 | 122.71 | 200.33 | 203.78 | 0.44 | 2.26 | 1.80 | 1.24 | 1.66 |
| March | 6.51 | 124.51 | 164.32 | 195.38 | 0.52 | 1.89 | 2.04 | 1.44 | 1.32 |
| April | 8.59 | 137.55 | 230.68 | 257.84 | 0.59 | 1.66 | 2.31 | 1.75 | 1.03 |
| May | 8.81 | 144.36 | 229.19 | 264.30 | 0.65 | 1.57 | 2.75 | 2.22 | 0.94 |
| June | 3.68 | 108.86 | 99.73 | 110.46 | 0.34 | 2.72 | 1.49 | 0.84 | 2.18 |
| July | 5.64 | 107.59 | 123.90 | 169.20 | 0.55 | 1.80 | 2.11 | 1.54 | 1.20 |
| August | 4.72 | 112.78 | 127.08 | 141.74 | 0.41 | 2.38 | 1.67 | 1.07 | 1.76 |
| September | 9.21 | 134.73 | 246.02 | 276.31 | 0.62 | 1.57 | 2.52 | 1.98 | 0.91 |
| October | 9.05 | 142.82 | 238.77 | 271.44 | 0.66 | 1.53 | 2.78 | 2.18 | 0.90 |
| November | 11.22 | 125.97 | 259.88 | 336.64 | 0.78 | 1.26 | 4.15 | 3.67 | 0.56 |
| December | 5.09 | 100.95 | 106.82 | 152.82 | 0.52 | 1.87 | 2.01 | 1.43 | 1.29 |

Station no.3217002

| Month | Mean Daily (mm) | Maximum (mm) | Variance (mm) | Mean Monthly (mm) | Wet-days (%) | Dry-Spell (day) | Wet-Spell (day) | Standard dev. Wet-Spell (day) | Standard dev. Dry-Spell (day) |
|---|---|---|---|---|---|---|---|---|---|
| January | 3.84 | 104.63 | 100.46 | 115.22 | 0.34 | 2.78 | 1.52 | 0.89 | 2.32 |
| February | 4.54 | 96.09 | 116.48 | 136.34 | 0.38 | 2.53 | 1.59 | 1.00 | 1.99 |
| March | 6.02 | 107.72 | 129.11 | 180.57 | 0.53 | 1.86 | 2.08 | 1.50 | 1.24 |
| April | 7.78 | 143.78 | 204.92 | 233.34 | 0.60 | 1.66 | 2.39 | 1.81 | 1.02 |
| May | 7.36 | 130.81 | 188.39 | 220.66 | 0.58 | 1.74 | 2.33 | 1.79 | 1.18 |
| June | 3.46 | 78.56 | 72.50 | 103.91 | 0.37 | 2.58 | 1.59 | 0.96 | 1.98 |
| July | 4.91 | 88.47 | 100.98 | 147.19 | 0.44 | 2.19 | 1.77 | 1.16 | 1.62 |
| August | 5.11 | 101.42 | 123.16 | 153.25 | 0.50 | 1.94 | 1.92 | 1.32 | 1.36 |
| September | 9.57 | 149.43 | 254.16 | 287.12 | 0.66 | 1.50 | 2.79 | 2.26 | 0.87 |
| October | 11.48 | 165.12 | 376.35 | 344.46 | 0.63 | 1.58 | 2.56 | 1.99 | 0.95 |
| November | 7.02 | 109.67 | 160.65 | 210.45 | 0.60 | 1.64 | 2.35 | 1.78 | 1.05 |
| December | 3.44 | 99.23 | 70.90 | 103.07 | 0.37 | 2.61 | 1.60 | 0.99 | 2.09 |

Station no.3217003

| Month | Mean Daily (mm) | Maximum (mm) | Variance (mm) | Mean Monthly (mm) | Wet-days (%) | Dry-Spell (day) | Wet-Spell (day) | Standard dev. Wet-Spell (day) | Standard dev. Dry-Spell (day) |
|---|---|---|---|---|---|---|---|---|---|
| January | 4.25 | 27.22 | 53.45 | 127.58 | 0.71 | 1.40 | 3.17 | 2.52 | 0.75 |
| February | 5.16 | 28.77 | 61.10 | 154.93 | 0.73 | 1.35 | 3.39 | 2.83 | 0.68 |
| March | 6.20 | 31.12 | 63.42 | 185.88 | 0.77 | 1.29 | 3.93 | 3.25 | 0.61 |
| April | 7.07 | 36.70 | 99.28 | 212.10 | 0.75 | 1.32 | 3.63 | 3.09 | 0.64 |
| May | 7.04 | 35.98 | 85.54 | 211.13 | 0.77 | 1.30 | 3.84 | 3.26 | 0.62 |
| June | 5.01 | 24.17 | 38.35 | 150.24 | 0.77 | 1.29 | 3.95 | 3.40 | 0.60 |
| July | 5.36 | 26.81 | 45.42 | 160.95 | 0.77 | 1.29 | 3.97 | 3.34 | 0.59 |
| August | 6.41 | 32.00 | 67.83 | 192.17 | 0.77 | 1.27 | 3.89 | 3.26 | 0.58 |
| September | 7.68 | 40.57 | 109.39 | 230.47 | 0.76 | 1.30 | 3.76 | 3.16 | 0.60 |
| October | 8.66 | 42.32 | 104.57 | 259.72 | 0.79 | 1.26 | 4.25 | 3.64 | 0.57 |
| November | 7.43 | 37.36 | 93.12 | 222.78 | 0.77 | 1.29 | 3.90 | 3.27 | 0.61 |
| December | 4.14 | 27.43 | 52.43 | 124.24 | 0.70 | 1.41 | 3.10 | 2.52 | 0.78 |

Station no.3217004

| Month | Mean Daily (mm) | Maximum (mm) | Variance (mm) | Mean Monthly (mm) | Wet-days (%) | Dry-Spell (day) | Wet-Spell (day) | Standard dev. Wet-Spell (day) | Standard dev. Dry-Spell (day) |
|---|---|---|---|---|---|---|---|---|---|
| January | 3.43 | 87.29 | 48.91 | 102.86 | 0.45 | 2.13 | 1.80 | 1.18 | 1.56 |
| February | 3.40 | 158.50 | 65.97 | 101.93 | 0.36 | 2.63 | 1.56 | 0.94 | 2.08 |
| March | 5.09 | 99.31 | 88.78 | 152.63 | 0.55 | 1.77 | 2.14 | 1.53 | 1.18 |
| April | 8.66 | 166.86 | 182.37 | 259.72 | 0.68 | 1.44 | 2.94 | 2.37 | 0.79 |
| May | 24.66 | 119.08 | 4460.60 | 739.82 | 0.68 | 1.45 | 2.88 | 2.33 | 0.78 |
| June | 5.63 | 88.69 | 105.01 | 168.90 | 0.54 | 1.83 | 2.09 | 1.52 | 1.25 |
| July | 5.44 | 96.97 | 104.42 | 163.06 | 0.55 | 1.75 | 2.16 | 1.57 | 1.14 |
| August | 5.50 | 97.98 | 160.71 | 164.87 | 0.37 | 2.54 | 1.56 | 0.97 | 2.00 |
| September | 8.35 | 106.94 | 170.09 | 250.46 | 0.70 | 1.41 | 3.06 | 2.40 | 0.77 |
| October | 10.12 | 121.22 | 195.78 | 303.50 | 0.78 | 1.29 | 4.12 | 3.51 | 0.61 |
| November | 10.34 | 112.40 | 190.69 | 310.12 | 0.85 | 1.17 | 5.76 | 5.02 | 0.45 |
| December | 5.05 | 99.94 | 76.69 | 151.57 | 0.61 | 1.59 | 2.45 | 1.88 | 0.98 |

Station no.3317004

| Month | Mean Daily (mm) | Maximum (mm) | Variance (mm) | Mean Monthly (mm) | Wet-days (%) | Dry-Spell (day) | Wet-Spell (day) | Standard dev. Wet-Spell (day) | Standard dev. Dry-Spell (day) |
|---|---|---|---|---|---|---|---|---|---|
| January | 2.37 | 66.90 | 42.46 | 70.84 | 0.30 | 3.08 | 1.41 | 0.74 | 2.50 |
| February | 5.66 | 81.23 | 141.82 | 169.60 | 0.48 | 2.00 | 1.89 | 1.33 | 1.42 |
| March | 6.33 | 86.79 | 149.13 | 189.80 | 0.56 | 1.75 | 2.21 | 1.64 | 1.14 |
| April | 10.44 | 117.04 | 318.62 | 313.20 | 0.60 | 1.61 | 2.40 | 1.82 | 0.99 |
| May | 12.70 | 844.54 | 416.19 | 380.90 | 0.68 | 1.61 | 3.17 | 3.04 | 1.08 |
| June | 2.54 | 88.49 | 76.25 | 76.01 | 0.21 | 4.55 | 1.34 | 0.70 | 4.71 |
| July | 6.37 | 98.01 | 192.92 | 191.00 | 0.43 | 2.25 | 1.73 | 1.11 | 1.64 |
| August | 5.99 | 122.49 | 199.67 | 180.00 | 0.38 | 2.57 | 1.60 | 0.98 | 2.05 |
| September | 11.86 | 122.91 | 376.41 | 355.70 | 0.64 | 1.53 | 2.64 | 2.09 | 0.91 |
| October | 6.73 | 122.42 | 146.22 | 201.80 | 0.57 | 1.73 | 2.29 | 1.76 | 1.13 |
| November | 9.56 | 114.71 | 235.86 | 286.90 | 0.71 | 1.41 | 3.17 | 2.64 | 0.76 |
| December | 4.86 | 77.29 | 109.40 | 145.80 | 0.49 | 2.01 | 1.91 | 1.31 | 1.41 |

## B- Projected rainfall for 2050s - A2 scenario

Station no.3116005

| Month | Mean Daily (mm) | Maximum (mm) | Variance (mm) | Mean Monthly (mm) | Wet-days (%) | Dry-Spell (day) | Wet-Spell (day) | Standard dev. Wet-Spell (day) | Standard dev. Dry-Spell (day) |
|---|---|---|---|---|---|---|---|---|---|
| January | 2.20 | 62.01 | 31.20 | 57.10 | 0.24 | 3.56 | 1.34 | 0.69 | 3.06 |
| February | 6.91 | 89.16 | 175.00 | 198.40 | 0.51 | 1.94 | 2.08 | 1.61 | 1.37 |
| March | 7.14 | 96.61 | 158.00 | 205.40 | 0.60 | 1.61 | 2.50 | 2.00 | 0.99 |
| April | 12.42 | 128.22 | 425.00 | 363.80 | 0.59 | 1.64 | 2.45 | 1.89 | 0.99 |
| May | 19.20 | 92.78 | 665.00 | 567.00 | 0.78 | 1.42 | 4.89 | 5.06 | 0.79 |
| June | 1.24 | 72.25 | 36.20 | 28.15 | 0.04 | 11.28 | 1.15 | 0.45 | 10.15 |
| July | 7.20 | 57.84 | 237.00 | 207.20 | 0.39 | 2.42 | 1.67 | 1.09 | 1.84 |
| August | 6.39 | 74.43 | 237.00 | 182.70 | 0.30 | 3.01 | 1.47 | 0.85 | 2.46 |
| September | 15.30 | 94.30 | 554.00 | 450.10 | 0.64 | 1.55 | 2.81 | 2.29 | 0.92 |
| October | 6.91 | 93.57 | 147.00 | 198.40 | 0.55 | 1.81 | 2.31 | 1.87 | 1.24 |
| November | 11.97 | 101.96 | 300.00 | 350.20 | 0.72 | 1.39 | 3.56 | 3.05 | 0.74 |
| December | 4.78 | 100.23 | 97.90 | 134.30 | 0.44 | 2.15 | 1.83 | 1.28 | 1.56 |

Station no.3116006

| Month | Mean Daily (mm) | Maximum (mm) | Variance (mm) | Mean Monthly (mm) | Wet-days (%) | Dry-Spell (day) | Wet-Spell (day) | Standard dev. Wet-Spell (day) | Standard dev. Dry-Spell (day) |
|---|---|---|---|---|---|---|---|---|---|
| January | 3.69 | 64.11 | 54.49 | 110.82 | 0.49 | 2.02 | 1.94 | 1.36 | 1.49 |
| February | 7.34 | 104.77 | 154.72 | 220.18 | 0.65 | 1.56 | 2.72 | 2.19 | 0.94 |
| March | 6.44 | 102.37 | 118.84 | 193.34 | 0.69 | 1.43 | 3.04 | 2.56 | 0.77 |
| April | 9.51 | 158.24 | 283.96 | 285.27 | 0.57 | 1.75 | 2.28 | 1.67 | 1.13 |
| May | 6.53 | 96.91 | 142.64 | 195.99 | 0.59 | 1.68 | 2.36 | 1.89 | 1.05 |
| June | 3.46 | 88.07 | 71.59 | 103.71 | 0.35 | 2.70 | 1.52 | 0.89 | 2.19 |
| July | 2.16 | 72.62 | 40.57 | 64.88 | 0.26 | 3.65 | 1.38 | 0.74 | 3.15 |
| August | 2.04 | 58.66 | 31.64 | 61.11 | 0.31 | 3.02 | 1.45 | 0.81 | 2.49 |
| September | 6.76 | 98.48 | 118.58 | 202.88 | 0.78 | 1.30 | 4.27 | 3.89 | 0.62 |
| October | 4.38 | 64.53 | 60.94 | 131.32 | 0.66 | 1.57 | 2.89 | 2.54 | 0.98 |
| November | 8.53 | 130.04 | 195.75 | 255.81 | 0.68 | 1.44 | 2.94 | 2.34 | 0.79 |
| December | 3.19 | 91.39 | 72.90 | 95.72 | 0.33 | 3.10 | 1.59 | 1.03 | 2.82 |

Station no.3117070

| Month | Mean Daily (mm) | Maximum (mm) | Variance (mm) | Mean Monthly (mm) | Wet-days (%) | Dry-Spell (day) | Wet-Spell (day) | Standard dev. Wet-Spell (day) | Standard dev. Dry-Spell (day) |
|---|---|---|---|---|---|---|---|---|---|
| January | 4.52 | 94.27 | 81.10 | 135.58 | 0.60 | 1.68 | 2.41 | 1.92 | 1.12 |
| February | 6.79 | 154.30 | 235.37 | 203.84 | 0.49 | 2.00 | 1.93 | 1.36 | 1.42 |
| March | 6.04 | 91.25 | 117.05 | 181.30 | 0.61 | 1.62 | 2.51 | 2.00 | 0.99 |
| April | 13.95 | 182.10 | 476.35 | 418.53 | 0.65 | 1.53 | 2.69 | 2.11 | 0.91 |
| May | 15.90 | 185.20 | 561.82 | 476.94 | 0.69 | 1.45 | 3.04 | 2.53 | 0.82 |
| June | 8.80 | 166.70 | 321.97 | 264.06 | 0.44 | 2.18 | 1.73 | 1.12 | 1.60 |
| July | 3.99 | 94.13 | 84.37 | 119.58 | 0.43 | 2.24 | 1.71 | 1.09 | 1.65 |
| August | 4.80 | 105.87 | 143.96 | 144.12 | 0.31 | 3.01 | 1.45 | 0.82 | 2.52 |
| September | 15.26 | 194.54 | 562.28 | 457.80 | 0.59 | 1.68 | 2.35 | 1.75 | 1.07 |
| October | 12.40 | 166.35 | 421.05 | 372.14 | 0.55 | 1.78 | 2.15 | 1.58 | 1.18 |
| November | 2.94 | 74.20 | 50.45 | 88.10 | 0.44 | 2.24 | 1.82 | 1.25 | 1.69 |
| December | 1.60 | 87.30 | 43.37 | 48.13 | 0.10 | 8.08 | 1.20 | 0.51 | 7.83 |

Station no. 3118069

| Month | Mean Daily (mm) | Maximum (mm) | Variance (mm) | Mean Monthly (mm) | Wet-days (%) | Dry-Spell (day) | Wet-Spell (day) | Standard dev. Wet-Spell (day) | Standard dev. Dry-Spell (day) |
|---|---|---|---|---|---|---|---|---|---|
| January | 5.21 | 42.57 | 34.69 | 156.31 | 0.74 | 1.38 | 3.63 | 3.27 | 0.74 |
| February | 5.61 | 55.59 | 58.09 | 168.44 | 0.65 | 1.61 | 2.91 | 2.82 | 1.03 |
| March | 7.41 | 67.70 | 82.86 | 222.16 | 0.72 | 1.39 | 3.37 | 2.79 | 0.74 |
| April | 5.91 | 52.93 | 55.65 | 177.35 | 0.71 | 1.44 | 3.21 | 2.78 | 0.80 |
| May | 6.65 | 63.39 | 70.31 | 199.54 | 0.72 | 1.42 | 3.39 | 2.95 | 0.77 |
| June | 3.53 | 37.46 | 25.90 | 106.05 | 0.59 | 1.69 | 2.34 | 1.80 | 1.11 |
| July | 3.55 | 52.79 | 35.64 | 106.45 | 0.60 | 1.65 | 2.42 | 1.85 | 1.05 |
| August | 4.04 | 58.67 | 50.68 | 121.30 | 0.48 | 2.11 | 1.93 | 1.43 | 1.53 |
| September | 6.00 | 69.82 | 73.45 | 179.89 | 0.70 | 1.43 | 3.16 | 2.76 | 0.80 |
| October | 7.49 | 80.59 | 104.13 | 224.58 | 0.72 | 1.38 | 3.39 | 2.88 | 0.71 |
| November | 6.66 | 90.01 | 103.27 | 199.72 | 0.65 | 1.57 | 2.80 | 2.39 | 0.94 |
| December | 4.49 | 45.80 | 32.88 | 134.60 | 0.72 | 1.42 | 3.38 | 2.94 | 0.78 |

Station no.3216001

| Month | Mean Daily (mm) | Maximum (mm) | Variance (mm) | Mean Monthly (mm) | Wet-days (%) | Dry-Spell (day) | Wet-Spell (day) | Standard dev. Wet-Spell (day) | Standard dev. Dry-Spell (day) |
|---|---|---|---|---|---|---|---|---|---|
| January | 1.89 | 62.03 | 31.08 | 56.80 | 0.26 | 3.53 | 1.36 | 0.68 | 3.04 |
| February | 6.60 | 123.22 | 174.40 | 198.06 | 0.53 | 1.91 | 2.11 | 1.60 | 1.35 |
| March | 6.83 | 119.64 | 158.10 | 205.05 | 0.62 | 1.58 | 2.52 | 1.99 | 0.97 |
| April | 12.11 | 187.17 | 425.38 | 363.44 | 0.61 | 1.61 | 2.47 | 1.88 | 0.98 |
| May | 18.89 | 221.72 | 665.18 | 566.69 | 0.80 | 1.39 | 4.91 | 5.05 | 0.77 |
| June | 0.93 | 94.66 | 36.07 | 27.84 | 0.06 | 11.25 | 1.17 | 0.44 | 10.14 |
| July | 6.89 | 158.82 | 236.42 | 206.84 | 0.41 | 2.39 | 1.69 | 1.08 | 1.83 |
| August | 6.08 | 158.26 | 237.07 | 182.34 | 0.32 | 2.98 | 1.49 | 0.84 | 2.45 |
| September | 14.99 | 209.65 | 554.32 | 449.75 | 0.66 | 1.52 | 2.83 | 2.28 | 0.90 |
| October | 6.60 | 111.72 | 147.26 | 198.04 | 0.57 | 1.78 | 2.33 | 1.86 | 1.22 |
| November | 11.66 | 143.66 | 299.96 | 349.93 | 0.74 | 1.36 | 3.58 | 3.04 | 0.72 |
| December | 4.47 | 102.55 | 97.74 | 133.98 | 0.46 | 2.12 | 1.85 | 1.27 | 1.54 |

Station no.3217001

| Month | Mean Daily (mm) | Maximum (mm) | Variance (mm) | Mean Monthly (mm) | Wet-days (%) | Dry-Spell (day) | Wet-Spell (day) | Standard dev. Wet-Spell (day) | Standard dev. Dry-Spell (day) |
|---|---|---|---|---|---|---|---|---|---|
| January | 1.05 | 59.11 | 17.36 | 31.47 | 0.17 | 5.26 | 1.27 | 0.59 | 5.07 |
| February | 7.85 | 134.90 | 223.13 | 235.59 | 0.52 | 2.02 | 2.14 | 1.80 | 1.50 |
| March | 6.55 | 116.19 | 158.39 | 196.41 | 0.54 | 1.83 | 2.14 | 1.54 | 1.18 |
| April | 8.97 | 148.97 | 254.66 | 269.21 | 0.57 | 1.73 | 2.28 | 1.70 | 1.12 |
| May | 11.56 | 140.26 | 295.09 | 346.94 | 0.75 | 1.39 | 3.88 | 3.45 | 0.76 |
| June | 2.78 | 95.59 | 71.97 | 83.44 | 0.28 | 3.35 | 1.39 | 0.74 | 2.87 |
| July | 6.08 | 104.28 | 127.51 | 182.32 | 0.63 | 1.59 | 2.59 | 2.02 | 0.97 |
| August | 3.91 | 97.49 | 101.68 | 117.43 | 0.37 | 2.54 | 1.57 | 0.95 | 1.95 |
| September | 10.09 | 150.05 | 290.73 | 302.75 | 0.61 | 1.60 | 2.45 | 1.87 | 1.00 |
| October | 9.23 | 153.23 | 246.73 | 276.98 | 0.67 | 1.48 | 2.86 | 2.32 | 0.85 |
| November | 13.20 | 161.20 | 312.86 | 395.86 | 0.85 | 1.20 | 5.92 | 5.62 | 0.51 |
| December | 5.22 | 88.97 | 103.25 | 156.51 | 0.55 | 1.79 | 2.14 | 1.54 | 1.20 |

Station no.3217002

| Month | Mean Daily (mm) | Maximum (mm) | Variance (mm) | Mean Monthly (mm) | Wet-days (%) | Dry-Spell (day) | Wet-Spell (day) | Standard dev. Wet-Spell (day) | Standard dev. Dry-Spell (day) |
|---|---|---|---|---|---|---|---|---|---|
| January | 4.19 | 102.80 | 113.41 | 125.66 | 0.36 | 2.67 | 1.56 | 0.91 | 2.15 |
| February | 4.59 | 107.81 | 109.40 | 137.78 | 0.38 | 2.49 | 1.61 | 0.99 | 1.91 |
| March | 6.07 | 110.71 | 124.61 | 182.20 | 0.54 | 1.80 | 2.08 | 1.49 | 1.24 |
| April | 7.77 | 133.19 | 202.91 | 233.10 | 0.59 | 1.67 | 2.31 | 1.69 | 1.05 |
| May | 8.35 | 127.90 | 210.42 | 250.60 | 0.64 | 1.58 | 2.68 | 2.15 | 0.98 |
| June | 3.30 | 84.09 | 66.64 | 98.89 | 0.37 | 2.57 | 1.58 | 0.97 | 1.97 |
| July | 5.49 | 98.93 | 120.42 | 164.72 | 0.46 | 2.10 | 1.77 | 1.15 | 1.56 |
| August | 4.51 | 96.02 | 91.62 | 135.39 | 0.53 | 1.82 | 2.07 | 1.50 | 1.22 |
| September | 10.59 | 141.46 | 273.74 | 317.77 | 0.70 | 1.43 | 3.12 | 2.65 | 0.77 |
| October | 13.27 | 188.35 | 468.92 | 398.04 | 0.64 | 1.53 | 2.68 | 2.06 | 0.91 |
| November | 6.36 | 109.31 | 137.73 | 190.73 | 0.56 | 1.77 | 2.18 | 1.62 | 1.17 |
| December | 3.83 | 96.63 | 87.15 | 115.02 | 0.38 | 2.54 | 1.60 | 0.98 | 1.97 |

Station no.3217003

| Month | Mean Daily (mm) | Maximum (mm) | Variance (mm) | Mean Monthly (mm) | Wet-days (%) | Dry-Spell (day) | Wet-Spell (day) | Standard dev. Wet-Spell (day) | Standard dev. Dry-Spell (day) |
|---|---|---|---|---|---|---|---|---|---|
| January | 4.17 | 26.75 | 53.18 | 125.10 | 0.70 | 1.42 | 3.10 | 2.55 | 0.77 |
| February | 4.94 | 29.58 | 61.38 | 148.09 | 0.72 | 1.37 | 3.30 | 2.67 | 0.68 |
| March | 6.23 | 31.91 | 63.62 | 186.76 | 0.77 | 1.30 | 3.99 | 3.39 | 0.60 |
| April | 6.87 | 36.34 | 97.90 | 206.11 | 0.74 | 1.33 | 3.56 | 3.00 | 0.66 |
| May | 7.04 | 35.73 | 84.83 | 211.29 | 0.77 | 1.29 | 3.88 | 3.25 | 0.59 |
| June | 5.18 | 25.65 | 37.61 | 155.29 | 0.78 | 1.29 | 4.23 | 3.48 | 0.60 |
| July | 5.43 | 26.85 | 45.64 | 162.79 | 0.77 | 1.29 | 3.98 | 3.33 | 0.60 |
| August | 6.60 | 30.73 | 65.82 | 198.07 | 0.78 | 1.28 | 4.07 | 3.42 | 0.59 |
| September | 7.69 | 40.31 | 109.38 | 230.57 | 0.76 | 1.30 | 3.77 | 3.17 | 0.60 |
| October | 9.04 | 41.59 | 104.34 | 271.32 | 0.80 | 1.24 | 4.44 | 3.74 | 0.55 |
| November | 7.26 | 36.48 | 94.58 | 217.74 | 0.76 | 1.31 | 3.85 | 3.23 | 0.65 |
| December | 4.15 | 26.53 | 51.29 | 124.53 | 0.70 | 1.41 | 3.11 | 2.58 | 0.75 |

Station no.3217004

| Month | Mean Daily (mm) | Maximum (mm) | Variance (mm) | Mean Monthly (mm) | Wet-days (%) | Dry-Spell (day) | Wet-Spell (day) | Standard dev. Wet-Spell (day) | Standard dev. Dry-Spell (day) |
|---|---|---|---|---|---|---|---|---|---|
| January | 3.15 | 93.58 | 43.27 | 94.40 | 0.43 | 2.29 | 1.73 | 1.12 | 1.72 |
| February | 3.15 | 146.50 | 60.62 | 94.57 | 0.35 | 2.68 | 1.54 | 0.92 | 2.19 |
| March | 5.29 | 106.43 | 89.42 | 158.82 | 0.58 | 1.70 | 2.29 | 1.83 | 1.11 |
| April | 9.09 | 165.91 | 193.54 | 272.61 | 0.70 | 1.43 | 3.07 | 2.49 | 0.76 |
| May | 25.68 | 134.92 | 4142.28 | 770.36 | 0.69 | 1.42 | 3.07 | 2.50 | 0.77 |
| June | 6.69 | 92.09 | 125.81 | 200.83 | 0.57 | 1.73 | 2.27 | 1.73 | 1.14 |
| July | 5.49 | 91.74 | 112.50 | 164.80 | 0.54 | 1.77 | 2.11 | 1.53 | 1.14 |
| August | 5.69 | 102.71 | 170.76 | 170.81 | 0.37 | 2.58 | 1.56 | 0.93 | 1.99 |
| September | 8.56 | 101.55 | 178.65 | 256.89 | 0.70 | 1.41 | 3.15 | 2.48 | 0.74 |
| October | 10.37 | 131.34 | 197.92 | 311.14 | 0.79 | 1.27 | 4.36 | 3.80 | 0.62 |
| November | 10.96 | 125.42 | 204.21 | 328.91 | 0.87 | 1.16 | 6.21 | 5.41 | 0.42 |
| December | 5.05 | 107.81 | 74.89 | 151.58 | 0.61 | 1.64 | 2.45 | 1.87 | 1.01 |

Station no.3317004

| Month | Mean Daily (mm) | Maximum (mm) | Variance (mm) | Mean Monthly (mm) | Wet-days (%) | Dry-Spell (day) | Wet-Spell (day) | Standard dev. Wet-Spell (day) | Standard dev. Dry-Spell (day) |
|---|---|---|---|---|---|---|---|---|---|
| January | 1.84 | 65.53 | 31.08 | 55.20 | 0.26 | 3.53 | 1.36 | 0.68 | 3.04 |
| February | 6.55 | 85.16 | 174.40 | 196.50 | 0.53 | 1.91 | 2.11 | 1.60 | 1.35 |
| March | 6.79 | 73.09 | 158.10 | 203.50 | 0.62 | 1.58 | 2.52 | 1.99 | 0.97 |
| April | 12.06 | 116.08 | 425.38 | 361.80 | 0.61 | 1.61 | 2.47 | 1.88 | 0.98 |
| May | 18.84 | 739.35 | 665.18 | 565.10 | 0.80 | 1.39 | 4.91 | 5.05 | 0.77 |
| June | 0.88 | 95.52 | 36.07 | 26.24 | 0.06 | 11.25 | 1.17 | 0.44 | 10.14 |
| July | 6.85 | 103.76 | 236.42 | 205.20 | 0.41 | 2.39 | 1.69 | 1.08 | 1.83 |
| August | 6.02 | 113.80 | 237.07 | 180.70 | 0.32 | 2.98 | 1.49 | 0.84 | 2.45 |
| September | 14.94 | 111.92 | 554.32 | 448.20 | 0.66 | 1.52 | 2.83 | 2.28 | 0.90 |
| October | 6.55 | 116.68 | 147.26 | 196.40 | 0.57 | 1.78 | 2.33 | 1.86 | 1.22 |
| November | 11.61 | 128.56 | 299.96 | 348.30 | 0.74 | 1.36 | 3.58 | 3.04 | 0.72 |
| December | 4.42 | 73.50 | 97.74 | 132.40 | 0.46 | 2.12 | 1.85 | 1.27 | 1.54 |

## C- Projected rainfall for 2080s - A2 scenario

Station no.3116005

| Month | Mean Daily (mm) | Maximum (mm) | Variance (mm) | Mean Monthly (mm) | Wet-days (%) | Dry-Spell (day) | Wet-Spell (day) | Standard dev. Wet-Spell (day) | Standard dev. Dry-Spell (day) |
|---|---|---|---|---|---|---|---|---|---|
| January | 1.66 | 66.11 | 23.90 | 43.70 | 0.18 | 4.32 | 1.24 | 0.64 | 3.99 |
| February | 7.43 | 90.57 | 193.00 | 216.90 | 0.54 | 1.83 | 2.30 | 2.03 | 1.29 |
| March | 7.21 | 98.98 | 143.00 | 210.20 | 0.67 | 1.44 | 3.23 | 2.85 | 0.77 |
| April | 15.55 | 126.45 | 596.00 | 460.50 | 0.57 | 1.65 | 2.39 | 1.94 | 0.99 |
| May | 30.00 | 90.43 | 1173.00 | 893.90 | 0.88 | 1.28 | 9.60 | 9.18 | 0.56 |
| June | 0.28 | 64.40 | 2.00 | 2.26 | -0.03 | 26.28 | 1.02 | 0.13 | 8.12 |
| July | 7.71 | 46.83 | 316.00 | 225.20 | 0.30 | 2.90 | 1.46 | 0.95 | 2.38 |
| August | 5.45 | 71.46 | 237.00 | 157.50 | 0.18 | 4.21 | 1.25 | 0.64 | 3.89 |
| September | 22.82 | 95.05 | 950.00 | 678.60 | 0.68 | 1.45 | 3.26 | 2.80 | 0.79 |
| October | 5.74 | 102.95 | 114.00 | 166.00 | 0.50 | 1.96 | 2.16 | 1.80 | 1.38 |
| November | 15.13 | 96.26 | 465.00 | 447.80 | 0.73 | 1.36 | 4.01 | 3.63 | 0.65 |
| December | 4.19 | 87.12 | 91.50 | 119.70 | 0.37 | 2.43 | 1.64 | 1.08 | 1.85 |

Station no.3116006

| Month | Mean Daily (mm) | Maximum (mm) | Variance (mm) | Mean Monthly (mm) | Wet-days (%) | Dry-Spell (day) | Wet-Spell (day) | Standard dev. Wet-Spell (day) | Standard dev. Dry-Spell (day) |
|---|---|---|---|---|---|---|---|---|---|
| January | 3.84 | 67.37 | 54.87 | 115.15 | 0.53 | 1.88 | 2.12 | 1.56 | 1.31 |
| February | 7.97 | 121.88 | 165.76 | 239.09 | 0.71 | 1.44 | 3.28 | 2.76 | 0.81 |
| March | 6.29 | 98.37 | 109.60 | 188.69 | 0.74 | 1.37 | 3.53 | 2.92 | 0.70 |
| April | 9.64 | 155.52 | 324.41 | 289.13 | 0.53 | 1.85 | 2.06 | 1.47 | 1.25 |
| May | 7.06 | 121.41 | 159.03 | 211.84 | 0.60 | 1.63 | 2.38 | 1.87 | 1.04 |
| June | 3.37 | 93.36 | 78.17 | 101.22 | 0.32 | 2.97 | 1.45 | 0.79 | 2.42 |
| July | 1.22 | 67.98 | 26.32 | 36.62 | 0.14 | 6.11 | 1.21 | 0.50 | 5.99 |
| August | 1.15 | 41.27 | 15.14 | 34.38 | 0.23 | 3.94 | 1.32 | 0.65 | 3.46 |
| September | 6.25 | 95.55 | 93.22 | 187.46 | 0.91 | 1.16 | 8.99 | 8.70 | 0.42 |
| October | 3.31 | 60.64 | 40.57 | 99.43 | 0.68 | 1.52 | 3.11 | 2.82 | 0.93 |
| November | 8.14 | 118.61 | 195.78 | 244.17 | 0.65 | 1.52 | 2.65 | 2.03 | 0.86 |
| December | 1.59 | 74.19 | 37.60 | 47.68 | 0.18 | 5.47 | 1.34 | 0.70 | 5.41 |

Station no.3117070

| Month | Mean Daily (mm) | Maximum (mm) | Variance (mm) | Mean Monthly (mm) | Wet-days (%) | Dry-Spell (day) | Wet-Spell (day) | Standard dev. Wet-Spell (day) | Standard dev. Dry-Spell (day) |
|---|---|---|---|---|---|---|---|---|---|
| January | 4.34 | 77.97 | 63.99 | 130.23 | 0.75 | 1.42 | 3.97 | 4.04 | 0.81 |
| February | 6.39 | 136.44 | 195.74 | 191.57 | 0.54 | 1.84 | 2.15 | 1.65 | 1.28 |
| March | 5.34 | 98.77 | 95.12 | 160.30 | 0.69 | 1.44 | 3.06 | 2.56 | 0.80 |
| April | 15.65 | 222.01 | 571.34 | 469.59 | 0.67 | 1.48 | 2.85 | 2.30 | 0.84 |
| May | 24.62 | 282.35 | 978.50 | 738.47 | 0.83 | 1.25 | 5.15 | 4.86 | 0.55 |
| June | 13.18 | 206.24 | 589.27 | 395.48 | 0.48 | 1.98 | 1.88 | 1.30 | 1.40 |
| July | 3.52 | 85.79 | 69.59 | 105.54 | 0.47 | 2.04 | 1.82 | 1.21 | 1.45 |
| August | 4.18 | 120.11 | 140.36 | 125.39 | 0.22 | 4.09 | 1.28 | 0.62 | 3.52 |
| September | 21.86 | 209.76 | 953.83 | 655.79 | 0.61 | 1.61 | 2.45 | 1.88 | 0.99 |
| October | 15.36 | 187.39 | 616.69 | 460.71 | 0.53 | 1.87 | 2.12 | 1.54 | 1.31 |
| November | 1.47 | 52.92 | 20.39 | 44.16 | 0.30 | 3.36 | 1.56 | 1.01 | 3.43 |
| December | 0.30 | 51.94 | 8.13 | 8.93 | 0.01 | 25.72 | 1.10 | 0.15 | 8.37 |

Station no.3118069

| Month | Mean Daily (mm) | Maximum (mm) | Variance (mm) | Mean Monthly (mm) | Wet-days (%) | Dry-Spell (day) | Wet-Spell (day) | Standard dev. Wet-Spell (day) | Standard dev. Dry-Spell (day) |
|---|---|---|---|---|---|---|---|---|---|
| January | 5.41 | 45.19 | 38.53 | 162.29 | 0.73 | 1.40 | 3.51 | 2.93 | 0.75 |
| February | 5.53 | 59.60 | 59.78 | 165.89 | 0.63 | 1.75 | 2.89 | 3.18 | 1.22 |
| March | 7.83 | 69.46 | 96.27 | 234.76 | 0.69 | 1.46 | 3.12 | 2.58 | 0.82 |
| April | 5.38 | 52.12 | 53.84 | 161.38 | 0.64 | 1.58 | 2.72 | 2.19 | 0.99 |
| May | 7.25 | 62.05 | 79.29 | 217.60 | 0.73 | 1.39 | 3.44 | 3.01 | 0.74 |
| June | 3.14 | 37.81 | 22.38 | 94.18 | 0.54 | 1.86 | 2.14 | 1.60 | 1.26 |
| July | 2.66 | 46.34 | 24.27 | 79.77 | 0.56 | 1.79 | 2.19 | 1.62 | 1.17 |
| August | 3.26 | 55.72 | 46.16 | 97.72 | 0.35 | 2.88 | 1.65 | 1.21 | 2.59 |
| September | 5.31 | 75.79 | 74.31 | 159.33 | 0.61 | 1.68 | 2.56 | 2.16 | 1.10 |
| October | 7.43 | 81.20 | 114.66 | 222.87 | 0.66 | 1.51 | 2.86 | 2.31 | 0.88 |
| November | 6.42 | 83.93 | 111.54 | 192.68 | 0.57 | 1.81 | 2.34 | 1.88 | 1.28 |
| December | 3.99 | 43.88 | 29.56 | 119.76 | 0.66 | 1.53 | 2.90 | 2.42 | 0.91 |

Station no.3216001

| Month | Mean Daily (mm) | Maximum (mm) | Variance (mm) | Mean Monthly (mm) | Wet-days (%) | Dry-Spell (day) | Wet-Spell (day) | Standard dev. Wet-Spell (day) | Standard dev. Dry-Spell (day) |
|---|---|---|---|---|---|---|---|---|---|
| January | 1.45 | 56.78 | 23.65 | 43.52 | 0.22 | 4.27 | 1.30 | 0.62 | 3.98 |
| February | 7.22 | 139.24 | 193.06 | 216.65 | 0.58 | 1.78 | 2.36 | 2.01 | 1.27 |
| March | 7.00 | 106.38 | 142.81 | 210.02 | 0.71 | 1.39 | 3.29 | 2.83 | 0.75 |
| April | 15.34 | 199.23 | 595.69 | 460.26 | 0.61 | 1.60 | 2.45 | 1.92 | 0.97 |
| May | 29.79 | 277.06 | 1172.79 | 893.68 | 0.92 | 1.23 | 9.66 | 9.16 | 0.54 |
| June | 0.07 | 25.18 | 1.77 | 2.05 | 0.01 | 26.23 | 1.08 | 0.11 | 8.10 |
| July | 7.50 | 173.20 | 315.29 | 224.97 | 0.34 | 2.85 | 1.52 | 0.93 | 2.36 |
| August | 5.24 | 146.53 | 237.00 | 157.28 | 0.22 | 4.16 | 1.31 | 0.62 | 3.87 |
| September | 22.61 | 240.73 | 950.18 | 678.35 | 0.72 | 1.40 | 3.32 | 2.78 | 0.77 |
| October | 5.53 | 98.02 | 113.67 | 165.75 | 0.54 | 1.91 | 2.22 | 1.78 | 1.36 |
| November | 14.92 | 189.50 | 464.94 | 447.63 | 0.77 | 1.31 | 4.07 | 3.61 | 0.63 |
| December | 3.98 | 96.99 | 91.26 | 119.50 | 0.41 | 2.38 | 1.70 | 1.06 | 1.83 |

Station no.3217001

| Month | Mean Daily (mm) | Maximum (mm) | Variance (mm) | Mean Monthly (mm) | Wet-days (%) | Dry-Spell (day) | Wet-Spell (day) | Standard dev. Wet-Spell (day) | Standard dev. Dry-Spell (day) |
|---|---|---|---|---|---|---|---|---|---|
| January | 0.56 | 36.71 | 7.55 | 16.75 | 0.11 | 7.55 | 1.21 | 0.49 | 7.13 |
| February | 10.06 | 139.02 | 260.42 | 301.72 | 0.65 | 1.68 | 2.99 | 3.05 | 1.14 |
| March | 6.99 | 117.25 | 167.94 | 209.74 | 0.58 | 1.68 | 2.33 | 1.74 | 1.06 |
| April | 9.51 | 152.30 | 289.49 | 285.31 | 0.55 | 1.79 | 2.15 | 1.56 | 1.22 |
| May | 16.35 | 169.64 | 454.05 | 490.48 | 0.87 | 1.23 | 6.78 | 6.75 | 0.52 |
| June | 1.96 | 98.63 | 53.71 | 58.81 | 0.20 | 4.51 | 1.27 | 0.60 | 4.15 |
| July | 6.27 | 87.24 | 103.29 | 187.96 | 0.76 | 1.34 | 3.81 | 3.36 | 0.69 |
| August | 3.18 | 87.35 | 73.38 | 95.33 | 0.35 | 2.69 | 1.52 | 0.89 | 2.09 |
| September | 11.49 | 162.32 | 360.47 | 344.81 | 0.61 | 1.61 | 2.42 | 1.88 | 0.97 |
| October | 9.60 | 167.96 | 303.27 | 287.93 | 0.68 | 1.45 | 2.94 | 2.35 | 0.78 |
| November | 15.73 | 158.45 | 368.80 | 471.84 | 0.93 | 1.15 | 10.89 | 9.24 | 0.40 |
| December | 5.54 | 99.81 | 112.51 | 166.14 | 0.59 | 1.66 | 2.35 | 1.76 | 1.07 |

Station no.3217002

| Month | Mean Daily (mm) | Maximum (mm) | Variance (mm) | Mean Monthly (mm) | Wet-days (%) | Dry-Spell (day) | Wet-Spell (day) | Standard dev. Wet-Spell (day) | Standard dev. Dry-Spell (day) |
|---|---|---|---|---|---|---|---|---|---|
| January | 4.53 | 115.50 | 115.88 | 136.05 | 0.38 | 2.55 | 1.61 | 1.01 | 2.05 |
| February | 4.68 | 100.92 | 117.17 | 140.26 | 0.38 | 2.50 | 1.60 | 0.98 | 1.95 |
| March | 6.32 | 107.72 | 135.03 | 189.61 | 0.55 | 1.78 | 2.13 | 1.51 | 1.18 |
| April | 7.81 | 126.83 | 207.71 | 234.24 | 0.57 | 1.71 | 2.21 | 1.62 | 1.12 |
| May | 9.72 | 150.56 | 237.37 | 291.56 | 0.72 | 1.45 | 3.40 | 3.04 | 0.82 |
| June | 3.29 | 82.15 | 64.11 | 98.60 | 0.39 | 2.45 | 1.61 | 1.02 | 1.88 |
| July | 6.21 | 95.34 | 138.22 | 186.32 | 0.47 | 2.03 | 1.83 | 1.21 | 1.47 |
| August | 3.76 | 87.38 | 67.84 | 112.79 | 0.56 | 1.73 | 2.21 | 1.66 | 1.11 |
| September | 12.95 | 160.49 | 356.88 | 388.61 | 0.76 | 1.33 | 3.96 | 3.53 | 0.69 |
| October | 17.35 | 207.96 | 730.87 | 520.59 | 0.66 | 1.50 | 2.75 | 2.17 | 0.85 |
| November | 5.62 | 111.85 | 134.43 | 168.53 | 0.48 | 2.04 | 1.93 | 1.39 | 1.47 |
| December | 3.93 | 80.43 | 90.74 | 117.99 | 0.37 | 2.59 | 1.57 | 0.94 | 2.04 |

Station no.3217003

| Month | Mean Daily (mm) | Maximum (mm) | Variance (mm) | Mean Monthly (mm) | Wet-days (%) | Dry-Spell (day) | Wet-Spell (day) | Standard dev. Wet-Spell (day) | Standard dev. Dry-Spell (day) |
|---|---|---|---|---|---|---|---|---|---|
| January | 4.08 | 26.14 | 53.91 | 122.44 | 0.69 | 1.44 | 3.06 | 2.46 | 0.79 |
| February | 4.74 | 29.13 | 60.30 | 142.17 | 0.71 | 1.40 | 3.21 | 2.63 | 0.73 |
| March | 6.37 | 30.88 | 63.45 | 191.03 | 0.77 | 1.28 | 3.95 | 3.36 | 0.61 |
| April | 6.64 | 37.68 | 96.28 | 199.32 | 0.74 | 1.34 | 3.49 | 2.90 | 0.66 |
| May | 7.30 | 35.70 | 84.12 | 218.95 | 0.78 | 1.29 | 4.02 | 3.32 | 0.60 |
| June | 5.71 | 24.69 | 37.79 | 171.28 | 0.81 | 1.22 | 4.57 | 3.94 | 0.52 |
| July | 5.38 | 26.22 | 45.73 | 161.35 | 0.77 | 1.29 | 4.04 | 3.34 | 0.58 |
| August | 7.06 | 32.47 | 66.73 | 211.77 | 0.79 | 1.26 | 4.32 | 3.83 | 0.59 |
| September | 7.82 | 40.70 | 109.44 | 234.54 | 0.76 | 1.32 | 3.81 | 3.15 | 0.65 |
| October | 9.54 | 40.78 | 105.54 | 286.13 | 0.82 | 1.24 | 4.86 | 4.33 | 0.53 |
| November | 7.24 | 38.25 | 92.43 | 217.27 | 0.76 | 1.30 | 3.84 | 3.21 | 0.61 |
| December | 3.72 | 25.95 | 51.20 | 111.50 | 0.68 | 1.45 | 2.96 | 2.41 | 0.79 |

Station no.3217004

| Month | Mean Daily (mm) | Maximum (mm) | Variance (mm) | Mean Monthly (mm) | Wet-days (%) | Dry-Spell (day) | Wet-Spell (day) | Standard dev. Wet-Spell (day) | Standard dev. Dry-Spell (day) |
|---|---|---|---|---|---|---|---|---|---|
| January | 2.80 | 99.77 | 41.66 | 84.11 | 0.38 | 2.52 | 1.62 | 0.99 | 1.97 |
| February | 2.78 | 148.82 | 49.72 | 83.29 | 0.33 | 2.89 | 1.51 | 0.89 | 2.41 |
| March | 5.88 | 109.05 | 99.62 | 176.26 | 0.63 | 1.59 | 2.59 | 2.10 | 0.95 |
| April | 9.21 | 163.62 | 186.66 | 276.43 | 0.72 | 1.38 | 3.23 | 2.62 | 0.74 |
| May | 28.92 | 131.50 | 5086.85 | 867.73 | 0.73 | 1.39 | 3.48 | 2.87 | 0.75 |
| June | 8.15 | 82.08 | 169.71 | 244.52 | 0.60 | 1.65 | 2.46 | 1.91 | 1.02 |
| July | 5.65 | 74.28 | 120.24 | 169.46 | 0.54 | 1.81 | 2.12 | 1.52 | 1.20 |
| August | 5.88 | 98.61 | 184.77 | 176.44 | 0.36 | 2.62 | 1.54 | 0.90 | 2.08 |
| September | 9.37 | 102.36 | 197.34 | 281.13 | 0.72 | 1.36 | 3.32 | 2.79 | 0.70 |
| October | 10.49 | 144.52 | 199.21 | 314.79 | 0.81 | 1.22 | 4.71 | 4.31 | 0.50 |
| November | 11.28 | 118.40 | 199.82 | 338.30 | 0.88 | 1.13 | 6.67 | 5.88 | 0.38 |
| December | 4.83 | 93.71 | 74.52 | 144.84 | 0.57 | 1.75 | 2.27 | 1.71 | 1.15 |

Station no.3317004

| Month | Mean Daily (mm) | Maximum (mm) | Variance (mm) | Mean Monthly (mm) | Wet-days (%) | Dry-Spell (day) | Wet-Spell (day) | Standard dev. Wet-Spell (day) | Standard dev. Dry-Spell (day) |
|---|---|---|---|---|---|---|---|---|---|
| January | 1.41 | 64.37 | 23.65 | 42.10 | 0.22 | 4.27 | 1.30 | 0.62 | 3.98 |
| February | 7.18 | 74.51 | 193.06 | 215.20 | 0.58 | 1.78 | 2.36 | 2.01 | 1.27 |
| March | 6.96 | 89.50 | 142.81 | 208.60 | 0.71 | 1.39 | 3.29 | 2.83 | 0.75 |
| April | 15.29 | 117.24 | 595.69 | 458.80 | 0.61 | 1.60 | 2.45 | 1.92 | 0.97 |
| May | 29.75 | 847.87 | 1172.79 | 892.30 | 0.92 | 1.23 | 9.66 | 9.16 | 0.54 |
| June | 0.33 | 108.53 | 1.77 | 9.79 | 0.01 | 26.23 | 1.08 | 0.11 | 8.10 |
| July | 7.46 | 102.69 | 315.29 | 223.60 | 0.34 | 2.85 | 1.52 | 0.93 | 2.36 |
| August | 5.19 | 122.73 | 237.00 | 155.90 | 0.22 | 4.16 | 1.31 | 0.62 | 3.87 |
| September | 22.56 | 108.82 | 950.18 | 676.90 | 0.72 | 1.40 | 3.32 | 2.78 | 0.77 |
| October | 5.48 | 110.66 | 113.67 | 164.30 | 0.54 | 1.91 | 2.22 | 1.78 | 1.36 |
| November | 14.87 | 112.45 | 464.94 | 446.20 | 0.77 | 1.31 | 4.07 | 3.61 | 0.63 |
| December | 3.94 | 80.84 | 91.26 | 118.10 | 0.41 | 2.38 | 1.70 | 1.06 | 1.83 |

### D- Projected rainfall for 2020s - B2 scenario

Station no.3116005

| Month | Mean Daily (mm) | Maximum (mm) | Variance (mm) | Mean Monthly (mm) | Wet-days (%) | Dry-Spell (day) | Wet-Spell (day) | Standard dev. Wet-Spell (day) | Standard dev. Dry-Spell (day) |
|---|---|---|---|---|---|---|---|---|---|
| January | 1.53 | 52.58 | 42.40 | 45.89 | 0.27 | 3.28 | 1.34 | 0.73 | 2.48 |
| February | 4.66 | 87.69 | 142.00 | 139.80 | 0.45 | 2.20 | 1.82 | 1.32 | 1.40 |
| March | 5.48 | 81.95 | 149.00 | 164.40 | 0.53 | 1.95 | 2.14 | 1.63 | 1.12 |
| April | 9.49 | 117.23 | 319.00 | 284.80 | 0.57 | 1.81 | 2.33 | 1.81 | 0.97 |
| May | 11.61 | 74.44 | 416.00 | 348.50 | 0.65 | 1.81 | 3.10 | 3.03 | 1.06 |
| June | 1.95 | 63.26 | 76.20 | 58.51 | 0.18 | 4.75 | 1.27 | 0.69 | 4.69 |
| July | 5.54 | 55.57 | 193.00 | 166.20 | 0.40 | 2.45 | 1.66 | 1.10 | 1.62 |
| August | 5.03 | 64.55 | 200.00 | 150.70 | 0.35 | 2.77 | 1.53 | 0.97 | 2.03 |
| September | 11.09 | 90.27 | 376.00 | 332.50 | 0.61 | 1.73 | 2.57 | 2.08 | 0.89 |
| October | 6.21 | 78.50 | 146.00 | 186.40 | 0.54 | 1.93 | 2.22 | 1.75 | 1.11 |
| November | 8.77 | 83.07 | 236.00 | 263.10 | 0.68 | 1.61 | 3.10 | 2.63 | 0.74 |
| December | 3.99 | 84.46 | 109.00 | 119.70 | 0.46 | 2.21 | 1.84 | 1.30 | 1.39 |

Station no.3116006

| Month | Mean Daily (mm) | Maximum (mm) | Variance (mm) | Mean Monthly (mm) | Wet-days (%) | Dry-Spell (day) | Wet-Spell (day) | Standard dev. Wet-Spell (day) | Standard dev. Dry-Spell (day) |
|---|---|---|---|---|---|---|---|---|---|
| January | 3.50 | 65.57 | 52.20 | 105.10 | 0.45 | 2.15 | 1.76 | 1.17 | 1.58 |
| February | 6.91 | 110.59 | 151.24 | 207.37 | 0.62 | 1.59 | 2.54 | 2.03 | 1.00 |
| March | 6.64 | 95.31 | 134.59 | 199.13 | 0.66 | 1.50 | 2.85 | 2.36 | 0.86 |
| April | 9.57 | 162.97 | 280.56 | 287.14 | 0.60 | 1.63 | 2.36 | 1.83 | 0.99 |
| May | 5.97 | 99.98 | 120.09 | 179.16 | 0.60 | 1.66 | 2.40 | 1.87 | 1.04 |
| June | 3.67 | 81.49 | 71.38 | 110.15 | 0.39 | 2.46 | 1.59 | 0.97 | 1.87 |
| July | 2.60 | 66.89 | 46.95 | 77.91 | 0.33 | 2.89 | 1.50 | 0.86 | 2.37 |
| August | 2.73 | 72.10 | 44.78 | 81.90 | 0.35 | 2.66 | 1.52 | 0.87 | 2.08 |
| September | 7.04 | 97.64 | 132.64 | 211.32 | 0.72 | 1.39 | 3.27 | 2.77 | 0.73 |
| October | 5.23 | 82.68 | 86.08 | 156.83 | 0.64 | 1.60 | 2.71 | 2.26 | 0.99 |
| November | 8.87 | 117.81 | 201.08 | 265.98 | 0.70 | 1.41 | 3.14 | 2.55 | 0.72 |
| December | 4.25 | 91.76 | 94.31 | 127.42 | 0.42 | 2.40 | 1.75 | 1.14 | 1.84 |

Station no.3117070

| Month | Mean Daily (mm) | Maximum (mm) | Variance (mm) | Mean Monthly (mm) | Wet-days (%) | Dry-Spell (day) | Wet-Spell (day) | Standard dev. Wet-Spell (day) | Standard dev. Dry-Spell (day) |
|---|---|---|---|---|---|---|---|---|---|
| January | 4.64 | 95.50 | 99.03 | 139.40 | 0.48 | 2.04 | 1.90 | 1.33 | 1.50 |
| February | 7.02 | 158.02 | 268.72 | 210.6 | 0.45 | 2.16 | 1.76 | 1.18 | 1.61 |
| March | 6.43 | 105.52 | 138.47 | 192.89 | 0.56 | 1.74 | 2.17 | 1.58 | 1.14 |
| April | 11.43 | 162.46 | 392.70 | 343.02 | 0.62 | 1.58 | 2.48 | 1.87 | 0.94 |
| May | 11.38 | 158.60 | 353.36 | 341.53 | 0.61 | 1.64 | 2.47 | 1.96 | 1.01 |
| June | 6.63 | 137.77 | 220.18 | 198.97 | 0.40 | 2.36 | 1.63 | 1.01 | 1.75 |
| July | 4.19 | 100.51 | 95.80 | 125.68 | 0.41 | 2.34 | 1.63 | 1.00 | 1.76 |
| August | 5.31 | 120.45 | 151.43 | 159.42 | 0.38 | 2.57 | 1.59 | 0.99 | 1.99 |
| September | 11.37 | 170.81 | 368.45 | 341.30 | 0.57 | 1.73 | 2.22 | 1.65 | 1.14 |
| October | 10.87 | 156.84 | 334.63 | 326.07 | 0.57 | 1.71 | 2.23 | 1.65 | 1.13 |
| November | 4.26 | 92.84 | 80.16 | 127.81 | 0.53 | 1.90 | 2.14 | 1.66 | 1.31 |
| December | 3.00 | 98.48 | 78.70 | 89.88 | 0.26 | 3.63 | 1.41 | 0.76 | 3.40 |

Station no. 3118069

| Month | Mean Daily (mm) | Maximum (mm) | Variance (mm) | Mean Monthly (mm) | Wet-days (%) | Dry-Spell (day) | Wet-Spell (day) | Standard dev. Wet-Spell (day) | Standard dev. Dry-Spell (day) |
|---|---|---|---|---|---|---|---|---|---|
| January | 4.81 | 39.71 | 33.97 | 144.54 | 0.73 | 1.41 | 3.46 | 3.01 | 0.76 |
| February | 5.66 | 60.14 | 58.43 | 169.82 | 0.65 | 1.54 | 2.70 | 2.21 | 0.94 |
| March | 6.73 | 63.17 | 72.88 | 201.86 | 0.71 | 1.39 | 3.14 | 2.50 | 0.73 |
| April | 6.03 | 53.23 | 56.22 | 181.02 | 0.73 | 1.38 | 3.42 | 2.91 | 0.75 |
| May | 6.08 | 55.94 | 60.68 | 182.51 | 0.71 | 1.42 | 3.33 | 2.92 | 0.77 |
| June | 3.64 | 36.08 | 23.81 | 109.10 | 0.64 | 1.54 | 2.67 | 2.11 | 0.91 |
| July | 4.02 | 55.8 | 40.59 | 120.53 | 0.63 | 1.58 | 2.58 | 1.96 | 0.95 |
| August | 4.50 | 55.97 | 50.88 | 134.92 | 0.57 | 1.80 | 2.34 | 2.00 | 1.24 |
| September | 6.16 | 73.52 | 73.67 | 184.96 | 0.71 | 1.43 | 3.29 | 2.84 | 0.81 |
| October | 7.29 | 74.38 | 90.39 | 218.71 | 0.77 | 1.31 | 3.90 | 3.37 | 0.63 |
| November | 6.95 | 80.67 | 103.16 | 208.37 | 0.70 | 1.43 | 3.15 | 2.75 | 0.78 |
| December | 4.68 | 42.46 | 34.85 | 140.42 | 0.72 | 1.40 | 3.42 | 3.07 | 0.76 |

Station no. 3216001

| Month | Mean Daily (mm) | Maximum (mm) | Variance (mm) | Mean Monthly (mm) | Wet-days (%) | Dry-Spell (day) | Wet-Spell (day) | Standard dev. Wet-Spell (day) | Standard dev. Dry-Spell (day) |
|---|---|---|---|---|---|---|---|---|---|
| January | 2.39 | 66.45 | 42.21 | 71.89 | 0.31 | 3.06 | 1.42 | 0.78 | 2.48 |
| February | 5.52 | 115.37 | 139.42 | 165.78 | 0.47 | 2.05 | 1.86 | 1.25 | 1.49 |
| March | 6.35 | 118.42 | 150.83 | 190.43 | 0.57 | 1.72 | 2.22 | 1.65 | 1.10 |
| April | 10.36 | 156.39 | 318.10 | 310.84 | 0.61 | 1.62 | 2.44 | 1.88 | 0.98 |
| May | 12.48 | 173.07 | 411.67 | 374.45 | 0.66 | 1.61 | 3.01 | 2.71 | 1.09 |
| June | 2.82 | 97.69 | 84.28 | 84.51 | 0.22 | 4.28 | 1.31 | 0.65 | 4.25 |
| July | 6.18 | 123.05 | 185.13 | 185.16 | 0.44 | 2.21 | 1.73 | 1.12 | 1.64 |
| August | 5.89 | 129.33 | 195.45 | 176.68 | 0.36 | 2.67 | 1.56 | 0.93 | 2.15 |
| September | 11.61 | 167.23 | 384.02 | 348.51 | 0.65 | 1.50 | 2.64 | 2.11 | 0.87 |
| October | 7.08 | 118.85 | 162.71 | 212.42 | 0.57 | 1.75 | 2.28 | 1.77 | 1.18 |
| November | 9.64 | 126.02 | 223.94 | 289.07 | 0.71 | 1.38 | 3.20 | 2.68 | 0.72 |
| December | 4.86 | 104.82 | 109.43 | 145.73 | 0.49 | 1.99 | 1.94 | 1.37 | 1.44 |

Station no. 3217001

| Month | Mean Daily (mm) | Maximum (mm) | Variance (mm) | Mean Monthly (mm) | Wet-days (%) | Dry-Spell (day) | Wet-Spell (day) | Standard dev. Wet-Spell (day) | Standard dev. Dry-Spell (day) |
|---|---|---|---|---|---|---|---|---|---|
| January | 1.62 | 63.39 | 28.01 | 48.77 | 0.24 | 3.87 | 1.34 | 0.68 | 3.37 |
| February | 6.73 | 134.23 | 192.95 | 201.83 | 0.44 | 2.23 | 1.79 | 1.24 | 1.70 |
| March | 6.74 | 120.87 | 167.05 | 202.14 | 0.54 | 1.82 | 2.09 | 1.48 | 1.21 |
| April | 8.59 | 134.21 | 231.33 | 257.74 | 0.59 | 1.65 | 2.30 | 1.73 | 1.04 |
| May | 9.11 | 134.24 | 245.96 | 273.25 | 0.66 | 1.54 | 2.82 | 2.37 | 0.96 |
| June | 3.64 | 103.29 | 96.58 | 109.10 | 0.35 | 2.78 | 1.52 | 0.91 | 2.25 |
| July | 5.79 | 101.39 | 128.87 | 173.57 | 0.55 | 1.80 | 2.17 | 1.67 | 1.21 |
| August | 4.95 | 111.75 | 135.79 | 148.64 | 0.40 | 2.40 | 1.65 | 1.04 | 1.80 |
| September | 9.24 | 133.84 | 258.37 | 277.50 | 0.62 | 1.58 | 2.48 | 1.88 | 0.94 |
| October | 9.34 | 140.16 | 256.92 | 280.05 | 0.66 | 1.48 | 2.79 | 2.20 | 0.83 |
| November | 10.56 | 138.60 | 271.38 | 316.57 | 0.78 | 1.29 | 4.25 | 3.70 | 0.62 |
| December | 4.88 | 95.58 | 104.80 | 146.40 | 0.52 | 1.86 | 2.05 | 1.44 | 1.26 |

Station no.3217002

| Month | Mean Daily (mm) | Maximum (mm) | Variance (mm) | Mean Monthly (mm) | Wet-days (%) | Dry-Spell (day) | Wet-Spell (day) | Standard dev. Wet-Spell (day) | Standard dev. Dry-Spell (day) |
|---|---|---|---|---|---|---|---|---|---|
| January | 4.06 | 99.32 | 105.30 | 122.03 | 0.36 | 2.66 | 1.52 | 0.90 | 2.06 |
| February | 4.55 | 102.56 | 111.88 | 136.66 | 0.38 | 2.53 | 1.60 | 1.01 | 1.97 |
| March | 6.03 | 111.30 | 126.44 | 180.90 | 0.54 | 1.84 | 2.12 | 1.52 | 1.21 |
| April | 7.75 | 132.56 | 210.47 | 232.47 | 0.59 | 1.66 | 2.37 | 1.79 | 1.04 |
| May | 7.49 | 124.91 | 198.52 | 224.63 | 0.58 | 1.71 | 2.32 | 1.77 | 1.16 |
| June | 3.55 | 84.60 | 72.25 | 106.53 | 0.38 | 2.54 | 1.58 | 0.95 | 1.95 |
| July | 5.07 | 89.96 | 102.44 | 151.92 | 0.45 | 2.13 | 1.76 | 1.14 | 1.52 |
| August | 5.15 | 122.58 | 115.93 | 154.43 | 0.50 | 1.95 | 1.97 | 1.40 | 1.38 |
| September | 9.63 | 137.34 | 254.95 | 289.14 | 0.67 | 1.48 | 2.85 | 2.31 | 0.85 |
| October | 10.96 | 179.11 | 368.97 | 328.74 | 0.63 | 1.56 | 2.59 | 1.97 | 0.92 |
| November | 6.99 | 108.39 | 152.55 | 209.62 | 0.59 | 1.70 | 2.42 | 1.89 | 1.10 |
| December | 3.83 | 81.28 | 86.78 | 114.80 | 0.38 | 2.52 | 1.60 | 1.02 | 1.98 |

Station no.3217003

| Month | Mean Daily (mm) | Maximum (mm) | Variance (mm) | Mean Monthly (mm) | Wet-days (%) | Dry-Spell (day) | Wet-Spell (day) | Standard dev. Wet-Spell (day) | Standard dev. Dry-Spell (day) |
|---|---|---|---|---|---|---|---|---|---|
| January | 4.17 | 27.38 | 54.43 | 125.06 | 0.70 | 1.42 | 3.08 | 2.45 | 0.75 |
| February | 4.99 | 29.93 | 61.76 | 149.79 | 0.72 | 1.38 | 3.34 | 2.72 | 0.73 |
| March | 6.00 | 31.31 | 63.63 | 180.01 | 0.76 | 1.31 | 3.78 | 3.09 | 0.64 |
| April | 7.03 | 37.40 | 97.53 | 210.97 | 0.75 | 1.32 | 3.69 | 3.04 | 0.62 |
| May | 6.95 | 35.91 | 84.29 | 208.55 | 0.76 | 1.30 | 3.85 | 3.18 | 0.63 |
| June | 5.00 | 25.10 | 38.15 | 149.96 | 0.77 | 1.29 | 4.01 | 3.41 | 0.60 |
| July | 5.36 | 26.48 | 46.18 | 160.80 | 0.77 | 1.29 | 3.88 | 3.22 | 0.60 |
| August | 6.35 | 32.12 | 65.63 | 190.37 | 0.77 | 1.30 | 3.97 | 3.36 | 0.63 |
| September | 7.69 | 40.28 | 108.72 | 230.75 | 0.76 | 1.30 | 3.74 | 3.07 | 0.63 |
| October | 8.85 | 40.62 | 105.16 | 265.56 | 0.79 | 1.24 | 4.31 | 3.65 | 0.55 |
| November | 7.45 | 36.16 | 93.35 | 223.61 | 0.77 | 1.29 | 3.91 | 3.30 | 0.61 |
| December | 4.37 | 26.27 | 51.72 | 131.09 | 0.71 | 1.39 | 3.27 | 2.77 | 0.75 |

Station no. 3217004

| Month | Mean Daily (mm) | Maximum (mm) | Variance (mm) | Mean Monthly (mm) | Wet-days (%) | Dry-Spell (day) | Wet-Spell (day) | Standard dev. Wet-Spell (day) | Standard dev. Dry-Spell (day) |
|---|---|---|---|---|---|---|---|---|---|
| January | 3.52 | 67.15 | 49.58 | 105.70 | 0.46 | 2.11 | 1.80 | 1.23 | 1.59 |
| February | 3.37 | 121.92 | 62.92 | 101.03 | 0.37 | 2.64 | 1.59 | 0.97 | 2.17 |
| March | 5.03 | 76.39 | 86.82 | 150.92 | 0.54 | 1.82 | 2.10 | 1.54 | 1.28 |
| April | 8.82 | 128.35 | 186.50 | 264.71 | 0.69 | 1.43 | 2.99 | 2.41 | 0.80 |
| May | 25.13 | 91.60 | 4252.80 | 723.82 | 0.68 | 1.45 | 2.98 | 2.41 | 0.82 |
| June | 5.93 | 68.22 | 113.65 | 178.02 | 0.55 | 1.77 | 2.17 | 1.58 | 1.18 |
| July | 5.55 | 74.59 | 114.36 | 166.48 | 0.54 | 1.80 | 2.09 | 1.52 | 1.19 |
| August | 5.60 | 75.37 | 166.77 | 167.99 | 0.37 | 2.54 | 1.57 | 0.95 | 2.00 |
| September | 8.38 | 82.26 | 167.05 | 251.41 | 0.70 | 1.41 | 3.11 | 2.53 | 0.76 |
| October | 10.20 | 93.24 | 196.98 | 305.95 | 0.78 | 1.27 | 4.11 | 3.60 | 0.58 |
| November | 10.22 | 86.46 | 190.53 | 306.55 | 0.86 | 1.16 | 5.84 | 5.05 | 0.43 |
| December | 4.78 | 76.88 | 77.21 | 143.36 | 0.62 | 1.59 | 2.50 | 1.98 | 0.97 |

Station no.3317004

| Month | Mean Daily (mm) | Maximum (mm) | Variance (mm) | Mean Monthly (mm) | Wet-days (%) | Dry-Spell (day) | Wet-Spell (day) | Standard dev. Wet-Spell (day) | Standard dev. Dry-Spell (day) |
|---|---|---|---|---|---|---|---|---|---|
| January | 1.06 | 61.04 | 42.30 | 31.89 | 0.26 | 3.10 | 1.35 | 0.75 | 2.51 |
| February | 4.20 | 72.75 | 142.00 | 125.80 | 0.44 | 2.02 | 1.83 | 1.34 | 1.43 |
| March | 5.01 | 79.07 | 149.00 | 150.40 | 0.52 | 1.77 | 2.15 | 1.65 | 1.15 |
| April | 9.02 | 113.09 | 318.00 | 270.80 | 0.56 | 1.63 | 2.34 | 1.83 | 1.00 |
| May | 11.15 | 766.11 | 416.00 | 334.50 | 0.64 | 1.63 | 3.11 | 3.05 | 1.09 |
| June | 1.48 | 94.50 | 76.10 | 44.51 | 0.17 | 4.57 | 1.28 | 0.71 | 4.72 |
| July | 5.08 | 98.49 | 193.00 | 152.20 | 0.39 | 2.27 | 1.67 | 1.12 | 1.65 |
| August | 4.56 | 123.63 | 200.00 | 136.70 | 0.34 | 2.59 | 1.54 | 0.99 | 2.06 |
| September | 10.62 | 119.52 | 376.00 | 318.50 | 0.60 | 1.55 | 2.58 | 2.10 | 0.92 |
| October | 5.74 | 115.05 | 146.00 | 172.40 | 0.53 | 1.75 | 2.23 | 1.77 | 1.14 |
| November | 8.31 | 120.32 | 236.00 | 249.10 | 0.67 | 1.43 | 3.11 | 2.65 | 0.77 |
| December | 3.53 | 78.37 | 109.00 | 105.70 | 0.45 | 2.03 | 1.85 | 1.32 | 1.42 |

## E- Projected rainfall for 2050s - B2 scenario

Station no.3116005

| Month | Mean Daily (mm) | Maximum (mm) | Variance (mm) | Mean Monthly (mm) | Wet-days (%) | Dry-Spell (day) | Wet-Spell (day) | Standard dev. Wet-Spell (day) | Standard dev. Dry-Spell (day) |
|---|---|---|---|---|---|---|---|---|---|
| January | 1.24 | 55.81 | 30.80 | 37.30 | 0.22 | 3.53 | 1.29 | 0.65 | 3.02 |
| February | 5.12 | 80.24 | 175.00 | 153.40 | 0.49 | 1.90 | 2.03 | 1.57 | 1.33 |
| March | 5.58 | 86.95 | 158.00 | 167.50 | 0.58 | 1.57 | 2.44 | 1.96 | 0.95 |
| April | 10.48 | 115.40 | 425.00 | 314.60 | 0.57 | 1.60 | 2.39 | 1.85 | 0.96 |
| May | 16.12 | 83.50 | 665.00 | 483.90 | 0.76 | 1.38 | 4.83 | 5.02 | 0.75 |
| June | 0.41 | 65.03 | 35.80 | 12.45 | 0.02 | 11.25 | 1.09 | 0.41 | 10.12 |
| July | 5.91 | 52.05 | 237.00 | 177.20 | 0.37 | 2.38 | 1.61 | 1.05 | 1.81 |
| August | 5.23 | 66.99 | 237.00 | 156.70 | 0.28 | 2.97 | 1.41 | 0.81 | 2.43 |
| September | 13.25 | 84.87 | 554.00 | 397.40 | 0.62 | 1.51 | 2.75 | 2.25 | 0.88 |
| October | 5.44 | 84.21 | 147.00 | 163.20 | 0.53 | 1.77 | 2.25 | 1.83 | 1.20 |
| November | 9.99 | 91.77 | 300.00 | 299.70 | 0.70 | 1.35 | 3.50 | 3.01 | 0.70 |
| December | 3.84 | 90.20 | 97.50 | 115.00 | 0.42 | 2.11 | 1.77 | 1.24 | 1.52 |

Station no.3116006

| Month | Mean Daily (mm) | Maximum (mm) | Variance (mm) | Mean Monthly (mm) | Wet-days (%) | Dry-Spell (day) | Wet-Spell (day) | Standard dev. Wet-Spell (day) | Standard dev. Dry-Spell (day) |
|---|---|---|---|---|---|---|---|---|---|
| January | 3.68 | 69.23 | 53.99 | 110.31 | 0.48 | 2.02 | 1.89 | 1.30 | 1.46 |
| February | 7.20 | 111.90 | 140.55 | 216.07 | 0.68 | 1.49 | 2.95 | 2.45 | 0.86 |
| March | 6.68 | 102.25 | 132.12 | 200.46 | 0.68 | 1.44 | 2.91 | 2.39 | 0.78 |
| April | 9.83 | 147.73 | 312.64 | 294.91 | 0.59 | 1.67 | 2.30 | 1.73 | 1.05 |
| May | 6.22 | 106.25 | 128.68 | 186.48 | 0.58 | 1.69 | 2.31 | 1.74 | 1.08 |
| June | 3.52 | 79.53 | 72.51 | 105.65 | 0.36 | 2.60 | 1.53 | 0.88 | 2.07 |
| July | 2.07 | 65.33 | 40.39 | 62.03 | 0.26 | 3.66 | 1.37 | 0.70 | 3.21 |
| August | 2.06 | 64.64 | 31.64 | 61.89 | 0.32 | 3.00 | 1.45 | 0.80 | 2.40 |
| September | 6.62 | 100.12 | 116.66 | 198.47 | 0.76 | 1.33 | 3.85 | 3.32 | 0.66 |
| October | 4.30 | 69.46 | 60.89 | 128.92 | 0.63 | 1.66 | 2.72 | 2.36 | 1.10 |
| November | 8.74 | 118.46 | 201.62 | 262.30 | 0.70 | 1.42 | 3.06 | 2.48 | 0.76 |
| December | 3.28 | 93.77 | 74.25 | 98.38 | 0.34 | 2.94 | 1.55 | 0.99 | 2.48 |

Station no. 3117070

| Month | Mean Daily (mm) | Maximum (mm) | Variance (mm) | Mean Monthly (mm) | Wet-days (%) | Dry-Spell (day) | Wet-Spell (day) | Standard dev. Wet-Spell (day) | Standard dev. Dry-Spell (day) |
|---|---|---|---|---|---|---|---|---|---|
| January | 4.52 | 90.58 | 81.10 | 135.58 | 0.58 | 1.72 | 2.33 | 1.78 | 1.16 |
| February | 6.79 | 151.57 | 235.37 | 203.84 | 0.47 | 2.09 | 1.84 | 1.27 | 1.52 |
| March | 6.05 | 88.85 | 117.05 | 181.30 | 0.59 | 1.66 | 2.32 | 1.70 | 1.03 |
| April | 13.38 | 180.48 | 476.35 | 401.53 | 0.65 | 1.54 | 2.69 | 2.12 | 0.92 |
| May | 15.89 | 183.92 | 561.82 | 476.94 | 0.67 | 1.49 | 2.86 | 2.29 | 0.85 |
| June | 8.46 | 153.38 | 321.97 | 254.06 | 0.43 | 2.24 | 1.71 | 1.09 | 1.67 |
| July | 3.99 | 93.87 | 84.37 | 119.58 | 0.43 | 2.20 | 1.70 | 1.10 | 1.58 |
| August | 4.80 | 111.30 | 143.96 | 144.12 | 0.32 | 2.95 | 1.46 | 0.82 | 2.40 |
| September | 14.59 | 190.06 | 562.28 | 437.80 | 0.58 | 1.69 | 2.32 | 1.73 | 1.06 |
| October | 12.41 | 161.54 | 421.05 | 372.14 | 0.56 | 1.76 | 2.19 | 1.62 | 1.15 |
| November | 2.94 | 77.36 | 50.45 | 88.10 | 0.47 | 2.12 | 1.90 | 1.35 | 1.55 |
| December | 1.61 | 83.78 | 43.37 | 48.13 | 0.15 | 5.94 | 1.20 | 0.48 | 5.47 |

Station no. 3118069

| Month | Mean Daily (mm) | Maximum (mm) | Variance (mm) | Mean Monthly (mm) | Wet-days (%) | Dry-Spell (day) | Wet-Spell (day) | Standard dev. Wet-Spell (day) | Standard dev. Dry-Spell (day) |
|---|---|---|---|---|---|---|---|---|---|
| January | 4.95 | 42.25 | 34.69 | 148.71 | 0.76 | 1.34 | 3.86 | 3.39 | 0.68 |
| February | 5.39 | 56.26 | 56.59 | 161.81 | 0.63 | 1.62 | 2.61 | 2.09 | 1.00 |
| March | 7.26 | 65.65 | 84.05 | 217.82 | 0.71 | 1.42 | 3.29 | 2.80 | 0.78 |
| April | 6.01 | 54.00 | 55.61 | 180.40 | 0.71 | 1.40 | 3.28 | 2.81 | 0.73 |
| May | 6.46 | 60.42 | 65.04 | 193.76 | 0.72 | 1.42 | 3.46 | 2.97 | 0.79 |
| June | 3.47 | 34.49 | 23.30 | 104.02 | 0.60 | 1.68 | 2.43 | 1.94 | 1.08 |
| July | 3.51 | 48.27 | 32.66 | 105.10 | 0.61 | 1.61 | 2.50 | 1.96 | 1.00 |
| August | 4.22 | 58.21 | 52.12 | 126.52 | 0.50 | 2.03 | 2.02 | 1.61 | 1.48 |
| September | 6.14 | 74.95 | 78.12 | 184.35 | 0.70 | 1.44 | 3.23 | 2.82 | 0.79 |
| October | 7.28 | 82.95 | 96.64 | 218.45 | 0.73 | 1.36 | 3.45 | 2.98 | 0.70 |
| November | 6.68 | 83.68 | 103.04 | 200.21 | 0.66 | 1.51 | 2.84 | 2.35 | 0.88 |
| December | 4.62 | 45.45 | 34.11 | 138.42 | 0.72 | 1.43 | 3.35 | 2.93 | 0.77 |

Station no. 3216001

| Month | Mean Daily (mm) | Maximum (mm) | Variance (mm) | Mean Monthly (mm) | Wet-days (%) | Dry-Spell (day) | Wet-Spell (day) | Standard dev. Wet-Spell (day) | Standard dev. Dry-Spell (day) |
|---|---|---|---|---|---|---|---|---|---|
| January | 4.95 | 42.25 | 34.69 | 148.71 | 0.76 | 1.34 | 3.86 | 3.39 | 0.68 |
| February | 5.39 | 56.26 | 56.59 | 161.81 | 0.63 | 1.62 | 2.61 | 2.09 | 1.00 |
| March | 7.26 | 65.65 | 84.05 | 217.82 | 0.71 | 1.42 | 3.29 | 2.80 | 0.78 |
| April | 6.01 | 54.00 | 55.61 | 180.40 | 0.71 | 1.40 | 3.28 | 2.81 | 0.73 |
| May | 6.46 | 60.42 | 65.04 | 193.76 | 0.72 | 1.42 | 3.46 | 2.97 | 0.79 |
| June | 3.47 | 34.49 | 23.30 | 104.02 | 0.60 | 1.68 | 2.43 | 1.94 | 1.08 |
| July | 3.51 | 48.27 | 32.66 | 105.10 | 0.61 | 1.61 | 2.50 | 1.96 | 1.00 |
| August | 4.22 | 58.21 | 52.12 | 126.52 | 0.50 | 2.03 | 2.02 | 1.61 | 1.48 |
| September | 6.14 | 74.95 | 78.12 | 184.35 | 0.70 | 1.44 | 3.23 | 2.82 | 0.79 |
| October | 7.28 | 82.95 | 96.64 | 218.45 | 0.73 | 1.36 | 3.45 | 2.98 | 0.70 |
| November | 6.68 | 83.68 | 103.04 | 200.21 | 0.66 | 1.51 | 2.84 | 2.35 | 0.88 |
| December | 4.62 | 45.45 | 34.11 | 138.42 | 0.72 | 1.43 | 3.35 | 2.93 | 0.77 |

Station no.3217001

| Month | Mean Daily (mm) | Maximum (mm) | Variance (mm) | Mean Monthly (mm) | Wet-days (%) | Dry-Spell (day) | Wet-Spell (day) | Standard dev. Wet-Spell (day) | Standard dev. Dry-Spell (day) |
|---|---|---|---|---|---|---|---|---|---|
| January | 1.16 | 53.62 | 19.66 | 34.73 | 0.19 | 4.72 | 1.29 | 0.63 | 4.37 |
| February | 7.36 | 137.33 | 215.33 | 220.77 | 0.49 | 2.03 | 1.97 | 1.45 | 1.50 |
| March | 6.90 | 113.20 | 172.71 | 206.92 | 0.55 | 1.78 | 2.14 | 1.54 | 1.17 |
| April | 9.07 | 134.88 | 265.17 | 272.06 | 0.58 | 1.68 | 2.26 | 1.65 | 1.09 |
| May | 11.38 | 148.99 | 305.17 | 341.47 | 0.73 | 1.38 | 3.47 | 2.91 | 0.76 |
| June | 3.05 | 98.94 | 80.50 | 91.55 | 0.29 | 3.19 | 1.39 | 0.75 | 2.59 |
| July | 6.05 | 108.19 | 123.20 | 181.34 | 0.62 | 1.60 | 2.51 | 1.91 | 0.99 |
| August | 4.03 | 101.98 | 100.20 | 120.86 | 0.37 | 2.57 | 1.59 | 0.97 | 2.00 |
| September | 9.90 | 149.81 | 283.75 | 297.08 | 0.62 | 1.57 | 2.45 | 1.87 | 0.94 |
| October | 8.91 | 132.09 | 242.32 | 267.04 | 0.67 | 1.48 | 2.80 | 2.25 | 0.81 |
| November | 12.74 | 151.87 | 306.42 | 381.99 | 0.83 | 1.21 | 5.17 | 4.54 | 0.52 |
| December | 5.18 | 87.30 | 101.27 | 155.33 | 0.54 | 1.83 | 2.10 | 1.51 | 1.20 |

Station no. 3217002

| Month | Mean Daily (mm) | Maximum (mm) | Variance (mm) | Mean Monthly (mm) | Wet-days (%) | Dry-Spell (day) | Wet-Spell (day) | Standard dev. Wet-Spell (day) | Standard dev. Dry-Spell (day) |
|---|---|---|---|---|---|---|---|---|---|
| January | 4.04 | 117.68 | 106.03 | 121.13 | 0.35 | 2.78 | 1.52 | 0.88 | 2.26 |
| February | 4.99 | 99.21 | 126.24 | 149.81 | 0.40 | 2.36 | 1.65 | 1.03 | 1.76 |
| March | 6.21 | 99.93 | 136.74 | 186.25 | 0.55 | 1.78 | 2.12 | 1.56 | 1.17 |
| April | 7.97 | 122.37 | 206.49 | 239.07 | 0.60 | 1.66 | 2.37 | 1.73 | 1.03 |
| May | 7.83 | 130.45 | 193.42 | 234.78 | 0.62 | 1.63 | 2.59 | 2.09 | 1.00 |
| June | 3.46 | 82.60 | 74.28 | 103.69 | 0.37 | 2.58 | 1.58 | 0.95 | 2.00 |
| July | 5.34 | 100.72 | 114.34 | 160.11 | 0.45 | 2.14 | 1.81 | 1.23 | 1.58 |
| August | 4.47 | 98.31 | 93.84 | 134.13 | 0.52 | 1.88 | 2.02 | 1.43 | 1.29 |
| September | 10.62 | 133.89 | 278.33 | 318.56 | 0.69 | 1.44 | 3.06 | 2.53 | 0.79 |
| October | 13.25 | 172.42 | 472.21 | 397.57 | 0.64 | 1.54 | 2.59 | 1.99 | 0.92 |
| November | 6.60 | 100.96 | 150.38 | 198.08 | 0.57 | 1.74 | 2.23 | 1.66 | 1.14 |
| December | 3.87 | 93.14 | 86.72 | 116.20 | 0.38 | 2.57 | 1.64 | 1.04 | 2.02 |

Station no. 3217003

| Month | Mean Daily (mm) | Maximum (mm) | Variance (mm) | Mean Monthly (mm) | Wet-days (%) | Dry-Spell (day) | Wet-Spell (day) | Standard dev. Wet-Spell (day) | Standard dev. Dry-Spell (day) |
|---|---|---|---|---|---|---|---|---|---|
| January | 4.19 | 25.70 | 53.81 | 125.63 | 0.70 | 1.41 | 3.10 | 2.56 | 0.74 |
| February | 5.18 | 29.25 | 62.23 | 155.43 | 0.73 | 1.36 | 3.41 | 2.80 | 0.70 |
| March | 6.19 | 31.07 | 63.27 | 185.69 | 0.76 | 1.28 | 3.77 | 3.04 | 0.60 |
| April | 6.97 | 38.08 | 95.95 | 209.19 | 0.75 | 1.33 | 3.65 | 3.01 | 0.65 |
| May | 7.09 | 35.54 | 83.09 | 212.82 | 0.77 | 1.29 | 3.89 | 3.27 | 0.61 |
| June | 5.16 | 23.95 | 38.19 | 154.77 | 0.78 | 1.27 | 4.11 | 3.44 | 0.57 |
| July | 5.30 | 26.78 | 44.91 | 159.14 | 0.77 | 1.30 | 3.91 | 3.28 | 0.61 |
| August | 6.56 | 32.31 | 66.86 | 196.77 | 0.78 | 1.26 | 4.01 | 3.52 | 0.57 |
| September | 7.80 | 39.38 | 109.43 | 233.96 | 0.76 | 1.31 | 3.83 | 3.24 | 0.65 |
| October | 9.14 | 40.39 | 105.21 | 274.14 | 0.80 | 1.23 | 4.49 | 3.88 | 0.52 |
| November | 7.37 | 38.20 | 92.58 | 220.98 | 0.77 | 1.28 | 3.84 | 3.25 | 0.61 |
| December | 4.20 | 26.09 | 51.43 | 125.87 | 0.71 | 1.40 | 3.17 | 2.56 | 0.75 |

Station no.3217004

| Month | Mean Daily (mm) | Maximum (mm) | Variance (mm) | Mean Monthly (mm) | Wet-days (%) | Dry-Spell (day) | Wet-Spell (day) | Standard dev. Wet-Spell (day) | Standard dev. Dry-Spell (day) |
|---|---|---|---|---|---|---|---|---|---|
| January | 3.24 | 82.35 | 47.24 | 97.44 | 0.43 | 2.24 | 1.73 | 1.14 | 1.66 |
| February | 3.43 | 128.92 | 67.48 | 102.82 | 0.38 | 2.54 | 1.58 | 0.96 | 1.98 |
| March | 5.21 | 93.66 | 85.87 | 156.12 | 0.56 | 1.75 | 2.17 | 1.63 | 1.18 |
| April | 8.96 | 146.00 | 182.96 | 268.96 | 0.70 | 1.42 | 3.06 | 2.47 | 0.78 |
| May | 23.82 | 118.73 | 4175.64 | 714.94 | 0.70 | 1.45 | 3.13 | 2.57 | 0.82 |
| June | 6.55 | 81.04 | 126.37 | 196.60 | 0.57 | 1.74 | 2.24 | 1.67 | 1.10 |
| July | 5.61 | 80.73 | 118.85 | 168.18 | 0.55 | 1.77 | 2.13 | 1.51 | 1.18 |
| August | 5.67 | 90.38 | 167.92 | 170.14 | 0.37 | 2.55 | 1.57 | 0.93 | 2.01 |
| September | 8.64 | 89.37 | 178.77 | 259.49 | 0.71 | 1.41 | 3.15 | 2.56 | 0.77 |
| October | 10.19 | 115.58 | 197.80 | 305.46 | 0.80 | 1.25 | 4.37 | 3.70 | 0.55 |
| November | 10.91 | 110.37 | 210.98 | 327.23 | 0.87 | 1.16 | 6.31 | 5.27 | 0.40 |
| December | 5.04 | 94.87 | 76.61 | 151.15 | 0.60 | 1.64 | 2.39 | 1.79 | 1.02 |

Station no. 3317004

| Month | Mean Daily (mm) | Maximum (mm) | Variance (mm) | Mean Monthly (mm) | Wet-days (%) | Dry-Spell (day) | Wet-Spell (day) | Standard dev. Wet-Spell (day) | Standard dev. Dry-Spell (day) |
|---|---|---|---|---|---|---|---|---|---|
| January | 0.84 | 58.14 | 30.90 | 25.30 | 0.28 | 3.51 | 1.32 | 0.67 | 3.03 |
| February | 4.72 | 78.82 | 174.00 | 141.40 | 0.55 | 1.89 | 2.07 | 1.59 | 1.34 |
| March | 5.18 | 85.07 | 158.00 | 155.50 | 0.64 | 1.56 | 2.48 | 1.98 | 0.96 |
| April | 10.08 | 120.59 | 425.00 | 302.60 | 0.63 | 1.59 | 2.43 | 1.87 | 0.97 |
| May | 15.72 | 714.49 | 665.00 | 471.90 | 0.82 | 1.37 | 4.87 | 5.04 | 0.76 |
| June | 0.01 | 88.48 | 35.90 | 0.45 | 0.08 | 11.23 | 1.13 | 0.43 | 10.13 |
| July | 5.51 | 94.46 | 236.00 | 165.20 | 0.43 | 2.37 | 1.65 | 1.07 | 1.82 |
| August | 4.83 | 127.88 | 237.00 | 144.70 | 0.34 | 2.96 | 1.45 | 0.83 | 2.44 |
| September | 12.85 | 117.73 | 554.00 | 385.40 | 0.68 | 1.50 | 2.79 | 2.27 | 0.89 |
| October | 5.04 | 117.91 | 147.00 | 151.20 | 0.59 | 1.76 | 2.29 | 1.85 | 1.21 |
| November | 9.59 | 116.95 | 300.00 | 287.70 | 0.76 | 1.34 | 3.54 | 3.03 | 0.71 |
| December | 3.44 | 71.59 | 97.60 | 103.00 | 0.48 | 2.10 | 1.81 | 1.26 | 1.53 |

## F- Projected rainfall for 2080s - B2 scenario

Station no. 3116005

| Month | Mean Daily (mm) | Maximum (mm) | Variance (mm) | Mean Monthly (mm) | Wet-days (%) | Dry-Spell (day) | Wet-Spell (day) | Standard dev. Wet-Spell (day) | Standard dev. Dry-Spell (day) |
|---|---|---|---|---|---|---|---|---|---|
| January | 1.49 | 58.84 | 23.20 | 25.03 | 0.15 | 4.28 | 1.18 | 0.58 | 3.95 |
| February | 0.80 | 80.60 | 192.00 | 192.90 | 0.51 | 1.79 | 2.24 | 1.97 | 1.24 |
| March | 0.94 | 88.09 | 142.00 | 178.40 | 0.64 | 1.39 | 3.17 | 2.79 | 0.72 |
| April | 0.80 | 112.54 | 595.00 | 393.80 | 0.54 | 1.61 | 2.33 | 1.88 | 0.94 |
| May | 0.67 | 80.48 | 1172.00 | 724.10 | 0.85 | 1.24 | 9.54 | 9.12 | 0.51 |
| June | 2.71 | 57.32 | 1.30 | 4.60 | 0.06 | 26.24 | 0.96 | 0.07 | 8.07 |
| July | 0.87 | 41.68 | 315.00 | 202.90 | 0.27 | 2.86 | 1.39 | 0.89 | 2.33 |
| August | 1.03 | 63.60 | 236.00 | 151.90 | 0.15 | 4.17 | 1.19 | 0.58 | 3.84 |
| September | 0.76 | 84.60 | 949.00 | 524.80 | 0.65 | 1.41 | 3.19 | 2.74 | 0.74 |
| October | 1.19 | 91.63 | 113.00 | 136.80 | 0.47 | 1.92 | 2.09 | 1.74 | 1.33 |
| November | 0.84 | 85.67 | 464.00 | 355.10 | 0.70 | 1.32 | 3.95 | 3.57 | 0.60 |
| December | 1.14 | 77.54 | 90.80 | 100.70 | 0.34 | 2.39 | 1.58 | 1.02 | 1.80 |

Station no.3116006

| Month | Mean Daily (mm) | Maximum (mm) | Variance (mm) | Mean Monthly (mm) | Wet-days (%) | Dry-Spell (day) | Wet-Spell (day) | Standard dev. Wet-Spell (day) | Standard dev. Dry-Spell (day) |
|---|---|---|---|---|---|---|---|---|---|
| January | 3.88 | 73.76 | 59.52 | 116.36 | 0.50 | 1.98 | 1.97 | 1.40 | 1.37 |
| February | 7.83 | 106.12 | 161.64 | 234.79 | 0.69 | 1.45 | 3.02 | 2.49 | 0.84 |
| March | 6.32 | 88.23 | 112.69 | 189.59 | 0.71 | 1.40 | 3.22 | 2.75 | 0.76 |
| April | 9.57 | 156.37 | 300.28 | 287.14 | 0.56 | 1.74 | 2.17 | 1.62 | 1.13 |
| May | 6.89 | 107.90 | 157.10 | 206.56 | 0.58 | 1.70 | 2.30 | 1.76 | 1.09 |
| June | 3.30 | 80.04 | 69.92 | 98.99 | 0.33 | 2.85 | 1.47 | 0.83 | 2.34 |
| July | 1.51 | 63.05 | 29.68 | 45.20 | 0.18 | 5.02 | 1.26 | 0.58 | 4.60 |
| August | 1.53 | 52.86 | 22.27 | 45.76 | 0.27 | 3.38 | 1.37 | 0.71 | 2.80 |
| September | 6.68 | 87.81 | 100.58 | 200.51 | 0.87 | 1.20 | 6.42 | 5.99 | 0.49 |
| October | 3.83 | 61.88 | 48.96 | 114.80 | 0.67 | 1.55 | 3.02 | 2.79 | 0.95 |
| November | 8.32 | 111.58 | 189.57 | 249.65 | 0.67 | 1.48 | 2.86 | 2.27 | 0.83 |
| December | 2.45 | 78.72 | 54.57 | 73.35 | 0.26 | 3.72 | 1.42 | 0.79 | 3.40 |

Station no. 3117070

| Month | Mean Daily (mm) | Maximum (mm) | Variance (mm) | Mean Monthly (mm) | Wet-days (%) | Dry-Spell (day) | Wet-Spell (day) | Standard dev. Wet-Spell (day) | Standard dev. Dry-Spell (day) |
|---|---|---|---|---|---|---|---|---|---|
| January | 4.34 | 73.35 | 63.99 | 130.23 | 0.68 | 1.49 | 3.05 | 2.60 | 0.91 |
| February | 6.38 | 139.33 | 195.74 | 191.57 | 0.52 | 1.93 | 2.08 | 1.52 | 1.36 |
| March | 5.35 | 89.79 | 95.12 | 160.30 | 0.65 | 1.54 | 2.78 | 2.29 | 0.93 |
| April | 14.65 | 200.49 | 571.34 | 439.59 | 0.66 | 1.52 | 2.78 | 2.21 | 0.87 |
| May | 24.61 | 249.75 | 978.50 | 738.47 | 0.76 | 1.33 | 3.81 | 3.31 | 0.68 |
| June | 12.94 | 209.26 | 589.27 | 388.48 | 0.47 | 2.05 | 1.83 | 1.20 | 1.46 |
| July | 3.52 | 86.23 | 69.59 | 105.54 | 0.44 | 2.18 | 1.76 | 1.15 | 1.58 |
| August | 4.18 | 126.84 | 140.36 | 125.39 | 0.26 | 3.55 | 1.36 | 0.69 | 3.12 |
| September | 21.85 | 224.30 | 953.83 | 655.79 | 0.61 | 1.62 | 2.50 | 1.94 | 1.01 |
| October | 15.36 | 196.23 | 616.69 | 460.71 | 0.55 | 1.80 | 2.14 | 1.62 | 1.22 |
| November | 1.47 | 57.13 | 20.39 | 44.16 | 0.37 | 2.73 | 1.64 | 1.08 | 2.33 |
| December | 0.30 | 49.02 | 8.13 | 8.93 | 0.03 | 16.74 | 1.08 | 0.28 | 11.05 |

Station no. 3118069

| Month | Mean Daily (mm) | Maximum (mm) | Variance (mm) | Mean Monthly (mm) | Wet-days (%) | Dry-Spell (day) | Wet-Spell (day) | Standard dev. Wet-Spell (day) | Standard dev. Dry-Spell (day) |
|---|---|---|---|---|---|---|---|---|---|
| January | 5.31 | 45.39 | 35.66 | 159.58 | 0.74 | 1.39 | 3.64 | 3.29 | 0.79 |
| February | 5.60 | 56.47 | 59.18 | 168.04 | 0.65 | 1.67 | 2.98 | 2.95 | 1.08 |
| March | 7.60 | 69.37 | 90.03 | 227.79 | 0.69 | 1.47 | 3.10 | 2.53 | 0.82 |
| April | 5.52 | 52.19 | 53.02 | 165.56 | 0.66 | 1.54 | 2.90 | 2.41 | 0.94 |
| May | 6.98 | 61.78 | 75.36 | 209.58 | 0.72 | 1.41 | 3.40 | 2.93 | 0.75 |
| June | 3.29 | 33.39 | 24.97 | 98.73 | 0.54 | 1.85 | 2.12 | 1.56 | 1.25 |
| July | 3.06 | 42.74 | 29.09 | 91.68 | 0.58 | 1.72 | 2.30 | 1.75 | 1.14 |
| August | 3.46 | 56.33 | 50.01 | 103.84 | 0.39 | 2.57 | 1.70 | 1.14 | 2.13 |
| September | 5.49 | 70.38 | 73.82 | 164.70 | 0.64 | 1.64 | 2.75 | 2.34 | 1.05 |
| October | 7.41 | 88.67 | 103.91 | 222.09 | 0.69 | 1.43 | 3.00 | 2.41 | 0.79 |
| November | 6.91 | 84.97 | 113.27 | 207.26 | 0.61 | 1.66 | 2.52 | 1.99 | 1.05 |
| December | 4.13 | 39.81 | 30.75 | 123.72 | 0.68 | 1.54 | 3.02 | 2.52 | 0.93 |

Station no. 3216001

| Month | Mean Daily (mm) | Maximum (mm) | Variance (mm) | Mean Monthly (mm) | Wet-days (%) | Dry-Spell (day) | Wet-Spell (day) | Standard dev. Wet-Spell (day) | Standard dev. Dry-Spell (day) |
|---|---|---|---|---|---|---|---|---|---|
| January | 1.72 | 58.80 | 28.85 | 51.73 | 0.25 | 3.72 | 1.32 | 0.65 | 3.27 |
| February | 7.32 | 137.80 | 198.59 | 219.57 | 0.57 | 1.79 | 2.33 | 1.86 | 1.22 |
| March | 6.84 | 113.40 | 146.14 | 205.10 | 0.67 | 1.49 | 2.91 | 2.30 | 0.85 |
| April | 14.01 | 191.51 | 527.91 | 420.47 | 0.61 | 1.59 | 2.47 | 1.86 | 0.97 |
| May | 25.02 | 245.75 | 896.04 | 750.76 | 0.90 | 1.23 | 8.65 | 8.07 | 0.52 |
| June | 0.20 | 68.25 | 10.15 | 5.86 | 0.01 | 23.58 | 1.11 | 0.23 | 9.69 |
| July | 6.99 | 155.47 | 299.08 | 209.59 | 0.37 | 2.62 | 1.62 | 1.02 | 2.07 |
| August | 5.85 | 154.78 | 248.89 | 175.59 | 0.27 | 3.46 | 1.37 | 0.73 | 2.95 |
| September | 18.37 | 230.67 | 713.55 | 551.50 | 0.69 | 1.45 | 3.06 | 2.55 | 0.82 |
| October | 5.45 | 99.36 | 115.92 | 163.54 | 0.53 | 1.91 | 2.12 | 1.68 | 1.32 |
| November | 12.73 | 156.44 | 336.10 | 381.84 | 0.76 | 1.32 | 3.86 | 3.25 | 0.63 |
| December | 4.25 | 93.54 | 91.85 | 127.36 | 0.45 | 2.20 | 1.78 | 1.19 | 1.64 |

Station no. 3217001

| Month | Mean Daily (mm) | Maximum (mm) | Variance (mm) | Mean Monthly (mm) | Wet-days (%) | Dry-Spell (day) | Wet-Spell (day) | Standard dev. Wet-Spell (day) | Standard dev. Dry-Spell (day) |
|---|---|---|---|---|---|---|---|---|---|
| January | 0.80 | 47.01 | 12.36 | 23.88 | 0.14 | 6.28 | 1.28 | 0.59 | 6.31 |
| February | 8.84 | 119.83 | 222.27 | 265.19 | 0.59 | 1.81 | 2.52 | 2.16 | 1.27 |
| March | 6.94 | 123.60 | 175.81 | 208.15 | 0.57 | 1.75 | 2.25 | 1.67 | 1.15 |
| April | 8.91 | 148.46 | 261.25 | 267.38 | 0.55 | 1.79 | 2.16 | 1.57 | 1.17 |
| May | 13.84 | 174.04 | 379.56 | 415.35 | 0.84 | 1.24 | 5.37 | 5.03 | 0.56 |
| June | 2.22 | 87.30 | 55.72 | 66.70 | 0.23 | 3.97 | 1.30 | 0.62 | 3.59 |
| July | 6.13 | 97.78 | 114.49 | 183.77 | 0.70 | 1.43 | 3.11 | 2.61 | 0.78 |
| August | 3.38 | 90.93 | 77.22 | 101.38 | 0.36 | 2.66 | 1.53 | 0.90 | 2.00 |
| September | 10.67 | 160.28 | 317.83 | 320.40 | 0.62 | 1.58 | 2.48 | 1.91 | 0.95 |
| October | 9.00 | 148.61 | 258.98 | 269.90 | 0.68 | 1.46 | 2.88 | 2.34 | 0.82 |
| November | 14.64 | 147.18 | 334.21 | 438.89 | 0.92 | 1.13 | 9.16 | 8.04 | 0.37 |
| December | 5.02 | 98.54 | 114.19 | 150.49 | 0.57 | 1.70 | 2.23 | 1.73 | 1.08 |

Station no. 3217002

| Month | Mean Daily (mm) | Maximum (mm) | Variance (mm) | Mean Monthly (mm) | Wet-days (%) | Dry-Spell (day) | Wet-Spell (day) | Standard dev. Wet-Spell (day) | Standard dev. Dry-Spell (day) |
|---|---|---|---|---|---|---|---|---|---|
| January | 4.50 | 99.54 | 129.38 | 135.15 | 0.36 | 2.65 | 1.58 | 0.99 | 2.13 |
| February | 4.69 | 103.10 | 115.13 | 140.67 | 0.39 | 2.47 | 1.61 | 1.01 | 1.87 |
| March | 6.15 | 106.26 | 132.33 | 184.34 | 0.55 | 1.78 | 2.13 | 1.57 | 1.18 |
| April | 7.79 | 124.55 | 197.13 | 233.76 | 0.58 | 1.69 | 2.26 | 1.68 | 1.08 |
| May | 9.38 | 135.24 | 254.86 | 281.48 | 0.69 | 1.47 | 3.14 | 2.67 | 0.85 |
| June | 3.19 | 78.74 | 63.67 | 95.79 | 0.37 | 2.57 | 1.59 | 0.94 | 2.01 |
| July | 5.90 | 102.08 | 128.45 | 176.73 | 0.47 | 2.09 | 1.84 | 1.28 | 1.51 |
| August | 3.57 | 81.18 | 71.91 | 107.14 | 0.55 | 1.78 | 2.13 | 1.53 | 1.13 |
| September | 12.10 | 152.34 | 329.93 | 363.20 | 0.74 | 1.35 | 3.53 | 2.94 | 0.68 |
| October | 15.31 | 221.60 | 586.15 | 459.06 | 0.65 | 1.50 | 2.69 | 2.07 | 0.87 |
| November | 6.10 | 107.54 | 149.34 | 182.94 | 0.50 | 1.96 | 1.98 | 1.40 | 1.39 |
| December | 3.85 | 94.34 | 80.95 | 115.32 | 0.38 | 2.55 | 1.59 | 0.95 | 1.97 |

Station no.3217003

| Month | Mean Daily (mm) | Maximum (mm) | Variance (mm) | Mean Monthly (mm) | Wet-days (%) | Dry-Spell (day) | Wet-Spell (day) | Standard dev. Wet-Spell (day) | Standard dev. Dry-Spell (day) |
|---|---|---|---|---|---|---|---|---|---|
| January | 4.03 | 26.81 | 54.65 | 120.83 | 0.69 | 1.41 | 3.02 | 2.39 | 0.74 |
| February | 4.90 | 28.60 | 62.14 | 146.93 | 0.71 | 1.38 | 3.22 | 2.69 | 0.73 |
| March | 6.36 | 30.26 | 62.93 | 190.91 | 0.77 | 1.27 | 3.96 | 3.28 | 0.57 |
| April | 6.84 | 37.97 | 96.72 | 205.26 | 0.74 | 1.34 | 3.52 | 2.89 | 0.66 |
| May | 7.26 | 36.82 | 85.53 | 217.89 | 0.77 | 1.27 | 3.95 | 3.35 | 0.57 |
| June | 5.27 | 24.66 | 37.64 | 158.14 | 0.79 | 1.27 | 4.17 | 3.69 | 0.57 |
| July | 5.35 | 26.55 | 45.87 | 160.37 | 0.77 | 1.29 | 3.87 | 3.17 | 0.60 |
| August | 6.58 | 32.80 | 67.68 | 197.28 | 0.77 | 1.28 | 4.00 | 3.29 | 0.58 |
| September | 7.80 | 38.99 | 107.77 | 233.86 | 0.76 | 1.30 | 3.84 | 3.26 | 0.62 |
| October | 9.26 | 40.66 | 103.38 | 277.93 | 0.81 | 1.23 | 4.69 | 4.11 | 0.52 |
| November | 7.31 | 37.17 | 92.80 | 219.24 | 0.76 | 1.31 | 3.85 | 3.18 | 0.65 |
| December | 4.04 | 26.59 | 51.23 | 121.14 | 0.70 | 1.41 | 3.07 | 2.46 | 0.76 |

Station no. 3217004

| Month | Mean Daily (mm) | Maximum (mm) | Variance (mm) | Mean Monthly (mm) | Wet-days (%) | Dry-Spell (day) | Wet-Spell (day) | Standard dev. Wet-Spell (day) | Standard dev. Dry-Spell (day) |
|---|---|---|---|---|---|---|---|---|---|
| January | 0.44 | 90.79 | 23.40 | 13.23 | 0.23 | 4.26 | 1.26 | 0.57 | 3.94 |
| February | 6.04 | 135.42 | 193.00 | 181.10 | 0.59 | 1.77 | 2.32 | 1.96 | 1.23 |
| March | 5.55 | 99.23 | 143.00 | 166.60 | 0.72 | 1.38 | 3.25 | 2.78 | 0.71 |
| April | 12.73 | 148.90 | 595.00 | 382.00 | 0.62 | 1.59 | 2.41 | 1.87 | 0.93 |
| May | 23.73 | 119.67 | 1173.00 | 712.30 | 0.93 | 1.22 | 9.62 | 9.11 | 0.50 |
| June | 0.12 | 74.69 | 1.54 | 3.64 | 0.02 | 26.22 | 1.04 | 0.06 | 8.06 |
| July | 6.38 | 67.59 | 315.00 | 191.10 | 0.35 | 2.84 | 1.48 | 0.88 | 2.32 |
| August | 4.67 | 89.73 | 237.00 | 140.10 | 0.23 | 4.15 | 1.27 | 0.57 | 3.83 |
| September | 17.11 | 93.15 | 950.00 | 513.00 | 0.73 | 1.39 | 3.28 | 2.73 | 0.73 |
| October | 4.16 | 131.51 | 113.00 | 125.00 | 0.55 | 1.90 | 2.18 | 1.73 | 1.32 |
| November | 11.45 | 107.74 | 465.00 | 343.30 | 0.78 | 1.30 | 4.03 | 3.56 | 0.59 |
| December | 2.96 | 85.28 | 91.00 | 88.90 | 0.42 | 2.37 | 1.66 | 1.01 | 1.79 |

Station no.3317004

| Month | Mean Daily (mm) | Maximum (mm) | Variance (mm) | Mean Monthly (mm) | Wet-days (%) | Dry-Spell (day) | Wet-Spell (day) | Standard dev. Wet-Spell (day) | Standard dev. Dry-Spell (day) |
|---|---|---|---|---|---|---|---|---|---|
| January | 2.99 | 60.55 | 43.41 | 89.59 | 0.41 | 2.35 | 1.65 | 1.05 | 1.79 |
| February | 3.09 | 76.08 | 58.38 | 92.71 | 0.35 | 2.75 | 1.52 | 0.90 | 2.15 |
| March | 5.54 | 81.36 | 89.50 | 166.26 | 0.60 | 1.67 | 2.43 | 1.88 | 1.08 |
| April | 9.10 | 105.88 | 179.91 | 273.08 | 0.71 | 1.40 | 3.22 | 2.64 | 0.75 |
| May | 25.09 | 749.96 | 4089.51 | 752.82 | 0.71 | 1.39 | 3.17 | 2.59 | 0.73 |
| June | 7.27 | 110.12 | 148.04 | 218.19 | 0.58 | 1.69 | 2.27 | 1.66 | 1.06 |
| July | 5.42 | 103.22 | 112.71 | 162.56 | 0.54 | 1.78 | 2.07 | 1.47 | 1.20 |
| August | 5.64 | 129.61 | 166.34 | 169.05 | 0.37 | 2.56 | 1.56 | 0.89 | 1.96 |
| September | 8.84 | 116.36 | 188.65 | 265.19 | 0.71 | 1.40 | 3.20 | 2.58 | 0.74 |
| October | 10.30 | 115.88 | 199.01 | 309.04 | 0.80 | 1.24 | 4.46 | 3.89 | 0.54 |
| November | 10.94 | 121.39 | 208.10 | 328.09 | 0.86 | 1.15 | 5.99 | 5.35 | 0.42 |
| December | 5.06 | 76.29 | 78.06 | 151.90 | 0.59 | 1.66 | 2.31 | 1.80 | 1.03 |

## Appendix N- The Maps of Infiltration Parameters for Klang Watershed

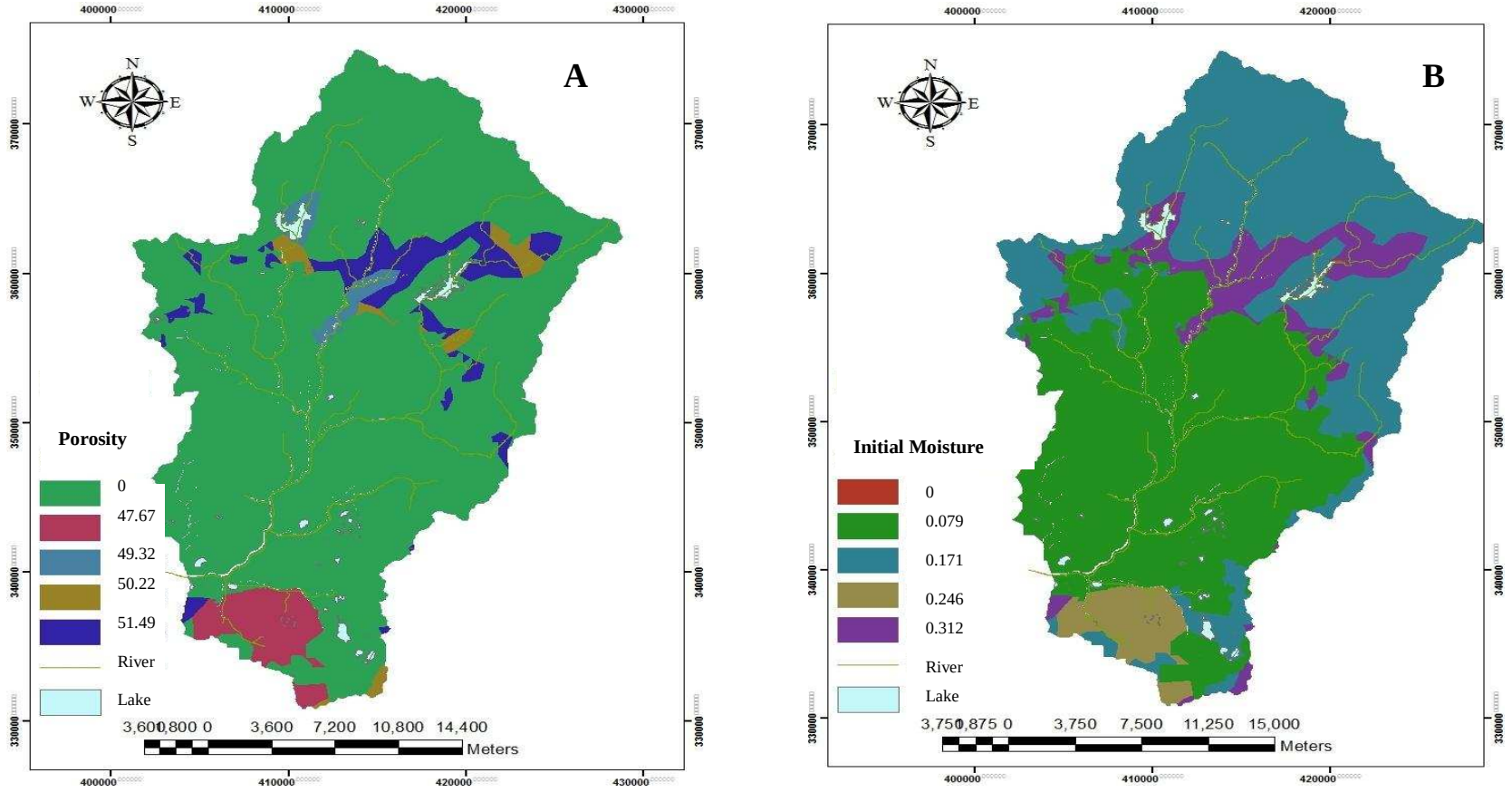


Infiltration parameters for Klang watershed **A :(** Porosity map: in %); **B:** (Initial moisture map: in volume ratio)

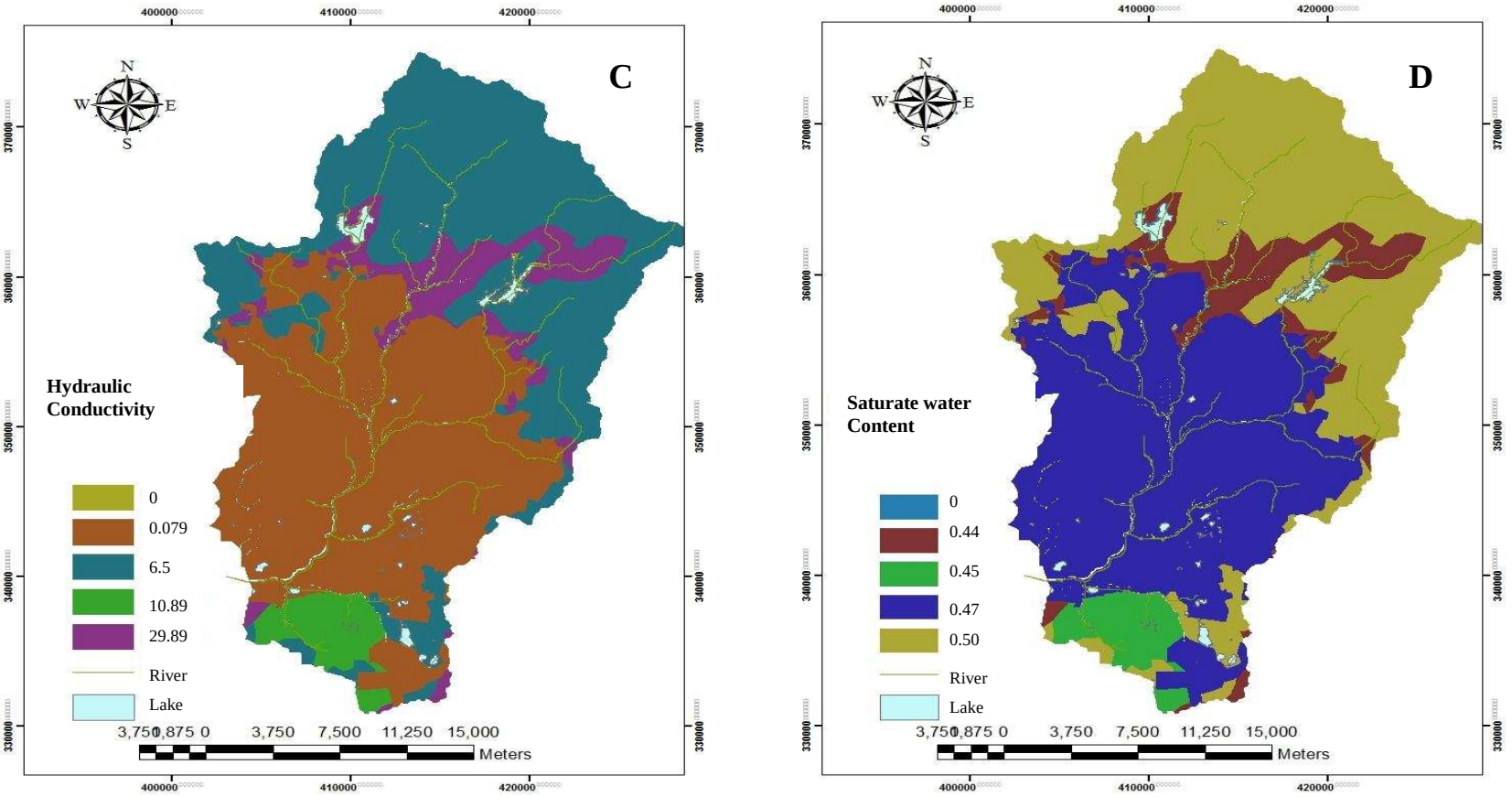


Infiltration parameters for Klang watershed **C :**( Hydraulic conductivity map in mm/h); **D:** (Saturate water content map in volume ratio**)**

## Appendix O- Storage-Discharge Relationships of Klang Gate Dam and Batu Dam

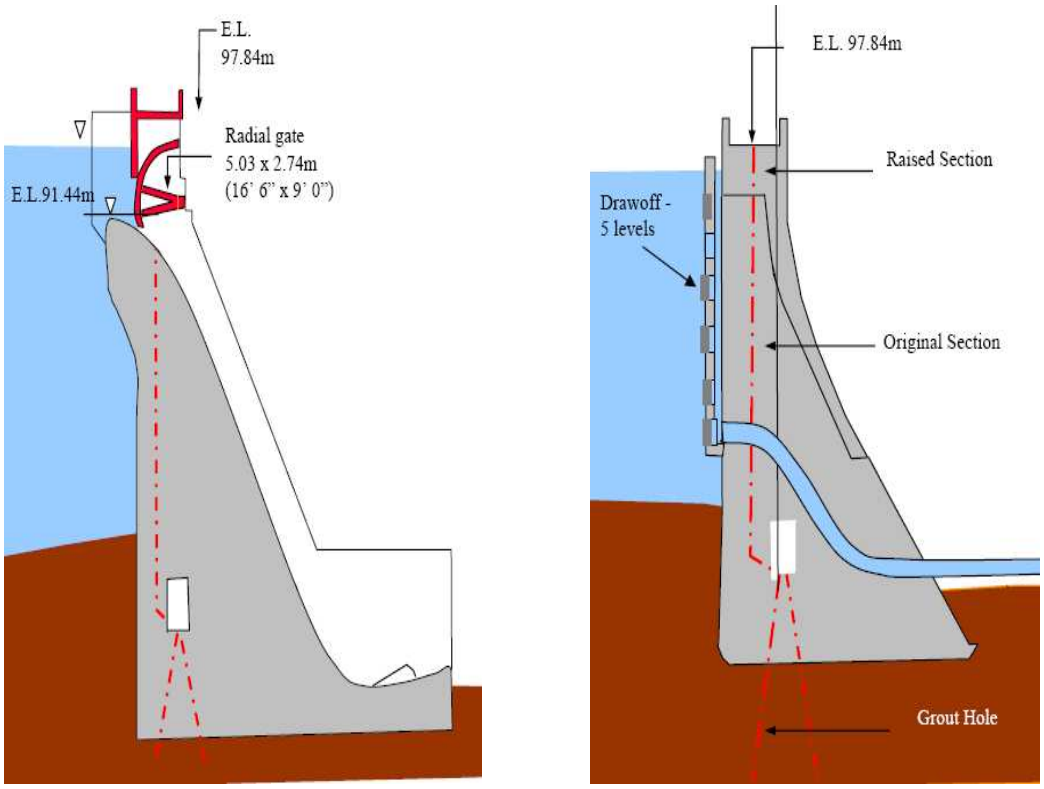


Cross section of Klang Gate dam. (Gibson Dodge ,1983)

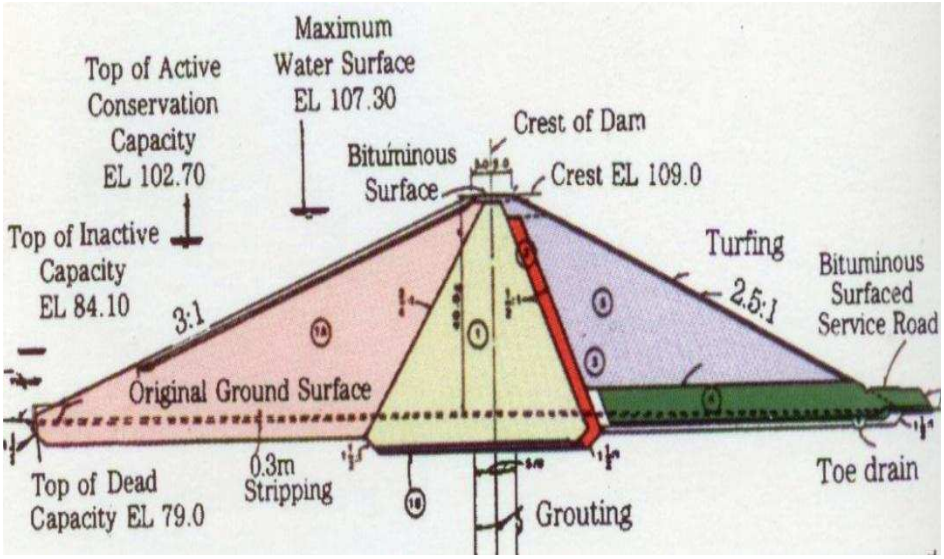


Cross section of Batu dam. (Obtained from DID).

**Appendix P- Performance of Daily and Monthly Discharges in the Calibration and Validation Periods in HEC-HMS**

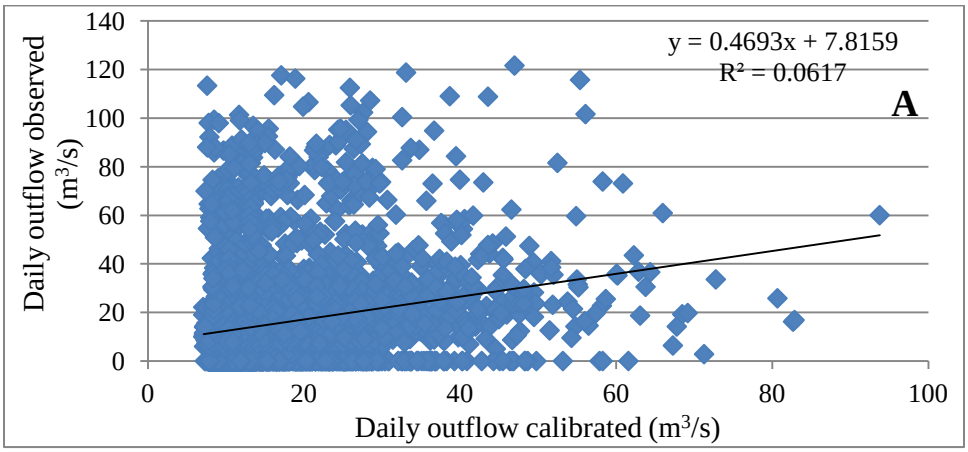


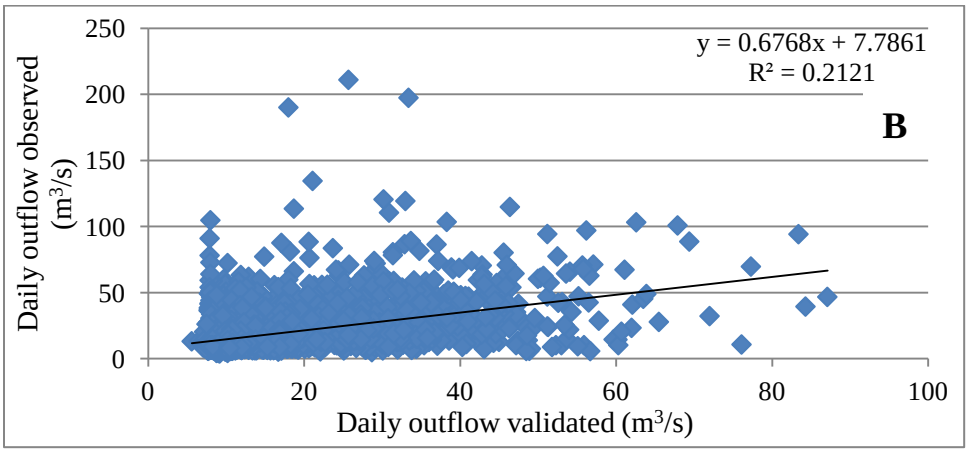


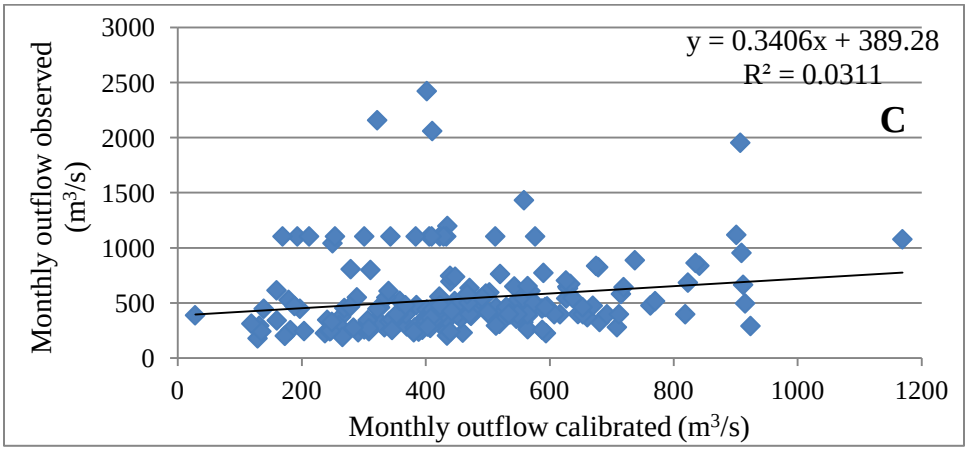

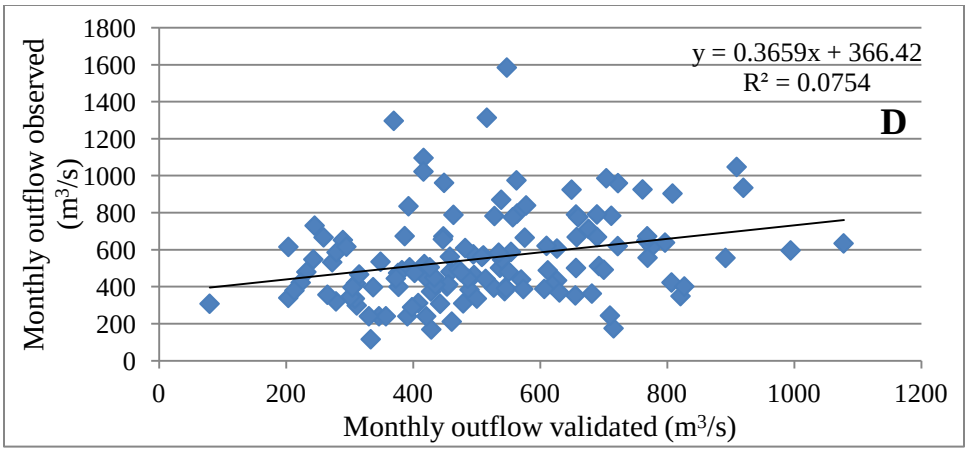


Scatter plots of calibrated and validated runoff against observed outflow at Sulaiman streamflow station, **A:** daily outflow calibrated, **B:** daily outflow validated, **C:** monthly outflow calibrated, **D:** monthly outflow validated

## Appendix Q- Maps of Rainfall Intensity for the Future Corresponding to A2 and B2 Scenarios

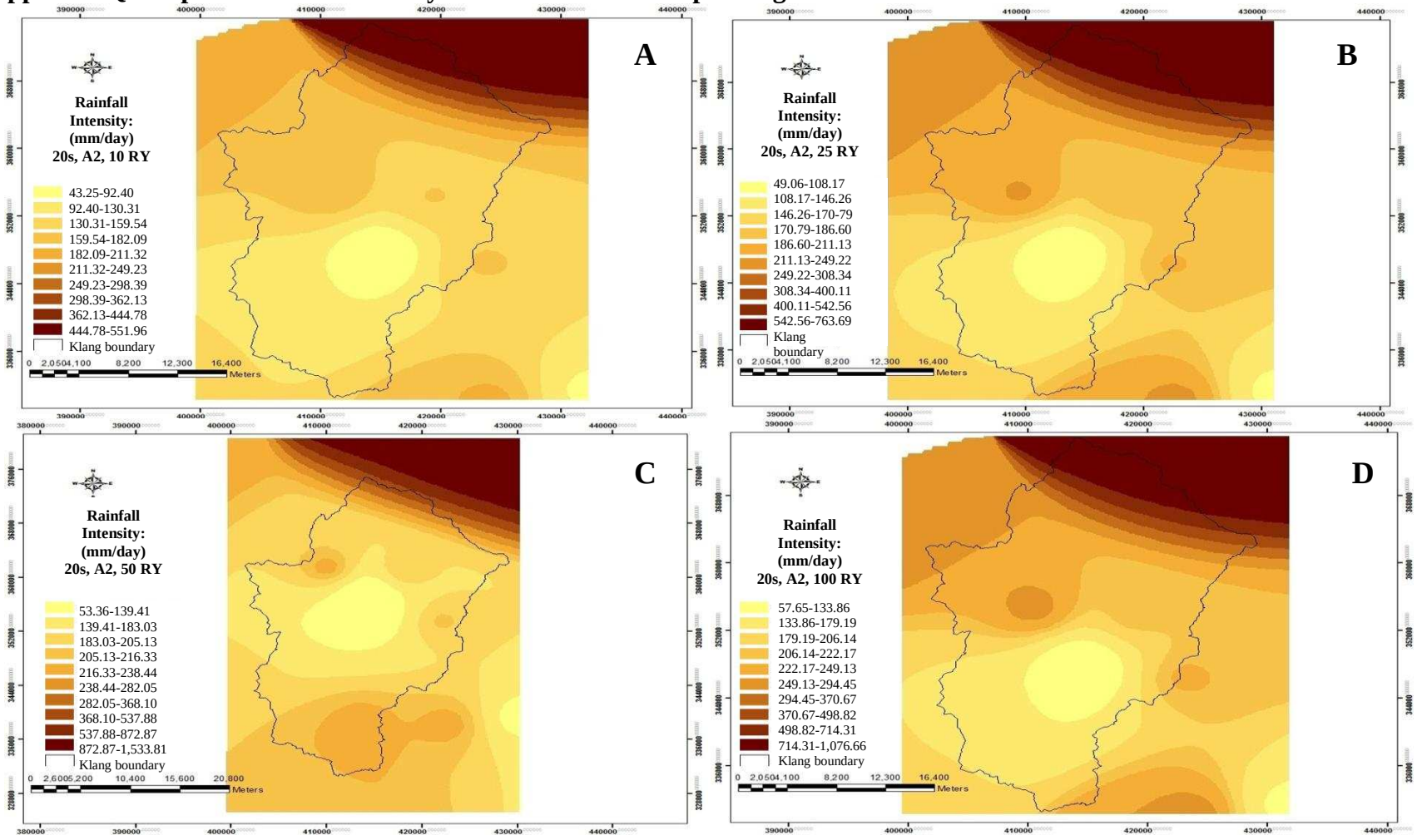


Rainfall Intensity for 2020s: **A:** (10 Return Year) ; **B:** (25 Return Year); **C:** (50 Return Year) and **D:** (100 Return Year) under A2 Scenario

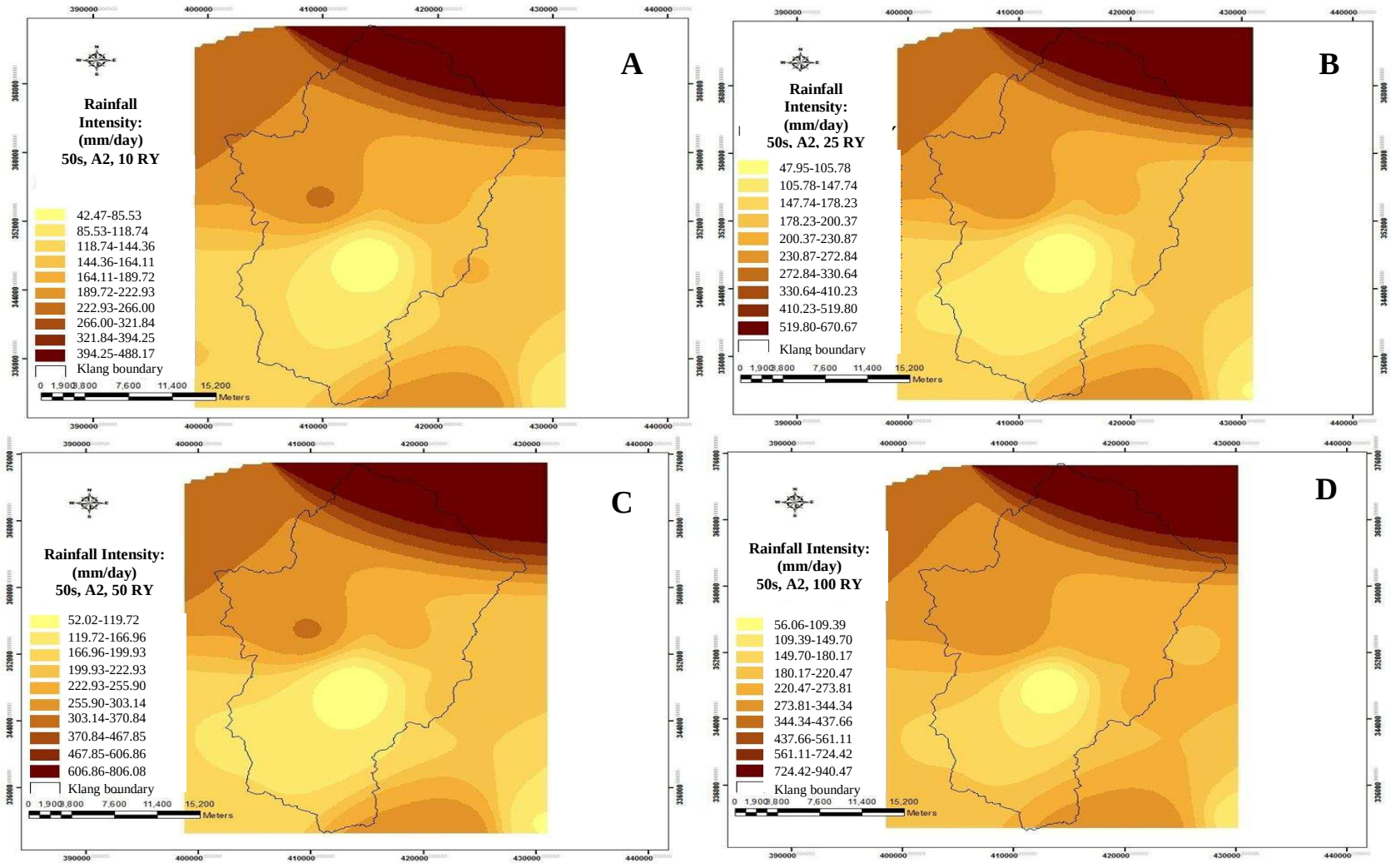


Rainfall Intensity for 2050s: **A:** (10 Return Year) ; **B:** (25 return Year); **C:** (50 Return Year) and **D:** (100 Return Year) under A2 Scenario

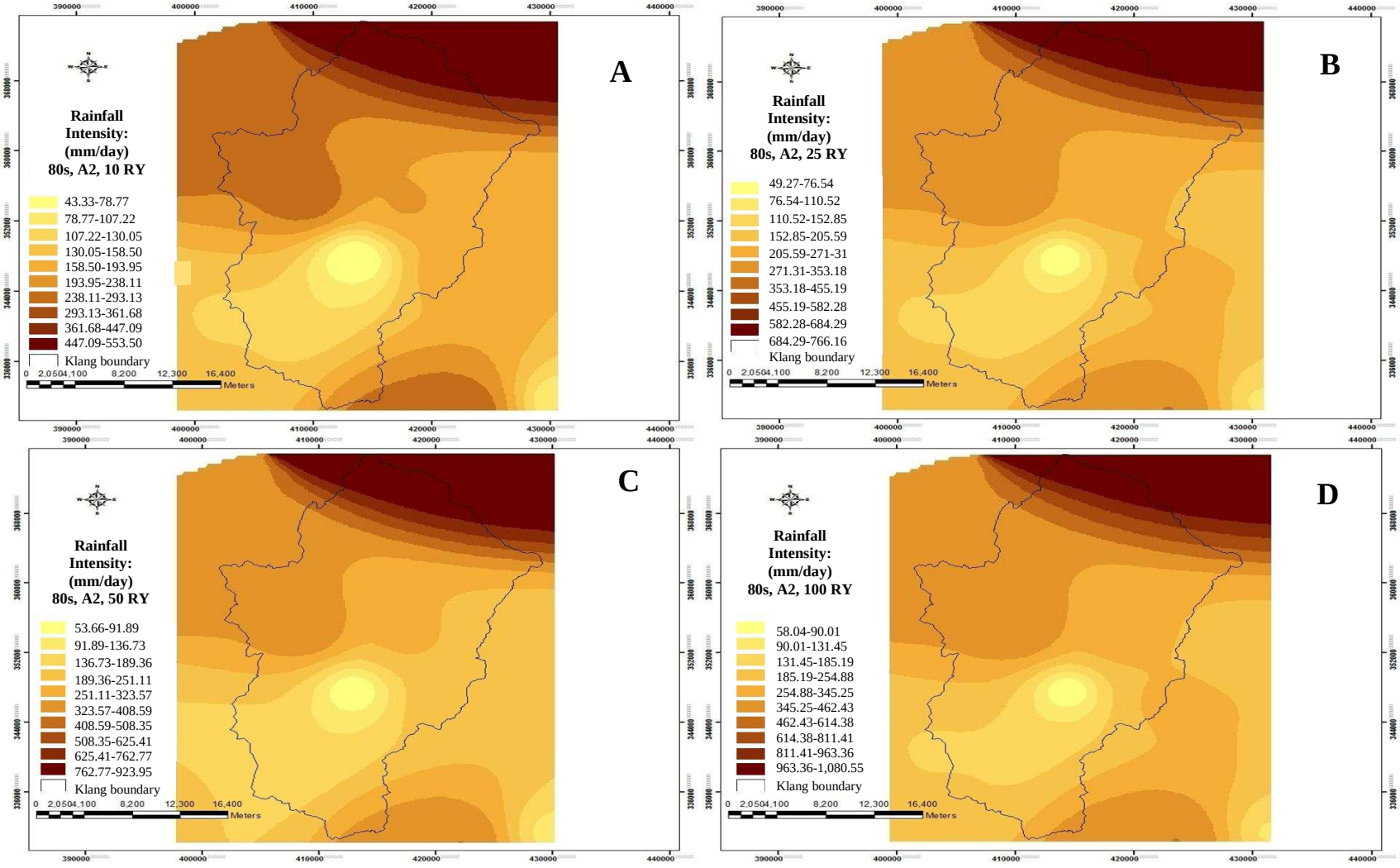


Intensity maps for 2080s: **A:** (10 Return Year) ; **B:** (25 return Year); **C:** (50 Return Year) and **D:** (100 Return Year) under A2 Scenario

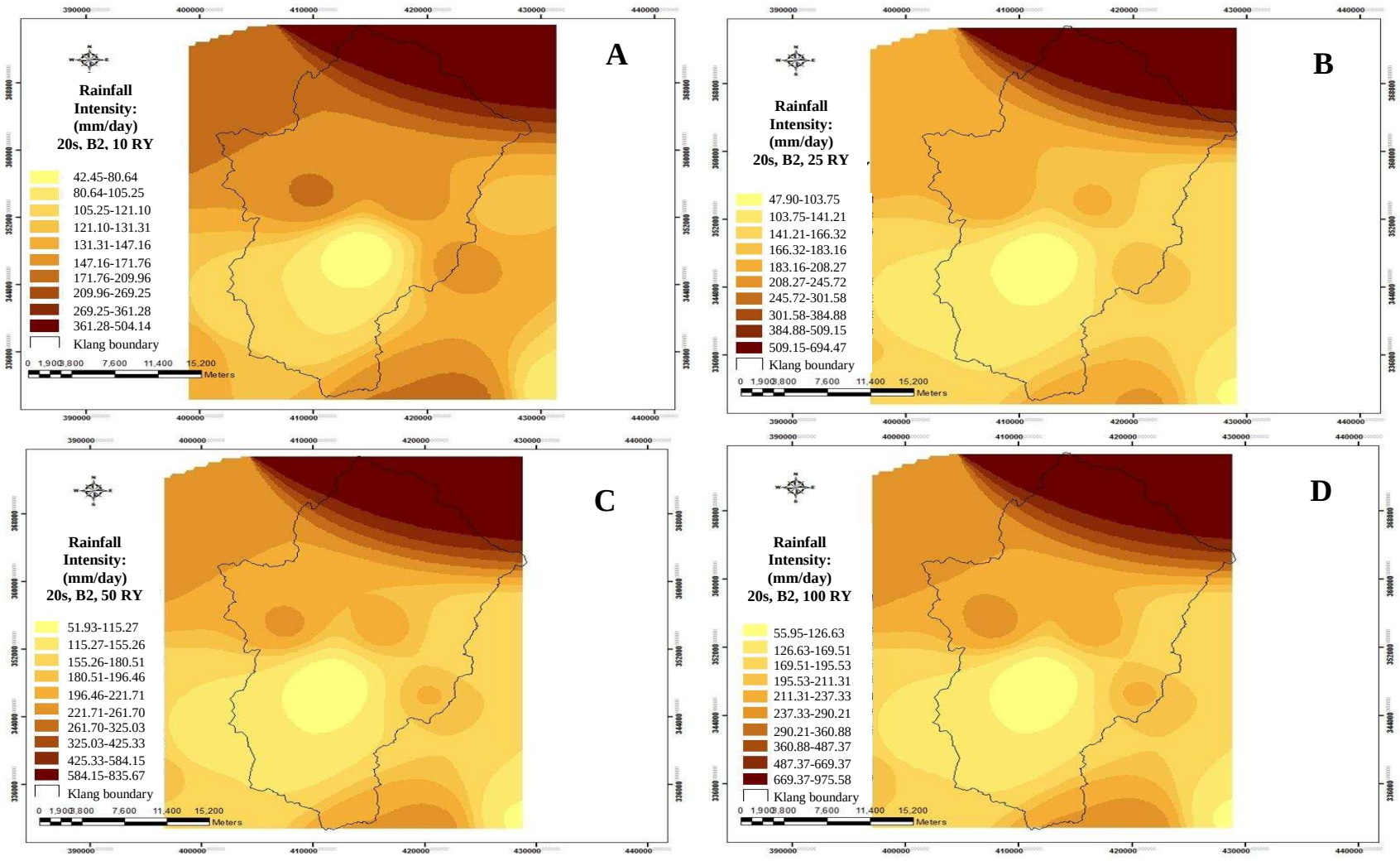


Rainfall Intensity for 2020s: **A:** (10 Return Year) ; **B:** (25 return Year); **C:** (50 Return Year) and **D:** (100 Return Year) under B2 Scenario

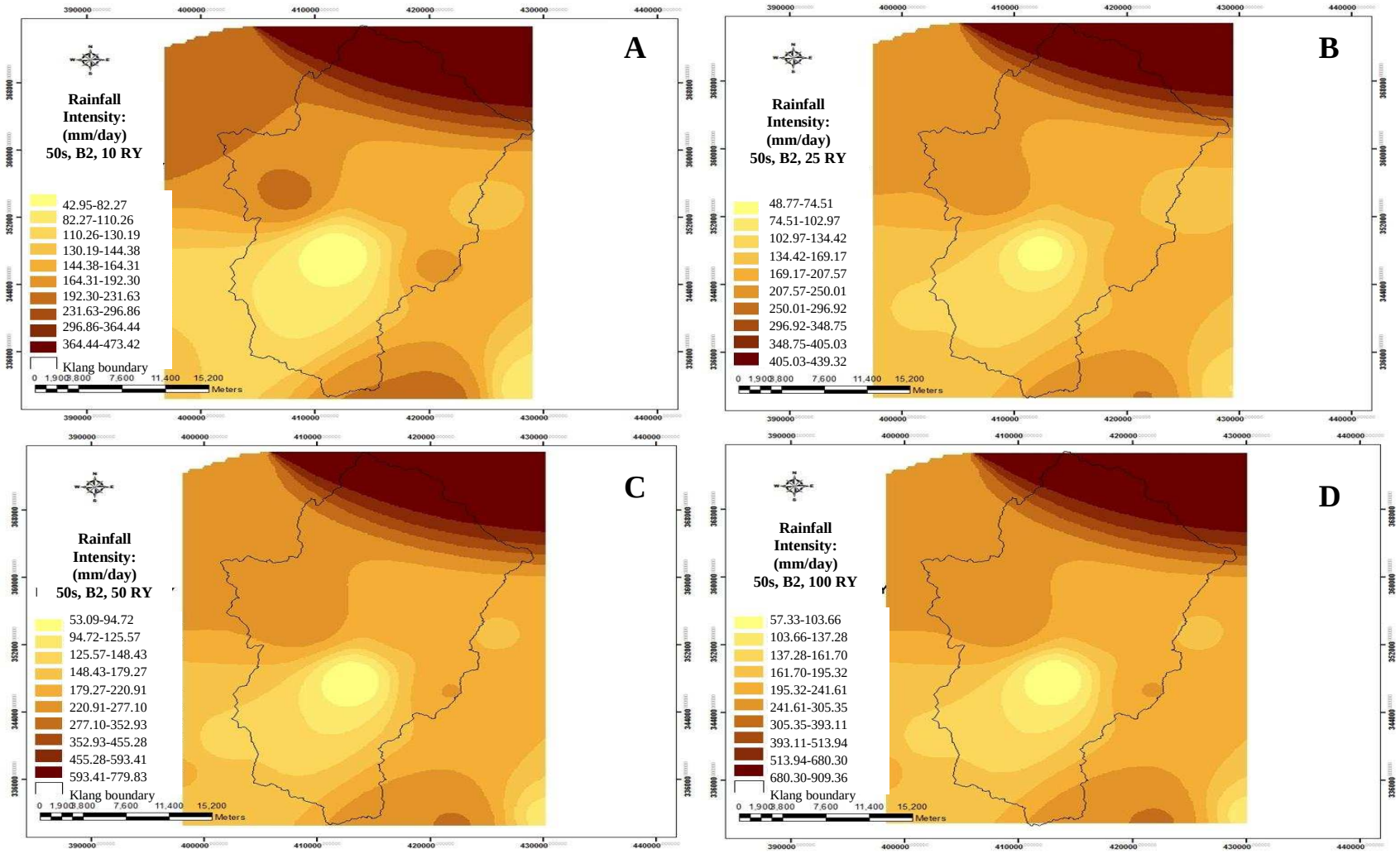


Rainfall Intensity for 2050s: **A:** (10 Return Year) ; **B:** (25 return Year); **C:** (50 Return Year) and **D:** (100 Return Year) under B2 Scenario

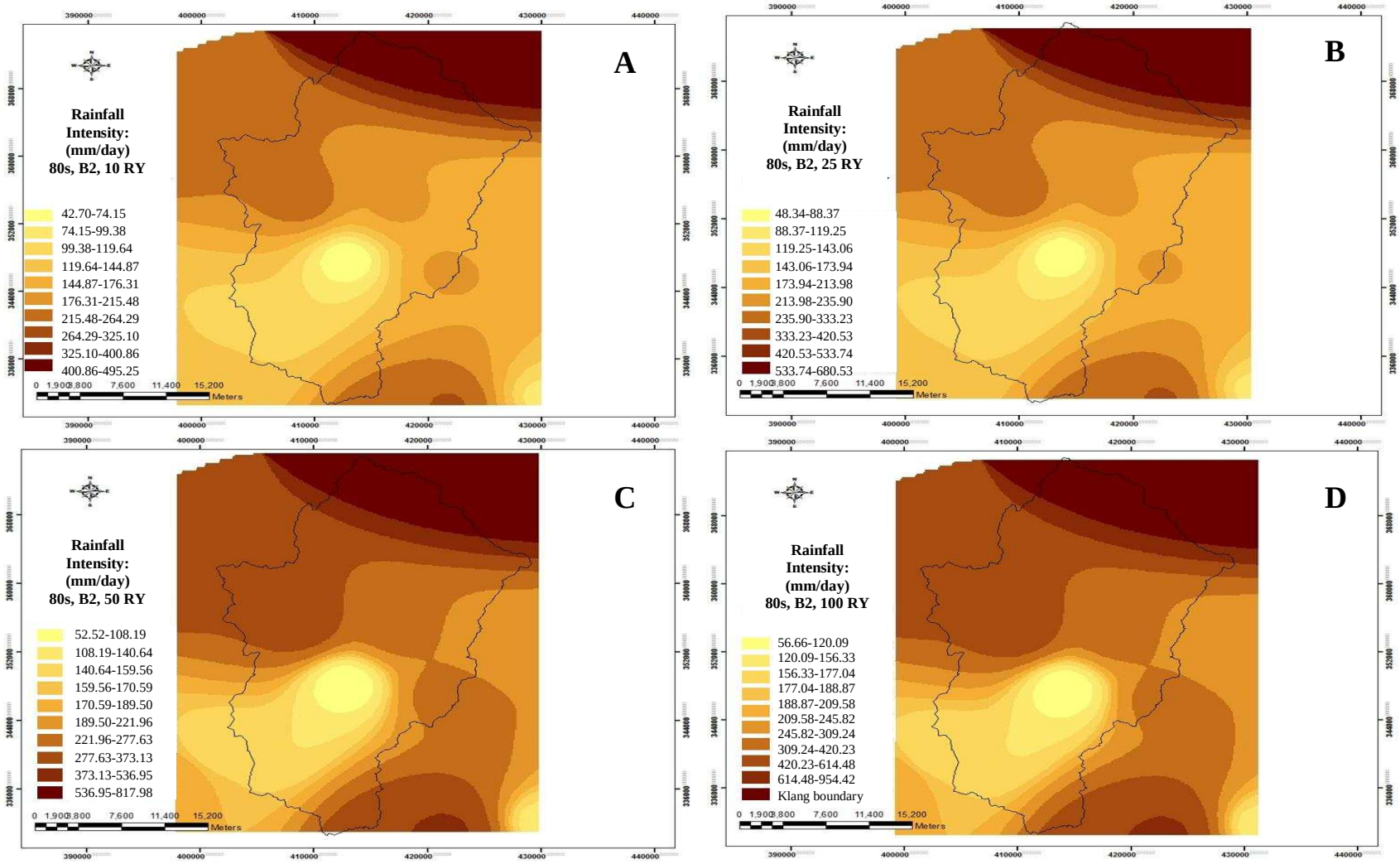


Rainfall Intensity for 2080s: **A:** (10 Return Year) ; **B:** (25 return Year); **C:** (50 Return Year) and **D:** (100 Return Year) under B2 Scenario

# Appendix R- Model Error in the Estimates of Mean and Variance

## A- Model errors in downscaled Mean daily precipitation with NCEP

Station no. 3116005

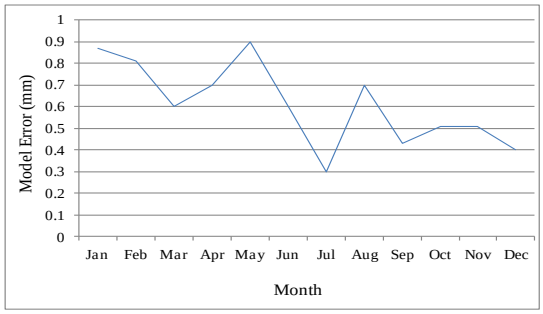


Station no. 3116006

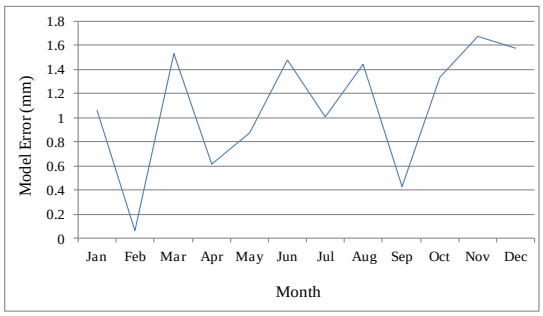


Station no. 3117070

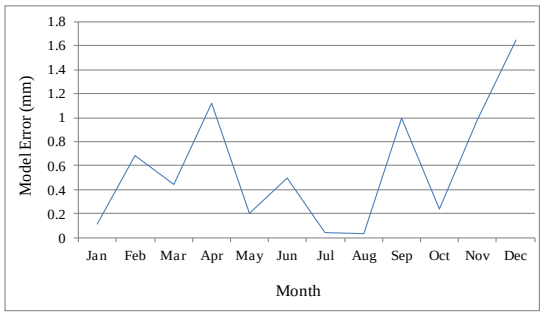


Station no. 3118069

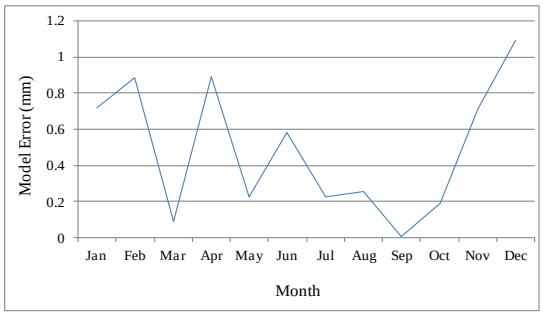


Station no. 3216001

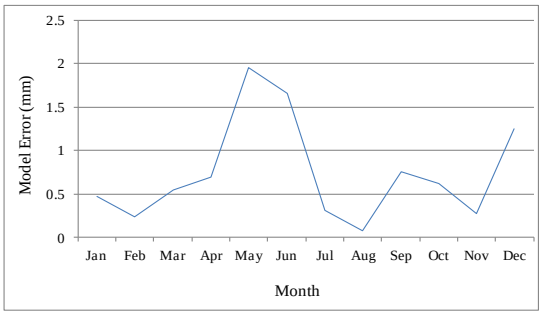


Station no. 3217001

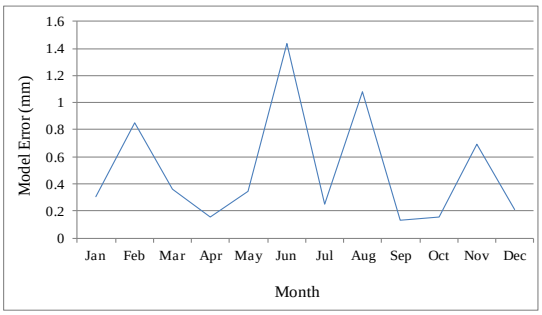


Station no. 3217002

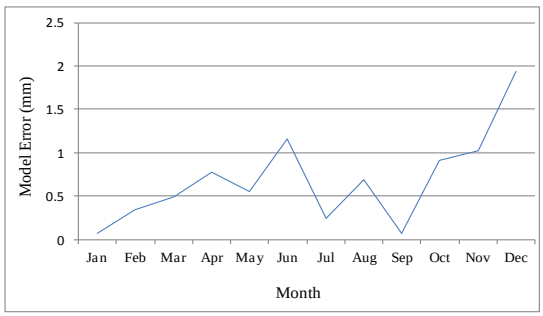


Station no. 3217004

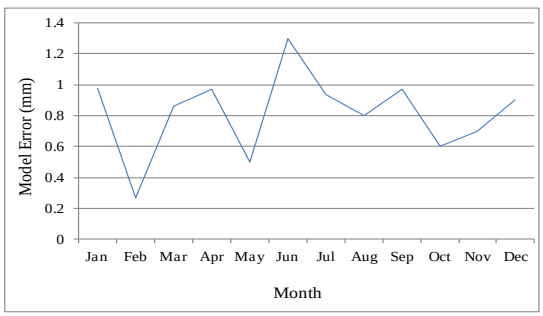

Station no. 3317004

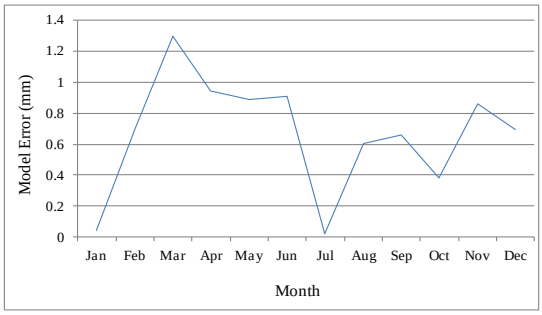


## B- Comparison between Variances of Observed and NCEP data

Station no. 3116005

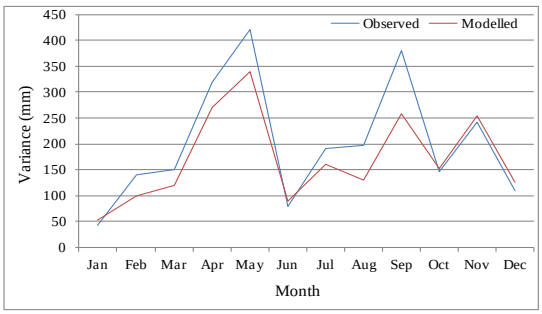


Station no. 3116006

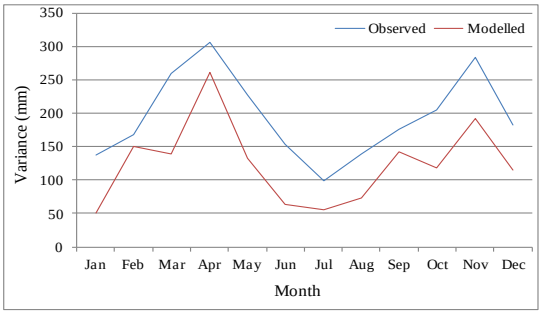


Station no. 3117070

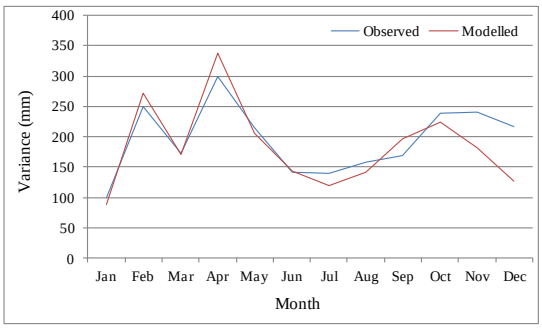


Station no. 3118069

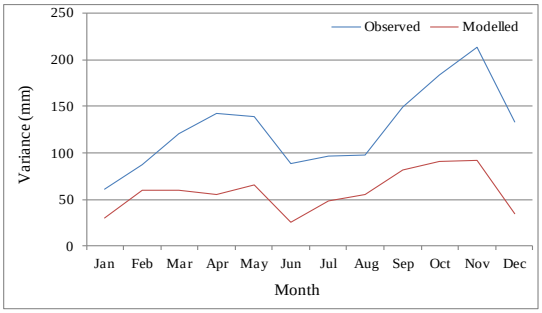


Station no. 3216001

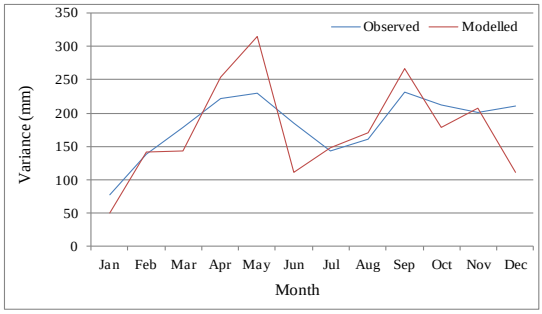


Station no. 3217001

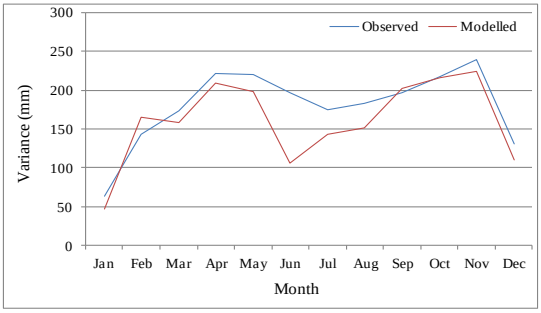

Station no. 3217002

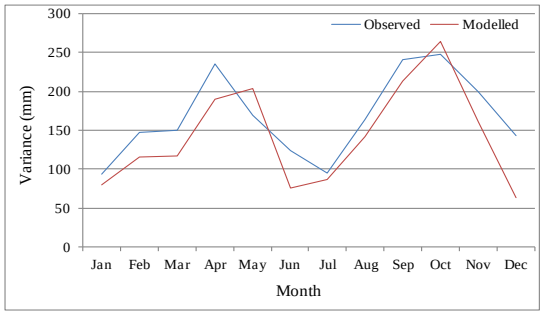


Station no. 3217004

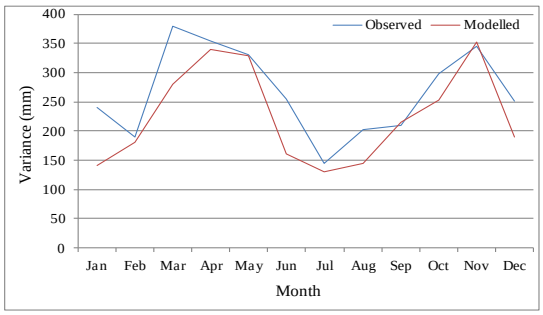


Station no. 3317004

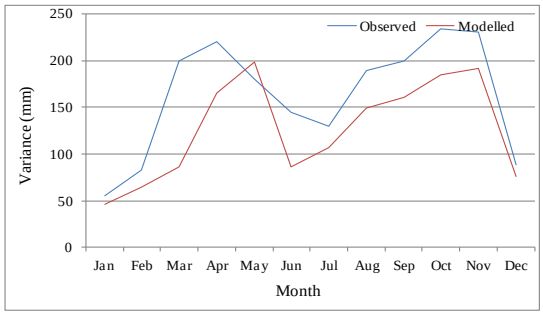

# Appendix S- Confidence Interval in the Estimates of Mean and Variance Daily Precipitation Downscaled with NCEP

## A- Confidence interval in the estimate of Mean

Station no. 3116005

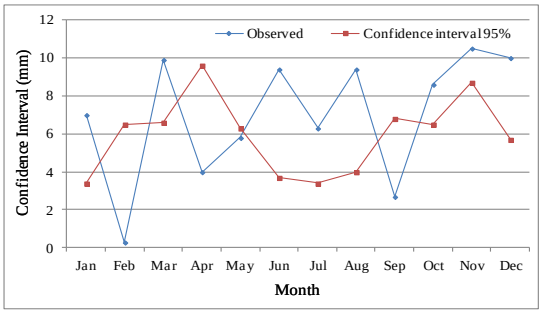


Station no 3116006

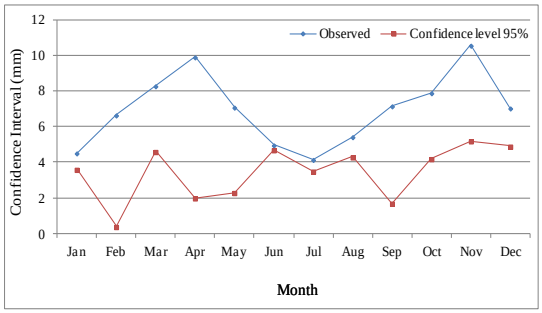


Station no. 3117070

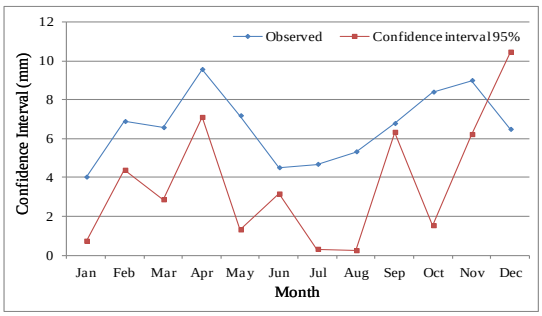


Station no. 3118069

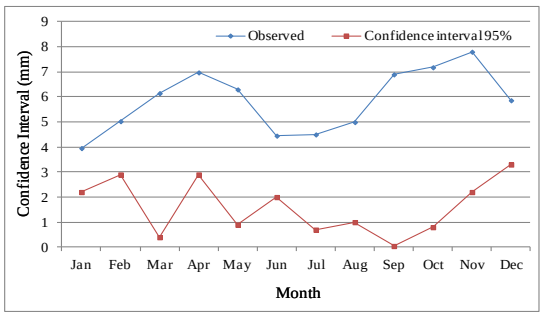


Station no. 3216001

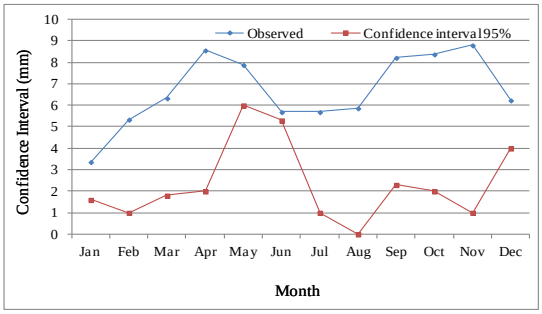


Station no. 3217001

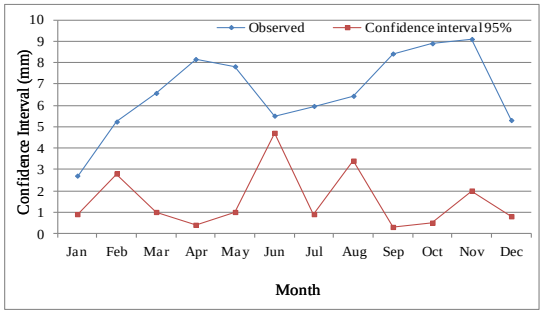


Station no. 3217002

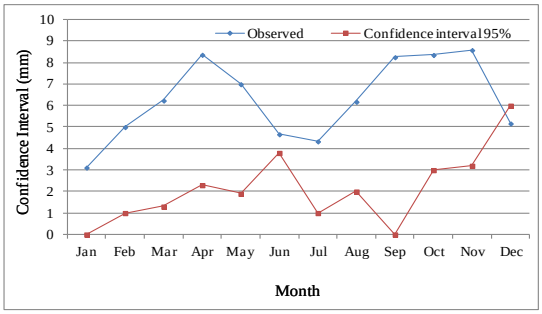


Station no. 3217004

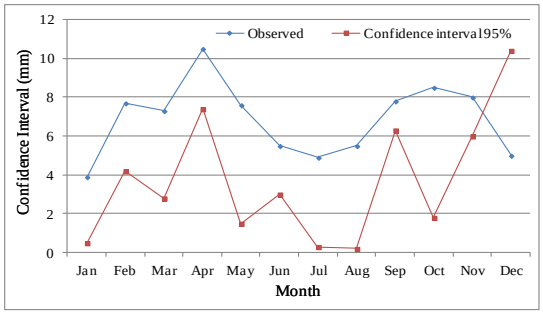

Station no. 3317004

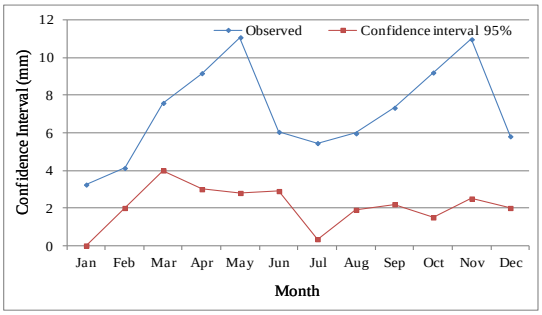


## B- Confidence interval in the estimate of Variance

Station no. 3116005

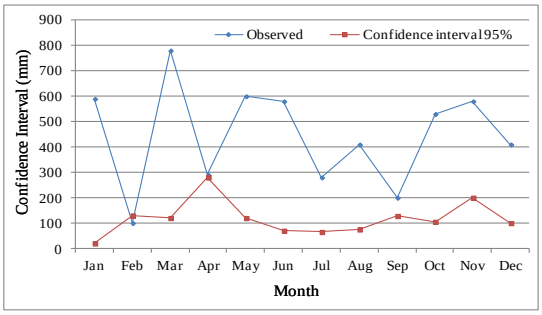


Station no. 3116006

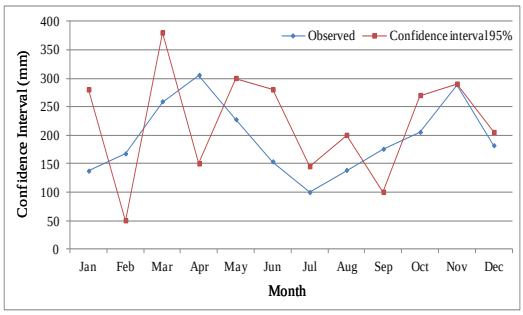


Station no. 3117070

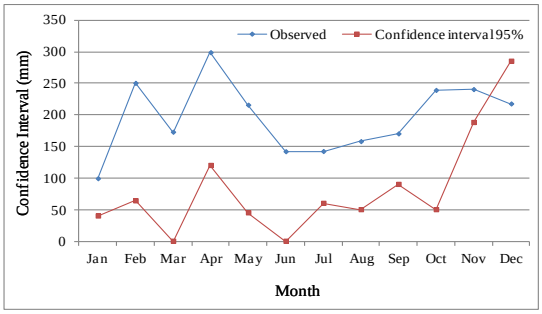


Station no. 3118069

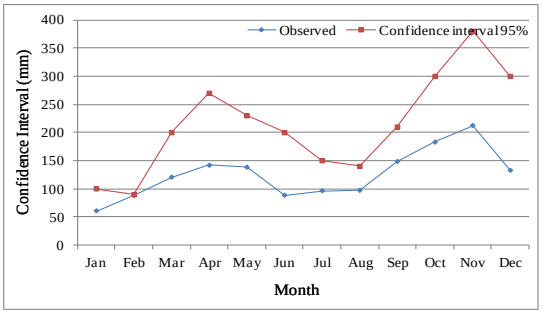


Station no. 3216001

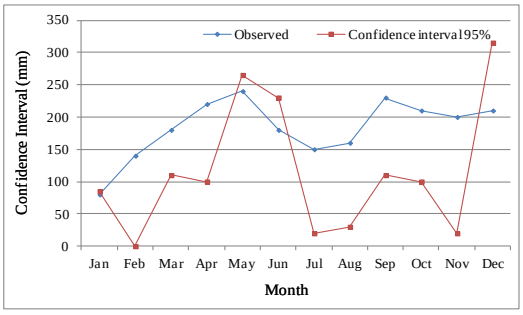


Station no. 3217001

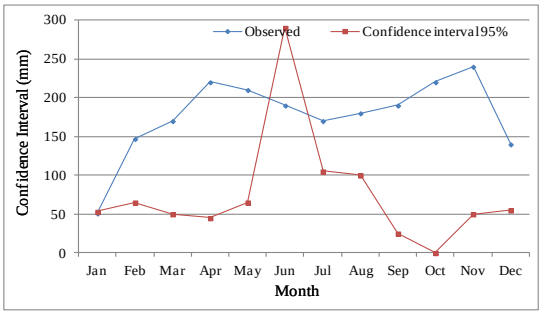

Station no. 3217002

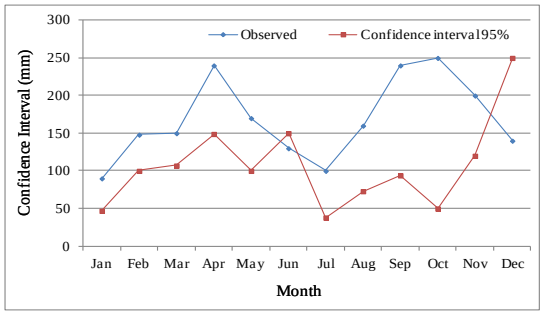


Station no. 3217004

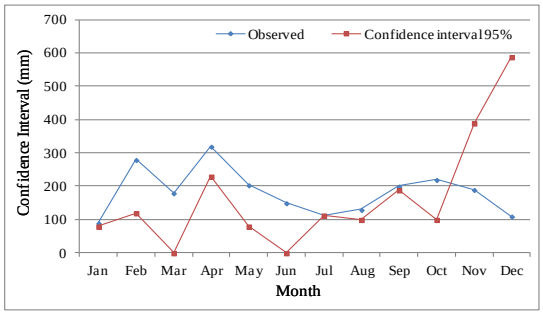


Station no. 3317004